A STUDY OF THE EFFECTS OF ORBITAL TOPOLOGY ON THE REGIOCHEMISTRY AND STEREOSPECIFICITY OF CYCLOPROPYL RING OPENING

A thesis

submitted in partial fulfilment

of the requirements for the Degree

of

Doctor of Philosophy in Chemistry

in the

University of Canterbury

New Zealand

by

Andrew Burritt

University of Canterbury

1993

"How would it be?" said Pooh slowly, "if, as soon as we're out of sight of this Pit, we try to find it again?"

"What's the good of that?" said Rabbit.

"Well," said Pooh, "we keep looking for Home and not finding it, so I thought that if we looked for this Pit, we'd be sure not to find it, which would be a Good Thing, because then we might find something that we *weren't* looking for, which might be just what we *were* looking for, really."

"I don't see much sense in that," said Rabbit.

"No," said Pooh humbly, "there isn't. But there was *going* to be when I began it. It's just that something happened to it on the way."

The House at Pooh Corner

ABSTRACT

The regiochemistry and stereochemistry of cyclopropane ring opening has been investigated by both theoretical and experimental methods to determine the factors which govern the selectivity of electrophilic addition to a cyclopropane ring.

The experimental work entailed the syntheses of compounds **I-VII** and the investigation of their reactions with electrophiles. The required tricyclic molecules were generally synthesised by literature procedures; however, for compounds **VI** and **VII** new synthetic routes were examined in an attempt to overcome the low yields and/or multiple step syntheses of the literature procedures. The cyclopropyl moieties were contained within tricyclo[3.2.1.$0^{2,4}$]octane **I-IV** or tricyclo[3.2.2.$0^{2,4}$]non-6-ene **V-VII** carbon skeletons to allow the stereochemical (edge verses corner) and regiochemical (which bond of the cyclopropane ring is broken) preferences of electrophilic addition to be determined. Incorporation of both a cyclopropane ring and an alkene functionality in the tricyclic hydrocarbons allowed the regiochemical preference for electrophilic addition to the cyclopropane ring or double bond to be elucidated. The structures of the products obtained from the electrophilic addition reactions were elucidated by detailed NMR studies using a variety of one and two dimensional NMR techniques and, in some cases, by X-ray crystallography.

The experimental results obtained indicate Br^+ addition for **I-III** to occur at the most substituted cyclopropyl bond with inversion of configuration at the site of electrophilic attack, and that substantial charge development occurs in the intermediate carbocations. For compounds **IV** and **V** Br^+ addition occurs predominantly at the double bond in preference to the cyclopropane ring. The reaction of **V** with H^+/D^+ gave predominantly electrophilic addition to the most substituted cyclopropyl bond with both edge and corner attack occurring to similar extents.

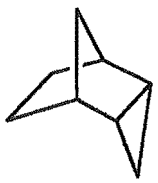

I

II

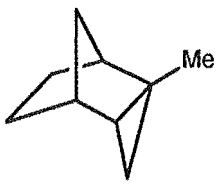

III

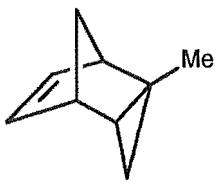

IV

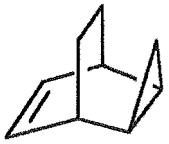

V

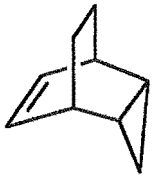

VI

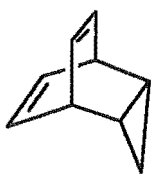

VII

Semiempirical and ab initio molecular orbital techniques were used to investigate the mechanisms of proton addition to cyclopropane and to *endo*- and *exo*-tricyclo-[3.2.1.$0^{2,4}$]octane (**I** and **II**, respectively) from both edge and corner trajectories. The effects of HOMO-LUMO interactions, orbital distributions, and secondary orbital interactions were found to be important in determining the stereoselectivity of electrophilic addition to a cyclopropane ring. The stabilities of the possible cations resulting from H^+ and Br^+ addition to cyclopropane and various saturated and unsaturated tricyclic hydrocarbons containing a cyclopropane ring were studied. The results of these investigations were used to evaluate the effect of cation stability in determining the regiochemical selectivity of electrophilic addition to a cyclopropane ring and the preference between addition to a double bond or cyclopropane ring. The results of these calculations were compared with those of experimental studies performed as part of the present work and with literature results. For the addition of H^+, the semiempirical calculations show cation stability to be important in determining the regiochemical selectivity of addition between a double bond or cyclopropane ring. However, for Br^+ addition the effects of carbocation stability are predicted not to be the dominant factor in determining the regiochemical selectivity between reaction at a double bond or cyclopropane ring.

CONTENTS

CHAPTER 1
Introduction

Section 1.1 BONDING IN CYCLOPROPANE

A number of theoretical descriptions of the bonding in cyclopropane have been suggested,[1-4] the first of which by Förster[1] in 1939 applied a valence bond (VB) approach which was later refined by Coulson and Moffit.[2] By applying the variation method in an approximate way, they concluded that the bonding consisted of three equivalent single bonds. Each bond was formed from the overlap of two *s-p* hybrid orbitals with each hybrid pointing outwards by 22° from the internuclear line, thus forming a bent bond.

In 1949 Walsh[3] adopted a Hartree-Fock (HF) molecular orbital (MO) viewpoint and suggested that the principal bonding resulted from the presence of three sp^2 hybridised carbons with one lobe of each carbon pointing toward the center of the cyclopropyl ring forming a three centre two electron bond. Extended Hückel (approximate HF theory) calculations performed by Hoffmann[4] in 1965 confirmed the presence of the orbitals described by Walsh (Figure 1.1).

The first ab initio HF treatment of cyclopropane was performed by Newton et al.[5,6] in 1970. Their calculations showed a delocalised bonding picture[7] consisting of a completely symmetrical doubly occupied orbital (2a' S, Figure 1.1) which makes up the electron deficient σ-bonding framework (the Hückel array of orbitals) and a degenerate pair of e' orbitals (3e' A, 3e' S, part of the Möbius array of orbitals) which form the electron rich π-bonding framework of cyclopropane. The symmetrical 2a' orbital resembled closely the principle bonding orbital suggested by Walsh. The molecular orbital methods[3,4,5,6] ascribe the stability of cyclopropane to σ-aromaticity and delocalisation[8,9] of electrons in the plane of the cyclopropane ring. Localisation[10] of the HF orbitals[5,6] gave three equivalent bent bonds which showed close agreement with the bonding description obtained by Coulson and Moffit. The bent bonds were formed from $sp^{3.81}$ hybridised carbons and have a calculated interorbital angle of 116°. The orbital amplitude is concentrated outside of the cyclopropane ring.

Recent high level self consistent field (SCF) VB calculations[11] incorporating a double-ζ plus *d* orbitals basis set of Slater type orbitals[11] have confirmed the general bonding picture described by Coulson and Moffit. The VB calculations[11] describe the carbon-carbon bonding in cyclopropane as being similar to that of ethene as both structures show similar features of the calculated anisotropy of the electron densities.

Thus, the VB predictions‡ show no evidence for the two electron three center bond obtained from the molecular orbital model. In any event,† the facility of cyclopropane to undergo ring opening with electrophiles and exhibit conjugation to a π system or carbocation centre is generally considered to result from the relative weakening of the σ-bonds in the carbon framework of cyclopropane by angle strain and thereby allowing greater interaction with electrophiles or an adjacent π system.[7,12]

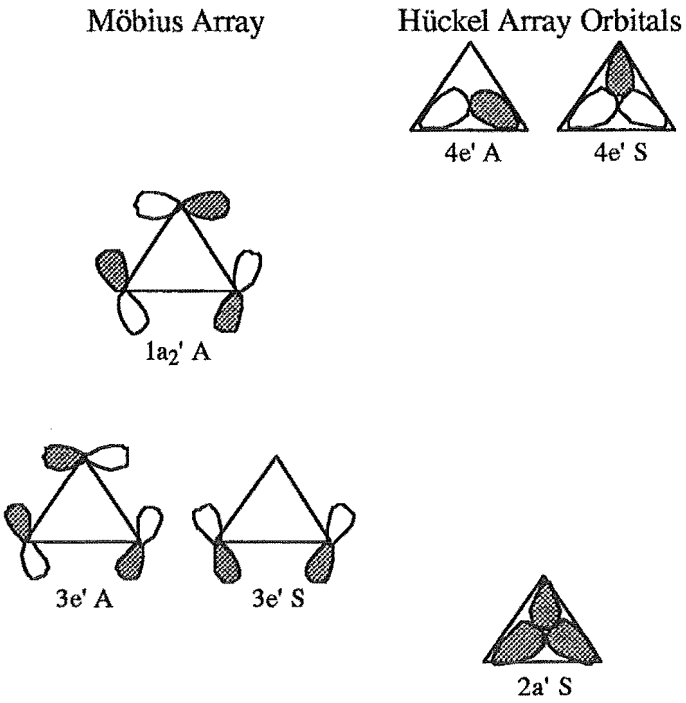

Figure 1.1. Walsh molecular orbitals of cyclopropane. The 2a', 3e' A, and 3e' S orbitals are occupied and the $1a_2'$, 4e' A, and 4e' S orbitals are unoccupied in ground state cyclopropane.

Section 1.2 REACTIVITY OF THE CYCLOPROPYL GROUP

Section 1.2.1 Reaction with Electrophiles

Section 1.2.1a Acid induced ring cleavage

Electrophilic attack on cyclopropanes has been suggested[7,13-16] to occur by either edge or corner attack of an electrophile, which leads to either retention or inversion, respectively, at the site of electrophilic addition (Figure 1.2). Reaction with retention may be considered[17,18] as cleavage of the carbon-carbon bond *syn* to the incoming electrophile and inversion as bond cleavage *anti* to the entering electrophile. Although, the direct formation of a primary cation has been shown[16,19-21] to be unlikely. A third

---

‡ VB theory does predict the existence of two electron three center bonds, for example, in diborane, but does not show[11] this to be the case for cyclopropane.

† For a discussion of VB versus MO descriptions see reference 11.

possible trajectory, face protonation (Figure 1.3), has also been proposed but this has consistently been rejected.[7]

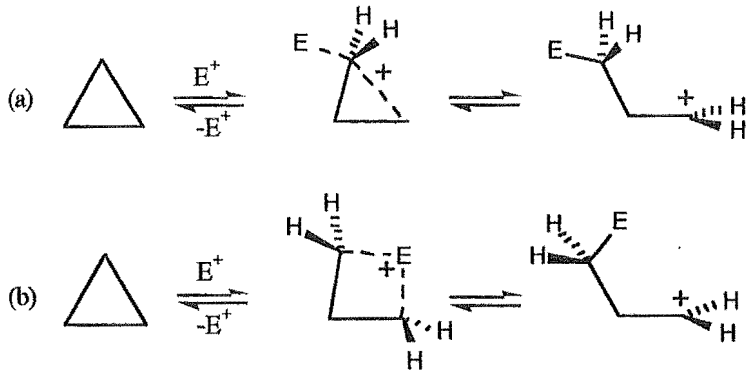

Figure 1.2. (a) Corner attack resulting in inversion of configuration. (b) Edge attack resulting in retention of configuration.

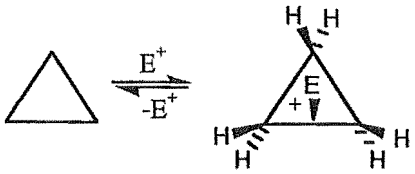

Figure 1.3. Face protonation of cyclopropane.

It is generally believed that the direction of bond cleavage can be accounted for by a modified version of Markovnikov's rule,[13;22] which states that the ring opens between the carbons bearing the largest number and smallest number of alkyl substituents. For cyclopropanes substituted at only one carbon, products may be rationalised by ring opening leading to the more substituted carbocation (Figure 1.4).

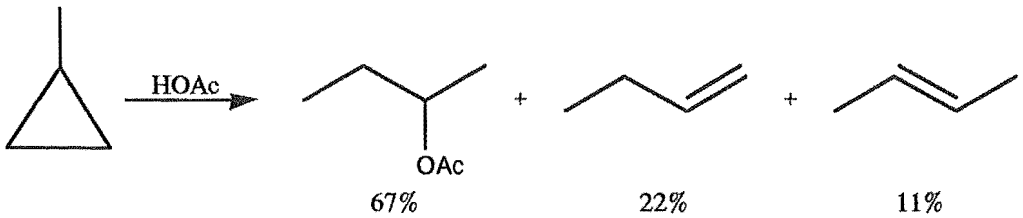

Figure 1.4. Cyclopropane ring opening by modified Markovnikov type cleavage.

When the cyclopropane is substituted at two carbons the products generally result[7,13] from both Markovnikov type addition and from cleavage of the most substituted carbon-carbon bond[18] (Figure 1.5). Generally, no products resulting from cleavage to the least substituted carbon[13] are observed. For example, Coxon et al.[18] have investigated the acid catalyzed reaction of *endo*-tricyclo[3.2.1.$0^{2,4}$]octane **1** with methanol and methanol-d_1. In this case only the most substituted carbon-carbon (C2-C4) bond was broken. Inclusion of the cyclopropane ring into a fused polycyclic ring system allows

definitive identification of the trajectory of electrophilic and subsequent nucleophilic attack. Thus the results of this study showed proton/deuteron addition to occur exclusively via a corner attack trajectory, followed by nucleophilic capture of the resulting cations **2a** (**2b**) and **3a** (**3b**) with inversion (Figure 1.6) to give the observed products **4a** (**4b**) and **5a** (**5b**) in a ratio of 62:38, respectively.

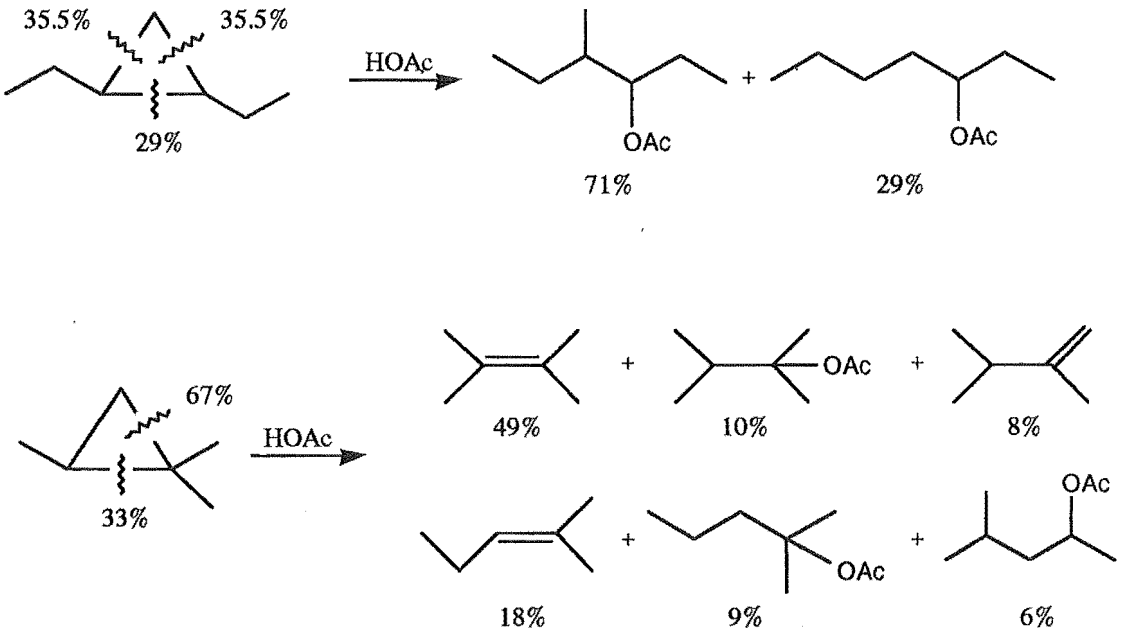

Figure 1.5. Cyclopropanes substituted at two carbons generally result in both Markovnikov type cleavage and ring opening resulting from cleavage of the most substituted carbon-carbon bond.[17]

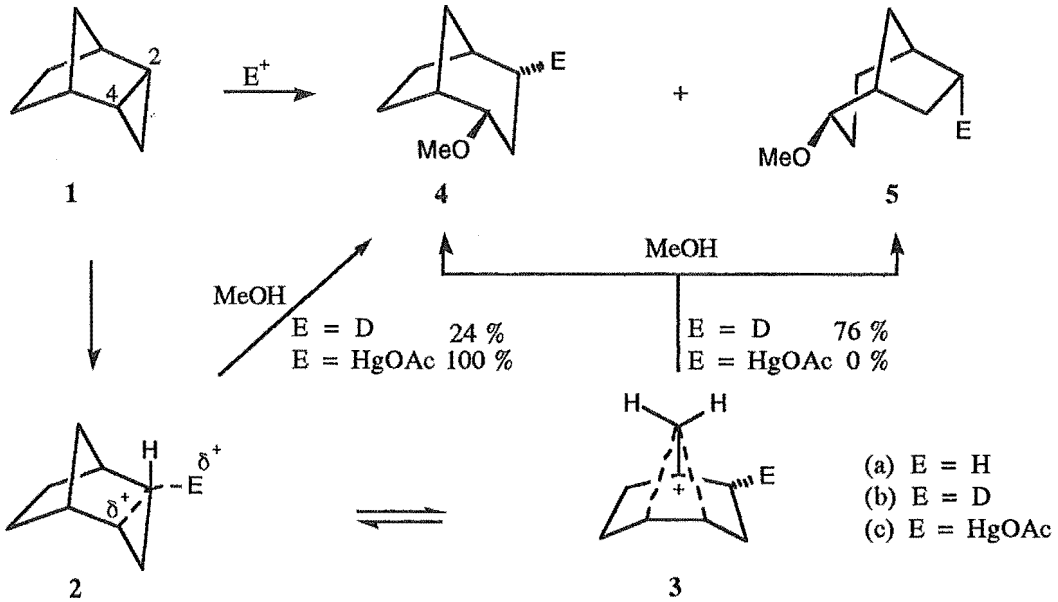

Figure 1.6. Reaction of *endo*-tricyclo[3.2.1.$0^{2,4}$]octane with (a) H^+, (b) D^+, and (c) $Hg(OAc)_2$.

Wiberg et al.[17,20,21] have investigated the acetolysis of a number of systems containing cyclopropane rings (Table 1.1) and concluded that the reaction proceeds towards the formation of the most stable carbocation with initial protonation being the rate determining step. The protonated cyclopropane reacts with the solvent, acting as a nucleophile, before it is cleaved to form an open carbocation. Relief of strain energy (SE) was shown to have only a small effect on the rate of reaction. For example, a plot of the relative rate of acetolysis (log k_{Rel}) for compounds **6** - **22** (Table 1.1) against ΔSE (Figure 1.7a)§ shows a poor correlation, indicating that strain relief is not an important factor in determining the rate of reaction.

Although the stability of the resulting carbocation is important in determining product formation[21] it does not show a major effect on the rate of reaction. This can be seen by comparison of the rates of acetolysis of **10** and **11** where the rates differ by only a factor of two even though they form secondary and tertiary carbocations,‡ respectively. This conclusion is supported by consideration of the propellanes **18** - **21** where all would result in the formation of tertiary carbocations but the rates of acetolysis[21] span a range of 10^7 (k_{Rel} : 0.36 - 1.9×10^6). Wiberg et al.[21] also considered a frontier molecular orbital[23] (FMO) explanation for the observed reactivities. By this theory the reactivity would be expected to be proportional to the degree of interaction of the empty *s* orbital of the proton and the highest occupied molecular orbital (HOMO) of the cyclopropane derivative. A plot of log k_{Rel} against vertical ionisation potential (Figure 1.7b) gives a reasonable correlation, with the exception of [3.2.1]propellane **18**. The [3.2.1] and [4.2.1] propellane systems, although having similar ionisation potentials (8.41 and 8.50 eV, respectively) show a relative rate difference of 10^4. Although the difference in strain energy may account for some of the observed rate difference, Wiberg et al.[21] concluded that it was unlikely that it could account for such a large difference in reactivity. Wiberg et al.[21] found the polarisability of the cyclopropane bonds to be important in rationalising the relative rates of reaction. A plot of log k_{Rel} versus electron population† (Figure 1.7c) showed a reasonable correlation.

---

§ ΔSE is the difference in strain energy between compounds **6** - **22** and the corresponding ring opened hydrocarbon products, for example, ΔSE for compound **18** = SE(**18**) - SE(bicyclo[3.2.1]octane) = 280.3 - 37.7 = 242.6 kJ mol^{-1} ≈ 243 kJ mol^{-1}.[21]

‡ This effect may also be interpreted to support the idea that an open cation is not formed before solvent capture occurs.

† The electron population was calculated by placing a proton along the axis of a carbon-carbon bond, 2.0 Å from the nearest carbon, in the cyclopropane derivative and evaluating the electron population of the incoming hydrogen. The electron density donated by each MO was also evaluated. The HOMO was estimated to contribute approximately 50% of the electron density.

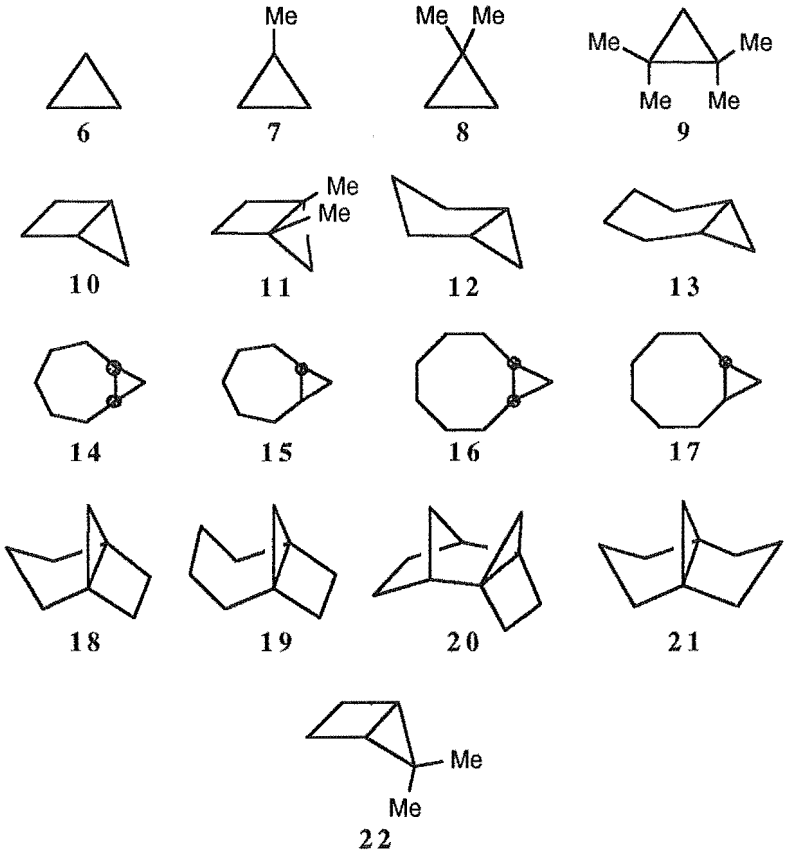

Compound	k_{Rel}	log k_{Rel}	I.P.	$\Delta SE^{\ddagger}$
tetracyclo[4.2.1.1^{2,5}.0^{1,6}]dodecane **20**	1.9x10^{6}	6.3		
[3.2.1]propellane **18**	1.2x10^{6}	6.1	8.41	243
[4.2.1]propellane **19**	93	2.0	8.50	201
5,5-dimethylbicyclopentane **22**	79	1.9		117
1,4-dimethylbicyclopentane **11**	2	0.30	8.8	213
bicyclo[2.1.0]pentane **10**	1.0	0.0	9.55	213
[3.3.1]propellane **21**	0.36	-0.44		121
1,1,2,2-tetramethylcyclopropane **9**	0.29	-0.54	9.18	117
trans-bicyclo[5.1.0]octane **15**	0.27	-0.57		138
1,1-dimethylcyclopropane **8**	0.65	-1.2	9.72	117
bicyclo[4.1.0]heptane **13**	0.032	-1.5	9.46	113
cis-bicyclo[6.1.0]nonane **16**	0.018	-1.7		100
cis-bicyclo[5.1.0]octane **14**	0.017	-1.8		96
trans-bicyclo[6.1.0]nonane **17**	0.015	-1.8		105
bicyclo[3.1.0]hexane **12**	0.011	-2.0	9.65	113
methylcyclopropane **7**	5.6x10^{-3}	-2.3	10.1	117
cyclopropane **6**	4.9x10^{-5}	-4.3	10.9	117

Table 1.1. Data for relative rates of acetolysis (k_{Rel}), ionisation potential (I.P. in eV), and relief of strain energy (ΔSE in kJ mol^{-1}) for selected compounds containing a cyclopropyl ring.[21] (‡ Values do not take into account the difference in energy between secondary and tertiary cations)

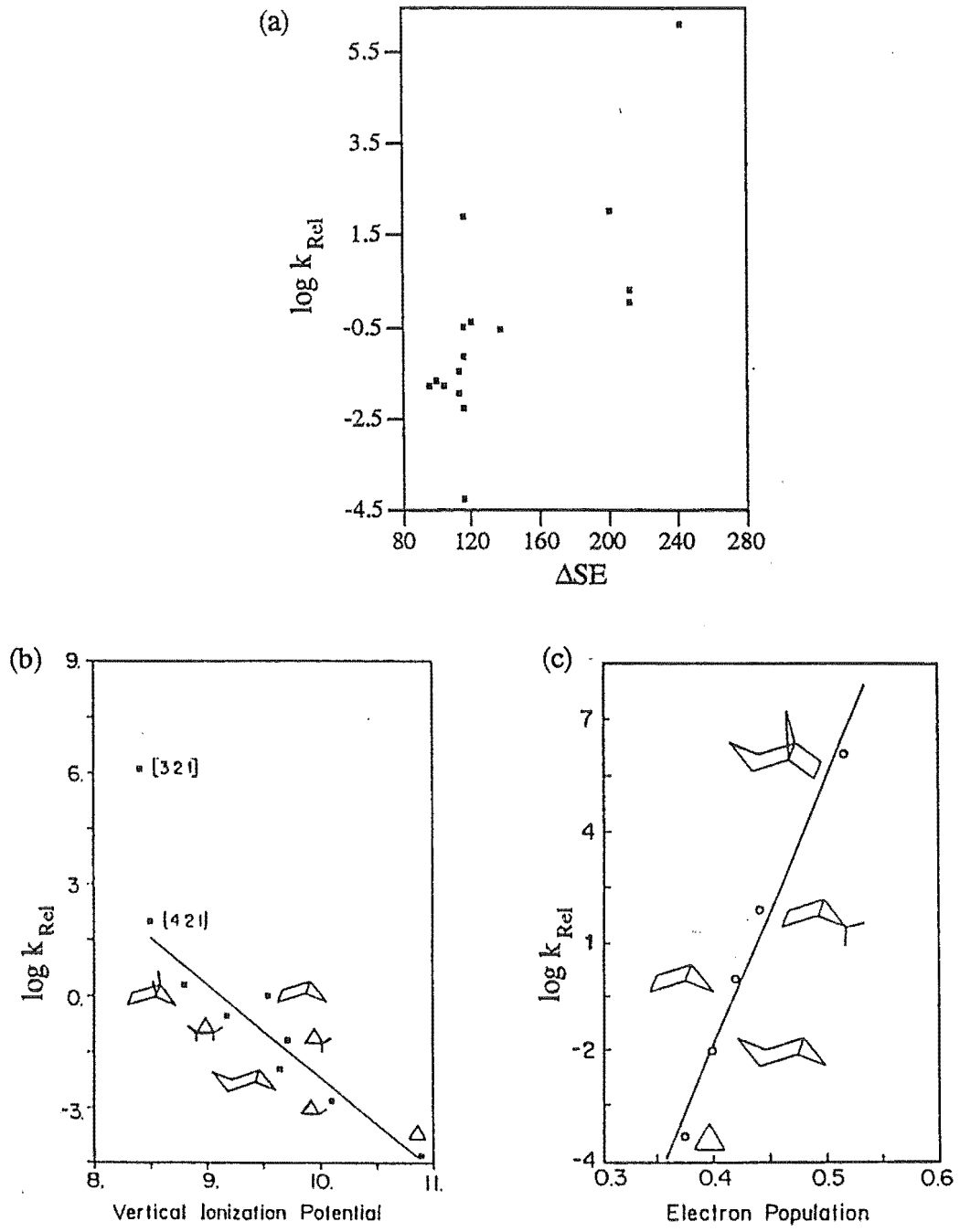

Figure 1.7. (a) Correlation of the relative rate of acetolysis (log k_{Rel}) with ΔSE (in kJ mol^{-1}). (b) Correlation of the relative rate of acetolysis (log k_{Rel}) with vertical ionisation potential (in eV). (c) Correlation of the relative rate of acetolysis (log k_{Rel}) with electron population.

These results show the importance of considering bond polarisation in the reaction of charged species with neutral molecules. Not only the HOMO is involved in electron donation to an incoming electrophile. This therefore explains why FMO theory gives a reasonable explanation for the rates of acetolysis but is not extremely accurate and some anomalies are observed, for example the reactivity of the [3.2.1]propellane system. Wiberg et al concluded that proton transfer to cyclopropane depends primarily on the ease of polarisation of one (or more) of the carbon-carbon bonds. The reaction proceeds towards the most stable carbocation, and at the product forming transition state the structure has not relaxed to a large degree. This is consistent with a poor correlation between reactivity and strain energy. The products formation by capture of the protonated species before it becomes an acyclic carbocation is consistent with the often stereoselective capture of the nucleophile, and stereoselective hydrogen transfer or proton loss. The above observations are consistent with the results obtained by Coxon[13,18] and Baird.[19]

Section 1.2.1b Bromination of cyclopropanes

Reaction of cyclopropanes with bromine is often slow in the absence of light or Lewis acid catalysts for example, cyclopropane and bromine do not react in the dark [24-28] in the absence of a Lewis catalyst. Methyl and ethylcyclopropane react slowly (3 days at room temperature) to produce at least seven and twelve products,[24] respectively. In contrast, reaction of cyclopropanes with HBr occurs rapidly. Alkenes, on the other hand react rapidly with bromine but more slowly with HBr. Radical reactions of Br_2 with cyclopropanes are also known.[24,29]

Skell et al.[24] have investigated the bromination of a number of cyclopropanes, using N-bromosuccinimide as an acid scavenger to minimise the reaction with HBr, precluding radical reactions by conducting the reactions in the dark. They concluded that bromine addition takes place predominantly at the least substituted carbon (Figure 1.8) and with Markovnikov ring opening.[24]

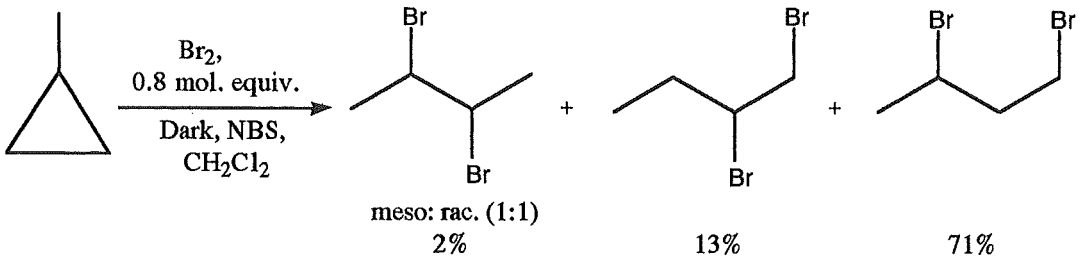

Figure 1.8. Bromination of methylcyclopropane with exclusion of radical pathways and reaction with HBr.

The rate of bromination is complicated by a concentration dependence[24,30,31] of the mechanism.‡ The rate of bromination of a number of cyclopropanes with low concentrations of bromine (0.25-0.50 M) has been investigated (Table 1.2).[24] Alkyl substitution results in a marked increase in rate (e.g. 1,1-dimethylcyclopropane > methylcyclopropane > cyclopropane) which is consistent with carbocation ion stability. Introduction of further alkyl groups at the unsubstituted carbon leads only to a modest increase in reactivity. Steric effects are generally not believed to effect the rate of bromination to a great extent.[24]

In order to determine the trajectory of bromine attack Skell investigated the reaction of dehydroadamantane **23**. The reaction of **23** with bromine in the absence of light† gave two products (**24** and **25**, Figure 1.9), in an approximate ratio of 3:2, which are consistent with the reaction occurring via equatorial attack on the cyclopropane ring, followed by reaction with the bromide ion (nucleophile) with axial attack being favoured. If electrophilic bromine attack had occurred from an axial trajectory the diaxial dibromide product **26** should have been observed.[24] The lack of selectivity of nucleophilic attack is consistent with formation of an "open" cation which contrasts with protonation[21] where nucleophilic addition is thought to occur before the structure has relaxed to a classical cation.

Cmpd	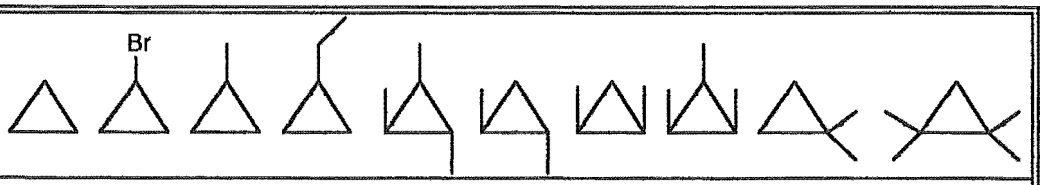
k_{Rel}	~0 ~0.0 ~1.0 (1.0) 4.3 10.8 20.8 23.8 ~10^2 >10^3

Table 1.2. Relative rates of bromination of various substituted cyclopropanes (Br_2, NBS, 25 °C, dark, CH_2Cl_2).[24]

The stereochemical and rate results[24] suggest that bromination of alkyl-cyclopropanes occurs at the least substituted carbon with inversion of configuration to produce a bromocarbonium ion - bromide pair which can undergo extensive sequential rearrangement characteristic of reactions where carbocations are considered to be intermediates (Figure 1.10).

---

‡ Halogenation of cyclopropanes, as with alkenes, is thought to have low concentration domains where the kinetic term is $[Br_2]^1$. At higher concentrations (> 1.0 M) the reaction is at least second order with respect to the bromine concentration.[24,30,31]

† Dehydroadamantane is very susceptible to radical addition.

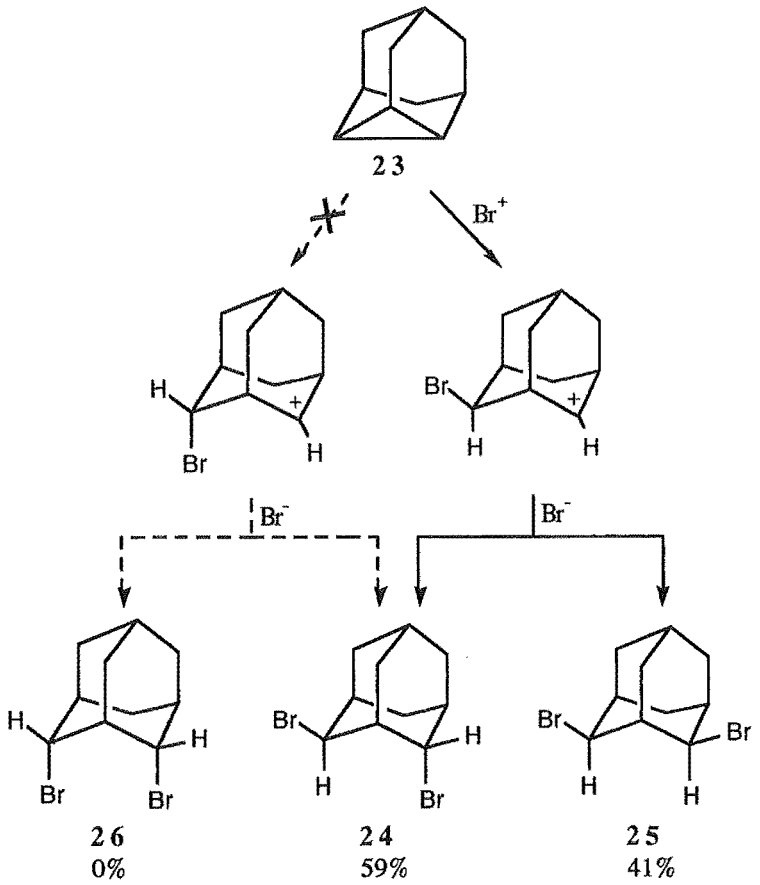

Figure 1.9. Reaction of dehydroadamantane 23 with bromine (Br_2, dark, -78 °C, CH_2Cl_2).

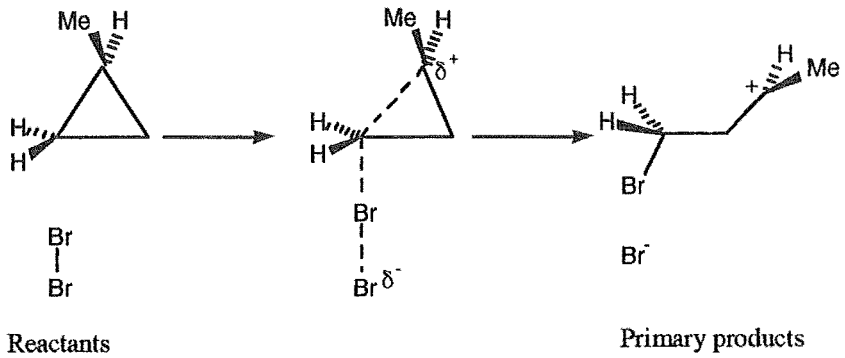

Figure 1.10. Possible mechanism for the bromination of alkyl cyclopropanes.

Further evidence for the formation of carbocation intermediates comes from the reaction of *n*-butylcyclopropane with bromine where 1,X-dibromoheptanes (X=2-6) are formed (Figure 1.11).[24] Since hydride migration is considered to be fast compared with nucleophilic capture, if a free carbocation were formed it would be expected to undergo rearrangement before nucleophilic capture thus leading to a number of products. The presence of a "free" bromonium has also recently been suggested[30,31] for the bromination of alkenes.

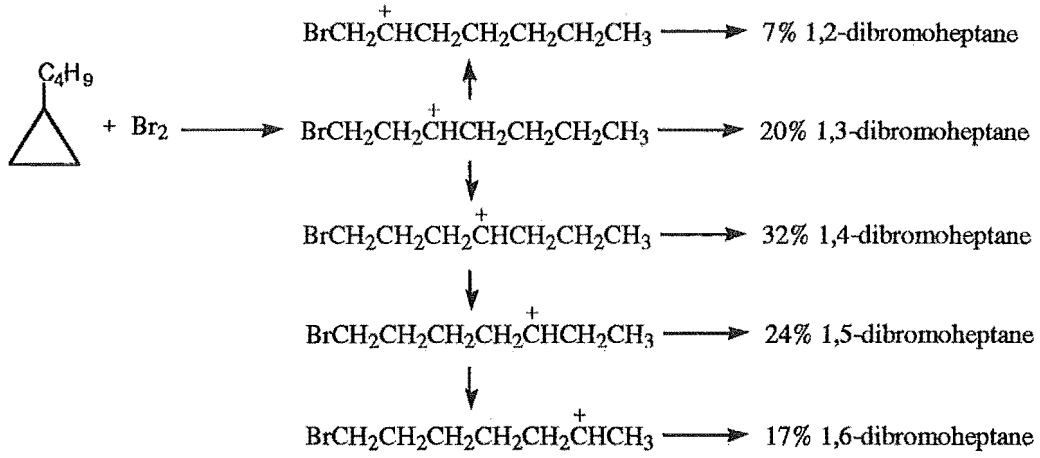

Figure 1.11. Bromination of *n*-butylcyclopropane.

A direct comparison of the reactivity of an alkene and cyclopropane towards bromine can be seen in the reactions of *endo*- and *exo*-tricyclo[3.2.1.$0^{2,4}$]oct-6-ene.[32] Reaction with bromine in carbon tetrachloride and methanol was found to occur at the alkene group in preference to the cyclopropane moiety.‡

Lambert et al.[33] have examined the reaction of *cis*-1,2,3-d_3-cyclopropane with bromine and determined the trajectory of bromine addition from an examination of the temperature dependence of the ^{1}H-^{1}H vicinal coupling constants of the products obtained. Bromine attack was found to occur with retention at the edge of the cyclopropane ring. Nucleophilic attack occurs with inversion. This is different from the mechanism proposed by Skell[24] (see Figure 1.10). However, Skell's results do not preclude the possibility that an initial edge brominated structure collapses rapidly to a corner brominated species† (see Figure 1.12).

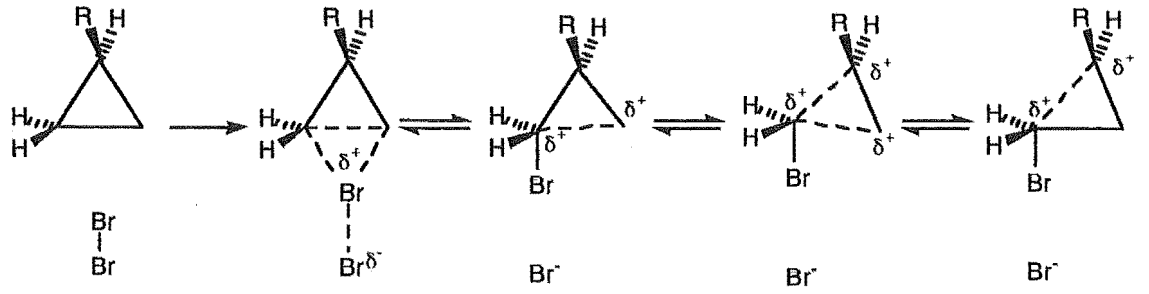

Figure 1.12. Rearrangement of an initial edge brominated cyclopropane may lead to formation of corner brominated structures (R = alkyl).

---

‡ This will be discussed in detail in Chapter 8.

† This is discussed in more detail in Chapters 3 and 6. Also see reference 26 and references cited therein.

Section 1.2.1c Mercuration of cyclopropanes

The first stereochemical study of a mercuric salt addition to cyclopropane derivatives was reported by DePuy et al.[34] in 1970. This widely reported investigation showed that 1-phenyl-*cis,trans*-2,3-dimethylcyclopropanol **27** and 1-phenyl-*trans,trans*-2,3-dimethylcyclopropanol **28**, as well as their methyl esters, react with mercuric acetate in acetic acid to give exclusively inversion of configuration at the carbon where mercury attacks (Figure 1.13).

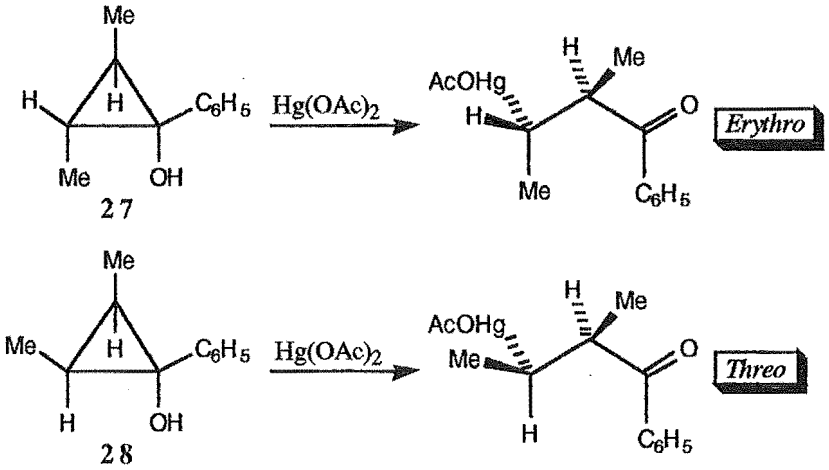

Figure 1.13. Oxymercuration of **27** and **28** gave exclusively *erythro* and *threo* products, respectively.[34]

A series of reactions of cyclopropanes using mercuric trifluoroacetate in methanol led to the conclusion that the trajectory of electrophilic attack was highly dependent on steric factors and hence the substitution pattern of the cyclopropane.[35] The electrophile was found to attack the least substituted bond of the cyclopropane and that ring opening occurred to give the most stable carbocation. If the bonds are equally substituted attack occurs at a *cis* substituted bond in preference to a *trans* substituted bond. For example, the three isomers of 1,2,3-trimethyl-1-phenylcyclopropane react exclusively with inversion of configuration and with cleavage of the C2-C3 disubstituted bond, rather than the trisubstituted C1-C2 or C1-C3 bonds. The ring opening process gives complete inversion at the site of electrophilic attack and results in formation of a tertiary benzylic cation. It was also shown that subsequent nucleophilic attack occurs with inversion of configuration (Figure 1.14).

The equivalent reaction with *trans,trans*- and *cis,cis*-2,3-dimethyl-1-phenylcyclopropane (**29** and **30**, respectively) resulted in the configuration at the site of mercury attack (72% and 81%, respectively) being inverted with attack occurring at the C2-C3 bond which is less sterically hindered than the C1-C2 or C1-C3 bonds (Figure 1.15). However, *cis,trans*-2,3-dimethyl-1-phenylcyclopropane **31** reacted predominantly with retention (88%) of configuration at the site of electrophilic attack at the *cis* substituted C1-

C2 bond.§ The regiochemistry of mercuric ion attack is therefore strongly dependent upon the stereochemistry of the starting hydrocarbon. Another example[26] of this effect is shown by reaction of the isomeric 2,3-dimethylcyclopropyl methyl ethers **32**, **33**, and **34** (Table 1.3).

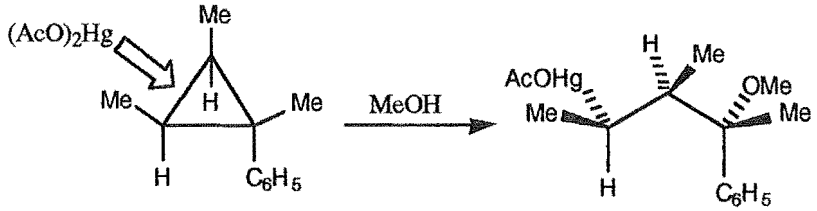

Figure 1.14. Mercuration of *cis,cis,cis*-1,2,3-trimethyl-1-phenylcyclopropane in methanol (Ac = CF_3CO).

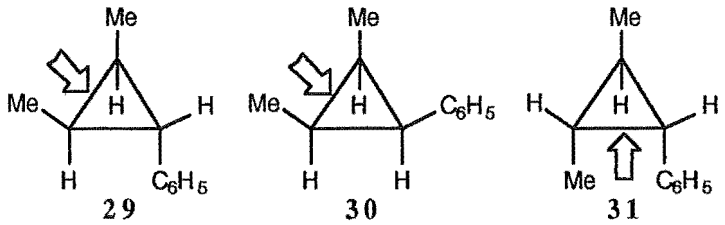

Figure 1.15. Mercuric trifluoroacetate addition to **29**, **30**, **31** results in cleavage of the bond indicated by an arrow in each case.

Compound	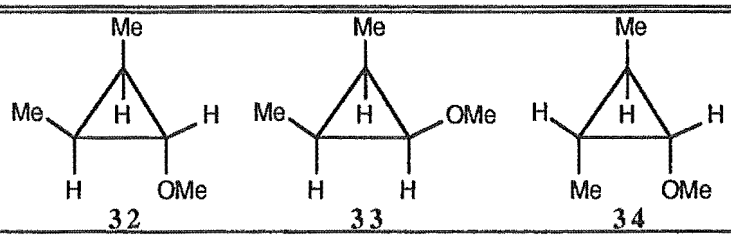		
	32	33	34
% Inversion	90	40	5
% Retention	10	60	95

Table 1.3. Competition between inversion and retention in oxymercuration of cyclopropyl ethers **32**, **33**, and **34**.

In all of the above examples the trajectory of electrophilic attack varies with the stereochemical features of the molecule. To determine the stereochemical demand of electrophilic attack it is necessary to consider cyclopropane derivatives where the carbon-carbon bonds are both chemically and structurally identical. DePuy et al.[35] have investigated the reaction of *cis,cis,cis*-1,2,3-trimethylcyclopropane **35** with mercuric trifluoroacetate in methanol and shown that electrophilic attack occurs with a small

§ In all these reactions nucleophilic attack occurred with inversion of configuration.[26]

preference for inversion (62:38). Inversion of configuration was exclusively observed for the addition of the nucleophile (Figure 1.16).

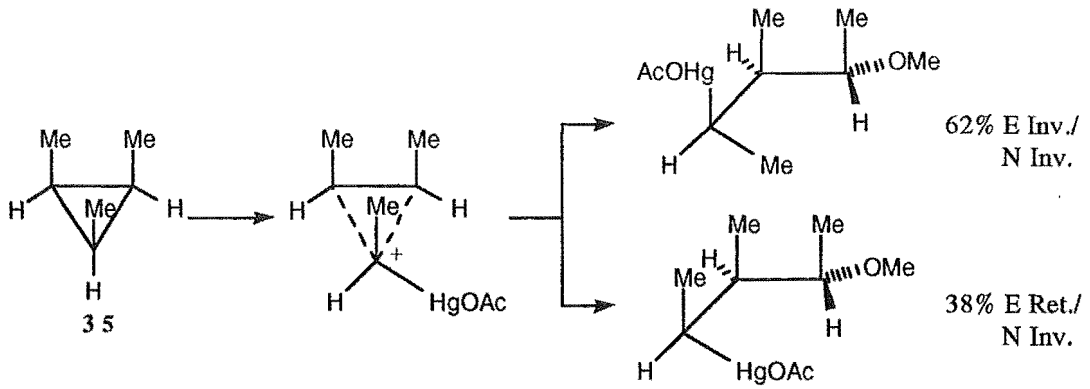

Figure 1.16. Mercuration of **35** followed by nucleophilic attack of methanol. Electrophilic attack proceeds by both retention and inversion pathways. E = Electrophilic, N = Nucleophilic, Inv. = Inversion of configuration, Ret. = Retention of configuration

DePuy has argued[26] that a corner mercurated intermediate **36a** (Figure 1.17) is formed. A corner mercurated structure **36a** would allow development of positive charge at C2 and C3; hence nucleophilic attack would be expected to occur at both C2 and C3 with inversion resulting in what appeared to be both retention and inversion of configuration at the site of electrophilic attack. A small preference for nucleophilic attack at one position would be expected since **36a** is not completely symmetrical. If C1, the pentavalent mercurated carbon atom, rotates the stereochemical results do not change.[26] If an edge mercurated cyclopropane **37a** were the sole intermediate, ring opening with retention would require a large amount of atomic reorganisation to obtain an inversion product and it is therefore unlikely that edge and corner mercurated pathways would be similar in energy.‡

Lambert et al.[36] have recently investigated the mercuric acetate promoted ring opening of 1,2,3-d_3-cyclopropane and concluded, in contrast to DePuy's[35] result for **35**, that attack of the mercury electrophile occurs exclusively with inversion of configuration. Lambert suggested that the mechanism of the reaction may proceed either by formation of an unsymmetrical corner mercurated cyclopropane **38b** (Figure 1.17) which is opened by acetate attack or by initial edge attack followed by fast rearrangement of the mercury from the edge to corner prior to nucleophilic attack (**37b** ⇔ **38b** or **39b**). The latter two step process or the closely related Zig-Zag collapse mechanism[37] could account for the double inversion process observed. Lambert suggests that **38b** is not interconverting with its mirror image **39b** (Figure 1.17) or with the "symmetrical" corner mercurated structure

‡ See Chapter 6 for a further discussion of corner versus edge attack.

36b since this process would be expected to result in both retention and inversion at the site of electrophilic attack as subsequent nucleophilic attack could occur at either C2 or C3. This could explain the difference in the observed electrophilic trajectory between the DePuy and Lambert results, if DePuy's corresponding structure **38a** was interconverting (as suggested by DePuy[26]) with its mirror image **39a**, although this seems unlikely since the barrier to rearrangement would be expected to be greater for the more substituted *cis,cis,cis*-1,2,3-trimethylcyclopropane from steric considerations. However, the methyl groups may induce strain in the originally formed corner mercurated structure **38a** which may drive the rearrangement process towards the more "symmetrical" and less strained structure **36a**.

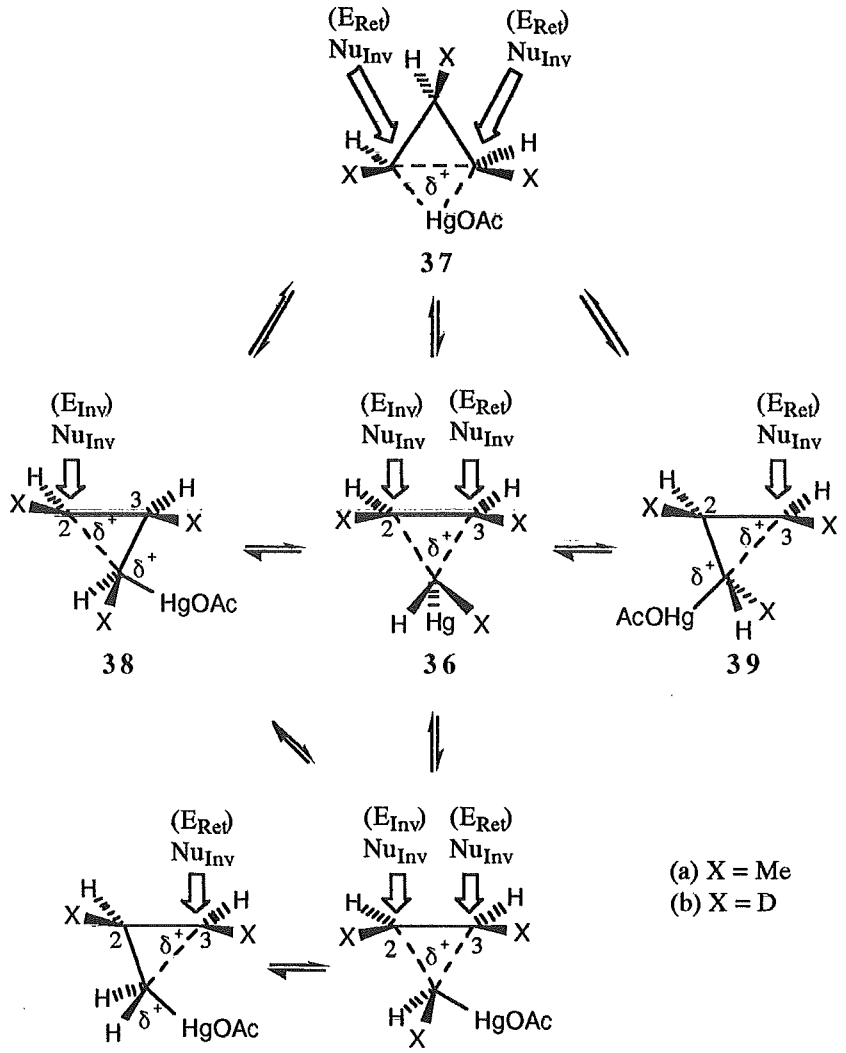

Figure 1.17. Possible rearrangements of mercurated cyclopropanes. The large arrows indicate the configuration resulting from nucleophilic attack ($Nu_{Inv.}$ = inversion at the site of nucleophilic attack) and electrophilic attack (in brackets) ($E_{Inv.}$ = inversion at the site of electrophilic attack, $E_{Ret.}$ = retention at the site of electrophilic attack).

The methyl groups of **35** may also affect the electron donating ability[37] of the π system in the corner mercurated charge transfer complex **38a** which may also affect the barrier to interconversion of the structures (see Chapter 6 for a further discussion of the factors affecting the stability of the π complex).

The exact nature and properties of the corner mercurated species remain unclear since a variety of structures and possible rearrangement pathways, which may be delicately balanced energetically, are possible (Figure 1.17). Both DePuy's and Lambert's results do however show inversion to be the dominant reaction pathway of electrophilic attack, but to varying extents.

In agreement with the stereochemical studies outlined above the rate of mercuric acetate addition to cyclopropanes is sensitive to substitution on the bond attacked. For example, the relative rates of reaction of the cyclopropanols **40, 41, 42** (Table 1.4) are in the ratio of $1:10^{-3}:10^{-6}$; therefore increased substitution leads to a decrease in the rate. The stability of the carbocations has however been shown[26,35,38-40] to have some effect on the rate of reaction, but is generally small. This can be seen from the rates of the reactions of mercuric acetate with 1,1-dimethyl, *trans*-1,2-dimethyl-, 1,1,2-trimethyl-, and 1,1,2,2-tetramethylcyclopropane which are similar (Table 1.5).[32,39,40] For these structures electrophilic attack occurs at the least substituted carbon and the ring opens to the most stable cation. There is a small increase in rate in going to a potential tertiary cation from a secondary cation.

Compound	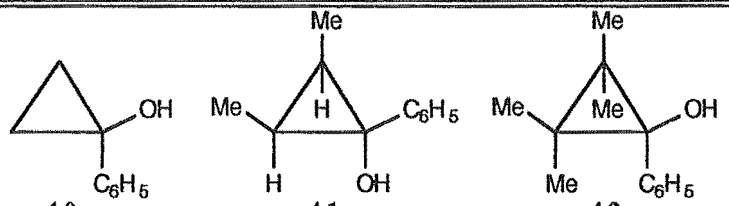		
	40	**41**	**42**
k_{Rel}	1	10^{-3}	10^{-6}

Table 1.4. Relative rates (k_{Rel}) of reaction with mercuric acetate.

Compound	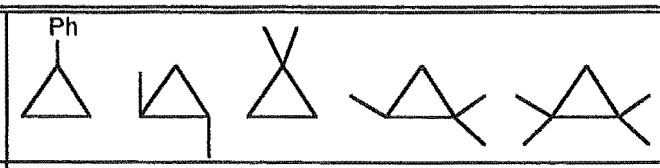				
k_{Rel}	1.0	1.1	2.0	2.2	2.5

Table 1.5. Relative rate of oxymercuration of various substituted cyclopropanes (MeOH, $Hg(OAc)_2$, 20 °C).

The predominance of nucleophilic attack with inversion may indicate the involvement of nonclassical cations and the absence of an "open" cation. An open cation would undergo nucleophilic attack by both retention and inversion. The formation of

substantial positive charge at one centre would be expected to give products resulting from rearrangement.

For mercuric acetate addition to *endo*-tricyclo[3.2.1.$0^{2,4}$]octane[18] (Figure 1.6) no rearrangement products were observed. A high degree of orbital interaction between C2 and C4 of cation 2c results in little charge development at C4 or rearrangement via cation 3c, as was observed for the deuterated analogue 2b.[13,18] The reaction is similar to the reaction of mercuric acetate with alkenes[41,42] where rearrangement is not normally observed. The results of this study contrast with those obtained from the smaller monocyclic cyclopropane systems[18] since in this case the internal and most substituted cyclopropyl bond is cleaved. For polycyclic systems it is therefore likely that it is not just steric effects which dictate the course of the reaction.

The stereochemistry of nucleophilic attack on the mercurated cyclopropanes can be affected by the solvent and the mercuric salt used in the reaction.[43] Generalisations about the trajectory of nucleophilic attack on the resulting mercurated cyclopropanes should therefore be made with caution.

Section 1.2.2 Reactivity of Cyclopropanes towards Nucleophiles

In contrast to electrophilic addition, nucleophilic attack on a cyclopropane is not usually a facile[44,45] process. Two electron withdrawing substituents on a carbon of the cyclopropane ring are required to obtain significant reactivity although some nucleophilic additions to cyclopropanes with one electron withdrawing group[46-49] have been reported.

Reactivity of a cyclopropane towards nucleophilic attack appears to be determined by a number of factors[44,45] including the type of nucleophile, the substitution pattern of the nucleophile, amount of substitution of the cyclopropane ring, and structure of the molecule in which the cyclopropyl ring is situated. For example, the rate of isomerisation of 43 is strongly dependent upon the nature of the substituents R_1 and R_2 (Figure 1.18).

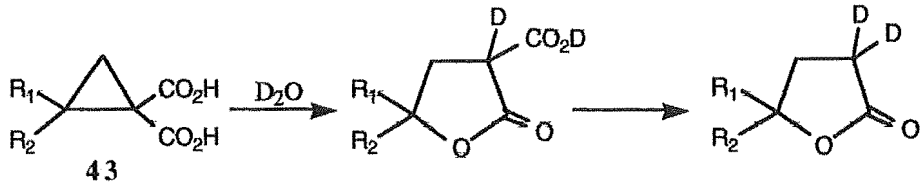

43

k_{Rel}	R_1	R_2
1	H	H
31	H	Me
81000	Me	Me

Figure 1.18. Butyrolactone synthesis by rearrangement of 1,1-cyclopropanedicarboxylic acid to the corresponding γ-butyrolactonecarboxylic acid which decarboxylates to the corresponding butyrolactone.

The effect of the substitution pattern of the nucleophile can be seen by comparison of the products obtained from the reactions of **44**. Reaction[50,51] of **44** with a secondary amine leads to ring opening while reaction with a primary amine results in the formation of N-substituted amides (Figure 1.19).

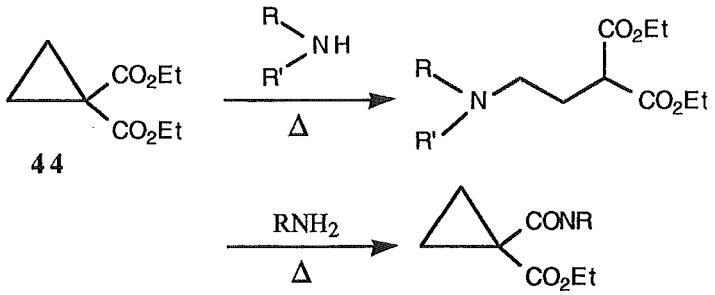

Figure 1.19. Products obtained from reaction of 1,1-cyclopropanedicarboxylic acid **44** with primary and secondary amines.

The reactivity of cyclopropane derivatives is increased by the inclusion of the ring into polycyclic compounds[44,49] and particularly by the presence of a spiroacylal[51,52] linkage. In this case, not only is there an increase in reactivity of the cyclopropane towards nucleophilic attack, but a high degree of selectivity[53] in the opening of unsymmetrical systems, where the nucleophile predominantly attacks the more hindered carbon (Figure 1.20). The increase in reactivity is generally attributed to the ability of both alkoxycarbonyl groups to participate in the delocalisation of the emerging carbanion when the plane of the cyclopropane ring is orthogonal to the O=C-OR planes of both esters.

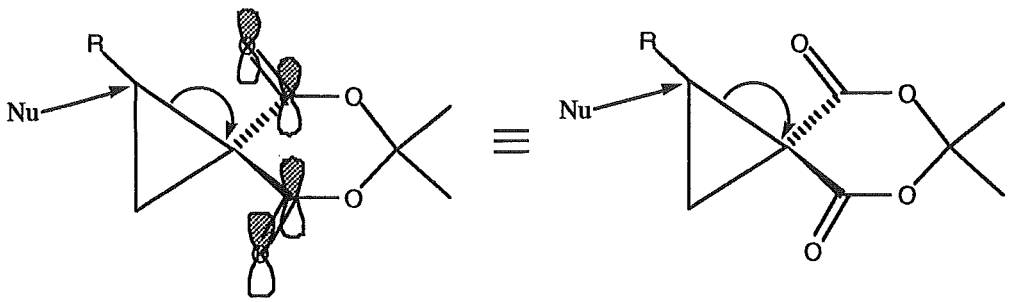

Figure 1.20. Activation of a cyclopropane ring to nucleophilic attack by inclusion in a spiro linkage.

Figure 1.21 shows some examples[45] of products that can be obtained from nucleophilic attack on spirosubstituted cyclopropanes with a variety of nucleophiles,[45] including sulphur, nitrogen, carbon, and oxygen (Figures 1.21(a)-(d), respectively).

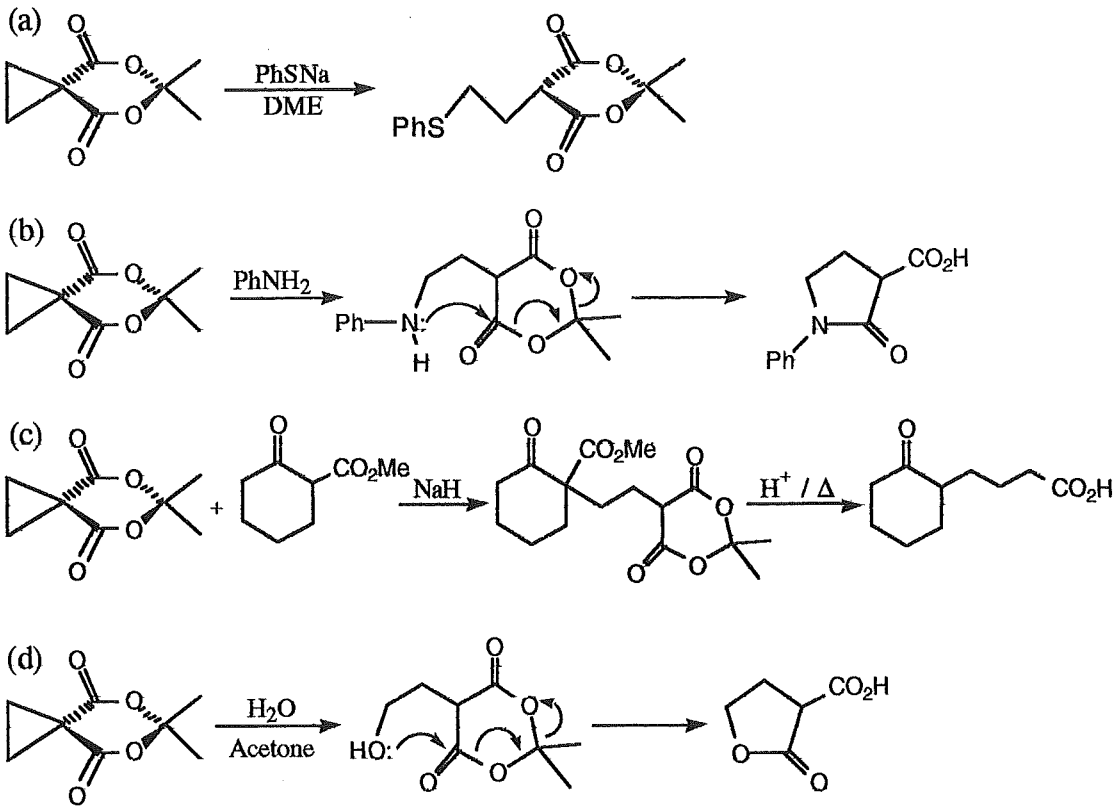

Figure 1.21. Examples of nucleophilic attack on cyclopropane derivatives.

Although few studies directed towards elucidating the stereochemistry of nucleophilic attack have been reported,[45,48,49] the data to date suggest that nucleophilic addition occurs predominantly with inversion of configuration at the site of attack (Figure 1.22). Thus, nucleophilic addition to activated cyclopropanes allows stereochemical control of the ring opening process. This has been exploited in a number of syntheses of prostaglandins[54] and other natural products.[44,45,55]

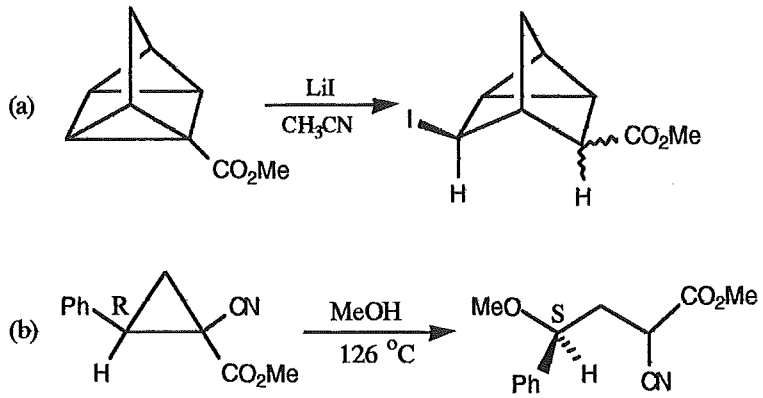

Figure 1.22. (a) Reaction[49] of 1-carbomethoxyquadricyclene with LiI in acetonitrile at room temperature. (b) Methanolysis[45] of (+)-(*R*)-methyl-1-cyano-2-phenylcyclopropane-carboxylate to give (-)-(*S*)-methyl-2-cyano-4-methoxy-4-phenylbutanote.

Section 1.3 USE OF CYCLOPROPANES IN ORGANIC SYNTHESIS

A detailed review of the use of cyclopropane derivatives in synthesis has recently been published[56] and hence will be dealt with only briefly here.

Due to the unusual bonding properties of cyclopropanes their chemical reactivity resembles that of alkenes more than that of other cyclic hydrocarbons.[57] Both show pericyclic, radical, and ionic reactions whose occurrence and outcome are dependent upon the cyclopropane substituents, reagents and conditions. The influence of the cyclopropane substituents on geometry[58] and orbital properties[59-61] have been a matter of extensive investigation[56] and have been shown to be important in determining reactivity.

With the exception of vinylcyclopropane-cyclopentene rearrangements[56] (Figure 1.23) there have been relatively few examples of the use of cyclopropyl radicals in organic synthesis. This is also true of pericyclic reactions involving cyclopropanes which are generally restricted to the divinylcyclopropane-cycloheptadiene[56] interconversion (Figure 1.24).

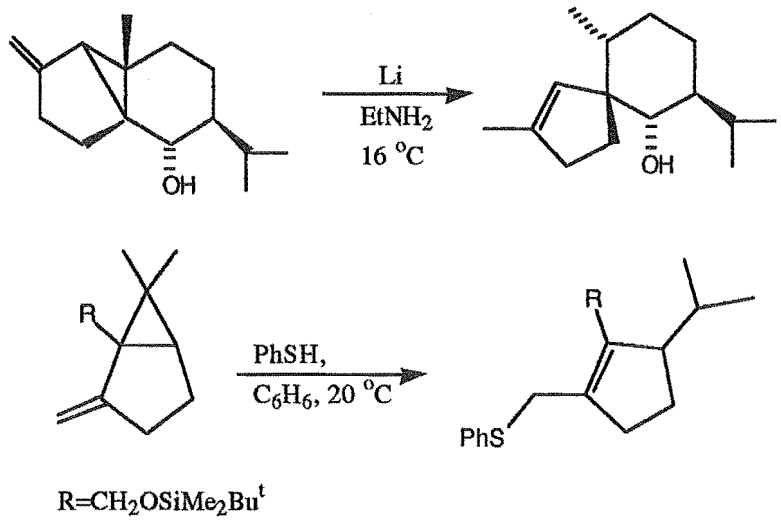

Figure 1.23. Examples of vinylcyclopropane-cyclopentene rearrangements.

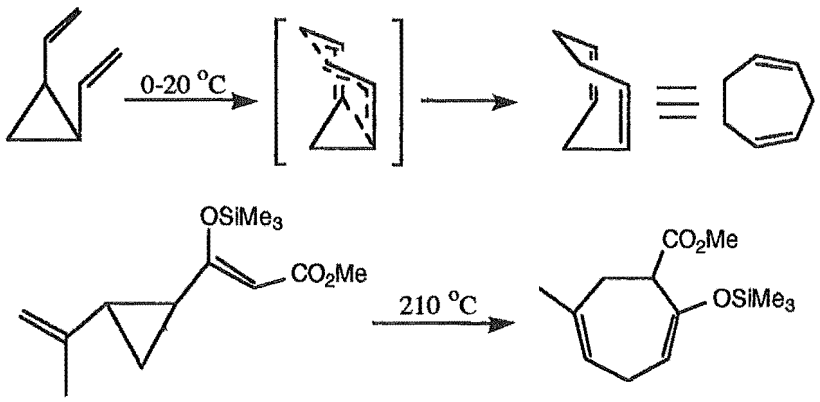

Figure 1.24. Examples of thermal divinylcyclopropane-cycloheptadiene rearrangements.

The majority of synthetically useful reactions of cyclopropanes proceed via polar intermediates[56] or at least via transition states which are thought to be polar in nature. The general reactivity of cyclopropanes has been classified into eleven major groups (Table 1.6). Equations 1-3 (Table 1.6) represent homoalkene, homo-Michael, and homoenolate systems, respectively, and clearly demonstrate the close relationship to alkene reactivity. This justifies the analogy of cyclopropanes as homoalkenes. Generally, addition of donor or acceptor groups to the cyclopropanes not only results in the ability to use more mild reaction conditions for the ring opening process but also allows incorporation of additional functional groups which may be used for further transformations (equations 4,6,7 Table 1.6). Reductive or electrocyclic ring opening can afford 1,4-dienes (equation 8) or allyl substituted products (equation 9). A donor group can also be created by deprotonation of an α-acceptor-substituted derivative, and when combined with the presence of a suitable acceptor or leaving group brings about ring cleavage (equations 10 and 11, Table 1.6).

Table 1.7 shows examples of cyclopropane derivatives used in synthesis and emphasises the wide range and versatility of organic transformations that are available via use of cyclopropanes. The reactions range from simple functionalisation reactions (entries 1-4, Table 1.7), to syntheses of molecules of more theoretical interest, such as semibullvalenes and cyclobutanes (entries 5-7, Table 1.7), to the preparation of building blocks useful for the synthesis of natural products (entries 8-10, Table 1.7).

Entry	General Reaction
1	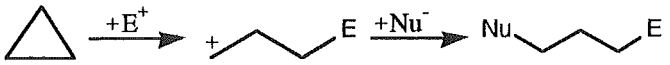
2	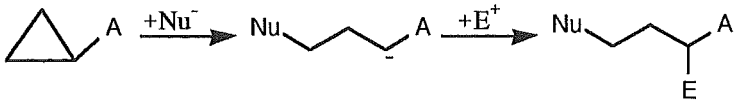
3	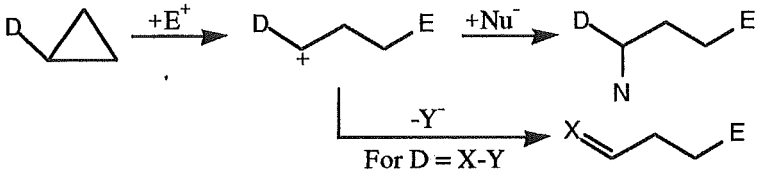
4	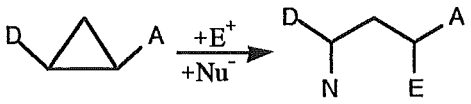
5	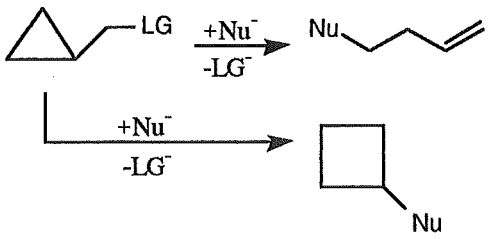
6	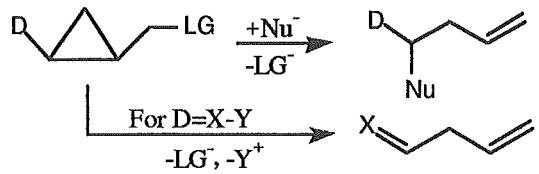
7	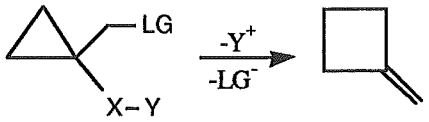
8	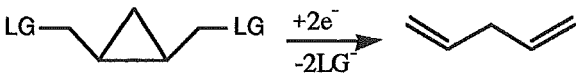
9	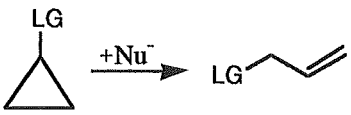
10	
11	

Table 1.6. General synthetic methodologies involving a cyclopropane group. A = Acceptor, D = Donor.

Entry	Example Reaction
1 (2)	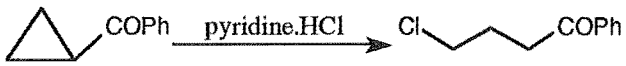
2 (3)	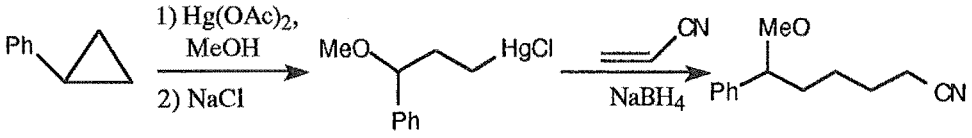
3 (5)	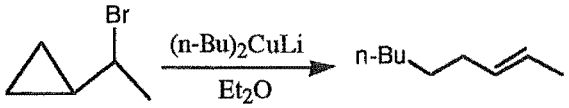
4 (6)	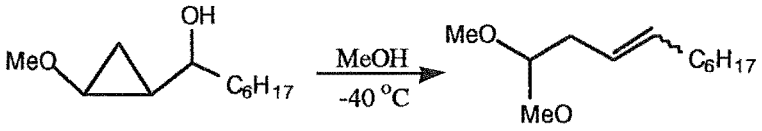
5 (5)	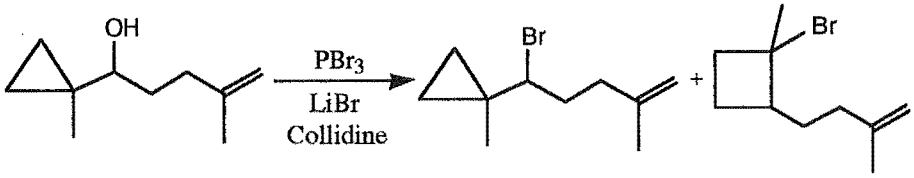
6 (7)	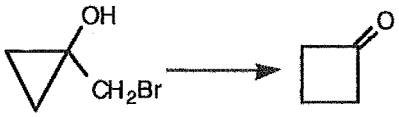
7 (8)	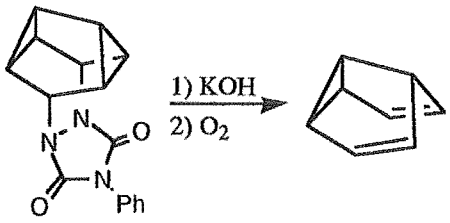
8 (3)	
9 (10)	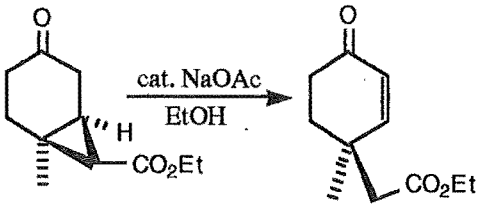
10 (4)	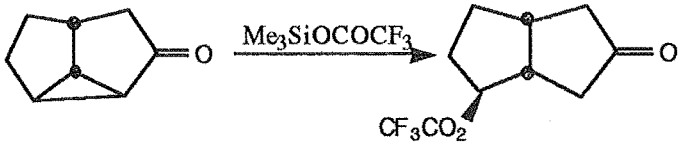

Table 1.7. Examples of the use of cyclopropane derivatives in synthesis. Numbers in brackets refer to the corresponding entry number for the general reaction type shown in Table 1.6.

Section 1.4 AIMS OF THIS WORK

Due to the importance of the cyclopropyl group both as a precursor in organic synthesis and the wide variety of natural products[62] which contain cyclopropane rings,‡ it is important to understand the factors which effect the stereochemistry and regiochemistry of cyclopropyl ring opening. Recent studies have considered the reaction of *exo*- and *endo*-tricyclo[3.2.1.$0^{2,4}$]octane and -oct-6-ene systems with a variety of electrophiles, and identified the stereochemistry of cyclopropane ring opening and the regiochemical preference of electrophilic attack between a double bond and cyclopropane ring. It was the intention of this work to further the investigations on these systems and to extend the work to systems with the general structure of tricyclo[3.2.2.$0^{2,4}$]non-6-ene. Both practical and theoretical studies were undertaken in an attempt to further elucidate the factors which are important in determining the stereochemistry of ring opening and also to attempt to explain the regioselectivity observed between different electrophiles.

‡ The cyclopropyl functionality may be present as part of a stable structural entity in secondary metabolites, while in others it may be generated transiently as a connecting element between a substrate and a final product in both primary and secondary metabolism.

CHAPTER 2
Syntheses of the Tricyclic Starting Materials

Section 2.1 SYNTHESES OF *endo*-TRICYCLO[3.2.1.$0^{2,4}$]OCTANE AND 2-METHYL-*endo*-TRICYCLO[3.2.1.$0^{2,4}$]OCTANE

The synthesis of *endo*-tricyclo[3.2.1.$0^{2,4}$]octane **1** was performed according to the literature procedure[14] by hydrogenation of *endo*-tricyclo[3.2.1.$0^{2,4}$]oct-6-ene which was produced from the Diels-Alder reaction of cyclopropene and cyclopentadiene.[63] Cyclopropene was generated by the standard method of Closs et al.[63] by reaction of allyl chloride with sodium amide.

2-Methyl-*endo*-tricyclo[3.2.1.$0^{2,4}$]octane[16] **45** was synthesised by hydrogenation of 2-methyl-*endo*-tricyclo[3.2.1.$0^{2,4}$]oct-6-ene which was prepared from the Diels-Alder reaction of 1-methylcyclopropene[64] with cyclopentadiene.[16] Compounds **1** and **45** were identified by comparison of their ^{1}H and ^{13}C NMR spectra with those reported.[14,16] The syntheses of **1** and **45** are shown in Figure 2.1.

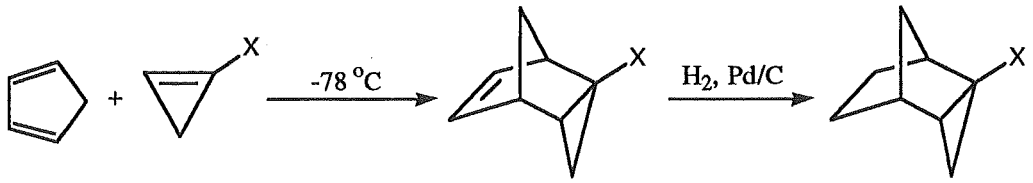

Figure 2.1. Syntheses of *endo*-tricyclo[3.2.1.$0^{2,4}$]octane **1** and 2-methyl-*endo*-tricyclo[3.2.1.$0^{2,4}$]-octane **45**.

Section 2.2 PREPARATION OF *exo*-TRICYCLO[3.2.1.$0^{2,4}$]OCTANE

exo-Tricyclo[3.2.1.$0^{2,4}$]octane **46** was prepared by the literature procedure of methylene carbene addition to norbornene[65] (Figure 2.2). The zinc/copper couple used in the reaction was prepared by the method of Rawson and Harrison.[66] Compound **46** was identified by comparison of its ^{1}H and ^{13}C NMR spectra with those reported.[14]

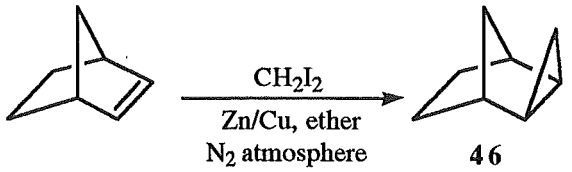

Figure 2.2. Synthesis of *exo*-tricyclo[3.2.1.$0^{2,4}$]octane **46** by carbene addition to norbornene.

Section 2.3 SYNTHESIS OF *exo*-TRICYCLO[3.2.2.$0^{2,4}$]NON-6-ENE

exo-Tricyclo[3.2.2.$0^{2,4}$]non-6-ene **47** was synthesised by the reported procedure[67,68] (Figure 2.3). Diels-Alder reaction of cycloheptatriene with maleic

anhydride in refluxing xylene[68,69] gave *exo*-tricyclo[3.2.2.0^{2,4}]non-8-en-6-*exo*-7-*exo*-dicarboxylic acid anhydride **48**, which was hydrogenated over 5% Pd on carbon until one equivalent of hydrogen was taken up.[68,69] The saturated anhydride **49** was then hydrolysed with an aqueous sodium bicarbonate solution to give the diacid **50**. Decarboxylation of **50** was effected by reaction with lead tetraacetate in benzene[67,68] to give *exo*-tricyclo[3.2.2.0^{2,4}]non-6-ene **47**. The identity of **47** was confirmed by comparison of its ^{1}H NMR spectrum with that reported.[67,68]

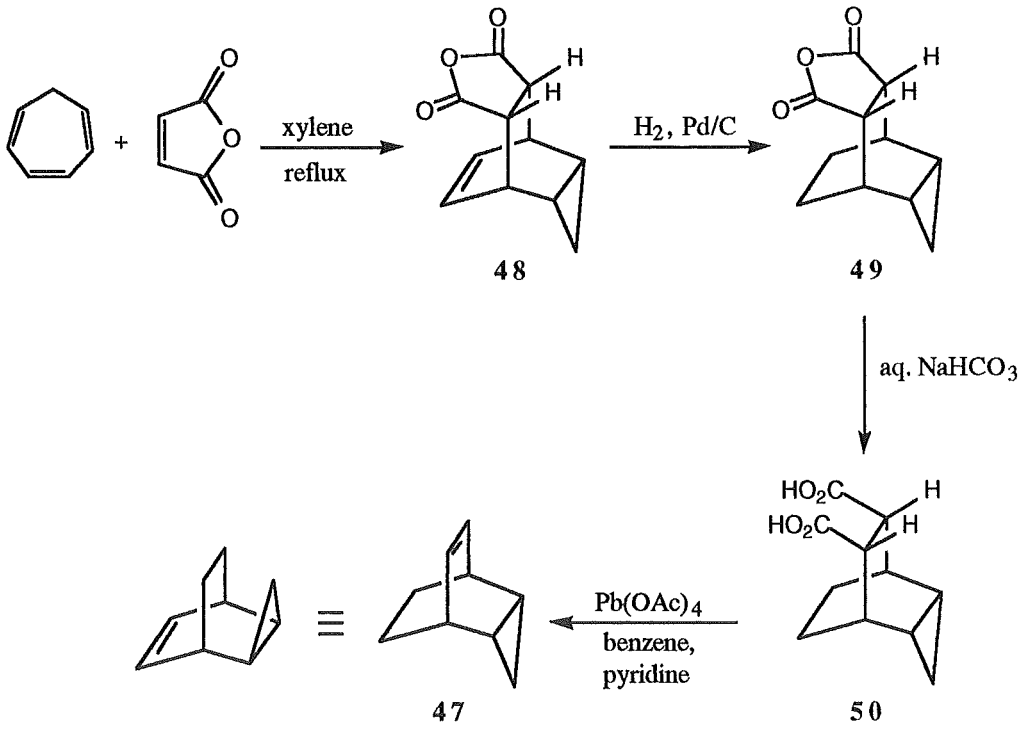

Figure 2.3. Synthesis of *exo*-tricyclo[3.2.2.0^{2,4}]non-6-ene **47**.

Section 2.4 PREPARATION OF TRICYCLO[3.2.2.0^{2,4}]NONA-6,8-DIENE

A number of methods for the preparation of tricyclo[3.2.2.0^{2,4}]nona-6,8-diene **51** have been reported,[67,70-74] but most involve a large number of steps and result in poor overall yields. The most direct method for the synthesis of 1,4-dienes of this type is by Diels-Alder reaction of acetylene and an appropriate 1,3-diene. However, due to the low dienophilic reactivity of acetylene, and the hazards involved in handling this compound at high temperatures and pressures, this direct route can only be used for the most reactive dienes.[75] In the present case, the low reactivity of both the required dienophile (acetylene) and diene (cycloheptatriene) would lead to poor yields and necessitate the use of forcing reaction conditions‡ (high temperatures and pressures). As a consequence of this, a

‡ Reaction of ethylene with 1,3-cyclohexadiene is reported[76] to require forcing reaction conditions (250 °C, 550 kg pressure, 50% yield). Both acetylene and cycloheptatriene are less reactive than ethylene and

number of procedures[75,77-81] have been developed to mimic the addition of acetylene; these are the so called acetylene dienophile equivalents (Figure 2.4).

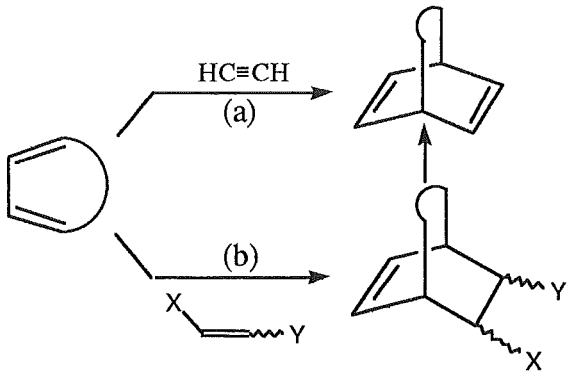

Figure 2.4. Synthesis of 1,4-dienes[75] via (a) direct Diels-Alder reaction of acetylene or (b) acetylene dienophile equivalents.

These procedures are characterised by high dienophilic reactivity and by the ease of removal of the activating groups to give the required second double bond. De Lucchi et al.[75,77] have reported a two step process for the synthesis of **51** (Figure 2.5) based on the Diels-Alder reaction of cycloheptatriene with (*E*)- or (*Z*)-1,2-bis(phenylsulphonyl)-ethene[82-84] (**52** and **53**, respectively), which are highly reactive and readily accessible (Figure 2.6) dienophiles. The resulting disulphone products 8-*anti*-9-*syn*-bis-(phenylsulphonyl)-*endo*-tricyclo[3.2.2.$0^{2,4}$]non-6-ene **54** or 8-*anti*-9-*anti*-bis(phenyl-sulphonyl)-*endo*-tricyclo[3.2.2,$0^{2,4}$]non-6-ene **55** undergo reductive desulphonation on treatment with sodium amalgam in sodium dihydrogen phosphate buffered methanol[75,77] to give diene **51** (Figure 2.5).

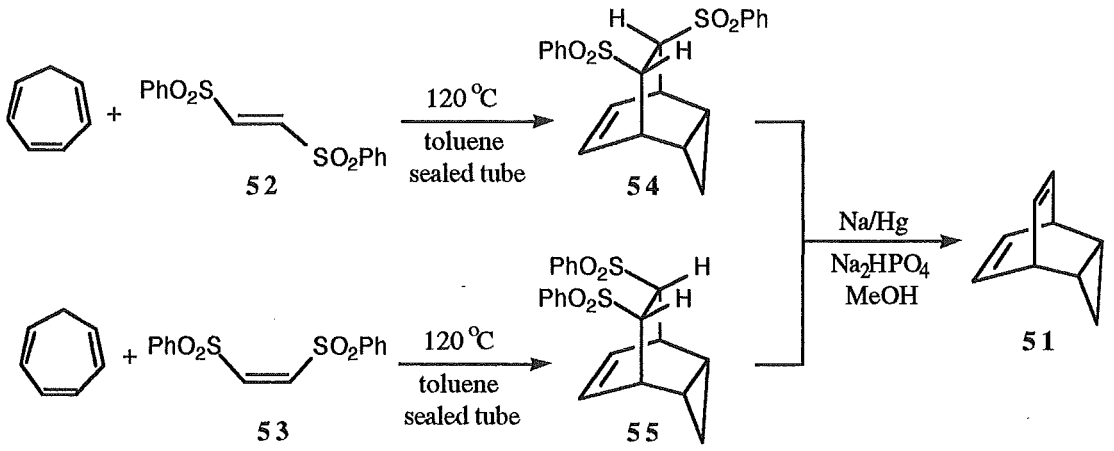

Figure 2.5. Syntheses of disulphones **54** and **55**.[75,76]

1,3-cyclohexadiene, respectively, and hence the reaction would be expected to proceed (if at all) in low yield. The reaction of acetylene and cycloheptatriene has not been reported in the literature.

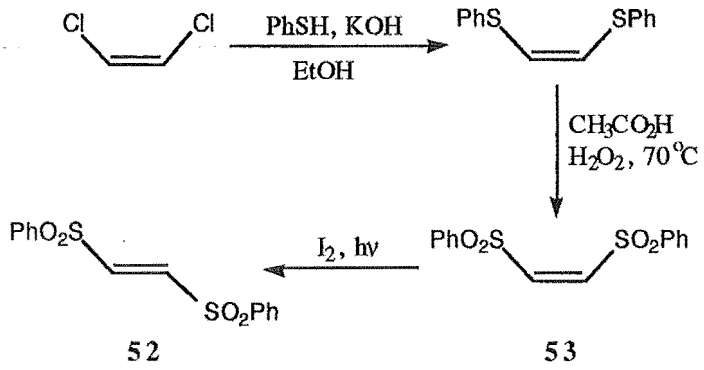

Figure 2.6. Preparation of (*E*)-1,2-bis(phenylsulphonyl)ethene **52** and (*Z*)-1,2-bis(phenylsulphonyl)-ethene **53**.[75,82-84]

Although De Lucchi's procedure[75] was reported to give **51** in reasonable yield (56% overall, from the vinyl sulphone **53**), the use of large quantities of toxic mercury is best avoided. Another procedure for reductive desulphonation of 1,2-disulphones has been reported[85] but results in the formation of a mixture of alkene and corresponding dihydro products (Figure 2.7). The reaction was also shown[85] to be sensitive to the purity of the magnesium used.†

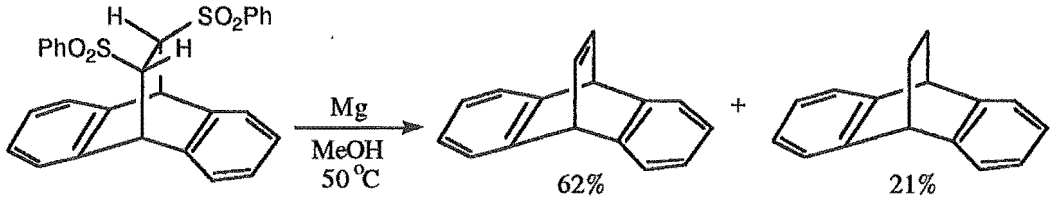

Figure 2.7. Magnesium in methanol reduction[85] of a 1,2-disulphone.

While attempting to synthesise *endo*-tricyclo[3.2.2.$0^{2,4}$]non-6-ene **56** using the method of De Lucchi et al.,[86] by lithium in ammonia reduction of disulphones **54** or **55**‡ (see Section 2.5), it was found that the reaction gave a mixture of diene **51** and the required alkane **56** (Figure 2.8). By increasing the "concentration" of lithium in the liquid ammonia the proportion of **56** formed also increased, although at higher lithium concentrations a third unidentified product was also formed. The ratio of products formed was however not always reproducible (Table 2.1). The required diene **51** could therefore

---

† As part of the present work, attempts to synthesise bicyclo[2.2.2]octa-2,5-diene (not reported here) by this method led to the formation of mixtures of diene and the corresponding dihydro derivative. Obtaining magnesium of high enough reactivity was also a problem, even after following the activation procedure described.[85]

‡ De Lucchi et al.[86] indicated that both disulphone isomers (*cis* or *trans*) were reduced to the corresponding alkane.

be prepared by the Li/NH_3 procedure, with little or no formation of **56**, when low lithium concentrations were employed and was therefore synthesised by this method in preference to the sodium amalgam reduction procedure.[75]

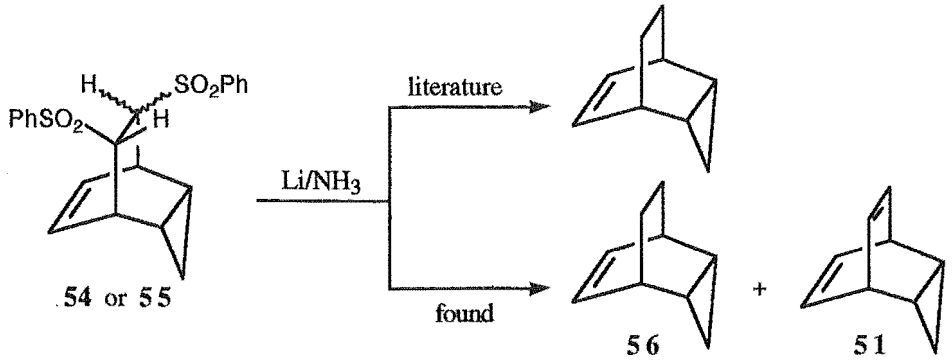

Figure 2.8. Attempted synthesis of *endo*-tricyclo[3.2.2.$0^{2,4}$]non-6-ene **56** by Li/NH_3 reduction of **54** or **55** gave a mixture of **56** and tricyclo[3.2.2.$0^{2,4}$]nona-6,8-diene **51**.

Sulphone		NH_3	Li	"[Li]"	Product Ratio			Time
Isomer	wgt (g)	(ml)	(g)	(M)	**51**	**56**	unknown	(h)
55	1.0	25	0.46	2.7	2	2	3	2.8
55	1.0	25	0.45	2.7	1	9	20	1.8
55	0.5	50	0.10	0.3	>10	1	0	1.1
54	4.0	300	0.86	0.4	1	0	0	4.3

Table 2.1. Reaction conditions and product ratios obtained from Li/NH_3 reduction of disulphones **54** and **55**. Product ratios are estimated from the ^1H NMR spectra of the crude reaction mixtures.

Although the reason for the difference in reported products from the Li/NH_3 reaction is not clear, and was not investigated further, it may be due to the presence of trace metal impurities present in the lithium. The reactivity of lithium in some reactions is known to be dependent on the amount of sodium impurity present.[87] Alkene and diene products were invariably formed when Na/NH_3 reductions of disulphones were attempted.[86]

Section 2.5 SYNTHESIS OF *endo*-TRICYCLO[3.2.2.$0^{2,4}$]NON-6-ENE

The standard literature procedure[67,68] for the synthesis of *endo*-tricyclo-[3.2.2.$0^{2,4}$]non-6-ene **56** is by Diels-Alder reaction of cyclopropene with 1,3-cyclohexadiene (Figure 2.9); however, the reaction proceeds in only low yield (2-5%).

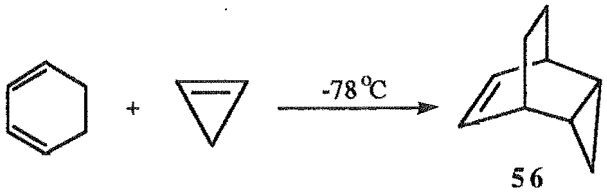

56

Figure 2.9. Diels-Alder reaction of 1,3-cyclohexadiene and cyclopropene to give *endo*-tricyclo-[3.2.2.$0^{2,4}$]non-6-ene **56**.

As described previously, the method of De Lucchi et al.[86] represented an attractive route to the synthesis of **56**, but attempts to repeat their procedure resulted in the formation of a mixture of **56** and **51**. Since separation of the diene **51** and alkene **56** would be difficult, it would be preferable to use a method which results exclusively in the formation of **56**. An alternative procedure for the synthesis of **56** could be envisioned by Diels-Alder reaction of cycloheptatriene and ethene, but this procedure would suffer from similar problems to those encountered for the reaction of cycloheptatriene and acetylene (see Section 2.4). In this case a dienophilic equivalent of ethene is required. Although a number of ethene synthetic equivalents have been reported,[88-91] recently published methods for decarboxylation[92-94] have made methyl acrylate **57** an attractive possibility.

The reaction of methyl acrylate with cycloheptatriene is slow even under forcing conditions (sealed tube, toluene, 140 °C, 30 days). Lewis acid catalysts are known to increase the rate of Diels-Alder reactions[95-98] and the $AlCl_3$ catalysed reaction of **57** with cycloheptatriene, using a procedure similar to that of Bellus et al.,[99] gave the required methyl esters in 44% isolated yield. The resulting methyl esters, 8-*anti*-methoxycarbonyl-*endo*-tricyclo[3.2.2.$0^{2,4}$]non-6-ene **58** and 8-*syn*-methoxycarbonyl-*endo*-tricyclo-[3.2.2.$0^{2,4}$]non-6-ene **59** were separated by TLC mesh column chromatography[100] and identified by comparison of their ^{1}H NMR spectra with those reported.[99] The ratio of **58** to **59** was determined (by ^{1}H NMR) to be 9:1, compared with the 3:1 ratio of these products obtained from the uncatalysed procedure. This is consistent with the known preference of Lewis acid catalysts to enhance *endo* (*anti*) selectivity.[98]

A number of new methods for the removal of carboxyl groups have recently appeared in the literature.[92-94] The procedure of Hasebe et al.[94] appeared most suitable as the required reagents were readily available and the procedure was amenable to large scale preparations. This method requires the preparation of the corresponding benzophenone oxime ester. Esters **58** and **59** were hydrolysed by treatment with an ethanolic potassium hydroxide solution to give a mixture of 8-*anti*-carboxy-*endo*-tricyclo[3.2.2.$0^{2,4}$]non-6-ene **60** (identified by comparison with the reported ^{1}H NMR data[101]) and 8-*syn*-carboxy-*endo*-tricyclo[3.2.2.$0^{2,4}$]non-6-ene **61** in 71% yield. The acids were used without further purification to prepare the corresponding acid chlorides by treatment with oxalyl chloride and DMF in dry benzene.[92] The acid chlorides were not isolated but reacted immediately

with benzophenone oxime to give the required benzophenone oxime esters.[102] Separation of the oxime esters was effected by TLC mesh column chromatography to give *exo*-tricyclo[3.2.2.0^{2,4}]non-8-en-6-*exo*-carboxylic acid benzophenone oxime ester **62** (52%) and *exo*-tricyclo[3.2.2.0^{2,4}]non-8-en-6-*endo*-carboxylic acid benzophenone oxime ester **63** (6%). The oxime esters **62** and **63** were characterised by their ^{1}H and ^{13}C NMR spectra and showed satisfactory mass spectral and elemental (for **62**) analyses. The orientation of the ester functionality in **62** and **63** followed from the stereochemistry of the starting methyl esters **58** and **59**, respectively, and was confirmed by nOe experiments and from examination of the relevant coupling constants.†

Compounds **62** and **63** (9:1 mixture) were dissolved in a 10% thiophenol/ isopropyl alcohol mixture and photolysed at 0 °C with a 450 W low-pressure mercury vapour lamp with a pyrex filter[94] until all the starting material had been consumed (TLC analysis). After workup **56** was obtained as a colourless glassy solid but in only 3% isolated yield from the oxime esters **62** and **63**. Figure 2.10 summarises the procedure for the synthesis of **56** via the benzophenone oxime ester route.

Due to the low yield of **56** obtained from the decarboxylation procedure, an alternative dienophile was considered. Paquette et al.[88,90] have reported the use of phenyl vinyl sulphone **64** as a synthetic equivalent of ethene. Synthesis of **64** was achieved by the literature procedure[88,103] (see Figure 2.11). Reaction of **64** with cycloheptatriene proceeded slowly under forcing conditions§ (170 °C, xylene, sealed tube, 14 days) to give a 4:1 ratio of 8-*anti*-phenylsulphonyl-*endo*-tricyclo[3.2.2.0^{2,4}]non-6-ene **65** and 8-*syn*-phenylsulphonyl-*endo*-tricyclo[3.2.2.0^{2,4}]non-6-ene **66** (Figure 2.11). Attempts to catalyse Diels-Alder reactions of **64** by the use of Lewis acids have been reported[88] to give no rate enhancement and therefore were not attempted.

---

† Compound **62**: Irradiation of H6 gave a 1.7% enhancement of the H2/H4 multiplet centred at 0.86 ppm (2.4% enhancement was observed for the reverse process). Relevant ^{1}H-^{1}H coupling constants: $^{3}J_{6,7endo}$ = 9.8 Hz ($^{3}J_{7endo,6}$ = 9.7 Hz), $^{3}J_{6,7exo}$ = 4.9 Hz ($^{3}J_{7exo,6}$ = 4.9 Hz).

Compound **63**: Irradiation of the multiplet at 1.92 ppm gave a 1.2% enhancement of the multiplet centred at 0.86 ppm (H2, H4) which established this proton as H7*endo* and the orientation of the cyclopropane ring as *exo*. Relevant ^{1}H-^{1}H coupling constants: $^{3}J_{6,7endo}$ = 4.9 Hz ($^{3}J_{7endo,6}$ = 4.9 Hz), $^{3}J_{6,7exo}$ = 10.7 Hz ($^{3}J_{7exo,6}$ =10.8 Hz). The coupling constants confirm a distorted *trans* relationship of H6 to the proton assigned to H7*endo* and a *cis* relationship of H6 to the multiplet at 1.45 ppm (H7*exo*), which was confirmed by a 2.7% enhancement of H7*exo* (1.45 ppm) on irradiation of H6, compared with the 0.8% enhancement of the multiplet centered at 1.92 ppm and previously assigned to H7*endo*.

§ Konovalov has reported the reactivity of phenyl vinyl sulphone to be approximately 50% that of methyl acrylate.[104]

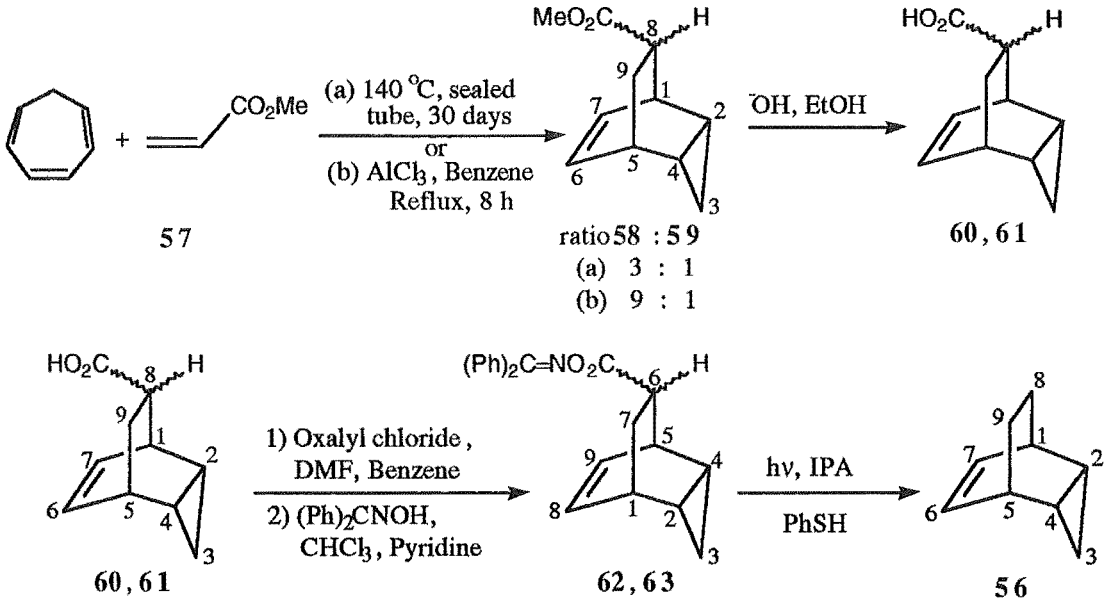

Figure 2.10. Synthesis of *endo*-tricyclo[3.2.2.$0^{2,4}$]non-6-ene **56** via Diels-Alder reaction of methyl acrylate with cycloheptatriene followed by decarboxylation.

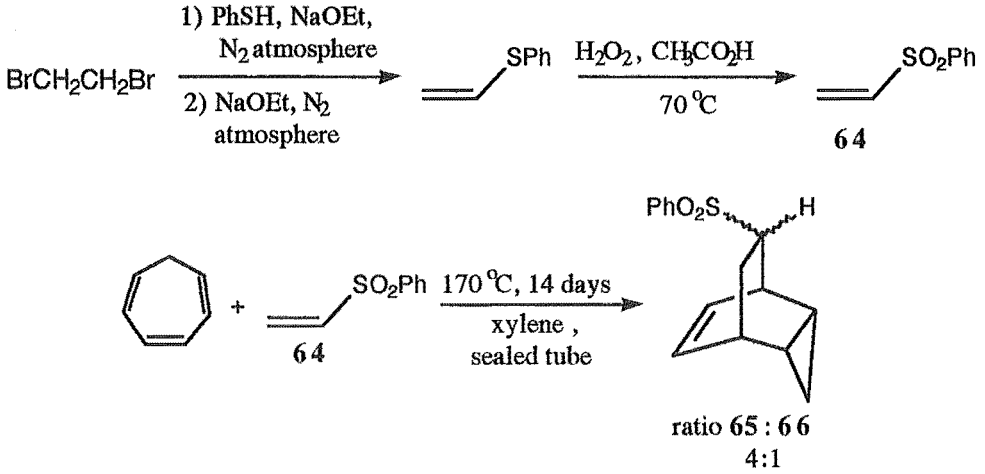

Figure 2.11. Synthesis of phenyl vinyl sulphone **64** followed by Diels-Alder reaction with cycloheptatriene.

Due to the low reactivity of **64** with cycloheptatriene a more reactive dienophile or another route to the formation of **65** and/or **66** was required. De Lucchi et al.[86] have recently reported the conversion of 1,2-disulphones to the corresponding monosulphone. Two procedures were reported, firstly, direct reduction of the disulphone to the monosulphone by treatment with sodium borohydride, and secondly, reaction of the disulphone with base to give a vinyl sulphone which was then reduced to the corresponding dihydro derivative (see Figure 2.12). Both procedures were reported to give the product in similar yields.

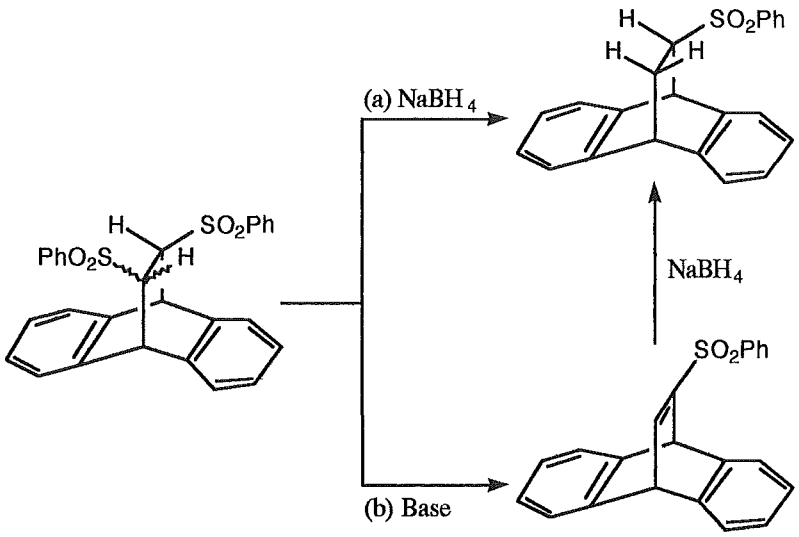

Figure 2.12. Reductive elimination of a single sulphone group from a 1,2-disubstituted sulphone.[86] Path (a) direct reduction or (b) base induced elimination followed by reduction of the vinyl sulphones double bond.

Reduction of **55** with $NaBH_4$ in refluxing THF gave **65** and **66** in a ratio of 2:1 (32% isolated yield) along with a small amount (3%) of the *trans* disulphone **54**. Due to the low yield of monosulphones **65** and **66** obtained from the direct reduction method, the second pathway was investigated.

Reaction of **55** with potassium carbonate in aqueous dioxan[86] at 50 °C for 3.5 h gave no formation 6-phenylsulphonyl-*exo*-tricyclo[3.2.2.$0^{2,4}$]nona-6,8-diene **67**. Likewise, treatment of **55** with NaOH in aqueous dioxan at room temperature or reflux, gave none of the desired product and resulted in the recovery of starting material and *trans* disulphone **54**. Although these conditions have been reported[86] to give good yields of elimination products, the low solubility of **55** in the reaction solvent may have been responsible for the failure to react. Compound **55** was found to be soluble in pyridine and therefore the reaction was repeated using pyridine as the solvent. Reaction of **55** with NaOH in pyridine, with a small amount of water, gave **67** in 53% yield. Attempted reaction of **55** with pyridine alone, and with pyridine in the presence of water, gave no observable (^{1}H NMR) product formation after prolonged stirring at room temperature (7 and 9 days, respectively).

Compound **67** was reduced with $NaBH_4$ in refluxing THF to give a mixture of **66** and **65** in a ratio of 3:2 (58% isolated yield). This equates to a 31% overall yield (from **55**) of the required monosulphones **66** and **65**, which is similar to the yield obtained from the one step reduction procedure. The two isomers were separated by TLC mesh column chromatography.

Reductive elimination of the sulphonyl group of **65** was accomplished according to the general procedure of Paquette,[88] by sodium amalgam reduction‡ in disodium hydrogen phosphate buffered anhydrous methanol, and gave the *endo* alkene **56** in an isolated yield of 39%. This corresponds to a 9% overall yield of **56** based on De Lucchi's[75] reported yield (80%) of **53**. Although the yield was low, it represented a 2-5 fold improvement on the yield obtained from the Diels-Alder procedure[67,68] and gives **56** cleanly without any significant formation of diene **51**, as was found with the Li/NH_3 reduction pathway.[86] The synthesis of **56** from the disulphone **55** is summarised in Figure 2.13.

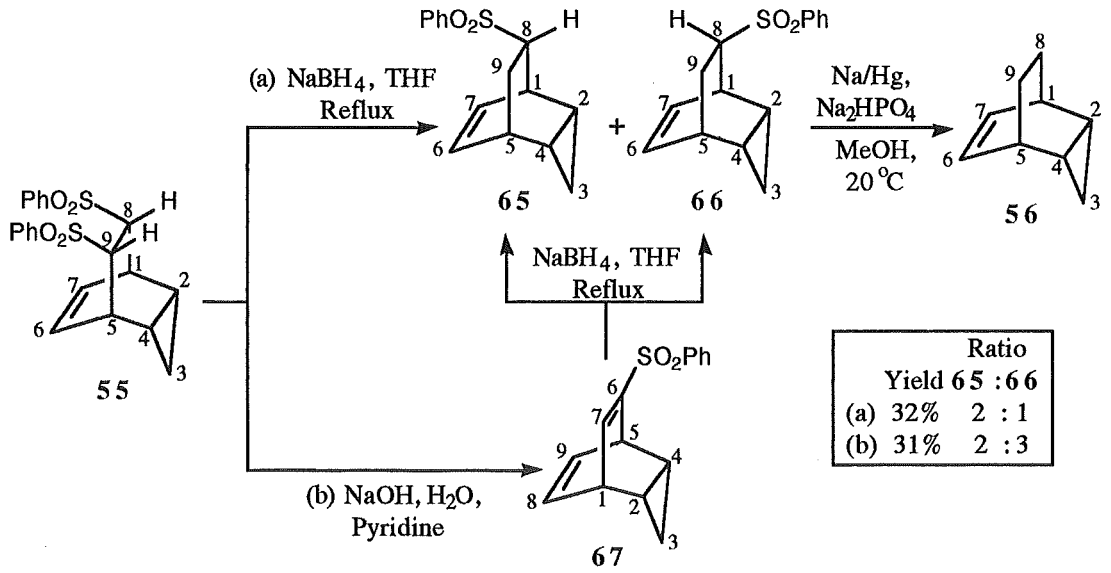

Figure 2.13. Synthesis of *endo*-tricyclo[3.2.2.$0^{2,4}$]non-6-ene **56** by sodium amalgam reduction of **65**. The monosulphones **65** and **66** result from reduction of **55** via a one step (path a) or two step (path b) procedure.

The identity of **67** was determined from its ^1H and ^{13}C NMR spectra. The compound also showed satisfactory mass spectral and elemental analyses. A homonuclear correlation experiment (DQCOSY) established the proton-proton connectivity, and identified a correlation from H1 (3.87 ppm) to H7 (7.56 ppm) (Figure 2.14). The chemical shift of H7 is consistent[86] with that of an olefinic proton shifted downfield by the presence of a β sulphonyl substituent.

‡ The desulphurisation procedure reported by Becker et al.[105] avoids the use of large quantities of toxic mercury but was not readily amenable to large scale preparations.

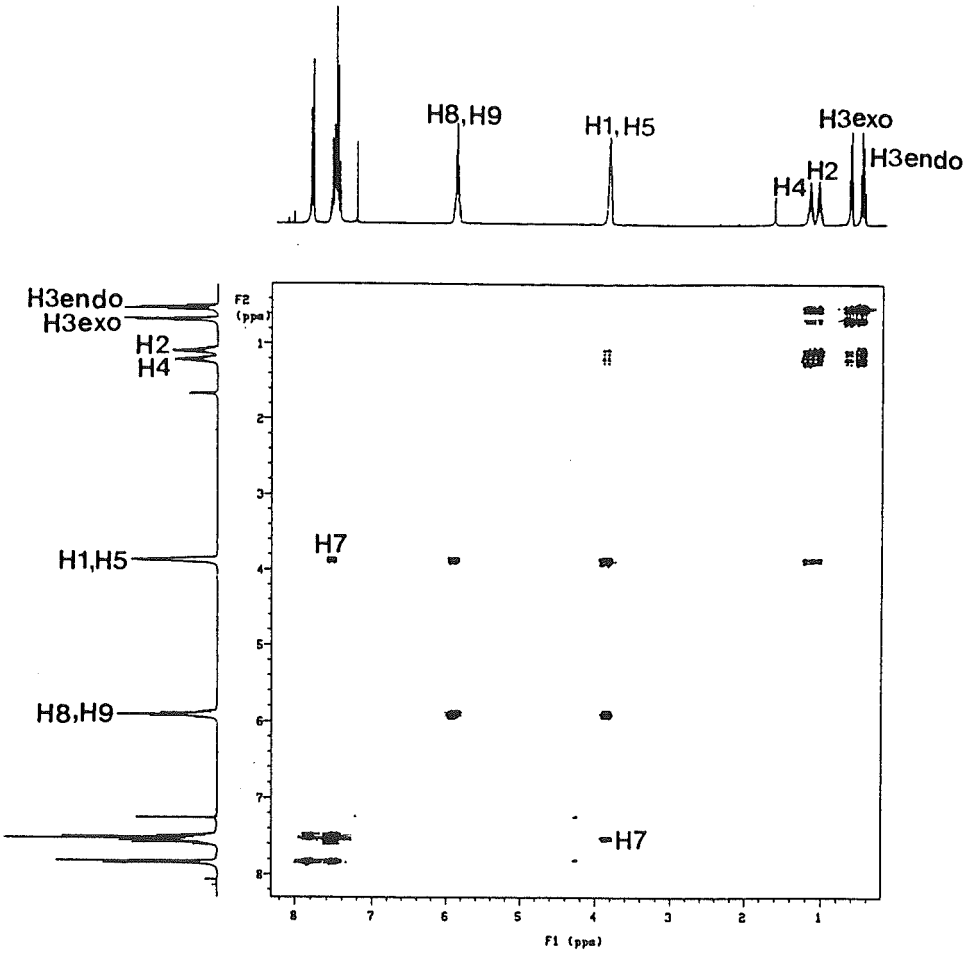

Figure 2.14. DQCOSY of 6-phenylsulphonyl-*exo*-tricyclo[3.2.2.0^{2,4}]nona-6,8-diene **67**.

Monosulphones **65** and **66** were characterised by their ^{1}H and ^{13}C NMR spectra and mass spectral analyses. The identity of **65** was determined as follows; the proton-proton connectivity was established from selective ^{1}H decoupling experiments and a Heteronuclear Multiple Quantum Coherance (HMQC) experiment allowed determination of the ^{1}H-^{13}C connectivity (Figure 2.15). The *anti* orientation of the phenylsulphonyl group was determined by the presence of an nOe to the multiplet at 3.34 ppm (H8) upon irradiation of H2 and H4 (multiplet centered at 0.89 ppm).† This conclusion was also supported by the presence of a 9.7 Hz coupling constant from H9*syn*‡ to H8, consistent with a *cis* vicinal coupling. The shielding of C7, by 4 ppm relative to C6, is consistent with that expected[106] for a gauche interaction of the *anti* phenylsulphonyl group. This effect is also observed for the equivalent carbons in the *anti*-methyl ester **58** and *anti*-

† Enhancements of H2 and H4 were also observed on irradiation of H8. No percent enhancement could be reported as the multiplets corresponding to H8 and H1 were partially overlapping. Irradiation of this multiplet would therefore be expected to show an enhancement to H2 via both H1 and H8.

‡ The proton at 1.89 ppm was assigned to H9*syn* from the proton-proton decoupling experiments and by the presence of a 1.7% nOe to H2/H4 on irradiation of this multiplet.

benzophenone oxime ester 62 (see Table 2.2). The *endo* orientation of the cyclopropane ring follows from the nOe data and from the *endo* stereochemistry of the cyclopropane ring in the starting material 55.

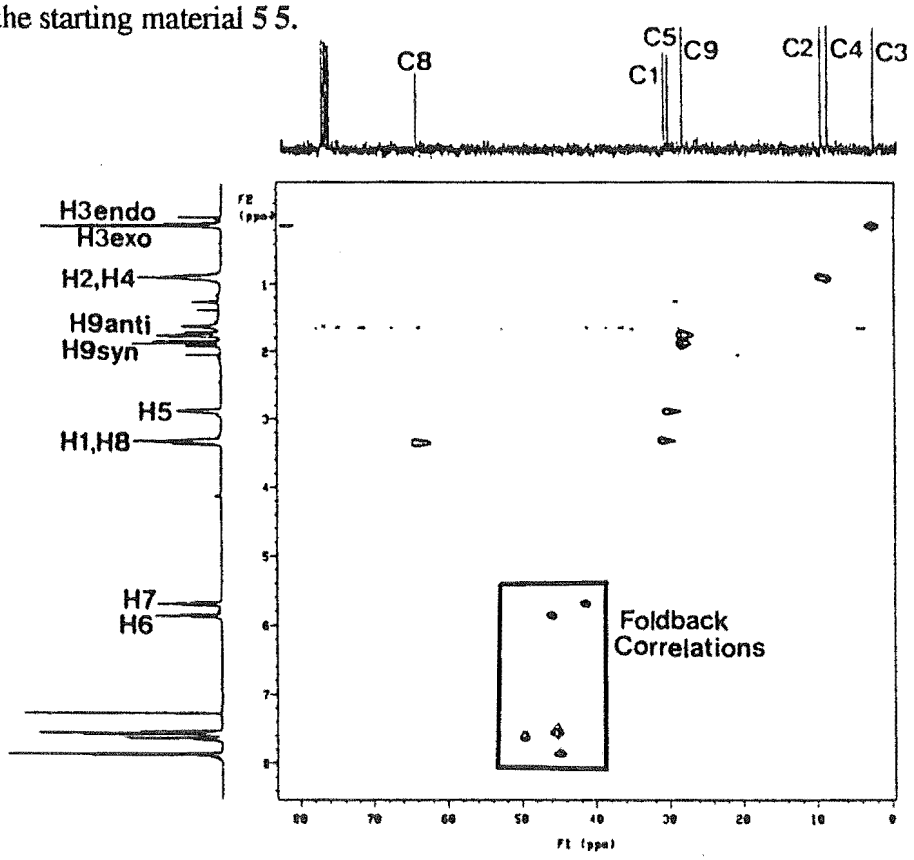

Figure 2.15. HMQC experiment of 8-*anti*-phenylsulphonyl-*endo*-tricyclo[3.2.2.$0^{2,4}$]non-6-ene 65.

For 66 the ^{1}H-^{1}H connectivity was determined from selective decoupling experiments and the ^{1}H-^{13}C connectivity established from an HMQC experiment. The *syn* stereochemistry of the C8 phenylsulphonyl group was assigned from the presence of a 5.8 Hz coupling constant from H9*syn* to H8 and a 10.3 Hz *cis* coupling from H9*anti* to H8. Irradiation of the multiplet centered at 2.07 ppm gave a 2.5% nOe to H4 (1.4% enhancement of the multiplet at 2.07 was observed on irradiation of H4), which identified this multiplet as H9*syn* (no enhancement of the multiplet at 1.53 ppm, identified as the second proton of the C9 methylene from the HMQC experiment, was observed on irradiation of H4).

The C2 signal of 66 showed an upfield shift of approximately 5 ppm, relative to the chemical shift of C4, and a 5 ppm shift from the equivalent carbon in 65. This is consistent with a γ shielding effect of the *syn* phenylsulphonyl group of C8. Shielding of the equivalent carbon in the *syn*-methyl ester 59 and *syn*-benzophenone oxime ester 63 was also observed (see Table 2.3). The steric compression which results in an upfield shift of C2 would also be expected to result in a downfield (deshielding) shift of the attached proton H2. The observed chemical shift of H2 at 1.44 ppm is shifted downfield by 0.3 ppm relative to that of H4 (1.15 ppm) and hence is also consistent with the *syn*

orientation of phenylsulphonyl group of C8. The inductive deshielding effect of this group would not be expected to give such a large difference in chemical shift between H2 and H4. This can be seen from comparing the chemical shifts of H6 and H7, 5.79 and 5.78 ppm, respectively (the chemical shifts of H2 and H4 in **65** were also almost identical, overlapping multiplet centred at 0.89 ppm).

Tables 2.2 and 2.3 summarise the ^{13}C NMR data of **65** and **66** and the related compounds **58**, **59**, **62**, and **63**. The assignment of the carbons for all six compounds was determined independently, that is, the carbon assignments were established from HMQC and HMBC ^{1}H-^{13}C heteronuclear correlation experiments, in conjunction with ^{1}H-^{1}H homonuclear correlation methods (COSY, DQCOSY) or selective proton decoupling experiments, which were performed for each compound.

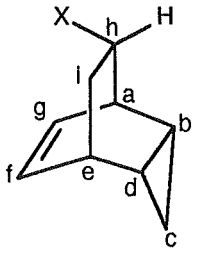

58 X = CO_2Me
62 X = $CO_2NC(Ph)_2$
65 X = SO_2Ph

	Carbon (a-i) and chemical shifts (ppm)								
Cmpd	a	b	c	d	e	f	g	h	i
58	33.9	9.8*	2.9	9.6*	30.5	130.4	126.4	42.9	29.7
62	33.5	9.7*	2.8	9.6*	30.3	130.3	126.3	42.1	29.6
65	31.3	9.9	2.9	9.0	30.7	129.8	125.2	64.7	28.8

Table 2.2. ^{13}C chemical shifts (ppm) of *anti /exo* substituted compounds **58**, **62**, and **65**.
(* = Assignments of carbons b and d may be reversed.)

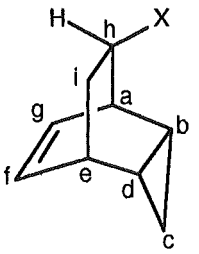

59 X = CO_2Me
63 X = $CO_2NC(Ph)_2$
66 X = SO_2Ph

	Carbons (a-i) and chemical shifts (ppm)								
Cmpd	a	b	c	d	e	f	g	h	i
59	33.7	5.5	1.5	9.4	30.1	130.1	128.5	42.8	28.3
63	33.3	5.4	1.5	9.3	30.0	130.9	128.3	41.9	28.1
66	31.7	4.8	2.1	10.0	30.4	130.5	127.8	63.7	26.6

Table 2.3. ^{13}C chemical shifts (ppm) of *syn/endo* substituted compounds **59**, **63**, and **66**.

CHAPTER 3
Bromination of *exo*- and *endo*-Tricyclo[3.2.1.0^{2,4}]octane

Section 3.1. INTRODUCTION

Bromination reactions of simple cyclopropanes have been extensively studied.[24-27] The reactions are generally believed to occur by a two step process in which initial electrophilic addition occurs with inversion of configuration at the site of attack and results in the formation of a "free" carbocation which may then undergo rearrangement or nucleophilic capture. In some systems however, attack exclusively with retention[33] or both retention and inversion pathways[107] has been observed. As an extension of work carried out by Coxon et al. to investigate the stereochemistry of electrophilic (proton, deuteron, mercuric acetate) addition to *endo*- and *exo*-tricyclo[3.2.1.0^{2,4}]octane (**1** and **46**, respectively)[13,14,15] and related compounds,[16,18] the bromination reactions of **1** and **46** were investigated.

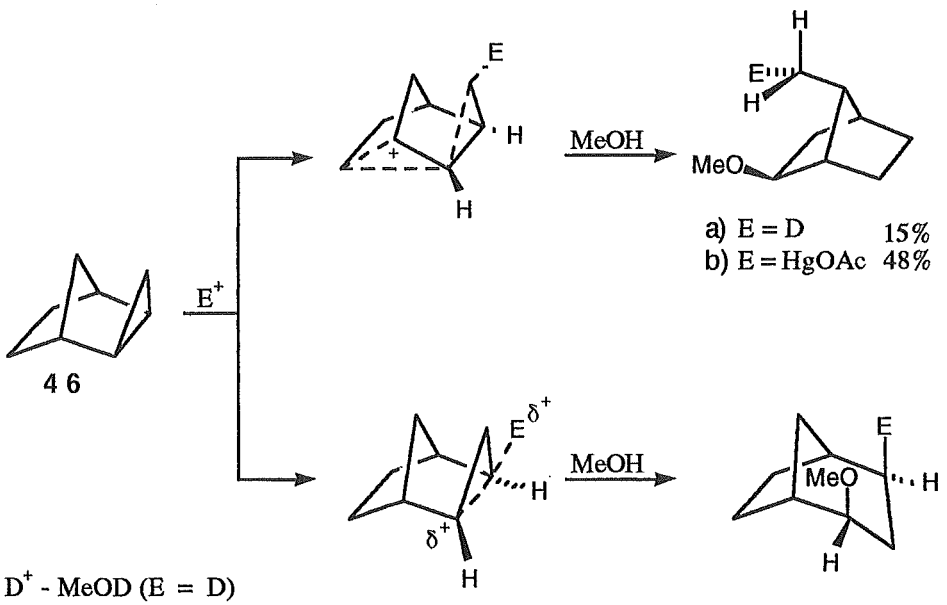

Figure 3.1. Reaction of *exo*-tricyclo[3.2.1.0^{2,4}]octane **46** with H^+, D^+, and $Hg(OAc)_2$.[13,18]

The differing geometrical constraints imposed on the cyclopropane ring in structures **1** and **46** would be expected to result in different orbital interactions of the cyclopropane with the rest of the hydrocarbon skeleton and thus also with incoming electrophiles. The compounds are therefore expected to give different products upon reaction with bromine, as observed in the reactions of **1** and **46** with a variety electrophiles[13,14,18] (proton, deuteron, mercuric acetate, see Figures 1.6 and 3.1).

Whittington et al.[32] have studied the bromination of *endo*- and *exo*-tricyclo[3.2.1.$0^{2,4}$]-oct-6-ene **68** and **69** (see Figures 3.2 and 3.3). From comparison of Figures 3.2 and 3.3 it can be seen that a Wagner-Meerwein rearrangement is observed to a significant extent for **68**, whereas less rearrangement is observed for **69**. For both **68** and **69** bromine addition preferentially occurs at the double bond. This contrasts with the reactions with acid and mercuric acetate which occur exclusively at the cyclopropane ring. Structures **1** and **46**, which have no double bonds, should therefore serve as good probes as to the importance of edge verses corner attack of bromine on the cyclopropane moiety.

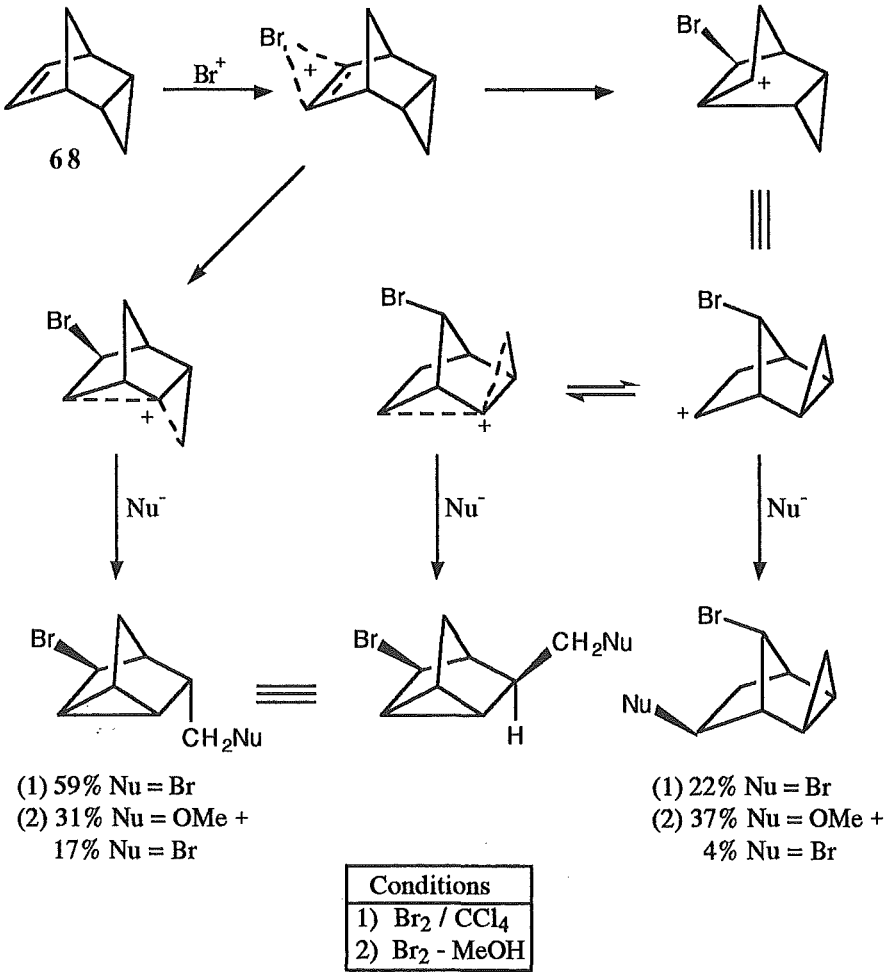

Figure 3.2. Bromination of *endo*-tricyclo[3.2.1.$0^{2,4}$]oct-6-ene **68**.[32]

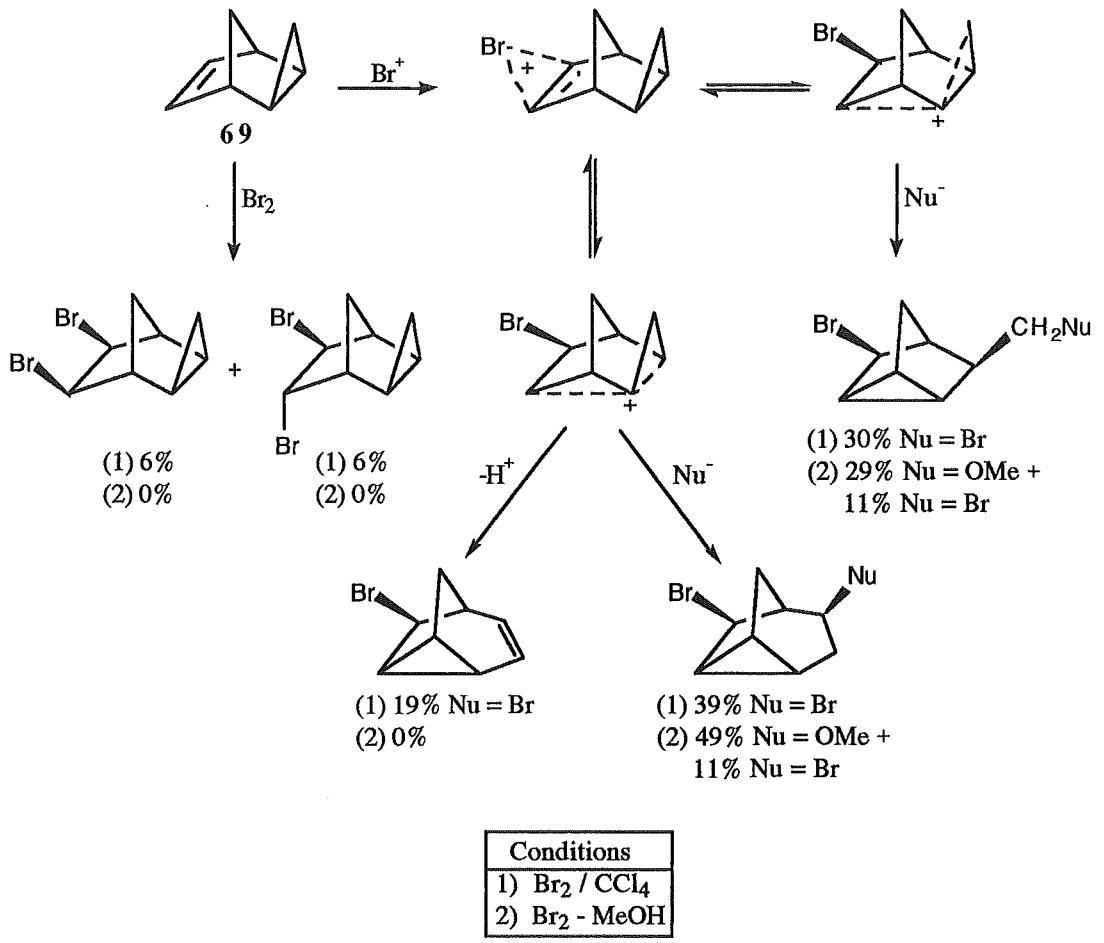

Figure 3.3. Bromination of *exo*-tricyclo[3.2.1.$0^{2,4}$]oct-6-ene **69**.[32]

Section 3.2 BROMINATION OF *exo*-TRICYCLO[3.2.1.$0^{2,4}$]OCTANE

The reaction of *exo*-tricyclo[3.2.1.$0^{2,4}$]octane **46** with bromine (0.8 mole equivalents) in carbon tetrachloride occurred relatively rapidly at room temperature‡ with only a faint bromine colour observable after 3 h. GLC analysis showed the presence of two major products, 2-*exo*-4-*endo*-dibromobicyclo[3.2.1]octane **70a** (58%) and 2-*exo*-4-*exo*-dibromobicyclo[3.2.1]octane **71a** (36%), as well as one minor product (6%) which was not identified. The major products were separated by column chromatography on silica gel (pentane elution).

‡ Addition of the bromine solution was carried out without complete exclusion of light but subsequent stirring was carried out in the complete absence of light.

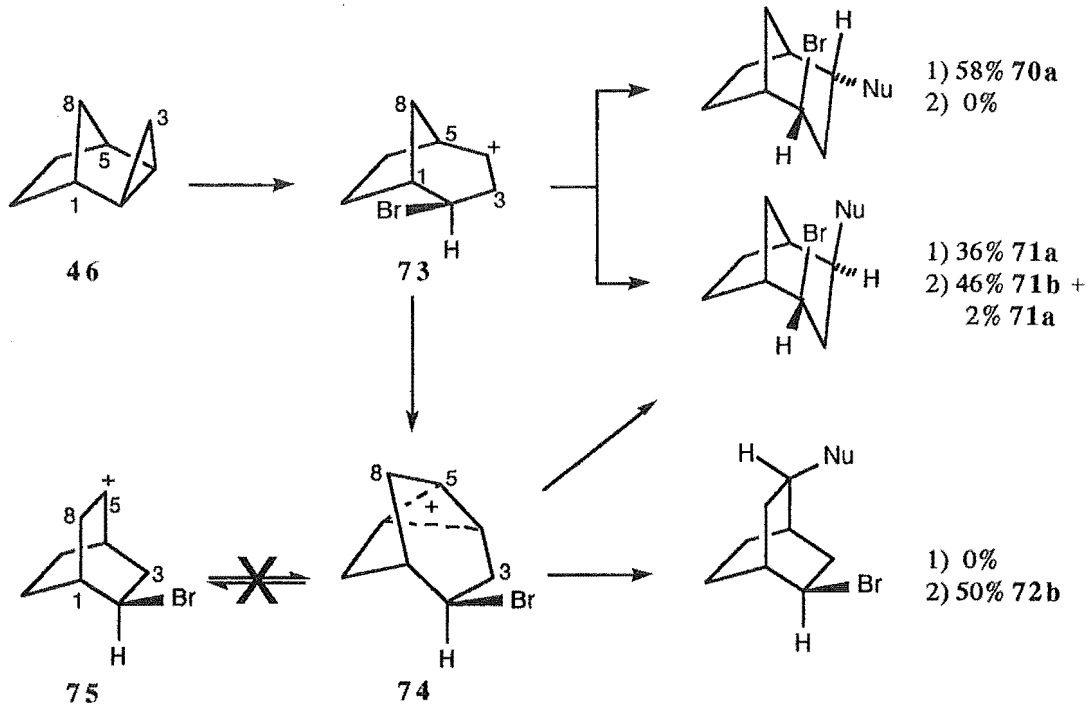

Figure 3.4. Reaction *exo*-tricyclo[3.2.1.$0^{2,4}$]octane **46** with bromine.

The identity of 2-*exo*-4-*endo*-dibromobicyclo[3.2.1]octane **70a** was determined as follows: a COSY experiment established the ^{1}H-^{1}H connectivity and a heteronuclear correlation experiment (HETCOR) established the ^{1}H-^{13}C one bond connectivities. The presence of two CHBr groups was determined from the presence of two protons with chemical shifts of 4.24 ppm (H2) and 4.52 ppm (H4) and from the chemical shifts of the associated carbons at 53.0 ppm (C2) and 55.9 ppm (C4). The *exo* stereochemistry of H4 was determined by the presence of a 2.9% nOe to a multiplet centred at 2.30 ppm on irradiation of H4.† The multiplet at 2.30 ppm had previously been determined from the HETCOR experiment to be a proton attached to C8. Enhancement of the multiplet at 2.30 ppm (H8*syn*) also established the *syn* orientation of this proton with respect to the largest bridge and this was confirmed by the absence of a measurable coupling from H1 or H5 to this proton which is consistent with results observed[32] for other bicyclo[3.2.1]octane systems. Carbon C2 was established as having an *exo*

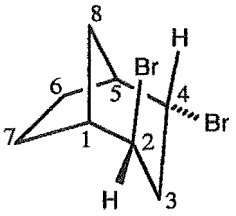

† The reverse nOe was observed but could not be quantified due to the partial overlap of H8*syn* with the multiplet assigned to H3*endo* and H3*exo*. The enhancement of H8*syn* on irradiation of H4 was identified by the multiplicity of this proton (a doublet).

bromine by the lack of symmetry in the molecule (eight carbon resonances were observed in the ^{13}C spectrum). The presence of a 2.0 Hz coupling from H2 to H8*anti* is consistent with a four bond 'W' coupling of these protons‡ and hence supports the assigned *endo* orientation of H2.

For 2-*exo*-4-*exo*-dibromobicyclo[3.2.1]octane **71a** structure elucidation was assisted by the observation that when the sample was run in benzene-d_6, instead of $CDCl_3$, all of the protons were resolved. Of particular note were the shifts of H3*endo* and H8*anti* which were overlapping with H1/H5 and H6*endo*/H7*endo*, respectively, in $CDCl_3$ (Figure 3.5a) but were completely resolved when the ^1H NMR spectrum was acquired in benzene-d_6 (Figure 3.5b). The ^{13}C NMR spectrum of **71a** showed only five signals and hence established the presence of symmetry in the molecule. The ^1H-^1H connectivity was determined by selective decoupling experiments and a HETCOR established the one bond ^1H-^{13}C connectivity. A 6.2% enhancement of the multiplet at 1.84 ppm in a difference nOe experiment, on irradiation of the proton centred at 0.80 ppm, established these protons as H3*endo* and H6*endo*/H7*endo*, respectively. The presence of a four bond 2.1 Hz coupling from H6*endo*/H7*endo* to a doublet centred at 3.03 ppm (H8*syn*) established a 'W' arrangement of these protons and therefore the *syn* orientation of the proton attached to C8. The second proton attached to C8 (identified from the HETCOR experiment), centred at 1.10 ppm, showed a small (1.5 Hz) coupling to H2 and H4 and hence allowed the assignment of these protons to an *endo* orientation, and therefore established an *exo* orientation of the bromine substituents at C2 and C4. Consideration of the chemical shift of H8*syn* (3.03 ppm) also supports the assignment of an *exo* orientation of the bromines since this would lead to an expected downfield shift of this proton due to steric compression effects[109-111] which are also reflected by an upfield shift of C8 (29.8 ppm).† The structure of **71a** was confirmed by X-ray crystal structure analysis (Figure 3.6).

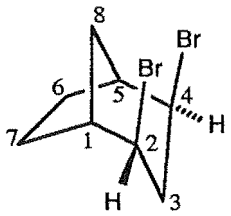

Although radical reactions of bromine with cyclopropanes are known to occur rapidly in nonpolar solvents[24] the possibility of radical reactions of bromine with **46** was minimized by exclusion of light. The Br-Br bond is weaker than the Cl-C bond of CCl_4 (the bond dissociation energies of the Br-Br and Cl-CCl_3 bonds are 193 kJ mol^{-1} and 306 kJ mol^{-1}, respectively) and is therefore more susceptible to radical attack. Any alkyl radical generated from **1** or **46** would be expected to be sufficiently reactive to react with whatever it collided with first. As CCl_4 was the reaction solvent (CCl_4 itself is a

---

‡ Although other four bond coupling patterns such as sickle or fork couplings[108] are possible, the size of the coupling constant (2.0 Hz) precludes any other four bond coupling pathway for these systems.[108]

† The NMR of these compounds will be discussed in more detail in Section 3.4.

reasonable radical scavenger[112]) and the probability of collision would be much greater than that of the radical with bromine, significant amounts of chloride containing products would be expected. No products containing chlorine were observed in the reaction. The reaction was therefore considered to be predominantly electrophilic in character.

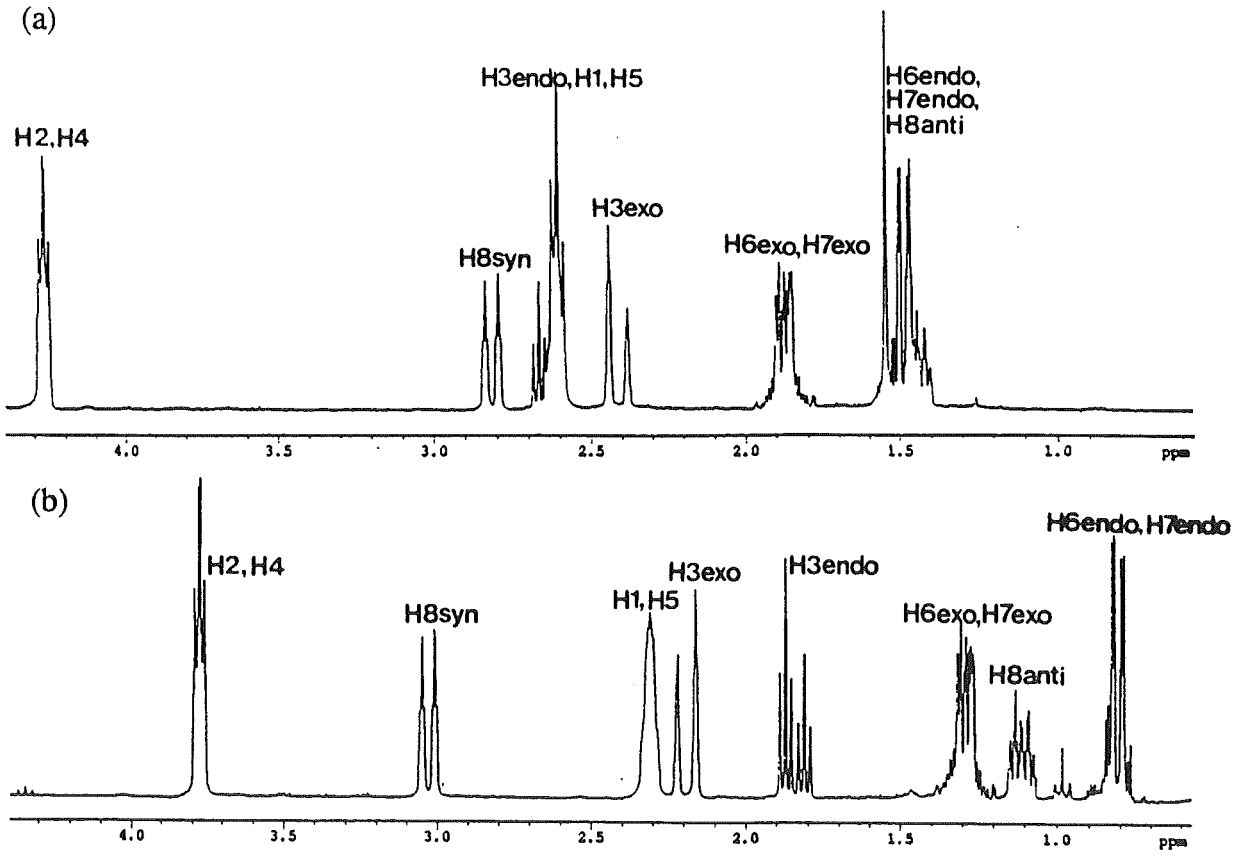

Figure 3.5. (a) ^{1}H NMR spectrum of **71a** in $CDCl_3$. (b) ^{1}H NMR spectrum of **71a** in benzene-d_6.

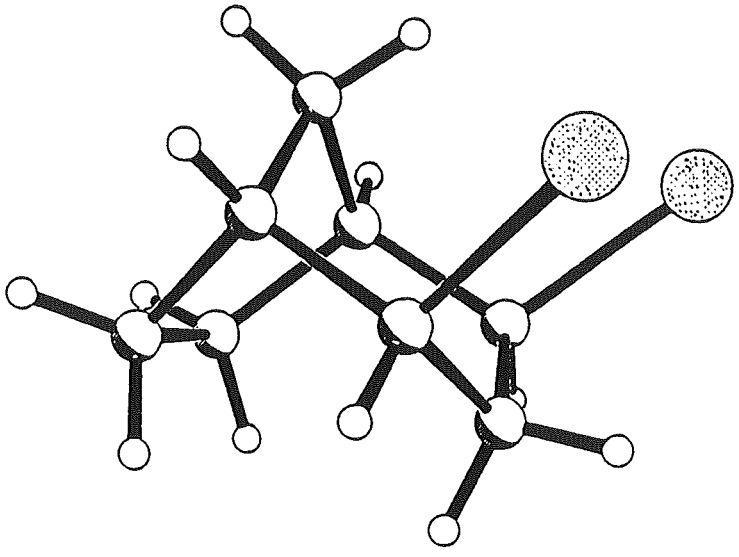

Figure 3.6. X-Ray crystal structure of 2-*exo*-4-*exo*-dibromobicyclo[3.2.1]octane **71a**.

In order to determine the trajectory of electrophilic attack and subsequent nucleophilic attack, the reaction of **46** with bromine was repeated using methanol as the reaction solvent. In this case the electrophile and nucleophile are different, hence allowing the trajectory of electrophilic attack to be differentiated from that of nucleophilic attack. GLC analysis of the product mixture obtained from reaction of **46** with bromine (0.8 mole equivalents) in dry methanol showed four products, 2-*endo*-bromo-5-*endo*-methoxybicyclo[2.2.2]octane **72b** (50%), 2-*exo*-bromo-4-*exo*-methoxybicyclo[3.2.1]-octane **71b** (46%), 2-*exo*-4-*exo*-dibromobicyclo[3.2.1]octane **71a** (2%) and one other minor product (2%) which was not identified. A crude separation was effected by radial chromatography on silica. The major products were then further purified by column chromatography.

The identity of 2-*endo*-bromo-5-*endo*-methoxybicyclo[2.2.2]octane **72b** was determined from the following: a COSY experiment established the proton-proton connectivity and a HETCOR allowed assignment of the one bond ^{1}H-^{13}C attachments. Carbons C7 and C8 were confirmed as methylene carbons by a DEPT135 experiment. Irradiation of the multiplet (1.14-1.23 ppm) corresponding to H7*syn* and H7*anti* gave a 4.8% enhancement of H2 (4.07 ppm) in a difference nOe experiment and therefore established the *exo* orientation of this proton and hence the *endo* orientation of the bromine attached to C2. The same irradiation showed a 2.8% enhancement of H6*exo* (multiplet centred at 1.72 ppm). Irradiation of the multiplet corresponding to H8*syn* and H8*anti* gave a 2.0% nOe to H5 (multiplet 3.12 ppm) and a 2.0 % enhancement of H3*exo* (multiplet 1.91 ppm), thus confirming the *exo* orientation of H5 and hence the *endo* orientation of the methoxy group. The protons H2 and H5 were identified as being attached to carbons bearing bromine and methoxy substituents, respectively, by consideration of their chemical shifts (4.07 ppm and 3.12 ppm) and from the chemical shifts of the attached carbons (53.2 ppm and 78.1 ppm, respectively), which were determined from the HETCOR experiment. The stereochemical assignments at C5 and C2 were supported by consideration of the coupling constants of H2 and H5 to the protons of the adjacent methylene groups ($^{3}J_{2,3exo}$ = 10.3 Hz, $^{3}J_{2,3endo}$ = 6.2 Hz, $^{3}J_{6exo,5}$ = 9.5 Hz) and from the long range four bond coupling constants ($^{4}J_{2,6exo}$ = 2.1 Hz, $^{4}J_{3exo,5}$ = 1.7 Hz)‡ which are consistent with 'W' couplings from H3*exo* to H5 and H6*exo* to H2.

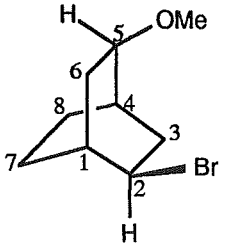

For 2-*exo*-bromo-4-*exo*-methoxybicyclo[3.2.1]octane **71b** a COSY established the

‡ Coupling constants were not calculated from H5 due the complexity of the multiplet and lack of a completely resolved coupling pattern.

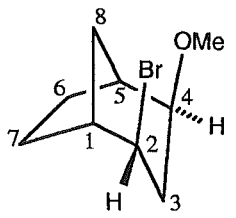

^{1}H-^{1}H connectivity and an HMQC experiment established the ^{1}H-^{13}C one bond connectivities. Protons H2 (multiplet 4.21 ppm) and H4 (multiplet 3.26 ppm) were identified as protons of CHBr and CHOMe groups, respectively, by consideration of their chemical shifts. The similarity of the shape of the H2 and H4 multiplets suggested the orientation of these protons to be the same and comparison with the multiplets of H2 and H4 in **71a** suggested an *endo* orientation of these protons. This was confirmed by the vicinal coupling constants of H2 and H4 to H3*endo*† ($^3J_{3endo,2}$ = $^3J_{3endo,4}$ = 5.0 Hz) and the presence of long range couplings to H8*anti* ($^4J_{8anti,2}$ = $^4J_{8anti,4}$ = 1.8 Hz) which are consistent with 'W' couplings. Irradiation of H7*endo* gave an nOe (2.7%) to H2 (reverse nOe 1.5% on irradiation of H2) which also supports the assignment of H2 to an *endo* configuration. On irradiation of H6*endo* a 4.7% nOe to H4 (2.7% on reverse irradiation) was observed, suggesting an *endo* orientation of H4. Finally, comparison of the chemical shifts of C8 in **71b** and the corresponding carbon in bicyclo[3.2.1]octane[106] (27.9 ppm and 39.7 ppm, respectively) shows a large (12 ppm) upfield shift in **71b** which is consistent with two gauche eclipsed interactions of C8 (H8*syn*) with the bromine of C2 and the methoxy of C4, thus confirming the *exo* orientation of the two substituents.

Analysis of the products resulting from the bromination of **46** shows initial electrophilic attack of bromine to occur from a corner attack trajectory, resulting in inversion of configuration, for both reactions. When CCl_4 is the reaction solvent no carbon skeleton rearrangement is observed. Nucleophilic attack occurs with both retention and inversion of configuration, with a small preference (1.6:1) for the inversion pathway. This implies the formation of a fully formed classical carbocation, in agreement with the results of Skell,[24] with a significant barrier to rearrangement as nucleophilic capture occurs rapidly, with respect to the rearrangement, with no products resulting from rearrangement reactions being observed. The products from the reaction therefore result from kinetic and not thermodynamic control, as would be expected in a nonpolar medium which would not stabilise the intermediate carbocation.

When the reaction is performed in methanol approximately 50% of the products result from Wagner-Meerwein rearrangement followed by nucleophilic capture. It therefore appears that under more polar conditions rearrangement becomes more favourable. If nucleophilic addition of methanol occurred to a classical open cation **75** (Figure 3.4) then both nucleophilic attack with inversion and retention would be expected

---

† The orientation of H3*endo* (d of t centred at 2.05 ppm) was determined by the presence of a 2.5% nOe to this proton on irradiation of the multiplet centred at 1.45 ppm (H7*endo*). On irradiation of H3*endo* a 1.7% nOe to H7*endo* was observed.

as both faces of cation **75** would be similar.‡ It therefore appears likely that nucleophilic attack occurs either to a nonclassical cation **74** or that two classical cations are interconverting rapidly and hence directing nucleophilic attack to occur with inversion[113,114] at either C4 or C5.†

Section 3.3 BROMINATION OF *endo*-TRICYCLO[3.2.1.$0^{2,4}$]OCTANE

The reaction of *endo*-tricyclo[3.2.1.$0^{2,4}$]octane **1** with bromine (0.8 mole equivalents) in carbon tetrachloride gave four products (GLC analysis), 2-*exo*-3-*endo*-dibromobicyclo[3.2.1]octane **75a** (48%), 2-*endo*-4-*endo*-dibromobicyclo[3.2.1]octane **76a** (29%), 2-*endo*-6-*endo*-dibromobicyclo[3.2.1]octane **77a** (15%) and a minor product (8%) which was not identified (Figure 3.7). A crude separation was effected by radial chromatography on polyethylene glycol (PEG, MW = 6000 g mol^{-1}) coated silica. Compound **75a** was further purified by preparative gas liquid chromatography. The other major products **76a** and **77a** were separated by preparative TLC (multiple elution, 3% ethyl acetate/pentane, silica).

The identity of 2-*exo*-3-*endo*-dibromobicyclo[3.2.1]octane **75a** was determined from the following: a double quantum filtered COSY (DQCOSY) experiment in conjunction with proton decoupling experiments established the ^1H-^1H connectivity and an HMQC experiment established the one bond ^1H-^{13}C connectivity. The DQCOSY (Figure 3.8) showed a strong coupling of H1 (2.64 ppm) and H5 (2.34 ppm) to the multiplets centred at 1.85 ppm and 1.77 ppm, respectively, thereby establishing these two protons as H7*exo* and H6*exo*, respectively. From the DQCOSY and HMQC experiments the multiplet at 2.19-2.29 ppm was assigned to H6*endo* and H7*endo*. Irradiation of this multiplet gave a small enhancement (1.1%) of H2 in a difference nOe experiment and hence determined H2 to have an *endo* orientation.§ This therefore requires an *exo* orientation of the bromine attached to C2.

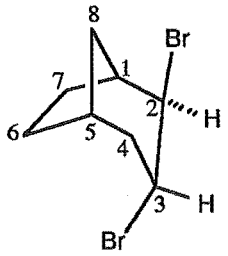

---

‡ If the bromine atom of C2 had an effect on the trajectory of nucleophilic attack it would be expected to direct the incoming nucleophile to the opposite side of the cation from both steric and electronic repulsion considerations, and hence give a different product from that observed.

† For discussions of classical versus nonclassical cations see references 113-123 and references cited therein.

§ This conclusion was supported by decoupling experiments which showed a fine coupling of H2 to the multiplet at 1.44 ppm (H8*anti*) suggesting a 'W' arrangement of these protons. The size of the coupling constant could not be quantified due to the complexity of the H8*anti* multiplet.

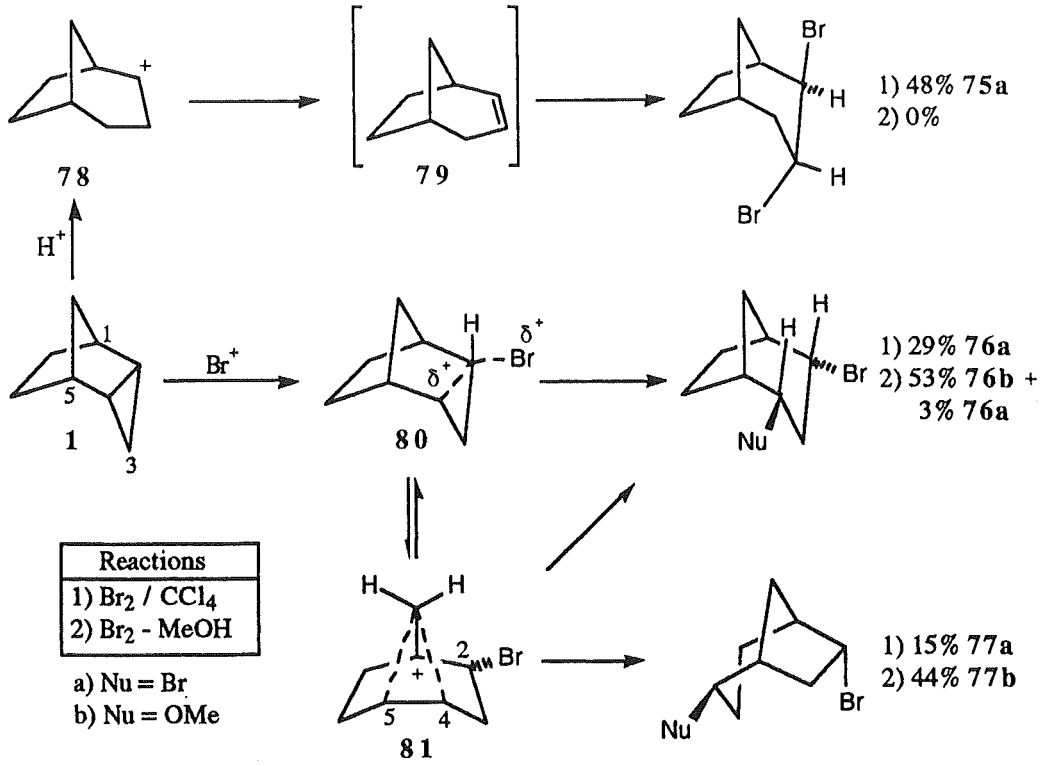

Figure 3.7. Possible mechanism for the bromination of *endo*-tricyclo[3.2.1.$0^{2,4}$]octane **1**.

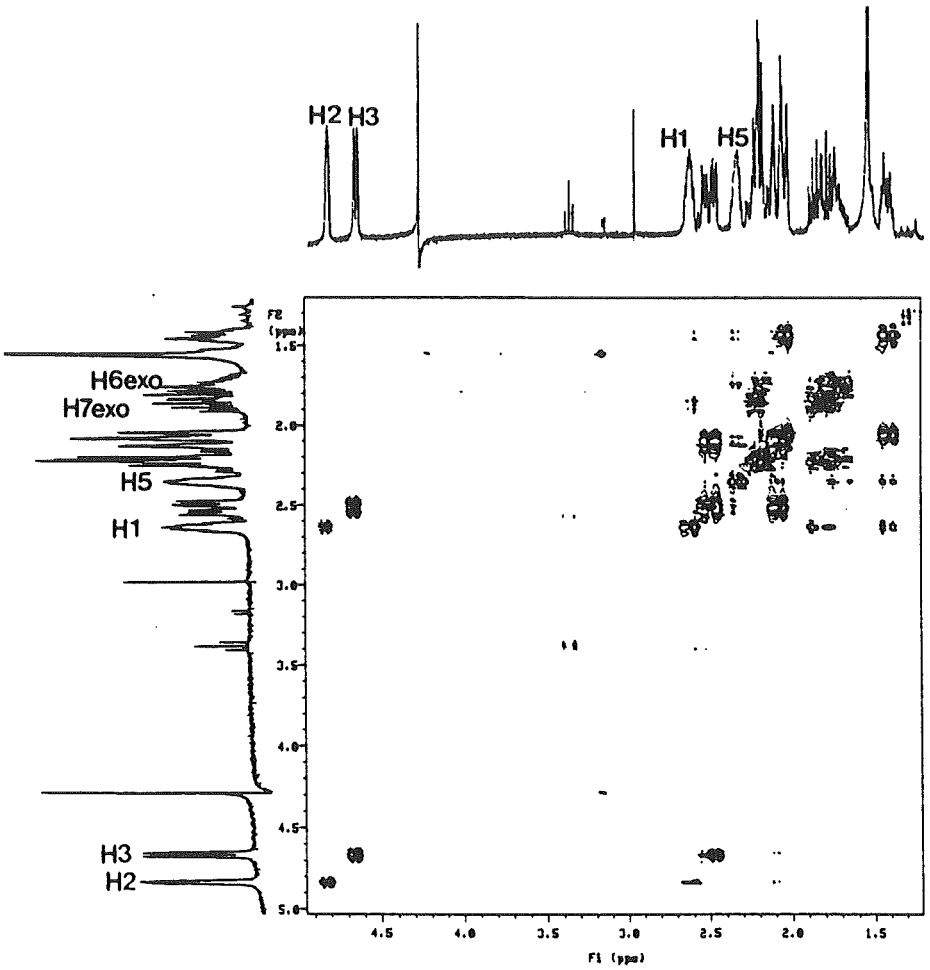

Figure 3.8. DQCOSY of 2-*exo*-3-*endo*-dibromobicyclo[3.2.1]octane **75a**.

The stereochemistry of C3 in **75a** was determined from consideration of the coupling constant of H3 to H4*exo* ($^3J_{3,4exo}$ = 6.2 Hz, $^3J_{4exo,3}$ = 6.4 Hz) and the lack of a measurable coupling to H4*endo*, thus no large *trans* coupling was observed. The coupling constants of H4*exo* and H4*endo* to H5 ($^3J_{4exo,5}$ = 3.2 Hz, $^3J_{4endo,5}$ = 3.4 Hz), and the lack of a *trans* coupling to H3 established the *exo* orientation of H3 and hence an *endo* orientation of the bromine at the C3 position. The chemical shifts of H8*syn*, H6*endo*, and H7*endo* all show significant downfield shifts (Section 3.4) which are also consistent with the proposed stereochemistry at both C2 and C3.

The identity of 2-*endo*-4-*endo*-dibromobicyclo[3.2.1]octane **76a** was determined from analysis of a DQCOSY experiment which established the ^{1}H-^{1}H connectivity and an HMQC which determined the ^{1}H-^{13}C one bond connectivity. The ^{13}C NMR spectrum showed five peaks indicating the presence of symmetry in the molecule. Compound **71a** could be ruled out as this was identified from the bromination of **46**, therefore since the 2D-NMR experiments had identified a bicyclo[3.2.1]octane structure and carbons C2 and C4 were assigned as having a bromine substituent from their chemical shifts (53.2 ppm), the only possibility was an *endo* orientation of the bromine at these centres giving **76a**. This assignment was confirmed by the presence of a 2.3% enhancement of H2/H4 upon irradiation of H8*syn* (doublet 1.55 ppm) in a difference nOe experiment (1.6 % enhancement of H8*syn* was observed on irradiation of H2/H4). The *syn* orientation of the doublet centred at 1.55 ppm was confirmed by the presence of only a small coupling to H1 and H5, whereas H8*anti* showed a 5.3 Hz coupling to both H1 and H5 which is diagnostic in bicyclo[3.2.1]octane compounds.[32]

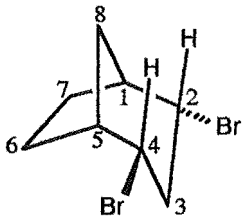

The structure of 2-*endo*-6-*endo*-dibromobicyclo[3.2.1]octane **77a** was elucidated from the following: as far as was possible a DQCOSY experiment established the ^{1}H-^{1}H connectivity. The ^{1}H-^{13}C one bond connectivities were established from HMQC and HMQC-DEPT experiments. The presence of a bicyclo[3.2.1]-octane structure was determined from HMBC and HMQC-TOCSY experiments which also allowed the assignment of C4 and C3 at 30.4 ppm and 30.9 ppm, respectively, from a correlation of H6 to C4 in the HMBC experiment and a correlation from H2 to C3 observed in the HMQC-TOCSY experiment when the spectrum was acquired using a short mixing time (ca. 10 ms). The orientation of H2 was confirmed by the presence of a 1.5% enhancement of the proton assigned to H8*syn* (1.65

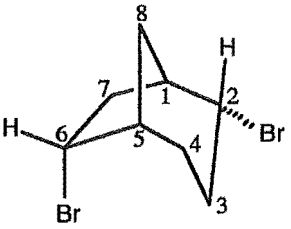

ppm) on irradiation of H2 in a difference nOe experiment.† The *exo* orientation of H6 was confirmed by nOe experiments which showed a 1.8% enhancement of H6 on irradiation of H8*anti* (1.77 ppm).

The formation of **75a**, with a 1,2-dibromo substitution pattern in a bicyclo[3.2.1]-octane skeleton, appeared unlikely to have arisen from bromine addition to the cyclopropane ring of **1**. As described earlier (see Chapter 1, Section 1.2.1b) bromination of cyclopropanes frequently occurs slowly in comparison with the acid promoted ring cleavage. If a catalytic amount of HBr were present under the reaction conditions this may compete with the bromination of the cyclopropane ring and since the reaction was performed in carbon tetrachloride, elimination in the resulting cation **78** (Figure 3.7) would be expected to dominate nucleophilic capture. This process would be expected to result in formation of bicyclo[3.2.1]oct-2-ene **79** which could then add bromine in a 1,2 relationship to give **75a**. Attempts to test the mechanism of formation of **75a** by reaction of **1** with trifluoroacetic acid (TFA) and HBr-acetic acid in CCl_4 at room temperature and 70 °C failed to give any observable (^{1}H NMR) formation of **79**.

To investigate the mechanism of formation of the two other major products, **76a** and **77a**, the reaction of **1** with bromine was repeated using methanol as the reaction solvent. Reaction of **1** with bromine (0.9 mole equivalents) in dry methanol gave three products (GLC). A crude separation of the products was effected by radial chromatography on PEG coated silica. The products were further purified by preparative TLC to give 2-*endo*-bromo-4-*endo*-methoxybicyclo[3.2.1]octane **76b** (53%), 6-*endo*-bromo-2-*endo*-methoxybicyclo[3.2.1]octane **77b** (44%), and 2-*endo*-4-*endo*-dibromo-bicyclo[3.2.1]octane **76a** (3%) (Figure 3.7).

The identification of 2-*endo*-bromo-4-*endo*-methoxybicyclo[3.2.1]octane **76b** was hampered by only six protons (including three of the methoxy group) being clearly isolated in the ^{1}H NMR spectrum when run in $CDCl_3$ (Figure 3.9); thus determination of the ^{1}H-^{1}H connectivity and even the ^{1}H-^{13}C one bond connectivity in some cases was difficult. In this case both 1D- and 2D-TOCSY experiments proved invaluable. Figure 3.10a shows how a DQCOSY experiment gave little information about the ^{1}H-^{1}H connectivity as the connectivity is lost due to the overlap of three protons (H1, H3*exo*, H5) as a multiplet at 2.41-2.48 ppm. A 2D-TOCSY experiment (Figure 3.10b) established the 1,3 relationship of the C<u>H</u>Br and C<u>H</u>OMe protons (H2 and H4, respectively), which were identified from their chemical shifts, 4.12 ppm and 3.17 ppm,

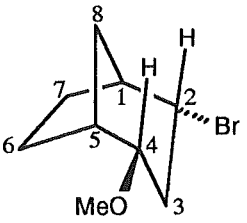

† The reverse nOe could not be measured due to the partial overlap of H8*syn* and H4*exo*, both of which would be expected to give enhancements of H2 on irradiation of this multiplet in a difference nOe experiment.

respectively. A 1D-TOCSY performed by irradiation of H2 (Figure 3.11a) allowed determination of the chemical shift and multiplicity of H3*endo* (d of t, 1.69 ppm) and also allowed the coupling constants of this proton to H3*exo*, H4, and H2 to be calculated ($^2J_{3endo,3exo}$ = 13.0 Hz, $^3J_{3endo,2}$ = $^3J_{3endo,4}$ = 10.9 Hz). Analysis of the coupling constants calculated from this proton and from H2 ($^3J_{2,3endo}$ = 11.3 Hz, $^3J_{2,3exo}$ = 5.4 Hz) and H4 ($^3J_{4,3endo}$ = 12.2 Hz, $^3J_{4,3exo}$ = 5.2 Hz) confirmed the assignment of the proton at 1.69 ppm as H3*endo* and, from the size of the coupling constants from H2 and H4 to H3*endo* (ca. 11 Hz), showed a *trans* relationship of these protons.

The ^{1}H-^{13}C one bond connectivity was determined by an HMQC experiment. However, the experiment was not performed at high enough resolution to distinguish the proton correlations to the carbons at 37.1 ppm and 37.0 ppm and was also complicated by both carbons correlating to the multiplet at 2.41-2.48 ppm. A DEPT135 experiment established the carbon resonance at 37.1 ppm to be a methine carbon and the carbon at 37.0 ppm to be a methylene carbon. The use of an HMQC-DEPT experiment enabled the resolution of the proton correlations as CH groups show correlations with a "positive" phase and the methylene correlations have a "negative" phase in this experiment.

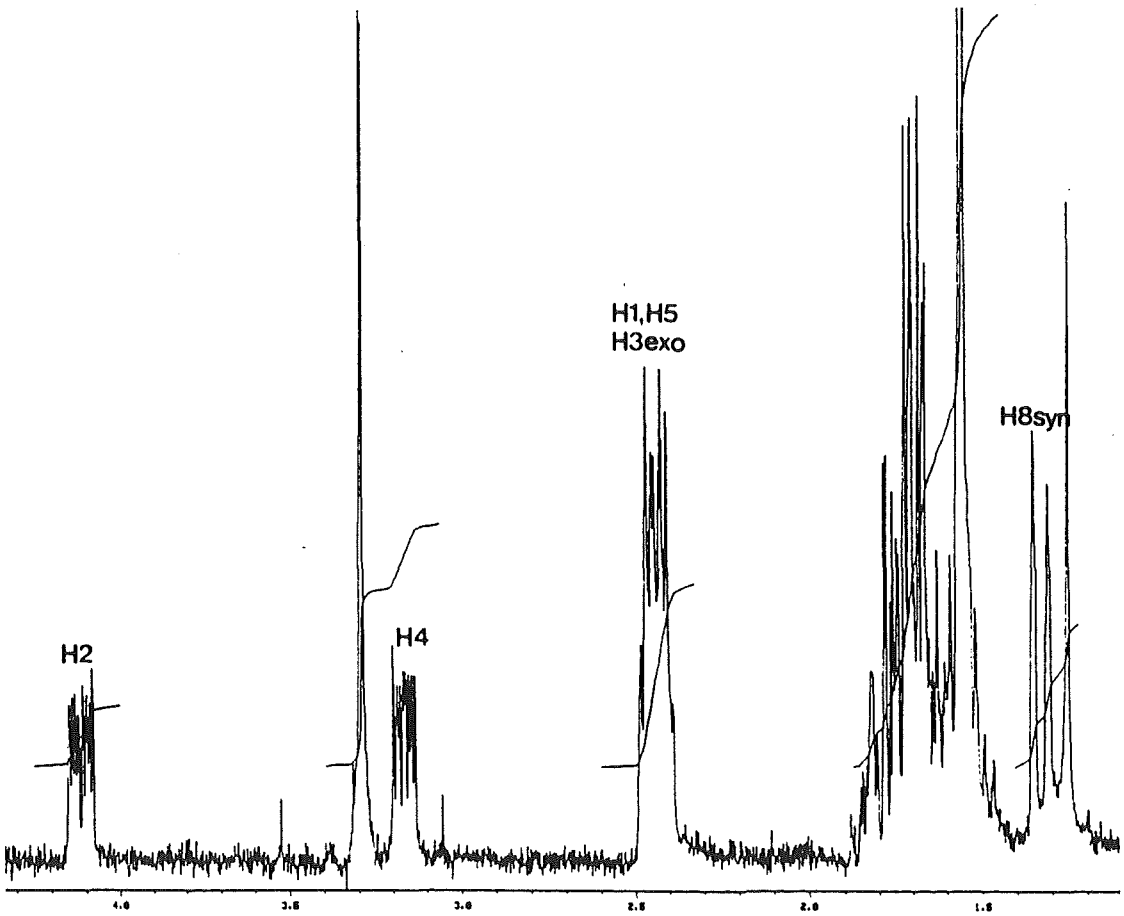

Figure 3.9. ^{1}H NMR spectrum of 2-*endo*-bromo-4-*endo*-methoxybicyclo[3.2.1]octane **76b**.

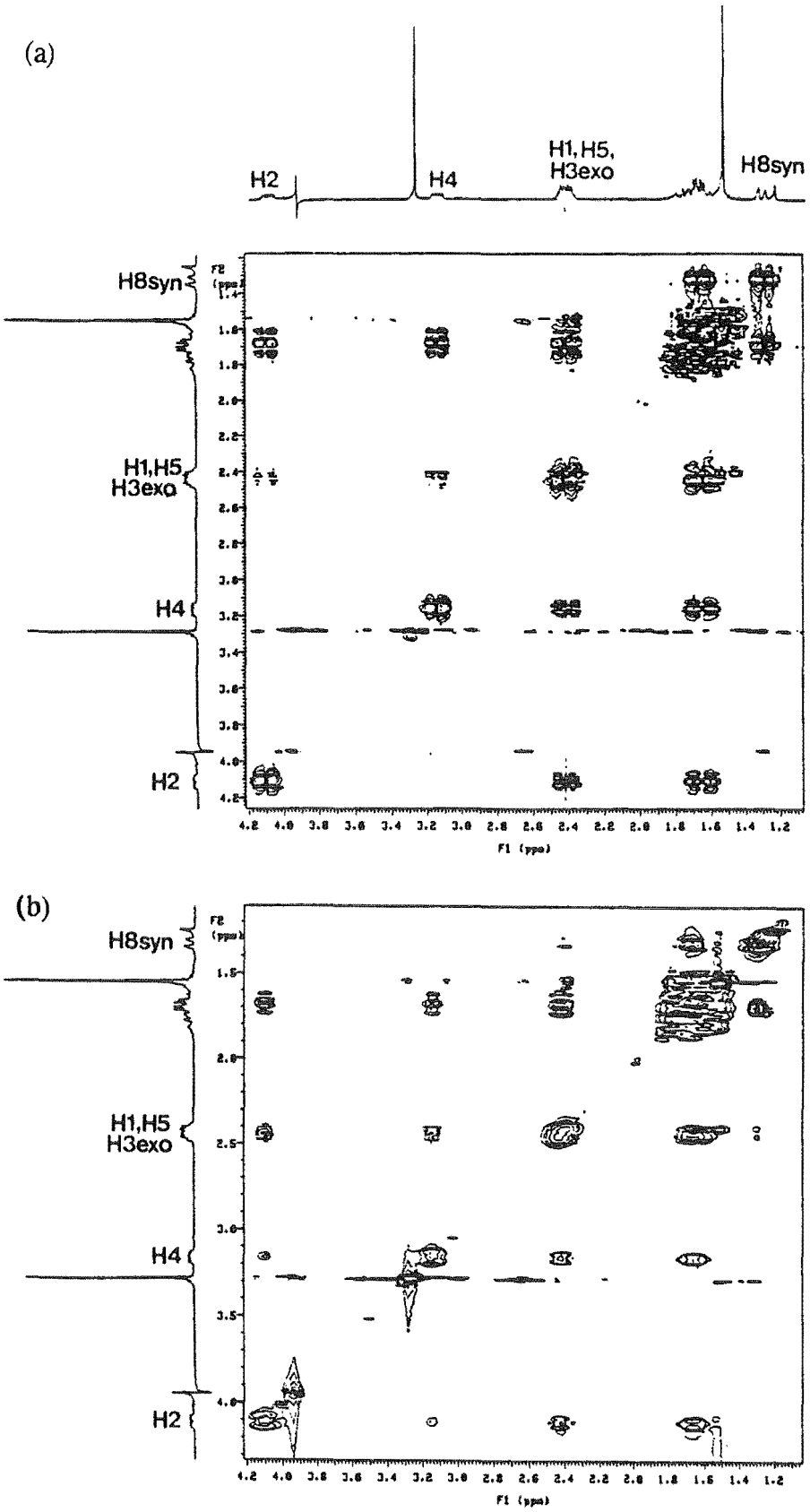

Figure 3.10 (a) DQCOSY of **76b** and (b) 2D-TOCSY of **76b**.

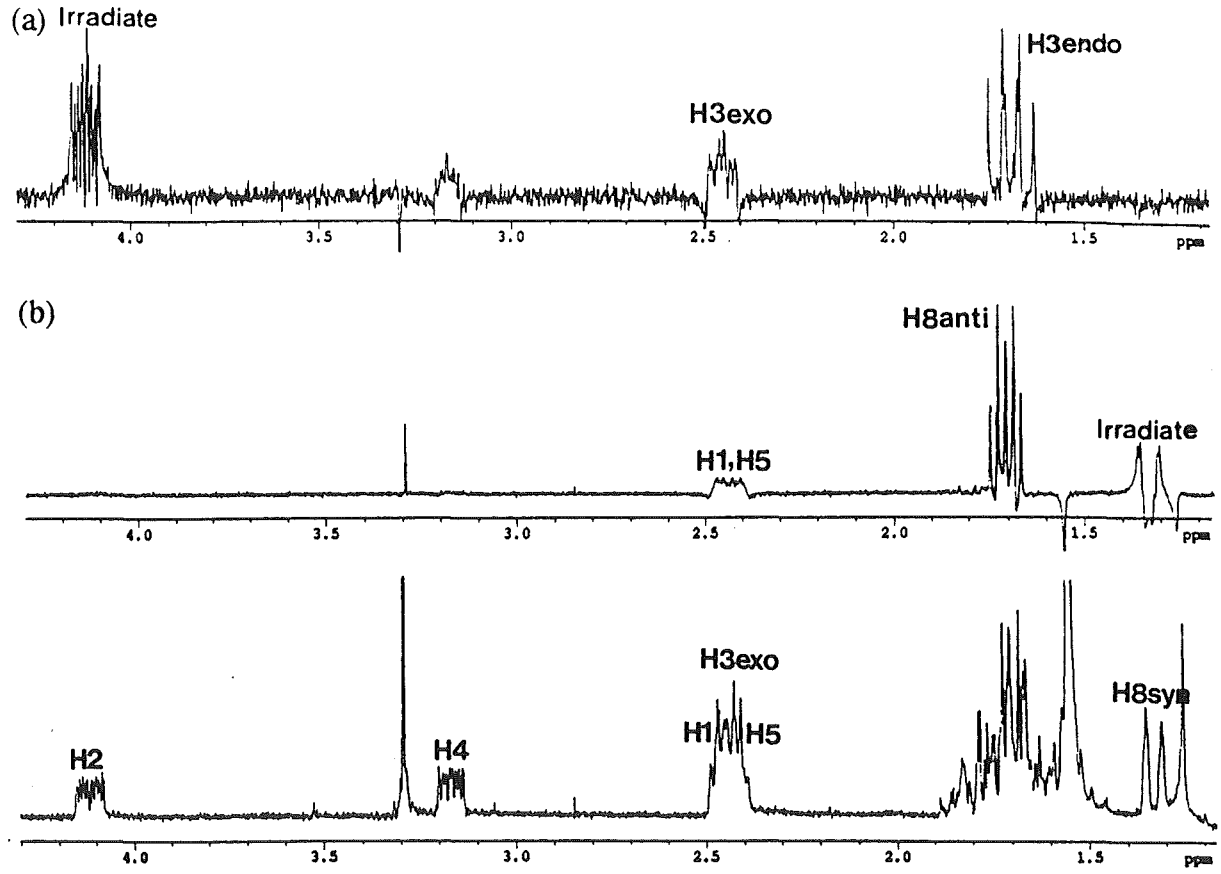

Figure 3.11. 1D-TOCSY of **76b** (a) Irradiation of H2 and (b) Irradiation of H8*syn*.

After establishing the one bond ^{1}H-^{13}C connectivities of **76b**, an HMBC experiment was used to obtain information about the long range ^{1}H-^{13}C correlations (two and three bond ^{1}H-^{13}C couplings). The doublet at 1.33 ppm, which was shown (HMQC) to be part of a methylene group, showed correlations to four carbons. Two of these carbons were methylene carbons and the other two were the CHBr and CHOMe carbons which had previously been determined to have a 1,3 relationship. This established the general bicyclo[3.2.1]octane carbon skeleton‡ and thus all that remained to be assigned was the stereochemistry of C2 and C4. The DQCOSY and the correlations to the doublet at 1.33 ppm in the HMBC established this proton to be one of the C8 methylene group protons. A 1D-TOCSY (Figure 3.11b) on this proton showed a correlation to the second proton of the C8 methylene group (d of t centred at 1.71 ppm). From this experiment the coupling constants of the proton centred at 1.71 ppm (H8*anti*) to H1 and H5 could be extracted ($^{3}J_{8anti,1}$ = $^{3}J_{8anti,5}$ = 5.9 Hz). This therefore established the proton at 1.71 ppm as H8*anti*[32] and the doublet at 1.33 ppm as H8*syn*. A

‡ No other carbon skeleton with the given number of methine and methylene carbons could account for the observed two and three bond correlations to the proton at 1.33 ppm in the HMBC experiment.

difference nOe experiment showed a 3.2% enhancement of H2 and a 1.7% enhancement of H4 on irradiation of H8*syn* (2.2% and 1.9%, respectively, in the reverse irradiations). This therefore establishes the orientation of both H2 and H4 as *exo* and hence the orientation of the bromine attached to C2 and the methoxy attached to C4 (identified from their chemical shifts of 53.8 ppm and 80.5 ppm, respectively, and from the HMQC experiment) as being *endo*.

The identity of 6-*endo*-bromo-2-*endo*-methoxybicyclo[3.2.1]octane **77b** was determined as follows: an HMQC experiment established the one bond ^{1}H-^{13}C connectivity and a DQCOSY established the proton-proton connectivity. An HMBC experiment confirmed the general bicyclo[3.2.1]octane carbon skeleton. The chemical shift of C2 at 80.8 ppm established this carbon as being attached to a methoxy group† and this was reflected in the chemical shift of H2 at 3.24 ppm. The proton signal of the CHBr group was evident at 4.36 ppm and the corresponding carbon signal C6 at 52.5 ppm. The *exo* orientation of H2 was determined from the presence of a 1.2% enhancement of H8*syn* (1.44 ppm) on irradiation of H2 in a difference nOe experiment (1.6% enhancement was observed for the reverse irradiation) and the assignment was supported by a 10.3 Hz coupling constant to H3*endo* (1.51 ppm) and a 3.4 Hz coupling to both H3*exo* and H1. This therefore establishes an *endo* orientation of the methoxy group attached to C2. Irradiation of H8*anti* (1.70 ppm, established from an HMQC experiment as geminal to the multiplet at 1.44 ppm previously assigned to H8*syn*) gave a 1.6% enhancement of H6 in a difference nOe experiment and hence determined this proton to have an *exo* orientation. This was confirmed by consideration of the coupling constants of H6 to H7*exo* ($^{3}J_{6,7exo}$ = 10.7 Hz) and H7*endo* ($^{3}J_{6,7endo}$ = 5.7 Hz).‡

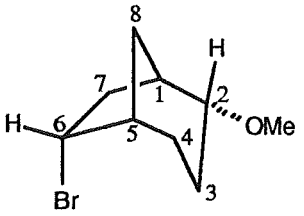

Analysis of the products obtained from bromination of **1** suggests that when bromine addition occurred to the cyclopropane, corner attack of the electrophile was observed in both CCl_4 and methanol solvents, resulting in inversion of configuration of the carbon attacked. Nucleophilic addition occurred exclusively with inversion of

---

† The methoxy CH_3 signal was clearly evident as a singlet ($W_{h/2}$ = 0.6 Hz) at 3.30 ppm in the ^{1}H NMR spectrum and showed a ^{13}C resonance at 55.4 ppm.

‡ The assignment of the multiplet centred at 1.99 ppm as H7*endo* follows from the DQCOSY and HMQC experiments. The orientation of the multiplet at 1.99 ppm was confirmed by the presence of a 2.5 Hz coupling to H8*syn* which is consistent with a 'W' arrangement of these protons and hence an *endo* orientation of this proton. H7*exo* was identified as being connected to the same carbon as H7*endo* from the HMQC experiment and also showed a stronger coupling to H1 than did H7*endo* in the DQCOSY which is consistent with an *exo* orientation.

configuration. When the reaction was performed in CCl_4 the rearrangement product **77a** was formed in approximately a 1:2 ratio with the product resulting from nucleophilic capture of the carbocation before rearrangement. In this case the lack of products resulting from nucleophilic capture of the cation with retention of configuration would suggest that nucleophilic attack does not occur to an open cation. The predominance of products resulting from nucleophilic capture before rearrangement would therefore suggest that either a corner brominated intermediate is formed (similar to that suggested by Coxon et al.[13,14,18] for the protonation and mercuration of **1**) or that due to the unsymmetrical nature of the cation formed, a higher amount of positive charge develops at C4 than at C5 in either a nonclassical cation **81** or rapidly equilibrating classical cations **82** and **83** (Figure 3.12). The unsymmetrical charge distribution may be due to the inductive effect of the bromine at C2 which would be expected to increase charge development at C4. For the reaction in methanol a larger proportion of rearrangement product **77b** was observed (1.0:1.2‡) and hence may reflect the stabilisation of the rearrangement process, and lowering of the activation barrier, by the presence of a more polar solvent. This was also observed in the bromination of **46**.

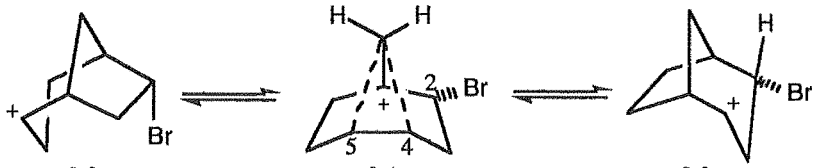

83 **81** **82**

Figure 3.12. Interconversion of classical cations **82** and **83** occurs rapidly or via a nonclassical cation intermediate **81**.

It is interesting to note that *exo*-**46** and *endo*-**1** hydrocarbons lead to different rearrangements on ring opening. The *exo* hydrocarbon **46** leads to a Wagner-Meerwein rearrangement and hence to the formation of a bicyclo[2.2.2]octane structure, but the *endo* hydrocarbon **1** leads to a 1,2 methylene migration which retains the bicyclo-[3.2.1]octane structure. For simplicity, if the extreme situations are considered where open carbocations are formed (although the same would be expected for partially formed cations or brominated cyclopropane intermediates), molecular mechanics§ calculations suggest a distinct difference in geometry between the cations resulting from cyclopropane ring opening of **1** and **46**. The carbocation formed on cyclopropane ring opening of **46**

---

‡ This ratio includes the products resulting from methanol capture only and does not include the small amount of **76a** isolated in this reaction, as a similar amount of **77a** may also have been present but not isolated.

§ Using PCMODEL with an MMX forcefield.

shows an *exo* orientation of the three membered bridge (Figure 3.13a) which allows a greater interaction of the vacant C4 *p* orbital of cation **73** with the C5-C6 bond and less favorable interaction with the C5-C8 bond, hence a Wagner-Meerwein rearrangement to give a bicyclo[2.2.2]octane system is observed. In the case of **1**, the carbocation resulting from cyclopropane ring opening **82** (Figure 3.13b) was shown by the molecular mechanics calculations to have an *endo* orientation of three membered bridge. This would allow better alignment of the vacant *p* orbital of C4 with the C5-C8 bond rather than the C5-C6 bond and hence more facile rearrangement via migration of the C5-C8 bond would be expected, resulting in the retention of a bicyclo[3.2.1]octane geometry. The observed rearrangements are also consistent with minimisation of steric interactions, as migration of C8 in *exo* cation **73** would result in significant interaction of the C8 methylene carbon with C3, and migration of C6 in a Wagner-Meerwein rearrangement of the *endo* structure **82** would also result in significant steric interaction with C3.

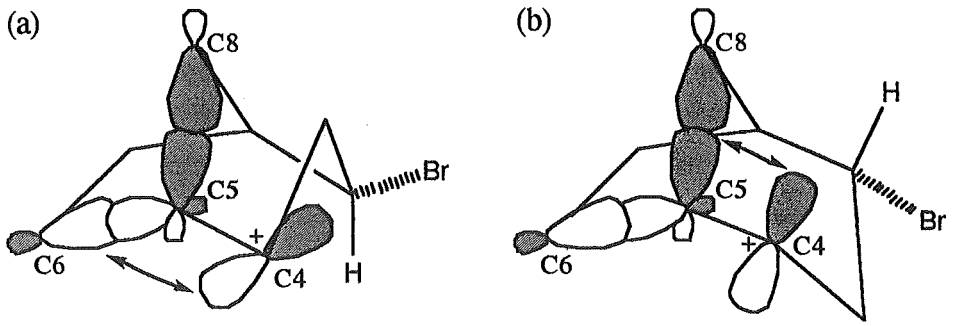

73 **82**

Figure 3.13. Cations resulting from ring opening of (a) *exo*-tricyclo[3.2.1.$0^{2,4}$]octane **46** and (b) *endo*-tricyclo[3.2.1.$0^{2,4}$]octane **1** on reaction with bromine. The double headed arrows indicate the most favourable orbital interactions.

Section 3.4 COMPARISON OF THE NMR SPECTRA OF SUBSTITUTED BICYCLO[3.2.1]OCTANE STRUCTURES

The substituted bicyclo[3.2.1]octane compounds obtained from the bromination reactions described earlier in this chapter provide an opportunity to examine the effects of the substituent groups on the ^{13}C and ^{1}H NMR spectra of these compounds and, as suggested by Kato,[124] provide an opportunity to investigate the effects of 1,3-diaxial interactions on the relative energies of the chair and boat conformations of the three membered bridge. For example, **71a** would be expected to experience significant 1,3-diaxial interaction between the bromine substituents of C2 and C4 in the chair conformation. The 1,3-diaxial interaction would be minimised in the boat conformation, but this conformation of the ring system is generally higher in energy than the chair conformation (Figure 3.14).

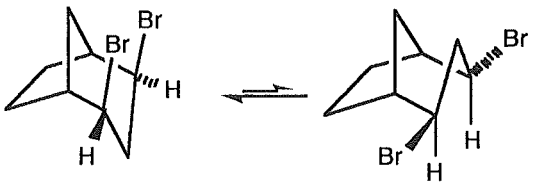

71a
CHAIR

71a
BOAT

Figure 3.14. Chair and boat conformations of **71a**.

Conformational searches of compounds **70a, 71a, 71b, 75a, 76a,** and **76b** were performed using the BKM† program and the MM2 force field. In all cases the *endo* conformation was found to be preferred.‡ For **70a, 71a, 75a,** and **76a** only one conformation within a 12.5 kJ mol^{-1} energy window was found and would therefore be expected to be populated to greater than 99% from a Boltzman distribution. Thus for **71a** and **71b** the stability gained from the chair conformation of the ring formed by the one and three membered bridges dominates the repulsive 1,3-diaxial interaction of the two bromines or bromine and methoxy group. This was confirmed by the X-ray crystal structure of **71a** (Figure 3.6) which showed an *endo* orientation of the three membered bridge. The steric interaction of the axial bromine substituents of **71a** was evident from the interatomic distance of 3.798 Å determined from the X-ray crystal structure (MMX calculated Br-Br distance = 3.756 Å).

Table 3.1 summarises the ^{13}C NMR data obtained for compounds **70a, 71a, 71b, 75a, 76a, 76b** and the parent compound bicyclo[3.2.1]octane **84**. The Δδ values of each carbon from the corresponding carbon of **84** are also shown. From Table 3.1 it can be seen that introduction of each axial bromine substituent at C2 or C4 results in an upfield shift of C8 by approximately 5 ppm due to an γ-eclipsed interaction.§ An equatorial bromine at C2 or C4 has little effect on the shift of C8 but shows a similar (ca. 5 ppm) upfield shift of either C6 or C7 due to an γ-eclipsed interaction. As was observed for the effect of an equatorial bromine on the shift of C8, the γ *anti* interaction of axial bromine substituents on carbons C6 and/or C7 are small (ca. -0.3 ppm). The upfield shift of C8 (6.6 ppm) in **75a** is substantially larger than the effect observed for **70a** and **71a**. This is presumably due to the presence of the bromine substituent at C3, which may affect the conformation of the molecule and increase the interaction of the C2 bromine and

---

† BAKMDL (BKM) Version KS 2.99 (1992).

‡ This is in agreement with the results of Kato[124] who also found the *endo* conformation of **71a** and **76a** to be lower in energy.

§ Also see references 125 and 126 for a discussion of shielding effects in bicyclo[3.2.1]octane and bicyclo[2.2.1]heptane systems.

C8 (H8) causing the observed upfield shift. The distances calculated from the molecular mechanics conformational searches show the axial bromine of C2 (Br(C2)) in **75a** is 0.02 to 0.03 Å closer to C8 and H8*syn* than in **71a** (Distances: **71a** : Br(C2)-H8syn = 2.95 Å, Br(C2)-C8 = 3.39 Å. **75a** : Br(C2)-H8syn = 2.92 Å, Br(C2)-C8 = 3.37 Å).

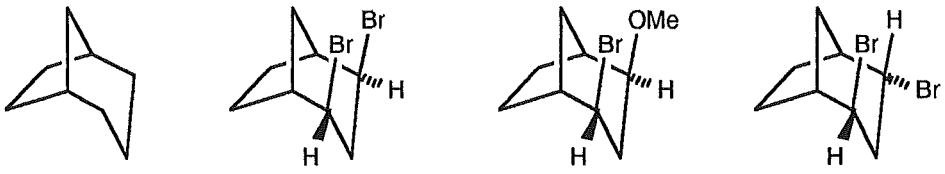

84 **71a** **71b** **70a**

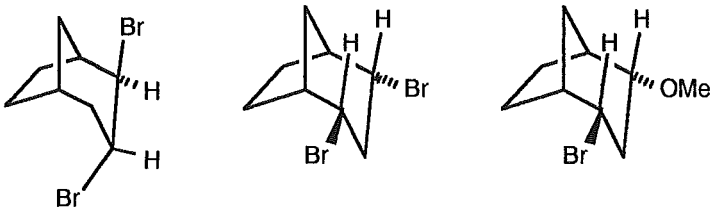

75a **76a** **76b**

Cmpd	C1	C2	C3	C4	C5	C6	C7	C8	OMe
84	35.2	32.8	19.1	32.8	35.2	28.9	28.9	39.7	
71a§	43.4	52.0	35.2	52.0	43.4	28.6	28.6	29.4	
	(8.2)	(19.2)	(16.1)	(19.2)	(8.2)	(-0.3)	(-0.3)	(-10.3)	
71b	43.3	53.7	30.6	79.7	38.0	25.9	28.1	27.9	56.0
	(8.1)	(20.9)	(11.5)	(46.9)	(2.8)	(-3.0)	(-0.8)	(-11.8)	
70a	42.1	53.0	39.7	55.9	44.1	23.8	28.8	35.2	
	(6.9)	(20.2)	(20.6)	(23.1)	(8.9)	(-5.1)	(-0.1)	(-4.5)	
75a	43.6	60.1	48.8	36.7	33.9	27.4	29.1	33.1	
	(8.4)	(27.3)	(29.7)	(3.9)	(-1.3)	(-1.5)	(0.2)	(-6.6)	
76a	42.7	53.2	41.3	53.2	42.7	24.4	24.4	38.7	
	(7.5)	(20.4)	(22.2)	(20.4)	(7.5)	(-4.5)	(-4.5)	(-1.0)	
76b	43.4	53.8	37.0	80.5	37.1	22.8	24.7	35.6	55.8
	(8.2)	(21.0)	(17.9)	(47.7)	(1.9)	(-6.1)	(-4.2)	(-4.1)	

Table 3.1. ^{13}C NMR chemicals shifts and $\Delta\delta$ values ($CDCl_3$) from the equivalent carbons in **84** in ppm for the compounds shown.

§ The ^{13}C chemical shifts shown in this table for **71a** were observed using $CDCl_3$ as the NMR solvent and not benzene-d_6 in which the values reported in the experimental section were measured.

Of particular note is the chemical shift of C7 in **75a**; here the chemical shift of this carbon is almost identical (+0.2 ppm) to that of the parent compound **84** and hence supports the *exo* assignment of the C2 bromine substituent, as an *endo* orientation of the bromine would be expected to result in an upfield shift of C7 similar to that observed for C6 of **70a**.

In agreement with the shielding/deshielding effects found in bicyclo[2.2.1]heptane systems[106] substituent effects of the methoxy group are larger for γ-eclipsed interactions than those of the corresponding bromine derivatives. This is evident from the shift of C8 in **71a** (-10.3 ppm) and **71b** (-11.8 ppm), and similarly leads to an increased shielding effect via γ *anti* interactions, for example the Δδ of C6 in **71a** and **71b** are -0.3 ppm and -3.0 ppm, respectively (Table 3.1).

The bicyclo[3.2.1]octane series also results in larger shielding effects due to the axial substituents at C2 and C4 than those of substituents at C2 and C3 in the bicyclo[2.2.1]heptane series. Thus an axial bromine substituent at C2 of norbornane results in an upfield shift of approximately 2.8 ppm[106] of C7 compared with that of approximately 5 ppm for C8 in the bicyclo[3.2.1]octane series. This is presumably due to the closer proximity of the axial substituents to the one carbon bridge as shown by the molecular mechanics calculations for **71a** and 2-*exo*-3-*exo*-dibromobicyclo[2.2.1]-heptane **85** (Figure 3.15).

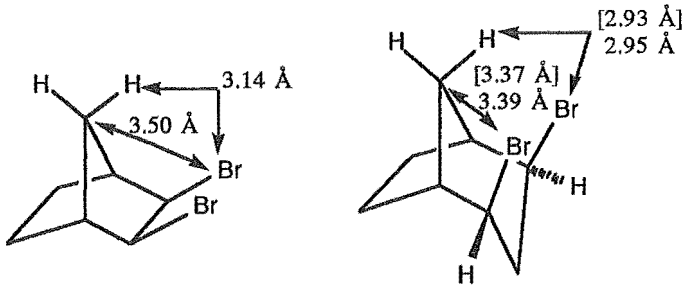

85 **71a**

Figure 3.15. Distances predicted by molecular mechanics calculations for 2-*exo*-3-*exo*-dibromobicyclo-[2.2.1]heptane **85** and 2-*exo*-4-*exo*-dibromobicyclo[3.2.1]octane **71a**. Numbers in square brackets are the values determined from X-ray crystal structure analysis. The X-ray value for the Br-H interatomic distance was determined from adding the hydrogens to the carbon skeleton at fixed C-H bond lengths of 0.96 Å.

Steric compression effects (γ-eclipsed interactions and gauche interactions) lead to shielding of the carbon involved but lead to a deshielding effect of the attached protons which are directly involved in the spatial interactions.[106] The effect is generally believed to result from the interaction of electron density of the γ substituent, whether it be from lone pairs or electron density associated with the substituent bonds, with the hydrogens

attached to the γ carbon which results in a shift of σ bond electron density towards the carbon[106] thus resulting in a shielding effect of the carbon and a deshielding effect of the hydrogen "overlapping" with the substituent. In the case of the bicyclo[3.2.1]octane systems with one or two axial substituents at C2 and/or C4 the effects are dramatic. Table 3.2 shows the chemical shifts of C8 and its attached protons H8*anti* and H8*syn* for compounds **70a**, **71a**, **71b**, and **76b**. For **71a**, with axial bromine substituents at C2 and C4, H8*syn* shows a large downfield shift of approximately 1.3 ppm with respect to the equivalent proton in **76a**.† The effect on H8*anti* however is in the opposite direction; that is, it is significantly shielded and hence the signal appears upfield by 0.4 ppm from the equivalent proton in **76a**. Successively removing an axial bromine substituent (**71a** to **70a** to **76a**) moves H8*syn* upfield by approximately 0.4-0.8 ppm , whereas the H8*anti* proton shifts by approximately 0.2 ppm downfield for each axial bromine removed. The shielding of H8*anti* presumably results from the movement of electron density towards the carbon and hence to the H8*anti*-C8 bond due to the γ-eclipsed interactions. This effect has been observed in a number of other systems.[110,111,127,128]

Structure	C8	H8*syn*	H8*anti*
84	39.7	not reported	not reported
71a	29.4	2.82	ca. 1.42
71b	27.9	2.53	1.22
70a	35.2	2.30	1.58
75a	33.1	2.06	1.44
76a	38.7	1.55	1.83
76b	35.6	1.33	1.71

Table 3.2. Chemical shifts ($CDCl_3$) of C8 and its attached protons for the compounds shown.

As a further test of the structure assignments the coupling constants extracted from the ^1H NMR spectra were compared with those predicted from molecular mechanics calculations.‡ Table 3.3 shows the results obtained from analysis of the ^1H NMR spectra, the values calculated by Kato et al.[124] (where applicable), and the coupling constants calculated from the BKM conformational searches.

---

† The chemical shifts for H8*anti* and H8*syn* of **84** have not been reported in the literature.

‡ Observed values are compared with the values calculated by Kato[124] and to the values obtained from conformational searches using the BKM program with the MM2 forcefield. The results of Kato[124] shown are for the chair conformer only, as *J* values calculated for the boat conformation of the structures showed large errors and conformational searches showed a large preference for the chair conformation (>99%).

	$^3J_{a,b}$ Coupling Constant (Hz) (*n=endo, x=exo, s=syn, a=anti*)								
Cmpd	1,8*s*	1,8*a*	1,2	2,3*x*	2,3*n*	4,3*x*	4,3*n*	4,5	5,8*a*
71a Calc	1.7	4.6	3.2	2.0 (0)	5.5 (5.8)	2.0 (0)	5.5 (5.8)	3.2	4.6
Obs	small	5.6		NO	5.5	NO	5.5		5.6
70a Calc	1.8	4.4	3.4 (3.4)	2.0 (2.0)	5.1 (5.1)	5.1 (5.1)	11.2 (11.2)	2.6 (2.6)	4.4
Obs	small	5.0				5.8	11.1		5.0
76a Calc	1.6	4.5	2.7 (2.7)	5.3 (5.3)	11.1 (11.1)	5.3 (5.3)	11.1 (11.1)	2.7 (2.7)	4.5
Obs		5.3	2.8	5.3	11.7	5.3	11.7	2.8	5.3

Table 3.3. Comparison of observed and calculated coupling constants for the compounds shown. Coupling constants in brackets were taken from reference 124. (NO = Not observed)

In general the calculated and experimental values are in good agreement ($|error| \leq 1.0$ Hz) and therefore provide supporting evidence for the assignment of structures of this type and hence provide a useful tool for structure elucidation where other methods, such as nOe data, are inconclusive.

CHAPTER 4

Bromination of 2-Methyl-*endo*-tricyclo[3.2.1.0^{2,4}]oct-6-ene and 2-Methyl-*endo*-tricyclo[3.2.1.0^{2,4}]octane

Section 4.1 INTRODUCTION

The reactions of 2-methyl-*endo*-tricyclo[3.2.1.0^{2,4}]octane **45** and 2-methyl-*endo*-tricyclo[3.2.1.0^{2,4}]oct-6-ene **86** with acid and mercuric acetate have been reported[13,16] (see Figures 4.1 and 4.2). For both **45** and **86** electrophilic attack was found to occur exclusively with inversion of configuration (corner attack) at the internal (C2-C4) cyclopropyl bond.[13,16]

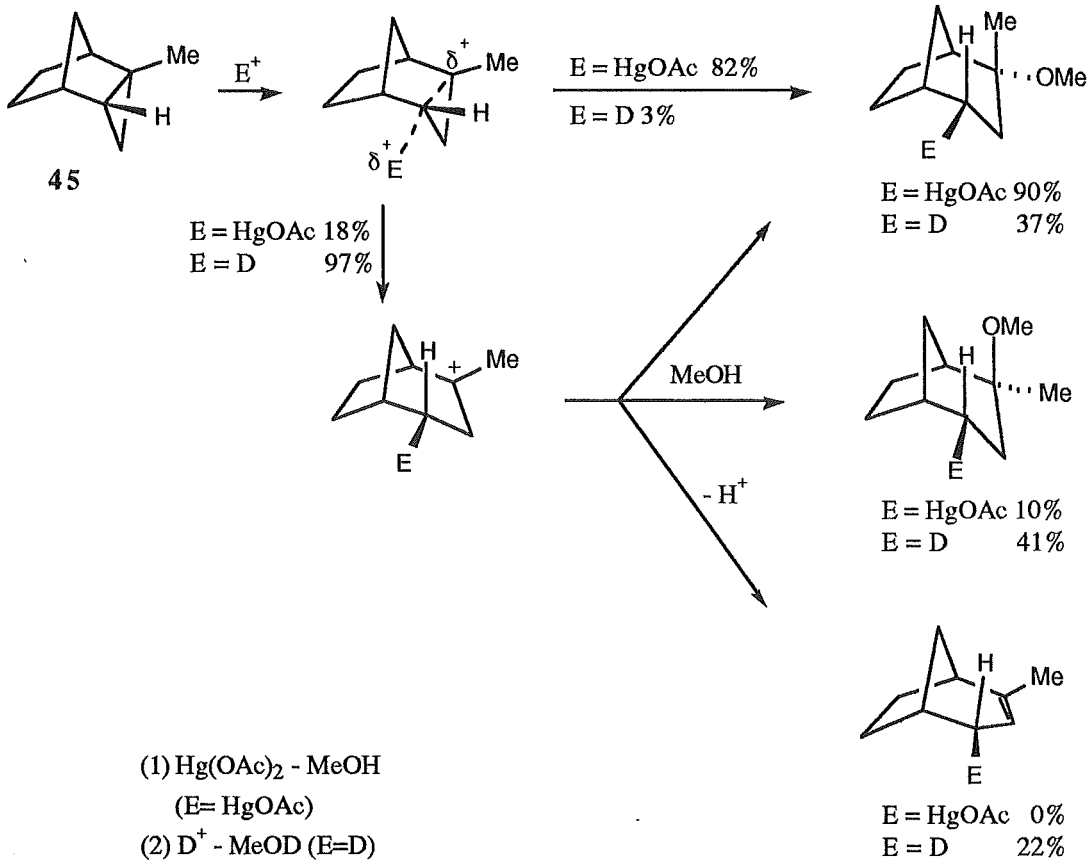

Figure 4.1. Reaction of 2-methyl-*endo*-tricyclo[3.2.1.0^{2,4}]octane **45** with D$^+$-MeOD and mercuric acetate.[13,16]

For compound **86** both acid and mercuric acetate showed a regiochemical preference for attack at the cyclopropane ring instead of at the double bond. The observation of exclusive protonation at the cyclopropane ring reflects the kinetic favourability of this process[13] which is enhanced by the presence of the methyl group at

C2. Mercuration similarly occurs at the cyclopropyl ring as a consequence of the greater charge stabilisation possible with the C2 methyl.[13]

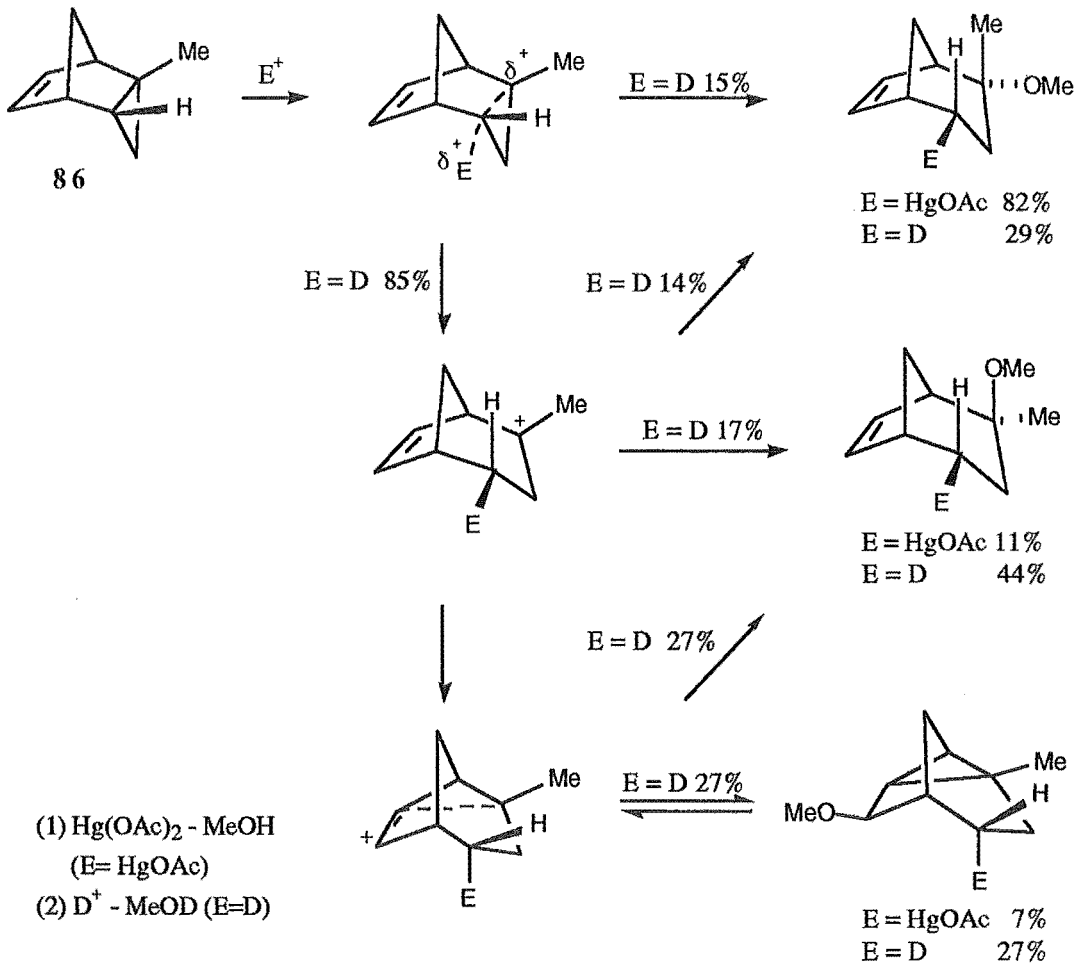

Figure 4.2. Reaction of 2-methyl-*endo*-tricyclo[3.2.1.$0^{2,4}$]oct-6-ene **86** with D^+-MeOD and mercuric acetate.[13,16]

To extend the scope of these studies, the bromination reactions of **45** and **86** were investigated. The presence of the methyl substituent of C2 would also be expected to enhance the reactivity of the cyclopropyl group[24] of both **45** and **86** towards bromine. For compounds containing a carbon-carbon double bond and a cyclopropane ring, reaction with bromine generally takes place at the double bond, as was observed[32] in the bromination of **68** and **69**, but due to the activating methyl substituent in **86** the cyclopropyl group may compete more effectively with the double bond. However, it is unlikely that the activating ability of the methyl group would be large enough to show a major effect on the regioselectivity of bromination. The activating effect of the methyl group is presumably due to its ability to donate electron density to the HOMO-1 orbital of **86** or the HOMO orbital of **45**, which are predominantly formed by contributions from

C2 and C4, which raises the energy of the orbital and therefore makes it more susceptible to electrophilic attack.

Section 4.2 BROMINATION OF 2-METHYL-*endo*-TRICYCLO[3.2.1.$0^{2,4}$]-OCT-6-ENE

The reaction of 2-methyl-*endo*-tricyclo[3.2.1.$0^{2,4}$]oct-6-ene **86** with bromine (0.9 mole equivalents) in CCl_4 proceeded essentially instantaneously at room temperature. A ^{1}H NMR spectrum of the crude reaction mixture showed the presence of one major product (ca. 80%)† and a number of minor products (1-5% each). GLC analysis showed the presence of five products in 10-20% yields and hence the major product (as shown by ^{1}H NMR) proved to be unstable to the GLC conditions used. The major product was isolated by rapid radial chromatography (2 mm silica plate, 10% ether/pentane elution) and was identified as 7-*exo*-8-*anti*-dibromo-2-methylbicyclo[3.2.1]oct-2-ene **87**.

The identity of **87** was determined as follows: a HETCOR established the ^{1}H-^{13}C one bond connectivities and a COSY experiment determined the proton-proton connectivity. The chemical shift of H7 at 4.27 ppm established this proton as part of a CHBr group and the absence of a measurable coupling to H1 established the *endo* orientation of this proton and hence an *exo* orientation of the bromine substituent of C7. The *endo* orientation of H7 was confirmed from consideration of its coupling constants to H6*endo* (2.43 ppm) and H6*exo* (2.88 ppm) ($^3J_{7,6endo}$ = 8.3 Hz, $^3J_{7,6exo}$ = 3.8 Hz, $^3J_{6endo,7}$ = 8.3 Hz).‡ The *anti* stereochemistry of the bromine at C8 (55.9 ppm) was established by the lack of coupling of H8 (4.42 ppm) to H5 or H1 which is characteristic of a proton attached to C8 in a *syn* orientation with respect to the largest bridge in bicyclo[3.2.1]octane systems.[32]

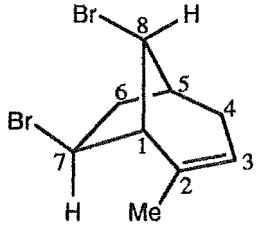

A possible mechanism for the formation of **87** (outlined in Figure 4.3) is from the initial formation of 7-*exo*-8-*anti*-dibromo-2-methyl-*exo*-tricyclo[3.2.1.$0^{2,4}$]octane **88** which underwent further reaction with acid (HBr) followed by elimination to give the cyclopropane ring opened product **87**. Attack of the bromine nucleophile on cation **89** from an *exo* trajectory is consistent with that observed for norbornane systems.[42,129-131] It is important to note that no definite conclusions about the mechanism for formation of

---

† The yield of this product was not always reproducible and ranged from approximately 50-80%.

‡ The *exo* orientation of the C6 proton centred at 2.88 ppm was assigned due to the presence of a correlation to H5 in the COSY. No correlation from H5 to the multiplet centred at 2.43 ppm was observed in the COSY, hence this proton was assigned to H6*endo*. The HETCOR experiment had previously established the geminal relationship of these protons.

87 can be made, as electrophilic and nucleophilic addition cannot be differentiated since both species are identical (i.e. bromines).

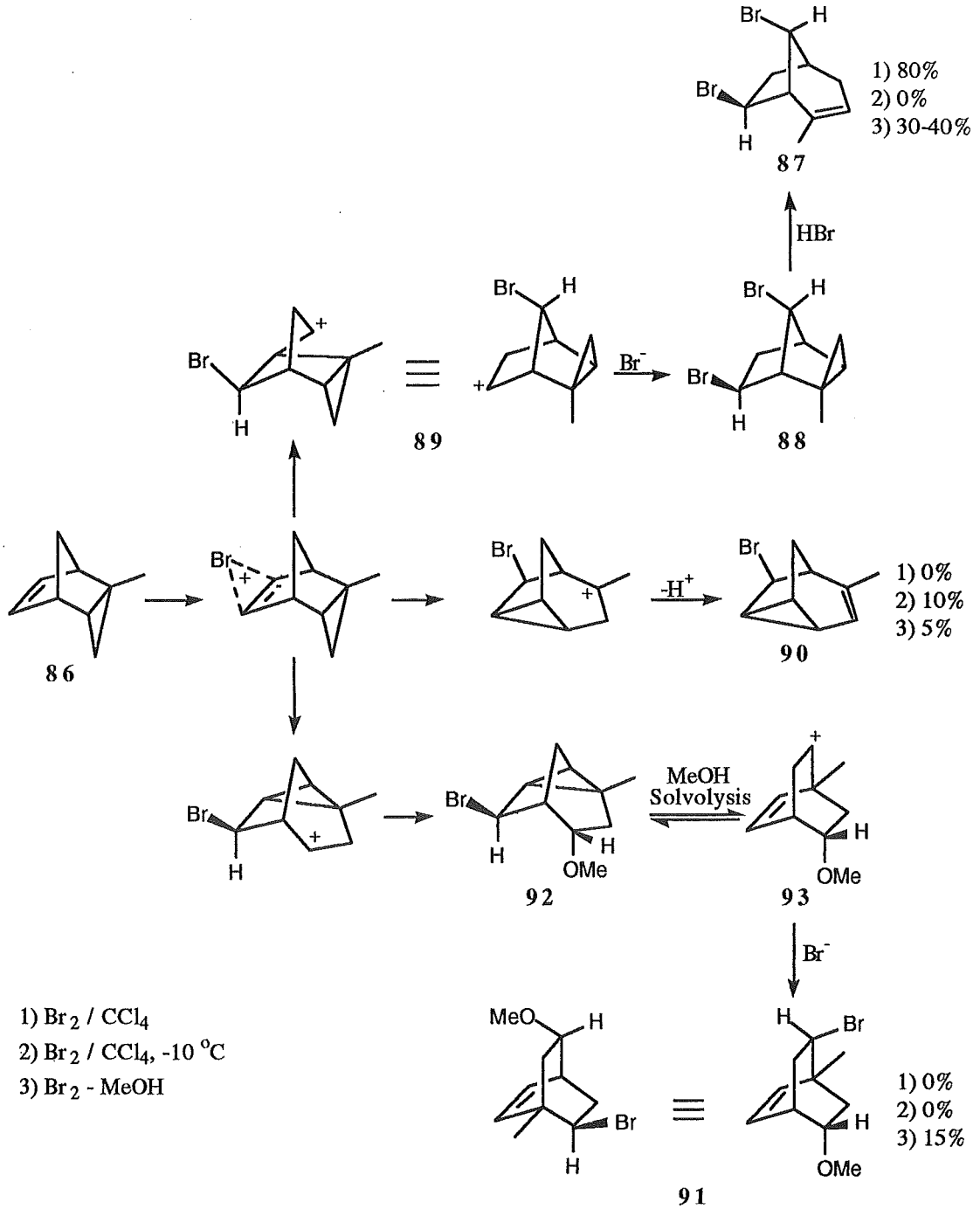

Figure 4.3. Possible mechanism for the bromination of 2-methyl-*endo*-tricyclo[3.2.1.$0^{2,4}$]oct-6-ene **86** in MeOH and CCl_4.

Attempts to isolate **88** by performing the reaction at -10 °C resulted in the formation of **87** in reduced yields (30-40%) along with 6-*exo*-bromo-4-methyl-

tricyclo[3.2.1.$0^{2,7}$]oct-3-ene **90** (ca. 5%)† and a number of other products. Column chromatography (silica gel, ether/pentane gradient elution) gave little separation and the products were not further investigated. Due to the freezing point of CCl_4 (-23 °C) the reaction temperature could not be significantly further lowered and hence no further attempts to isolate **88** were made.

The identity of 6-*exo*-bromo-4-methyltricyclo[3.2.1.$0^{2,7}$]oct-3-ene **90** was determined from the following: a COSY experiment in conjunction with difference nOe experiments established the ^{1}H-^{1}H connectivity and a HETCOR allowed determination of the one bond ^{1}H-^{13}C connectivities. The presence of a cyclopropane ring was established by the chemical shift of C1 and C2 at 15.4 ppm and 18.5 ppm, respectively.§ The proton of the CHBr group (H6) appeared as a singlet at 3.69 ppm ($W_{h/2}$ = 2.5 Hz) with no apparent coupling to H5 (2.53 ppm) or H7 (1.68 ppm) which is consistent with an *endo* orientation of this hydrogen. The chemical shift of 3.69 ppm is significantly upfield from that usually observed for protons of CHBr groups‡ and is consistent with the close proximately of this proton to a cyclopropane ring and with its relationship to the double bond. The chemical shift is also similar to that reported for H6 (3.64 ppm) of 6-*exo*-bromotricyclo[3.2.1.$0^{2,7}$]oct-3-ene.[32,132] The connectivity of H6 to H5 and H7 was confirmed by the presence of a small enhancement of these protons on irradiation of H6 in a difference nOe experiment. Further support for the *exo* orientation of the bromine at C6 came from the downfield shift of H8*anti* (2.22 ppm) which is consistent with deshielding due to steric compression effects of the bromine in this orientation and from comparison of the chemical shift of C8 in **90** (25.5 ppm) with C8 in 6-*exo*-bromotricyclo[3.2.1.$0^{2,7}$]oct-3-ene (25.4 ppm).[32]

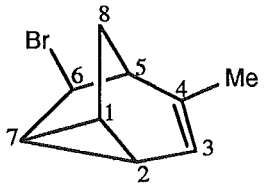

In order to distinguish electrophilic from nucleophilic attack, bromination of **86** was repeated using methanol as the reaction solvent. Reaction of **86** with bromine (0.9 mole equivalents) in methanol gave a complex reaction mixture consisting of numerous products. Attempted separation by radial chromatography (2 mm silica plate, ether/pentane gradient elution) followed by further purification by dry column flash chromatography gave two products, 7-*anti*-bromo-5-*endo*-methoxy-1-methylbicyclo-

---

† Compound **90** was not isolated from this reaction but was identified from a ^{1}H NMR spectrum of the crude reaction mixture, as it was isolated from the reaction of **86** with bromine in methanol (see later this section).

§ The third carbon of cyclopropane ring, C7 (22.5 ppm), was shifted downfield due the presence of an α CHBr group.

‡ The HETCOR confirmed this proton as part of a CHBr group by the presence of a correlation to C6 at 56.5 ppm. The downfield chemical shift of C6 identified this carbon a having a bromine substituent.

[2.2.2]oct-2-ene **91** (ca. 15%) and 6-*exo*-bromo-4-methyltricyclo[3.2.1.$0^{2,7}$]oct-3-ene **90** (ca. 10%);‡ no other products were isolated in high purity.

The identity of 6-*exo*-bromo-4-methyltricyclo[3.2.1.$0^{2,7}$]oct-3-ene **90** was determined as outlined earlier. For 7-*anti*-bromo-5-*endo*-methoxy-1-methylbicyclo-[2.2.2]oct-2-ene **91** the structure was identified from the following: a COSY established the ^{1}H-^{1}H connectivity and a HETCOR determined the one bond ^{1}H-^{13}C assignments. Irradiation of H5 (3.69 ppm) showed a 2.2% enhancement of the multiplet at 1.81 ppm in a difference nOe experiment (3.4% enhancement of H5 was observed in the reverse irradiation) and hence established the *exo* orientation of H5 and determined the multiplet at 1.81 ppm to be H8*anti*. The chemical shift of H5 (3.69 ppm) and its attached carbon C5 (80.1 ppm) is diagnostic of a CHOMe group, with the methoxy group clearly evident as a singlet in the ^{1}H NMR at 3.29 ppm and its corresponding carbon at 55.8 ppm in the ^{13}C NMR spectrum. The HETCOR experiment established a geminal relationship between the protons at 2.25 ppm and 1.81 ppm and hence in conjunction with the nOe data allowed the assignment of the multiplet at 2.25 ppm as H8*syn*. The chemical shift of C7 at 58.1 ppm and its attached proton H7 at 3.80 ppm (determined from the HETCOR experiment) established the presence of a CHBr group. The stereochemistry of the bromine substituent at C7 was determined from the coupling constants of H7 to H8*syn* ($^3J_{7,8syn}$ = 10.1 Hz, $^3J_{8syn,7}$ = 10.2 Hz) and H8*anti* ($^3J_{7,8anti}$ = 4.3 Hz, $^3J_{8anti,7}$ = 4.3 Hz) which established a *cis* relationship of H7 and H8*syn* and therefore determined the orientation of the bromine substituent at C7 to be *anti* with respect to the carbon-carbon double bond. A possible mechanism for the formation of **91** (shown in Figure 4.3) is by solvolysis of 6-*exo*-bromo-4-*endo*-methoxy-2-methyltricyclo[3.2.1.$0^{2,7}$]octane **92** followed by nucleophilic addition of bromine to cation **93**.

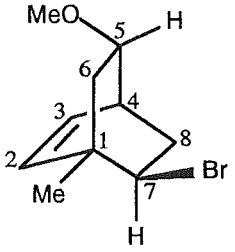

Due to the low percentage of products isolated from the reaction of **86** with bromine in methanol at room temperature and the complexity of the reaction mixture obtained, the reaction was repeated at lower temperatures (-20 °C, -78 °C) in an attempt to stop the rearrangements occurring. However, when the reactions were performed in methanol or methanol-d_4 (to allow direct examination of the reaction mixture by ^{1}H NMR without workup) the ^{1}H NMR spectra of the products obtained still showed the formation of a complex mixture. The reactions were therefore not investigated further.

---

‡ The percentage composition of the products was estimated from a ^{1}H NMR spectrum of the crude reaction mixture due to the overlap of peaks on GLC analysis and also due to the possible instability of the products to the GLC conditions, as was observed for the major product from bromination of **86** in CCl_4.

From the limited amount of products that were isolated from the bromination of **86** is appears likely that bromine addition to the double bond was favoured over addition to the cyclopropane. This is consistent with the observations of Whittington et al.[32] for the bromination of *endo*- and *exo*-tricyclo[3.2.1.$0^{2,4}$]oct-6-ene (**68** and **69**) and therefore the activating effect of the methyl group at C2 of **86** was insufficient to direct attack predominantly to the cyclopropane ring, although, due to the small percentage of products isolated, no definite conclusions can be drawn.

Section 4.3 BROMINATION OF 2-METHYL-*endo*-TRICYCLO[3.2.1.$0^{2,4}$]OCTANE

Reaction of 2-methyl-*endo*-tricyclo[3.2.1.$0^{2,4}$]octane **45** with bromine (0.9 mole equivalents) in CCl_4 in the absence of light gave one major product (ca. 80%)‡ and a number of minor products (all less than 5%). Attempted purification by column chromatography on silica gel (pentane elution) resulted in complete conversion of the initial product to 2-*exo*-6-*endo*-dibromo-1-methylbicyclo[2.2.2]octane **93**. The reaction was repeated and this time purification was effected by radial chromatography on a PEG coated silica plate to give 2-*exo*-3-*endo*-dibromo-2-*endo*-methylbicyclo[3.2.1]octane **94**, which was identified as the initial product formed from the bromination reaction by comparison of its ^{1}H NMR with that of the crude reaction mixture before chromatography (Figure 4.4).

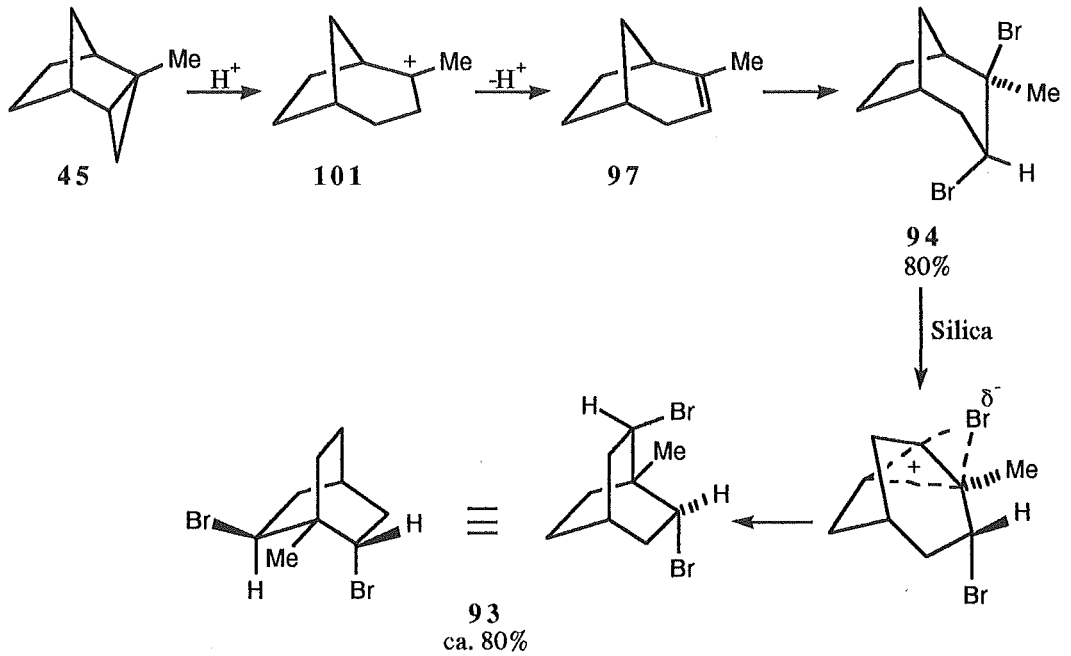

Figure 4.4. Bromination of 2-methyl-*endo*-tricyclo[3.2.1.$0^{2,4}$]octane **45** in CCl_4.

‡ Product ratios were estimated from a ^{1}H NMR spectrum of the crude reaction mixture due to the instability of the major product to GLC analysis.

The identity of 2-*exo*-6-*endo*-dibromo-1-methylbicyclo[2.2.2]octane **93** was determined from the following: the proton-proton connectivity was established as far as possible from DQCOSY and 2D-TOCSY experiments. An HMBC confirmed the general bicyclo[2.2.2]octane skeleton, and the presence of four correlations from the methyl group protons to carbons in a two or three bond relationship established the methyl group to be attached to a bridgehead carbon. The methyl group correlations in the HMBC experiment (Figure 4.5) established the molecular connectivity around the C1 (37.8 ppm) quaternary carbon where connectivity was lost in the DQCOSY experiment due to the lack of a proton at C1. The C1 carbon was shown to be quaternary by the absence of a correlation in an HMQC experiment and the suppression of this signal in a DEPT135 experiment. The ability of an HMBC experiment to correlate equally well to protonated and nonprotonated carbons, due to the experiment being independent of the T_1 relaxation time of the carbons, is advantageous over other long range proton-carbon correlation experiments, such as XCORFE. The latter are carbon detected experiments and hence are dependant on the T_1 relaxation time of the carbon atoms involved. The HMBC is also an intrinsically more sensitive experiment as it is proton detected.

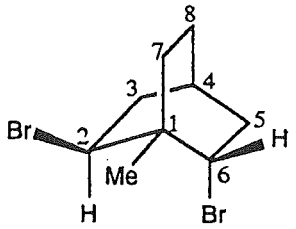

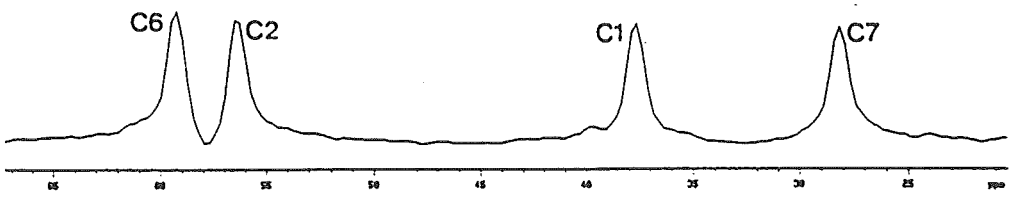

Figure 4.5. Trace through F2 of an HMBC experiment of **93** at 1.08 ppm, which corresponds to the methyl substituent of C1, showing correlations to C1(37.8 ppm), C2 (56.4 ppm), C6 (59.2 ppm), and C7 (28.3 ppm).

The one bond ^1H-^{13}C connectivities of **93** were determined from both decoupled and coupled HMQC experiments (Figures 4.6a and 4.6b, respectively). Coupled HMQC experiments allow the determination of one bond ^1H-^{13}C coupling constants† and may also allow resolution of correlations which overlap in decoupled HMQC experiments

† One bond ^1H-^{13}C coupling constants have been shown to be useful in stereochemical analysis of rigid bicyclic systems,[133] such as norbornene systems, but have not been necessary to use in this work.

(Figure 4.6a) if the one bond couplings are significantly different. In this case however, little improvement in resolution was gained.

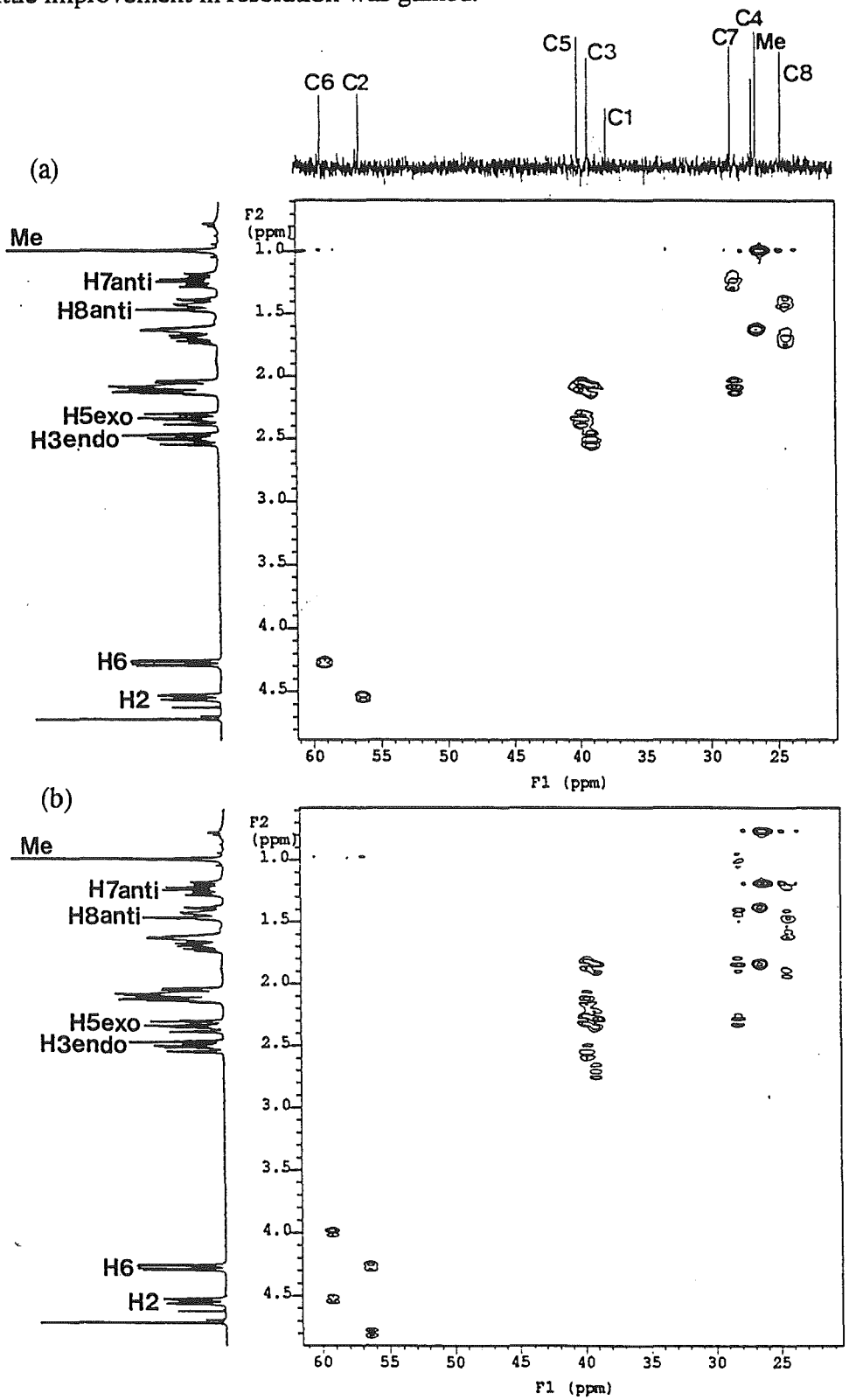

Figure 4.6. (a) Decoupled HMQC of 2-*exo*-6-*endo*-dibromo-1-methylbicyclo[2.2.2]octane **9 3**.
(b) Coupled HMQC of **9 3** showing the ^{1}H-^{13}C one bond coupling constants.

Having determined the general structure of the molecule, the presence of two CHBr groups was established from the chemical shifts of H2 (4.63 ppm) and H6 (4.36 ppm) and from the chemical shifts of the carbons (C2, 56.4 ppm and C6, 59.2 ppm) to which they are attached, as determined from the HMQC experiments. The presence of a 1.5% enhancement of the multiplet at 1.32 ppm on irradiation of H6 in a difference nOe experiment, established the *exo* orientation of H6 and the *anti* configuration of the proton at 1.32 ppm (H7*anti*) to the highest priority bridge.‡ The *exo* configuration of H6 was also supported by consideration of its coupling constants to H5*exo*† (2.43 ppm) and H5*endo* (2.18 ppm) ($^3J_{6,5exo}$ = 9.8 Hz, $^3J_{6,5endo}$ = 3.9 Hz). The stereochemistry of C2 was assigned as having an *exo* bromine substituent due to the lack of symmetry in the molecule (nine carbon signals were observed in the ^{13}C NMR spectrum). An *endo* orientation of the bromine at C2 would result in C_s symmetry of the molecule by the presence of a vertical mirror plane through C1, C7, C8, and C4, and hence only seven signals would be expected in the ^{13}C NMR spectrum. The stereochemical assignment of C2 was also supported by the presence of a 2.5 Hz coupling of H7*anti* to H2 ($^4J_{7anti,2}$ = 2.5 Hz, $^4J_{2,7anti}$ = 2.5 Hz), consistent with a 'W' coupling of these protons and hence an *endo* orientation of H2.

The identity of 2-*exo*-3-*endo*-dibromo-2-*endo*-methylbicyclo[3.2.1]octane **94** was established from the following: an HMQC experiment allowed assignment of the ^1H-^{13}C one bond connectivities and a DQCOSY experiment determined the ^1H-^1H connectivity as far as was possible. However, due to the overlap of a number of protons, a definite structural assignment (i.e. bicyclo[3.2.1]octane or bicyclo[2.2.2]octane, etc) could not be made. A number of HMBC experiments were performed and allowed assignment of a bicyclo[3.2.1]octane carbon skeleton. Of particular note were the correlations of the methyl group (2.08 ppm) to C1, C2, and C3 and the correlations of H3 (4.85 ppm) to C1, C2, C4, and C5 which also established the molecular connectivity through the quaternary carbon C2. The presence of an nOe to the multiplet at 2.30-2.38 ppm (H1 and H8*syn* or H8*anti*) on irradiation of the multiplet centred at 2.47 ppm (H4*exo* or H4*endo*) established an *exo* orientation of this proton and a *syn* orientation of the proton attached to C8 in the multiplet at 2.30-2.38

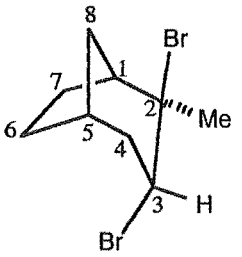

‡ Although the bridges are all of equal size, once the structure of the compound has been established the highest priority bridge was assigned the lowest carbon numbering and hence the main bridge protons descriptors are defined with respect to the lowest numbered carbon bridge.

† The multiplet at 2.43 ppm in the ^1H NMR spectrum was assigned to H5*exo* by the presence of a small nOe (1.0%) to the multiplet at 1.52 ppm (H8*anti*) on irradiation of H5*exo*. A 1.0% enhancement of H5*exo* was observed on irradiation H8*anti* in the reverse nOe experiment.

ppm (H8*syn*, centred at 2.33 ppm from the HMQC). The presence of a proton at 4.85 ppm attached to a carbon with a chemical shift of 56.6 ppm identified this proton and carbon as being part of a CHBr group. The DQCOSY and HMBC experiments established this proton and carbon to be H3 and C3. A 5.9 Hz coupling from H4*exo* (2.47 ppm) to H3 and a 1.2 Hz coupling from H4*endo* (2.04 ppm)§ to H3 is consistent with an *exo* orientation of H3 and hence an *endo* orientation of the C3 bromine substituent. The quaternary carbon at 76.7 ppm was identified as having methyl and bromine substituents from its chemical shift and was assigned as C2 from the HMBC experiments. The stereochemistry of C2 was more difficult to assign due to the similarity of the chemical shifts of the methyl group (2.08 ppm) with H7*endo* (2.12 ppm), H5 (2.03 ppm), and H4*endo* (2.04 ppm), and hence irradiation of the methyl group in nOe experiments could lead to ambiguous results as any enhancements observed may be due to the partial irradiation of the other protons. Consideration of the effects expected from steric interactions of the bromine or methyl group on the ^{13}C chemical shifts of C8 and C7 also proved fruitless, as the effects may be similar in magnitude. This can be seen from Table 4.1 where the ^{13}C chemical shifts and $\Delta\delta$ values of 2-*endo*- and 2-*exo*-methylbicyclo[3.2.1]octane (**95** and **96**, respectively)[106] and various bromine substituted bicyclo[3.2.1]octane structures are compared with the parent compound bicyclo[3.2.1]-octane **84**.

Of particular note is the similarity in shielding effects ($\Delta\delta$ values) of an axial methyl or bromine at C2 which result in 6.8 ppm and 4.5-6.6 ppm upfield shifts of C8, respectively. A γ eclipsed interaction from an equatorial methyl or bromine at C2 also result in similar shielding effects of C7 (4.7 pm and 4.5-5.1 ppm,‡ respectively). Neither substituent shows significantly different γ *anti* effects. Consideration of the chemical shift of H8*syn* (see later this section) shows an axial methyl group to result in a much smaller downfield shift of this proton than does a bromine in the same position. The chemical shift of H8*syn* in **94** was established to be 2.22 ppm when the sample is run in $CDCl_3$† (the chemical shifts of protons in this molecule, reported above in the structure elucidation, were recorded using benzene-d_6 as the NMR solvent unless otherwise stated) which compares well with the chemical shift of H8*syn* of **70a** (2.30 ppm) and **75a** (2.06

---

§ H4*endo* was identified from the HMQC experiment as the second proton of the C4 methylene group. The assignment of H4*endo* (2.04 ppm) was also consistent with the presence of a 2.4 Hz four bond coupling of this proton to H8*anti* (1.32 ppm) which shows a 'W' relationship of these protons and hence an *endo* orientation of the multiplet at 2.04 ppm.

‡ An equatorial bromine at C4 in **70a** results in a 5.1 ppm shielding of C6.

† A sample of **94** was run in $CDCl_3$ and the HMQC, HMBC, etc experiments were rerun to obtain the assignments of the protons and carbons.

ppm) both of which have one axial bromine substituent. The stereochemistry of the bromine substituent of C2 was therefore assigned as *exo* and the methyl group as *endo*.

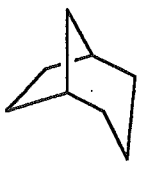

84

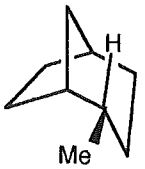

95

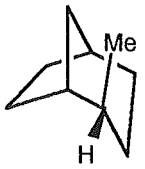

96

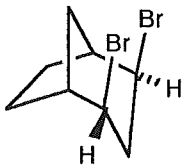

71a

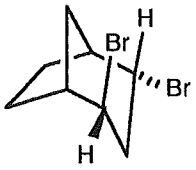

70a

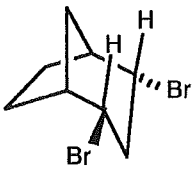

76a

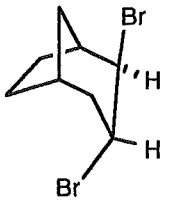

75a

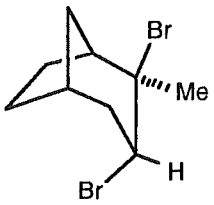

94

Cmpd	C1	C2	C3	C4	C5	C6	C7	C8
84	35.2	32.8	19.1	32.8	35.2	28.9	28.9	39.7
95	42.0	36.9	28.4	32.9	35.0	29.3	24.2	40.8
	(6.8)	(4.1)	(9.3)	(0.1)	(-0.2)	(0.4)	(-4.7)	(1.1)
96	41.8	35.0	25.2	30.8	35.7	28.9	27.7	32.9
	(6.6)	(2.2)	(6.1)	(-2.0)	(0.5)	(0.0)	(-1.2)	(-6.8)
71a§	43.4	52.0	35.2	52.0	43.4	28.6	28.6	29.4
	(8.2)	(19.2)	(16.1)	(19.2)	(8.2)	(-0.3)	(-0.3)	(-10.3)
70a	42.1	53.0	39.7	55.9	44.1	23.8	28.8	35.2
	(6.9)	(20.2)	(20.6)	(23.1)	(8.9)	(-5.1)	(-0.1)	(-4.5)
76a	42.7	53.2	41.3	53.2	42.7	24.4	24.4	38.7
	(7.5)	(20.4)	(22.2)	(20.4)	(7.5)	(-4.5)	(-4.5)	(-1.0)
75a	43.6	60.1	48.8	36.7	33.9	27.4	29.1	33.1
	(8.4)	(27.3)	(29.7)	(3.9)	(-1.3)	(-1.5)	(0.2)	(-6.6)
94§	49.9	76.7	56.0	38.2	34.0	27.2	26.2	37.9
	(14.7)	(43.9)	(36.9)	(5.4)	(-1.2)	(-1.7)	(-2.7)	(-1.8)

Table 4.1. ^{13}C chemical shifts (ppm) and $\Delta\delta$ values (shown in brackets) of carbons C1-C8 of bromine (**70a**, **71a**, **75a**, **76a**, and **94**) and methyl substituted (**95**, **96**) bicyclo[3.2.1]octanes compared with the parent compound bicyclo[3.2.1]octane **84**.

§ The chemical shifts shown for these compounds were recorded using $CDCl_3$ as the NMR solvent and not benzene-d_6 in which the values reported in the experimental section were recorded.

The *trans* 1,2-relationship of the two bromine substituents in **94** is identical to that found for **75a** and appeared to have arisen from bromine addition to a double bond rather than to the cyclopropane ring. Reaction of **45** with a catalytic amount of TFA in CCl_4 gave, after stirring at room temperature for 3 h, approximately 50% conversion (^{1}H NMR) to 2-methylbicyclo[3.2.1]oct-2-ene‡ **97** (Figure 4.4). After a further 1 h bromine was added and the reaction stirred for another 15 minutes after which time a ^{1}H NMR spectrum showed complete consumption of **45**. The major product from the reaction was **94** in approximately 80% yield. It therefore appears likely that **94** results from the rapid reaction of **45** with HBr, present in the bromine or derived from elimination reactions of minor products, followed by elimination to give **97** which then adds bromine across the double bond to form **94** (Figure 4.4). Since bromine addition to nonconjugated alkenes generally occurs with a *trans* stereochemistry§ this adds further support to the assignment of the stereochemistry of C2 in **94** as an *exo* bromine, since the bromine at C3 was assigned as *endo*. Due to rapid reaction of **45** with HBr it may have been advantageous to have carried out the reaction in the presence of an acid scavenger, such as N-bromosuccinimide,[24] however this was not investigated.

The reaction of **45** with bromine (0.9 mole equivalents) in dry methanol in the absence of light gave four products (GLC analysis), 4-*endo*-bromo-2-*exo*-methoxy-2-*endo*-methylbicyclo[3.2.1]octane **98** (50%), 4-*endo*-bromo-2-*endo*-methoxy-2-*exo*-methylbicyclo[3.2.1]octane **99** (45%), and two minor products which not identified (Figure 4.7). The major products were separated by preparative GLC.

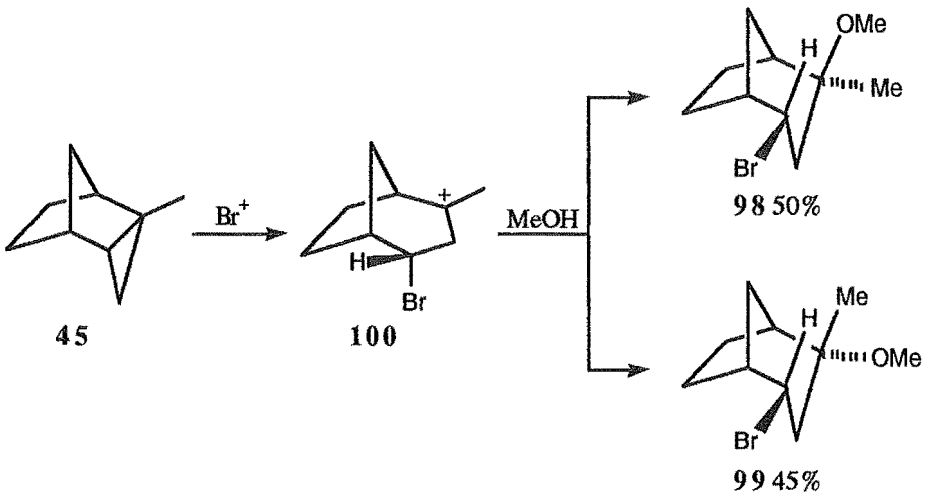

Figure 4.7. Reaction of 2-methyl-*endo*-tricyclo[3.2.1.0^{2,4}]octane **45** with bromine in methanol.

‡ The identity of **97** was determined by comparison with the ^{1}H and ^{13}C NMR data reported.[16]

§ Although examples of *cis* bromine additions are known.[134]

The identity of 4-*endo*-bromo-2-*exo*-methoxy-2-*endo*-methylbicyclo[3.2.1]octane **98** was determined as follows: a DQCOSY experiment established the ^{1}H-^{1}H connectivity and an HMQC determined the one bond ^{1}H-^{13}C assignments. An HMBC experiment confirmed the general bicyclo[3.2.1]octane structure from the presence of correlations from H8*anti*‡ (1.37 ppm) to C1 (42.0 ppm), C5 (43.2 ppm), C4 (55.7 ppm), and C2 (78.2 ppm) and from H8*syn* (2.04 ppm) to C6 (24.2 ppm) and C7 (26.2 ppm). The HMBC also showed correlations to C1, C2, C4, and C5 from H3*exo* (2.14 ppm) and hence established the molecular connectivity through the quaternary carbon C2. The presence of the C(OMe)Me (C2) and CHBr (C4) groups were determined from consideration of the ^{13}C chemical shifts and from the chemical shift of H4 (4.40 ppm). Table 4.2 summarises the HMQC and HMBC correlations observed for **98.**

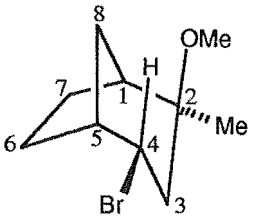

		C1	C2	C3	C4	C5	C6	C7	C8	Me	OMe
	ppm	42.0	78.2	41.5	55.7	43.2	24.2	26.2	33.5	21.5	48.6
H1	2.17	O					X				
H3*x*	2.14	X	X	O	X	X					
H3*n*	1.62			O							
H4	4.40				O						
H5	2.49					O					
H6*n*	1.84						O				
H6*x*	1.64						O				
H7*x*	1.69							O			
H7*n*	1.42							O			
H8*a*	1.37	X	X		X	X			O		
H8*s*	2.04						X	X	O		
Me	1.08	X	X							O	
OMe	3.16										O

Table 4.2. Heteronuclear shift correlation data obtained from HMQC (O) and HMBC (X) experiments for 4-*endo*-bromo-2-*exo*-methoxy-2-*endo*-methylbicyclo[3.2.1]octane **98**. Chemical shifts are in ppm with $CDCl_3$ as the NMR solvent. Abbreviations for proton descriptors are as follows: *x* = *exo*, *n* = *endo*, *a* = *anti*, and *s* = *syn*.

‡ The assignment of the multiplet at 1.37 ppm as H8*anti* stemmed from the presence of a 5.1 Hz coupling of this proton to H1 and H5. The proton at 2.04 ppm was established from the HMQC to be the second proton of the C8 methylene group and hence was assigned to H8*syn*.

The stereochemistry of C4 was assigned by the presence of a 1.8% enhancement of the multiplet at 2.04 ppm on irradiation of H4 (4.40 ppm) in a difference nOe experiment and therefore establishes the multiplet centred at 2.04 ppm as H8*syn* and the *exo* orientation of H4 (a 1.7% enhancement of H4 was observed on irradiation of H8*syn*). This therefore requires an *endo* orientation of the C4 bromine substituent. The axial orientation of H4 was also supported by the presence of a 12.0 Hz coupling to H3*endo* (1.62 ppm), consistent with a *trans* relationship of these protons, and a smaller 5.4 Hz coupling to H3*exo* (2.14 ppm). An *exo* orientation of the methoxy group of C2 was established from the presence of an nOe (1.2 %) to H8*syn* on irradiation of the methoxy group at 3.16 ppm and the presence of a 1.7% enhancement of H7*endo* (1.42 ppm) on irradiation of the methyl group attached to C2, hence confirming an *endo* orientation of this group. The chemical shift of H8*syn* showed a significant downfield shift to 2.04 ppm similar to that observed for **75a** and **70a** (2.06 ppm and 2.30 ppm, respectively), both of which have a single axial bromine substituent at C2, and hence supports the *exo* assignment of the methoxy group (see later this section).

The structure of the second major product, 4-*endo*-bromo-2-*endo*-methoxy-2-*exo*-methylbicyclo[3.2.1]octane **99** was determined from the following: a DQCOSY and selective decoupling experiments established the proton-proton connectivity and an HMQC experiment established the ^{1}H-^{13}C one bond connectivities. The one bond ^{1}H-^{13}C connectivities of the carbons at 23.9_4 ppm and 23.8_5 ppm could not be resolved due to the similarity of the chemical shifts of both the carbons and their attached protons, whose correlations overlapped in the HMQC.‡ An HMBC experiment confirmed the general bicyclo[3.2.1]octane structure of the molecule and also identified the chemical shift of the quaternary carbon (C2, 76.8 ppm) which was not observed in the ^{13}C NMR spectrum.† The connectivities determined from the DQCOSY and selective decoupling experiments are summarised in Table 4.3 and correlations found from the HMQC and HMBC experiments are shown in Table 4.4.

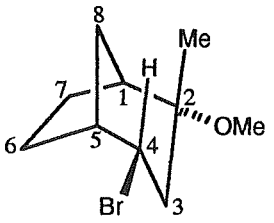

‡ The carbons at 23.9_4 ppm and 23.8_5 ppm were confirmed as the carbons of methylene groups by a DEPT135 experiment. The chemical shifts of the protons of each CH_2 were identified from the DQCOSY.

† The H3*exo* (2.10 ppm) proton showed correlations to C1 (42.0 ppm), C4 (54.6 ppm), C5 (44.0 ppm) and a fourth carbon which, after taking into account foldback, was calculated to have a chemical shift of 76.8 ppm, which is similar to that observed for C2 (78.2 ppm) of **98**, and is consistent with a quaternary carbon with methoxy and methyl substituents.

Proton	ppm												
H4	4.18	4.18											
OMe	3.16		3.16										
H5	2.50	V(2.4)		2.50									
H1	2.18				2.18								
H3x	2.10	V(5.4)		L4(1.4)	L4(1.4)	2.10							
H6n	1.84						1.84						
H3n	1.83	V(12.2)				G(13.2)		1.83					
H7n	1.82								1.82				
H7x	1.65				V				G	1.65			
H8a	1.55			V	V						1.55		
H8s	1.55											1.55	
H6x	1.50			V			G			V			1.50	
Me	1.20				L4 (1.2)									1.20

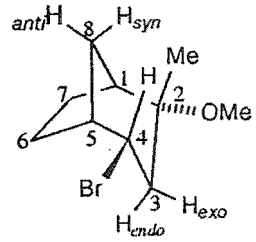

99

Table 4.3. ^{1}H-^{1}H Homonuclear connectivities obtained from DQCOSY and selective decoupling experiments for 4-*endo*-bromo-2-*endo*-methoxy-2-*exo*-methylbicyclo-[3.2.1]octane **99**. Coupling constants, if obtained, are shown in brackets. G = Geminal, V = Vicinal, Lx = Long range through "x" bonds. Abbreviations used in proton descriptors: *x = exo, n = endo, a = anti, s =syn.*

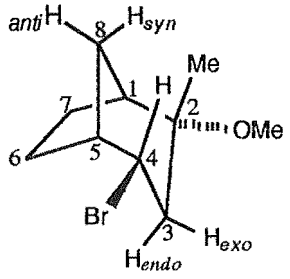

99

		C2	C4	OMe	C5	C3	C1	C8	C7*	C6*	Me
	ppm	76.8	54.6	48.5	44.0	43.0	42.0	34.7	23.9	23.9	21.3
H4	4.18		O								
OMe	3.16			O							
H5	2.50				O						
H1	2.18						O				
H3*x*	2.10	X	X		X	O	X				
H6*n*	1.84									O	
H3*n*	1.83					O					
H7*n*	1.82								O		
H7*x*	1.65								O	X	
H8*a*†	1.55		X					O	(X)	(X)	
H8*s*†	1.55		X					O	(X)	(X)	
H6*x*	1.50									O	
Me	1.20	X				X	X				O

Table 4.4. Heteronuclear shift correlation data obtained from HMQC (O) and HMBC (X) experiments for 4-*endo*-bromo-2-*endo*-methoxy-2-*exo*-methylbicyclo[3.2.1]octane **99**. Abbreviations for proton descriptors are as follows: *x* = *exo*, *n* = *endo*, *a* = *anti*, and *s* = *syn*.

* Chemical shifts of the carbons at 23.9_4 ppm and 23.8_5 ppm, C6 and C7, were not distinguishable from the 2D-NMR experiments. HMBC correlations in brackets are from H8*syn* or H8*anti* to C6 or C7.

† Chemical shifts of H8*anti* and H8*syn* could not be distinguished.

Irradiation of the multiplet corresponding to H8*syn* and H8*anti*§ at 1.55 ppm in a difference nOe experiment gave a 0.7% enhancement of the methyl group of C2 and a 2.7% enhancement of H4, thereby establishing the *exo* orientation of H4 and giving a

§ C8 showed only one correlation in the HMQC experiment, to a multiplet centred at 1.55 ppm, but was confirmed as the carbon of a methylene group from a DEPT135 experiment. Therefore the chemical shifts of H8*syn* and H8*anti* are similar.

tentative assignment of an *exo* orientation of the methyl substituent of C2. Irradiation of H4 gave an enhancement to the multiplet centred at 1.55 ppm but this could not be measured due to the presence of water in the ^{1}H NMR spectrum which partially obscured the multiplet. In the same irradiation a 0.9% nOe to the methyl group of C2 was observed. Irradiation of the methyl signal at 1.20 ppm gave a 2.6% enhancement of H4, an enhancement of the multiplet centred 1.55 ppm was also observed. This confirmed the *exo* orientation of the methyl substituent and hence an *endo* orientation of the methoxy group attached to the same carbon. The assignment of an axial orientation of H4 was also supported by the presence of a 12.2 Hz coupling to H3*endo*, consistent with a *trans* arrangement of the two protons.

Of note is the chemical shift of H8*syn* at approximately 1.55 ppm which is significantly (0.5 ppm) upfield from H8*syn* in compound **98**. Thus the presence of an axial methyl group leads to a smaller downfield shift of this proton than does an axial methoxy group (and bromine substituent, see Chapter 2, Section 3.4) and hence further supports the assignment of an *exo* bromine at C2 in **94** due to the large downfield shift of H8*syn* observed (2.22 ppm in $CDCl_3$ solution).

The products obtained from bromination of **45** in methanol are consistent with corner attack of the bromine electrophile at the C2-C4 bond of the cyclopropane ring, followed by nucleophilic attack with both inversion and retention, with a small preference (5%) for the latter.† This is consistent with the formation of an open tertiary carbocation intermediate **100** (Figure 4.7) which then undergoes nucleophilic attack. Electrophilic attack of bromine therefore resulted in cleavage of the most substituted cyclopropyl bond (C2-C4 bond) and the formation of the most stable carbocation. Corner attack of the bromine electrophile was also observed in the bromination of **1** and **46** (Chapter 3) and is consistent with results of Skell[24] for the bromination of substituted cyclopropanes. However, the corner attack trajectory contrasts with the mechanism suggested by Lambert et al.[33] from investigations of the bromination of *cis-cis-cis-d*$_3$-cyclopropane.

The competition of acid induced ring opening with bromination in CCl_4 and the absence of competition in methanol may indicate greater stabilisation of the open cation **100** in methanol than in CCl_4. However, the acid induced ring opening would also be expected to form an intermediate carbocation **101** (Figure 4.4), before elimination to give **97** occurs. Although **101** would also be stabilised in methanol, cation **100** would be expected to be less stable than **101** due to the inductive effect of the bromine substituent and hence bromination may be significantly less favourable and not compete with the acid catalysed reaction in CCl_4. Thus in methanol cation **101** may be sufficiently stabilised to compete with proton attack at the cyclopropane ring, and since the bromine was present in

† This was also observed for the reaction of **45** with MeOD-D$^+$.[13,16]

higher concentrations than the acid it would be expected to be the dominant reaction pathway. Another possible reason for the predominance of acid promoted ring opening in nonpolar solvents may be that an open cation is not formed, and hence a synchronous addition-elimination of a proton may be observed, or the protonated cyclopropane formed could be significantly stabilised with respect to an equivalent brominated cyclopropane, if indeed an intermediate brominated cyclopropane is formed.†

† Bromination and protonation of cyclopropane is discussed further in Chapter 6.

CHAPTER 5
Reactions of Tricyclo[3.2.2.0^{2,4}]non-6-ene Systems with Electrophiles

Section 5.1 INTRODUCTION

A number of reactions involving electrophilic addition to compounds containing a tricyclo[3.2.2.0^{2,4}]non-6-ene carbon skeleton have been reported[22,135-137] with both modified Markovnikov (Figures 5.1a and b)‡ and modified *anti*-Markovnikov (Figure 5.1c) addition being observed. For compounds **102** and **103** (Figures 5.1a and b, respectively) the presence of a bridgehead methoxy substituent complicates the analysis of orbital effects on the trajectory of electrophilic addition to the cyclopropane ring.[22] The use of unsubstituted and/or symmetrical systems should therefore result in considerable simplification of orbital/electronic and steric factors which determine the mechanism of product formation.

Reaction of tricyclo[3.2.2.0^{2,4}]nona-6,8-diene **51** with mercuric acetate (Figure 5.1d)[137] gave predominantly mercuric ion addition to the C6-C7 double bond, similar to that found for the reaction of $Hg(OAc)_2$ with *exo*-tricyclo[3.2.1.0^{2,4}]oct-6-ene **69**,[13,15] in preference to addition to the cyclopropane ring as was observed for *endo*-tricyclo-[3.2.1.0^{2,4}]oct-6-ene **68**.[13,15] This result has been attributed[13] to the increased size of the orbital coefficients[138] of C6 and C7 in **51** due to the large through space interaction with the e_s orbital of the cyclopropyl ring (overlap integral[139] $\langle\pi/\sigma_s\rangle$ = 0.061 for **51** compares with 0.052 and 0.012 for hydrocarbons **69** and **68**, respectively). This results in better overlap of the hydrocarbon π orbitals with the Hg^{2+} LUMO. A similar explanation has been proposed for the reactivity of **69**. In the case of **68** the smaller π orbital coefficients in the HOMO of the double bond result in exclusive cyclopropyl ring opening.[13,15]

To extend the scope of the above reactions and to further elucidate the factors which determine the regiochemistry and stereochemistry of electrophilic addition, a number of reactions with symmetrically substituted and unsubstituted tricyclo[3.2.2.0^{2,4}]non-6-enes (*endo* and *exo*) were studied.

---

‡ The reaction products shown in equations (a) and (b) of Figure 5.1 were those from the original paper[136] and are the reverse of the products reported by Zimmerman.[22]

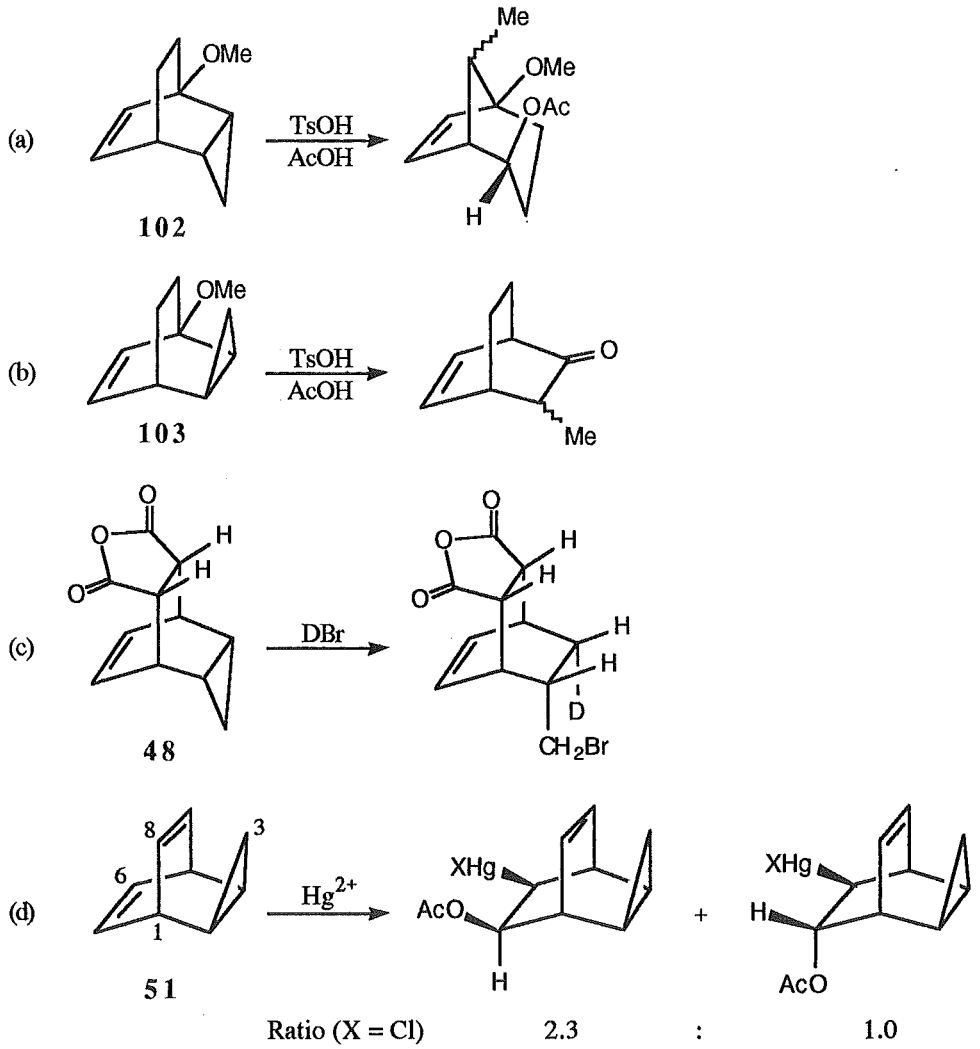

Figure 5.1. Example reactions of molecules containing tricyclo[3.2.2.0^{2,4}]non-6-ene carbon skeletons with electrophiles.[22,135-137]

Section 5.2 BROMINATION OF *exo*-TRICYCLO[3.2.2.0^{2,4}]NON-8-EN-6-*exo*-7-*exo*-DICARBOXYLIC ACID ANHYDRIDE

The bromination of *exo*-tricyclo[3.2.2.0^{2,4}]non-8-en-6-*exo*-7-*exo*-dicarboxylic acid anhydride **48** in CCl_4 under conditions which favour radical addition (light catalyzed reaction) has been reported[140] (Figure 5.2). As part of the present work, the bromination of **48** was performed in the absence of light and hence under conditions which favour electrophilic addition; however, little product formation was observed.‡

Reaction of bromine (0.9 mole equivalents) with **48** in dry methanol showed almost complete decolourisation after stirring at room temperature for 23 h. A ^{1}H NMR spectrum of the crude reaction mixture showed complete consumption of the starting

‡ The reaction was less than 10% complete after stirring at room temperature for 50 days. The product(s) obtained were not identified.

material and the presence of three products. The products were separated by flash dry column chromatography and identified as *exo*-tricyclo[3.2.2.0^{2,4}]non-8-en-6-*exo*-7-*exo*-dicarboxylic acid monomethyl ester **104** (62%), *exo*-tricyclo[3.2.2.0^{2,4}]non-8-en-6-*exo*-7-*exo*-dicarboxylic acid dimethyl ester **105** (11%), and 8-*syn*-bromo-9-*anti*-methoxy-*exo*-tricyclo[3.2.2.0^{2,4}]nona-6-*exo*-7-*exo*-dicarboxylic acid anhydride **106** (9%) (Figure 5.3). No other products were isolated. The identity of **105** was determined by comparison of its melting point and ^{1}H NMR data with those reported.[140-142] Product **105** also showed identical ^{1}H NMR data to the product obtained from Diels-Alder reaction of dimethyl maleate with cycloheptatriene.

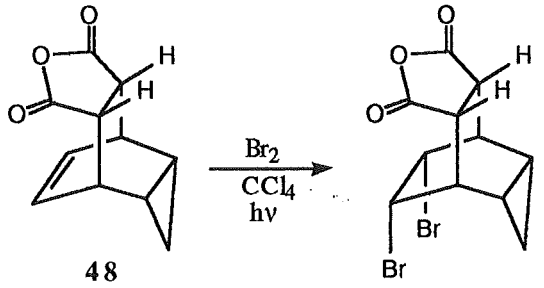

48

Figure 5.2. Radical bromination of *exo*-tricyclo[3.2.2.0^{2,4}]non-8-en-6-*exo*-7-*exo*-dicarboxylic acid anhydride **48**.[140]

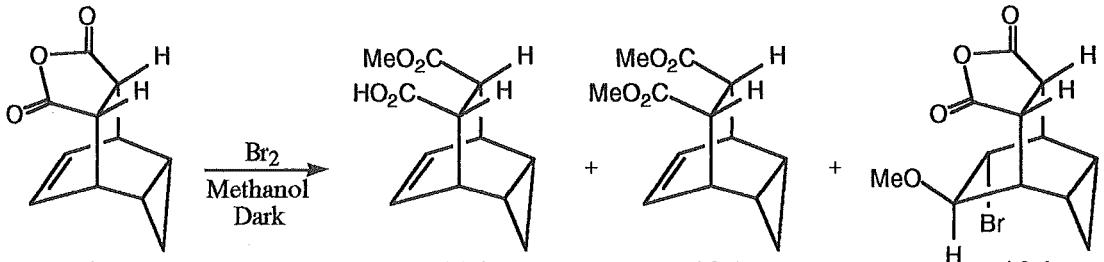

48 **104** 62% **105** 11% **106** 9%

Figure 5.3. Reaction of *exo*-tricyclo[3.2.2.0^{2,4}]non-8-en-6-*exo*-7-*exo*-dicarboxylic acid anhydride **48** with bromine in dry methanol.

The structure of the major product **104** was determined from the following: the presence of two carbonyl groups was ascertained from examination of the ^{13}C NMR spectrum which showed signals at 179.1 ppm and 173.5 ppm which are indicative of carboxylic acid and ester carbonyl groups, respectively. An IR spectrum showed strong absorptions at 1739 cm^{-1} and 1701 cm^{-1} which are also consistent with the presence of two carbonyl groups. An HMQC experiment established the one bond ^{1}H-^{13}C NMR connectivities. The presence of a cyclopropyl group was determined from the ^{13}C NMR which showed carbon signals at 9.4 ppm (C2), 9.2 ppm (C4), 2.8 ppm (C3). The general tricyclo[3.2.2.0^{2,4}]non-6-ene structure

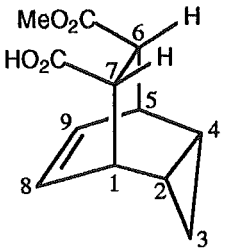

was confirmed by an HMBC experiment as, due to the significant overlap of protons in the ^{1}H NMR spectrum, little information could be gained from ^{1}H-^{1}H connectivity experiments. The integral of the OMe signal (3.59 ppm) in the ^{1}H NMR spectrum was consistent with three protons and hence only one methoxy group. Compound **104** also showed satisfactory mass spectral and elemental analyses and showed identical ^{1}H NMR data to the product obtained from refluxing **48** in dry methanol for 48 h. Anhydride ring opening on reaction with methanol under these conditions would be expected to give the monomethyl ester.[143]

The identity of the third product 8-*syn*-bromo-9-*anti*-methoxy-*exo*-tricyclo-[3.2.2.0^{2,4}]nona-6-*exo*-7-*exo*-dicarboxylic acid anhydride **106** was established as follows: a DQCOSY in conjunction with selective decoupling experiments established the ^{1}H-^{1}H connectivity and a HETCOR experiment established the one bond ^{1}H-^{13}C connectivities. An nOe (4.2%) to H9 (4.58 ppm) on irradiation of H3*exo* (1.27 ppm)‡ established the *syn* orientation of the cyclopropane ring towards the main bridge (C8C9 bridge). A 2.1% enhancement of H3*exo* was observed on irradiation of H9 in the reverse difference nOe experiment. Having established the general structure of the molecule, the stereochemistry of C8 was determined from the presence of a small coupling ($^3J_{9,8}$ = 2.5 Hz, $^3J_{8,9}$ = 2.2 Hz) from H8 (4.67 ppm) to H9 which eliminated the possibility of a *cis* relationship of these protons and hence determined an *anti* orientation of H8 and a *syn* orientation of the C8 bromine substituent. The assignment of the C8 bromine as *syn* to the three membered bridge was supported by comparison of the chemical shifts of C2 and C4 (8.1 ppm and 11.5 ppm, respectively) which shows a significant (3 ppm) upfield shift of C2 and is consistent with a γ-eclipsed interaction with the C8 bromine substituent. The presence of a four bond 1.2 Hz coupling of H8 to H2, consistent with a 'W' arrangement of these protons, also supports an *endo* assignment of H2 and an *anti* orientation of H8. The *exo* configuration of the anhydride moiety follows from that of the starting material and was supported by the presence of a four bond coupling of H9 to H6 ($^3J_{9,6}$ = 1.3 Hz) which is consistent with a 'W' arrangement of these protons and hence an *endo* orientation of H6 and *syn* orientation of H9.

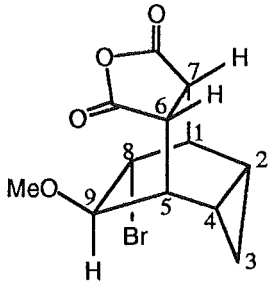

‡ The multiplet centred at 1.27 ppm in the ^{1}H NMR spectrum of **106** was established as H3*exo* from consideration of the coupling constants of this proton to H2 and H4 (multiplet 1.13-1.20 ppm) ($^3J_{3exo,2}$ = $^3J_{3exo,4}$ = 3.9 Hz) which are significantly smaller than the 8.0 Hz vicinal coupling constants of H2 and H4 to H3*endo* (doublet of triplets centred at 0.78 ppm, $^3J_{3endo,2}$ = $^3J_{3endo,4}$ = 8.0 Hz) which are characteristic of *cis* couplings found in cyclopropane rings.[32]

The products obtained from bromination of **48** in methanol show bromination of the double bond to be slow in the absence of light. This is consistent with the deactivation of the double bond by the inductive effect of the anhydride moiety and also due to steric hindrance on both sides of alkene by the anhydride and cyclopropyl groups. The small amount of bromination which did occur resulted in a *trans* addition of the electrophile (Br^+) and nucleophile (MeOH) in contrast to the *cis* addition of bromine observed under radical conditions.[140] Presumably the *trans* addition of Br^+ and methanol reflects the formation of a bromonium ion which directs nucleophilic capture to the opposite side of the alkene. The preference for *cis* addition under radical conditions may reflect the greater ease of attack from the *syn* face of the resulting radical rather than from the more sterically crowded *anti* face which is shielded by the anhydride group. The inductive effect of the anhydride group presumably also deactivates the cyclopropane ring to an extent where bromination does not occur to a significant extent.

Section 5.3 BROMINATION OF 8-*anti*-9-*anti*-BIS(HYDROXYMETHYL)-*endo*-TRICYCLO[3.2.2.$0^{2,4}$]NON-6-ENE

Due to the low reactivity of **48** towards bromination a more reactive starting material was required. Reduction of **48** with $LiAlH_4$ gave two products, 8-*anti*-9-*anti*-bis(hydroxymethyl)-*endo*-tricyclo[3.2.2.$0^{2,4}$]non-6-ene **107** (62%)[144] and 7-*exo*-hydroxymethyl-*exo*-tricyclo[3.2.2.$0^{2,4}$]non-8-en-6-*exo*-carboxylic acid lactone **108** (38%) (Figure 5.4). The latter product presumably results from incomplete reduction of the anhydride group followed by cyclisation on workup. The diol product **107** was identified by comparison of its melting point and ^1H NMR data with those reported.[144] Diol **107** would be expected to have a smaller inductive deactivating effect and provide less steric hindrance to bromination than the anhydride **48** and hence be more reactive towards bromine.

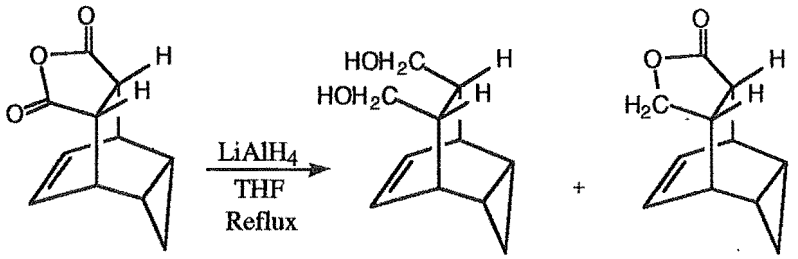

48 **107** 62% **108** 38%

Figure 5.4. $LiAlH_4$ reduction of *exo*-tricyclo[3.2.2.$0^{2,4}$]non-8-en-6-*exo*-7-*exo*-dicarboxylic acid anhydride **48**.

Reaction of **107** with bromine (0.9 mole equivalents) in dry methanol at room temperature for 25 h resulted in the formation of one major product, 7-*endo*-bromo-11-

anti-hydroxymethyl-9-oxa-*endo*-tetracyclo[4.4.1.0.^{2,8}0^{3,5}]undecane **109** (78%) and a number of minor products which were not identified; starting material **48** (11%) was also recovered.

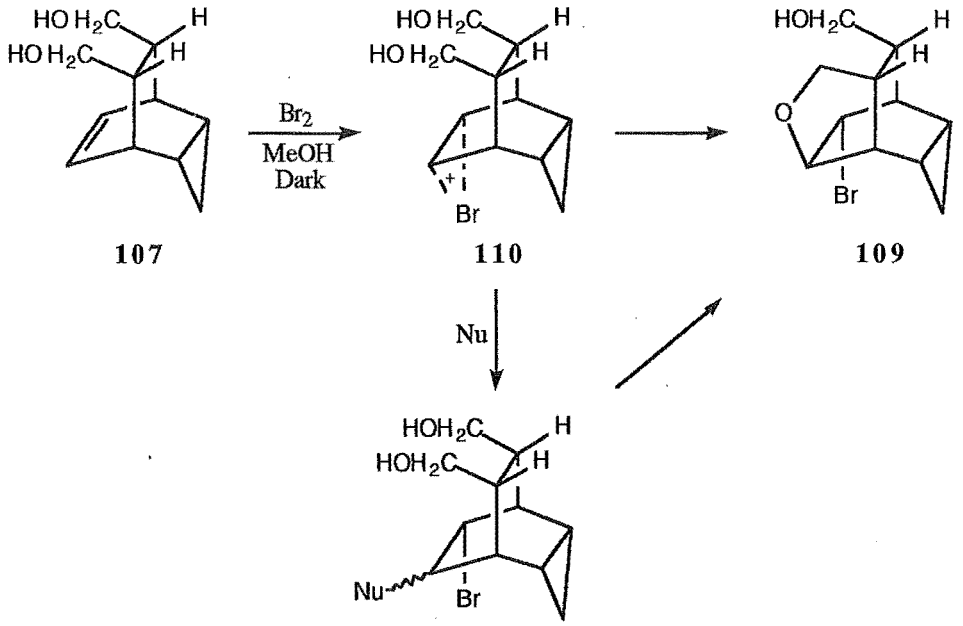

107 **110** **109**

111a Nu = Br
111b Nu = OMe

Figure 5.5. Bromination of 8-*anti*-9-*anti*-bis(hydroxymethyl)-*endo*-tricyclo[3.2.2.0^{2,4}]non-6-ene **107** in dry methanol in the absence of light.

The identity of **109** was determined from the following: a COSY in conjunction with selective decoupling experiments established the ^{1}H-^{1}H connectivity and a HETCOR determined the one bond ^{1}H-^{13}C connectivities. The presence of a CHBr group was established from the chemical shift of C7 (53.7 ppm) and its attached proton H7 (3.78 ppm). Three downfield signals in the ^{13}C NMR spectrum showed three carbons attached to an oxygen and hence determined the presence of an alcohol and an ether linkage. The chemical shift of C8 (83.6 ppm) was indicative of an ether carbon of a polycyclic ring system and the chemical shift of C10 (67.8 ppm) was close to that observed for the chemical shift of the corresponding carbon in THF[145] (68.4 ppm), and hence in conjunction with the COSY and decoupling experiments established the presence of a five membered cyclic ether. The HETCOR experiment showed only one correlation to C10 and the carbon assigned to the $\underline{C}H_2OH$ group; however, these carbons were confirmed as methylene group carbons from a DEPT135 experiment. The presence

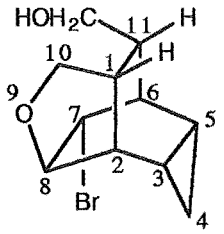

of an nOe‡ to H4*endo* on irradiation of H8 and the observation of 4.3% enhancement of H8 in the reverse irradiation at 1.03 ppm (H4*endo*)† confirmed the *endo* orientation of H8 with respect to the cyclopropane ring and established the *endo* orientation of both the cyclopropane ring and the proton centred at 1.03 ppm (H4*endo*). The proton at 0.61 ppm was established as H4*exo* from consideration of the coupling constants of this proton to H3 and H5 ($^3J_{4exo,3} = {}^3J_{4exo,5} = 7.6$ Hz) which are consistent with a *cis* arrangement of these protons. A small coupling of H7 to H8 ($^3J_{7,8} = 1.0$ Hz) established an axial-equatorial arrangement of these protons and hence an *exo* orientation of H7. A larger coupling would be expected if a *cis* diaxial arrangement of H7 and H8 was present.

The bromination products of **48** and **107** are consistent with bromine addition to the double bond in preference to the cyclopropane, as was observed for the reaction of *exo*- and *endo*-tricyclo[3.2.1$0^{2,4}$]oct-6-ene[32] (**68** and **69**), with electrophilic addition taking place from the less hindered face of the double bond. In the case of **107**, formation of the major product **109** is consistent with intramolecular capture of carbocation **110** by a hydroxymethyl substituent of C8 or C9. This has also been observed in the addition of electrophilic species to norbornene derivatives[42,146-149] and various other carbocycles[150] with an appropriately oriented nucleophilic group (Figure 5.6). Some formation of **109** may also have occurred from intramolecular nucleophilic substitution of an initially formed dibromide adduct **111a** (Figure 5.5). Similar substitution reactions have been observed in lactonisation of 5,6- and 5,7-dibromo-bicyclo[2.2.1]hepta-2,3-dicarboxylic acid derivatives.[151-154] Attempts to displace the bromine substituent of **109** by intramolecular substitution with the hydroxymethyl group, by treating **109** with KOBu^t or $NaNH_2$ in dry ether, were unsuccessful. No products resulting from addition of methanol to cation **110**, to give **111b**, were isolated.

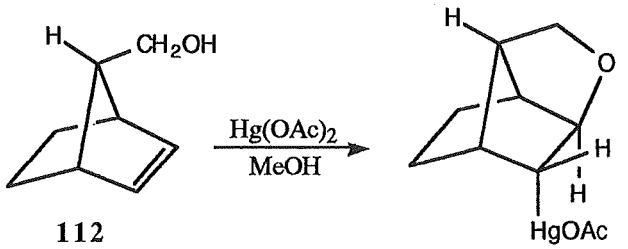

112

Figure 5.6. Addition of mercuric acetate to 7-*syn* hydroxymethylbicyclo[2.2.1]hept-2-ene **112**.[42,147]

---

‡ The size of the enhancement of H4*endo* could not be measured due to the partial overlap of this proton with H5 and H3.

† The chemical shifts of H3, H4*endo*, and H5 were determined from the HETCOR and COSY experiments as the three protons were overlapping in the ^{1}H NMR (multiplet 0.96-1.11 ppm).

Section 5.4 REACTIONS OF *exo*-TRICYCLO[3.2.2.$0^{2,4}$]NON-6-ENE WITH BROMINE

Section 5.4.1 Bromination of *exo*-Tricyclo[3.2.2.$0^{2,4}$]non-6-ene in CCl_4

The reaction of bromine (0.9 mole equivalents) with *exo*-tricyclo[3.2.2.$0^{2,4}$]non-6-ene **47** in CCl_4 proceeded essentially instantaneously at room temperature. GLC analysis of the resulting product mixture showed the presence of four major products, 5-*endo*-9-*syn*-dibromo-*endo*-tricyclo[4.2.1.$0^{2,4}$]nonane **113** (38%), 4-*endo*-9-*anti*-dibromotricyclo[3.3.1.$0^{2,8}$]nonane **114** (26%), and 6-*exo*-7-*endo*-dibromo-*exo*-tricyclo-[3.2.2.$0^{2,4}$]nonane **115** (15%) (Figure 5.7). The fourth major product (10%) was not identified. A number of minor products were also present, of which 5-*endo*-9-*syn*-dibromobicyclo[4.2.1]non-2-ene **116** (ca. 5%) was the only one isolated.

Column chromatography on silica gel (pentane elution) gave pure **115** and **116** but led to rearrangement of **113** and **114**. Pure **113** was obtained from radial chromatography on a PEG coated silica plate followed by recrystallisation from pentane. The second major product was not isolated in high purity but was tentatively assigned to **114** from NMR studies of an enriched fraction obtained from radial chromatography on a PEG coated silica plate.

The identity of 5-*endo*-9-*syn*-dibromo-*endo*-tricyclo[4.2.1.$0^{2,4}$]nonane **113** was established from the following: the proton-proton connectivity was determined from DQCOSY and 2D-TOCSY experiments and an HMQC experiment established the one bond ^1H-^{13}C connectivities. The HMQC also allowed estimation of the chemical shifts of a number of protons which were overlapping in the ^1H NMR spectrum.

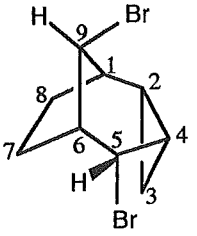

The TOCSY experiments were particularly useful as they allowed the ^1H-^1H connectivity of almost the entire ring system to be traced (Figure 5.8). As can be seen from Figure 5.8 the traces through the proton centred at 5.28 ppm (H5) showed initial correlations to H6 and H4 which gradually traced around the cyclopropyl ring and through the main bridge with increased mixing times. An HMBC experiment confirmed the tricyclo[4.2.1.$0^{2,4}$]-nonane carbon skeleton and showed a correlation to the carbon signal at 23.5 ppm which, in conjunction with the HMQC and ^1H-^1H correlation experiments, established this carbon as C7.‡

The presence of a cyclopropane ring was established from the DQCOSY experiment and the *endo* orientation was assigned from the presence of a 1.8% enhancement of

---

‡ Differentiation of C8 and C7 was complicated by the nearly identical chemical shifts of H7*exo* and H8*exo*, hence the DQCOSY and HMQC experiments were not able to distinguish the positions of the carbons at 23.5 ppm and 25.7 ppm.

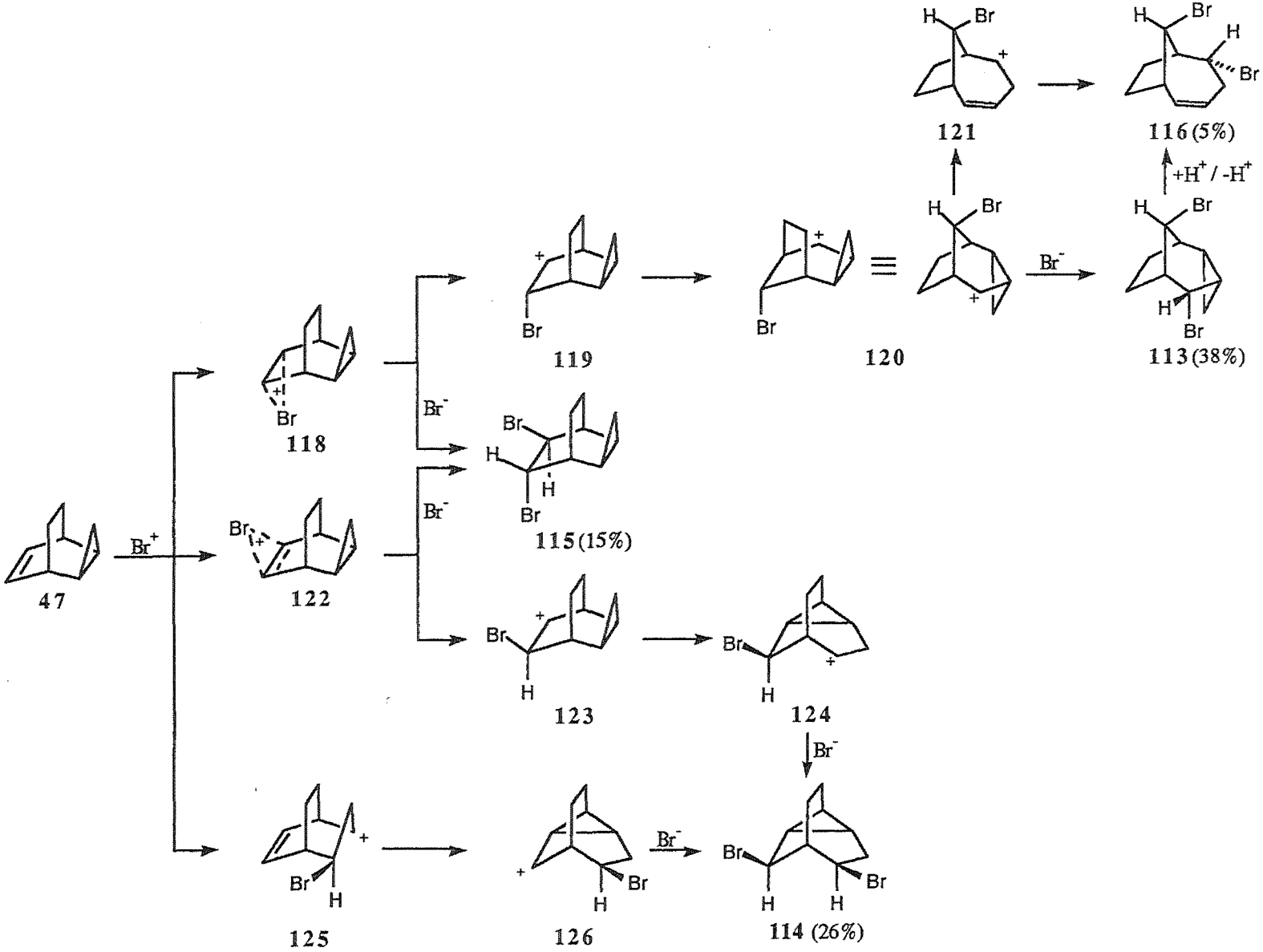

Figure 5.7. Possible mechanism for the bromination of *exo*-tricyclo[3.2.2.0^{2,4}]non-6-ene 47 in CCl_4.

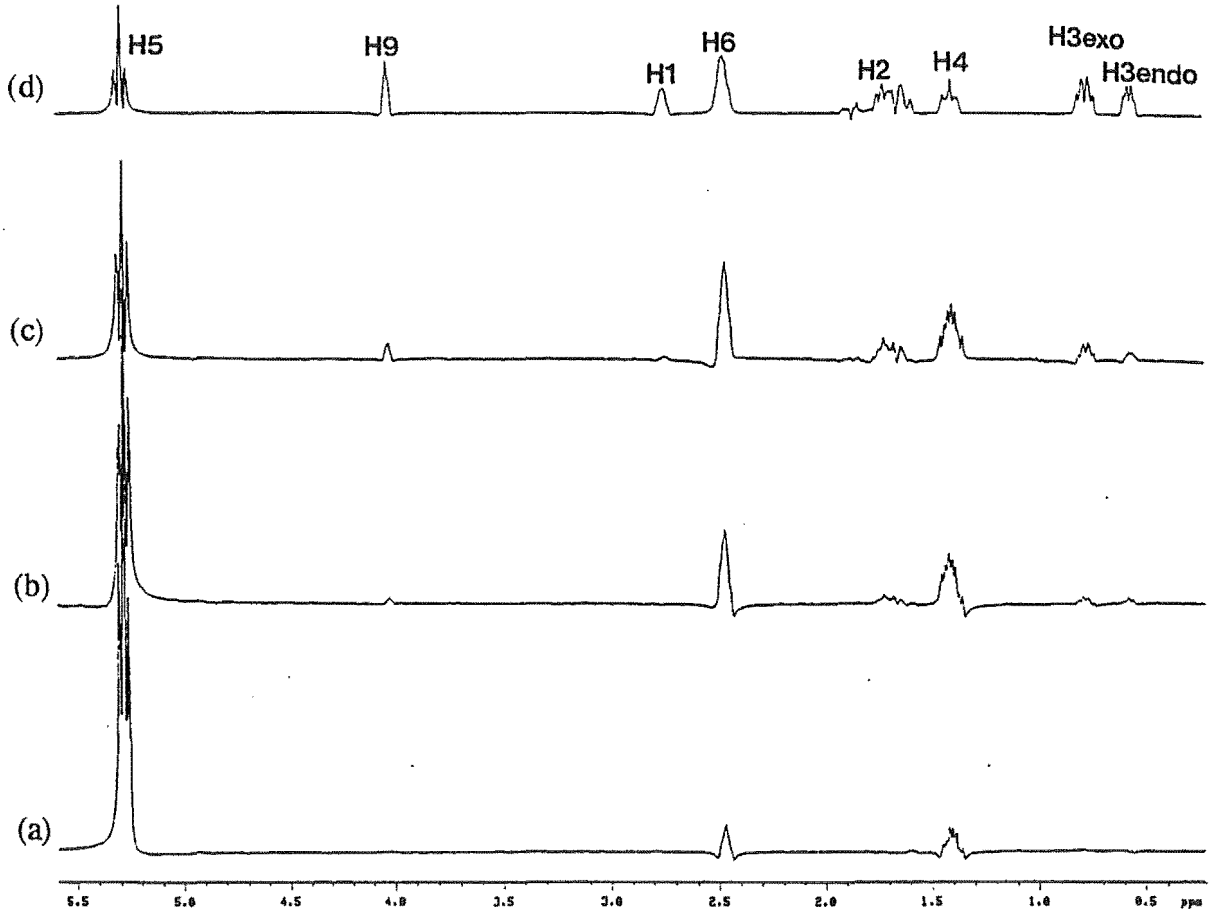

Figure 5.8. Traces through H5 of 2D-TOCSY experiments with mixing times of (a) 5 msec, (b) 15 msec, (c) 25 msec, and (d) 50 msec of 5-*endo*-9-*syn*-dibromo-*endo*-tricyclo[4.2.1.$0^{2,4}$]-nonane **113**.

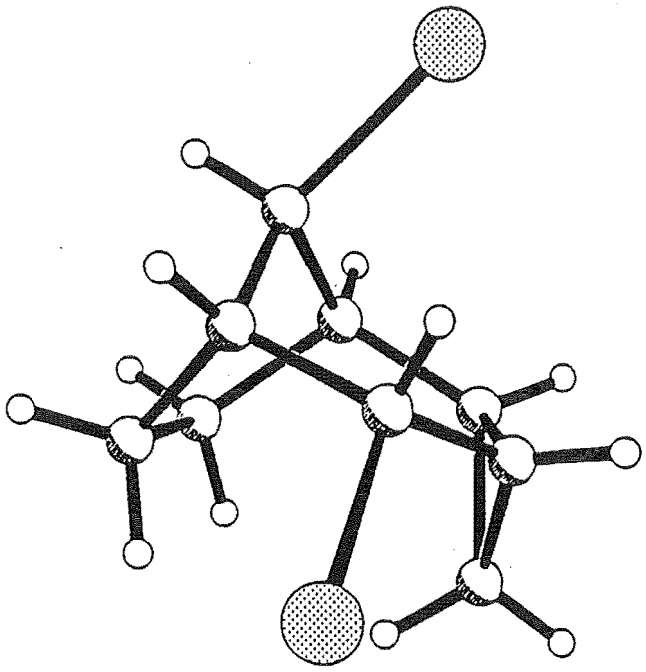

Figure 5.9. X-Ray crystal structure of 5-*endo*-9-*syn*-dibromo-*endo*-tricyclo[4.2.1.$0^{2,4}$]nonane **113**.

H7*endo* and 1.2% enhancement of H8*endo* on irradiation of H3*endo*† in a difference nOe experiment. A 1.2% enhancement of H3*endo* was observed on irradiation of H7*endo* in a further difference nOe experiment. The presence of two CHBr groups was determined from consideration of the chemical shifts of C5 (59.0 ppm) and C9 (56.9 ppm) and their attached protons H5 (5.28 ppm) and H9 (4.03 ppm). The stereochemistry of H5 was determined as *exo* from consideration of the coupling constants of this proton to H4 and H6 ($^3J_{5,4}$ = 7.4 Hz, $^3J_{5,6}$ = 5.7 Hz) which are similar to those observed for H5 of 5-*endo*-methoxy-*endo*-tricyclo[4.2.1.$0^{2,4}$]nonane[101] ($^3J_{5,4}$ = $^3J_{5,6}$ = 6.0 Hz). A *syn* orientation of the bromine substituent of C9 was determined from consideration of the observed coupling constants of H9 to H1 and H6 ($^3J_{9,1}$ = $^3J_{9,6}$ = 4.3 Hz). This is diagnostic of an H8*anti* proton in bicyclo[3.2.1]octane systems and a tricyclo-[4.2.1.$0^{2,4}$]nonane skeleton would be expected to show similar coupling characteristics of the *syn* and *anti* protons of the methylene main bridge. The *syn* stereochemistry of the C9 bromine substituent was also supported by the large downfield shift of H5, which is consistent with the through space deshielding effects of bromine substituents (see Chapters 3 and 4). The structure of compound **113** was confirmed by single crystal X-ray analysis (Figure 5.9).

The second major product 4-*endo*-9-*anti*-dibromotricyclo[3.3.1.$0^{2,8}$]nonane **114** was not isolated in high purity due to the instability of the compound. Attempts to purify **114** by chromatography on silica, basic alumina, florosil, and PEG coated silica led to either complete or partial decomposition of this compound. The product also degraded at room temperature and if left in $CDCl_3$ solution at 0 °C for prolonged periods. The compound was therefore assigned as far as possible by NMR methods from an enriched (ca. 70%) fraction obtained from radial chromatography on a PEG coated silica plate. The following assignments were made: an HMQC determined the one bond ^1H-^{13}C connectivities of C9 (54.0 ppm), C4 (51.0 ppm), C5 (42.1 ppm), and C3 (28.2 ppm). A DQCOSY showed correlations from H9 (4.76 ppm) to H1 (1.50 ppm), H9 to H5 (2.34 ppm), H5 to H4 (4.15 ppm), H4 to H3*endo* (2.12 ppm),‡ and H3*exo* (2.60 ppm) to H2 (1.21-1.27 ppm, multiplet

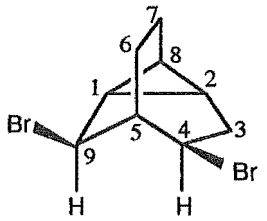

† The multiplet centred at 0.57 ppm was assigned as H3*endo* by consideration of its coupling constants with H2 and H4 ($^3J_{3endo,2}$ = $^3J_{3endo,4}$ = 5.8 Hz). The multiplet at 0.78 ppm (H3*exo*) was determined to be bonded to the same carbon as H3*endo* from the HMQC experiment and the presence of a 9.4 Hz coupling to H2 and H4 confirmed the *exo* orientation of this proton.

‡ The assignment of H3*exo* and H3*endo* was determined from the presence of a correlation from H3*exo* to H2 and the absence of any correlation of H3*endo* to H2 in the DQCOSY experiment. This is consistent

overlapping with H8). The presence of an internal cyclopropane ring was deduced from the number of ^{13}C signals at high field (although these carbons could not be assigned): 18.1, 16.1, 15.9, 14.4, and 14.0 ppm.† The presence of two CHBr groups was determined from the chemical shifts of C5 and C9 and from the chemical shifts of their attached protons H5 and H9. The stereochemistries of C4 and C9 were assigned as having *endo* and *anti* bromine substituents, respectively, from the presence of a 3.7% enhancement of H4 on irradiation of H9 in a difference nOe experiment. Irradiation of H4 in the reverse difference nOe experiment gave a 1.9% enhancement of H9 confirming the *exo* and *syn* orientations of these protons. Further support for the *exo* orientation of H4 came from the presence of a 10.7 Hz coupling to H3*endo* which is consistent with a *trans* arrangement of these protons.

The identity of 6-*exo*-7-*endo*-dibromo-*exo*-tricyclo[3.2.2.$0^{2,4}$]nonane **115** was established as follows: the ^{1}H-^{1}H connectivity was determined from a COSY experiment and a HETCOR established the ^{1}H-^{13}C one bond connectivities. The presence of a cyclopropane ring was determined from the COSY experiment and from consideration of the chemical shifts of C2 (9.2 ppm), C3 (6.3 ppm), and C4 (14.5 ppm) which reflect the characteristic shielding effects observed in cyclopropane rings. The orientation of the cyclopropyl group was determined as *exo* by the presence of 3.6% enhancement of H4 (1.10 ppm) on irradiation of H6 (4.53 ppm) in a difference nOe experiment (3.0% enhancement of H6 was observed on irradiation of H4 in the reverse nOe experiment). This also confirmed the *endo* orientation of H6 and hence an *exo* orientation of the C6 bromine substituent.§ The assignment of an *exo* orientation of the cyclopropane group was supported by the presence of a small coupling from H4 to H9*anti* (1.80 ppm, $^{4}J_{9anti,4}$ = 1.1 Hz), which is consistent with a 'W' arrangement of the two protons, and from the presence of an enhancement of H8*syn* (multiplet 1.43-1.54 ppm overlapping with H8*anti*) and H9*syn* (1.29 ppm)‡ on irradiation of H3*exo* in a difference nOe experiment. A 'W' coupling of 2.5 Hz was also observed between H6 and

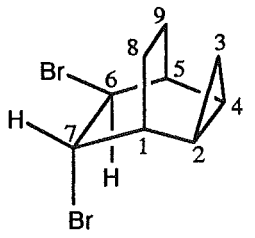

---

with the observations made from similar compounds obtained from the bromination of **47** in methanol (see Section 5.4.2).

† The ^{13}C signals listed are similar to those obtained for similar structures found from the bromination of **47** in methanol (see Section 5.4.2).

§ Carbons C6 and C7 were established as the carbons of CHBr groups from the observed chemical shifts (61.7 ppm and 61.1 ppm, respectively) and from the chemical shift of their attached protons H6 (4.53 ppm) and H7 (4.39 ppm).

‡ The size of the enhancement could not be measured due to the overlap of H8*syn* with H8*anti* and H9*syn* with H2.

H9*syn*, which further supports the *endo* and *syn* assignments of these protons. The stereochemistry of C7 was assigned as having an *endo* bromine substituent due to the lack of symmetry in the molecule (nine signals were observed in the ^{13}C NMR spectrum). This was also supported by the presence of only a small coupling from H6 to H7 ($^3J_{6,7}$ = 3.3 Hz) which would be inconsistent with a *cis* arrangement of the two protons. The shielding of C9 (17.3 ppm compared with 24.4 ppm for C8) and the deshielding of H2 (1.34 ppm compared to 1.10 ppm of H4) are also consistent with the stereochemical assignments of C6 and C7, respectively.

The identity of 5-*endo*-9-*syn*-dibromobicyclo[4.2.1]non-2-ene **116** was determined from the following: a COSY established the ^1H-^1H connectivity and a HETCOR established the one bond ^1H-^{13}C connectivities. The presence of a carbon-carbon double bond was deduced from the chemical shifts of C2 and C3 (137.0 ppm and 127.5 ppm, respectively) and from the chemical shifts of H2 and H3 (5.85 ppm and 5.59 ppm, respectively). Carbon signals at 56.6 ppm (C9) and 52.0 ppm (C5) with attached protons at 4.25 ppm (H9) and 4.74 ppm (C5) established the presence of two CHBr groups. The *syn* stereochemistry of the C9 bromine substituent was determined from the presence of a 6.7 Hz coupling of H9 to H1 and H6 which is consistent with an *anti* orientation of this proton. An *endo* orientation of the C5 bromine was assigned from consideration of the chemical shift of H5 (4.74 ppm) which is significantly deshielded from the chemical shift usually found for protons of a CHBr group and hence is consistent with the deshielding effect of the *syn* C9 bromine substituent, as was observed for H5 of **113**. The *exo* orientation of H5 was also supported by the presence of an 11.2 Hz coupling of this proton to H4*endo* (2.80 ppm)† which is consistent with a *trans* arrangement of these protons. The *endo* assignment of the C5 bromine is also supported by the chemical shift of C7 (23.7 ppm) which shows a 6.0 ppm upfield shift relative to C8 (29.7 ppm) and is consistent with an γ-eclipsed interaction with the C5 bromine substituent. Further support for the stereochemical assignment of C5 and for the overall structure assignment was gained from comparison of the observed coupling constants with those calculated for **116** and 5-*exo*-9-*syn*-

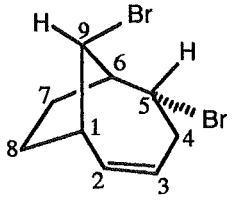

† The assignment of H4*endo* (2.80 ppm) and H4*exo* (2.70 ppm) was determined from the presence of an nOe (approximately 3% but could not be measured accurately due to the partial overlap of H4*endo* and H4*exo*) to H4*endo* on irradiation of H7*endo*/H8*exo* (multiplet 2.04-2.20 ppm) in a difference nOe experiment and from consideration of the coupling constants of H4*endo* and H4*exo* to H3 ($^3J_{4endo,3}$ = 3.3 Hz, $^3J_{4exo,3}$ = 8.5 Hz). The presence of a small coupling of H4*exo* to H6 ($^4J_{4exo,6}$ = 1.0 Hz) is consistent with a 'W' arrangement of these protons and hence an *exo* stereochemistry of the multiplet centred at 2.70 ppm..

dibromobicyclo[4.2.1]non-2-ene **117** (Table 5.1) from conformational searches using the BKM program. This program implements an empirical generalisation of the Karplus equation developed by Haasnoot et al.[155] for calculation of H-C(sp^3)-C(sp^3)-H couplings and the method of Garbisch[156] for calculation of H-C(sp^2)-C(sp^3)-H coupling constants. As can be seen from Table 5.1 the calculated coupling constants for **116** show a closer agreement (average error = 1.1 Hz) than do those calculated for **117** (average error = 2.3 Hz). The larger errors found in calculation of the three bond H-C(sp^2)-C(sp^3)-H coupling constants are consistent with the errors reported for other systems[156] and may reflect the deficiencies of this method when applied to systems of this type.

	Vicinal Coupling Constants (Hz)								
Compound	2,1	3,4*x*	3,4*n*	5,4*x*	5,4*n*	5,6	9,1	9,6	A.E.
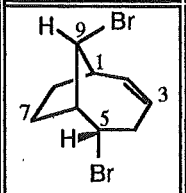 **116** Calc.	6.6 (2.1)	6.4 (2.2)	3.0 (0.4)	4.1 (1.1)	11.7 (0.5)	2.2 (0.2)	5.9 (0.8)	5.4 (1.3)	1.1
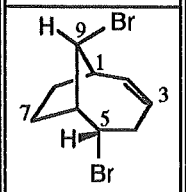 **116** Obs.	8.7	8.6	3.4	5.2	11.2	2.0	6.7	6.7	
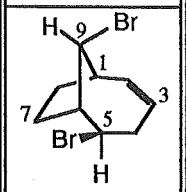 **117** Calc.	6.5 (2.2)	6.5 (2.1)	3.3 (0.1)	3.3 (1.5)	3.7 (7.5)	3.9 (1.9)	5.6 (1.1)	5.1 (1.6)	2.3

Table 5.1. Calculated vicinal coupling constants for **116** and **117** compared to those observed for **116**. A.E. = Average absolute error. Numbers in brackets are the absolute value of the differences between the observed and calculated values. All values are in Hertz. *x* = *exo*, *n* = *endo*.

Possible mechanisms for the formation of **113-116** are outline in Figure 5.7. The major product **113** appears to arise from *endo* addition of Br^+ to form a bromonium ion **118** or open carbocation **119** which rearranges to form the cyclopropylcarbinyl cation‡ **120**. Cation **120** then undergoes nucleophilic capture to give **113**. Nucleophilic attack to cation **120** appears to occur predominantly from the *endo* ("bottom") face of the cation.

‡ For reviews of cyclopropylcarbinyl cation species see references 157-159.

This may be due to the orientation of the vacant *p*-orbital of C5 and/or to a large amount of electronic or steric interaction of the incoming nucleophile with the C9 bromine substituent.† This has also been observed in the reactions of other tricyclo[4.2.1.$0^{2,4}$]-nonane derivatives.[101] Formation of **116** may occur either by acid catalyzed ring opening of **113** followed by elimination, or from opening of the cyclopropane ring in **120** to give cation **121** which then undergoes nucleophilic addition to give **116**.

Product **115** arises from *trans* addition of bromine to the alkene group of **47**. In this case both the electrophile and nucleophile are bromines (Br^+, Br^-) and hence the facial selectivity of addition to the double bond cannot be determined. The formation of structure **114** could proceed by either of the two mechanisms outline in Figure 5.7. Initial electrophilic attack could occur via *exo* addition of Br^+ to the alkene moiety to form bromonium ion **122** or the classical cation **123** which then undergoes rearrangement to give cation **124**. Nucleophilic addition of Br^- to **124** could then result in the formation of **114**. In the second pathway, electrophilic attack could occur at the cyclopropane ring to give cation **125** which then rearranges to give the cyclopropylcarbinyl stabilised cation **126**. Cation **126** may then undergo nucleophilic attack to give **114**. The former pathway may be more likely as bromine addition to the double bond is generally faster than to cyclopropanes; however, the second pathway cannot be completely discounted. Another possibility is that both mechanisms are operating to varying extents. For cations **120**, **121**, and **124** or **126** nucleophilic addition to the opposite face to that proposed for the formation of **113**, **116**, and **114**, respectively, cannot be excluded since approximately 15% of the reaction mixture was not accounted for. However, for **120** and **124** or **126** addition from the observed face to give products **113** and **114** must be the predominant trajectory due to the large proportion of these products formed.

Section 5.4.2 Bromination of *exo*-Tricyclo[3.2.2.$0^{2,4}$]non-6-ene in Methanol

The reaction of bromine (0.8 mole equivalents) with *exo*-tricyclo[3.2.2.$0^{2,4}$]non-6-ene **47** in methanol occurred rapidly at room temperature. Analysis of a ^{1}H NMR spectrum‡ of the crude reaction mixture showed the presence of three major products, 9-*syn*-bromo-5-*endo*-methoxy-*endo*-tricyclo[4.2.1.$0^{2,4}$]nonane **127** (34%), 4-*endo*-9-*anti*-dimethoxytricyclo[3.3.1.$0^{2,8}$]nonane **128** (24%), and 4-*endo*-9-*syn*-dimethoxy-tricyclo[3.3.1.$0^{2,8}$]nonane **129** (14%) (Figure 5.10). Numerous minor products were also present, of which the following were isolated, 4-*endo*-bromo-9-*anti*-methoxytri-

† This will be discussed in more detail in Chapter 8.

‡ GLC analysis of the crude reaction mixture using a variety of conditions proved unsuccessful due to the coincident retention times of a number of products. The product ratios were therefore estimated from integration of the methoxy signals in the ^{1}H NMR spectrum where possible.

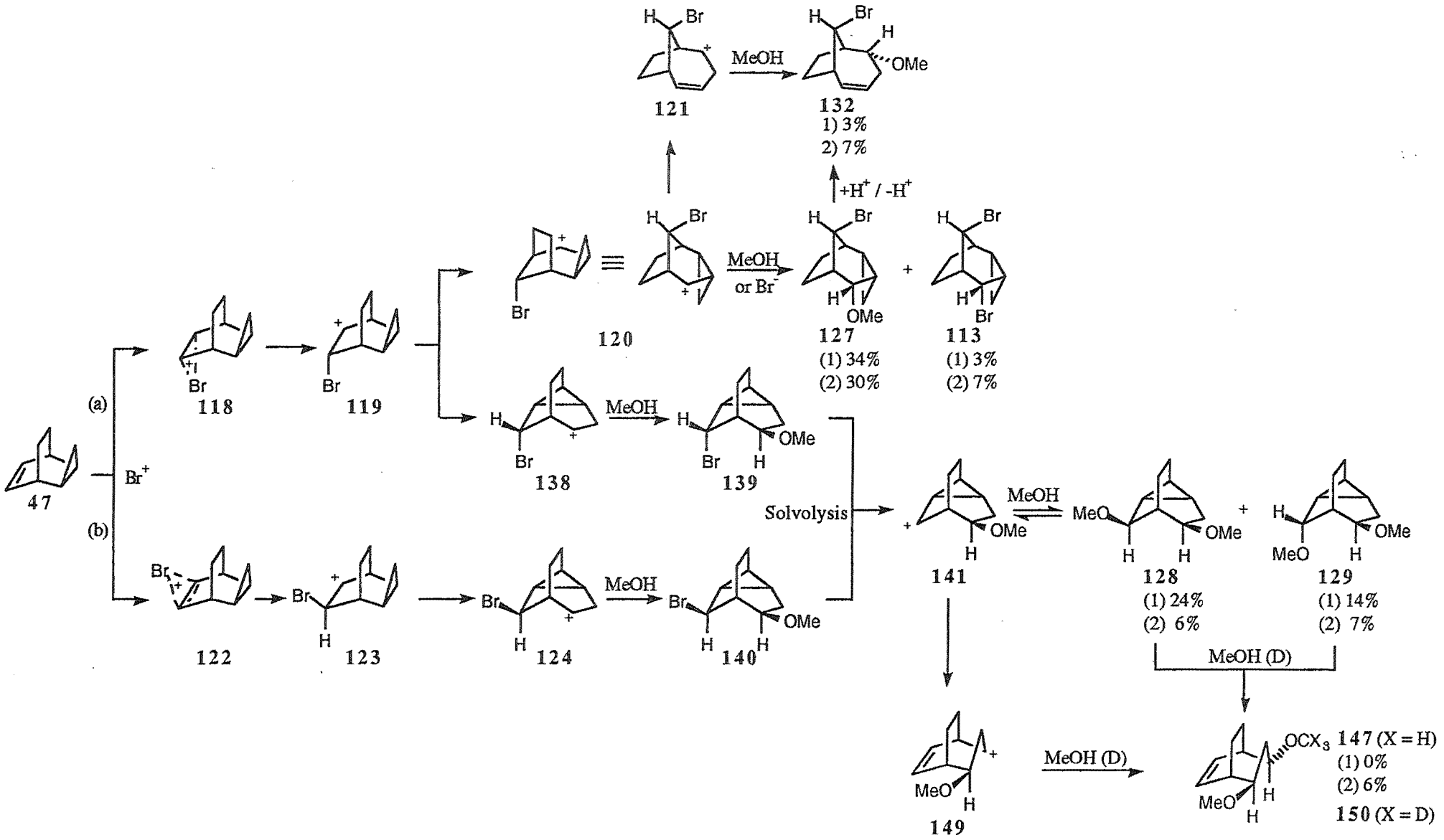

Figure 5.10. Possible mechanism for the bromination of *exo*-tricyclo[3.2.2.0^{2,4}]non-6-ene **47** at the alkene moiety in methanol at (1) room temperature and (2) 0 °C.

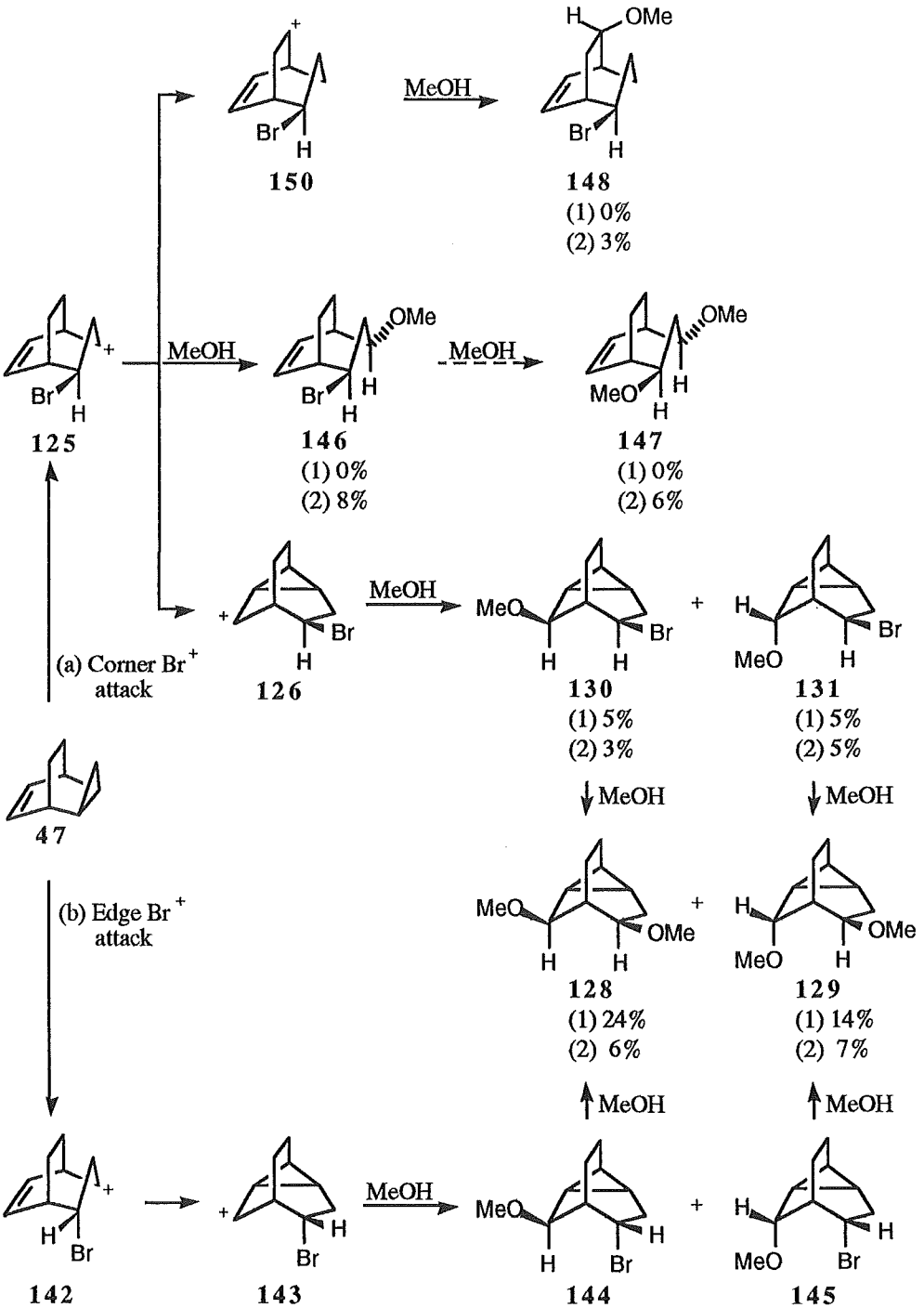

Figure 5.11. Possible mechanisms for product formation from bromination of *exo*-tricyclo[3.2.2.$0^{2,4}$]-non-6-ene at the cyclopropane ring in methanol at (1) room temperature and (2) 0 °C.

cyclo[3.3.1.$0^{2,8}$]nonane **130** (5%), 4-*endo*-bromo-9-*syn*-methoxytricyclo[3.3.1.$0^{2,8}$]-nonane **131** (5%), 9-*syn*-bromo-5-*endo*-methoxybicyclo[4.2.1]non-2-ene **132** (3%), and 5-*endo*-9-*syn*-dibromo-*endo*-tricyclo[4.2.1.$0^{2,4}$]nonane **113** (3%) (Figures 5.10 and 5.11). A crude separation of the products was obtained from radial chromatography on PEG coated silica.§ The resulting fractions were further purified by preparative gas liquid chromatography.

The identity of 9-*syn*-bromo-5-*endo*-methoxy-*endo*-tricyclo[4.2.1.$0^{2,4}$]nonane **127** was determined from the following: a DQCOSY experiment established the ^{1}H-^{1}H connectivity and an HMQC allowed determination of the one bond ^{1}H-^{13}C connectivities. A DEPT135 experiment established the carbon at 19.9 ppm (C7) to be part of a methylene group and the carbon at 19.6 ppm (C2) to be a methine carbon. An HMBC experiment confirmed the presence of a tricyclo[4.2.1.$0^{2,4}$]nonane carbon skeleton and also supported the assignment of C7 from a correlation observed from H5 (4.12 ppm) to the carbon signal at 19.9 ppm. The assignments of C7 and C8 had previously been assigned from the DQCOSY and HMQC experiments but due to the close proximity of H7*exo* (1.34 ppm) and H8*exo* (1.40 ppm) only tentative assignments could be made. The presence of CHBr and CHOMe groups was determined from the chemical shifts of C9 (56.5 ppm) and C5 (76.4 ppm) and from the chemical shifts of their associated protons at 4.04 ppm (H9) and 4.12 ppm (C5). The methoxy group appeared as a singlet at 3.40 ppm in the ^{1}H NMR with a corresponding carbon signal at 55.0 ppm in the proton decoupled ^{13}C NMR spectrum. The presence of a cyclopropane ring was determined from the DQCOSY experiment.

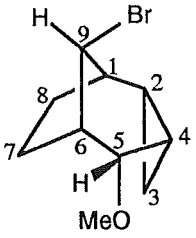

An nOe to the multiplet corresponding to H7*endo* and H8*endo* on irradiation of H3*endo*† in a difference nOe experiment indicated an *endo* orientation of the cyclopropane ring. The stereochemistry of C9 was determined from the coupling constants of H9 to H1 (2.63 ppm, $^{3}J_{9,1}$ = 4.9 Hz) and H6 (2.44 ppm, $^{3}J_{9,6}$ = 4.9 Hz) which were similar to those observed in **113** ($^{3}J_{9,1}$ = $^{3}J_{9,6}$ = 4.3 Hz). This therefore established an *anti* orientation of H9 and hence a *syn* configuration of the C9 bromine substituent. The stereochemistry of C5 was determined from the coupling constants of H5 to H4 and H6

---

§ Compounds **128** and **129** proved unstable to chromatography on silica gel and attempted separation by HPLC resulted in large handling losses on solvent removal due to the volatility of the compounds.

† The size of the nOe could not be measured accurately due to the partial overlap of H7*endo* and H8*endo* but was approximately 2%. The H3*endo* (0.44 ppm) and H3*exo* (0.58 ppm) protons were assigned on the basis of their coupling constants with H2 and H4 ($^{3}J_{3endo,2}$ = $^{3}J_{3endo,4}$ = 5.4 Hz, $^{3}J_{3exo,2}$ = $^{3}J_{3exo,4}$ = 8.8 Hz) and from the enhancement of H2 observed on irradiation of H3*endo* and H3*exo* in difference nOe experiments (0.9% and 2.9%, respectively).

($^3J_{5,4}$ = $^3J_{5,6}$ = 6.7 Hz) which are consistent with an *endo* orientation of the methoxy group and similar in magnitude to those observed in **113** ($^3J_{5,4}$ = 7.4 Hz, $^3J_{5,6}$ = 5.7 Hz). The assignment of an *exo* orientation to H5 was also consistent with the deshielding of this proton to 4.12 ppm due to a through space interaction with the C9 bromine substituent. Carbon C7 showed a 5.6 ppm upfield shift relative to C8 which is consistent with an equatorial orientation of the C5 methoxy group and shows a similar trend to that observed for C7 in **113** (2.2 ppm upfield shift).

For 4-*endo*-9-*anti*-dimethoxytricyclo[3.3.1.0^{2,8}]nonane **128** a DQCOSY (Figure 5.12a) in conjunction with selective proton decoupling experiments established the ^{1}H-^{1}H connectivity and an HMQC determined the one bond ^{1}H-^{13}C connectivities. An HMBC experiment supported the assignment of a tricyclo[3.3.1.0^{2,8}]nonane carbon skeleton. The presence of an internal cyclopropane ring was deduced from the DQCOSY and from consideration of the ^{13}C chemical shifts of C1 (13.7 ppm), C2 (11.4 ppm), and C8 (13.1 ppm) and from the chemical shifts of the attached protons 1.15 ppm (H1), 0.96 ppm (H2), and 0.97 ppm (H8). Due to the similarity in chemical shifts of C1 (13.7 ppm) and C6 (13.8 ppm) a DEPT135 experiment was performed to confirm the methine and methylene assignments of the two carbons.

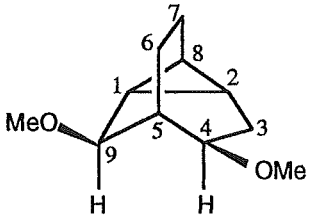

The presence of two CHOMe groups was established from signals at 76.7 ppm (C9) and 78.8 ppm (C4) in the ^{13}C NMR spectrum and from the chemical shifts of the attached protons at 3.57 ppm (H9) and 3.23 ppm (H4), respectively. The two methoxy groups were observed as singlets at 3.41 ppm and 3.31 ppm in the ^{1}H NMR and the corresponding carbons appeared at 55.6 ppm and 55.7 ppm, respectively, in the ^{13}C NMR spectrum. The stereochemical assignments of C4 and C9 were determined from the presence of a 3.0% enhancement of H4 on irradiation of H9 and 2.8% enhancement of H9 on irradiation of H4 in difference nOe experiments which established an *exo* orientation of H4 and a *syn* orientation of H9. This therefore requires *endo* and *anti* orientations of the C4 and C9 methoxy groups, respectively.

The identity of 4-*endo*-9-*syn*-dimethoxy[3.3.1.0^{2,8}]nonane **129** was determined as follows: an HMQC experiment determined the one bond ^{1}H-^{13}C connectivities and a DQCOSY in conjunction with selective decoupling experiments and an HMBC established the presence of a tricyclo[3.3.1.0^{2,8}]nonane carbon skeleton. The similarity of the correlations in the DQCOSY experiments of **129** (Figure 5.12b) and **128** (Figure 5.12a) also supported the assignment the general tricyclo-[3.3.1.0^{2,8}]nonane structure. The presence of two CHOMe groups was determined from the chemical shifts of C9 (78.7 ppm) and C4 (73.0 ppm) and from the chemical shifts of

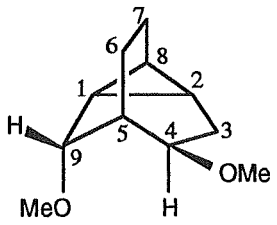

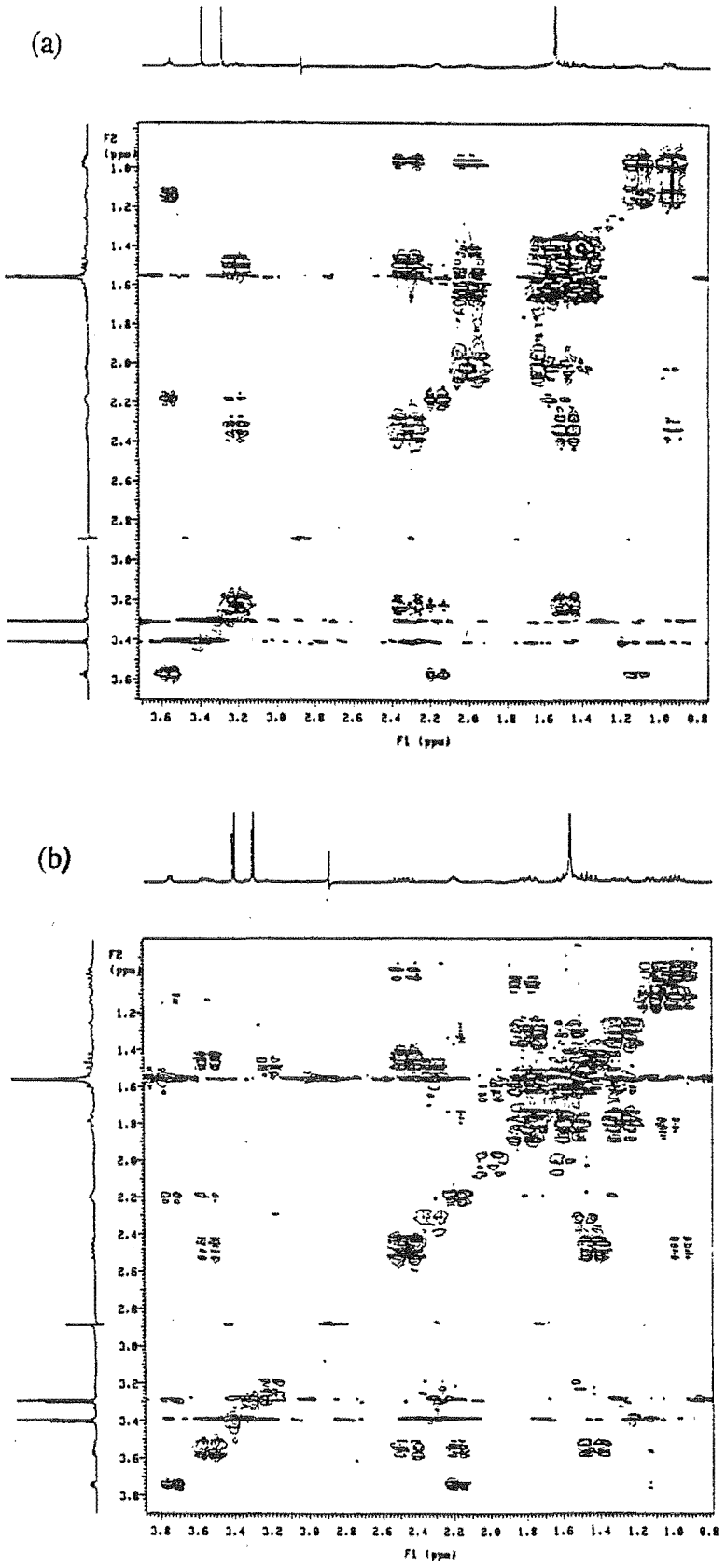

Figure 5.12. DQCOSY experiments of (a) 4-*endo*-9-*anti*-dimethoxytricyclo[3.3.1.$0^{2,8}$]nonane **128** and (b) 4-*endo*-9-*syn*-dimethoxytricyclo[3.3.1.$0^{2,8}$]nonane **129**

the associated protons at 3.75 ppm (H9) and 3.55 ppm (H4), respectively. The stereochemistry of C9 was assigned from the presence of a 2.3% enhancement of H9 on irradiation of H6*exo* (1.32 ppm)‡ in a difference nOe experiment which established an *anti* orientation of H9 and also confirmed the *exo* orientation of the multiplet at 1.32 ppm in the ^{1}H NMR spectrum as H6*exo*. A 1.2% enhancement of H6*exo* was observed on irradiation of H9 in the reverse difference nOe experiment. This therefore established a *syn* orientation of the C9 methoxy substituent. Consideration of the coupling constants of H4 to H5 (2.21 ppm), H3*endo* (1.46 ppm), and H3*exo* (2.48 ppm) ($^3J_{4,5}$ = 4.2 Hz, $^3J_{4,3exo}$ = 9.2 Hz, $^3J_{4,3endo}$ = 7.7 Hz) and of H2 (1.00 ppm) to H3*endo* and H3*exo* ($^3J_{3endo,2}$ < 1.0 Hz, $^3J_{3exo,2}$ = 6.8 Hz) established the *exo* orientation of H4 and hence an *endo* orientation of the C4 methoxy group. The chemical shift of C6 (21.4 ppm) showed a downfield shift of 7.6 ppm from the equivalent carbon in **128** (13.8 ppm) which supports the assignment of a *syn* configuration of the C9 methoxy group due to the loss of a γ-eclipsed interaction of the methoxy group with C6.† Similar sized shielding effects have been observed for γ-eclipsed interactions in bicyclo[2.2.2]octan-2-ol (7.5 ppm upfield shift) and in bicyclo[3.3.1]nonan-9-ol (7.0 ppm upfield shift) (see Figure 5.13).

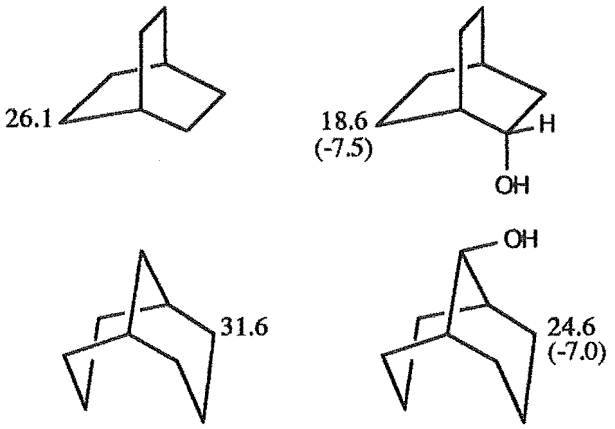

Figure 5.13. Effects of a γ-eclipsed interaction of an hydroxy group on ^{13}C chemical shifts in bicyclo-[2.2.2]octane and bicyclo[3.3.1]nonane systems.

Further support for the structure assignments of **128** and **129** came from comparison of the coupling constants observed from the two products with those calculated for the four 4,9-dimethoxytricyclo[3.3.1.0^{2,8}]nonane isomers **128**, **129**, **133**, and **134** (Table 5.2). For each isomer the conformational space was searched using

---

‡ Established as being bonded to C6 from the HMQC experiment.

† The parent compound tricyclo[3.3.1.0^{2,8}]nonane has been synthesised[160] but the ^{13}C NMR has not been reported and hence the chemical shift of C6 in **128** and **129** could not be compared with the chemical shift of C6 in the parent compound.

Monte Carlo mechanics techniques. In each case the smallest average error is obtained for the assigned structure with respect to the calculated values (0.5 Hz average error between the calculated and observed coupling constants for **129** and a 0.4 Hz average error for **128**). The calculated coupling constants in conjunction with the nOe data outlined earlier serve to exclude the other possible structures. For compound **129** the larger difference in calculated and observed coupling constants for $^3J_{3endo,4}$ may be due to to the calculation method, which was derived empirically[155] without a good representative number of bicyclic and tricyclic molecules. The effects of substituent orientation on the size of the coupling constants may therefore not be well represented in these systems.[155]

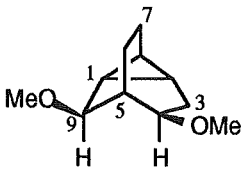

128

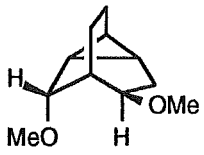

129

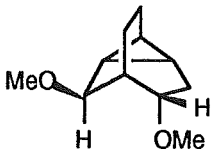

133

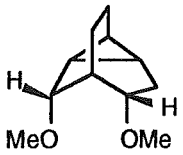

134

Compound	^3J Vicinal Coupling Constants							
	3*n*,2	3*n*,4	3*x*,2	3*x*,4	4,5	9,1	9,5	A.E.
128 Obs.	NO	8.8	NM	8.8	3.0	3.7	3.7	
128 Calc.		8.7	8.2	7.5	2.9	4.0	3.4	
		(0.1)	(---)	(1.3)	(0.1)	(0.3)	(0.3)	(0.4)
		[0.9]	[1.4]	[1.8]	[1.3]	[0.6]	[0.0]	[1.0]
133 Calc.	1.6	6.4	7.6	2.6	3.3	4.0	3.3	
		(2.4)	(---)	(6.2)	(0.3)	(0.3)	(0.4)	(1.9)
		[1.4]	[0.8]	[6.7]	[0.9]	[0.6]	[0.1]	[1.8]
134 Calc.	3.4	9.0	3.7	5.9	0.9	4.3	3.8	
		(0.2)	(---)	(2.9)	(2.1)	(0.6)	(0.1)	(1.2)
		[1.2]	[3.1]	[3.4]	[3.3]	[0.9]	[0.4]	[2.1]
129 Calc.	1.3	5.5	6.8	9.2	4.4	3.7	3.5	
		(3.3)	(1.4)	(0.4)	(1.4)	(0.0)	(0.2)	(1.1)
		[2.3]	[0.0]	[0.1]	[0.2]	[0.3]	[0.1]	[0.5]†
129 Obs.	NO	7.8	6.8	9.3	4.2	3.4	3.4	

Table 5.2. Comparison of observed and calculated coupling constants of products **128** and **129** with the four 4,9-dimethoxytricyclo[3.3.1.$0^{2,8}$]nonane isomers.

A.E. = average error = $\frac{\Sigma\,|\text{Calc.} - \text{Obs.}|}{\text{number coupling constants observed}}$, Obs. = Observed, Calc. = Calculated, NO = none observed, NM = could not be measured, *x* = *exo*, *n* = *endo*. Numbers in curved brackets '( )' and square brackets '[ ]' are the absolute value of the differences from the observed values for **128** and **129**, respectively.

† = Average error is 0.1 Hz if $^3J_{3endo,4}$ is ignored.

The identity of 4-*endo*-bromo-9-*anti*-methoxytricyclo[3.3.1.$0^{2,8}$]nonane **130** was determined from the following: a DQCOSY experiment established the ^{1}H-^{1}H connectivity and an HMQC established the ^{1}H-^{13}C one bond connectivities. The general tricyclo-[3.3.1.$0^{2,8}$]nonane structure was determined from the DQCOSY experiment and supported by the correlations observed in an HMBC experiment. The presence of the CHBr and CHOMe groups was determined from the chemical shifts of C4 (52.0 ppm) and C9 (76.9 ppm) and from the chemical shifts of the corresponding protons H4 (4.09 ppm) and H9 (3.64 ppm). The methoxy group was evident as a singlet ($W_{h/2}$ = 0.7 Hz) at 3.39 ppm in the ^{1}H NMR and as a signal at 55.8 ppm in the ^{13}C NMR spectrum. The stereochemistry of C4 and C9 was determined from the presence of a 3.2% enhancement of H4 on irradiation of H9 in a difference nOe experiment, with a 2.8 % enhancement of H9 observed on irradiation of H4 in a further difference nOe experiment. The nOe results are therefore consistent with *syn* and *exo* orientations of H9 and H4, respectively. This therefore requires an *anti* configuration of the methoxy group of C9 and an *endo* orientation of the bromine substituent of C4. The chemical shift of C6 (ca. 14.7 ppm)‡ is similar to that observed for C6 (13.8 ppm) of **128**, which had *anti* and *endo* orientations of the C9 and C4 methoxy groups, and hence is consistent with the stereochemical assignments determined from the nOe experiments.

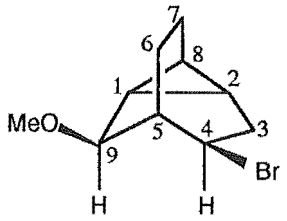

For 4-*endo*-bromo-9-*syn*-methoxytricyclo[3.3.1.$0^{2,8}$]nonane **131** a DQCOSY established the proton-proton connectivity and an HMQC established the one bond proton-carbon connectivities. A DEPT135 experiment showed the carbon at 14.9 ppm (C7) to be part of a methylene group and the signal at 14.5 ppm to be a methine carbon (C8). The presence of a CHBr group at C4 was determined from the presence of a ^{13}C signal at 49.5 ppm with its attached proton at 4.56 ppm in the ^{1}H NMR. A CHOMe group was determined to be present from the appearance of a ^{13}C signal at 78.7 ppm (C9) with an attached proton at 3.76 ppm (H9). The stereochemistry of C9 was determined from the presence of an enhancement of H6*exo* (1.51 ppm) on irradiation of H9 in a difference nOe experiment.† Examination of the

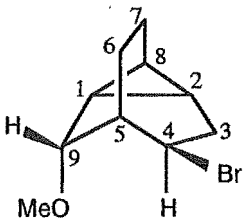

‡ Carbons C6 and C7 could not be differentiated due to the similarity of their chemical shifts (14.7_6 ppm and 14.7_2 ppm) and of the similar chemical shifts of their attached protons (multiplet 1.65-1.78 ppm corresponding to H6*endo*, H6*exo*, and H7*endo*).

† The size of the enhancement of H6*exo* could not be measured due to the presence of water in the ^{1}H NMR spectrum which partially obscured the H6*exo* multiplet. Irradiation of H6*exo* gave a 1.6% enhancement of H9 in a further difference nOe experiment.

coupling constants of H4 to H5, H3*endo*, H3*exo* and from H3*endo* and H3*exo* to H2 determined an *exo* orientation of H4 and hence an *endo* orientation of the C4 bromine substituent.§ An *exo* orientation of H4 was also supported by the presence of a small coupling to H6*exo* ($^4J_{4,6exo}$ = 1.0 Hz) which is consistent with the proposed 'W' arrangement of these protons; however, the size of the coupling constant is too small to rule out other possible coupling pathways, such as 'sickle' or 'fork' couplings which may be as large as 1.5 Hz.[108] The 8.0 ppm downfield shift of C6 (22.7 ppm) relative to C6 (ca. 14.7 ppm) of **130** is also consistent with elimination of a γ-eclipsed interaction with one of the substituents at C9 or C4. This is similar to the 7.6 ppm downfield shift observed for C6 in **129** relative to C6 in **128**.

Further support for the structure of **131** came from comparison of the observed coupling constants for this molecule with those calculated for the four possible isomeric 4-bromo-9-methoxytricyclo[3.3.1.$0^{2,8}$]nonane structures **130**, **131**, **135**, and **136** (Table 5.3). The conformational space of each isomer was searched using Monte Carlo molecular mechanics techniques. The coupling constants reported are the Boltzman averaged coupling constants from the conformations of each isomer found within a 12.5 kJ mol^{-1} energy window. For both structures **130** and **131** the calculated coupling constants are in best agreement with the observed values for the structures assigned, with average errors between the calculated and observed coupling constants of 0.6 Hz and 0.7 Hz, respectively.

Table 5.4 summarises the ^{13}C chemical shifts observed for compounds **128**, **129**, **130**, and **131** and shows the similarity in chemical shifts of this series of compounds. Of particular note, as mentioned previously, is the chemical shift of C6 in the four compounds which reflects the shielding of this carbon due to the number of γ-eclipsed interactions with the C4 and C9 substituents (two for **128** and **130** and one for **129** and **131**). Both C3 and C5 are approximately 5 ppm further downfield in **130** (28.6 ppm, 39.2 ppm) and **131** (28.7 ppm, 39.3 ppm) than in **128** (23.7 ppm, 33.9 ppm) and **129** (23.9 ppm, 34.0 ppm) and hence reflects the larger β inductive effect of the bromine substituent than that of the methoxy substituent at C4.[106]

The similarity of the chemical shifts of C3 and C5 in **128** and **129**, and in **130** and **131** also supports the constant assignment of an *exo* substituent at C4 for each pair as a change from an *exo* to *endo* orientation would be expected to result in a significant change in chemical shift of carbons C3 and C5.[106]

---

§ The relevant coupling constants are : $^3J_{4,5}$ = 2.9 Hz, $^3J_{4,3endo}$ = $^3J_{4,3exo}$ = 9.3 Hz, $^3J_{3exo,2}$ = 7.1 Hz; the coupling of H3*endo* to H2 was small and could not be resolved (< 1.0 Hz).

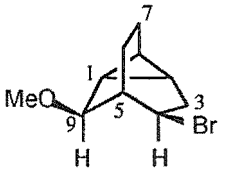

130

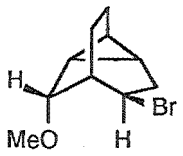

131

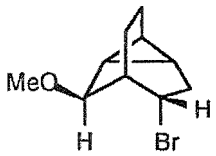

135

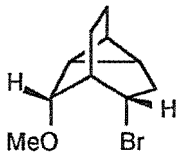

136

Compound	Vicinal Coupling constants (Hz)									
	3*endo*,2	3*exo*,2	4,3*endo*	4,3*exo*	4,5	7*endo*,6*endo*	7*endo*,6*exo*	9,1	9,5	A.E.
130 Obs.	NO	NM	10.4	8.6	2.4	NM	NM	3.9	3.9	
130 Calc.	1.0	8.7 (---) [1.6]	10.3 (0.1) [1.0]	6.3 (2.3) [3.0]	2.3 (0.1) [0.6]	11.9 (---) [2.8]	2.8 (---) [6.3]	4.3 (0.4) [0.9]	3.6 (0.3) [0.2]	(0.6) [2.1]
135 Calc.	1.0	9.0 (---) [1.9]	6.3 (4.1) [3.0]	1.5 (7.1) [7.8]	3.7 (1.3) [0.8]	11.8 (---) [2.7]	2.5 (---) [6.6]	4.6 (0.7) [1.2]	3.8 (0.1) [0.4]	(2.7) [3.1]
136 Calc.	3.6	3.5 (---) [3.6]	7.0 (3.4) [2.3]	9.0 (0.4) [0.3]	0.8 (1.6) [2.1]	7.1 (---) [2.0]	11.3 (---)[2.2]	4.4 (0.5) [1.0]	3.9 (0.0) [0.5]	(1.2) [1.8]
131 Calc.	1.0	7.8 (---) [0.7]	8.2 (2.2) [1.1]	8.1 (0.5) [1.2]	3.3 (0.9) [0.4]	9.7 (---) [0.6]	8.3 (---) [0.8]	3.3 (0.6) [0.1]	3.1 (0.8) [0.3]	(1.0) [0.7]
131 Obs.	NO	7.1	9.3	9.3	2.9	9.1	9.1	3.4	3.4	

Table 5.3. Comparison of the calculated and observed coupling constants of **130** and **131** with the four possible 4-bromo-9-methoxytricyclo[3.3.1.$0^{2,4}$]nonane isomers. A.E. = average error = $\frac{\Sigma\ |\text{Calc.} - \text{Obs.}|}{\text{number coupling constants observed}}$, Obs. = Observed, Calc. = Calculated, NO = none observed, NM = could not be measured. Numbers in curved brackets '( )' and square brackets '[ ]' are the absolute value of the differences from the observed values for **130** and **131**, respectively.

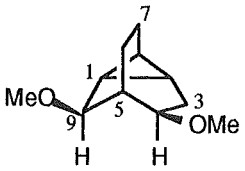

128

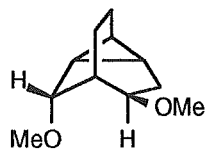

129

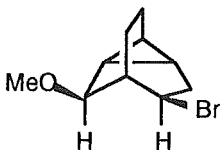

130

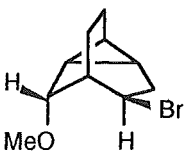

131

Cmpd.	^{13}C Chemical Shifts (ppm, $CDCl_3$)								
	C1	C2	C3	C4	C5	C6	C7	C8	C9
128	13.7	11.4	23.7	78.8	33.9	13.8	15.0	13.1	76.7
129	13.5	11.6	23.9	73.0 (-5.8)*	34.0	21.4 (7.6)*	15.2	14.7	78.7
130	13.4	13.2	28.6	52.0	39.2	14.7	14.7	14.3	76.9
131	13.0	14.0	28.7	49.5 (-2.5)†	39.3	22.7 (8.0)†	14.9	14.5	78.7

Table 5.4. Comparison of ^{13}C chemical shifts of **128**, **129**, **130**, and **131**.

* Δδ values from the equivalent carbons of **128**. † Δδ values from the equivalent carbons in **130**.

The identity of 9-*syn*-bromo-5-*endo*-methoxybicyclo[4.2.1]non-2-ene **132** was determined from an enriched mixture (ca 70:30) of this compound with **127** as they were not separated after attempts at purification by preparative GLC and repeated column or radial chromatography. A DQCOSY in conjunction with 1D-TOCSY experiments established the ^{1}H-^{1}H connectivity and an HMQC determined the one bond ^{1}H-^{13}C assignments. The presence of an alkene group was identified from the ^{13}C chemical shifts of C2 (136.2 ppm) and C3 (125.3 ppm) and from the chemical shifts of the associated protons H2 (5.84 ppm) and H3 (5.63 ppm) and a CHBr group was identified from the chemical shifts of C9 (55.8 ppm) and H9 (4.31 ppm). A CHOMe group was evident from the chemical shifts of C5 (75.9 ppm) and H5 (3.63 ppm). The presence of a methoxy group was shown by the appearance of a singlet in the ^{1}H NMR at 3.35 ppm and a ^{13}C resonance at 56.9 ppm.

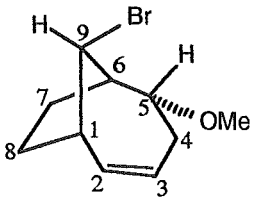

The *anti* orientation of H9 was determined from examination of its coupling constants with H1 and H6 ($^3J_{9,1}$ = $^3J_{9,6}$ = 6.9 Hz) and therefore established a *syn* orientation of the bromine substituent of C9. The presence of a small nOe (1.5%) to the multiplet at 2.26 ppm, which had previously been assigned to a proton of the C4

methylene group, on irradiation of H7*endo* (2.00 ppm)‡ assigned this multiplet as H4*endo* and confirmed the assignment of the multiplet centred at 2.00 ppm as H7*endo*. A 1.2% enhancement of H7*endo* was observed on irradiation of H4*endo* in the reverse difference nOe experiment. The *endo* orientation of the proton multiplet at 2.26 ppm was also consistent with the observed coupling constants of this proton (H4*endo*) and H4*exo* (2.43 ppm) to H3 ($^3J_{4endo,3}$ = 3.1 Hz, $^3J_{3,4endo}$ =3.2 Hz, $^3J_{3,4exo}$ = 8.8 Hz). Carbon C5 was assigned as having an *endo* orientation of the methoxy substituent by examination of the coupling constants of H5 to H6, H4*exo*, and H4*endo* ($^3J_{5,6}$ = 2.5 Hz, $^3J_{5,4exo}$ = 4.4 Hz, $^3J_{5,4endo}$ = 10.7 Hz). A 10.7 Hz coupling of H5 to H4*endo* indicated a *trans* arrangement of the two protons and hence an *exo* orientation of H5. Further support for the structure assignment of **132** and for the stereochemistry of C5 was gained from comparison of the coupling constants observed for this structure with those of compound **116** and from comparison of the observed coupling constants with those calculated for the geometries resulting from molecular mechanics conformational searches of **132** and its isomer 9-*syn*-bromo-5-*exo*-methoxybicyclo[4.2.1]non-2-ene **137** (Table 5.5). The average deviation of the calculated coupling constants from those observed for **132** is 1.0 Hz compared with an average deviation of 2.2 Hz for **137**. Of particular note is the coupling constant of H5 to H4*endo* which shows a 0.5 Hz deviation between the observed and calculated values for **132** but shows a large 8.1 Hz error for **137**.

Possible mechanisms for the formation of the products obtained from bromination of **47** in methanol at room temperature are outlined in Figures 5.10 and 5.11. Figure 5.10 shows possible mechanisms for product formation if bromine addition occurs to the double bond. Some products may also arise from electrophilic attack at the cyclopropane ring and these mechanisms are summarised in Figure 5.11.

Formation of **127** and **132** (Figure 5.10) may occur by similar mechanisms to those outlined for the formation of **113** and **116** (Figure 5.7), in this case a small amount of product arising from Br^- addition was also identified (**113**, 3%). The other major products obtained showed no indication of the presence of a bromine substituent (^1H, ^{13}C NMR, mass spectroscopic analysis) and thus appear to have arisen from further reaction with methanol which displaced the bromine substituent. Figure 5.10 outlines a number of possible pathways for the formation of **128** and **129** whereby reaction with bromine may occur by either *exo* or *endo* addition to the double bond resulting in the formation of cations **118** or **122** which undergo rearrangement to give **138** and **124**, respectively. Nucleophilic attack of methanol then gives **139** and **140**, respectively.

---

‡ H7*endo* (2.00 ppm) was determined from the HMQC to be one proton of the C7 methylene and was assigned an *endo* configuration due to the lack of a correlation to H6 in the DQCOSY. A correlation of H6 to H7*exo* (1.71 ppm) was observed.

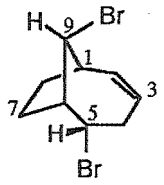

116

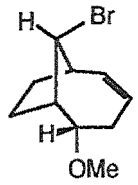

132

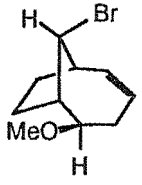

137

Compound	Vicinal Coupling Constants (Hz)								
	2,1	3,4*endo*	3,4*exo*	4*endo*,5	4*exo*,5	5,6	6,9	9,1	A.E.
116 Obs.	8.7	3.4	8.6	11.2	5.2	2.0	6.7	6.7	
132 Obs.	8.3	3.2	8.8	10.7	4.4	2.5	6.9	6.9	
132 Calc.	6.6 (1.7)	3.0 (0.2)	6.5 (2.3)	11.2 (0.5)	4.3 (0.1)	2.1 (0.4)	5.5 (1.4)	5.8 (1.1)	1.0
137 Calc.	6.5 (1.8)	3.3 (0.1)	6.5 (2.3)	2.6 (8.1)	4.1 (0.3)	4.5 (2.0)	5.3 (1.6)	5.6 (1.3)	2.2

Table 5.5. Comparison of coupling constants observed for **116** and **132** and of the calculated values for **132** and **137**. Numbers in brackets are the absolute differences of observed and calculated values. A.E. = Average Error = $\frac{\Sigma\ |\text{Calc.} - \text{Obs.}|}{\text{number coupling constants observed}}$, Obs. = Observed, Calc. = Calculated.

Compounds **139** and **140** may not be stable to the reaction conditions and could undergo solvolysis to the cyclopropylcarbinyl stabilised cation **141** which adds methanol to give products **128** and **129**, with a small preference for *anti* attack favoured (*anti*:*syn* ratio 1.7:1).‡ However, due to elimination of the bromine substituent any information about the regiochemistry of electrophilic attack leading to the formation of **128** and **129** could not be ascertained and hence the possibility of electrophilic attack of bromine to the cyclopropyl group (Figure 5.11) could not be ruled out. The mechanism shown in Figure 5.11 path (a) shows the derivation of **128** and **129** from corner attack of bromine at the cyclopropyl group of **47** to give cation **125** which then rearranges to give **126** and undergoes nucleophilic capture to form products **130** and **131**. Solvolysis of the C4 bromine substituent could give rise to **128** and **129**, respectively. The possibility of edge attack of bromine at the cyclopropane ring (Figure 5.11 path (b)) followed by rearrangement and nucleophilic capture of cations **142** and **143**, respectively, could give rise to **144** and **145** which may undergo solvolysis to form **128** and **129**. No products with an orientation of bromine at C4 that could have arisen from edge bromine addition were isolated (although not all of the reaction mixture was accounted for) and hence this pathway seems less likely than that of pathway (a) in Figure 5.11.§ Solvolysis of the bromine substituent of C4 in **130/131** and **144/145** would be expected to be a less facile process than solvolysis of the C9 bromine substituent of **139** and **140** as formation of a stabilised cyclopropylcarbinyl cation intermediate would not occur. However, the ability of a cation to reach planarity may be enhanced at the C4 position relative to the C9 position and this may offset the stabilising effect of the cyclopropylcarbinyl cation to some extent.

In an attempt to stop the solvolysis processes, the reaction of **47** with bromine in methanol was repeated at 0 °C. In this case a complex reaction mixture was obtained which was identified as containing,† 9-*syn*-bromo-5-*endo*-methoxy-*endo*-bicyclo-[4.2.1.$0^{2,4}$]nonane **127** (30%), 2-*exo*-bromo-4-*exo*-methoxybicyclo[3.2.2]non-6-ene

---

‡ For a discussion of solvolysis reactions involving cyclopropylcarbinyl cations and the factors which effect the rate of reaction and the stereochemical outcome see reference 158 and references cited therein.

§ This is supported by the results obtained from bromination of *endo*- and *exo*-tricyclo[3.2.1.$0^{2,4}$]octane (**1** and **46**, respectively) and 2-methyl-*endo*-tricyclo[3.2.1.$0^{2,4}$]octane **45** which occurred via corner attack. However, the effect of a double bond, in this geometric relationship to the cyclopropane ring, on edge bromination has not been determined.

† GLC analysis of the crude reaction mixture showed the presence of one major product and numerous minor products but due to the overlap of the peaks a reliable estimate of the product ratios could not be obtained. The product composition was therefore estimated from a ^{1}H NMR spectrum of the reaction mixture by integration of the methoxy peaks where possible.

146 (8%), 4-*endo*-9-*syn*-dimethoxytricyclo[3.3.1.$0^{2,8}$]nonane **129** (7%), 9-*syn*-bromo-5-*endo*-methoxybicyclo[4.2.1]non-2-ene **132** (7%), 5-*endo*-9-*syn*-dibromo-*endo*-tricyclo[4.2.1.$0^{2,4}$]nonane **113** (7%), 2-*exo*-4-*exo*-dimethoxybicyclo[3.2.2]non-6-ene **147** (6%), 4-*endo*-9-*anti*-dimethoxytricyclo[3.3.1.$0^{2,8}$]nonane **128** (6%), 4-*endo*-bromo-9-*syn*-methoxytricyclo[3.3.1.$0^{2,8}$]nonane **131** (5%), 4-*endo*-bromo-9-*anti*-methoxytricyclo[3.3.1.$0^{2,8}$]nonane **130** (3%), and 2-*exo*-bromo-9-*syn*-methoxy-bicyclo-[3.2.2]non-6-ene **148** (3%). A crude separation was effected by radial chromatography on PEG coated silica. Further purification by preparative GLC gave compounds **127, 128, 129, 130, 131,** and **147.** TLC mesh column chromatography of fractions obtained from the radial chromatography gave compounds **146** and **148.** Compounds **113, 127, 128, 129, 130, 131,** and **132** were identified by comparison of their ^{1}H NMR with those products isolated from the reaction of **47** with bromine in methanol at room temperature.

The identity of 2-*exo*-bromo-4-*exo*-methoxybicyclo[3.2.2]non-6-ene **146** was determined from the following: a DQCOSY established the ^{1}H-^{1}H connectivity as far as possible and an HMQC established the one bond ^{1}H-^{13}C connectivities. The carbon signals at 19.7_2 ppm and 19.6_8 ppm assigned to C8 or C9 could not be distinguished in the HMQC experiment due to the similarity of their chemical shifts. An HMBC showed a correlation from H9*syn* (2.02 ppm) to C6 (133.3 ppm) and allowed assignment of C6 and C7 (133.7 ppm) whose protons were overlapping (multiplet 6.13-6.17 ppm, H6 and H7). The presence of a CHBr group was established from the chemical shifts of C2 (52.7 ppm) and H2 (4.17 ppm). Likewise, the presence of a CHOMe group was established from the ^{13}C and ^{1}H chemical shifts of C4 (78.8 ppm) and H4 (3.08 ppm). The methoxy group appeared as a singlet in the ^{1}H NMR at 3.29 ppm with its associated carbon at 56.3 ppm in the ^{13}C NMR spectrum. The connectivity of H2 to H1 and H4 to H5 was determined from difference nOe experiments and a correlation of H9*syn* to C4 in an HMBC experiment confirmed the connectivity of H9*syn*-C9-C5-C4.

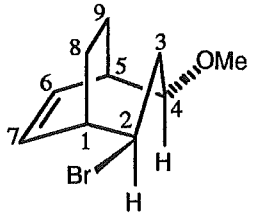

A 2.1% enhancement of the proton centred at 2.28 ppm, which had previously been assigned as a proton of the C3 methylene group, on irradiation of H9*syn* established this proton as H3*exo*. The reverse irradiation of H3*exo* showed an enhancement of H9*syn* but due to the close proximity of H3*exo* and H8*syn* (2.18 ppm), which would also be expected to give an enhancement of H9*syn*, the enhancement could not be measured accurately. The lack of coupling of H2 (4.17 ppm) to H1 (2.73 ppm) and H4 (3.08 ppm) to H5 (2.50 ppm) established an axial orientation of these protons. The multiplicity of H3*exo* as a doublet of triplets was established from a 1D-TOCSY experiment on irradiation of H2 and allowed calculation of the coupling constant of H3*exo* to H3*endo*

($^2J_{3endo,3exo}$ = 13.2 Hz, $^3J_{3exo,3endo}$ = 13.2 Hz) and confirmed the values of the coupling constants calculated from H2 and H4 to H3*exo* ($^3J_{2,3exo}$ = 11.7 Hz, $^3J_{4,3exo}$ = 10.8 Hz, $^3J_{3exo,2} = {}^3J_{3exo,4}$ = 11.2 Hz). The 11 Hz coupling of H3*exo* to H2 and H4 established a *trans* arrangement of these protons and hence an *endo* orientation of H2 and H4. This therefore requires an *exo* orientation of the bromine substituent of C2 and the methoxy group of C4. The similarity of the coupling constants of H2 and H4 to H3*endo* and H3*exo* are consistent with both protons having the same orientation and the similar chemical shifts of C6 and C7 are consistent with both the methoxy and bromine substituents having similar orientations.

For 2-*exo*-4-*exo*-dimethoxybicyclo[3.2.2]non-6-ene **147** the appearance of only six carbons in the ^{13}C NMR spectrum indicated the presence of symmetry in the molecule. A DQCOSY established the proton-proton connectivity and identified the presence of two nonequivalent methylene groups. Integration of an ^{1}H NMR spectrum of **147** showed the methylene groups to be present in a 2:1 ratio. This therefore established the presence of three methylene groups in the molecule, two of which were equivalent. The ^{1}H-^{13}C assignment was determined by examination of the ^{13}C and ^{1}H chemical shifts and by comparison with similar molecules. The presence of two equivalent CHOMe groups was determined from the integration of the proton NMR spectrum and were identified from the chemical shifts of C2/C4 (78.8 ppm) and those of H2/H4 (3.11 ppm). A signal corresponding to the methoxy groups was evident as a singlet in the ^{1}H NMR spectrum at 3.31 ppm and that of the corresponding carbons at 56.2 ppm. An alkene moiety was evident from the chemical shifts of C6/C7 at 132.8 ppm and of H6/H7 at 6.11 ppm. The absence of a significant coupling of H1/H5 (2.46 ppm) to H2/H4 determined an axial orientation of H2/H4.

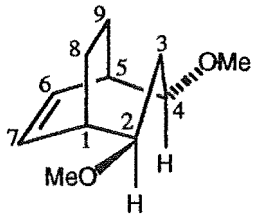

A 3.5% enhancement of the multiplet at 1.61 ppm‡ on irradiation of the multiplet at 1.91 ppm in a difference nOe experiment confirmed an *exo* orientation of the H3 proton at 1.61 ppm (H3*exo*) and a *syn* orientation of the protons at 1.91 ppm (H8*syn*/H9*syn*). The reverse irradiation of H3*exo* in a difference nOe experiment was not attempted† due to the partial overlap of H3*exo* with H8*anti*/H9*anti* (1.52 ppm). The stereochemistry of C2 and C4 was determined from consideration of the coupling constants of H2/H4 to

---

‡ The assignment of the multiplet at 1.61 ppm as an H3 proton was determined from the presence of a strong coupling of this proton to the multiplet at 2.40 ppm (H3*endo*). The chemical shift of both of these protons is consistent with the C3 position of the carbon skeleton due to the deshielding effects expected from the methoxy groups of C2 and C4.

† The nOe to H3*exo* on irradiation of H8*syn*/H9*syn* was clearly evident from the part of the H3*exo* multiplet that was not overlapping with H8*anti*/H9*anti*.

H3*endo* and H3*exo* ($^3J_{2,3endo} = {}^3J_{4,3endo} = 5.1$ Hz, $^3J_{2,3exo} = {}^3J_{4,3exo} = 11.5$ Hz). An 11.5 Hz coupling of H2/H4 to H3*exo* is consistent with a *trans* arrangement of H2/H4 with H3*exo* and hence an *endo* orientation of H2 and H4. This therefore establishes an *exo* orientation of the C2 and C4 methoxy substituents. The chemical shifts of C6/C7 (132.8 ppm) are also similar to those of C6 (133.3 ppm) and C7 (133.7 ppm) of **146** which was also assigned as having *exo* substituents at C2 and C4.

The identity of 2-*exo*-bromo-9-*syn*-methoxybicyclo[3.2.2]non-6-ene **148** was established from the following: a DQCOSY experiment determined the ^{1}H-^{1}H connectivity and a difference nOe experiment established the connectivity of H2 to H1 as no coupling of these protons was apparent from the DQCOSY experiment. An HMQC established the ^{1}H-^{13}C one bond connectivities. The presence of CHBr and CHOMe groups was determined from the chemical shifts of carbons C2 and C9 (55.4 ppm and 78.3 ppm, respectively) and from the chemical shift of the corresponding protons H2 and H9 (4.32 ppm and 3.67 ppm, respectively). The presence of an alkene group was apparent from signals in the ^{13}C NMR at 132.4 ppm (C7) and 136.3 ppm (C6) and from the chemical shift of the associated protons at 6.09 ppm (H7) and 6.19 ppm (H6). The *exo* orientation of the C3 proton centred at 2.78 ppm and the *syn* orientation of the proton at 2.12 ppm attached to C8 was confirmed by the presence of a 1.9% enhancement of the multiplet at 2.78 ppm on irradiation of the H8 proton in a difference nOe experiment. The reverse enhancement of H8*syn* was observed on irradiation of H3*exo* but could not be measured accurately due to the partial overlap of H8*syn* with H8*anti*.

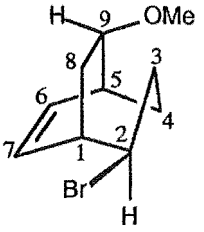

The stereochemistry of H2 was determined from examination of the coupling constants of H2 to H3*endo* and H3*exo* ($^3J_{2,3endo} = 5.4$ Hz, $^3J_{2,3exo} = 11.3$ Hz). The large 11.3 Hz coupling of H2 to H3*exo* is consistent with a *trans* arrangement of these protons and hence an *endo* orientation of H2 which therefore requires an *exo* configuration of the C2 bromine substituent. The *syn* orientation of the C9 methoxy group was established from consideration of the coupling constants of H9 to H8*anti* and H8*syn* ($^3J_{9,8anti} = 9.8$ Hz, $^3J_{9,8syn} = 4.9$ Hz). The 9.8 Hz coupling of H9 to H8*anti* is consistent with a *cis* arrangement of these protons in the C8C9 two carbon bridge and hence established the *anti* orientation of this proton. The stereochemical assignments of C2 and C9 were supported by examination of the ^{13}C chemical shifts of C7 and C6 (132.4 ppm and 136.3 ppm). The C7 chemical shift is similar to that observed for C7 of **146** and **147** (133.7 ppm and 132.8 ppm, respectively) both having equatorial substituents at C2. If the C9 methoxy group were *anti* to the three membered bridge then a large shielding effect and hence an upfield shift of C6 would be expected. The C6 chemical shift of 136.3 ppm is downfield from that of C7 and hence does not appear to be consistent with a γ-eclipsed interaction of an *anti* substituent at C9.

The yields of the products isolated from the bromination reactions of **47** in methanol are summarised in Table 5.6. As can be seen from Table 5.6, when the reaction was performed at 0 °C the formation of **128** and **129** was decreased‡ and three new products were isolated. However, compounds **139** and **140**, which were postulated as precursors to **128** and **129**, were not isolated.

Possible mechanisms for the formation **146**, **147**, and **148** are outlined in Figures 5.10 and 5.11. The formation of **147** may occur by either solvolysis of **128** and/or **129** to give cation **141** followed by ring opening to give **149** which undergoes nucleophilic attack to form **147**. A more direct route to **147** could be envisaged by direct nucleophilic attack on the cyclopropane ring of **128** and/or **129** which may occur if the elimination process is thermodynamically favourable and the ring sufficiently activated. When a mixture of **127-132** was heated in methanol-d_4 for 1 h, a ^{1}H NMR of the resulting products showed the complete disappearance of **128** and approximately 60% loss of **129**. The main product resulting from this reaction was not isolated but from inspection of the NMR spectra was found to have similar ^{1}H and ^{13}C NMR data to those of **147**. The assignment of this product to 4-*exo*-methoxy-2-*exo*-trideuteriomethoxybicyclo-[3.2.2]non-6-ene **150** was supported by GCMS results which showed the molecule to have incorporated three deuterium atoms ($C_9H_{15}{}^2H_3O_2$ requires 185.1495; Found 185.1492, D_0 1%, D_1 0%, D_2 0%, D_3 99%). The presence of only three deuterium atoms in product **150** precludes the possibility of acid induced ring opening as this would be expected to result in incorporation of four deuterium atoms into the product. Compounds **127** and **132** appeared to be stable to the reflux conditions. The ratios of the products shown in Table 5.7 and were derived from comparison to **132**.†

The instability of **128** and **129** towards reflux in methanol can be seen from comparison of the ^{1}H NMR spectrum between approximately 3.20 ppm and 3.50 ppm where one methoxy group of **128** appears as a singlet at 3.41 ppm before refluxing in methanol (Figure 5.14a) and completely disappears after refluxing for 1 h in methanol-d_4 (Figure 5.14b). The second methoxy of **128** at 3.31 ppm appears to remain but this is due to the accidental equivalence of the chemical shift of this methoxy group with that of the methoxy group of **150**.§ For **129** one methoxy group appears at 3.29 ppm and the second, at 3.40 ppm, is partially overlapping with the methoxy group of **127**.

---

‡ This reaction proved to be very sensitive to the reaction conditions and was not always reproducible.

† Compound **132** was assumed to be stable to the reflux conditions as the ratio of **132** to **127** and **131** appeared to remain constant before and after the reflux. A reasonable error (ca. 10%) is involved in the experiment from estimation of the integrals in the ^{1}H NMR spectra.

§ The absence of compound **128** after reflux was also shown from the ^{13}C NMR of the reaction mixture and from the disappearance of H4 (3.23 ppm) in the ^{1}H NMR. The possibility of solvolysis at both C4

113

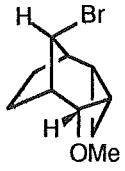

127

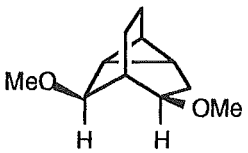

128

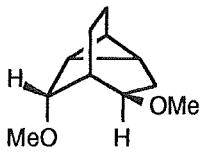

129

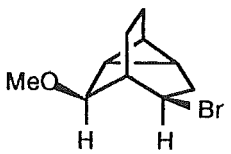

130

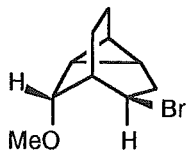

131

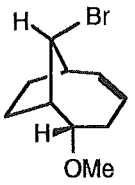

132

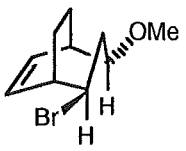

146

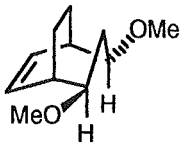

147

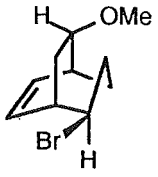

148

	Compounds										
Rxn	113	127	128	129	130	131	132	146	147	148	Total
(a)	3%	34%	24%	14%	5%	5%	3%	NI	NI	NI	88%
(b)	7%	30%	6%	7%	3%	5%	7%	8%	6%	3%	82%

Table 5.6. Products formed from bromination of *exo*-tricyclo[3.2.2.0^{2,4}]non-6-ene **47** in dry methanol at (a) room temperature and (b) 0 °C. NI = Not isolated.

	Compounds					
Rxn	150	127	128	129	131	132
(a)	0.0	9.0	6.3	3.2	0.6	1.0
(b)	5.9	8.5	0.0	1.0	0.5	1.0

Table 5.7. Composition of products relative to **132** from bromination of **47** (a) before refluxing in methanol-d_4 and (b) after a 1 h reflux in methanol-d_4.

Although a substantial error is involved in estimating the product ratios a reasonable correlation can be seen between the loss of **128** and **129** and the formation of **150**. Some other products were also formed on reflux (as can be seen by comparison of Figures 5.14a and b) and these were assumed to make up the deficit between the loss of **128** and **129** and the formation of **150**. Also of note in this reaction was the apparent stability of **131** to the reflux in methanol-d_4, which therefore suggests that formation of **129** does not proceed by methanolysis of this compound and since **131** and **130** both

---

and C9 positions followed by capture of the resulting cation with CD_3OD, and hence resulting in the disappearance of the methoxy signals in the ^1H NMR, was eliminated. A ^2H NMR spectrum showed two main peaks (3.25 ppm and 3.36 ppm, the peaks were not well resolved) indicating that other products containing an OCD_3 group were formed. Some deuterium incorporation in **129** may have occurred.

have the same stereochemistry of the C4 bromine substituent it appears likely that **130** will not undergo solvolysis under these conditions to give **128**.‡

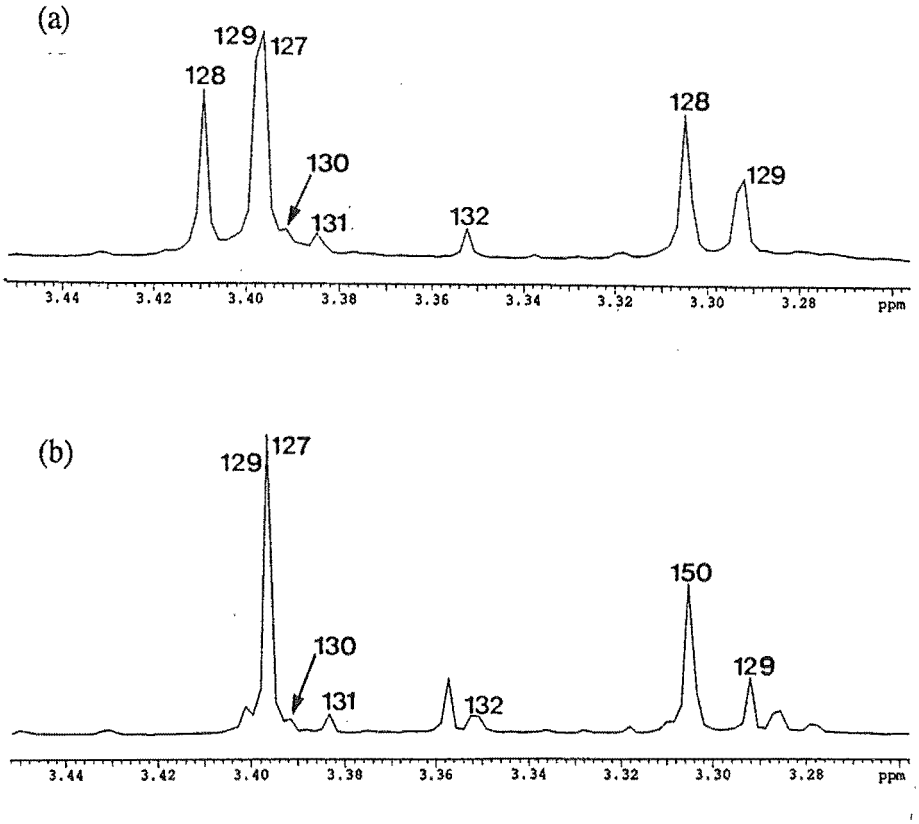

Figure 5.14. ^{1}H NMR (methoxy region) of products from the bromination of **47** (a) before refluxing in methanol-d_4 and (b) after 1 h reflux in methanol-d_4.

To check the stability of the products in methanol at room temperature and to determine whether product solvolysis was occurring on workup the reaction was performed at ca. -25 °C in an NMR tube and then rapidly inserted into the NMR spectrometers probe which was precooled to -20 °C. A ^{1}H NMR spectrum recorded after approximately 5 minutes showed the reaction to be complete.§ The sample was gradually

‡ This could not be confirmed from Figures 5.14a and b with certainty due to the close proximity of the chemical shifts of the methoxy group of **127** with that of **130**.

§ The reaction was most likely instantaneous even at -25 °C, although bromine colouration was still evident when the sample was inserted into the NMR probe and after warming to room temperature. An excess of bromine was therefore present.

warmed to room temperature in the probe and the reaction mixture monitored by ^{1}H NMR. No product degradation or change in product ratios was evident on warming. The solvent was removed and half of the residue redissolved in methanol-d_4 and a ^{1}H NMR spectrum obtained. No noticeable change was observed between the spectrum run before and after workup. The second half of the crude reaction mixture was taken up with $CDCl_3$ and the products identified from comparison with the data already determined. In this case the deuterated analogues of compounds **127**, **128**, and **129** were the major products. Thus the products **128** and **129** are formed from a facile solvolysis reaction that takes place in some cases even at -20 °C and therefore are not artefacts of the workup procedure.

The most direct pathway for the formation of **146** appears to be via corner addition of the bromine electrophile to **47** followed by capture of the resulting cation **125** by methanol before rearrangement occurs. However, solvolysis of **128** or **129** via **141** followed by nucleophilic capture of cation **149** by Br^- or direct nucleophilic attack on the cyclopropane ring cannot be ruled out. A possible pathway for the formation of **148** is via a 1,3-hydride shift† in cation **125** to give **150** which then undergoes nucleophilic attack to form **148**.

To summarise the results obtained from bromination of **47**, electrophilic addition appears to favour attack at the double bond in preference to the cyclopropane ring. Products **130**, **131**, and **148** appear to have arisen from bromination of the cyclopropane ring indicating that at least 10% of the reaction proceeds by this pathway. If it is assumed that **146** also results from initial electrophilic attack at the cyclopropane ring, and not from Br^- addition to cation **149** for example,§ then up to 18% of the reaction may proceed via this mechanism. The products obtained from the ring opening reactions are consistent with corner attack of Br^+ at the C2-C4 bond of the cyclopropyl group and no products arising from edge attack were isolated. The remainder of the reaction that was accounted for appears to proceed via reaction of bromine with the double bond, with at least 40% of the overall reaction occurring from *endo* addition of bromine to the double bond resulting in the formation of **113**, **116**, **127**, and **132**.

Section 5.5 ADDITION OF METHANOL TO *exo*-TRICYCLO[3.2.2.0^{2,4}]NON-6-ENE

The reaction of *exo*-tricyclo[3.2.2.0^{2,4}]non-6-ene **47** with a catalytic amount of *p*-toluenesulphonic acid (PTSA) in dry methanol at 80 °C for 21 days gave three products. GLC analysis showed the reaction to consist of 2-*exo*-methoxybicyclo[3.2.2]-

† See reference 161 for a review of hydride migrations in polycyclic systems.

§ A number of other pathways for the formation of **146** are also possible.

non-6-ene **152** (75%) and two other products (15% and 10%) which were not isolated (Figure 5.15). Compound **152** was isolated by preparative GLC.

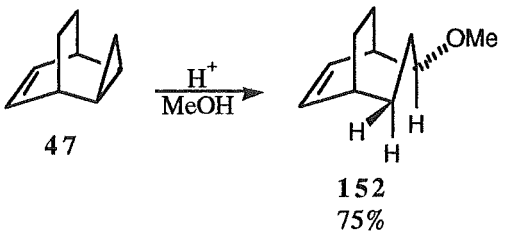

47

152
75%

Figure 5.15. Reaction of *exo*-tricyclo[3.2.2.0^{2,4}]non-6-ene **47** with H^+-MeOH.

The identity of **152** was determined‡ from the following: an HMQC-DEPT experiment established the one bond ^1H-^{13}C connectivities and a DQCOSY experiment determined the ^1H-^1H connectivity as far as was possible. A DEPT135 experiment established the carbons at 30.3 ppm (C4) and 30.6 ppm (C3) to be methylene carbons and showed the ^{13}C resonance at 30.5 ppm to be that of a methine carbon. An HMBC showed correlations from H2 (3.08 ppm) to carbons C7 (131.1 ppm) and C8 (20.3 ppm). Correlations from H7 to C1 (36.1 ppm), C8, and C6 (138.5 ppm) and from H6 to C9 (24.3 ppm) and C1 in conjunction with the DQCOSY experiment established the bicyclo[3.2.2]non-6-ene carbon skeleton. The presence of a CHOMe group was determined from the chemical shift of C2 (79.5 ppm) and from its corresponding proton H2 (3.08 ppm). The methoxy group appeared as a singlet at 3.30 ppm in the ^1H NMR spectrum with the corresponding ^{13}C resonance at 56.0 ppm in the ^{13}C NMR spectrum.

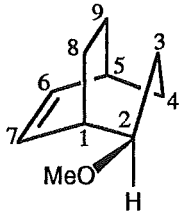

In this case difference nOe experiments were of little help in the assignment of the stereochemistry at C4 due to the similarity of the chemical shifts of the protons attached to C3 (1.79 ppm, 1.99 ppm) with those of the C8 (1.57 ppm, 2.03 ppm) and C9 (1.58 ppm, 1.72 ppm) methylene groups. The absence of a significant coupling of H1 to H2 determined an axial orientation of H2. This was also observed for compounds **146** and **147** which had an *endo* orientation of H2 and showed little or no coupling to the bridgehead proton H1. The axial orientation of H2 was confirmed from the coupling constants of H2 to H3*endo* (1.99 ppm, $^3J_{2,3endo}$ = 5.3 Hz) and H3*exo* (1.79 ppm, $^3J_{2,3exo}$ = 10.4 Hz) which are consistent with a *trans* arrangement of H2 and H3*exo*. A 1D-TOCSY allowed identification of the H3*exo* multiplet (d of d of t) and also allowed conformation of the size of the coupling constants of H3*exo* to H2 and determination of the coupling constants of H3*exo* to H4*endo* and H4*exo* ($^3J_{3exo,2} = {}^3J_{3exo,4endo}$ = 9.8 Hz,

‡ 2-*exo*-Hydroxybicyclo[3.2.2]non-6-ene and 2-*endo*-hydroxybicyclo[3.2.2]non-6-ene have been reported[162] but no NMR data have been published.

$^3J_{3endo,4exo}$ = 6.0 Hz). The 1D-TOCSY also allowed determination of the geminal coupling constant of H3*exo* to H3*endo* ($^2J_{3exo,3endo}$ =13 .3 Hz) and also established the assignment of the protons of the C4 methylene group. To confirm the stereochemistry of C2 conformational searching of the two possible isomers **152** and 2-*endo*-methoxy-bicyclo[3.2.2]non-6-ene **153** was performed and the Boltzman averaged coupling constants of H1 to H2 calculated. The calculated values of $^3J_{1,2}$ were found to be 1.4 Hz for structure **152** and 5.2 Hz for **153** (Table 5.8). It therefore seems likely that the orientation of H2 is *endo*, which requires an *exo* orientation of the C2 methoxy group. Apparently an *exo* conformation of the three membered bridge is more favourable (populated to greater than 95% for **152** and more than 85% for **153** from the Boltzman distribution of the conformers found within a 12.5 kJ mol^{-1} energy window in the conformational searches) for both isomers **152** and **153** and hence explains the larger 5.2 Hz coupling constant of H1 to H2 predicted for **153**.

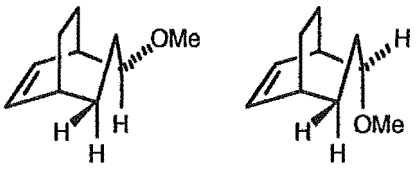

152 **153**

Compound	Vicinal Coupling Constants (Hz)		
	1,2	2,3*exo*	2,3*endo*
152 Obs.	< 1.0	10.4	5.3
152 Calc.	1.4	10.4	5.3
153 Calc.	5.2	3.7	4.2

Table 5.8. Comparison of the calculated coupling constants of **152** and **153** to those observed for the major product from the reaction of *exo*-tricyclo[3.2.2.0^{2,4}]non-6-ene **47** with H$^+$-MeOH.

Comparison of the observed† and calculated values for the $^3J_{2,3endo}$ and $^3J_{2,3exo}$ couplings shows good agreement for structure **152** but shows significant deviation, especially for $^3J_{2,3exo}$, from those values calculated for **153**. This therefore adds further support to the stereochemical assignment of C2.

Comparison of the chemical shift of C6 (133.3 ppm) of **146** and C6/C7 (132.8 ppm) of **147**, both with *exo* methoxy groups at C2 or C4, shows close agreement with the ^{13}C chemical shift of C7 (131.1 ppm) in **152** and hence further supports the

† The observed values shown for the coupling of H2 to H3*endo* and H3*exo* were extracted from the H2 multiplet.

configurational assignment of C2 in **152**. The chemical shift of H8*syn* (2.03 ppm) is also consistent with an *exo* orientation of the C2 methoxy group as it would be expected to show a downfield shift due to steric compression effects on interaction with the methoxy group.

To establish the trajectory of electrophilic attack on the cyclopropane ring the reaction of **47** with a catalytic amount of PTSA was repeated using methanol-d_1 as the reaction solvent. GLC analysis of the products showed three peaks in a similar ratio to that observed for the reaction in methanol (71%, 16%, 13%). The peak corresponding to the major product(s) was collected by preparative GLC and shown from a ^{2}H NMR spectra to contain two products, 4-*exo*-deuterio-2-*exo*-methoxybicyclo[3.2.2]non-6-ene **154** (40% overall yield) and 4-*endo*-deuterio-2-*exo*-methoxybicyclo[3.2.2]non-6-ene **155** (31% overall yield) in a ratio of 1.3:1.0 (Figure 5.16).

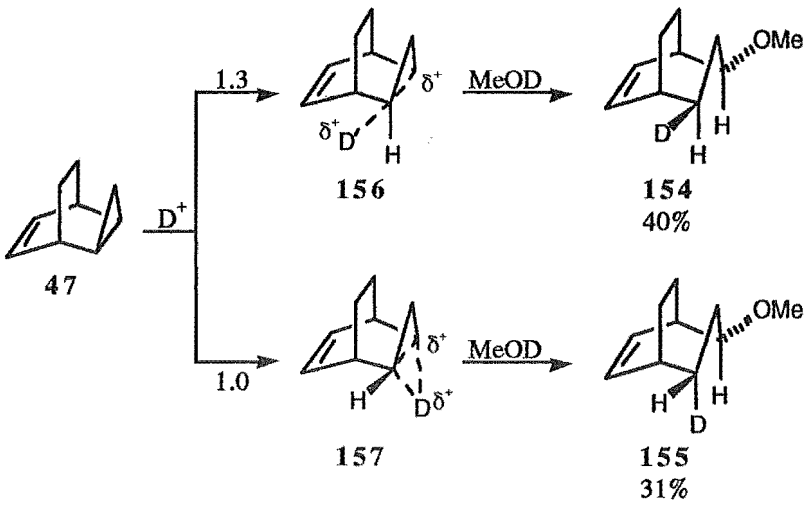

Figure 5.16. Reaction of *exo*-tricyclo[3.2.2.0^{2,4}]non-6-ene **47** with D$^+$-MeOD.

The identity of **154** and **155** was determined from the following: the compounds showed identical retention times to that of **152** on GLC and the ^{1}H NMR of the mixture of **154** and **155** appeared nearly identical to that of **152**.‡ The ^{13}C NMR spectrum of the mixture of deuterated products showed thirteen signals due to deuterium isotope shift effects.[163,164] Signals at 137.9 ppm, 131.0$_8$ ppm, and 131.1$_1$ ppm in the ^{13}C NMR spectrum with the corresponding protons at 6.21 ppm and 5.97 ppm in the ^{1}H NMR spectrum established the presence of the alkene groups. The presence of a

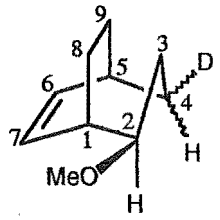

‡ The chemical shift values reported above for **154** and **155** were determined with CCl_4 as the NMR solvent and those of **152** in $CDCl_3$. The ^{1}H NMR and ^{13}C NMR spectra of **154** and **155** were also obtained in $CDCl_3$ for comparison to those of **152**. The ^{1}H and ^{13}C NMR spectra of **152** were also run in CCl_4 for comparison to those of **154** and **155**.

^{13}C signal at 78.8 ppm and a proton at 2.98 ppm confirmed the presence of a CHOMe group. The methoxy group was evident as a singlet in the ^{1}H NMR spectrum at 3.20 ppm with the methoxy carbon resonance at 55.4 ppm in the ^{13}C NMR spectrum. The bridgehead protons H1 and H5 were evident at 2.42 ppm (H1) and 2.28 ppm (H5) and the bridgehead C1 carbon at 35.9 ppm in the ^{13}C NMR spectrum. The C9 carbons of **154** and **155** appeared at 24.4 pm and the C8 carbons 20.1 ppm and 20.0 ppm.† The appearance of four carbons in the range 30.0 ppm to 30.3 ppm were attributed to C3 and C4 of **154** and **155** and one signal showing line broadening, which was identified as a methine carbon from a DEPT135 experiment, was assigned to C5 of **154** and **155**.‡ The chemical shifts of H4*exo* of **155** and H4*endo* of **154** (1.59 ppm and 1.46 ppm, respectively) were identified from a 1D-TOCSY experiment on irradiation of H2. The ^{2}H NMR spectrum§ of the two deuterio isomers showed two signals (1.80 ppm and 1.65 ppm) in a ratio of 1.3:1.0 (**154**:**155**).

The products obtained from addition of methanol to **47** are consistent with both edge and corner addition of the electrophile at the C2-C4 bond of the cyclopropane ring, which results in retention and inversion, respectively, at the site of electrophilic attack. The product ratio of 1.3:1.0 (**154**: **155**) is consistent with both corner and edge trajectories having similar energies. This contrasts with the results reported for methanol addition to **1**, **46**, **68**, and **69** where electrophilic addition to the cyclopropane ring occurs exclusively with inversion.[13-15] As no other products were isolated no exact determination of the regiochemical preference for attack at the cyclopropane ring over the alkene can be made but it appears that at most approximately 25% of the reaction mixture could proceed via attack at the double bond. For **69** 15% of the reaction was found to occur at the double bond.[13,15]

Nucleophilic attack occurred exclusively with inversion to form products **154** and **155** which is consistent with the formation of corner **156** and edge **157** protonated intermediates with little open carbocation formation (Figure 5.16).

---

† The appearance of carbons C7 and C8 as separate signals for **154** and **155** reflects the stereochemical dependence of the four bond isotope shift effects, whereas C6 and C9, which are in a three bond relationship to the deuterium atoms of C4, do not show different isotope shift effects as three bond isotope shift effects are not stereochemically dependent and hence both D4*exo* and D4*endo* of **154** and **155**, respectively, would be expected to show similar isotope shift effects on C6 and C9.[163,164]

‡ Three ^{13}C signals arising from C3 and C4 of **154** and **155** were presumably due to the weak triplet signals of C4 (which were not observed separately) overlapping with each other and/or the C3 and C5 signals.

§ ^{2}H NMR spectra were run unlocked with CCl_4 as the solvent.

As the deuterium-carbon attachment could not be assigned (due to the similarity of the chemical shifts of C3 and C4) deuterium scrambling[161] (Figure 5.17) cannot be ruled out but this may be considered unlikely as methoxy capture of the resulting cations would be expected and, as outlined above, only limited charge development at the carbon where nucleophilic addition takes place appears to occur in the protonated cyclopropane intermediate. The greater strength of the C-D bond than that of the C-H bond would be expected to make deuterium scrambling less facile.

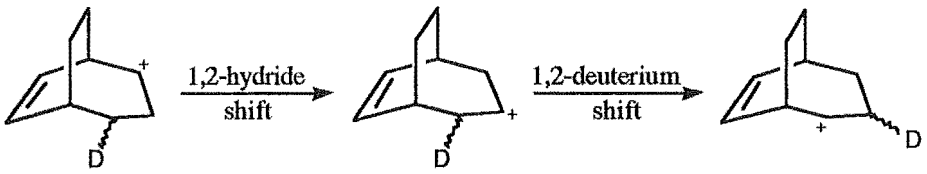

Figure 5.17. Possible mechanism for deuterium scrambling around the three membered bridge.

For **47** the major product of methanol addition does not result from rearrangement of the hydrocarbon skeleton. The overlap integrals of the π orbital of **47** with the symmetric and antisymmetric Walsh orbital of the cyclopropane ring $<\pi/\sigma_s>$ and $<\pi/\sigma_a>$ have been calculated[139] and were found to be larger than those for the corresponding orbitals in **69** (**47**: $<\pi/\sigma_s> = 0.061$, $<\pi/\sigma_a> = 0.037$; **69**: $<\pi/\sigma_s> = 0.052$, $<\pi/\sigma_a> = 0.031$) where rearrangement was observed.[13,15] Assuming the orbital overlap calculations are correct then, if significant charge development occurred during the proton/deuteron addition to the cyclopropane ring, rearrangement involving the alkene moiety would be expected to be more likely than in **69**. Therefore, since the major product does not result from rearrangement it appears likely that significant charge development at the carbon where nucleophilic capture takes place does not occur during protonation of the cyclopropane ring. However, it may be that the structural reorganisation of the bicyclo[3.2.2]non-6-ene carbon skeleton is not as energetically facile as the corresponding rearrangement in the bicyclo[3.2.1]oct-6-ene systems, and hence charge localisation may not be the dominant factor contributing to rearrangement.

The increased interaction of alkene π orbitals with the cyclopropane ring σ_a and σ_s orbitals of the internal C2-C4 bond may in fact enhance the reactivity of the cyclopropane group by increasing the size of the contribution of the C2 and C4 orbital coefficients to the HOMO-1 orbital as has been suggested[13] for the enhanced reactivity of the C6-C7 bond of tricyclo[3.2.2.$0^{2,4}$]nona-6,8-diene **51** towards reaction with $Hg(OAc)_2$ and hence may also enhance edge addition of a proton to **47**.

Section 5.6 REACTION OF MOLECULES CONTAINING A TRICYCLO[3.2.2.$0^{2,4}$]-NON-6-ENE SKELETON WITH TETRACYANOETHENE

Tetracyanoethene (TCNE) has been reported to act as an electrophile in additions to alkenes and cyclopropanes.[165,166] For example, reaction of *endo*-tricyclo[3.2.1.$0^{2,4}$]-oct-6-ene **68** and 2-methyl-*endo*-tricyclo[3.2.1.$0^{2,4}$]oct-6-ene **86** with TCNE under mild conditions (CH_2Cl_2, room temperature) give products resulting from reaction of both the cyclopropane ring and the double bond (Figure 5.18).[165,166]

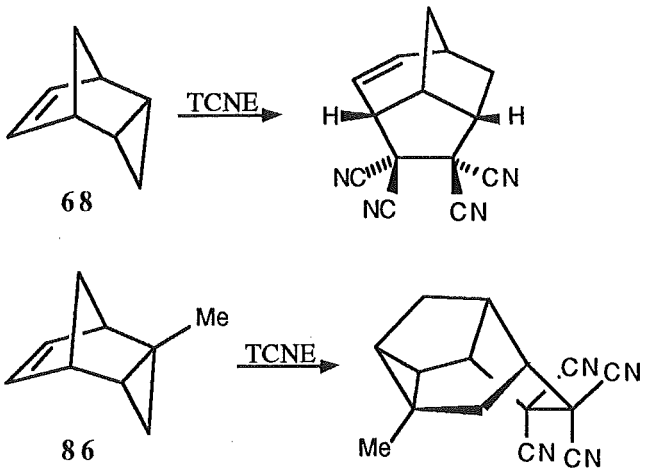

Figure 5.18. Reaction of *endo*-tricyclo[3.2.1.$0^{2,4}$]oct-6-ene **68** and 2-methyl-*endo*-tricyclo[3.2.1.$0^{2,4}$]-oct-6-ene **86** with TCNE.[165,166]

Reaction of tricyclo[3.2.2.$0^{2,4}$]nona-6,8-diene **51** with TCNE in $CHCl_2$ solution for eight days at room temperature gave one product 10,10,11,11-tetracyanopenta-cyclo[5.4.0.$0^{2,9}$.$0^{3,5}$.$0^{6,8}$]undecane **158** in 44% yield (Figure 5.19).

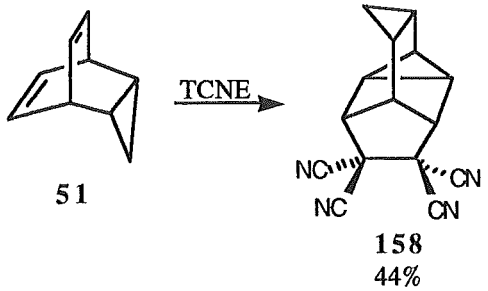

Figure 5.19. Reaction of tricyclo[3.2.2.$0^{2,4}$]nona-6,8-diene **51** with TCNE.

The identity of **158** was determined from the following: a COSY established the ^1H-^1H connectivity and a HETCOR determined the one bond ^1H-^{13}C connectivities. The presence of the nitrile groups was evident form an absorption at 2252 cm^{-1} in an IR spectrum and from the signals in the ^{13}C NMR spectrum (112.9 ppm, 112.8 ppm, 111.7 ppm, 111.5 ppm) which are characteristic of this functional group. Two cyclopropyl groups were evident from the COSY experiment

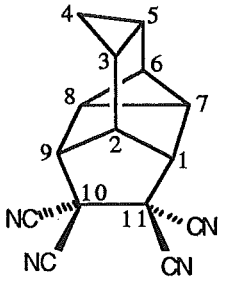

and from the ^{13}C NMR which showed six carbon resonances characteristic of the chemical shift of cyclopropane carbons (C6 15.7 ppm, C7 15.0 ppm, C8 14.9 ppm, C4 8.0 ppm, C3 6.6 ppm, C5 5.4 ppm). The chemical shifts of H1 and H9 (3.61 ppm and 3.58 ppm, respectively) are consistent with protons β to carbons bearing two nitrile groups. The presence of two quaternary carbons C10 and C11 (46.9 ppm and 47.6 ppm) with two α nitrile groups attached were evident from the ^{13}C NMR spectrum. Irradiation of H4*endo*† in a difference nOe experiment gave a large enhancement (17.1%) of H9 and therefore established a *syn* orientation of this proton with respect to the cyclopropane ring. A 9.3% enhancement of H4*endo* was observed on irradiation of H9 in a further difference nOe experiment.

In this case reaction occurred via TCNE addition to the 1,4-diene moiety of **56** in a homo-Diels-Alder reaction[167,168] rather than with the cyclopropane ring. The reason for this may be that either the homo-Diels-Alder reaction is an inherently more facile process than addition to the cyclopropyl ring, or that for similar reasons to those described‡ for mercuric acetate addition to **51**, the C6-C7 double bond is activated towards electrophilic attack.

Reaction of *exo*-tricyclo[3.2.2.$0^{2,4}$]non-6-ene **47** with TCNE in CH_2Cl_2 at room temperature gave no reaction. The reaction was repeated in refluxing benzene and toluene but again no significant reaction was observed.

When *endo*-tricyclo[3.2.2.$0^{2,4}$]non-6-ene **56** was stirred with TCNE at room temperature in CH_2Cl_2 or in refluxing benzene no reaction occurred. When the reaction was performed in refluxing toluene (9 days) a ^1H NMR spectrum of the crude reaction mixture showed a small amount of product formation (ca. 5%). TLC mesh column chromatography of the resulting product mixture gave 5-*exo*-methyl-9,9,10,10-tetracyanotricyclo[4.4.$0^{1,6}0^{2,8}$]dec-3-ene **159** (2%) and a mixture of two other products (5%) which were not identified (Figure 5.20).

For compound **159** a DQCOSY in conjunction with selective decoupling experiments established the proton-proton connectivity as far as was possible. However, due to the presence of a number of singlets in the ^1H NMR spectrum with only fine couplings, the complete skeletal structure of the molecule could not be deduced. An HMQC established the ^1H-^{13}C one bond connectivities. DEPT90 and DEPT135 experiments confirmed the presence of a

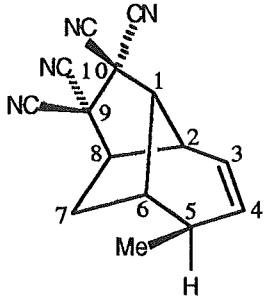

† Assignment of H4*endo* (0.30 ppm) and H4*exo* (0.60 ppm) was established by examination of the coupling constants of the two protons to H3 (1.16 ppm) and H5 (1.26 ppm): $^3J_{4endo,3} = {}^3J_{4endo,5} =$ 4.1 Hz, $^3J_{4exo,3} = {}^3J_{4exo,5} = 7.8$ Hz).

‡ See reference 13 and Section 5.1.

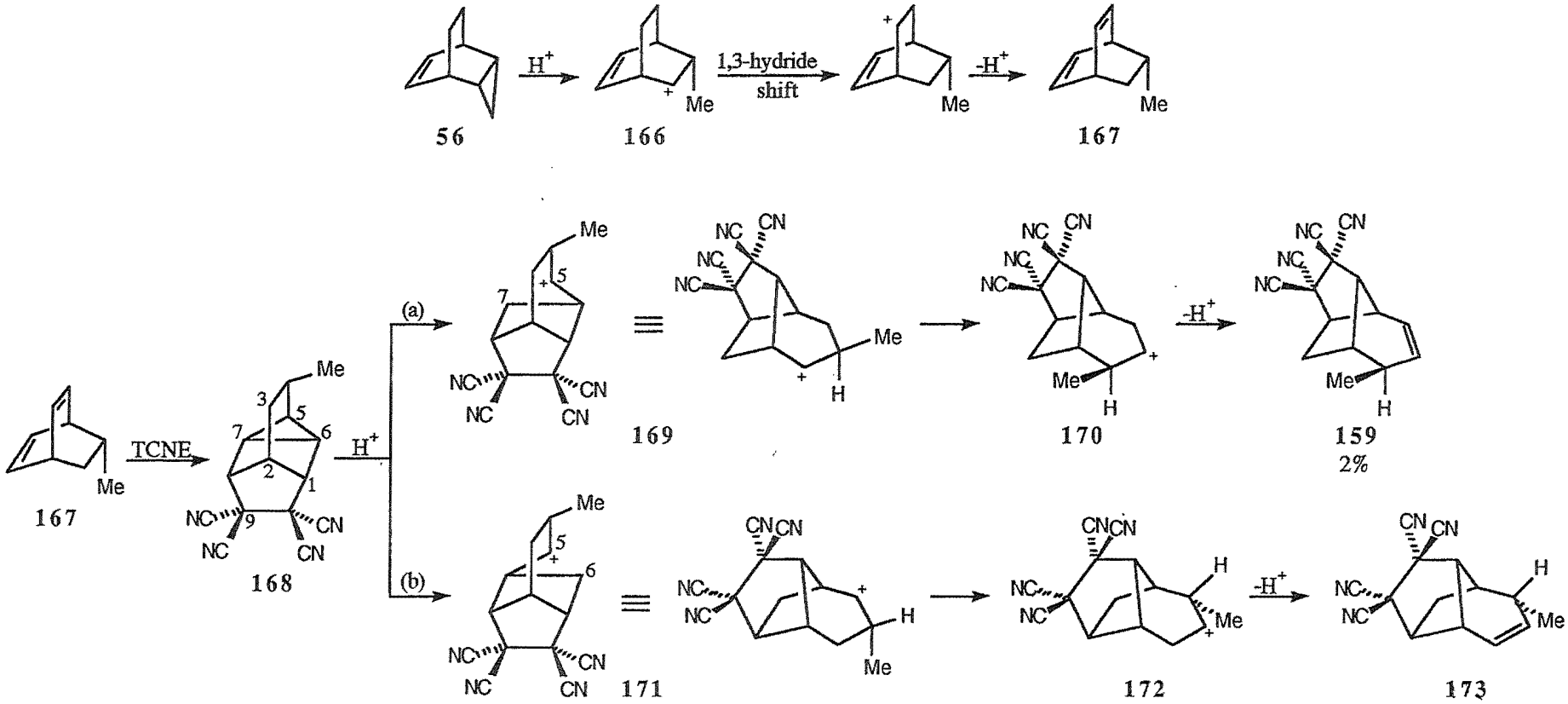

Figure 5.20. Possible mechanism for the formation of 5-*exo*-methyl-9,9,10,10-tetracyanotricyclo[4.4.0^{1,6}0^{2,8}]dec-3-ene **159**

methyl group. An HMBC experiment (correlations are shown in Table 5.9) in conjunction with the DQCOSY experiment allowed determination of the carbon skeleton and also allowed the chemical shifts of carbons C9 (45.8 ppm) and C10 (45.5 ppm) to be determined as these quaternary carbons were not observed in the ^{13}C NMR spectrum. The HMBC also allowed determination of the position of the 'TCNE' attachments which were confirmed from consideration of the chemical shift of the protons H1 (2.85 ppm) and H8 (3.18 ppm) and carbons C1 (48.8 ppm) and C8 (54.6 ppm). The presence of the nitrile groups was established from an absorption at 2256 cm^{-1} in the IR spectrum and the presence of four nitrogens was confirmed by mass spectroscopic analysis. An alkene moiety was evident from the chemical shifts of C3 (121.0 ppm) and C4 (134.8 ppm) and their attached protons H3 (5.74 ppm) and H4 (5.76 ppm). The *syn* orientation of H1 (singlet, $W_{h/2}$ = 3.8 Hz) towards the double bond was determined from the lack of a measurable coupling (< 1 Hz) to H2 and H6 and also from structural considerations.† The *exo* orientation of the C5 methyl group was determined from the presence of a 6.7% enhancement of H1 on irradiation of the methyl group in a difference nOe experiment; this also confirmed the *syn* orientation of H1. A 0.9% enhancement of the methyl group was observed on irradiation of H1 in a further difference nOe experiment. The assignment of an *exo* orientation of the C5 methyl was also supported by the presence of a 1.8% nOe to H7*endo*‡ (1.73 ppm) on irradiation of H2 and a 3.7% enhancement of H2 on irradiation of H7*endo* in difference nOe experiments.

From the position of the methyl group relative to the double bond and the TCNE moiety it seemed unlikely that **159** arose from similar addition mechanisms to those proposed for the additions to **68** and **86**.[165,166] The presence of a methyl group appeared to be consistent with an edge addition of TCNE to the cyclopropyl group of **56** with subsequent hydride migration (Figure 5.21) to give the tertiary carbocation **160**.§ However, if this mechanism occurred then formation of **161** or rearrangement to give **164** or **165** via carbocations **162** and **163** may be expected. None of the three products **161, 164,** or **165** show the observed relationship of the methyl group to the double

---

† It is unlikely that a two membered bridge could span between a *syn* orientation at C1 and an *exo* orientation at C8 from distance and strain considerations.

‡ The assignment of the multiplet at 1.73 ppm as H7*endo* was determined from examination of the proton coupling constants of H7*endo* and H7*exo* (2.08 ppm) to H6 (2.48 ppm) and H8 (3.18 ppm): $^3J_{7endo,6}$ = 2.4 Hz, $^3J_{7endo,8}$ = 5.3 Hz, $^3J_{7exo,6}$ = 7.8 Hz, $^3J_{7exo,2}$ = 1.5 Hz.

§ TCNE additions to tricyclic molecules containing a cyclopropyl group and double bond have been proposed to occur with the intermediate formation of a zwitterion since substantial carbon skeleton rearrangements have been observed before intramolecular nucleophilic capture of the carbocation occurs.[166]

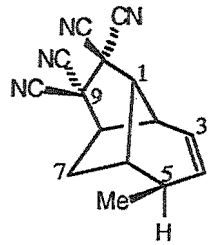

159

Proton Chemical Shifts (ppm)		^{13}C Chemical shifts (ppm)										
		C4 134.8	C3 121.0	C8 54.6	C1 48.8	$C9_q$ 45.8	$C10_q$ 45.5	C2 44.6	C5 41.0	C6 38.5	C7 28.9	CH_3 19.1
H4	5.76	O										
H3	5.74		O									
H8	3.18			O	X			X		X		
H2	3.02							O				
H1	2.85			X	O		X				X	
H6	2.48									O		
H5	2.31								O			
H7*exo*	2.08					X		X	X		O	
H7*endo*	1.73										O	
CH_3	1.14	X							X	X		O

Table 5.9. HMQC (O) and HMBC (X) correlations observed for 5-*exo*-methyl-9,9,10,10-tetracyanotricyclo[4.4.0^{1},^{6}0^{2},^{8}]dec-3-ene **159**. q = quarternary carbon.

bond and TCNE moiety observed in **159** and do not show any obvious possibility for rearrangement to **159**.

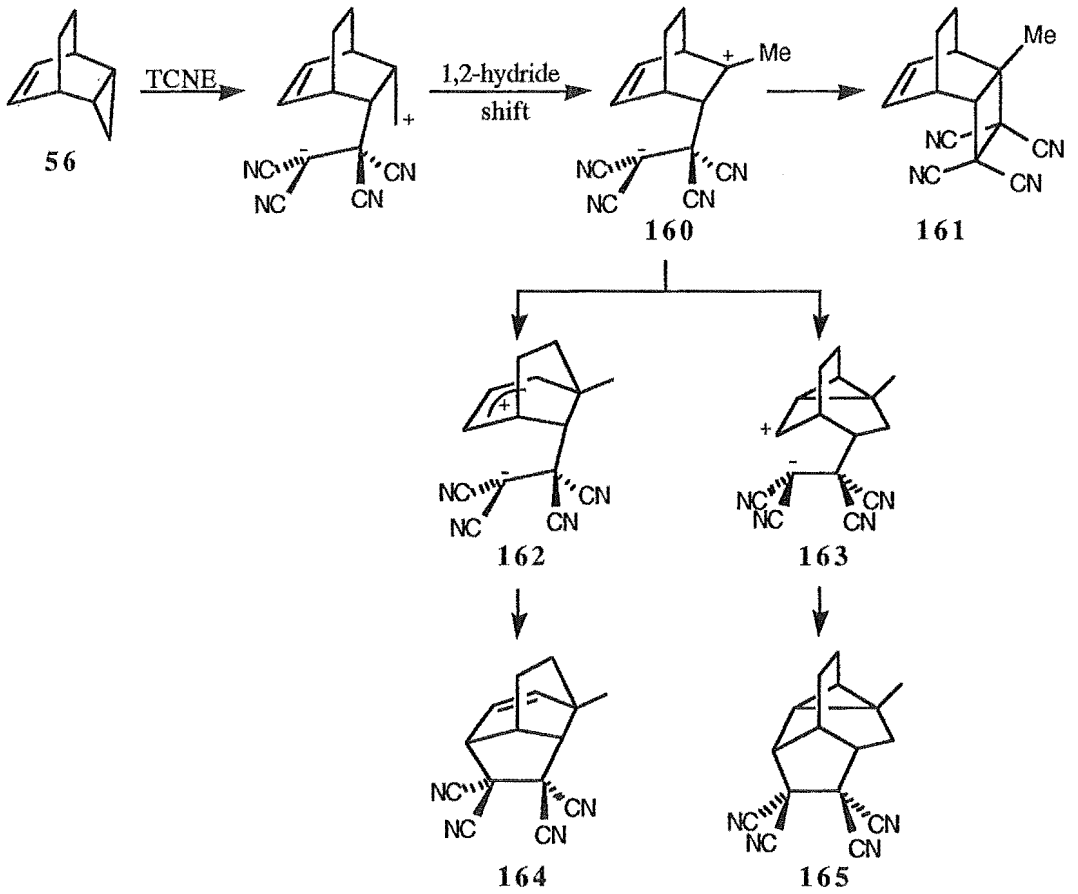

Figure 5.21. Possible products that may be expected to form from initial edge attack of TCNE on the cyclopropane ring of *endo*-tricyclo[3.2.2.$0^{2,4}$]non-6-ene **56**.

A possible mechanism for the formation of **159** is outlined on Figure 5.20. If a catalytic amount of acid were present, possibly from oxidation of TCNE, the cyclopropane ring of **51** may open to form the methyl group, as was observed[136] for the reactions of **102** and **103** (Figure 5.1), and secondary carbocation **166** which may then undergo a hydride shift, followed by elimination to give diene **167**. Diene **167** may then add TCNE in a homo-Diels-Alder reaction to give **168**. If **168** were unstable to the reaction conditions (toluene reflux) it may undergo ring opening by scission of the C5-C7 bond (path a, Figure 5.20) to give cation **169**. A methyl migration would then be required, resulting in the formation of **170** which could then eliminate H^+ to give **159**. A similar mechanism (path b, Figure 5.20) by scission of the C5-C6 bond would result in the formation of **173**, via cations **171** and **172**, which has the same general carbon

skeleton as **159** but would be expected to have a different stereochemistry of the C5 methyl group.‡

The direct reaction of **51** with TCNE does not appear to occur, unlike the facile reactions of **68** and **86** with TCNE which occur at room temperature. If the reaction of TCNE with the cyclopropane occurs via formation of a charged intermediate[166] then the cyclopropane ring of **51** appears to be much less reactive than that of **68**.† The reasons for the difference in reactivity may be related to the relative energy of the HOMO-1 orbitals of **51** and **68** (**86**) to the LUMO of TCNE and may also be due to the mixing of orbitals of the carbon skeleton with those of the cyclopropane ring, hence altering the orbital energies and/or distributions which are a function of the molecular geometry.

---

‡ Methyl migration would be expected to occur in a *cis* migration sense, that is, the methyl group would not be expected to migrate to the opposite side of the ring.[169]

† If the reaction was a concerted process then the relative distances of the cyclopropane ring and alkene moiety and the angle between the two groups may also be important.[167]

CHAPTER 6
Cyclopropane Ring Opening: a Semiempirical Molecular Orbital Study

Section 6.1 INTRODUCTION

The chemistry of cyclopropane ring opening has been of interest to both experimental and theoretical chemists for a number of years. The small size of the molecule itself and the difficulties involved in direct experimental investigation of this process (differentiation of corner and edge attack of the incoming electrophile, synthesis of a suitable substrate to differentiate between these two mechanisms, etc) have all contributed to the interest in the theoretical investigation of the ring opening process and characterisation of its potential energy (PE) surface. To date a large number of calculations have been undertaken, at a variety of levels of theory, to characterise the stationary points associated with the ring opening process. Although a number of ab initio results on various aspects of cyclopropane chemistry have been reported, no rigorous semiempirical investigations of the ring opening process have appeared in the literature.†

The intention of the present study has been to investigate the stereochemistry involved in the opening of a cyclopropyl ring contained within tricyclic molecules, by using semiempirical molecular orbital methods. A comparison of the results obtained from semiempirical calculations and those from ab initio studies for the ring opening processes of cyclopropane, may serve as a guide as to the accuracy of results obtained for the larger systems. It was therefore necessary to completely characterise the semiempirical potential energy surface for the addition of an electrophile to cyclopropane, and hence to identify any transition states and minima which may occur on the potential energy surface.

Section 6.2 PROTONATION OF CYCLOPROPANE

Section 6.2.1 Ab initio Results

The addition of an electrophile, in this case a proton, to cyclopropane has been proposed to occur by either edge or corner attack[13,14,18] (see introduction Section 1.2.1) resulting in the formation of an edge or corner protonated species **174** and **175**, respectively (Figure 6.1). A third possible trajectory, face protonation, has also been proposed but has been discounted as a viable possibility by recent investigations.[7]

---

† A number of papers[170-176] have reported semiempirical calculations of the heat of formation for the 1-propyl and 2-propyl cations but have not generally given detailed descriptions of the structure or type of the stationary points obtained.

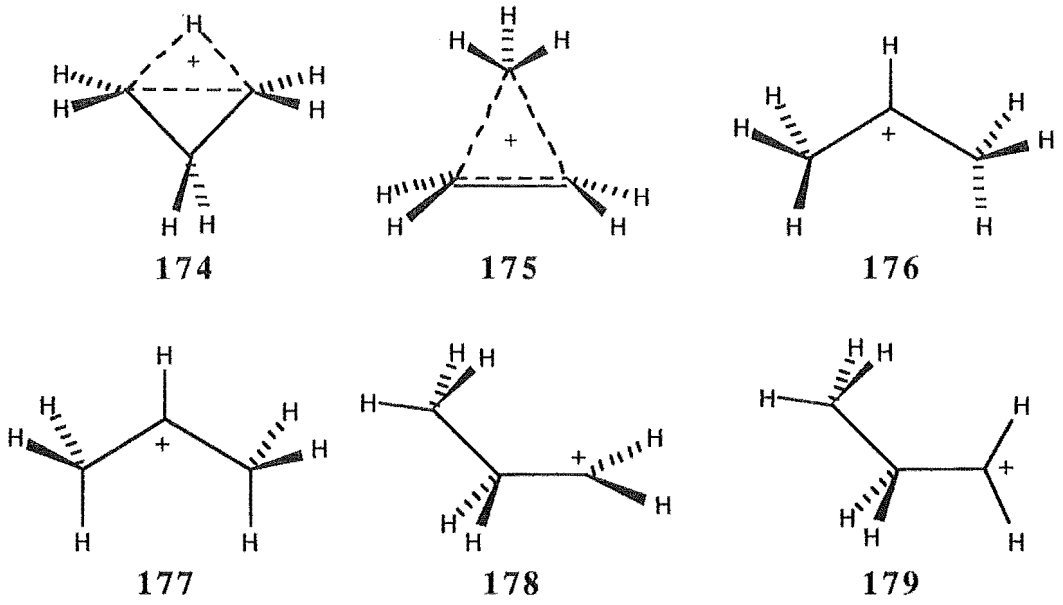

174 175 176

177 178 179

Figure 6.1. $C_3H_7^+$ cations identified by Pople.[181]

A number of ab initio studies have characterised these structures and also investigated the possible cations that may result from their collapse or rearrangement.[178-181] Pople et al.[181] were the first to use a Møller-Plesset (MP) perturbation treatment to include electron correlation effects which have been shown to be important in the characterisation of nonclassical cation species.[122] Pople characterised the six structures shown in Figure 6.1, which were calculated from geometry optimisation at the HF/6-31G* level of theory† and the energy determined by single point calculations with a 6-31G** basis set using both the Hartree-Fock (HF) and MP perturbation procedures.[182] The MP treatment was at full second-order theory (MP2)[183] and used "projected estimates" for the third (MP3)[184] and partial fourth-order theory[185] (MP4(SDQ)) which is correct to fourth-order in the space of single, double, and quadruple substitutions.

The 2-propyl cation **176** with C_2 symmetry was calculated to be the most stable of the six structures identified and was slightly lower in energy than the conformer **177** which has C_{2v} symmetry. Structure **177** was found to be a transition state (TS) on the PE surface with one imaginary frequency corresponding to the distortion from C_{2v} to C_2 symmetry by rotation about the C1-C2 and C2-C3 bonds.

The 1-propyl cation **178** was a local minimum when symmetry restrictions were imposed, but on complete optimisation collapsed to **175** with no activation barrier. The 1-propyl cation **179** was identified as being higher in energy by 82.4 kJ mol^{-1} than the

---

† HF/6-31G* = use of Restricted Hartree-Fock theory, with a basis set that has six primitive Gaussians for the core orbitals, a three/one split for the *s*- and *p*-valence orbitals, and a single set of six *d*-functions (indicated by the asterisk).

2-propyl cation **177**, in reasonable agreement with an experimental value[186] of 67 kJ mol^{-1}.

Pople et al. also attempted to characterise the edge protonated structure **174**, with C_{2v} symmetry imposed, and the corner protonated structure **175**, restricted to C_s symmetry, but concluded that the energy difference between the two structures was too small to make any definite prediction about the nature of the two cations with the level of theory available. The energy difference between **177** and **175** was calculated to be 34.3 kJ mol^{-1}, which is in good agreement with the experimental value of 33 kJ mol^{-1} observed as the difference in energy between the 2-propyl cation **177** and a species considered to be a "protonated cyclopropane".[187-189]

A number of years after Pople's paper was published Dewar et al.[190] repeated Pople's calculations using an identical basis set at both HF and MP4SDQ levels of theory. These results showed the corner protonated species **175** (Figure 6.2) to have one negative force constant, and thus identified the structure as a transition state (TS) and not a minimum on the PE surface as Pople et al. had implied. Rotation of the methyl group by 30° and reoptimisation gave a true minimum **180** (Figure 6.2) on the PE surface, with an energy 0.67 kJ mol^{-1} lower than **175** and a distinctly unsymmetrical structure. This demonstrates that **175** is a transition state for the rotation of the methyl group in the nonclassical charge transfer complex and that this process interconverts **180** with its mirror image. The observation that **180** is lower in energy than **175** is surprising considering the eclipsing of the adjacent methylene and methyl hydrogens. The stability of **180** is thought to be due to a stabilising hyperconjugative interaction between the C-H bonds of the apical methyl group and the antibonding π^* molecular orbital (MO) of the ethene moiety.[190,191]

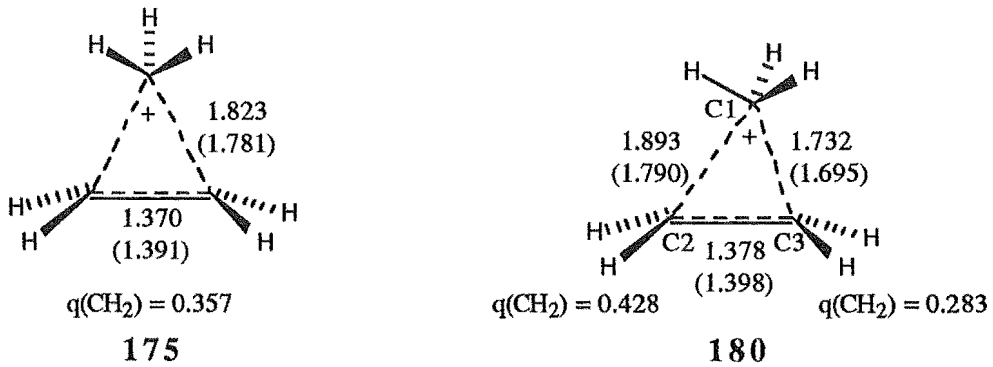

Figure 6.2. Bond lengths and charges (q) of corner protonated cyclopropanes **175** and **180**, from geometry optimization using a 6-31G* basis set using RHF procedures.[190] Bond lengths in brackets are taken from geometry optimization using MP2/6-311G** level of theory.[192] All bond lengths are in Angstroms and charges in atomic units.

Yamabe et al.[37] have also reported results of calculations attempting to characterise the $C_3H_7^+$ PE surface. Their results, using MIDI-1 optimised geometries, predict the edge protonated cation **174** to be a transition state for proton migration, and also suggest the presence of a charge transfer (CT) complex **181** (Figure 6.3) similar to **180**, but more unsymmetrical.†

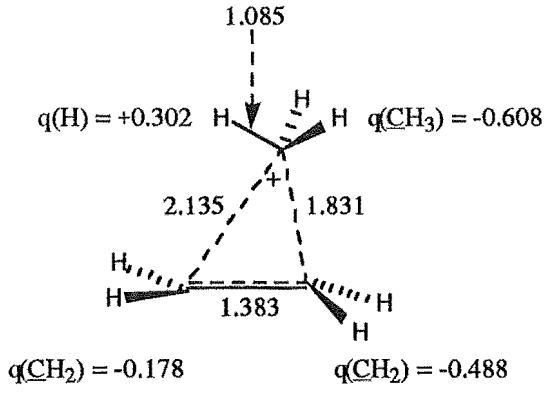

181

Figure 6.3. Geometry of the CT complex **181** optimized using a MIDI-1 basis set. Bond lengths are in Angstroms. Net atomic charges (q) are also shown.[37]

For the CT complex **181**, the incoming proton lies in the horizontal plane of the cyclopropane ring, with the front-side edge (2.135 Å) being longer than the back-side edge (1.831 Å). The structure therefore arises from edge attack of the incoming electrophile, resulting in retention of configuration at the site of attack (E-retention).[37] As Yamabe pointed out,[37] the unsymmetrical nature of **181** will lead to uneven charge development at the two carbons of the ethene moiety (Figure 6.3). Thus, a nucleophile would be expected to attack the back-side of ethene moiety at the least anionic (charge = -0.178 a.u.) carbon. This would result in inversion of configuration of the carbon at this center (N-inversion) and thus the overall result would be an E-retention/N-inversion process. However, since the barrier to methyl migration is calculated to be small[37] (less than 4 kJ mol^{-1}) the methyl group may migrate before the nucleophilic capture of the cation, resulting in a competing E-inversion/N-inversion process. The presence of substituents on the ethene moiety will influence the relative lengths of the edges and hence influence the partition between the E-inversion/N-inversion process. In the reaction of *cis*-1,2,3-trimethylcyclopropane with acid, DePuy et al.[7,17,193] observed that 68% of

† In order to distinguish geometries calculated at different levels of theory for each general structure, the new geometry has been assigned a different number. For example, structures **180** and **181** are both unsymmetrical corner protonated cyclopropanes but have been optimised using different basis sets (6-31G** and MIDI-1, respectively) and hence are calculated to have significantly different geometries.

electrophilic addition occurred with retention of configuration and 32% with inversion (Figure 6.4).

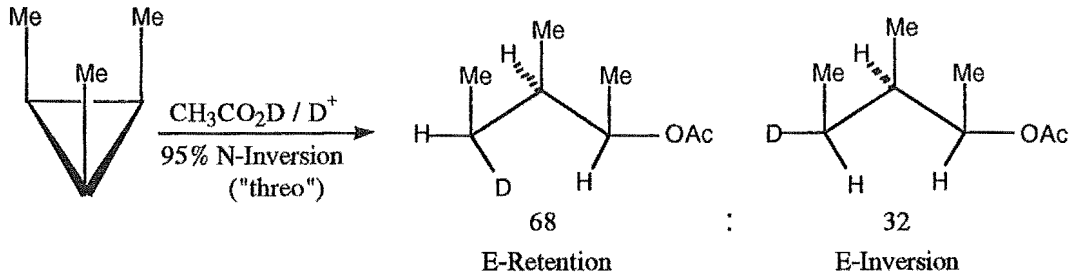

Figure 6.4. Addition of acetic acid-d_1 to *cis*-1,2,3-trimethylcyclopropane gave a 68:32 ratio of E-retention and E-inversion, respectively.[193]

DePuy et al. suggested that an unsymmetrical corner protonated species **182** (Figure 6.5) was formed (probably via an initial edge protonated structure[193]), since if nucleophilic attack occurred to an edge protonated structure a great deal of molecular motion and change in bonding would have to occur in order to obtain E-inversion. Hence it is unlikely that both E-retention and E-inversion pathways would have similar energies i.e. a much larger proportion of E-retention products would be expected. The possibility of both corner and edge protonated intermediates being formed on separate reaction pathways (i.e. two competing mechanisms which could give rise to the observed ratio) was also considered, but this seemed unlikely as the ratio of products formed from two independent pathways would not be expected to remain constant over a wide range of conditions,‡ as was observed experimentally.

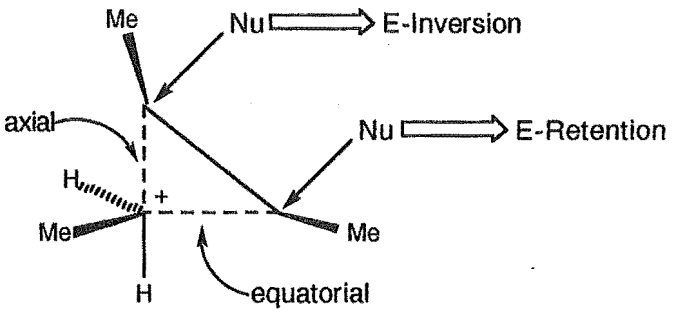

182

Figure 6.5. Unsymmetrical corner protonated structure suggested by DePuy.[193]

In structure **182** one bond of the three membered ring would be expected to be axial (see Figure 6.5) and another equatorial. Nucleophilic attack on the equatorial carbon

---

‡ Experiments investigating the ratio of products from the reaction of *cis*-1,2,3-trimethylcyclopropane with CF_3CO_2D/D^+, CH_3CO_2D/D^+, and CH_3OD/D^+ were carried out.[193]

would lead to retention of D^+ and attack on the axial carbon would give inversion of D^+. The carbons in such an intermediate are not identical and an exact 50:50 ratio of the products would not be expected.

The most definitive computational investigation of the $C_3H_7^+$ PE surface has recently been published by Koch and co-workers[192,194] using MP2/6-311G** optimised geometries. Energy differences and vibrational frequencies were determined from single point calculations (based on the MP2 optimised geometries) using the MP4(FC)/ 6-311G** level of theory.† The results of Koch's calculations for the 2-propyl cation **177**, in agreement with those of Pople,[181] show that the structure is not a minimum of the PE surface. The change in structure from C_{2v} to C_2 symmetry results in a small lowering in energy. Thus **176** is considered to be the true 2-propyl cation minimum, with a small (2 kJ mol^{-1}) barrier for rotation of the methyl groups.

Structure **180** was calculated to be the lowest energy corner protonated cyclopropane, in agreement with Dewar,[190] but the distortion was less after optimisation at the MP2 level (Figure 6.2). The barrier to rotation of the methyl group via **175** was found to be small (0.4 kJ mol^{-1}).

According to Koch, movement of hydrogens around the cyclopropane ring occurs via the edge protonated structure **174** which lies 5.9 kJ mol^{-1} above the unsymmetrical corner protonated species **180**. Although **174** appeared to be a shallow minimum, the exact nature of the stationary point could not be conclusively determined since the TS for the interconversion of **174** and **175** becomes a little lower in energy than **174** after zero-point energy corrections are applied.[192]

Koch et al. concluded that their results indicated the 1-propyl cations **183**§ (Figure 6.6) and **179** to be "isotope scrambling" structures. Structure **179** was slightly lower in energy than **183**, which is the transition structure for the interconversion of the unsymmetrical corner protonated structure **180** and the 2-propyl cation **176**. This process occurs by widening of the C1-C2-C3 or C1-C3-C2 bond angle of **180** with simultaneous rotation of the methyl group until **183** is reached. A hydrogen then migrates from C2 without an activation barrier. A twisting of the C1-C2 bond in **179** from the perpendicular geometry allows a 1,2-hydride migration, to give the 2-propyl cation **176**. Due to the small activation barrier (0.4 kJ mol^{-1}) **180** would interconvert rapidly at room temperature with its mirror image **180'**, therefore no marked preference for nucleophilic attack at C2 or C3 would be expected. This pathway would lead to both proton and carbon scrambling. The alternative rearrangement of **179** to **176** leads to proton but not carbon scrambling[192] (see Figure 6.7).

---

† FC indicates that the core 1*s* orbitals on the carbon atoms were frozen in the MP4 calculations.

§ Koch's structure **183** appears to have the positively charged methylene group twisted out of the horizontal plane resulting in C_1 symmetry unlike Pople's structure **178** which has C_s symmetry.

It is worthwhile noting that, although structure **183** is similar to cation **178** identified by Pople et al.,[181] the structures are distinctly different. Cation **178** has C_s symmetry and **183** has C_1 symmetry (Figure 6.6).

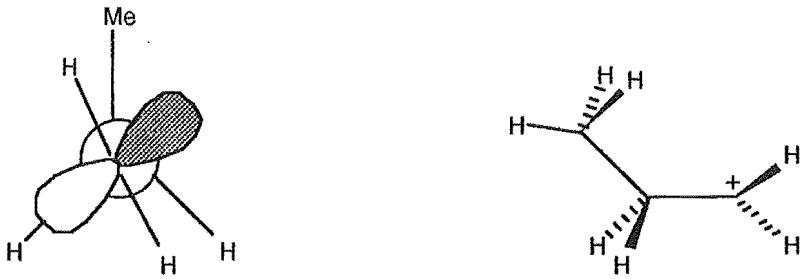

183 **183**

Figure 6.6. 1-Propyl cation **183**. The cation is similar to **178** but has C_1 rather than C_s symmetry.

Koch's calculations agree well with the observations of Saunders et al.[195,196] which show **183** to lie 3.3 kJ mol^{-1} above **179**, in agreement with the calculated value. Cation **179** is calculated[192] to lie 81 kJ mol^{-1} above the 2-propyl cation **176** which is substantially larger than the value determined in nonnucleophilic (super acid) media[186,195] of 68 ± 2 kJ mol^{-1}. Koch et al.[192] have suggested that this may be due to differential solvation; however, as they also pointed out, this is unlikely because both **176** and **179** are "classical" carbenium ions and recent studies[197,198] indicate that the differential solvation of carbocation structures is energetically small.

The experimental estimates of the energy differences between the 2-propyl cation and protonated cyclopropane (33 kJ mol^{-1}),[187,188] and the 1-propyl cation (84 kJ mol^{-1})[199] agree well the calculated values of 30 kJ mol^{-1} and 81 kJ mol^{-1}, respectively, for the most stable forms of the species. The results of Koch's calculations are shown in Figure 6.7.

Section 6.2.2 Results of the Semiempirical Molecular Orbital Calculations

Although the ab initio results would be expected to give a more accurate picture of the stabilities of the $C_3H_7^+$ cations and therefore of the processes involved in cyclopropane ring opening, it is important for the present study of larger systems to obtain an estimate of the reliability of the semiempirical molecular orbital methods in modelling the ring opening reactions of cyclopropane, and hence their value in modelling more complex systems containing a cyclopropane ring where the size of the system prohibits the use of ab initio methods.

Dewar et al.[174] have reported the MINDO/3 heat of formation for the 1-propyl, 2-propyl and "corner" protonated cations but did not publish the geometries. They did not report calculations for all the reasonable conformations of the 1-propyl and 2-propyl cations, or discuss the difference between the symmetrical and unsymmetrical corner

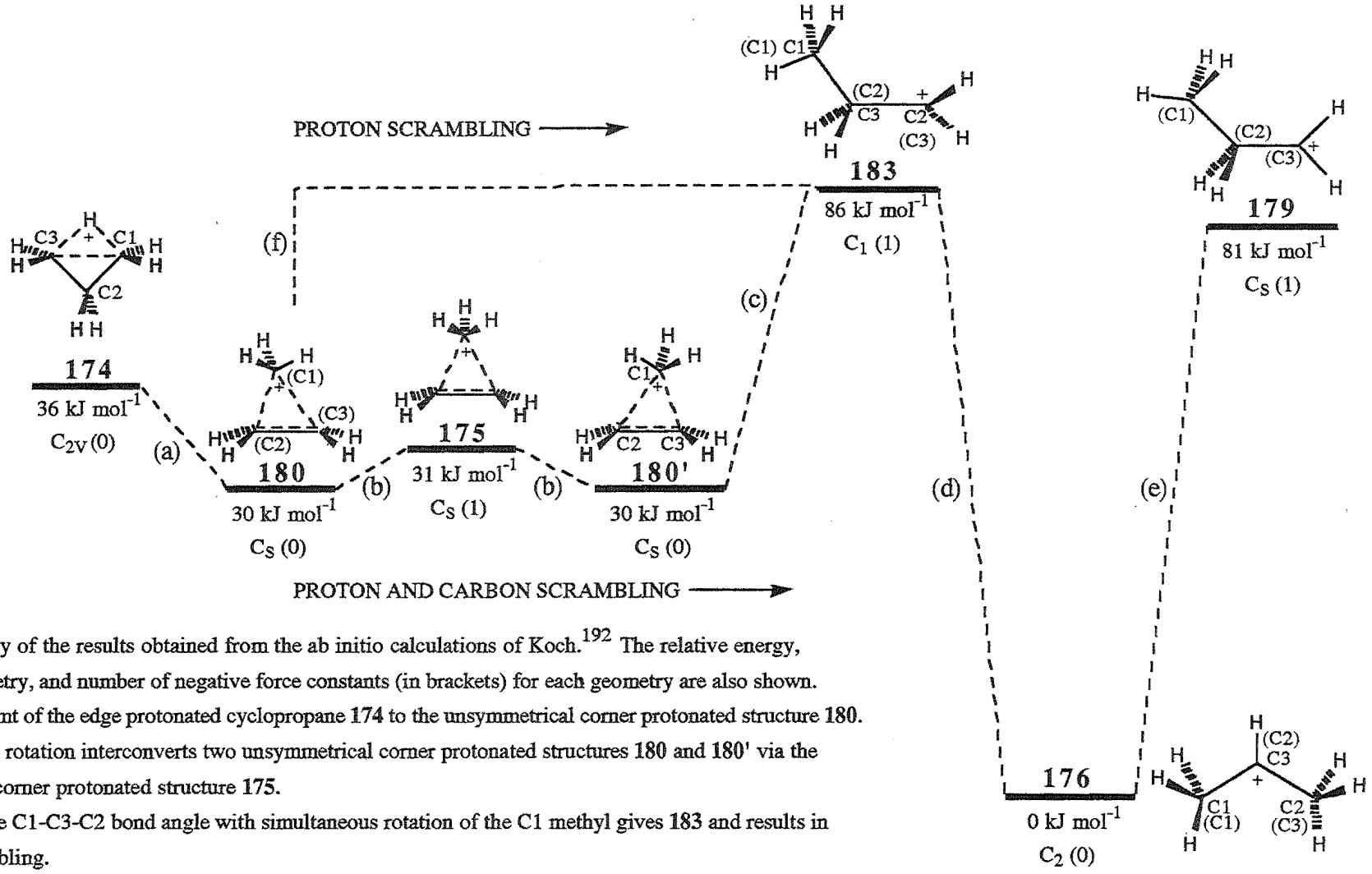

Figure 6.7. Summary of the results obtained from the ab initio calculations of Koch.[192] The relative energy, symmetry, and number of negative force constants (in brackets) for each geometry are also shown.

(a) Rearrangememt of the edge protonated cyclopropane **174** to the unsymmetrical corner protonated structure **180**.

(b) Methyl group rotation interconverts two unsymmetrical corner protonated structures **180** and **180'** via the symmetrical corner protonated structure **175**.

(c) Increase of the C1-C3-C2 bond angle with simultaneous rotation of the C1 methyl gives **183** and results in carbon scrambling.

(d) 1,2-Hydride shift with no activation barrier.

(f) Increase of the C1-C2-C3 bond angle with simultaneous rotation of the C3 methylene gives **183** without carbon scrambling (carbon numbers are shown in brackets).

(e) 1,2-Hydride shift with no activation barrier.

protonated species. Although they reported the structure and heat of formation of the edge protonated cyclopropane, the structure and symmetry constraints reported were inconsistent with the edge protonated structure.‡ It was therefore decided to repeat Dewar's MINDO/3 calculations but in a more rigorous manner.

For the PM3[172,200,201] (Parametric Method 3) and AM1[202] (Austin Model 1) semiempirical molecular orbital methods[203] the "cyclopropyl cation" ($C_3H_5^+$) is cited as the worst case, i.e. largest error in heat of formation calculations, the 1-propyl and 2-propyl cations give much better agreement with the experimental results.[170-172]

For the present study it is the relative energies and geometries obtained, which are important in studying the possible mechanisms of a reaction.

Section 6.2.2a The 2-propyl cation

To search the conformational space of the secondary cation both methyl groups were rotated through 120° by 10° increments and the PM3 energy† and geometry calculated at each point using the semiemipirical molecular orbital program MOPAC version 6.0.§ The results of this search are shown in Figure 6.8. Possible stationary points (A-D, Figure 6.8) were identified and the geometries then refined using Bartel's gradient norm minimisation method.[204] Frequency calculations were then performed on the stationary points to determine the force constants and hence characterise the structures as minima or transition states.

The geometries of the stationary points are shown in Figure 6.9 along with their calculated heats of formation. The three structures **184-186** are transition states and structure **184** was established as a second order saddle point by the presence of two imaginary frequencies. Structures **185** and **186** are identical, as expected from symmetry considerations (see Figure 6.8), and were shown to be transition states for the rotation of the eclipsed methyl group.

---

‡ One of the geometries described as "edge protonated cyclopropane" in the original paper was not that of edge protonated cyclopropane and the C_{3v} symmetry constraint reported is also inconsistent with the edge protonated structure (C_{2v} symmetry would be expected) although this may have been a type setting error.

† Although the AM1 method generally gives more accurate heats of formation for cations,[172,203] the PM3 parameterised Hamiltonian is used here since it tends to give a better treatment of the starting materials and products used in later chapters. PM3 also proved advantageous in the location of TS's for the larger systems (see Chapter 7).

§ Semiempirical calculations were performed using MOPAC Ver. 6.0 or SPARTAN Ver. 201 running on IBM 320 or 320H RISC computers.

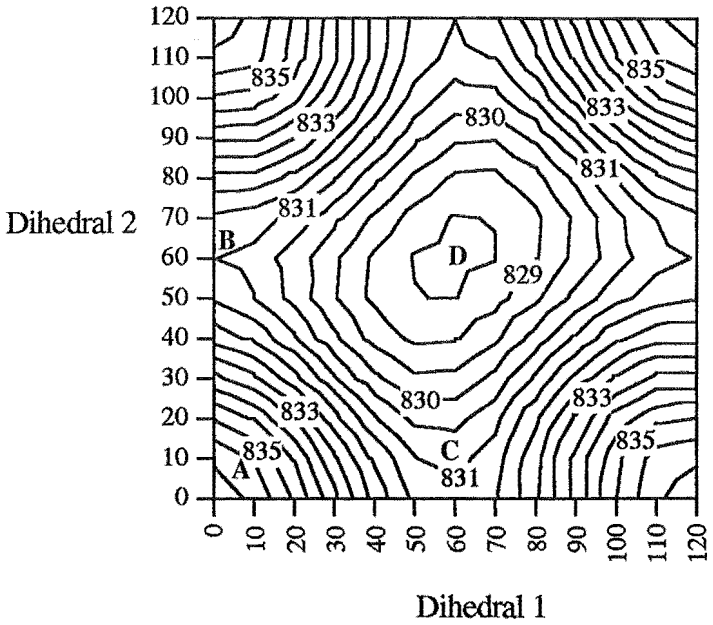

Figure 6.8. Contour plot showing PM3 energies upon rotation of both methyl groups of the 2-propyl cation. Heats of formation are in kJ mol^{-1}, angles are in degrees. Dihedrals 1 and 2 are the H2-C2-C1-H1 and H2-C2-C3-H3 dihedral angles (see Figure 6.9), respectively. The approximate positions of structures **184-187** on the PE surface are indicated by the labels **A-D**, respectively.

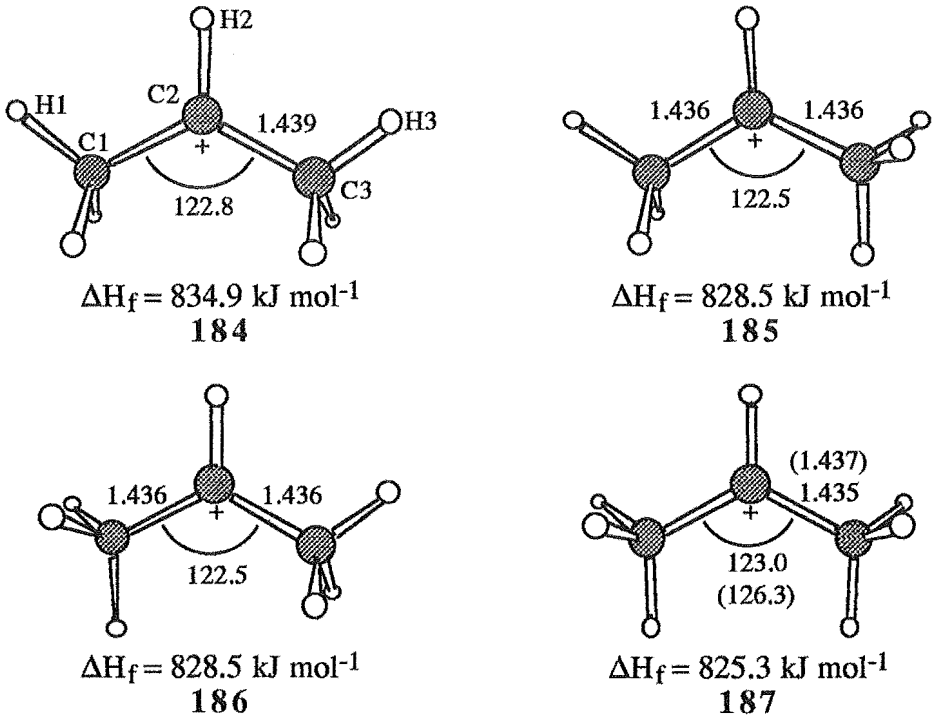

Figure 6.9. PM3 2-propyl cations resulting from the conformational search. Bond lengths and angles are in Angstroms and degrees, respectively. Numbers in brackets are the corresponding ab initio bond lengths and angles[192] for the similar structure **176** with C_2 symmetry. The position of structures **184-187** on the PE surface for the rotation of the methyl groups are indicated by labels **A-D** on Figure 6.8.

Structure **187** was characterised as a minimum on the PE surface (all force constants were positive and the six vibrations corresponding to the rotation and translation of the molecule as a whole were all small) and was the lowest energy structure. In contrast to the ab initio calculations, where the lowest energy 2-propyl cation **176** had C_2 symmetry, the lowest energy 2-propyl cation identified on the PM3 PE surface showed C_{2v} symmetry. The PM3 calculated carbon-carbon bond lengths of structure **187** were in good agreement with those obtained for **176** by the ab initio methods, 1.435 Å and 1.437 Å, respectively. The PM3 method underestimates the C1-C2-C3 bond angle, 123.0° compared to 126.3° from the ab initio calculations.[192] The twisted 2-propyl cation with C_2 symmetry was not observed as a stationary point on the PM3 PE surface (Figure 6.8).

The cations shown in Figure 6.9 were reoptimised using the MINDO/3[205] (Modified Intermediate Neglect of Differential Overlap) semiempirical molecular orbital method since such INDO[206] (Intermediate Neglect of Differential Overlap) based methods are known to perform somewhat differently to the NDDO[207] (Neglect of Diatomic Differential Overlap) based methods, such as PM3, AM1, and MNDO, in terms of geometries obtained and characterisation of stationary points.‡ Force constants were calculated for the resulting geometries and the stationary points characterised. The resulting structures are shown in Figure 6.10.

Structures **188-191** were all characterised as second order saddle points. No lower energy structure with C_2 symmetry was found upon reoptimisation using both gradient norm and energy minimisation criteria.

The carbon-carbon bond lengths of structure **191** compared well with those calculated for **176** in the ab initio studies, 1.439 Å and 1.437 Å, respectively, but the C1-C2-C3 bond angle was larger than predicted by the ab initio results, 133.5° compared with 126.3°.

Section 6.2.2b The 1-propyl cations

The 1-propyl cation was studied in a similar way to the 2-propyl cation. The two carbon-carbon bonds were rotated and the PM3 energy evaluated at each point. The results of the calculations are shown in Figure 6.11. The stationary points were identified, the geometries extracted, refined, force constants calculated, and the stationary points characterised. Figure 6.12 shows the resulting 1-propyl cation geometries.

---

‡ For a discussion of the differences between the various semiempirical molecular orbital methods see references 203 and 208.

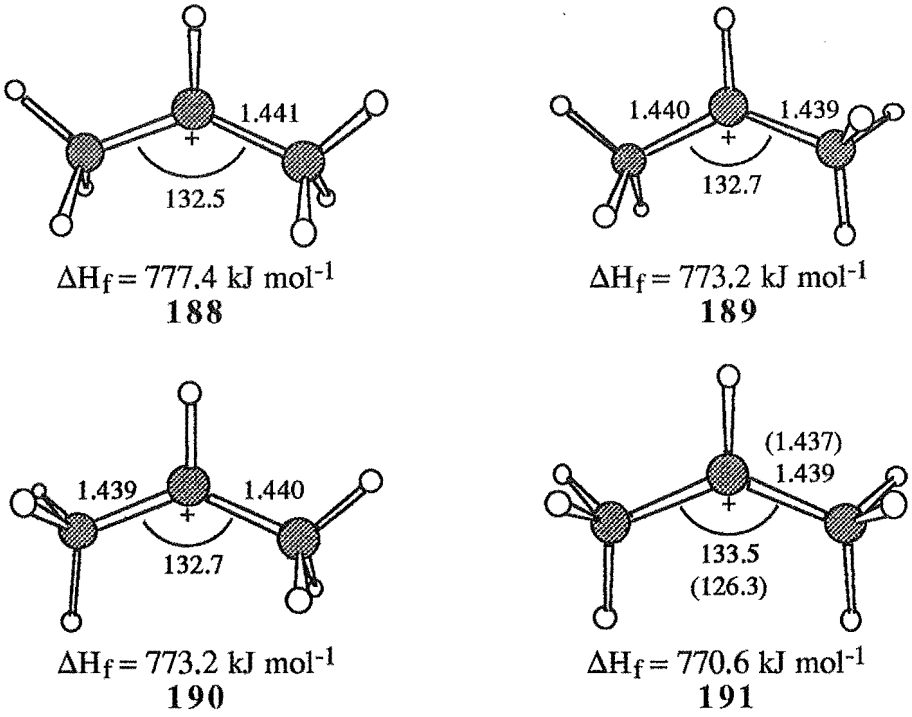

$\Delta H_f = 777.4$ kJ mol^{-1}
188

$\Delta H_f = 773.2$ kJ mol^{-1}
189

$\Delta H_f = 773.2$ kJ mol^{-1}
190

$\Delta H_f = 770.6$ kJ mol^{-1}
191

Figure 6.10. MINDO/3 2-propyl cations. Bond lengths and angles are in Angstroms and degrees, respectively. Numbers in brackets are the corresponding ab initio bond lengths and angles[192] for the similar structure **176** with C_2 symmetry.

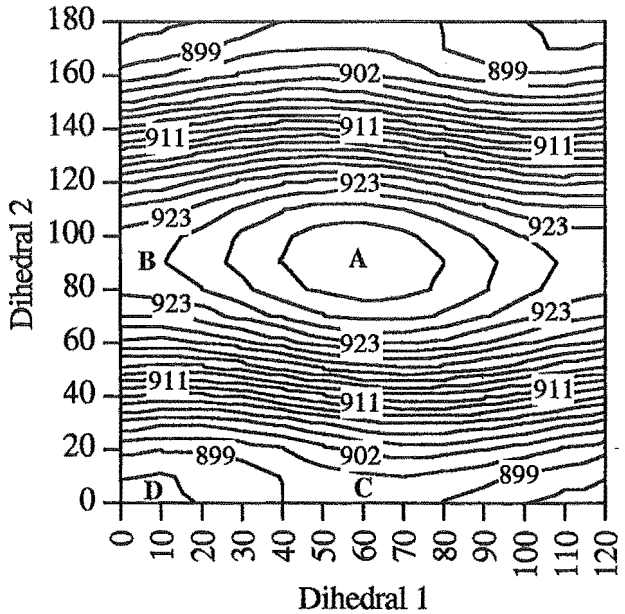

Figure 6.11. Contour plot of the PM3 results for the 1-propyl cations. ΔH_f is plotted against the dihedral angle of a reference proton on each of the terminal carbon atoms with respect to a dummy atom attached to C2. Heats of formation are in kJ mol^{-1}, angles are in degrees. The points labeled **A-D** correspond to structures **192-195**, respectively.

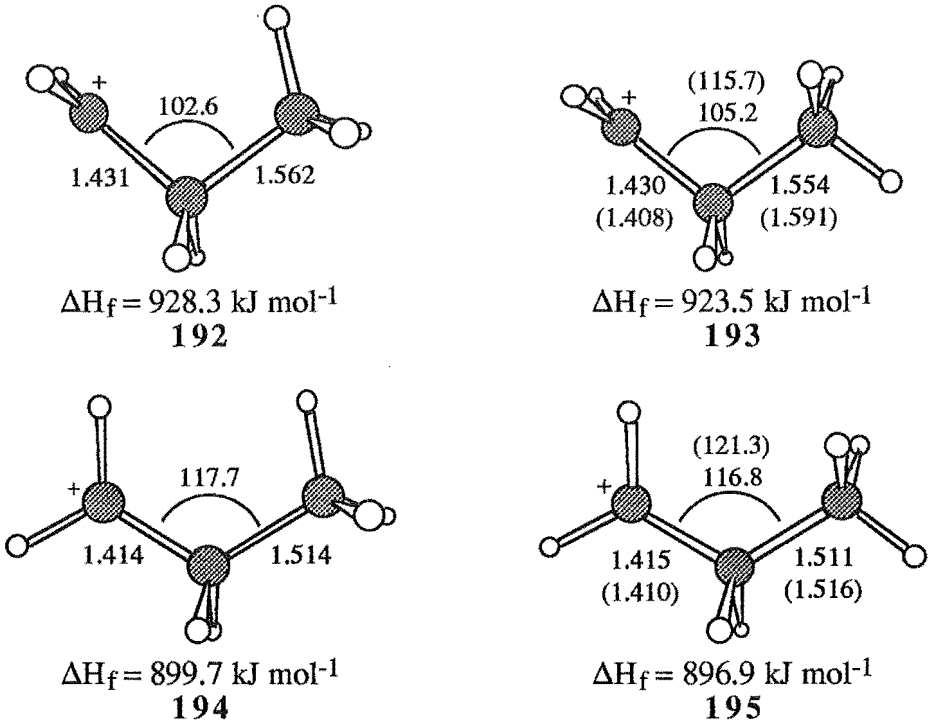

Figure 6.12. 1-Propyl cations on the PM3 potential energy surface. Distances are in Angstroms. Numbers in brackets are values taken from the ab initio results.[192]

Structure **192** is a second order saddle point. The two imaginary frequencies, -172 cm^{-1} and -139 cm^{-1}, correspond to rotation of the positively charged methylene group and rotation of the methyl group, respectively. The second highest energy 1-propyl cation **193** is the PM3 equivalent of **178**, identified from the ab initio calculations.[192] This structure was established as a TS (one imaginary frequency) in agreement with the ab initio result.[192] From analysis of the imaginary frequency contributions the structure was identified as a TS for the rotation of the positively charged methylene group. The lengths of the C1-C2 and C2-C3 bonds show deviations of +0.022 Å and -0.037 Å, respectively, from the ab initio structures (see Figure 6.12).

Structure **194** was characterised as a TS for methyl group rotation. No equivalent structure was reported in the ab initio calculations.

The lowest energy 1-propyl cation **195** is the PM3 equivalent of structure **179** and was identified as a minimum on the PM3 PE surface. In contrast, the ab initio results suggest **179** to be a "isotope scrambling structure".[192] The PM3 calculated bond lengths are in good agreement with the ab initio results, but the C1-C2-C3 bond angle is underestimated by 5°. The PM3 results show **195** to be higher in energy by 72 kJ mol^{-1} than the 2-propyl cation **187**. This compares well with the experimental[199] result of 84 kJ mol^{-1} and the ab initio value[192] of 81 kJ mol^{-1}.

Each of the structures **192-195** were reoptimised using the MINDO/3 parameterised Hamiltonian method and each of the resulting geometries characterised.

The final geometries obtained from these calculations are shown in Figure 6.13. All four structures **196-199** were identified as transition states on the MINDO/3 PE surface but structures **196** and **197** were second order transition states, both having two imaginary frequencies.

Structure **198** was identified as a TS for rotation of the C1 positively charged methylene and cation **199**, the lowest energy MINDO/3 1-propyl cation, showed one imaginary frequency which involved one proton on C2 and both the hydrogens attached to C1, consistent with a 1,2-hydride shift as described by Koch for structure **179**.[192]

As for the PM3 method, agreement of the MINDO/3 calculated bond lengths for **199** (**195** for PM3) and **179** is better than the agreement for the bond lengths of **197** (**193** for PM3) and **178**. The C1-C2-C3 bond angles for both structures show significant deviation from the ab initio results (see Figure 6.13).

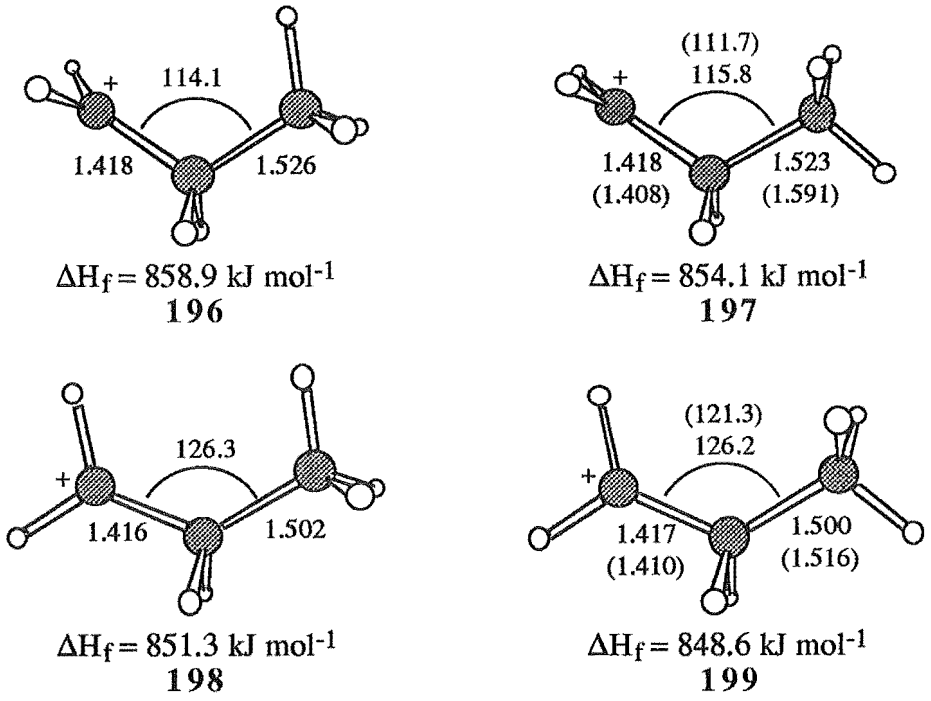

$\Delta H_f = 858.9$ kJ mol^{-1} **196**

$\Delta H_f = 854.1$ kJ mol^{-1} **197**

$\Delta H_f = 851.3$ kJ mol^{-1} **198**

$\Delta H_f = 848.6$ kJ mol^{-1} **199**

Figure 6.13. MINDO/3 1-propyl cations. Distances are in Angstroms. Numbers in brackets are values taken from the ab initio results.[192]

The MINDO/3 calculated difference in energy between the 1-propyl cation **199** and the lowest energy 2-propyl cation **191** is in good agreement with the ab initio value, 78 kJ mol^{-1} and 80.8 kJ mol^{-1}, respectively, and close to the experimental value[199] of 84 kJ mol^{-1}. Thus prediction of the relative stabilities of the secondary and primary carbocations is better using the MINDO/3 method than the PM3 method.

Section 6.2.2c The corner protonated cation

An initial approximate structure was obtained and minimised with the PM3 parameterised Hamiltonian using Bartel's gradient norm optimisation procedure. The resulting symmetrical structure **200** (Figure 6.14) showed one imaginary frequency, the vibration corresponding to the migration of the methyl group which interconverts two mirror image 1-propyl cations similar in structure to **193**.

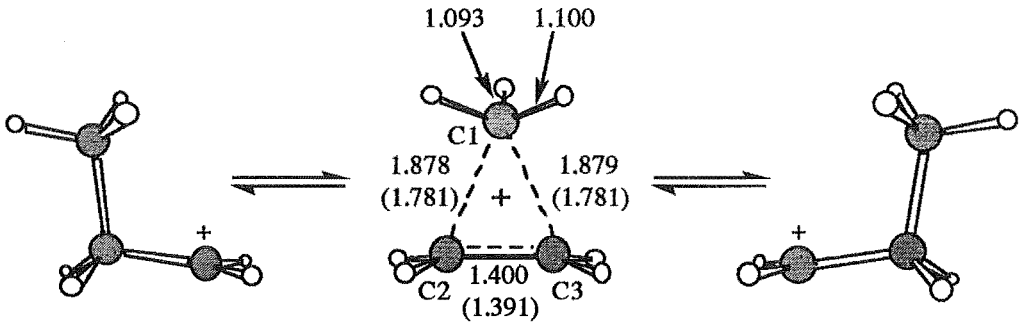

$\Delta H_f = 969.3$ kJ mol^{-1}

193 **200** **193**

Figure 6.14. Diagram showing the PM3 corner protonated cyclopropane **200** to be a transition state for the interconversion of two mirror image 1-propyl cations. Bond lengths in brackets are the corresponding ab initio values.[192]

Rotation of the methyl group of **200** showed a maximum energy when one hydrogen was in the plane of the three carbons (Figure 6.15). Gradient minimisation of this structure gave **201** (Figure 6.16) which corresponds to a second order saddle point for the rotation and migration of the methyl group. Thus, the PM3 results do not predict the presence of a distinctly unsymmetrical CT complex minimum, as found by the ab initio calculations.[181,192] The contour plot Figure 6.17a shows the heat of formation of the CT complex versus the C1-C2 and C1-C3 distances. The "lowest energy structures" correspond to the 1-propyl cation **193** (labelled A, Figure 6.17a). The symmetrical CT complex **200** (labelled B, Figure 6.17a) is a saddle point.

The difference in energy between the 2-propyl cation **187** and the corner protonated species **200** do not agree with the ab initio and experimental results. The PM3 calculated difference is 144 kJ mol^{-1} compared with the ab initio[192] and experimental[187,189] value of 30 kJ mol^{-1}.

The geometry of **200** obtained from the PM3 calculations is significantly different from the ab initio models. The C1-C2 bond length differs from Dewar's structure[190] by +0.056 Å and from Koch's structure[192] by +0.098 Å. The C2-C3 bond length shows a deviation of +0.030 Å from Dewar's geometry but shows much better agreement with Koch's structure, +0.009 Å. Thus, the results appear to reflect the inability of the PM3 method to deal with nonclassical structures of this type. The method does however

correctly predict a very small barrier to methyl rotation (approximately 0.1 kJ mol^{-1}) in agreement with the ab initio calculations.

The unsymmetrical CT complex **201** shows poor agreement with the ab initio calculated geometry (see Figure 6.16).

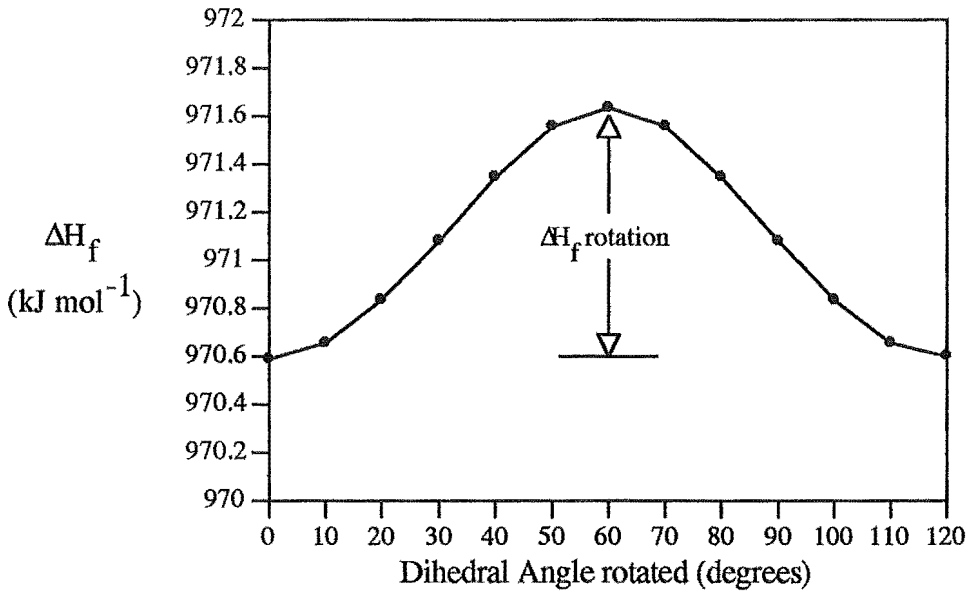

Figure 6.15. Rotation of the methyl group of the PM3 corner protonated cyclopropane **200**. The dihedral angle was defined with respect to two dummy atoms which were placed on the vertical mirror plane which bisects **200**. Values at 0° and 120° correspond to **200** and a value of 60° to structure **201**.

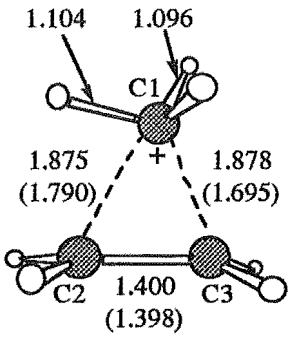

$\Delta H_f = 969.4$ kJ mol^{-1}

201

Figure 6.16. Rotation of the methyl group in **200** followed by optimization gave a transition state **201** for methyl rotation and migration on the PM3 PE surface. Distances are in Angstroms. Bond lengths in brackets are the corresponding ab initio values.[192]

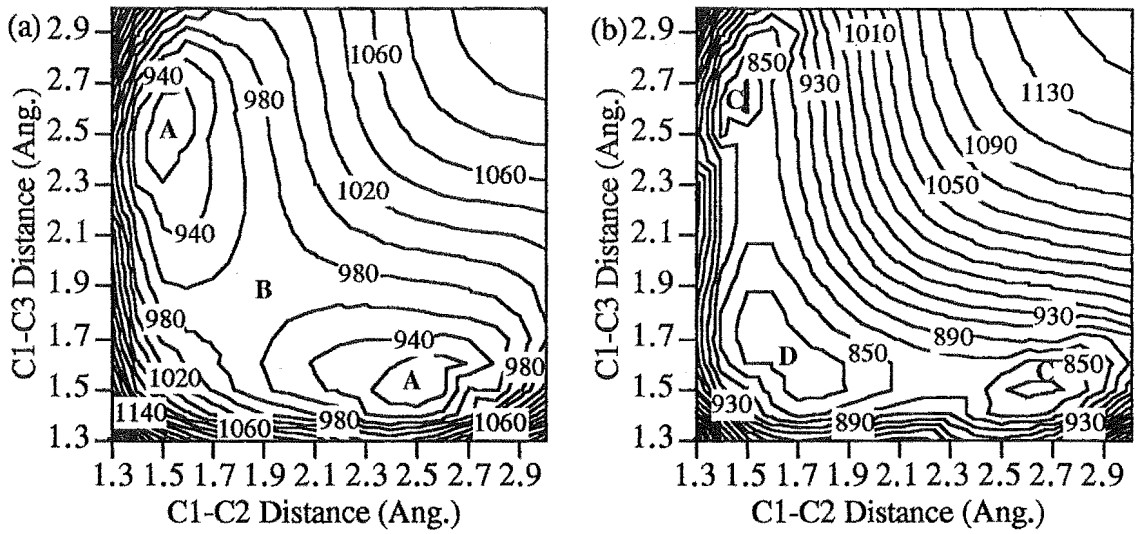

Figure 6.17. Contour plots of (a) PM3 and (b) MINDO/3 heats of formation for the structures obtained from varying the distance of the methyl group carbon from each of the carbons in the ethene moiety of the corner protonated cation **200**. Points **A** and **B** of (a) correspond to structures **193** and **200**, respectively. Points **C** and **D** of (b) correspond to structures **197** and **203**, respectively.

The corner protonated structure **200** was reoptimised using the MINDO/3 method and a frequency calculation performed. The resulting geometry **202** (Figure 6.18) was found to be a TS for the rotation of the methyl group, in agreement with the ab initio calculations, but the geometry was different, with a C1-C3 distance of 1.648 Å compared with 1.781 Å found by the ab initio calculations.[192] Rotation of the methyl group, followed by reoptimisation gave structure **203** which was demonstrated to be a true minimum on the PE surface but showed a markedly different geometry to that obtained from the ab initio calculations. For example, the C1-C3 distance of 1.586 Å and the C1-C2 distance of 1.700 Å show significant deviations from the ab initio bond lengths of 1.695 Å and 1.790 Å, respectively.

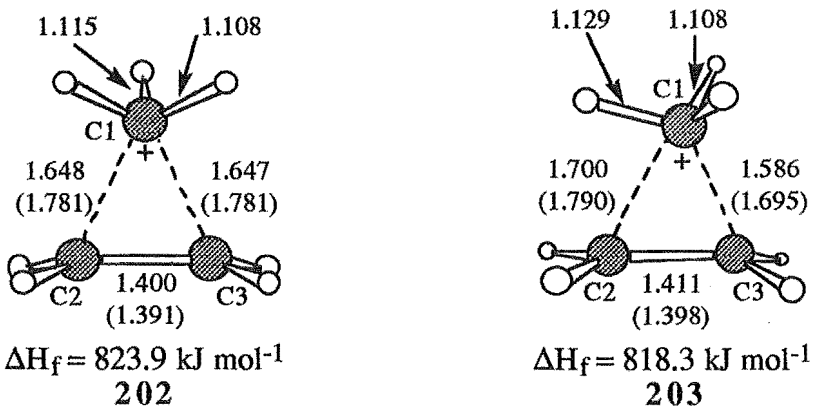

Figure 6.18. MINDO/3 symmetrical **202** and unsymmetrical **203** corner protonated cyclopropanes. Distances are in Angstroms. Numbers in brackets are the corresponding ab initio bond lengths.[192]

The reduced bond lengths of the MINDO/3 optimised geometries lead to an increase in bond order of the C1-C2 and C1-C3 bonds (Table 6.1). Presumably, both this and the larger steric interactions incurred, contribute to the increase in the calculated barrier to rotation of the methyl group (5.6 kJ mol^{-1}). Also of note is the elongated C-H bond of the hydrogen in the carbon-carbon plane (1.129 Å, see Figure 6.18). This is consistent with with a hyperconjugative interaction with the π^*-orbital of the ethene moiety as described by Dewar.[190] An elongation of the equivalent bond in the PM3 unsymmetrical corner protonated structure **201** was not observed (1.104 Å). The underestimation of the hyperconjugative interaction by the PM3 method would therefore account for some of the deviation from the ab initio results when calculating the energy of this nonclassical ion.

Method	Structure	Bond length C1-C2 (C1-C3)	Bond order C1-C2 (C1-C3)	Methyl Rotational Barrier (kJ mol^{-1})
PM3	**200**	1.878 (1.879)	0.529 (0.529)	0.1
MINDO/3	**202**	1.648 (1.647)	0.569 (0.569)	5.6

Table 6.1. PM3 and MINDO/3 calculated methyl rotational barriers, bond lengths, and bond orders for CT complexes **200** and **202**.

Although the geometries of the corner protonated cyclopropanes **202** and **203** were not in agreement with those obtained by the ab initio studies, the calculated difference in energy (48 kJ mol^{-1}) between the most stable corner protonated species **203** and the 2-propyl cation **191** was in better agreement with the ab initio and experimental value (30 kJ mol^{-1}) than that obtained from the PM3 method (144 kJ mol^{-1}). This presumably reflects the MINDO/3 and ab initio methods characterising the nonclassical cation **203** as a minimum, contrasting with the PM3 results which classify structure **201** as a second order transition state. Comparison of the PE surfaces shows a TS at approximately 1.9 Å, 1.9 Å on the PM3 PE surface (point B, Figure 6.17a) and a minimum at approximately 1.7 Å, 1.7 Å on the MINDO/3 surface (point D, Figure 6.17b).

Section 6.2.2d The edge protonated cation

An initial approximate structure was determined and refined by gradient minimisation to **204** (Figure 6.19) which was shown to be a TS for a 1,3-hydride migration between two 1-propyl cations, similar in structure to **192**. The potential energy surface for this hydride migration (Figure 6.20) shows the heat of formation plotted against the distance of H1 from C1 and C3.

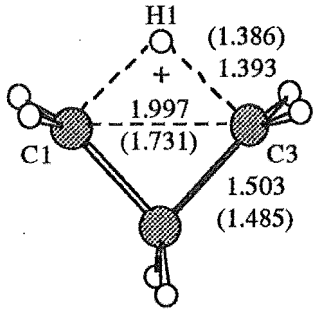

$\Delta H_f = 973.4$ kJ mol^{-1}

204

Figure 6.19. Diagram of PM3 edge protonated cyclopropane. Bond lengths are in Angstroms. Numbers in brackets are the corresponding bonds lengths from the ab initio results.[192]

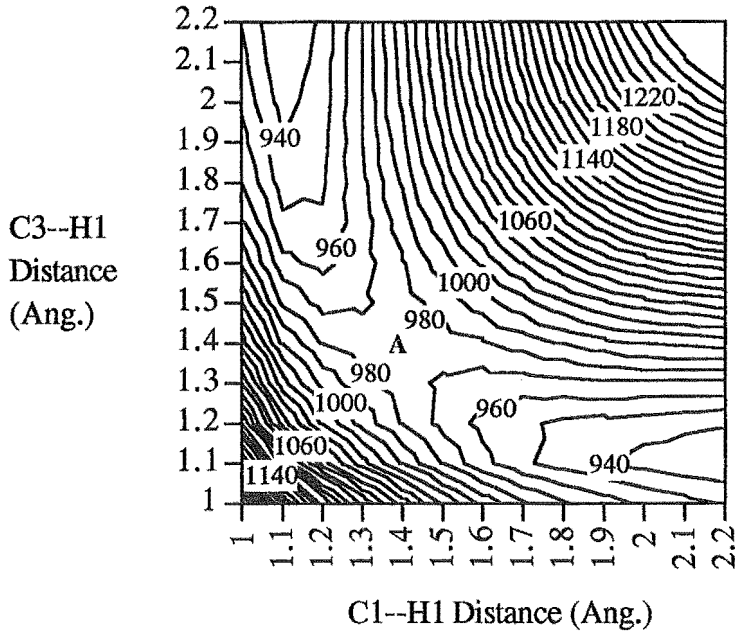

Figure 6.20. Contour plot showing the PM3 results for a 1,3-hydride migration. Heats of formation are in kJ mol^{-1}, distances are in Angstroms. Point A corresponds to the position of structure **204** on the PE surface.

The geometry calculated from the PM3 method was in reasonable agreement with the ab initio results. The C1-H1 and C1-C2 bond lengths of 1.393 Å and 1.503 Å, respectively, compare well with ab initio calculated distances of 1.386 Å (+0.007 Å) and 1.485 Å (+0.018 Å), respectively. However, the structure was characterised as a transition state rather than a minimum, as was found with the ab initio methods.[192]

The PM3 results predict the edge protonated structure **204** to lie 4 kJ mol^{-1} above the corner protonated species **205**, in agreement with the ab initio result of 5.9 kJ mol^{-1}. The MINDO/3 results for the edge protonated structure **205** (Figure 6.21), show it to be a minimum on a flat PE surface (Figure 6.22) in agreement with the ab initio results. The MINDO/3 method predicts the C1-H1 bond length (1.280 Å) to be shorter than the ab

initio calculated value (1.386 Å), although close agreement is obtained for the C1-C2 bond length[192] (1.486 Å and 1.485 Å, respectively).

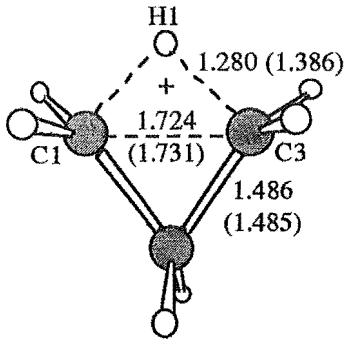

$\Delta H_f = 802.3$ kJ mol^{-1}

205

Figure 6.21. MINDO/3 edge protonated cation. Bond lengths are in Angstroms, numbers in brackets are taken from ab initio[192] results.

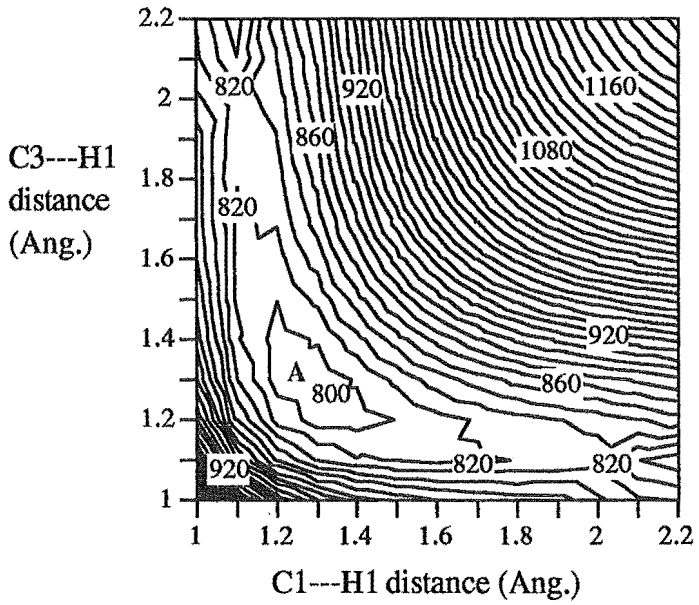

Figure 6.22. Contour plot showing the MINDO/3 results for a 1,3-hydride migration. Heats of formation are in kJ mol^{-1}, distances are in Angstroms. Point A corresponds to the position of structure **205** on the PE surface.

Comparison of Figures 6.20 and 6.22 shows the difference in the PE surface for the edge protonated species calculated by the two semiempirical methods. Figure 6.22 (MINDO/3 results) shows a minimum at approximately 1.3,1.3 Å, in contrast to Figure 6.20 (PM3 results) which shows a saddle point at this position.The MINDO/3 method therefore characterises the edge protonated structure **205** as a minimum, and the PM3 method identifies **204** as a transition state.

The MINDO/3 and ab initio methods give similar predictions for the relative energy of the edge protonated structure **205** with respect to the 2-propyl cation **191**, 32 kJ mol^{-1} and 36 kJ mol^{-1}, respectively. Unlike the MINDO/3 result, the PM3 method does not show good agreement with the ab initio calculations in prediction of the relative energies of the edge protonated **204** and 2-propyl **187** cations (PM3: $\Delta(\Delta H_f)$ = 148 kJ mol^{-1}, ab initio: ΔE = 36 kJ mol^{-1}). This is probably a reflection of the MINDO/3 method characterising the edge protonated structure **205** as a minimum on the PE surface, in agreement with the ab initio results, in contrast to the PM3 prediction of the edge protonated structure **204** as being a transition state for hydride migration.

Section 6.2.2e Discussion of semiempirical results for the $C_3H_7^+$ cations

Overall, as can be seen from Table 6.2, the PM3 semiempirical molecular orbital method gives a smaller average error for the geometries calculated with respect to the ab initio results than does the MINDO/3 method.

Average error§ in bond lengths of PM3 and MINDO/3 calculated structures with respect to the ab initio results.		
Ab initio	PM3	MINDO/3
174	0.013 (**204**, 2)†	0.054 (**205**, 2)
175	0.068 (**200**, 3)	0.092 (**202**, 3)
176	0.002 (**187**, 2)	0.002 (**191**, 2)
179	0.005 (**195**, 2)	0.012 (**199**, 2)
180	0.090 (**201**,3)	0.071 (**203**, 3)
183	0.030 (**193**, 2)	0.039 (**197**, 2)
Average	0.035	0.045

Table 6.2. Average deviations of the semiempirical calculated bond lengths from the corresponding ab initio values (MP2/6-311G** level of theory used for geometry optimisations).[192] Numbers in brackets are the structure number and number of bond lengths averaged, respectively. § Average error = $\frac{\Sigma(|\text{ab initio distance - semiempirical distance}|)}{\#\text{ of distances}}$. † This value excludes the C1-C3 distance which shows an uncharacteristically large deviation from the ab initio result (0.266 Å).

A summary of the relative energies of the 2-propyl, 1-propyl, corner protonated and edge protonated $C_3H_7^+$ cations from the PM3, MINDO/3, ab initio,[192] and experimental[187,195] results‡ is given in Table 6.3. Figures 6.23 and 6.24 show energy

‡ Also see reference 174 for the MINDO/3 relative energies.

level diagrams, relative to the 2-propyl cation, for the PM3 and MINDO/3 results, respectively.

An analysis of these results shows that although problems will arise in that the PM3 method does not characterise the nonclassical cations correctly, a problem not restricted to the PM3 semiempirical method alone,[122] the greater accuracy obtained in the geometries and the larger number of elements parameterised in the PM3 method (particularly bromine, see Chapter 8) substantiates the use of PM3 over MINDO/3 for further calculations on larger systems.

Cation	Relative Energy (kJ mol^{-1})			
	PM3	MINDO/3	AB INITIO[192]	EXPT.†
2-Propyl	0 (**187**, m)	0 (**191**, ts)	0 (**176**, m)	0
1-Propyl	72 (**195**, m)	78 (**199**, ts)	81 (**179**, ts)	84
Sym-Corner Protonated	144 (**200**, ts)	53 (**202**,ts)	31 (**175**, ts)	-------
Unsym-Corner Protonated	144 (**201**, ts)	48 (**203**, m)	30 (**180**, m)	30
Edge Protonated	148 (**204**, ts)	32 (**205**, m)	36 (**174**, m)	-------

Table 6.3. Relative energies of the 2-Propyl, 1-Propyl, corner protonated, and edge protonated $C_3H_7^+$ cations. PM3, MINDO/3, ab initio (energies calculated at the MP4(FC)/6-311G** level of theory) and experimental (EXPT.) results. Brackets enclose the corresponding structure number followed by the type of stationary point (ts = Transition state, m = minimum) predicted. † See references 187, 195, and 199.

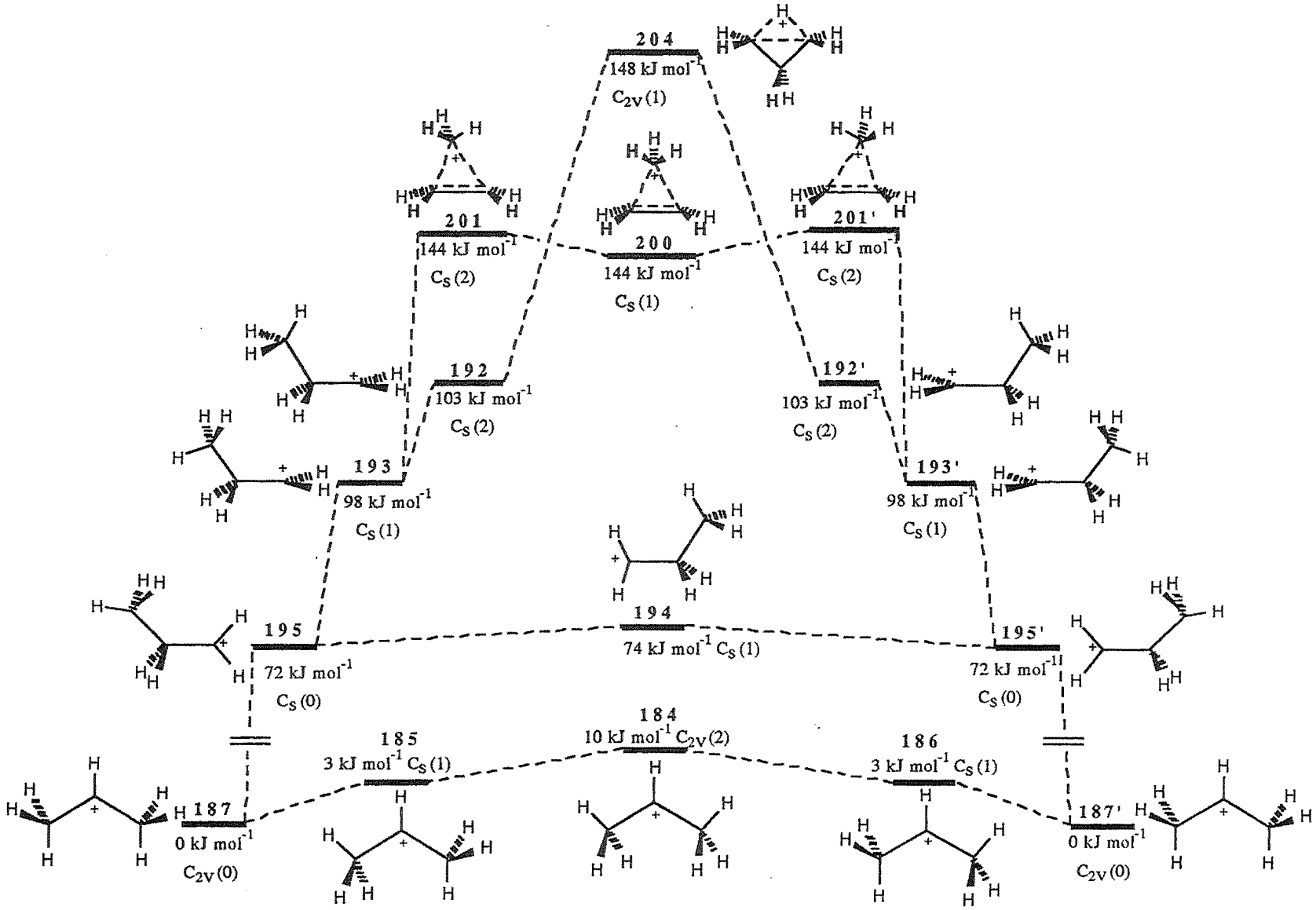

Figure 6.23. Summary of the PM3 energies of the $C_3H_7^+$ cations relative to the 2-propyl cation **187**. The relative energy (kJ mol^{-1}), symmetry, and number of negative force constants (in parentheses) are also shown.

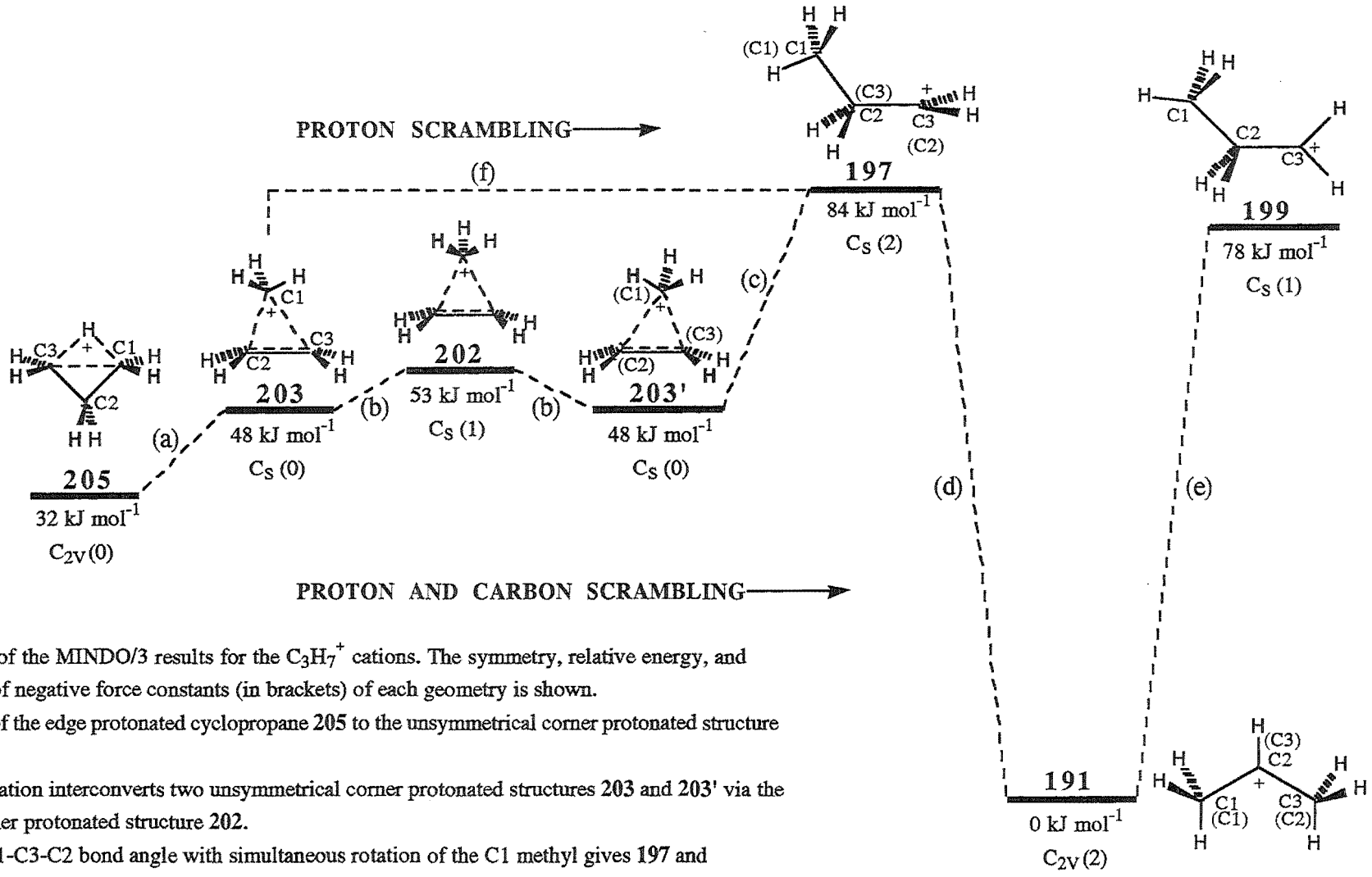

Figure 6.24. Summary of the MINDO/3 results for the $C_3H_7^+$ cations. The symmetry, relative energy, and number of negative force constants (in brackets) of each geometry is shown.

(a) Rearrangememt of the edge protonated cyclopropane **205** to the unsymmetrical corner protonated structure **203**.

(b) Methyl group rotation interconverts two unsymmetrical corner protonated structures **203** and **203'** via the symmetrical corner protonated structure **202**.

(c) Increase of the C1-C3-C2 bond angle with simultaneous rotation of the C1 methyl gives **197** and results in carbon scrambling (carbon numbers in brackets).

(d) 1,2-Hydride shift.

(f) Increase of the C1-C2-C3 bond angle with simultaneous rotation of the C3 methylene gives **197** without carbon scrambling.

(e) 1,2-Hydride shift.

Section 6.2.3 Reaction of Protonated Methanol with Cyclopropane

In the last section the addition of a proton to cyclopropane and the resulting $C_3H_7^+$ carbocation geometries were considered. While this may be a reasonable model for gas phase reactions, in solution an unsolvated proton is not a realistic electrophile. Solvation will effect the relative size of an electrophile and desolvation may be an integral and important part of the reaction mechanism.[209] This, and the fact that ion-neutral reactions have been proposed to occur without an activation barrier in the gas phase,[209] makes inclusion of "solvent" an important aspect in the study of reaction trajectories.

Yamabe et al.[37] considered the attack of an hydronium ion (H_3O^+) on cyclopropane and identified a TS for proton addition **206** (Figure 6.25) which converted smoothly to the charge transfer complex **181** and water.

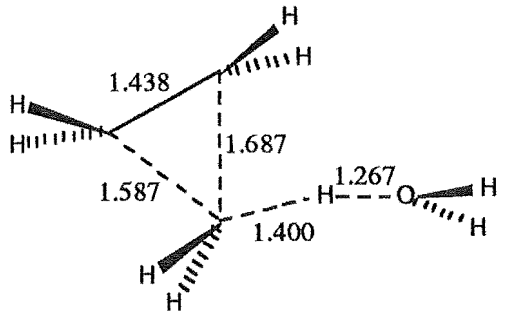

206

Figure 6.25. MIDI-1 optimised transition state for hydronium ion attack on cyclopropane. Distances are in Angstroms.

In the present case, a solvent molecule was explicitly included in the geometry specification of the molecule since the facilities to use semiempirical solvent inclusion models, such as AM1-SM1,[210] AM1-SM1a,[211] AM1-SM2,[212] PM3-SM3,[213] and SAM1[214] which are also computationally more demanding, were not available.

Methanol was used as the solvent molecule in the calculations to enable direct comparison of the results with those obtained for the larger tricyclic systems, which will be discussed later (Chapter 7), where reactions with a proton/deuteron have been examined experimentally using methanol as the reaction solvent.[13-15,18]

To model the reaction of protonated methanol ($CH_3OH_2^+$) with cyclopropane a number of grid calculations were performed by varying the distance of the attacking proton from C1 and C3 (see Figure 6.26) while constraining the O1-H1 distance to a particular value. The heat of formation was evaluated at each point using the PM3 semiempirical method.

The resulting grid calculations are shown in Figures 6.27a-c, for fixed O1-H1 distances of 1.3 Å, 1.4 Å, and 1.5 Å, respectively.

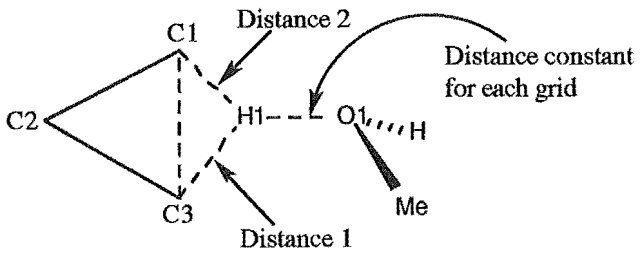

Figure 6.26. Geometry specification for the grid calculations involving protonated methanol and cyclopropane.

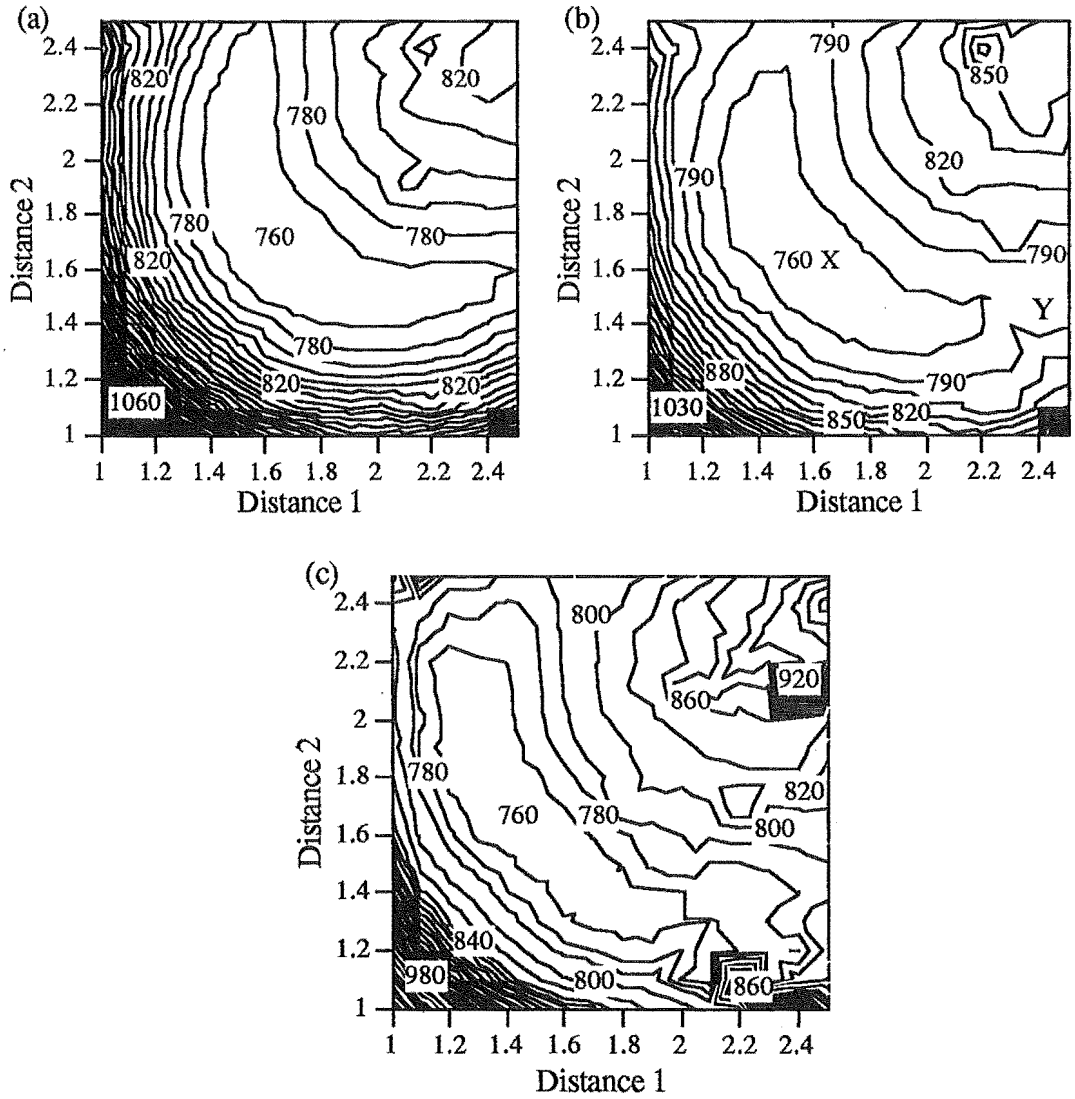

Figure 6.27. Contour plots showing heat of formation (kJ mol^{-1}) verses C1-H1 (Distance 2) and C3-H1 (Distance 1) for fixed O1-H1 distances of (a) 1.3 Å, (b) 1.4 Å, and (c) 1.5 Å. Distances 1 and 2 are in Angstroms.

Each contour plot showed a similar shaped PE surface. The heat of formation values for an O1-H1 distance of 1.4 Å were consistently lower than the values observed for the two other surfaces. From Figure 6.27b two potential stationary points (X and Y)

were identified. The geometry corresponding to point X was extracted and refined using Bartel's gradient norm minimisation routine. A frequency calculation performed on the resulting structure showed the presence of one imaginary frequency which corresponded to the opening of the C1-C3 bond and a symmetrical widening of the C1-C2-C3 bond angle with the simultaneous elongation of the O1-H1 bond and contraction of the C1-H1 and C3-H1 distances. The vibration was therefore consistent with that expected for a transition state for edge attack of protonated methanol on cyclopropane.

Although this structure was a TS for edge attack the presence of the protonated methanol group gave a degree of conformational flexibility and hence the minimum energy conformation of this group may not have been found. To investigate this, the transition state O1-H1, C1-H1, and C3-H1 distances were fixed and the O1-H1 and O1-CH_3 bonds rotated. The PM3 energy was evaluated for each point at 30° increments for a full 360° rotation of the O1-H1 bond and at 10° increments over a 120° range for the O1-CH_3 bond. A contour plot revealed a flat PE surface for the rotation of both bonds (see Figure 6.28). The minimum energy geometry was identified and refined using a gradient norm criterion. The resulting structure **207** (Figure 6.29) showed one imaginary frequency corresponding to an edge protonated transition state for the addition of $CH_3OH_2^+$ to cyclopropane.

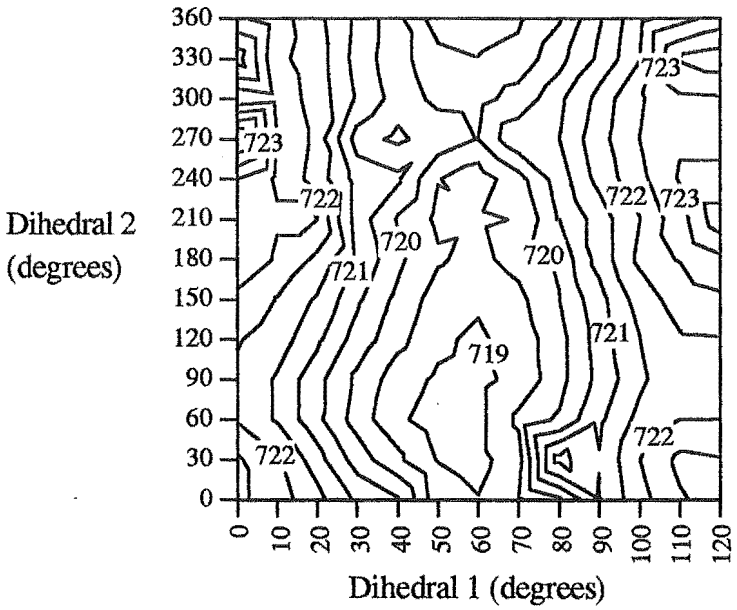

Figure 6.28. Contour plot for rotation of the O1-H1 transition state bond and O1-CH_3 bond. Dihedral angles are in degrees and heats of formation in kJ mol^{-1}.

The second potential stationary point Y (Figure 6.27b) was refined and characterised using an identical procedure to that described for point X. The resulting structure showed two imaginary frequencies (-1478 cm^{-1} and -5 cm^{-1}). The second imaginary frequency corresponded to a slight twisting of the methoxy group with respect

to the plane of cyclopropane ring, and did not appear to be involved in the major TS vibration. This combined with its small size (<1% of the major frequency) allowed the vibration to be ignored as an artifact of the method.

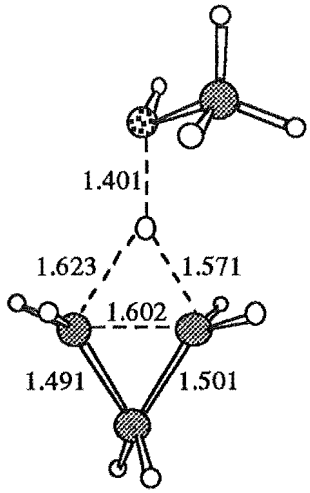

$\Delta H_f = 718.1$ kJ mol^{-1}

207

Figure 6.29. PM3 edge attack transition state for the reaction of protonated methanol and cyclopropane.

The large imaginary frequency corresponded to the symmetrical stretching of the C1-C2 and C1-C3 bonds with a simultaneous elongation of the breaking O1-H1 bond and contraction of the forming C1-H1 bond. The geometry was therefore consistent with a transition state leading to the formation of a corner protonated cyclopropane, resulting in proton transfer from $CH_3OH_2^+$ to cyclopropane. The presence of the methanol group again allows conformational flexibility, and so the O1-H1 and O1-CH_3 bonds were rotated. The lowest energy geometry was identified, refined, and characterised. The structure obtained **208** (Figure 6.30), showed the same characteristic imaginary frequency, as described above for a transition state of $CH_3OH_2^+$ attack on cyclopropane which leads to a corner protonated species.

The PM3 calculations predict the edge protonation pathway to be approximately 5 kJ mol^{-1} lower in energy than the corner attack trajectory. A Boltzman distribution would therefore predict approximately 85% edge attack and 15% corner attack.

Structures **207** and **208** were reoptimised in transition state searches using ab initio methods‡ with a 3-21G(*) basis set. On optimisation the edge TS **207** collapsed to a TS leading directly to a corner protonated structure **209** (Figure 6.31)† analogous to **208**.

---

‡ Ab initio calculations were performed using the program SPARTAN Ver. 2.01.

† Structure **209** shows significant deviation from the bond lengths found by Yamabe[37] for H_3O^+ attack on cyclopropane (see Figure 6.25).

Similarly, optimisation of **208** also led to structure **209**. Comparison of structures **208** and **209** showed a lengthening of the C1-C2 and C1-C3 distances and a contraction of the C2-C3 bond in the structure derived from the ab initio calculation. This is consistent with a lower bond order of the C1-C2 and C1-C3 bonds and hence less electron donation from the ethene C2C3 moiety due to the lower charge development at C1 in **209** than in **208** (Table 6.4).

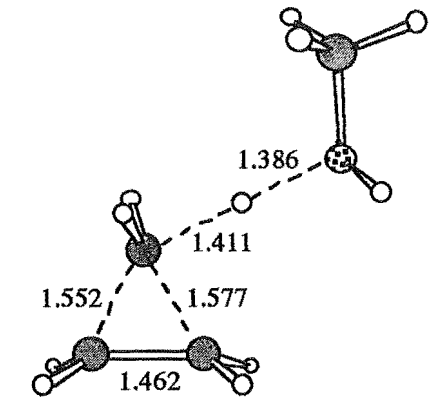

Figure 6.30. PM3 transition state for the reaction of protonated methanol with cyclopropane which leads to the formation of a corner protonated structure. Distances are in Angstroms.

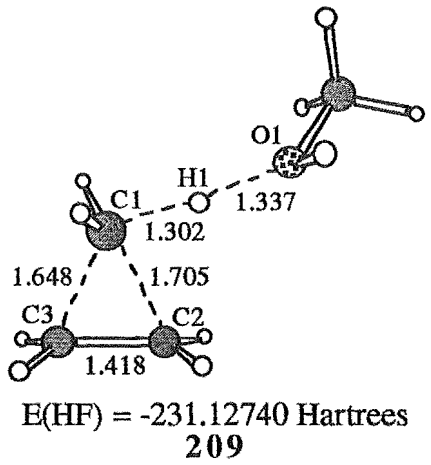

Figure 6.31. Ab initio (HF/3-21G(*) basis set) calculated transition state for proton transfer from protonated methanol to cyclopropane. Distances are in Angstroms.

The collapse of the PM3 edge addition TS to a TS leading to a corner protonated structure may indicate that the edge protonated structure **207** is an artifact of the semiempirical calculations or possibly that the PE surface for the interconversion of **207** and the TS leading directly to a corner protonated species **208** (**209**) is flat. However, the results are not conclusive and require further investigation of the PE surface.

Atom	Charge (a.u.)	
	208	**209**
O1	-0.234	-0.754
H1	0.381	0.492
C1	-0.377	-0.820
C2	-0.029	-0.281
C3	0.007	-0.354
	Mulliken Bond order	
	208	**209**
H1-O1	0.386	0.275
H1-C1	0.339	0.344
C1-C2	0.797	0.615
C1-C3	0.849	0.698
C9-C10	1.047	0.972

Table 6.4. Bond orders and charges (calculated from a natural population analysis) for transition states **208** and **209** (see Figure 6.31 for atom definitions).

Lengthening of the O1-H1 distance (Figure 6.31) of **209** to 1.5 Å and contraction of the H1-C1 distance to 1.2 Å followed by geometry optimisation by an energy criteria (HF/3-21G(*) basis set) resulted in collapse of TS **209** to structure **210** (Figure 6.32). Structure **210** is a minimum on the PE surface and corresponds to the structure formed from transfer of H1 from the methanol molecule to cyclopropane.

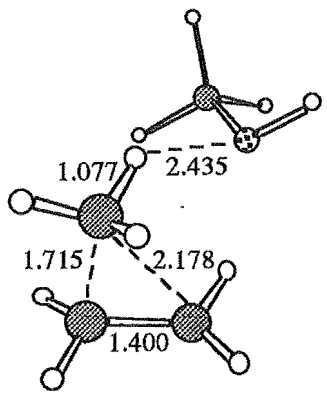

E(HF) = -231.13941 Hartrees

210

Figure 6.32. Minimum resulting from H^+ transfer from methanol to cyclopropane. Distances are in Angstroms.

When TS **209** was reoptimised (3-21G(*) basis set) by an energy criterion, after lengthening the C1-H1 distance and shortening the H1-O1 distance, another minimium **211** on the PE surface was obtained (Figure 6.33). This structure corresponded to a complex formed on approach of protonated methanol to cyclopropane before any significant bond disruption occurred. Of note is the relative symmetry of **211** which has similar H1-C1 and H1-C3 (2.015 Å and 2.017 Å, respectively) distances, thus an analogy may be drawn to edge attack.

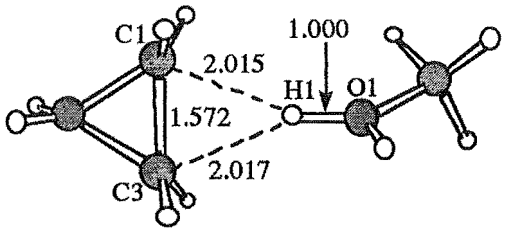

E(HF) = -231.14745 Hartrees
211

Figure 6.33. Complex formed on approach of protonated methanol and cyclopropane before proton transfer occurs. Distances are in Angstroms.

Structures **211**, **209**, and **210** are consistent with the formation of an edge attack complex **211** which leads to TS **209**. Transition state **209** then collapses to form the corner protonated cyclopropane - methanol complex **210** when proton transfer is almost complete. The initial edge attack of electrophiles to cyclopropane followed by rapid collapse to a corner protonated species has been suggested by DePuy[193] and is also consistent with the high level ab initio calculations which suggest an edge protonated cyclopropane to be a TS for proton migration around the cyclopropane ring, although this result is not conclusive.[192] The results of the ab initio calculations for proton transfer from protonated methanol to cyclopropane are summarised in Figure 6.34.

Figure 6.35 summarises possible reaction pathways for transition states **207** and **208**.§ If the electrophile initially attacks C1 (or C1 and C3 in the case of edge attack) both edge and corner attack transition states can give rise to the unsymmetrical corner protonated intermediate **180**. The edge attack TS leads to the edge protonated cyclopropane **174** which may undergo nucleophilic attack, presumably by an inversion process,[36] or collapse to a more stable cation, which from the ab initio calculations would appear to be the unsymmetrical corner protonated species **180**[192] (or **181**[37]). Nucleophilic attack on the edge protonated species would be expected to proceed by

§ The edge TS **208** has been included as, from the limited ab initio results obtained, it cannot be completely discounted as a viable possibility.

inversion at either C1 or C3, to give **212** or **213** respectively, and hence an E-retention/N-inversion process would result.

The corner protonated species would also be expected to undergo nucleophilic attack with inversion.[36,37] Due to the small barrier to interconversion of the unsymmetrical corner protonated structures[37,190,192] **180** and **180'** (Figure 6.35), nucleophilic attack would be expected to result in both E-retention (attack of the nucleophile at C3 resulting in cleavage of the C1-C3 bond) and E-inversion (attack of the nucleophile at C2 resulting in cleavage of the C1-C2 bond) processes giving **213** and **214**, respectively.

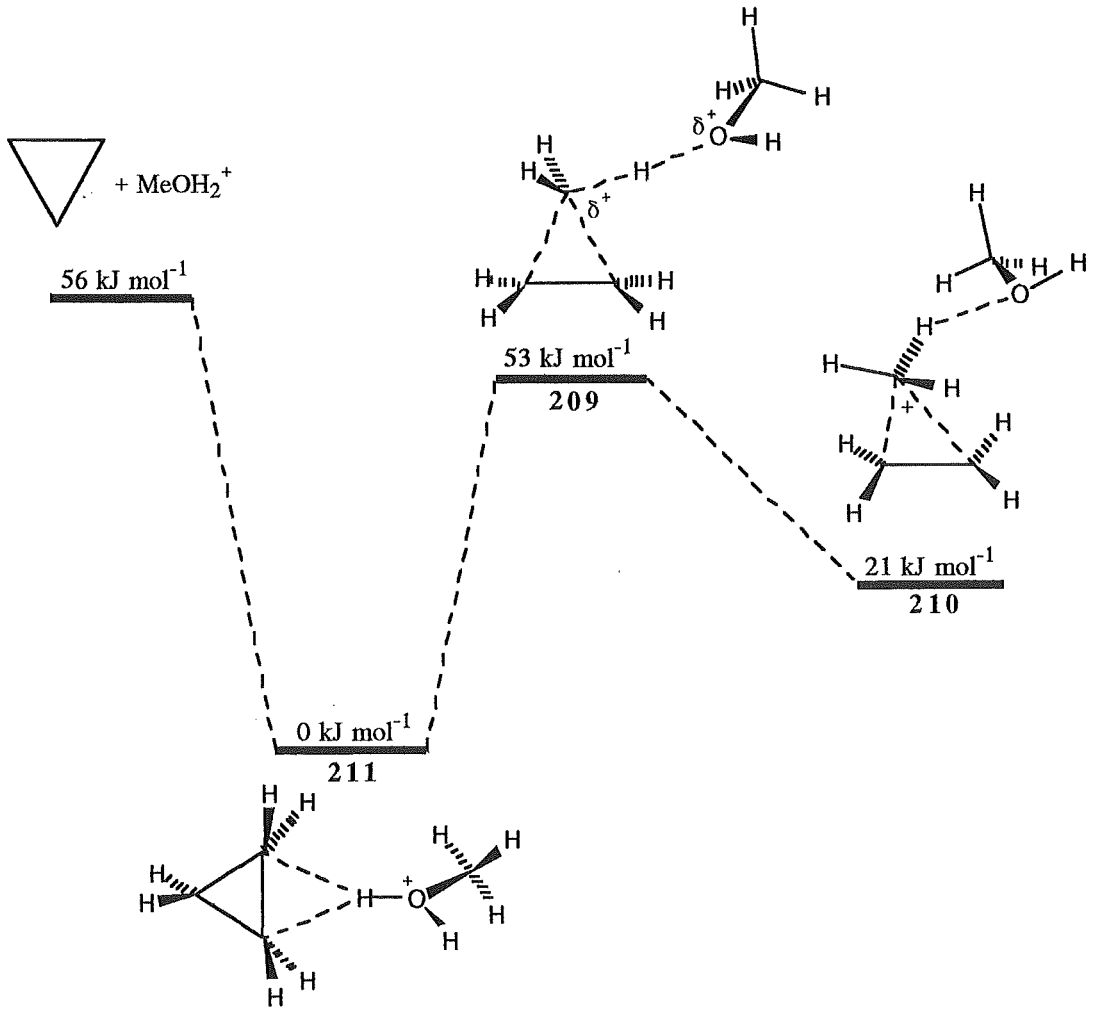

Figure 6.34. Energy diagram (relative to **211**) and possible reaction pathway summarising the ab initio (3-21G(*) basis set) results for proton transfer from $MeOH_2^+$ to cyclopropane (Cyclopropane: E(HF) = -116.4012 Hartrees, $MeOH_2^+$: E(HF) = -114.7249 Hartrees, 1 Hartree = 2625.5 kJ mol^{-1}).

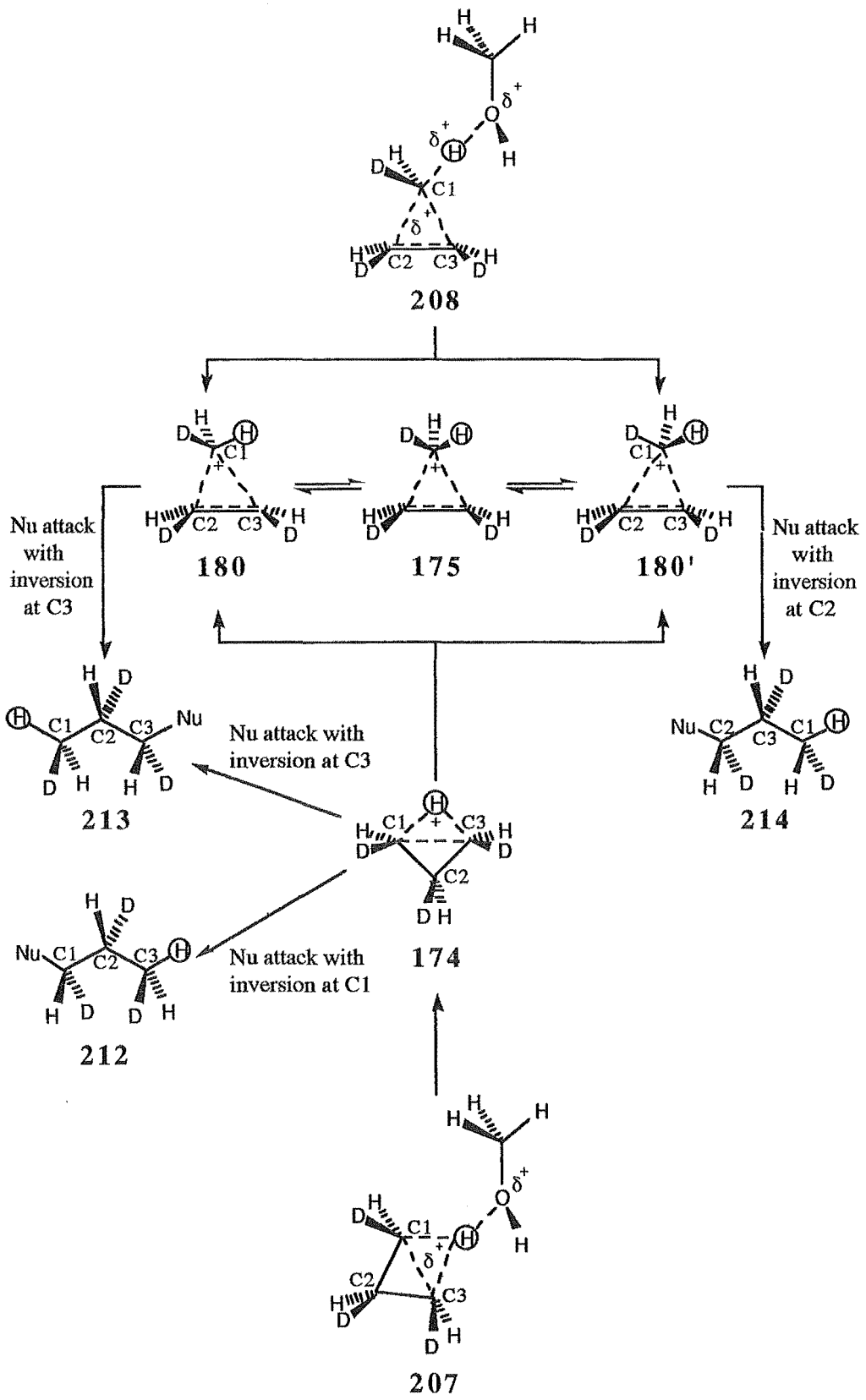

Figure 6.35. Diagram showing possible reaction pathways from transition states **207** and **208** formed from $CH_3OH_2^+$ attack on cyclopropane. For clarity, one hydrogen of each methylene group of cyclopropane has been indicated by D.

The Corner attack TS would lead to the unsymmetrical corner protonated structure **180** either directly or via the symmetrical corner protonated cyclopropane **175** and would be expected to give rise to a mixture of products resulting from E-retention/N-inversion and E-inversion/N-inversion pathways, as described above.

Section 6.3 BROMINATION OF CYCLOPROPANE

There are several experimental studies which have investigated the mechanism of cyclopropane ring opening on reaction with bromine.[28,33,215] The most recent study by Lambert et al.[33] considered the reaction of *cis*-1,2,3-d_3-cyclopropane with bromine and chlorine in the presence of a catalytic amount of iron. By consideration of the possible conformations of the 1,3-dihalogenated products and by analysis of their temperature dependent proton-proton coupling constants, Lambert concluded that an E-retention/N-inversion process was the dominant reaction pathway for both bromination and chlorination. The latest experimental study was an improvement on the previous investigation[215] as the use of *cis*-1,2,3-d_3-cyclopropane resulted in all three carbon-carbon bonds being both isotopically and structurally equivalent. A previous study[215] had considered the addition of bromine to *trans*-1,1,2,3-d_4-cyclopropane, but analysis of this system is complicated by the three carbon-carbon bonds being structurally but not isotopically equivalent and hence there may be different isotope effects on attack at CHD vs. CD_2.[33] At that time the major reaction pathway identified from the bromination of *trans*-1,1,2,3-d_4-cyclopropane was a double E,N-inversion process. This contrasts to the E-retention/N-inversion pathway established from the *cis*-1,2,3-d_3-cyclopropane bromination study.[7,33,216]

Section 6.3.1 Ab initio Results

Yamabe et al.[37] have carried out calculations on the bromination and chlorination of cyclopropane using the GUASSIAN 80 program. Geometries were optimised using a MIDI-1 basis set and the energies further refined by single point calculations performed at the MP2/MIDI-1 and MP2/MIDI-1* levels of theory. Their results showed a strong preference for edge halogenation as both the edge brominated **215** (Figure 6.36) and edge chlorinated **216** (Figure 6.37) structures were found to be significantly lower in energy than the corresponding open bromopropyl **217** (Figure 6.36) and open chloropropyl **218** (Figure 6.37) cations (see Table 6.5).

In this case no corner brominated or chlorinated minima were identified. In fact the corner chlorinated structure **219** was characterised as a transition state for the so called Zig-Zag collapse[37] of the cyclic chloronium ion **216** to the open chloropropyl cation **218** (see Figure 6.37). Although edge halogenation would be expected to result in E-retention,

if the rearrangement of the **216** to **218** occurred with rotation of the chloromethyl group an E-inversion process would result.

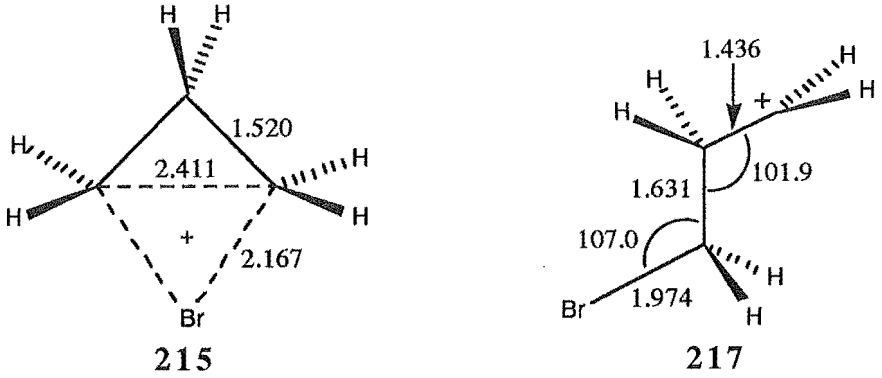

Figure 6.36. Edge brominated **215** and open 3-bromo-1-propyl **217** cations from MIDI-1 optimisation.[37] Bond lengths are in Angstroms and angles in degrees.

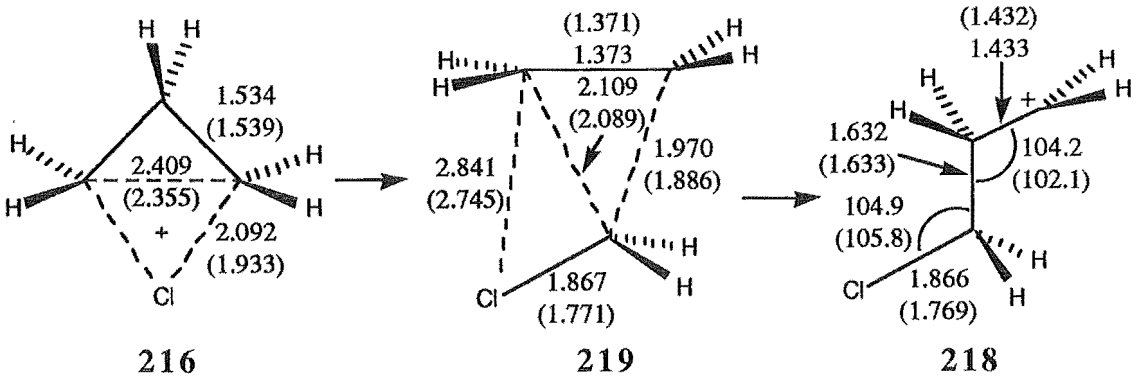

Figure 6.37. Edge chlorinated **216** and open 3-chloro-1-propyl **218** cations and the Zig-Zag collapse TS **219** from MIDI-1 and MIDI-1* optimisation. Bond lengths are in Angstroms and angles in degrees. Numbers in brackets are the MIDI-1* optimised values.

Structure	Yamabe[37]		Lambert[33]
	E_{Rel} RHF/MIDI-1	E_{Rel} MP2/MIDI-1	E_{Rel} RHF/6-31G*
215	0.0	0.0	----------
217	51.2	85.5	----------
216	0.0	0.0	0.0
218	52.8 (63.3)	74.1 (95.3)	45.6
219	84.1 (85.4)	69.5 (88.0)	138.9
220	60.3 (66.0)	74.6 (86.6)	----------

Table 6.5. Ab initio results for the relative energies (E_{Rel}) of the $C_3H_6Br^+$ and $C_3H_6Cl^+$ cations. Relative energies (E_{Rel}) are in kJ mol^{-1}. Numbers in brackets are the MIDI-1* energies.

The transition state character of the corner chlorinated **219** structure (and presumably the corner brominated, which was not characterised by Yamabe et al. due to its size) is thought to be due to the effect of the substituent. A lone pair on the halogen atom delocalises to the carbocation centre of the chloromethyl cation in the CT complex **219** and hence the electron accepting ability of the cation ($ClCH_2^+ \leftarrow C_2H_4$) is therefore lowered.

Yamabe et al. also identified another possible transition state **220** (Figure 6.38) for the interconversion of the edge chlorinated cation **216** and the open chloropropyl cation **218**. Structure **220** interconverts **216** and **218** by an out of plane rotation of one of the C-Cl bonds in **216**. At the RHF level **220** appears to be lower in energy than **219** by 24 kJ mol^{-1} but after electron correlation was included at the MP2 level, the order was reversed (see Table 6.5). The results therefore indicate that the Zig-Zag collapse mechanism occurs with comparable energy to rotation and that both rearrangements are facile processes.

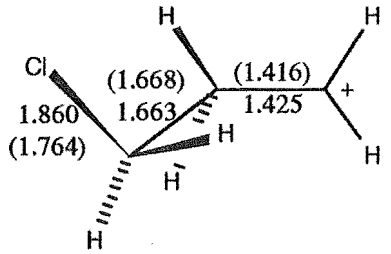

220

Figure 6.38. MIDI-1 transition state for the interconversion of edge chlorinated **216** and open 3-chloropropyl **218** cations.[37] Bond lengths are in Angstroms. Numbers in brackets are from MIDI-1* optimised geometries.

Surprisingly, **218** was calculated to be higher in energy (see Table 6.4) than the transition states (**219** and **220**) leading to it. Yamabe[37] suggests that the formation of the C-Cl covalent bond (from C^+--Cl^-), on approach of the Cl^- nucleophile to the methylene carbocation at the end of the rearrangement, stabilises the system and makes the reaction more exothermic.

Lambert et al.[33] have also examined the relative stabilities of the $C_3H_6X^+$ (X=Cl, Br, F) cations using geometries optimised at the RHF/3-21G level and energies calculated at the RHF/3-21G* level for the chloropropyl structures. The results of their calculations (see Table 6.5), with respect to the relative stability of the cations, are in agreement with those found by Yamabe.[37]

Section 6.3.2 Semiempirical Results

Section 6.3.2a The 3-bromo-2-propyl cation

A conformational search was carried out, as for the $C_3H_7^+$ secondary cation, by rotation of both carbon-carbon bonds. Only one true minimum **221** (Figure 6.39) was found on the potential energy surface, all other stationary points being characterised as transition states.

The MINDO/3 method has not been parameterised for bromine and hence the MINDO/3 energies of the $C_3H_6Br^+$ cations could not be evaluated.

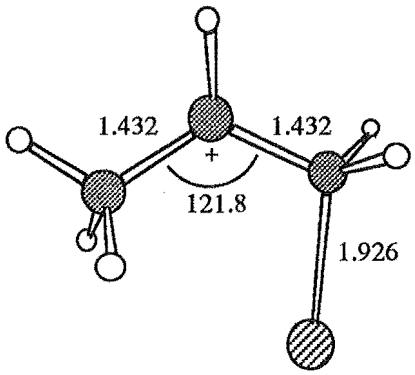

$\Delta H_f = 887.4$ kJ mol^{-1}

221

Figure 6.39. Lowest energy 3-bromo-2-propyl cation **221**. Bond lengths and angles are in Angstroms and degrees, respectively.

Section 6.3.2b The 3-bromo-1-propyl cation

Both carbon-carbon bonds, of an initial structure obtained from molecular mechanics calculations, were rotated and the potential stationary points located and further refined. The two resulting structures **222** and **223** (Figure 6.40) were minima on the PE surface and had open 1-propyl cation geometries.

The barrier to rotation of the CH_2Br group was estimated by rotation of the C2-C3 carbon-carbon bond to give an eclipsed conformation of the bromine atom with one proton of the C2 methylene group, and a single point calculation performed. The resulting heat of formation (951.8 kJ mol^{-1}) indicated the barrier to rotation to be approximately 6 kJ mol^{-1} (from **222** to **223**) and hence at room temperature "free" rotation of the CH_2Br group is expected.

No stationary point corresponding to the eclipsed 1-propyl cation **224** (Figure 6.41) was identified as this structure collapses to the edge brominated species upon optimisation (see later this section).

The open 1-propyl cation **225** (Figure 6.42) was characterised as a TS for the rotation of the C1 methylene group by PM3, in contrast to the ab initio calculations which

describe the structure as a minimum. The structure collapsed to **222** when optimised by an energy criteria.

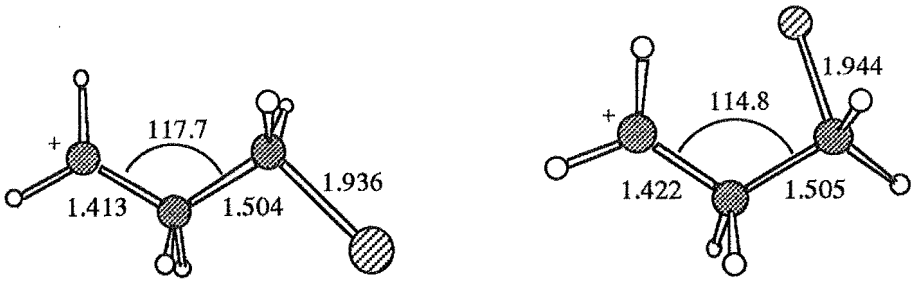

$\Delta H_f = 949.4$ kJ mol^{-1} **222**

$\Delta H_f = 946.1$ kJ mol^{-1} **223**

Figure 6.40. Geometries of the two lowest energy 3-bromo-1-propyl cations. Bond lengths and angles are in Angstroms and degrees, respectively.

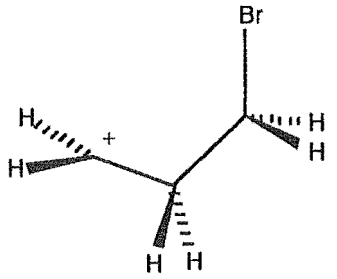

224

Figure 6.41. The eclipsed 3-bromo-1-propyl cation **224** was found to collapse to the edge brominated structure upon optimisation.

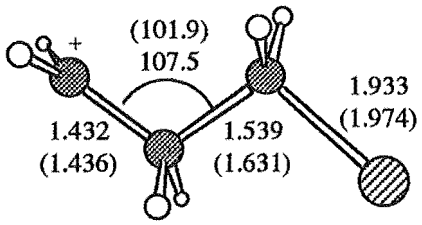

$\Delta H_f = 981.5$ kJ mol^{-1}

225

Figure 6.42. The PM3 transition state open 3-bromo-1-propyl cation **225**. Bond lengths and angles are in Angstroms and degrees, respectively. Numbers in brackets are the corresponding ab initio values.[37]

Section 6.3.2c The corner brominated cation

Structure **226** (Figure 6.43) was characterised as a TS for the interconversion of two open 3-bromopropyl cations. This was established from the vibrational analysis and from a contour plot (Figure 6.44) which shows the heat of formation verses the C1-C2 and C1-C3 bond lengths. Rotation of the bromine atom into the carbon plane, followed by reoptimisation, gave the unsymmetrical structure **227** (Figure 6.43). This structure was also identified as a TS for the interconversion of two open 3-bromopropyl type cations. In this case the symmetrical corner brominated structure **226** lay 7 kJ mol^{-1} lower in energy than the unsymmetrical structure **227**, in general agreement with results of Lambert et al.[33] who found the symmetrical corner chlorinated structure to be lower in energy than the unsymmetrical structure. This is in contrast to results obtained for the symmetrical **175** and unsymmetrical **180** corner protonated structures.[192]

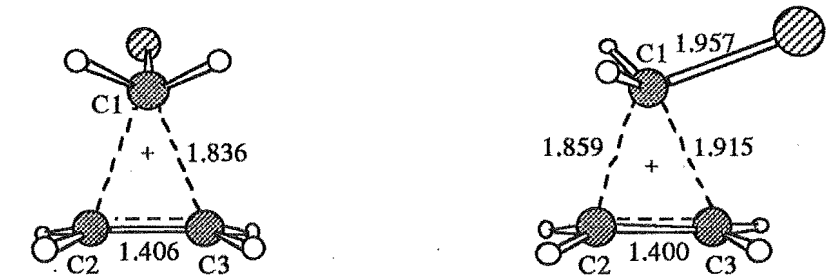

$\Delta H_f = 1037.1$ kJ mol^{-1} **226**

$\Delta H_f = 1044.2$ kJ mol^{-1} **227**

Figure 6.43. Symmetrical **226** and unsymmetrical **227** corner brominated cations. Distances are in Angstroms.

An approximate barrier to rotation of the CH_2Br group of the corner brominated species was estimated by rotating the CH_2Br group of **226** by 45° and calculating a single point energy (optimisation inevitably led to collapse of the structure to either **226** or **227**). The calculated rotational barrier was established as 9 kJ mol^{-1} which would indicate a relatively free interconversion of **226** and **227** at room temperature. The formation of a corner brominated species would therefore be expected to result in both E-retention and E-inversion products if the reaction were to proceed via this pathway.

Section 6.3.2d The edge brominated cation

From an initial approximate structure, the distance of the bromine from C1 and C3 was varied and the heat of formation evaluated at each point. The results of the grid calculation are shown in Figure 6.45. A minimum corresponding to the edge brominated structure can clearly be seen at C1-Br and C3-Br distances of approximately 2.1 Å (point A, Figure 6.45). The corresponding geometry was refined and a frequency calculation performed. The resulting structure **228** (Figure 6.46) was a minimum on the PE surface

and was significantly lower in energy than the corner brominated or 3-bromo-1-propyl cations (see Table 6.6).

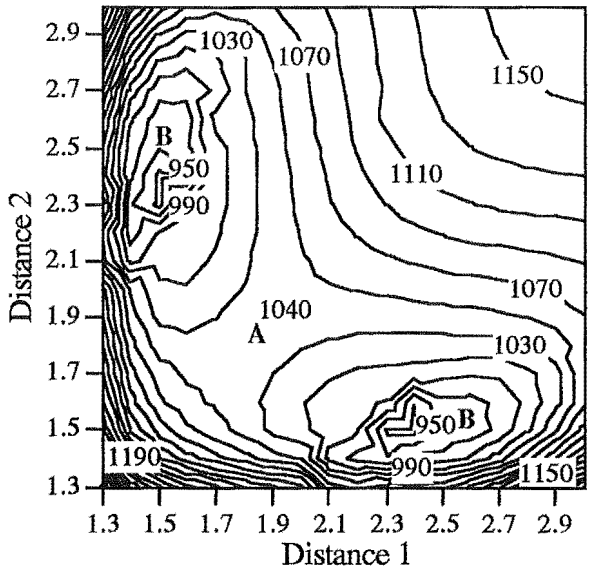

Figure 6.44. Contour plot showing heats of formation of the structures obtained from varying the C1-C2 (Distance 1) and C1-C3 (Distance 2) bond lengths in the corner brominated structure **226**. Energies are in kJ mol^{-1} and distances in Angstroms. Point **A** corresponds to structure **226**. Point **B** corresponds to an "open" 3-bromo-1-propyl cation (**222** and/or **223**).

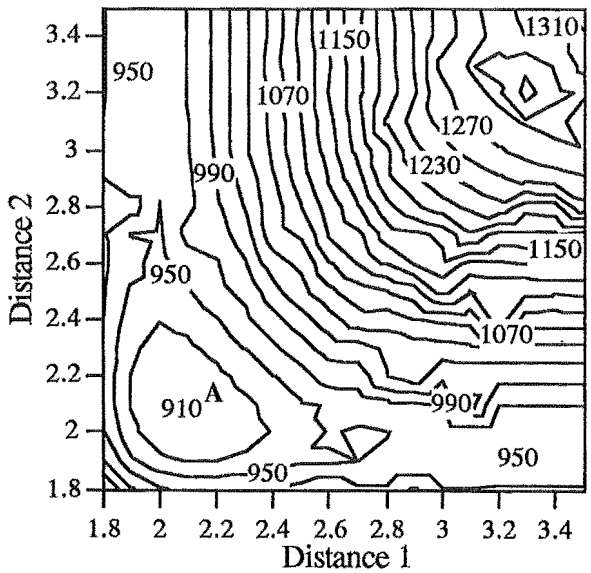

Figure 6.45. Contour plot showing the energies (kJ mol^{-1}) of the structures obtained from varying the Br-C1 (Distance 1) and Br-C3 (Distance 2) distances. Bond lengths are in Angstroms. Point **A** corresponds to position of structure **228** of the PE surface.

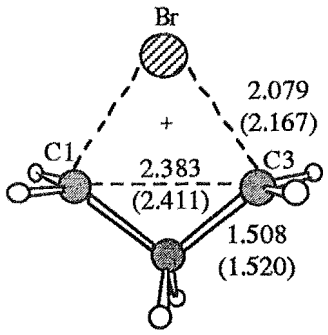

$\Delta H_f = 910.1$ kJ mol^{-1}

228

Figure 6.46. Edge brominated cyclopropane. Bond lengths and angles are in Angstroms and degrees, respectively. Numbers in brackets are the corresponding ab initio bond lengths.[37]

Structure	ΔH_f (kJ mol^{-1})	E_{Rel} (kJ mol^{-1})
221	887.4	0.0
223	946.1	58.7
226	1037.1	149.7
227	1044.2	156.8
228	910.1	22.7

Table 6.6. Table showing the heats of formation and relative energies for the 1-bromo-2-propyl **221**, 3-bromo-1-propyl **223**, symmetrical corner brominated **226**, unsymmetrical corner brominated **227**, and edge brominated **228** cations.

The bond lengths obtained from the PM3 calculations for structure **228** are in poor agreement with the MIDI-1 calculated values[37] (see Figure 6.46) as the PM3 method predicts a more tightly bound bromine atom than the ab initio methods (C-Br distances: PM3 2.079 Å, MIDI-1 2.167 Å, difference 0.088 Å). The difference in energy between the edge brominated **228** and open **225** cations is calculated to be 71 kJ mol^{-1} by the PM3 method, which is comparable with the value of 85.5 kJ mol^{-1} from the MP2/MIDI-1 results and shows an improvement on the value obtained from the RHF/MIDI-1 calculations of 51.2 kJ mol^{-1}.

Based on the relative energies of the possible cations, the PM3 results predict edge attack to be the dominant pathway for bromination. The 1,3-dibromopropane products would therefore be expected to be formed by E-retention/N-inversion processes, in agreement with the ab initio predictions[33,37] and with the experimental results obtained by Lambert.[33] Figure 6.47 shows an energy level diagram, relative to the 1-bromo-2-propyl cation, of the PM3 results for the $C_3H_6Br^+$ cations.

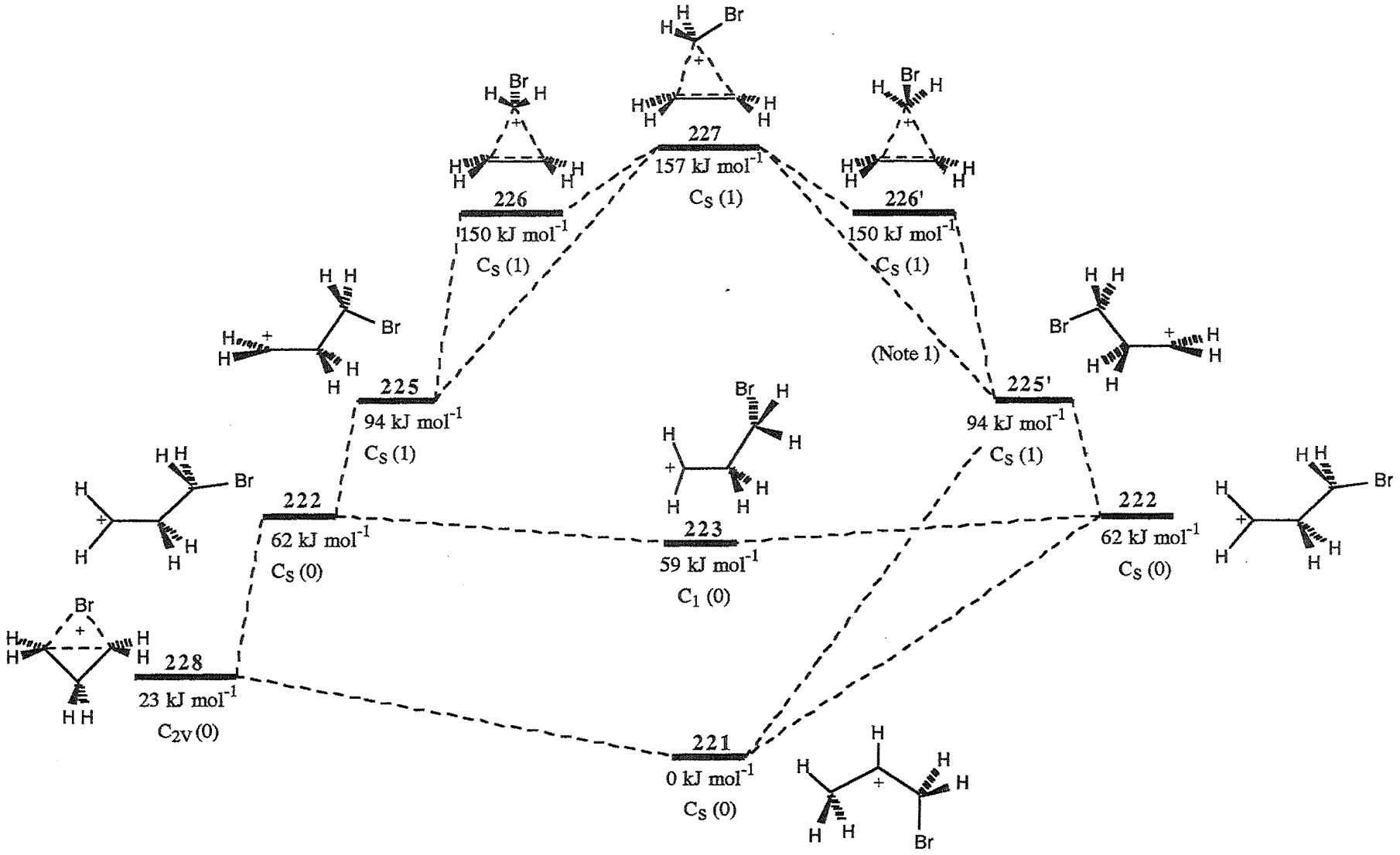

Figure 6.47. Relative energies and possible interconversion mechanisms for PM3 $C_3H_6Br^+$ cations. The symmetry of the cation and the number of negative force constants (in brackets) are also shown. Note 1: a number of rearrangements are possible depending on which terminal group (CH_2^+ or CH_2Br) rotates.

Section 6.3.3 PM3 Results for the Reaction of Molecular Bromine with Cyclopropane

The cations formed from the attack of a bromine electrophile on cyclopropane gave a clear indication of the preferred reaction pathway; however, since it is presumably Br_2 which is the attacking electrophile it was necessary to investigate the reaction of molecular bromine with cyclopropane.

A number of grid calculations were performed by varying the C1-Br1 and C3-Br1 distances while holding the Br1-Br2 bond length fixed at selected values. Figures 6.48a-d show the resulting heats of formation plotted versus the C1-Br1 and C3-Br1 bond lengths for fixed Br1-Br2 distances of 2.2 Å, 2.4 Å, 2.6 Å, and 2.8 Å, respectively.

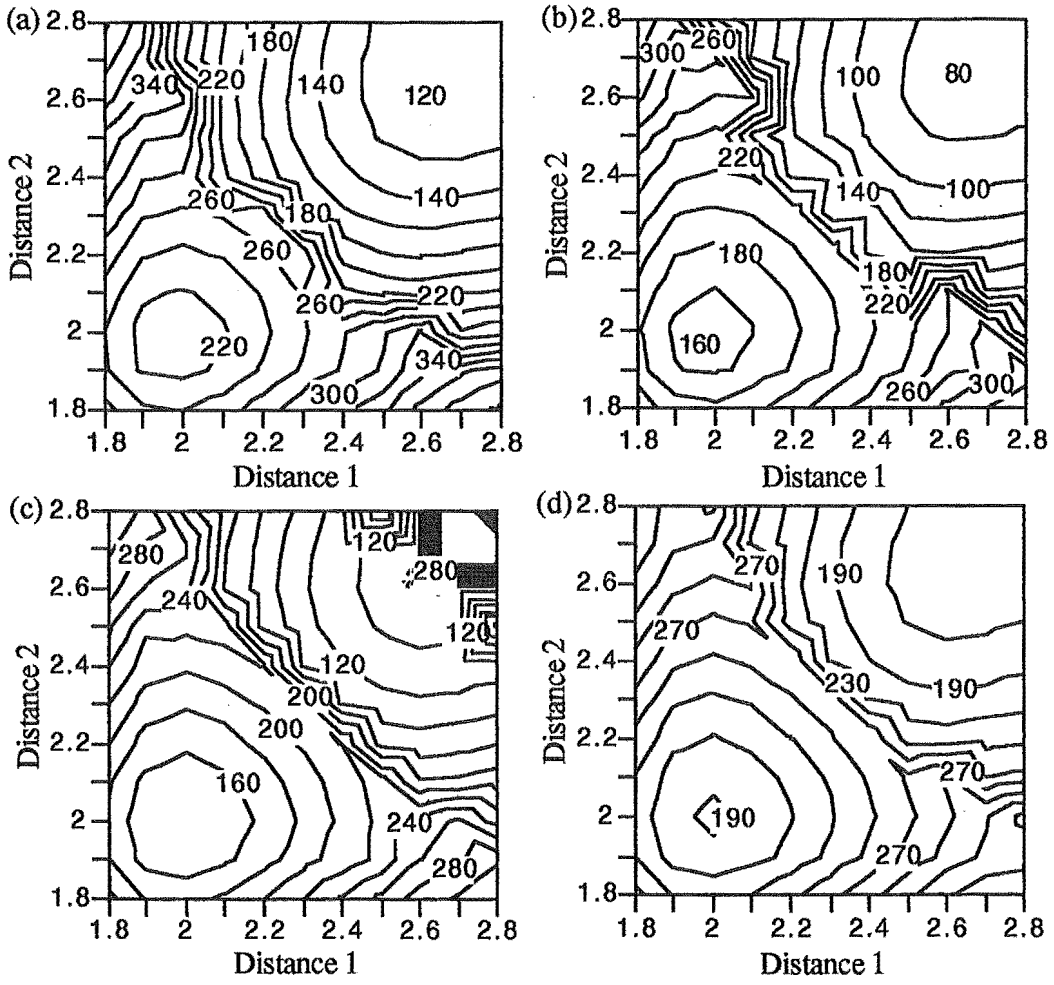

Figure 6.48. Contour plots showing heat of formation (kJ mol^{-1}) against C1-Br1 (Distance 2) and C3-Br1 (Distance 1) bond lengths (in Angstroms) for Br1-Br2 distances of (a) 2.2 Å, (b) 2.4 Å, (c) 2.6 Å, and (d) 2.8 Å.

A potential stationary point corresponding to a TS for edge attack of Br_2 on cyclopropane was identified at a value of approximately 2.3 Å for Distances 1 and 2 of Figures 6.48b and c. The geometry corresponding to this point on the surface with a fixed Br1-Br2 distance of 2.6 Å (Figure 6.48c) was refined and the resulting structure

229 (Figure 6.49) identified as a TS by the presence of one imaginary frequency. The corresponding vibration indicated the symmetrical stretching of the C1-C3 bond with simultaneous contraction of the C1-Br and C3-Br bonds and a lengthening of the Br1-Br2 bond, which is consistent with a TS for edge attack.

The stationary point observed on all plots (Figure 6.48a-d) at approximately 2.0 Å, 2.0 Å was optimised and the resulting structure **230** (Figure 6.49) identified as a minimum on the PE surface. The structure appeared to correspond to a charge transfer complex of the edge brominated cation **228** and an Br^- ion. In structures **229** and **230** both bromine atoms lay in the plane of the cyclopropane ring.

No point corresponding to a potential TS for the corner attack of Br_2 was identified from the surfaces.

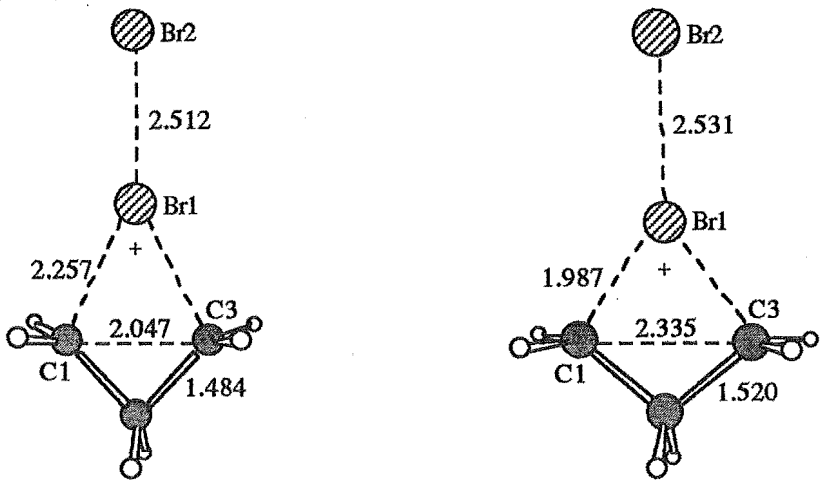

$\Delta H_f = 208.2$ kJ mol^{-1} — **229**

$\Delta H_f = 135.7$ kJ mol^{-1} — **230**

Figure 6.49. Edge transition state for Br_2 attack on cyclopropane **229** and charge transfer complex **230**.

The absence of a corner brominated TS on the PE surfaces reflects a marked preference for edge over corner bromination, which is in agreement with the experimental results.[33]

Section 6.4 DISCUSSION OF THE SEMIEMPIRICAL RESULTS

The results of these studies, show some deficiencies in the semiempirical molecular orbital methodology, particularly for nonclassical cations, but show reasonable agreement with the ab initio calculated geometries with the proviso of caution regarding nonclassical structures. This justifies their use in modelling of the possible reaction pathways that may occur in more complex molecules. Although the accuracy of the semiempirical methods is not generally considered as satisfactory as that obtained from ab initio calculations, their computational speed advantage and lesser demand on computational facilities (hardware, memory, etc) make their use feasible and advantageous.

CHAPTER 7

Molecular Modelling Studies of Proton Addition to *exo*- and *endo*-Tricyclo[3.2.1.$0^{2,4}$]octane

Section 7.1 INTRODUCTION

The previous chapter demonstrated that semiempirical molecular orbital techniques gave a reasonable indication of the geometries involved in proton addition to cyclopropane. As outline earlier (Sections 1.2.1 and 3.1) the reactions of *exo*- and *endo*-tricyclo[3.2.1.$0^{2,4}$]octane (**46** and **1**, respectively) with H^+/D^+ have been examined experimentally (see Figures 1.6 and 3.1).[13,14,18] It was therefore of interest to extend the semiempirical investigations to the larger tricyclic systems to further study the factors effecting the regiochemistry and stereochemistry of proton addition to a cyclopropane ring.

Section 7.2 CATION STABILITY

A starting point for the semiempirical calculations was to consider the stability of the possible cations resulting from opening of the cyclopropane ring of **1**. If one of the external cyclopropane bonds of **1** (C2-C3 or C3-C4) is broken on proton addition, then cations **231** or **232** (Figure 7.1) may be formed. Formation of cations **231** and **232** may occur from edge attack at either the C2-C3 or C3-C4 bond or, in the case of **232**, from corner attack at C3. Cation **78** may be formed from either corner attack at C2 (C4) or edge addition to the C2-C4 bond. Cations **78**, **231**, and **232** would be formed if complete bond rupture occurs to give an open carbocation and do not preclude the possibility of protonated cyclopropane intermediates.

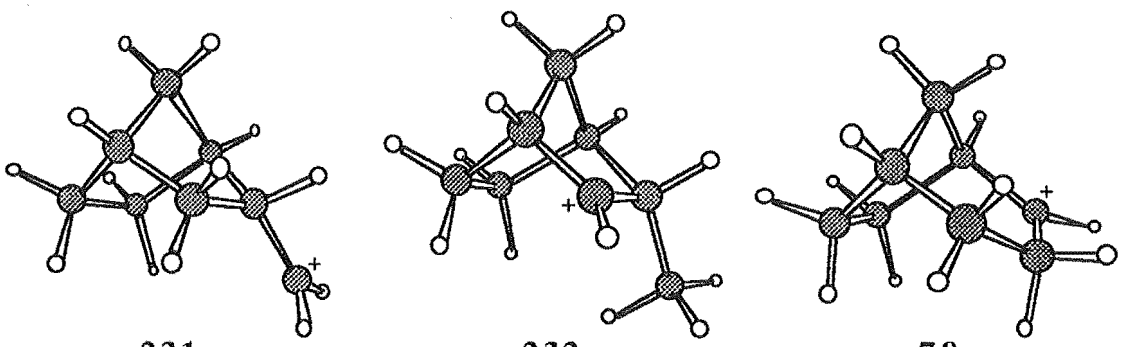

	231	**232**	**78**
ΔH_f(PM3) (kJ mol^{-1})	898.0	849.5	800.7

Figure 7.1. Possible cations resulting from acid induced cleavage of the cyclopropane ring of **1**.

Figure 7.1 shows the structure and heat of formation of cations **78**, **231**, and **232** calculated using the PM3 semiempirical molecular orbital method. Cation **78** was found

to be the most stable carbocation by approximately 49 kJ mol^{-1}, in general agreement with the experimental results[13,14,18] (Figure 1.6) which show cleavage exclusively of the C2-C4 internal bond of the cyclopropane ring on reaction with H^+.

The geometry of the three membered bridge in cation **78** is predicted to be essentially flat by the PM3 semiempirical method (Figure 7.1) but shows a distinctly *endo* orientation when the structure is optimised using ab initio methods with a 3-21G(*) basis set (Figure 7.2).

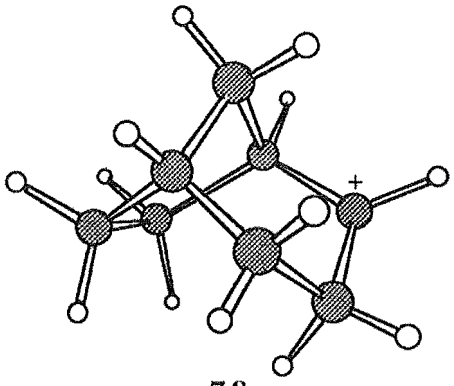

78

E(HF/3-21G(*)) = -308.52998 Hartrees

Figure 7.2. Cation **78** resulting from geometry optimisation using ab initio methods with a 3-21G(*) basis set.

Geometry optimisation of cation **78** starting with an *exo* or *endo* orientation of the three carbon bridge, using the PM3 method, gave an essentially planar arrangement of three membered bridge. The PM3 method therefore predicts the open cation formed from cleavage of the C2-C4 bond of **1** and **46** to be identical (Figure 7.3).

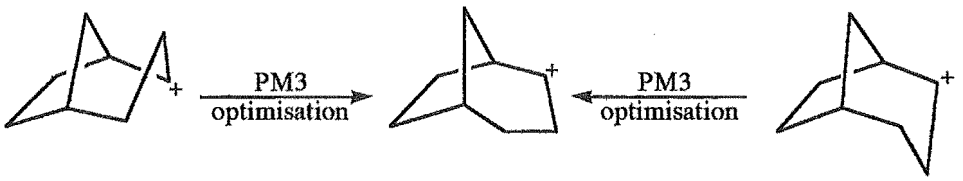

exo **78** *endo*

Figure 7.3. PM3 predicts an essentially flat three membered bridge in cation **78**.

However, optimisation of cation **78** with an *exo* orientation of the three carbon bridge by ab initio (3-21G(*) basis set) methods led to the collapse of the structure to a nonclassical cation **233** (Figure 7.4).

The experimental results[13,14,18] for the acid catalysed ring opening of **1** (Figure 1.6) indicate a facile rearrangement of the resulting cation to take place. This process may occur via a nonclassical cation **3a** with some nucleophilic capture occurring from a corner protonated cyclopropane intermediate **2a** (Figure 1.6) before rearrangement takes place, or by rapid interconversion of the classical cation **78** and its mirror image **78'** (Figure 7.5) with only a small activation barrier. Modelling of this rearrangement process by both

PM3 and ab initio (3-21G(*) basis set) methods indicated that cation **3a** was a TS for the interconversion process and hence not an intermediate on the PE surface (Figure 7.5).

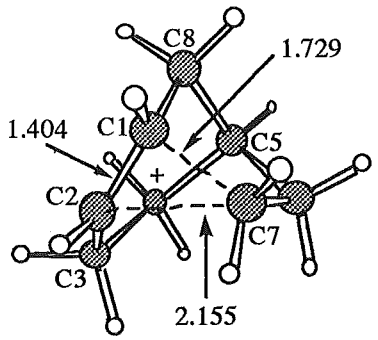

233

E(HF/3-21G(*)) = -308.52938 Hartrees

Figure 7.4. Nonclassical cation resulting from optimisation of **78** with an initial *exo* orientation of the three membered bridge by ab initio methods (3-21G(*) basis set). Distances are in Angstroms.

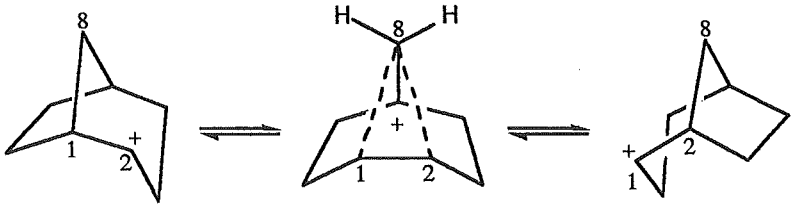

	78	**3a**	**78'**
ΔH_f(PM3)	800.7	855.1	800.7
E_{Rel}(PM3)	0.0	54.4	0.0
E_{Tot}(HF)*	-308.52998	-308.52730	-308.52998
E_{Rel}(HF)*	0.0	7.0	0.0

Figure 7.5. Rearrangement of cation **78** to its mirror image structure **78'** via cation **3a**. Relative energies (E_{Rel}) and heats of formation are in kJ mol^{-1}. Total energies (E_{Tot}) are in Hartrees.

* Results from ab initio calculations using a 3-21G(*) basis set at the Hartree-Fock level.

From Figure 7.5 it can be seen that the PM3 method predicts a large barrier to interconversion (54.5 kJ mol^{-1}) but the ab initio results show a much smaller barrier (7.0 kJ mol^{-1}) and therefore would predict the cations **78** and **78'** to interconvert rapidly at room temperature. The ab initio result may therefore explain the preference for nucleophilic attack with inversion due to the 'windscreen wiper' effect of two rapidly interconverting classical cations.[113-123] It should be noted that the ab initio result may in fact classify **3a** as an intermediate (minimum) if a larger basis set and electron correlation effects are included, as these have been found to be important in characterising other nonclassical cations, in particular, the 2-norbornyl cation.[119,123] Of particular note is that the MINDO/3 method characterises cation **3a** as a minimum on the PE surface.

Optimisation of cation **78** by an energy criteria using MINDO/3 leads to the collapse of this cation to the nonclassical structure **3a**. The contrasting characterisation of cation **3a** as a TS by PM3 and minimum by MINDO/3 can be seen by comparison of the PE surfaces derived from varying the C1-C8 and C2-C8 distances and calculating the heat of formation at each point (Figures 7.6a and b). From the PM3 surface a TS is observed at C1-C8 and C2-C8 distances of 2.0 Å (point A, Figure 7.6a) whereas a minimum is shown at C1-C8 and C2-C8 distances of 1.7 Å (point C, Figure 7.6b) on the MINDO/3 PE surface. The relevant bond lengths of the structures obtained from gradient minimisation of points A and C and the corresponding ab initio geometry (optimised using a 3-21G(*) basis set) are shown in Figure 7.7. The minima labelled B on Figure 7.6a correspond to cations **78** and **78'**. As can be seen from Figure 7.6b, cation **78** is not a stationary point on the MINDO/3 PE surface.

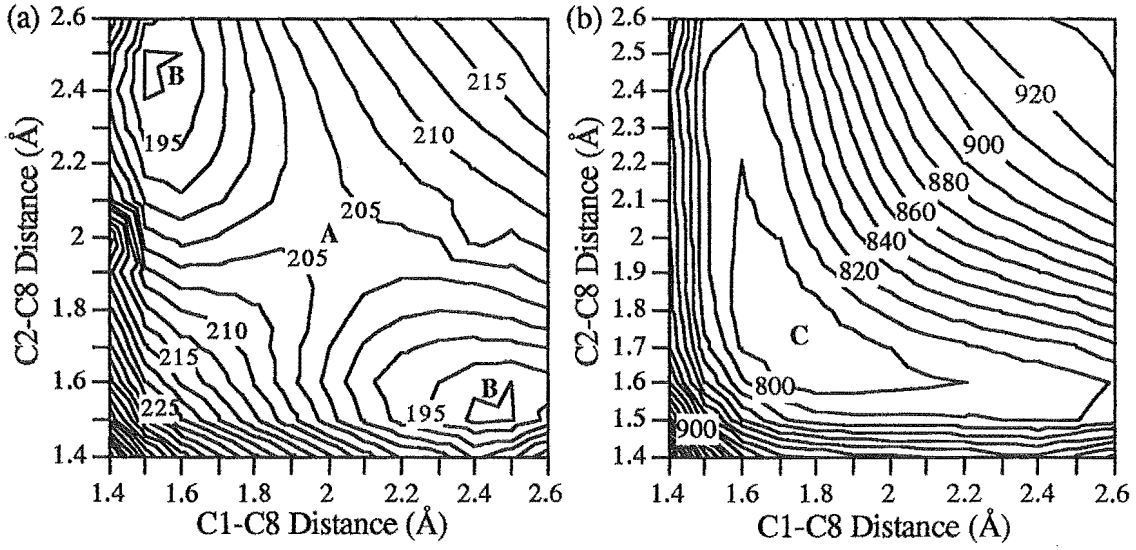

Figure 7.6. (a) PM3 and (b) MINDO/3 PE surfaces for the interconversion of **78** and **78'**.

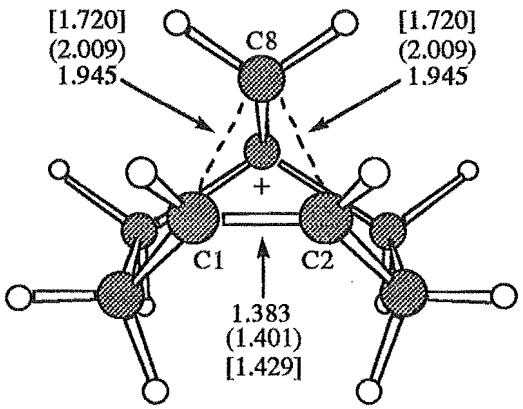

3a

Figure 7.7. Structure of cation **3a** from ab initio (3-21G(*) basis set), PM3 (bond lengths in curved brackets), and MINDO/3 (bonds lengths in square brackets) calculations. Distances are in Angstroms.

Comparison of the activation energy for the rearrangement of **78** to **78'** and to the bicyclo[2.2.2]octane cation **234**, shows similar activation barriers (E_a) for the two processes (Figure 7.8). The PM3 method predicts rearrangement via cation **3a** (E_a = 54.4 kJ mol^{-1}) to be slightly lower in energy then the Wagner-Meerwein rearrangement via TS **235** (E_a = 52.6 kJ mol^{-1}). This contrasts with the ab initio results, using a 3-21G(*) basis set, which show the Wagner-Meerwein pathway to be slightly more favourable (**78** → **78'**, E_a = 7.0 kJ mol^{-1}; **78** → **234**, E_a = 3.2 kJ mol^{-1}). Both methods would therefore predict the two pathways to occur to similar extents (see Figures 7.5 and 7.8). Both the ab initio and semiempirical methods predict little cation stabilisation to be gained from rearrangement of the bicyclo[3.2.1]octane cation **78** to the bicyclo[2.2.2]octane cation **234**. The experimental results[13,14,18] show no Wagner-Meerwein rearrangement to occur for reaction of **1** and 15% Wagner-Meerwein rearrangement to occur for **46** but only when proton/deuteron addition resulted in rupture of the C2-C3 or C4-C3 external cyclopropyl bond.

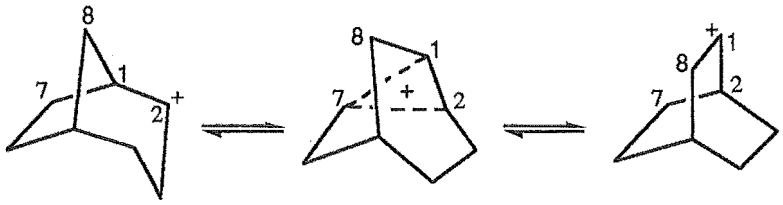

	78	**235**	**234**
ΔH_f(PM3)	800.7	853.3	796.8
E_{Rel}(PM3)	3.9	56.5 (52.6)	0.0
ΔH_f(AM1)	751.5	803.0	740.3
E_{Rel}(AM1)	11.2	62.7 (51.5)	0.0
E_{Tot}(HF)*	-308.52998	-308.52875	-308.52990†
E_{Rel}(HF)*	0.0	3.2 (3.2)	0.2

Figure 7.8. Wagner-Meerwein rearrangement of cation **78** via TS **235**. Relative energies (E_{Rel}) and heats of formation are in kJ mol^{-1}. Total energies (E_{Tot}) are in Hartrees.

* Results from ab initio calculations using a 3-21G(*) basis set at the Hartree-Fock level.

† Total energy for **234** with C_1 symmetry.

The relevant bond lengths from the PM3 and ab initio calculations of the Wagner-Meerwein transition states are shown in Figure 7.9. The corresponding AM1 TS bond lengths are also shown.

The absence of any products resulting from Wagner-Meerwein rearrangement on acid induced ring opening of **1** may be due to a number of factors. If the cation **78** has a distinctly *endo* conformation, as predicted by the ab initio calculations, then the vacant *p*-orbital of C2 will align more favourably with the C1-C8 bond (Figure 7.10a) than with

the C1-C7 bond (Figure 7.10b) thus migration of the C1-C8 bond would be favoured and rearrangement with retention of the bicyclo[3.2.1]octane carbon skeleton expected.† This was observed experimentally.[13,14,18]

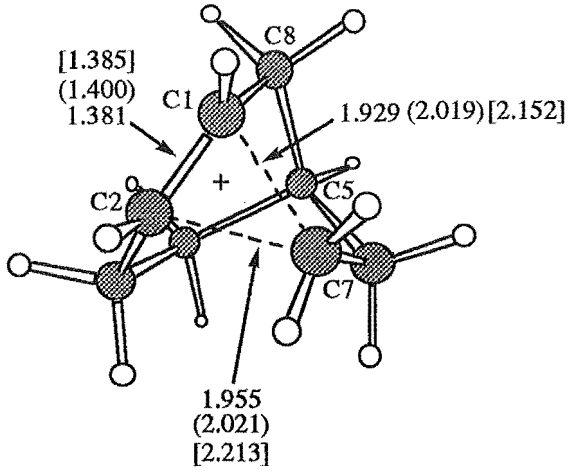

235

Figure 7.9. Structure of TS **235** from ab initio (3-21G(*) basis set), PM3 (bond lengths in curved brackets), and AM1 (bonds lengths in square brackets) calculations. Distances are in Angstroms.

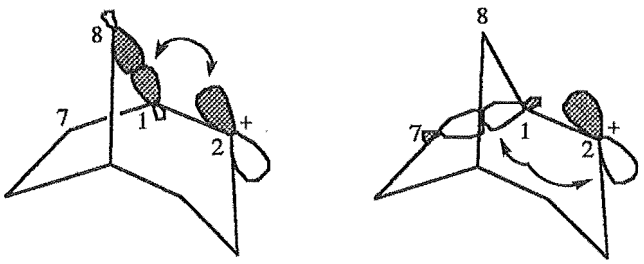

Figure 7.10. Orbital overlap diagrams for cation **78** (ab initio geometry) showing migration of the C1-C8 bond (Figure 7.10a) to be favoured over migration of the C1-C7 bond (Figure 7.10b).

Also of note is that the ab initio calculations predict cation **234** to have C_1 and not C_s symmetry. Optimisation of the geometry with C_s symmetry imposed resulted in convergence to a transition state whose imaginary frequency corresponded to a small distortion of the 'positively' charged carbon C1 of **234** (Figure 7.8) from the vertical

---

† If formation of a corner protonated cation **2a** (Figure 1.6) occurs[13] and not an open carbocation the same result would be expected. Equilibration of the *exo* and *endo* conformations of cation **78** would therefore either not occur or would be a higher energy process, due to the presence of a partial bond between C2 and C4

mirror plane. The energy difference between the C_1 and C_s geometries was small (2.8 kJ mol^{-1}).

In the case of **46** the cation resulting from cleavage of the C2-C4 bond was again the most stable of the three possible classical carbocations **78**, **236**, and **237** (Figure 7.11). Cleavage of the C2-C4 bond of **46** was the dominant pathway observed experimentally (76%).[13,14,18]

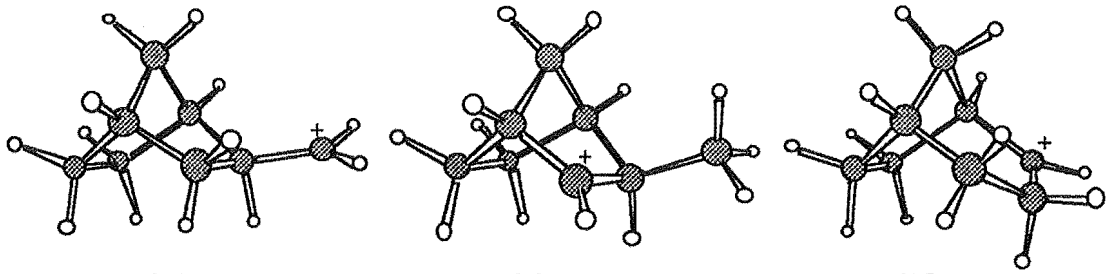

236	**237**	**78**
ΔH_f(PM3) 896.8 (kJ mol^{-1})	856.2	800.7

Figure 7.11. Possible cations resulting from the proton induced cleavage of the cyclopropane ring of **46**.

As outlined earlier, optimisation of cation **78** initially with an *exo* orientation of the of the three membered bridge led to a flattening of the ring when optimised using the PM3 Hamiltonian and collapse to a nonclassical cation **233** (Figure 7.4) when optimised by ab initio methods. Cation **233** is similar to TS **235** but has a shorter C1-C7 and longer C2-C7 bond length (**233**: C1-C7 1.729 Å, C2-C7 2.155 Å; **235**: C1-C7 1.929 Å, C2-C7 1.955 Å) and is lower in energy by 1.7 kJ mol^{-1}. Structure **233** is minimum on the PE surface whereas **235** has one negative force constant and hence is a transition structure. It seems unlikely that structure **233** is formed on the reaction pathway from H^+ induced ring opening of **46**, since no products resulting from a Wagner-Meerwein rearrangement of this type were observed.[13,14,18] The calculation may therefore be in error; however, charge development at C2 (0.252) is larger than at C1 (-0.135) and hence nucleophilic capture would be expected to occur predominantly at C2 and hence result in retention of the bicyclo[3.2.1]octane skeleton in the major product.

Section 7.3 PROTON TRANSFER FROM PROTONATED METHANOL TO *endo*-TRICYCLO[3.2.1.$0^{2,4}$]OCTANE

Section 7.3.1 Corner Attack

Having established that rupture of the internal cyclopropyl bond (C2-C4) is preferred due to cation stability, the relative energies of the edge versus corner trajectories remained to be examined.

As with proton addition to cyclopropane, attack of a charged species (H^+) on a neutral molecule (**1**) is predicted by PM3 to occur without an activation barrier in the gas phase. This can be seen from Figure 7.12 where the heat of formation was evaluated when a proton was placed at a fixed distance from C2 (C4) of **1**.

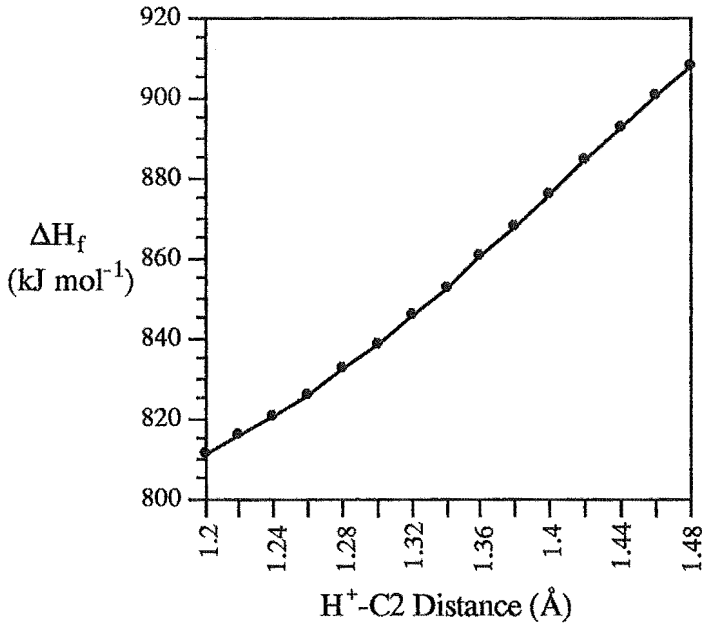

Figure 7.12. Heat of formation (PM3) evaluated with a proton at a fixed distance from C2 of **1**.

As the distance of the proton to C2 was decreased the heat of formation continually decreased until the open cation **78** was reached. It was therefore necessary to consider the proton as being transferred from another molecule (MeOH) and not just as an isolated proton in the gas phase.

Corner attack was modelled by evaluating the PM3 heat of formation of geometries at varying lengths of the H2-O1 and H2-C2 distances (Figure 7.13), after initially placing the $MeOH_2^+$ moiety in the plane of the cyclopropane ring. The results of the calculations are shown as a PE surface in Figure 7.14.

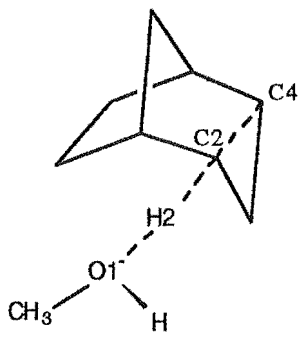

Figure 7.13. Input geometry of the grid calculation for corner attack of $MeOH_2^+$ on *endo*-tricyclo[3.2.1.$0^{2,4}$]octane **1**.

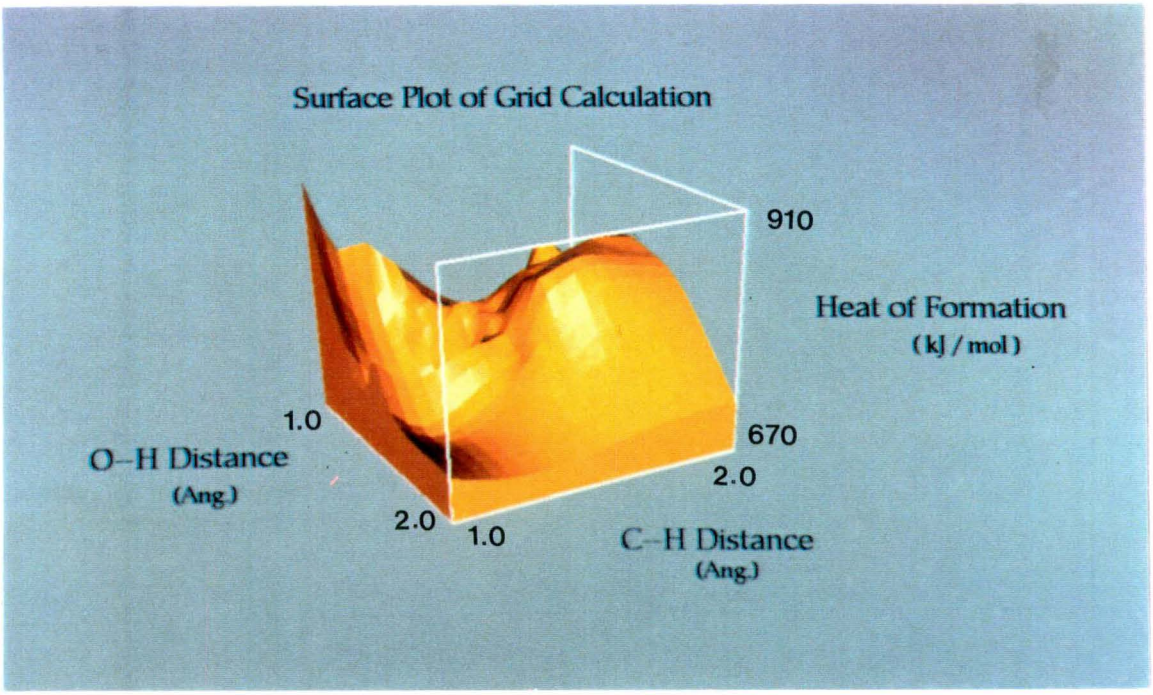

Figure 7.14. Potential energy surface obtained from the grid calculation for corner attack of $MeOH_2^+$ on *endo*-tricyclo[3.2.1.$0^{2,4}$]octane **1**.

The position of a possible transition state was identified at an O1-H2 distance of 1.3 Å and a C2-H2 distance of 1.5 Å. The geometry of this point was refined by a gradient norm minimisation procedure. The resulting structure showed one imaginary frequency characteristic of a TS. The six vibrational modes corresponding to the rotation and translation of the structure as a whole were all small and hence characteristic of a stationary point.

The oxygen of the methanol group was enantiotopic due to it being four coordinate in the transition state‡ and hence the oxygen was epimerised and the geometry reoptimised by a gradient norm criteria. The resulting structure, as before, showed one imaginary frequency. A degree of conformational flexibility was also present due to the methanol group. The O1-H2 and O1-CH_3 bonds were therefore rotated while the O1-H2 and C2-H2 distances were fixed at the TS values. The O1-H2 bond was rotated through 360° with 30° increments and the O1-CH_3 bond rotated through 120° with 10° increments with the heat of formation being evaluated at each point. From the contour plot of the resulting energies (Figure 7.15) the PE surface for the bond rotations was shown to be flat. The lowest energy structure (point A, Figure 7.15) was extracted and further refined by gradient minimisation with no geometric constraints imposed. The resulting structure **238** (Figure 7.16) was shown to be a TS from the presence of one negative force constant. The corresponding imaginary frequency showed a simultaneous

‡ Due to symmetry this was not the case for the addition of protonated methanol to cyclopropane.

elongation of the O1-H2, C2-C4, and C2-C3 bonds and contraction of the H2-C2 bond. The TS therefore corresponds to a structure which leads directly to a corner protonated cyclopropane.§

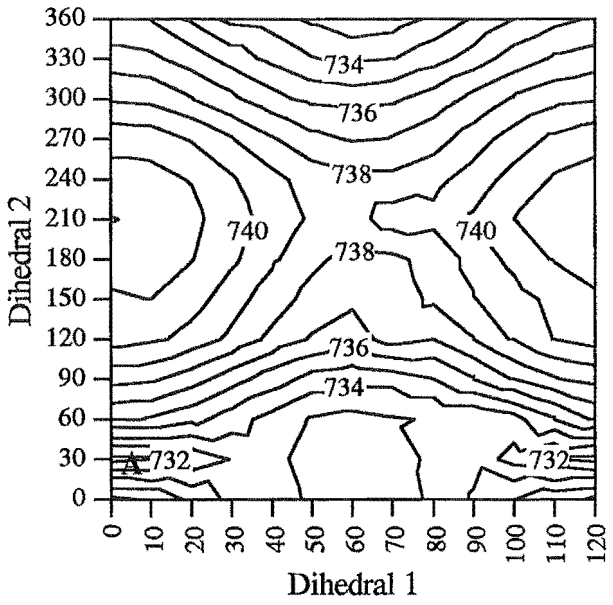

Figure 7.15. Contour plot for rotation of the O1-H2 and O1-CH_3 bonds. Heat of formation values are in kJ mol^{-1}. Dihedrals 1 and 2 correspond to the dihedral angles defining the rotation of the O1-CH_3 and O1-H2 bonds, respectively. The angles were defined with respect to dummy atoms.

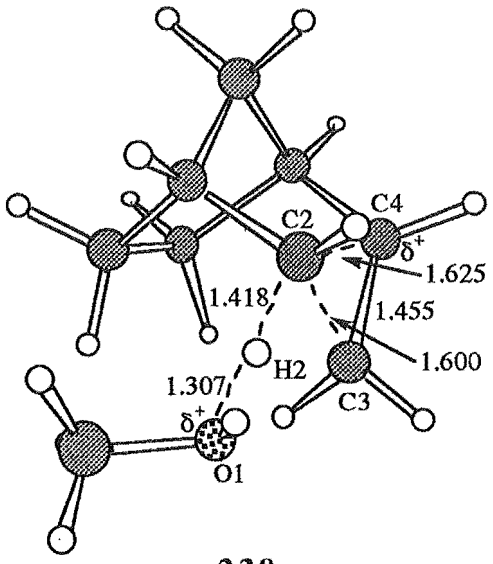

238

$\Delta H_f = 729.9$ kJ mol^{-1}

Figure 7.16. Lowest energy transition state found after epimerisation of the oxygen centre. Distances are in Angstroms.

§ Optimisation of this structure with AM1 failed to converge to a transition state.

Due to the relatively flat PE surface for the rotation of the methanol moiety found above, the conformation of the first TS found (before epimerisation of the oxygen) was searched by rotating the O1-H2 bond through 360° with 90° increments and reoptimising at each point. Three of the four initial structures converged to the same final geometry and the forth collapsed to a TS which was 0.8 kJ mol^{-1} higher in energy. The methanol moiety would therefore be freely rotating at room temperature. The lowest energy TS **239** (Figure 7.17) obtained from conformational searching of the first TS (before epimerisation) showed one negative force constant with a corresponding vibration identical to that described for structure **238**. Transition state **239** was 1.9 kJ mol^{-1} higher in energy than structure **238** and hence the configuration at the oxygen was shown to have little effect on the energy of the TS.

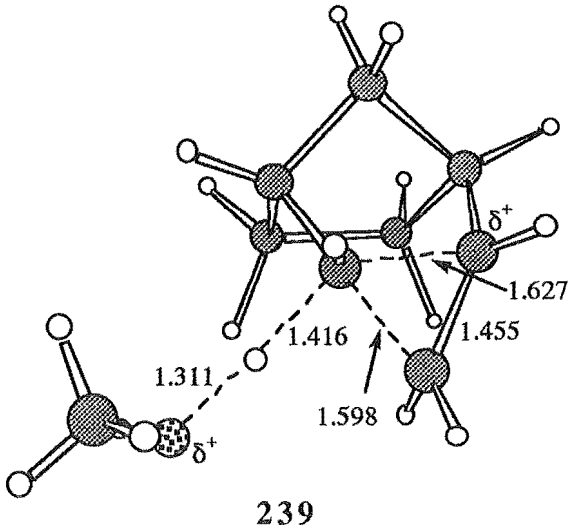

239

$\Delta H_f = 731.8$ kJ mol^{-1}

Figure 7.17. Lowest energy TS obtained for the corner attack of protonated methanol on *endo*-tricyclo-[3.2.1.$0^{2,4}$]octane **1** before epimerisation of the oxygen. Distances are in Angstroms.

When transition state **238** was reoptimised by an energy criteria, the resulting structure **240** (Figure 7.18) was a minimum (all force constants were positive) on the PE surface and corresponded to the complex formed by cation **78** and methanol after proton transfer had occurred. By lengthening the H2-C2 bond of **238** to 1.8 Å and decreasing the O1-H2 bond length to 1.2 Å, followed by geometry optimisation on an energy criteria, the TS collapsed to the $MeOH_2^+$-**1** complex **241** shown in Figure 7.19. This structure corresponded to a minimum on the potential energy surface formed on approach of protonated methanol to **1**.

The barrier to activation for proton transfer from $MeOH_2^+$ to **1** from a corner trajectory can be estimated from the difference in energy between structures **238** and **241** (ΔH_f(**238**) - ΔH_f(**241**)) and was calculated to be 23.8 kJ mol^{-1}. The overall enthalpy

change for proton transfer (ΔH_f(**240**) - ΔH_f(**241**) + Activation barrier) is -128.0 kJ mol^{-1}.

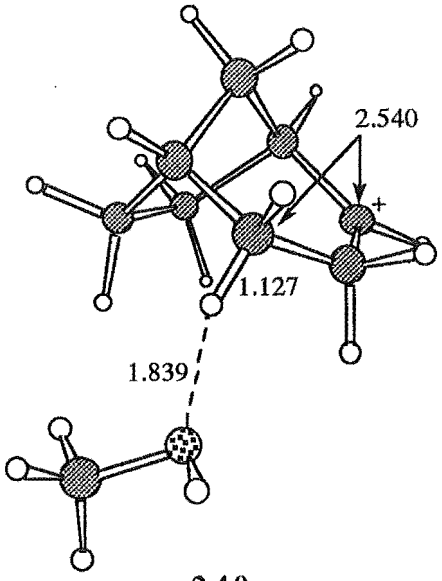

240

$\Delta H_f = 554.3$ kJ mol^{-1}

Figure 7.18. Minimum formed after proton transfer from $MeOH_2^+$ to **1** from a corner trajectory. Distances are in Angstroms.

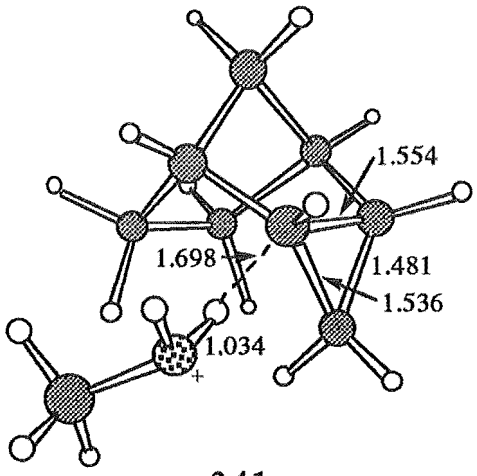

241

$\Delta H_f = 706.1$ kJ mol^{-1}

Figure 7.19. Minimum formed before proton transfer from $MeOH_2^+$ to **1** from a corner trajectory. Distances are in Angstroms.

Section 7.3.2 Edge Attack

To model the attack of $MeOH_2^+$ on **1** from an edge trajectory an approximation to the TS was derived from building the hydrocarbon skeleton around the edge transition state for $MeOH_2^+$ addition to cyclopropane **207**. The TS O1-H2, H2-C2, and H2-C4

(Figure 7.20) distances were fixed and the structure minimised using molecular mechanics methods. The resulting structure was then reoptimised by a gradient norm minimisation procedure using the PM3 parameterised Hamiltonian. The possible conformations of the methanol moiety in the TS obtained were searched in a similar way to those of **239** by rotation of O1-H2 bond by 90° increments through 360° with full TS optimisation at each point. The lowest energy TS obtained **242** is shown in Figure 7.20. The structure was shown to have one imaginary frequency which corresponded to the symmetrical contraction of the H2-C2 and H2-C4 distances and an elongation of the H2-O1 and C2-C4 distances and hence is consistent with a TS for edge attack of protonated methanol on the internal C2-C4 bond of **1**.

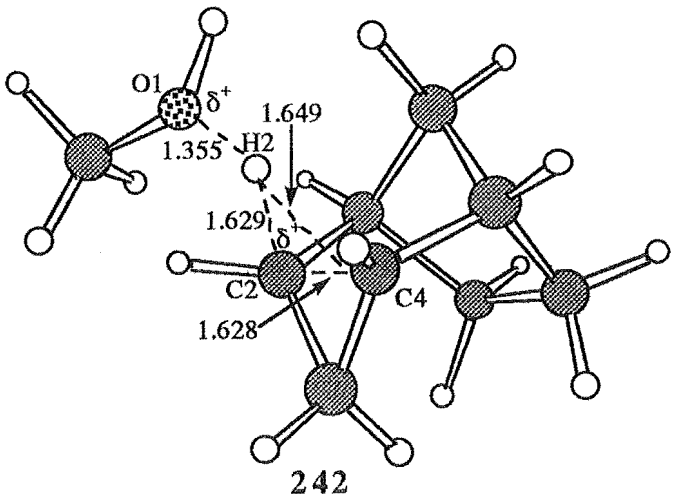

242

$\Delta H_f = 741.1$ kJ mol^{-1}

Figure 7.20. Edge TS for addition of $MeOH_2^+$ to the C2-C4 bond of **1**. Distances are in Angstroms.

In this case, although the oxygen is enantiotopic in TS **242** epimerisation of the oxygen would lead to a nonsuperimposable mirror image structure which would therefore have an identical energy to that of **242**. This is due to the presence of vertical mirror plane which passes through C3, C8, and bisects the C2-C4 and C6-C7 bonds of **1**. This was not the case with TS **238** as epimerisation of the oxygen did not lead to mirror image structures.

The minimum **243** (Figure 7.21) formed on approach of $MeOH_2^+$ to **1** and leading to the edge TS was located by optimisation of TS **242** on an energy criteria after lengthening the H2-C2 and H2-C4 distances to 1.8 Å and decreasing the H2-O1 distance to 1.2 Å. A minimum **244** (Figure 7.22a), which was formed after proton transfer to **1** from $MeOH_2^+$ had occurred, was found by geometry optimisation of TS **242**.

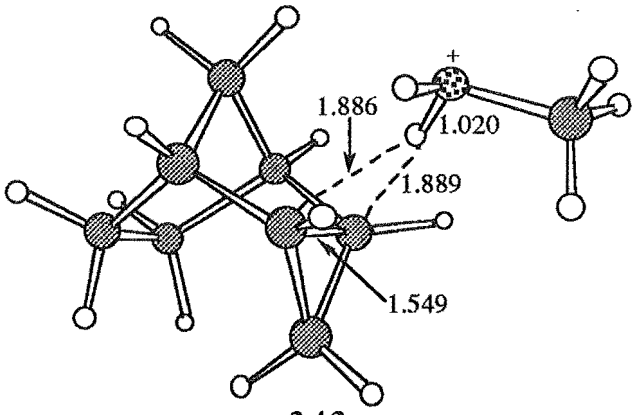

243

$\Delta H_f = 716.5$ kJ mol^{-1}

Figure 7.21. Minimum formed before proton transfer from $MeOH_2^+$ to **1** via TS **242**. Distances are in Angstroms.

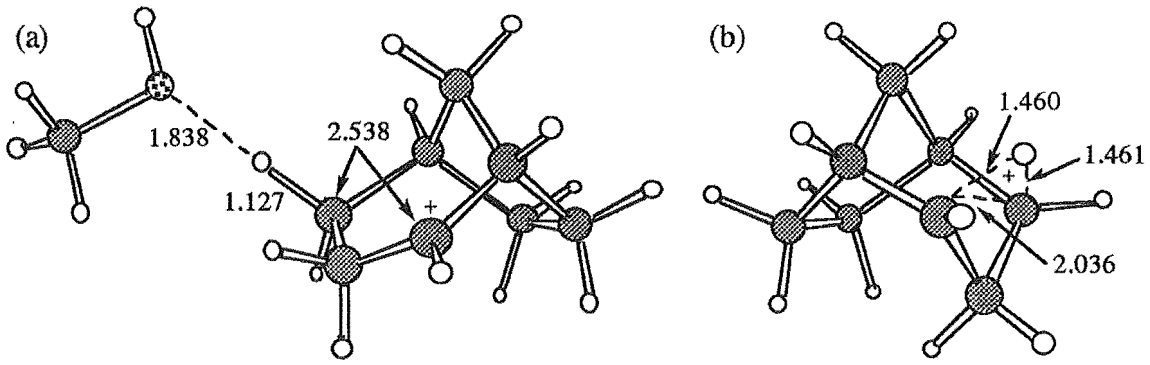

244 **245**

$\Delta H_f = 560.1$ kJ mol^{-1} $\Delta H_f = 971.2$ kJ mol^{-1}

Figure 7.22. (a) Minimum **244** formed after proton transfer from $MeOH_2^+$ to **1** via TS **242**.
(b) An edge protonated structure **245** was located but was identified as a TS and not a minimum. Distances are in Angstroms.

Structure **244** was unsymmetrical‡ and therefore may indicate that as the O1-H2 bond lengthens the H2-C2 and H2-C4 distances become less similar, that is, a symmetrical edge protonated intermediate **245** (Figure 7.22b) is not formed. Structure **245** was shown to be a TS for hydride migration from C2 to C4 of cation **78**.

The activation barrier for edge proton addition to **1** (ΔH_f(**242**) - ΔH_f(**243**)) is 24.6 kJ mol^{-1} and the overall enthalpy change for the proton transfer (ΔH_f(**244**) - ΔH_f(**243**) + Activation barrier) is -131.8 kJ mol^{-1}.

---

‡ Attempts to locate a minimum formed by an edge protonated structure **245** and methanol after proton transfer were unsuccessful.

Section 7.4 DISCUSSION OF THE RESULTS OBTAINED FOR THE ADDITION OF PROTONATED METHANOL TO *endo*-TRICYCLO[3.2.1.$0^{2,4}$]OCTANE

The results of Sections 7.3.1 and 7.3.2 indicate that the activation barrier for addition of $MeOH_2^+$ to the internal cyclopropane bond of **1** is similar for both the corner and edge trajectories, 23.8 kJ mol^{-1} and 24.6 kJ mol^{-1}, respectively. However, the activation barriers were calculated from consideration of the TS and minima formed before proton transfer in each case. Since the energies of the two minima **241** and **243** differ significantly (706.1 kJ mol^{-1} and 716.5 kJ mol^{-1}, respectively) a better indication of the relative energies of the two processes may be gained by direct comparison of the energies of the transition states **238** and **242**. The difference in heat of formation of **242** and **238** ($\Delta Hf(242) - \Delta Hf(238)$) is 11.2 kJ mol^{-1}. A Boltzman distribution would therefore predict TS **238** to be 99% populated compared with 1% for **242**. This is in agreement with the experimental results (Figure 1.6) which show exclusively corner addition of an electrophile (H^+/D^+) to occur.[13,14,18] The relative energies of the transition states and minima found for both corner and edge attack of $MeOH_2^+$ on **1** are summarised in Figure 7.23.

Consideration of the CPK models of **1** (Figures 7.24a and b) shows that edge addition (Figure 7.24a) may be a little more hindered than corner attack (Figure 7.24b) but it seems unlikely that this alone would be sufficient to completely disfavour edge attack as both trajectories are reasonably open.† Likewise, consideration of the distribution of the HOMO of **1** (Figures 7.25a and b) shows no discernible reason for the large predominance of corner attack (Figure 7.25b) over edge attack (Figure 7.25a). This can be seen more clearly from consideration of Figures 7.26c and d which show the HOMO of **1** mapped onto the electron density surface (Figures 7.26a and b). The blue/purple areas show a high correlation between electron density and the HOMO and the red areas show low correlation. Thus for both edge (Figure 7.26c) and corner attack (Figure 7.26d) a similar size and colour blue/purple area can be seen, therefore both edge and corner attack would be expected to occur.

The HOMO-1 orbital (Figures 7.27a and b) of **1** forms the C2-C3 (C4-C3) bond. If the HOMO-1 orbital is mapped onto the electron density surface (Figures 7.28a and b) only one purple area is observed and this is at the edge of the C2-C3 (C4-C3) bond (Figure 7.28b). This region of high correlation of electron density and HOMO-1 orbital overlaps with that of the purple area corresponding to the position of corner attack at the C2-C4 bond (Figure 7.29b). No contribution of the HOMO-1 orbital to the area where edge addition to the C2-C4 bond takes place was observed (Figure 7.29a).

---

† Figures 7.24-7.29 show compound **1** in similar orientations. The descriptions "edge" and "corner" refer to the C2-C4 bond.

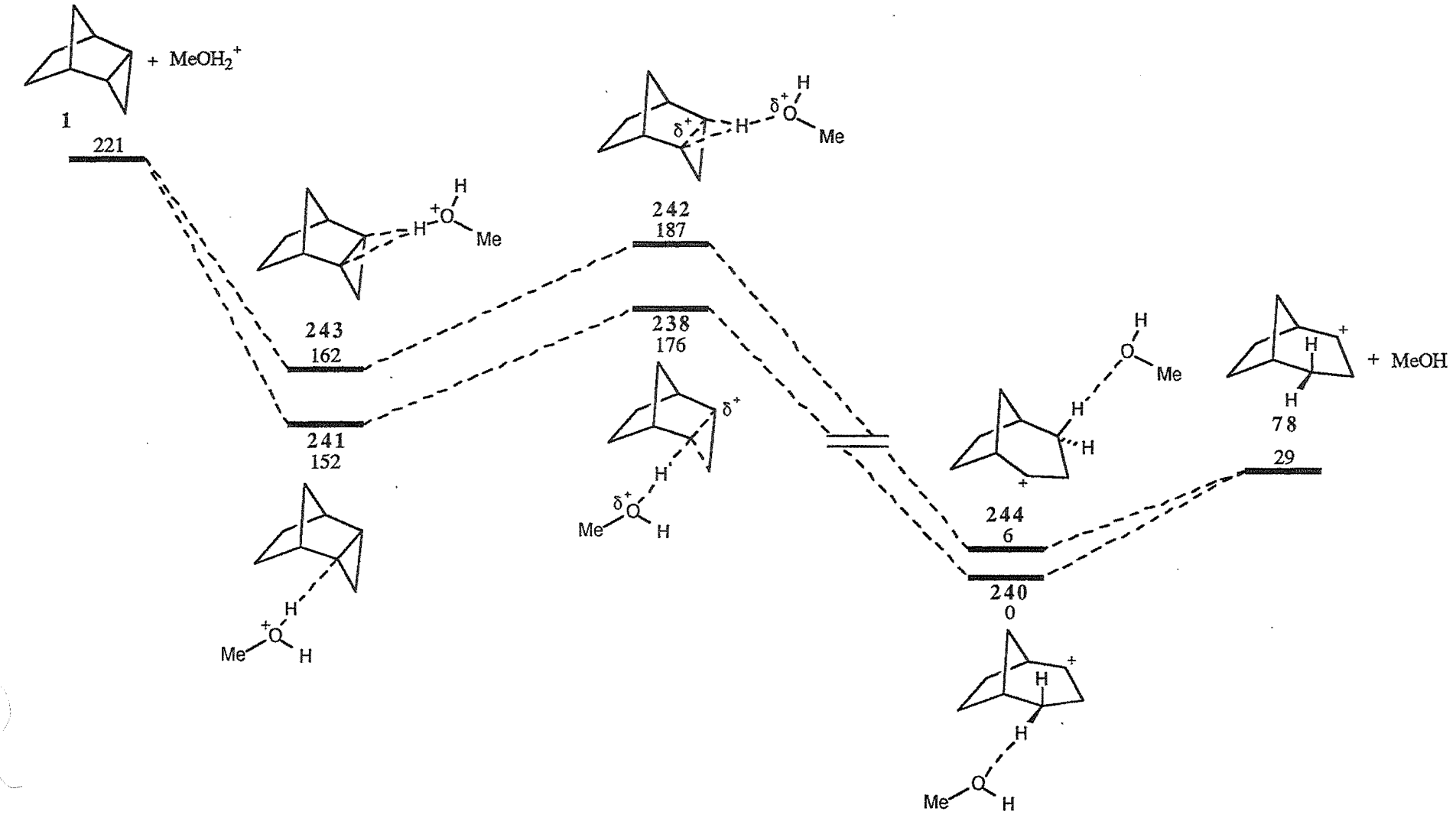

Figure 7.23. PM3 results for the relative energies of the species involved in edge and corner protonation of *endo*-tricyclo[3.2.1.$0^{2,4}$]octane **1**. Energies are in kJ mol^{-1} relative to intermediate **240**.

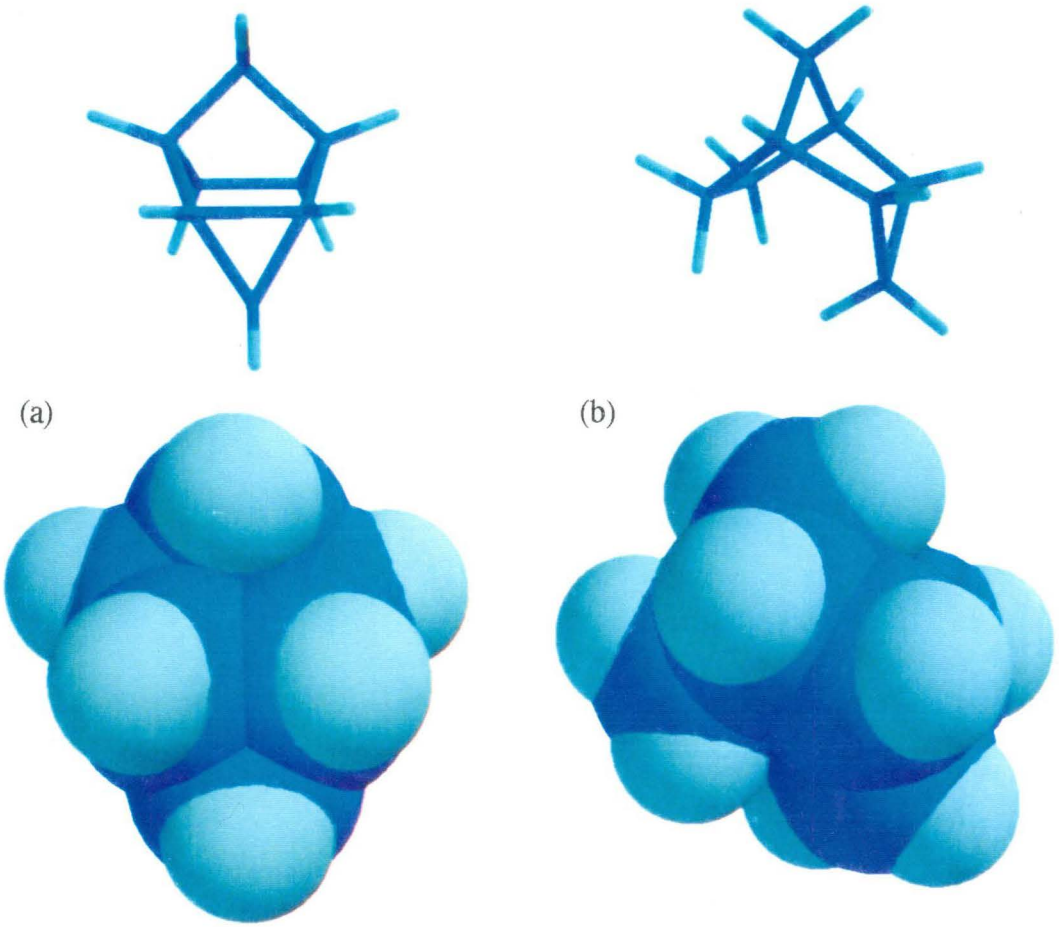

Figure 7.24. CPK models showing (a) edge and (b) corner trajectories for addition to the C2-C4 bond of **1**. The "tube" representations from identical perspectives are also shown.

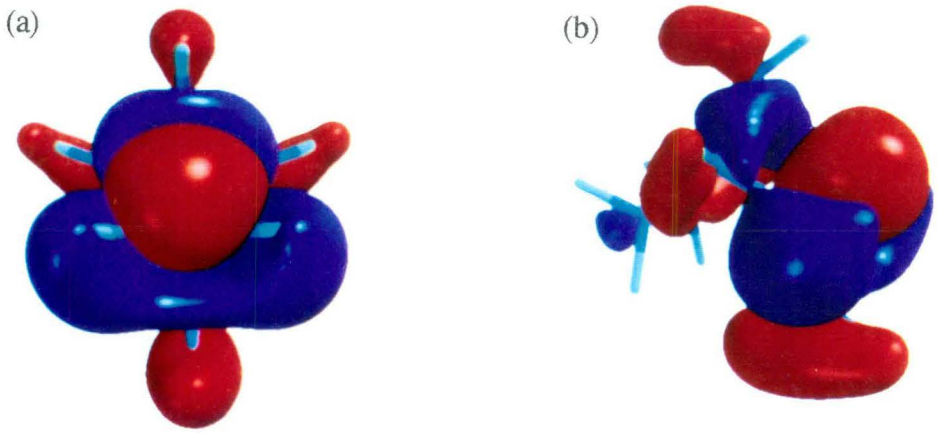

Figure 7.25. HOMO orbital of **1** from two orientations, (a) edge and (b) corner addition trajectories to the C2-C4 bond of **1**.

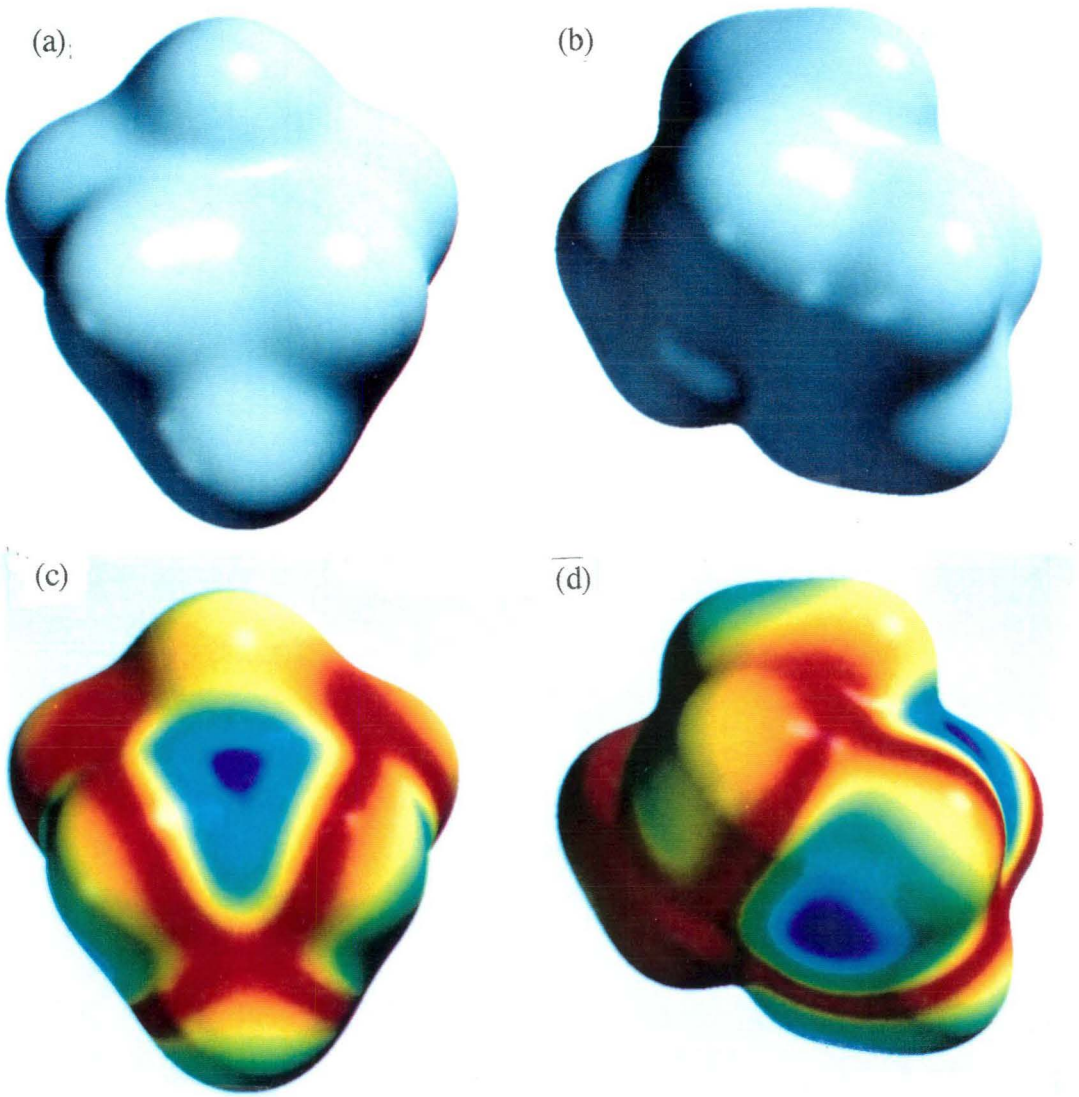

Figure 7.26. Electron density surface of **1** from (a) edge and (b) corner of the C2-C4 bond. Figures (c) and (d) show the HOMO orbital of **1** mapped onto its electron density surface from the edge and corner trajectories, respectively.

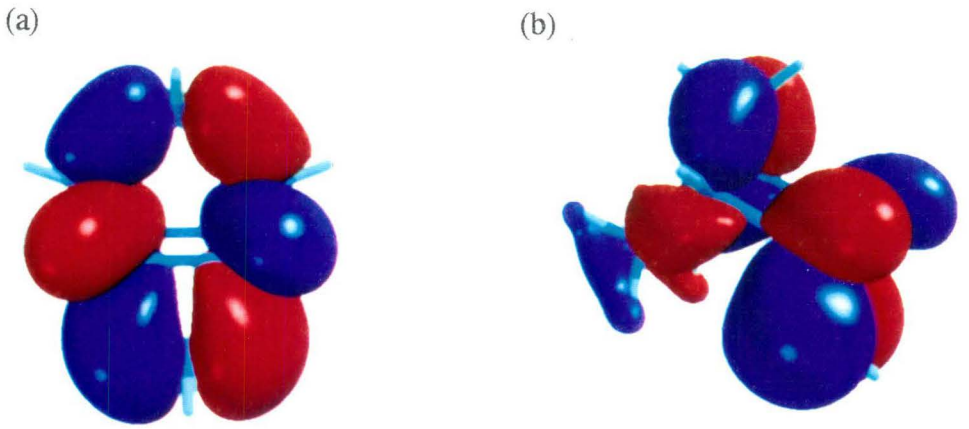

Figure 7.27. HOMO-1 orbital of **1** viewed from (a) the edge and (b) the corner of the C2-C4 bond.

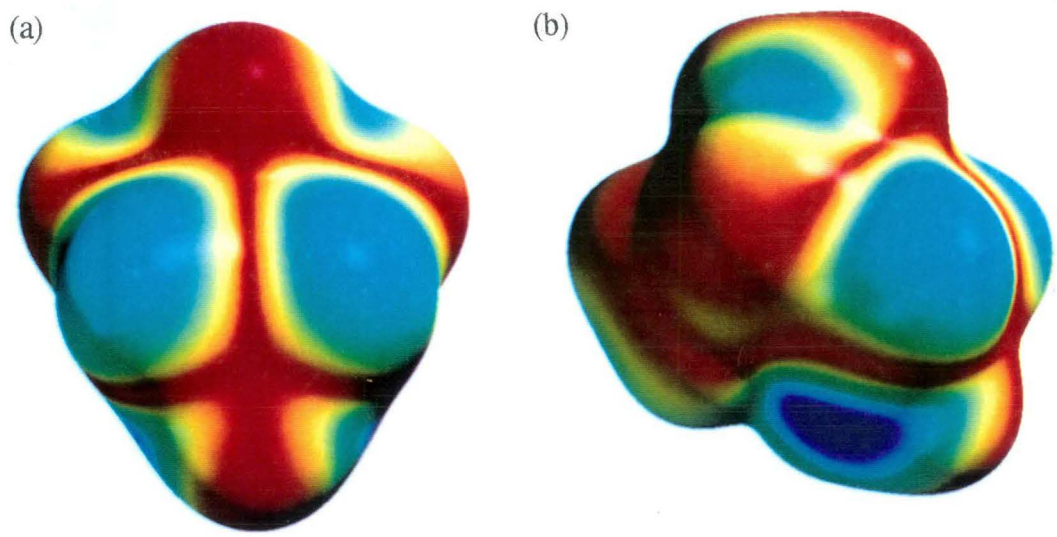

Figure 7.28. HOMO-1 orbital mapped onto the electron density surface of **1**. (a) Edge and (b) corner views of the C2-C4 bond.

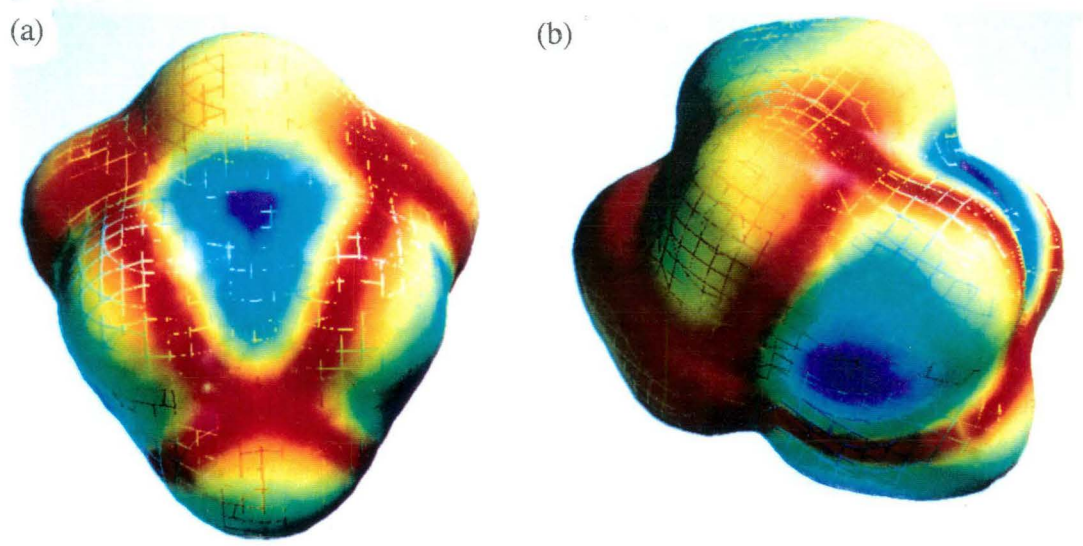

Figure 7.29. HOMO-1 (mesh) and HOMO (transparent) orbitals mapped onto the electron density plot of **1**. (a) Edge and (b) corner views of the C2-C4 bond.

This therefore suggests that as $MeOH_2^+$ approaches the cyclopropane ring, from a corner attack trajectory at the C2-C4 bond, it not only interacts with the HOMO but also with the HOMO-1 orbital. Interaction with the HOMO-1 orbital would result in a stabilising effect on the corner attack trajectory which is not present in edge attack pathway. This, in conjunction with corner attack being more sterically favoured, results in attack exclusively from a corner trajectory. However, this is not formally corner attack as both the C2-C4 and C2-C3 bonds are partially broken at the transition state and not just the bond (C2-C4) *anti* to the incoming electrophile.[13,15] In TS **238** both the C2-C4 and C2-C3 bond lengths are lengthened, 1.625 Å and 1.600 Å, respectively, and the C4-C3 bond is significantly shortened (1.455 Å). Thus the TS may be considered to be leading to a corner protonated cyclopropane structure. The increased bond length of the C2-C3 bond (1.503 Å in **1**) supports the assumption that the HOMO-1 orbital is involved in the proton transfer, as this orbital is predominantly responsible for formation of the C2-C3 bond.

The importance of the interaction of orbitals other than the HOMO with incoming electrophiles has previously been suggested by Wiberg,[17,20,21] who found that in some cases the HOMO is responsible for only 50% of the electron density contributed to the attacking proton on addition to a cyclopropane ring.

Attempts to locate a corner protonated intermediate, analogous to corner protonated cyclopropane **180**, were unsuccessful. However, a TS **246** (Figure 7.30) similar in structure to that expected for a corner protonated species was identified. Structure **246** showed both the C2-C4 and C2-C3 bonds to be lengthened (1.875 Å and 2.217 Å, respectively) with charge development greater at C3 than C4 (0.239 an -0.133, respectively). It therefore appears unlikely that structure **246** would lead to cation **78** and seems more likely to lead to the formation of the primary cation **231** on the PM3 PE surface.

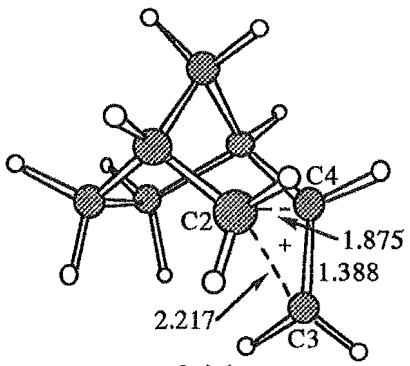

246

$\Delta H_f = 915.7$ kJ mol^{-1}

Figure 7.30. Corner protonated cation **246**. Distances are in Angstroms.

Since optimisation of TS **238** by an energy criteria gave **240**, it appears that the PM3 semiempirical method predicts the TS to collapse to an open carbocation as the O1-H2 distance increases. Comparison of the charges of C3 and C4 (-0.002 and 0.030, respectively) of **238** shows considerably more charge development at C4. This is presumably due to the greater ability of C4 to stabilise the positive charge via electron density donation from the rest of the hydrocarbon skeleton. Transition state **238** therefore collapses to form the most stable open carbocation **78**. Formation of an open carbocation contrasts with the conclusions drawn from experimental results.[13,14,17,18,21,22] In this system the possibility of rearrangement to a nonclassical species **3a** or rapid interconversion of two classical cations, **78** and **78'** (Figure 7.5), may explain the observation that nucleophilic attack occurs exclusively with inversion. However, the geometry of cation **78** when optimised at the ab initio 3-21G(*) level shows the LUMO (Figures 7.31a and b) to clearly be more susceptible to 'bottom' face attack (*anti* to the main bridge, Figure 7.31a) than from 'top' face attack (*syn* to the main bridge, Figure 7.31b). Consideration of CPK models (Figures 7.32a and b) and of the colour coded contour plot of the LUMO mapped onto the electron density surface (Figures 7.33a and b) also supports this conclusion.‡ Nucleophilic capture would therefore be expected to occur with inversion of configuration as was observed by experiment.[13,14,18] This would be consistent with cation **78** being an intermediate with a small barrier to interconversion, via TS cation **3a** with its mirror image **78'** with a small amount of nucleophilic capture of cation **78** before leakage to cation **78'** occurs. However, since the nature of cations **3a** and **78** is not known categorically, as higher levels of theory may be required to properly characterise these cations,[119,122,123] the possibility of a corner protonated intermediate[13,14,17,18,21,22] cannot be ruled out.

‡ Cation **78** when optimised at the PM3 level, using the same analysis, predicts the opposite result, that is, 'top' face attack on cation **78** would be favoured.

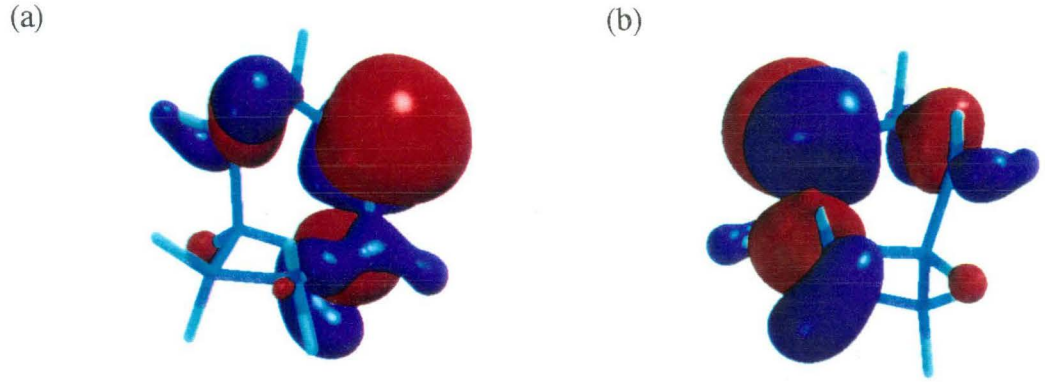

Figure 7.31. LUMO of **78** obtained from the ab initio 3-21G(*) optimised geometry from (a) 'bottom' face and (b) 'top' face views of the cation.

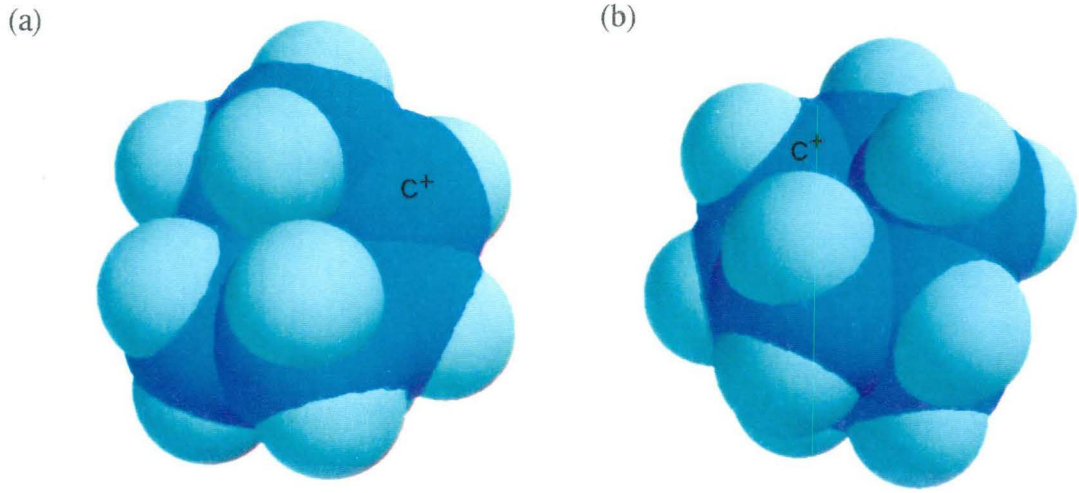

Figure 7.32. CPK model showing (a) 'bottom' face and (b) 'top' face of cation **78** (ab initio geometry).

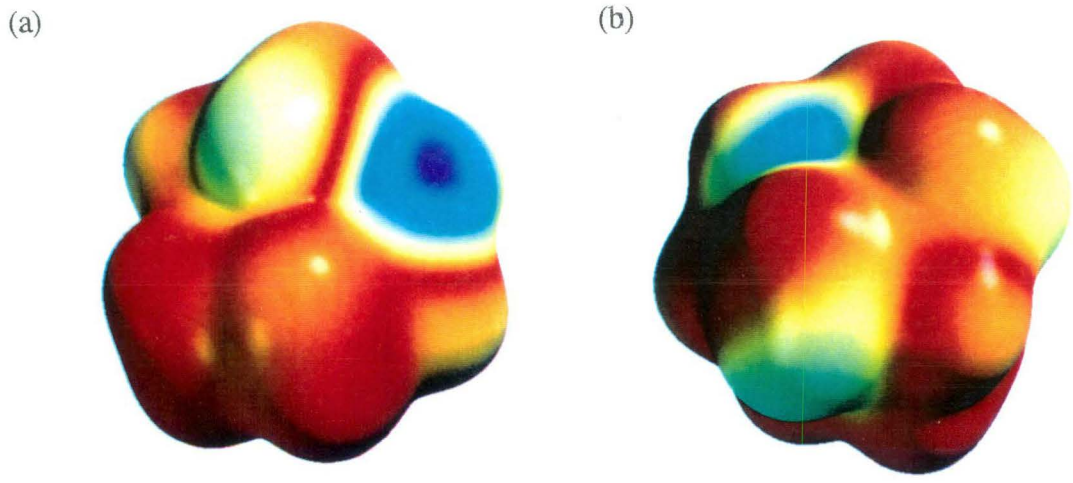

Figure 7.33. LUMO of **78** mapped onto electron density plot showing (a) the 'bottom' face and (b) the 'top' face of the cation.

Section 7.5 PROTON TRANSFER FROM PROTONATED METHANOL TO *exo*-TRICYCLO[3.2.1.$0^{2,4}$]OCTANE

Section 7.5.1 Corner Attack

The cations resulting from cleavage of the C2-C4 or C2-C3 (C3-C4) bonds of **46** were examined in Section 7.2 (Figure 7.11). Rupture of the C2-C4 bond was found to result in formation of the most stable carbocation **78**.

An approximate transition structure for corner addition of protonated methanol to **46** was constructed by using the TS obtained for cyclopropane **208** and building the rest of the hydrocarbon framework around this structure. The TS distances were fixed and the structure minimised with molecular mechanics. The resulting structure was then optimised using the PM3 semiempirical method without any geometrical constraints imposed. A TS was obtained and the structure conformationally searched by rotating the O1-H2 bond through 360° by 90° increments. Optimisation of each conformer led to the collapse of all four structures to the same final geometry **247** (Figure 7.34). The PE surface for rotation of this bond was therefore assumed to flat.

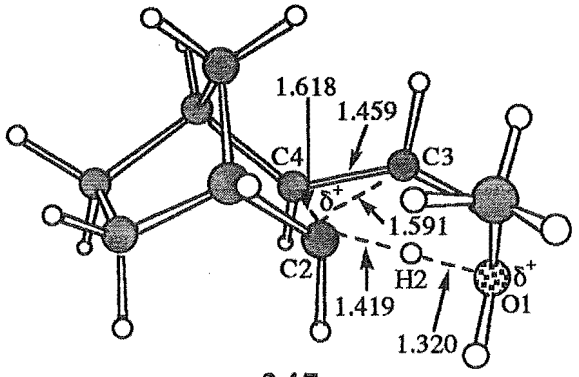

247

$\Delta H_f = 725.4$ kJ mol^{-1}

Figure 7.34. Lowest energy corner protonated TS for addition of $MeOH_2^+$ to *exo*-tricyclo[3.2.1.$0^{2,4}$]-octane **46**.

The oxygen of **247** was epimerised and the above procedure repeated to search for the lowest energy conformation of the TS. The lowest energy geometry obtained **248** is shown in Figure 7.35. Structures **247** and **248** have nearly (0.4 kJ mol^{-1}) identical energies and hence little lowering of the energy was obtained from epimerisation of the oxygen atom in the transition states. Both structures showed one imaginary frequency which corresponded to an increase in length of the C2-C3, C2-C4, and H2-O1 bonds and a decrease in length of the C3-C4 and C2-H2 bonds (Figure 7.34). The structures are therefore consistent with transition states leading directly to a corner protonated species. Geometry optimisation of **247** after decreasing the H2-C2 and increasing the H2-O1

bond lengths gave structure **249** (Figure 7.36) which is a minimum on the potential surface and is the structure formed after proton transfer from protonated methanol to **46.**

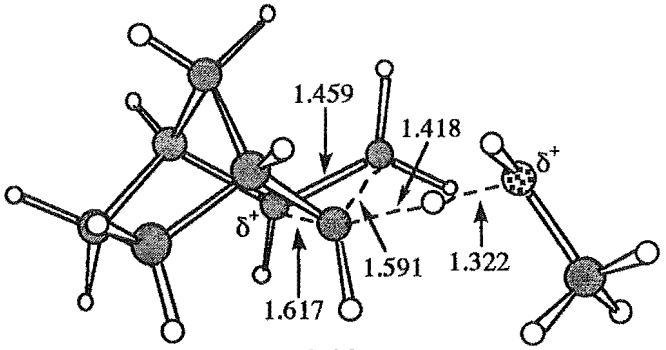

248

$\Delta H_f = 725.8$ kJ mol^{-1}

Figure 7.35. Lowest energy corner protonated TS for addition of $MeOH_2^+$ to *exo*-tricyclo[3.2.1.$0^{2,4}$]-octane **46** after epimerisation of the oxygen. Distances are in Angstroms.

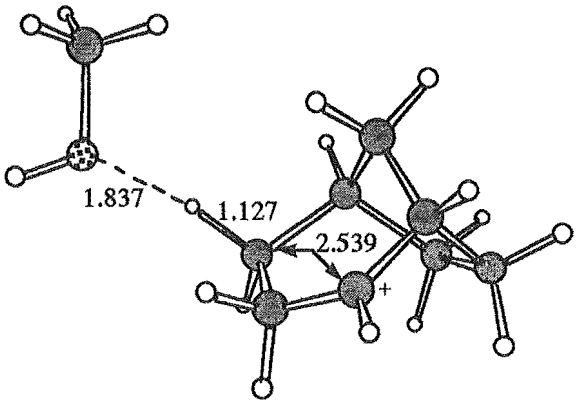

249

$\Delta H_f = 559.0$ kJ mol^{-1}

Figure 7.36. Minimum formed after proton transfer from $MeOH_2^+$ to **46** via TS **247.** Distances are in Angstroms.

Geometry optimisation of **247** by an energy criteria after increasing the H2-C2 distance to 1.6 Å and decreasing the H2-O1 distance to 1.2 Å gave structure **250** (Figure 7.37) the minimum formed on approach of $MeOH_2^+$ and **46** before proton transfer occurs. The barrier to activation for proton transfer from $MeOH_2^+$ to **46** from a corner trajectory (ΔH_f(**247**) - ΔH_f(**250**)) was calculated to be 32.1 kJ mol^{-1} and the overall enthalpy change is -102.2 kJ mol^{-1} (ΔH_f(**249**) - ΔH_f(**250**) + Activation barrier).

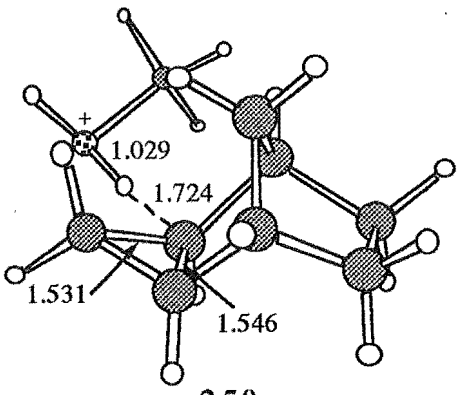

250

$\Delta H_f = 693.3$ kJ mol^{-1}

Figure 7.37. Minimum formed before proton transfer occurs as $MeOH_2^+$ and **46** approach from a corner trajectory. Distances are in Angstroms.

Section 7.5.2 Edge Attack

Edge attack of protonated methanol on the C2-C4 bond of **46** was modelled in a similar way to that of edge attack on **1**, by using the edge TS obtained from addition of protonated methanol to cyclopropane **207** and building the rest of the hydrocarbon skeleton around this structure. Optimisation by a gradient norm minimisation procedure gave a TS which was conformationally searched by rotation of the O1-H2 bond through 360° in 90° increments with complete structure optimisation performed for each conformer. The lowest energy TS **251** is shown in Figure 7.38.

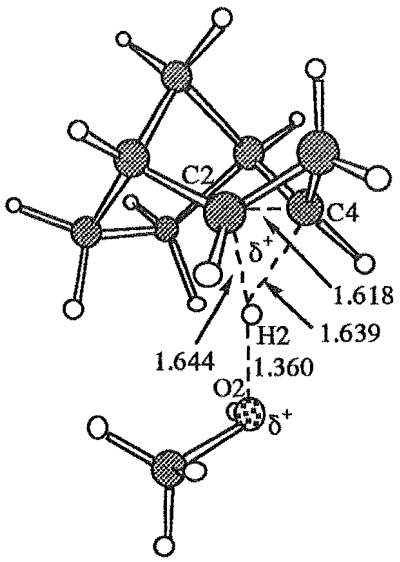

251

$\Delta H_f = 723.1$ kJ mol^{-1}

Figure 7.38. Lowest energy edge attack TS for addition of $MeOH_2^+$ to *exo*-tricyclo[3.2.1.$0^{2,4}$]octane **46**. Distances are in Angstroms.

Structure **251** showed one imaginary frequency which corresponded to the simultaneous decrease of the H2-C2 and H2-C4 bond lengths and an increase in length of the H2-O2 and C2-C4 bonds. The vibration is therefore consistent with a TS for edge attack of protonated methanol on **46**. The minimum **252** (Figure 7.39), formed on approach of $MeOH_2^+$ to **46** before H^+ transfer occurred, was located by increasing the C2-H2 and C4-H2 distances and shortening the H2-O1 distance of **251**, followed by geometry optimisation by an energy criterion.

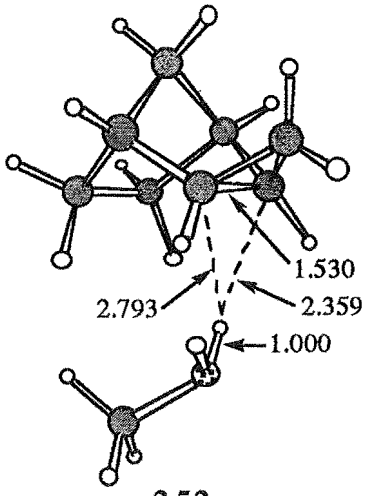

252

$\Delta H_f = 694.6$ kJ mol^{-1}

Figure 7.39. Minimum formed before proton transfer as $MeOH_2^+$ and **46** approach from an edge trajectory. Distances are in Angstroms.

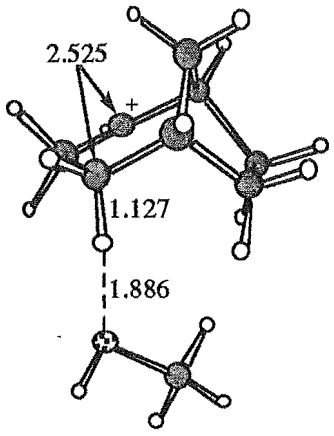

253

$\Delta H_f = 563.6$ kJ mol^{-1}

Figure 7.40. Minimum formed after proton transfer from $MeOH_2^+$ to **46** from an edge trajectory. Distances are in Angstroms.

Increasing the H2-O1 distance and decreasing the H2-C2 and H2-C4 bond lengths of **251** followed by geometry optimisation by an energy criteria gave **253** (Figure 7.40).

Structure **253** was identified as a minimum on the PE surface and corresponded to the structure formed after proton transfer from $MeOH_2^+$ to **46** was complete.

The activation barrier for edge addition of $MeOH_2^+$ to the C2-C4 bond of **46** was calculated to be (ΔH_f(**251**) - ΔH_f(**252**)) 28.5 kJ mol^{-1} and the overall enthalpy change for the reaction to be -102.5 kJ mol^{-1} (ΔH_f(**253**) - ΔH_f(**252**) + Activation Barrier).

Section 7.6 DISCUSSION OF THE RESULTS OBTAINED FOR THE ADDITION OF PROTONATED METHANOL TO *exo*-TRICYCLO[3.2.1.0^{2,4}]OCTANE

The results obtained from the semiempirical calculations of Sections 7.5.1 and 7.5.2 are summarised in Figure 7.41. From this diagram it can be seen that the corner and edge trajectories for addition to the C2-C4 bond are predicted to have similar activation barriers, 32.1 kJ mol^{-1} and 28.5 kJ mol^{-1}, respectively, with only 2.3 kJ mol^{-1} difference in the heat of formation of the transition states **247** and **251**. From a Boltzman distribution the transition states would be expected to be populated in a ratio of 71:29 (**251**:**247**) in favour of the edge TS **251**. This contrasts with the experimental results where attack predominantly from a corner trajectory at the C2-C4 bond was observed.[13,14] The reason for the failure of the semiempirical calculations in this case is not clear but from inspection of a CPK model of **46** it would appear that the corner trajectory (Figure 7.42a) would be sterically more favourable than the edge trajectory (Figure 7.42b). This can also be seen from comparison of the surfaces obtained by mapping the HOMO orbital of **46** onto the electron density surface (Figure 7.43). As can be seen from Figure 7.43 the blue/purple area, corresponding to a high correlation of the electron density with the HOMO, for corner attack (Figure 7.43a) is more susceptible to electrophilic attack than the blue/purple area at the edge of the C2-C4 bond (Figure 7.43b). The semiempirical calculations may therefore be underestimating the steric effects (i.e. nuclear - nuclear repulsions) in this case or overestimating the electronic stabilisation gained from attack at the edge of the C2-C4 bond.

As was the case for $MeOH_2^+$ attack on **1**, no edge or corner protonated intermediates were located. Cations **254** and **255** (Figure 7.44), the edge and corner protonated structures, respectively, were identified but were shown to be transition states. Structure **254** was a TS on the PM3 PE surface for a 1,3-hydride migration from C2 to C4 and **255** was identified as a TS leading to the primary cation **236** rather than cation **78**. Both edge and corner trajectories therefore appear to proceed to open carbocation intermediates. As outlined earlier, the PM3 method predicts the cations resulting from proton addition to **46** and **1** with cleavage of the C2-C4 bond to be **78**, and that nucleophilic capture of this cation would be favoured from 'top' face addition. However, the ab initio (3-21G(*)) optimised geometry of **78** favoured nucleophilic addition from the 'bottom' face (as was observed experimentally[13,14,18] for the reaction of **1** with H^+).

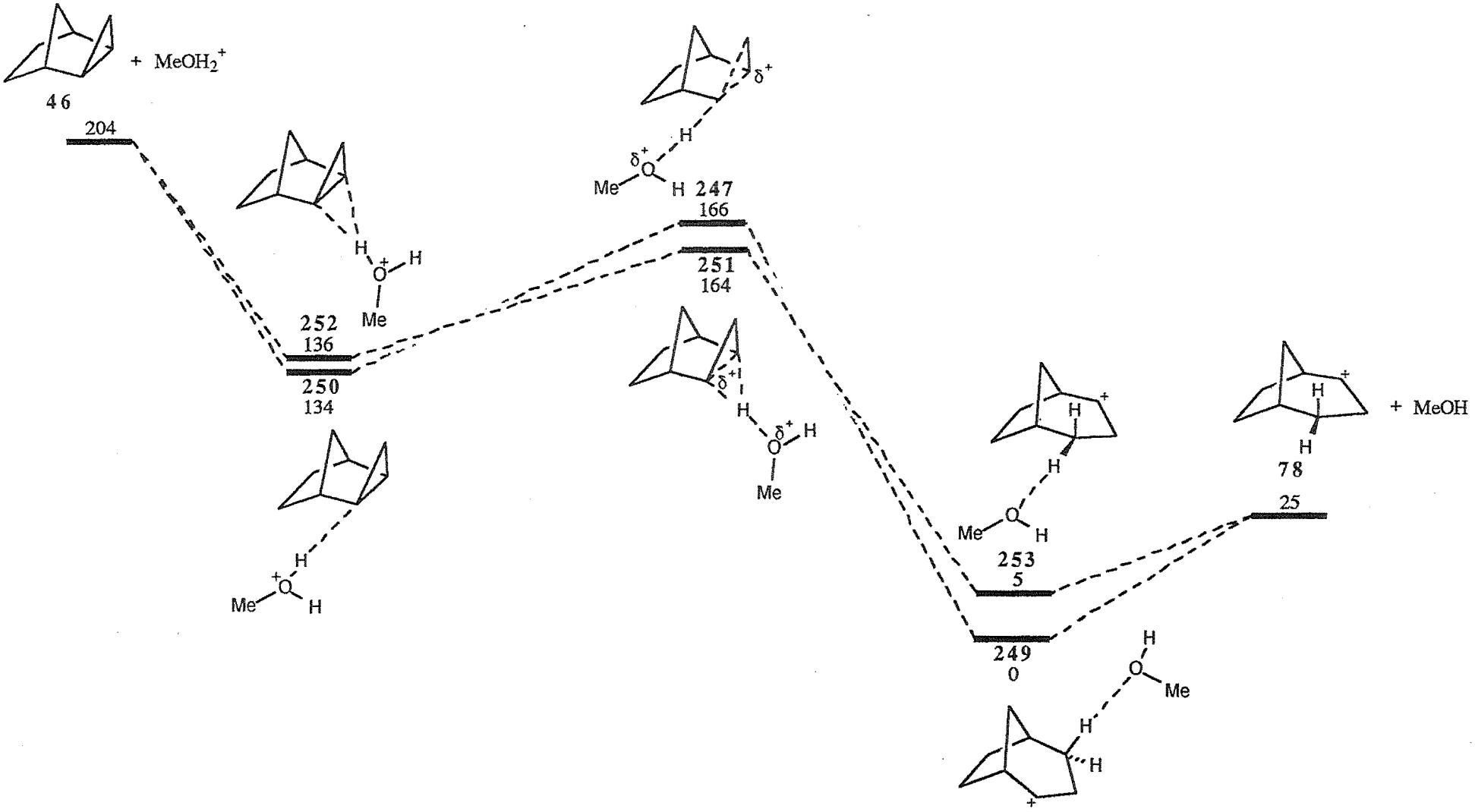

Figure 7.41. PM3 results for the relative energies of the species involved in edge and corner addition of $MeOH_2^+$ to *exo*-tricyclo[3.2.1.$0^{2,4}$]octane **46**. Energies are in kJ mol^{-1} relative to intermediate **249**.

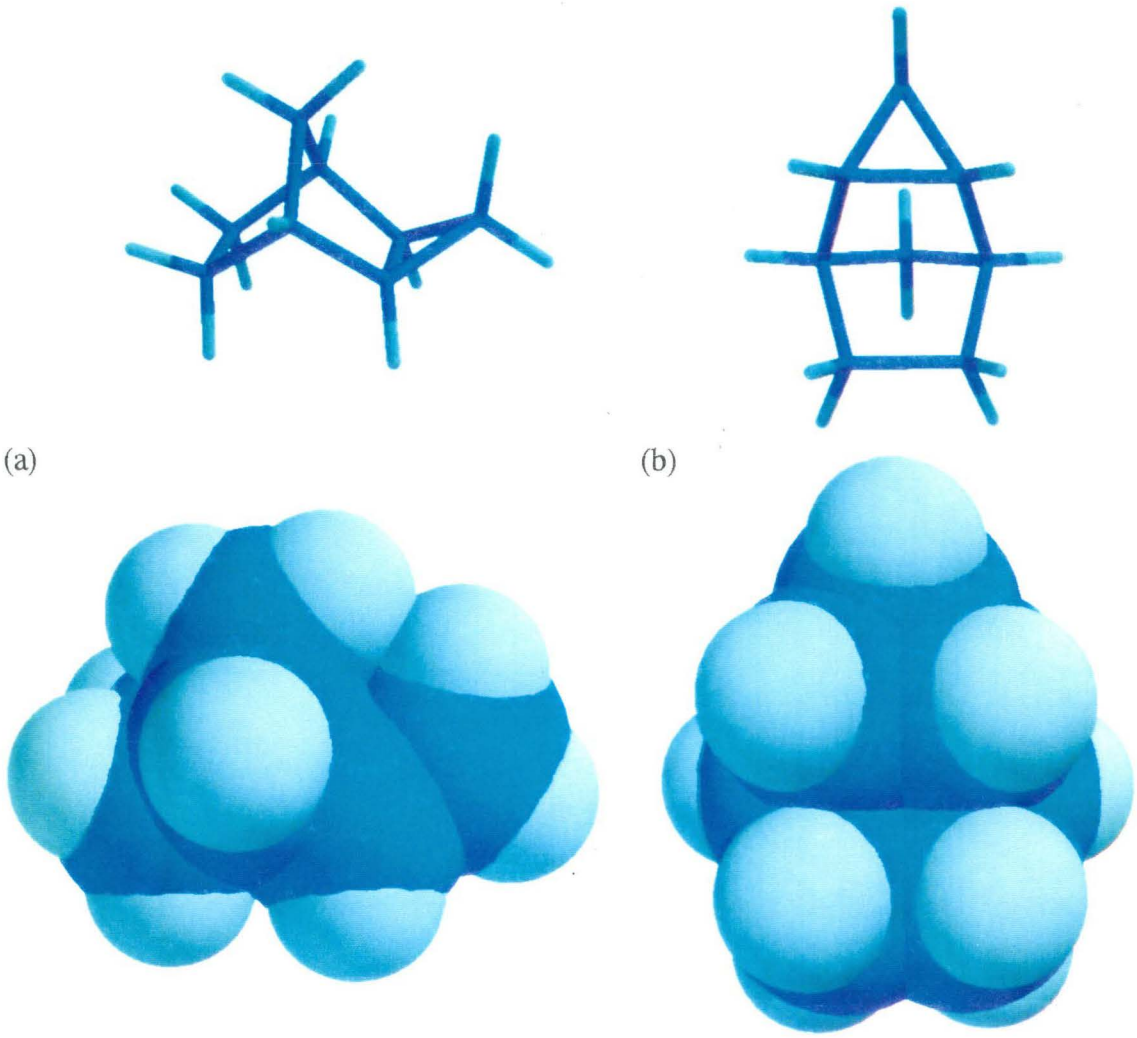

Figure 7.42. CPK model of *exo*-tricyclo[3.2.1.$0^{2,4}$]octane **46**. (a) Corner trajectory and (b) edge trajectory. The corresponding tube representations are also shown from identical orientations

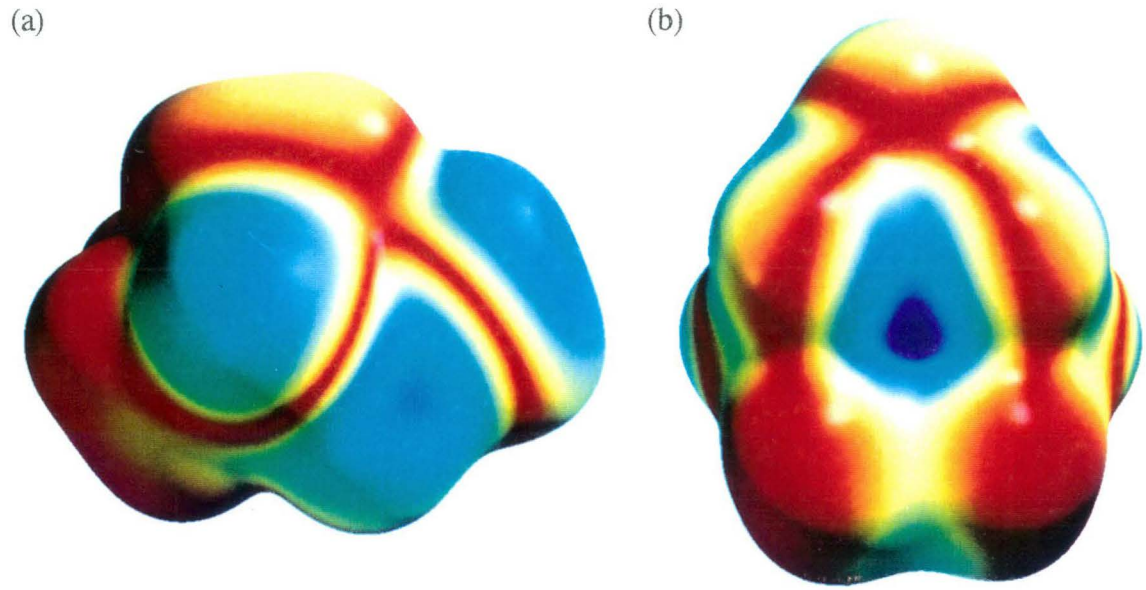

Figure 7.43. HOMO orbital mapped onto the electron density surface of **46**. (a) Corner trajectory and (b) edge trajectory of electrophilic attack on the C2-C4 bond.

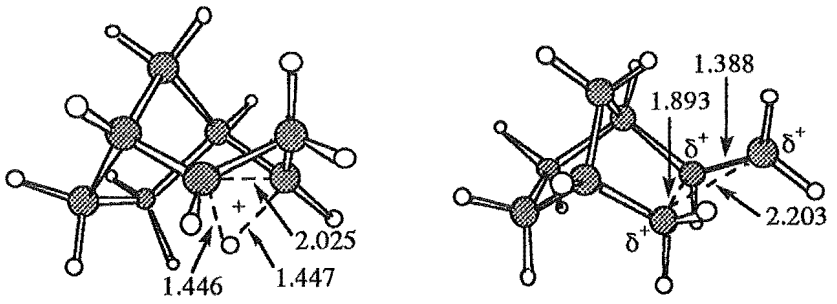

254 $\Delta H_f = 960.0$ kJ mol^{-1}

255 $\Delta H_f = 917.9$ kJ mol^{-1}

Figure 7.44. PM3 edge and corner protonated structures of **46**. Distances are in Angstroms.

As outlined earlier (Section 7.2) optimisation of the open carbocation **78** with an *exo* orientation of the three membered bridge by ab initio methods (3-21G(*) basis set) gave cation **233** (Figure 7.4). Consideration of the carbon charges in **233** showed C2 to be more highly charged than C1 (0.252 and -0.315, respectively). Therefore nucleophilic capture would be expected to occur at C2 in preference to C1 and retention of the bicyclo[3.2.1]octane carbon skeleton would be expected. Comparison of the possible trajectories (Figure 7.45) of nucleophilic attack on C2 showed attack with inversion to be favoured. This can be seen by comparison of Figures 7.45a and b where the area of high correlation of electron density with the LUMO can be seen as a blue/purple area on Figure 7.45a. The view from the opposite side shows no blue/purple area (Figure 7.45b) and hence is less favourable. If nucleophilic addition took place with the trajectory depicted by Figure 7.45a then inversion of configuration at C2 would occur. Nucleophilic attack with inversion was observed experimentally.[13,14]

The corner attack TS **247** showed an increase in length of both the C2-C3 and C2-C4 bonds (Figure 7.34) (C2-C3 1.591 Å, C2-C4 1.618 Å) similar to those observed for **238** and hence showed significant contribution of electron density of both bonds, and hence from both the HOMO and HOMO-1 orbitals, to the incoming proton. This can be seen from comparison of Figures 7.43a and 7.46a which show the HOMO and HOMO-1 orbitals, respectively, of **46** mapped onto the electron density surface. As with **1**, the HOMO-1 and HOMO orbitals show significant overlap of the high correlation (blue/purple) areas. Figure 7.47 shows the HOMO (transparent) and HOMO-1 (mesh) orbital maps overlapped on the same structure to further illustrate this point.‡

‡ The orbitals and orbital map pictures shown are from the ab initio optimised geometry of **46**.

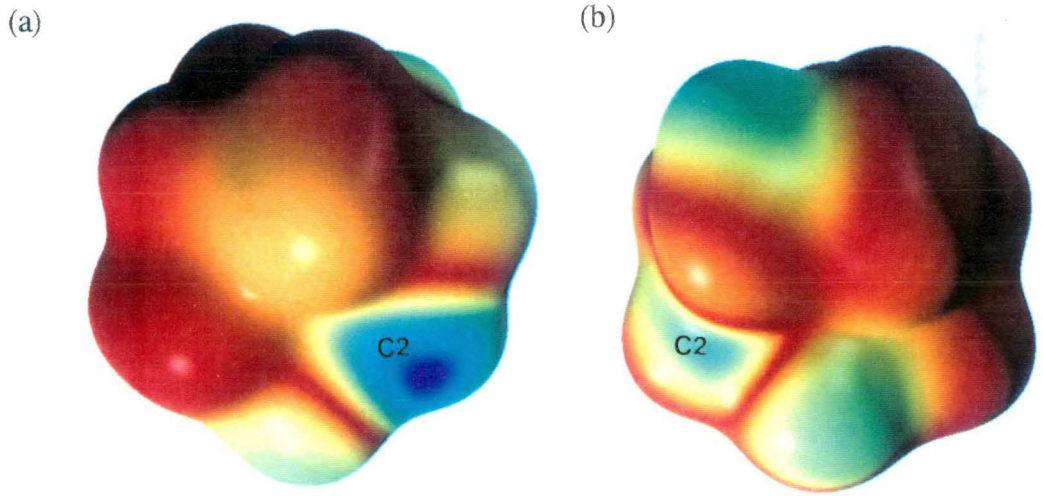

Figure 7.45. (a) LUMO of **233** mapped onto the electron density surface showing an area of high correlation (blue/purple) and (b) opposite face showing lower correlation.

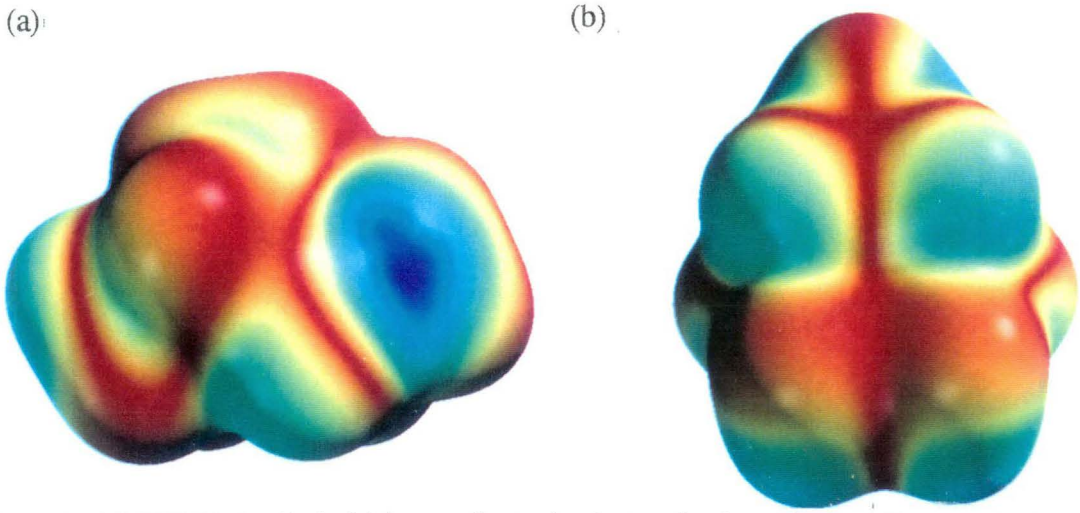

Figure 7.46. HOMO-1 orbital of **46** mapped onto the electron density surface. (a) Corner and (b) edge views of the C2-C4 bond.

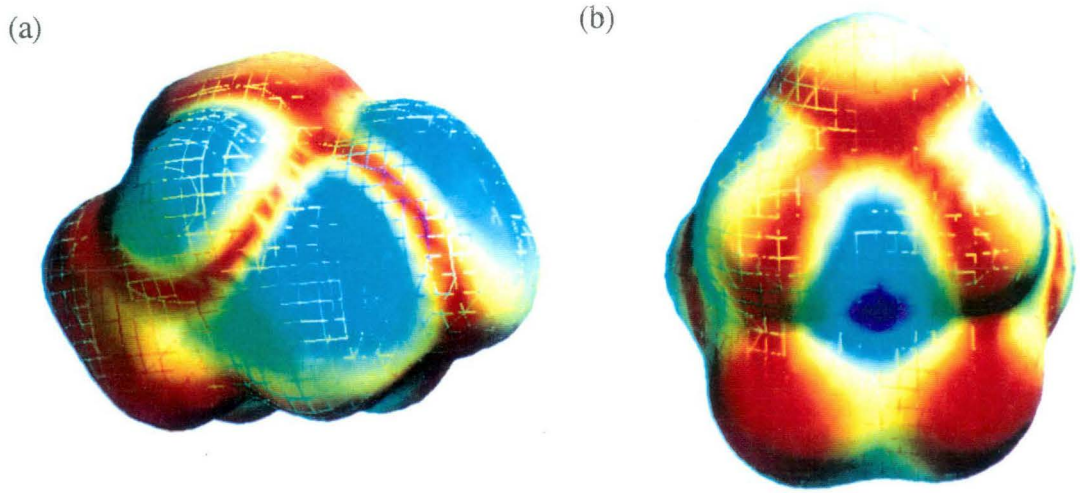

Figure 7.47. Overlapping maps of the HOMO (transparent) and HOMO-1 (mesh) on the electron density surface showing (a) corner and (b) edge attack trajectories for addition to the C2-C4 bond of **46**.

Single point calculations† performed on transition states **251** and **247** using ab initio methods (3-21G(*) basis set) showed **251** to be 59.5 kJ mol^{-1} higher in energy than **247**. Although this energy difference does not necessarily reflect the energies of the optimised ab initio structures (if both are stationary points on the ab initio PE surface) such a large difference in energy may indicate that ab initio calculations would find the corner TS to be more stable than the edge, in agreement with the experimental results.[13,14,18] Also of note is that the PM3 edge TS **207**, for addition of $MeOH_2^+$ to cyclopropane, did not appear to be a stationary point on ab initio PE surface (3-21G(*) basis set optimisation).

The experimental results[13,14] for the acid catalysed ring opening of **46** showed some cleavage of the C2-C3 (C3-C4) bond to also occur. Preliminary results of PM3 calculations to model edge addition to the C2-C3 bond indicate the TS **256** (ΔH_f = 726.9 kJ mol^{-1}, Figure 7.48) to be similar in energy to transition states **247** and **251** (ΔH_f = 725.4 kJ mol^{-1}, ΔH_f = 723.1 kJ mol^{-1}, respectively) and hence some addition from this trajectory would be expected. Attempted conformational searches of **256** led to the collapse of the structure to TS **247**, indicating a flat PE energy surface for the interconversion of the two transition states and possibly that the two may interconvert by rotation of the methanol group.

Attempts to locate a TS for corner addition of $MeOH_2^+$ to the C2-C3 (C4-C3) bond of **46** have so far been unsuccessful as an approximate TS structure, obtained from building the hydrocarbon framework around the edge TS for $MeOH_2^+$ addition to cyclopropane **207**, invariably collapsed to the TS for corner attack on the C2-C4 bond **247**.

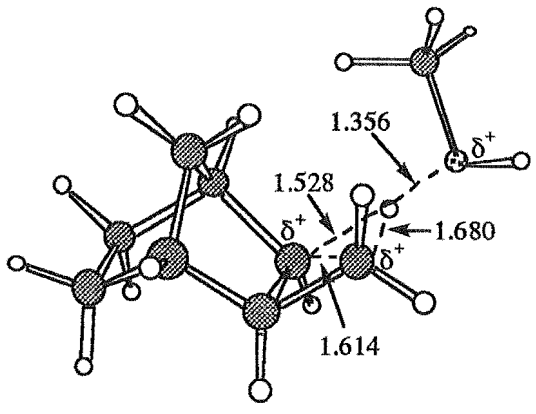

256

ΔHf = 726.9 kJ mol^{-1}

Figure 7.48. TS for edge attack of $MeOH_2^+$ on the C2-C3 bond of **46**. Distances are in Angstroms.

† At present the computational facilities required to optimise the structures with ab initio methods using large basis sets are not available.

CHAPTER 8

Regioselectivity of Electrophilic Addition in Tricyclo[3.2.1.$0^{2,4}$]oct-6-ene and Tricyclo[3.2.2.$0^{2,4}$]non-6-ene Systems

Section 8.1 INTRODUCTION

Whittington[32] has suggested that the major factor in determining the regioselectivity of electrophilic addition between a double bond and a cyclopropane ring is the stability of the cations formed. A number of studies[32] have examined the regioselectivity of electrophilic addition to *endo*- and *exo*-tricyclo[3.2.1.$0^{2,4}$]oct-6-ene (**68** and **69**, respectively) and concluded that bromination occurs exclusively at the double bond (Figures 3.2 and 3.3) while proton and mercuric(II) addition takes place predominantly at the cyclopropane ring.[13,15] It was therefore of interest to use semiempirical MO methods to study the cations resulting from H^+ and Br^+ addition to **68** and **69** and also the cations resulting from addition of the above electrophiles to *exo*-tricyclo[3.2.2.$0^{2,4}$]non-6-ene **47**, as this system has also been studied experimentally (see Chapter 5).

Section 8.2 PROTON ADDITION TO *exo*- AND *endo*-TRICYCLO[3.2.1.$0^{2,4}$]-OCT-6-ENE.

The possible cations resulting from proton addition to **68** and **69** are shown in Figures 8.1 and 8.2, respectively.

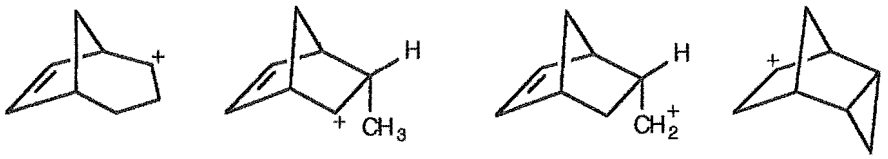

	257	**258**	**259**	**260**
ΔH_f(PM3) kJ mol^{-1}	936.8	1007.1	1047.8	1051.8

Figure 8.1. Possible cations resulting from proton addition to *endo*-tricyclo[3.2.1.$0^{2,4}$]oct-6-ene **68**.

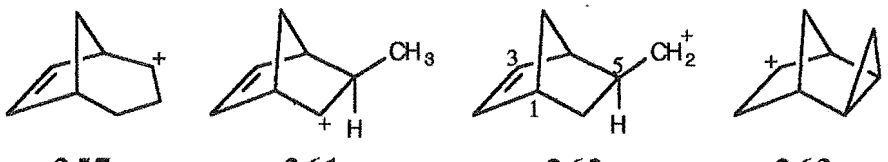

	257	**261**	**262**	**263**
ΔH_f(PM3) kJ mol^{-1}	936.8	1011.6	1169.9‡	1036.2

Figure 8.2. Possible cations resulting from proton addition to *exo*-tricyclo[3.2.1.$0^{2,4}$]oct-6-ene **69**.

‡ Estimated by fixing the C4-C5, C5-C6, and C1-C6 bond lengths. Complete optimisation using PM3 led to the break up of the carbon skeleton.

For **68**, the cations resulting from cleavage of the cyclopropane ring **257-259** were calculated by the PM3 semiempirical MO method to be more stable than the cation resulting from proton addition to the double bond **260**. Cation **257**, which results from rupture of the C2-C4 bond of **68**, was found to be the most stable of the four cations. This is in general agreement with the experimental results[13,15] which show proton addition to occur exclusively with cleavage of the C2-C4 bond. Similarly, for **69** the lowest energy cation **257** results from rupture of the C2-C4, in preference to cleavage of one of the external cyclopropyl bonds (C2-C3 or C3-C4), which would form cations **261** or **262**, or from addition to the double bond to give **263**. The dominant reaction pathway found by experiment was that of H^+/D^+ addition to the C2-C4 bond of **69**; however, in this case a significant amount (18%) of addition occurred to the alkene moiety. Of note, is that the PM3 method predicts the classical cation **257** to result from rupture of the C2-C4 bond of both **68** and **69**.

The PM3 calculations show agreement with the conclusions of Whittington[32] and Wiberg,[17,20,21] that carbocation stability may be important in determining the regiochemistry of proton addition.

Section 8.3 STABILITY OF THE CATIONS RESULTING FROM BROMINE ADDITION TO *exo*- AND *endo*-TRICYCLO[3.2.1.$0^{2,4}$]OCT-6-ENE

The possible classical cations resulting from Br^+ addition to the double bond or cyclopropane ring of **68** and **69** are shown in Figures 8.3 and 8.4, respectively.

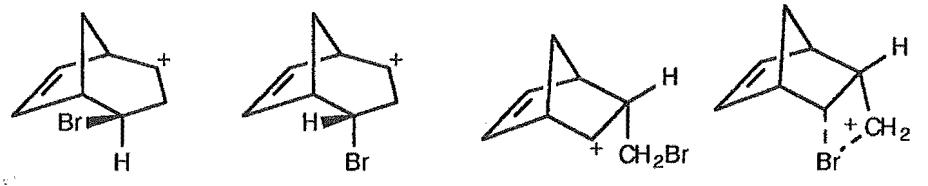

	264	**265**	**266**	**267**
ΔH_f(PM3) kJ mol^{-1}	974.5	973.6	1055.8	1045.3

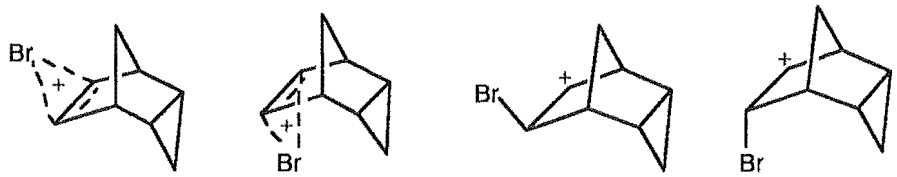

	270	**271**	**274**	**275**
ΔH_f(PM3) kJ mol^{-1}	1126.9 (ts)	1198.5 (ts)	1105.1 (m)	1121.4 (m)

Figure 8.3. Possible cations resulting from Br^+ addition to *endo*-tricyclo[3.2.1.$0^{2,4}$]oct-6-ene **68**. The type of stationary point of **270**, **271**, **274**, and **275** predicted by PM3 is shown in brackets (ts = transition state, m = minima).

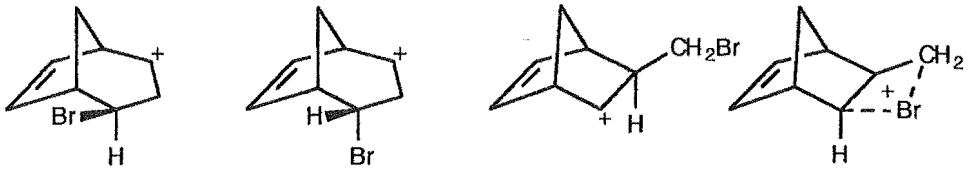

	264	265	268	269
ΔH_f(PM3) kJ mol^{-1}	974.5	973.6	1061.4	1040.8

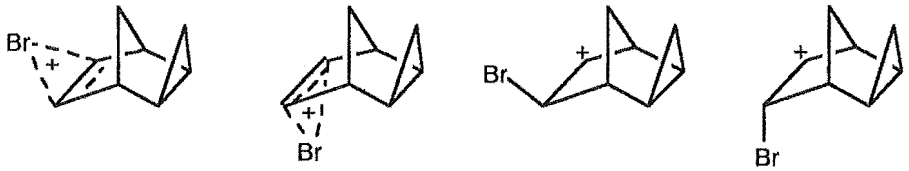

	272	273	276	277
ΔH_f(PM3) kJ mol^{-1}	1113.1 (ts)	1115.1 (ts)	1090.3 (m)	1095.3 (m)

Figure 8.4. Possible cations resulting from Br^+ addition to *exo*-tricyclo[3.2.1.$0^{2,4}$]oct-6-ene **69**. The type of stationary point of **272**, **273**, **276**, and **277** predicted by PM3 is shown in brackets (ts = transition state, m = minima).

In both cases the cations resulting from cleavage of the C2-C4 bond, **264** and **265**, are calculated to give the most stable carbocations, with the cation **265**, resulting from edge addition to **69** or corner attack to **68**, being slightly lower in energy than **264**. The other possible cations **266-269** resulting from cleavage of the C2-C3 (C3-C4) external cyclopropyl bond were also calculated to be of lower energy than the nonclassical **270-273** or classical **274-277** cations resulting from bromine addition to the double bond of **68** or **69**. The primary cations **278** and **279** (Figure 8.5) could not be located as optimisation of these structures using PM3 led to collapse of the initial structure (derived from molecular mechanics) to the bromine bridged intermediates **267** and **269**, respectively.

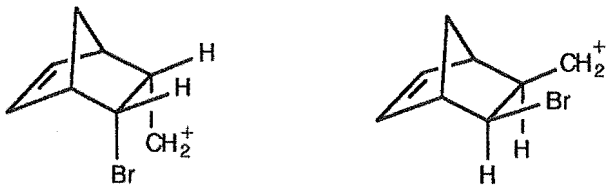

278 **279**

Figure 8.5. Primary cations **278** and **279** resulting from Br^+ addition to **68** and **69**, respectively, with cleavage of the C2-C3 (C3-C4) external cyclopropyl bond.

Of note is that PM3 predicts the nonclassical cations **270-273** to be transition states for the interconversion of the classical cations **274-277**, respectively, and their mirror images. It was therefore possible that the PM3 method underestimates the stability gained

from formation of a nonclassical bromonium ion. To determine whether the stability gained from formation of a bromonium ion may significantly lower the energy of the cations arising from Br^+ addition to the double bond of **68** and **69**, the classical **274-277** and nonclassical **270-273** cations were reoptimised using the AM1 and MNDO semiempirical methods which are known to give reasonable agreement with ab initio estimates of the stability gained from bromonium ion formation.[217-219,‡] The PM3, AM1, and MNDO energies of cations **270-277** are shown in Table 8.1. In each case the classical cation was found to be lower in energy than the corresponding nonclassical structure (Table 8.1). However, for nonclassical structures **270**, **272**, and **273** AM1 and MNDO classify the cations as minima, whereas PM3 characterised the structures as transition states. All three methods (PM3, AM1, and MNDO) characterise cation **271** as a transition state for the interconversion of classical cation **275** with its mirror image structure. It therefore appears that the PE surface for the interconversion of classical and nonclassical cations of this type, shows a double minima with the classical cation lower in energy than the corresponding bromonium ions. This contrasts with the results obtained for ethene and various substituted ethenes where no 'double minima' PE surfaces[217] or only a shallow minima corresponding to an open $C_2H_4Br^+$ cation were observed.[219]

The transition states which interconvert nonclassical cations **270**, **272**, and **273** with their respective classical cation isomers **274**, **276**, and **277** were located from AM1 optimisation, by a gradient norm minimisation procedure, of approximate transition states derived from linear synchronous TS approximation procedures.[†] The AM1 energies and relevant distances of the transition states **271**, **278-280**, and the corresponding cation intermediates are summarised in Table 8.2. From Table 8.2 it can be seen that as the Br-C7-C1 bond angle of the nonclassical cations **270-273** increases the activation energy (E_a) and the difference in energy between the classical and nonclassical structures (shown in brackets in Table 8.2) also increases. The equivalent angle in the ethene bromonium ion **281** (Figure 8.6) is 110.7° and thus as the deviation from this value increases (ΔA_1, Table 8.2) the difference in energy between the classical and nonclassical species also increases and hence the stabilisation of the nonclassical species decreases. An extreme of this situation is cation **271** where the deviation from the most favourable value of 110.7°, which is free from any steric effects, is 16.6° and the structure is classified as a TS. Thus once the Br-C7-C1 angle is only 16.6° from that of the ethene bromonium ion, no stabilisation is gained from formation of a bridged nonclassical cation. This presumably reflects the greater stabilisation and better orbital interaction gained when the electrophile may approach the double bond perpendicular to the plane of the double bond

---

‡ Also see references 220-222 for related calculations.

† Available in the program SPARTAN Ver. 2.01.

and its attached hydrogens. For **68** and **69** steric effects presumably restrict the electrophile from approaching perpendicular to the horizontal plane of the double bond and hence less orbital interaction of the LUMO of the electrophile with the HOMO of the double bond results in less stabilisation (Figure 8.7).

	Nonclassical cation (NC) ΔH_f	Classical cation (C) ΔH_f	$\Delta(\Delta H_f)$ $(\Delta H_f(NC)-\Delta H_f(C))$
	270	**274**	
PM3	1126.9 (ts)	1105.1 (m)	21.8
AM1	1109.8 (m)	1104.1 (m)	5.7
MNDO	1131.8 (m)	1113.9 (m)	17.9
	271	**275**	
PM3	1198.5 (ts)	1121.4 (m)	77.1
AM1	1173.3 (ts)	1108.9 (m)	64.4
MNDO	1177.7 (ts)	1120.2 (m)	57.5
	272	**276**	
PM3	1113.1 (ts)	1090.3 (m)	22.8
AM1	1104.0 (m)	1095.8 (m)	8.2
MNDO	1122.3 (m)	1102.5 (m)	19.8
	273	**277**	
PM3	1115.1 (ts)	1095.3 (m)	19.8
AM1	1113.9 (m)	1095.8 (m)	18.1
MNDO	1128.9 (m)	1104.0 (m)	24.9

Table 8.1. Heats of formation of classical and nonclassical cations resulting from Br^+ addition to the double bond of **68** and **69** as calculated by the PM3, AM1, and MNDO semiempirical MO methods. Heats of formation are in kJ mol^{-1}. The type of stationary point of each structure is shown in brackets (ts = transition state, m= minima).

	Classical Cation	Transition State	Nonclassical Cation	General Structure	Nonclassical cation (continued) Br-C7-C1 angle	Br-C7-H7 angle	ΔA_1	ΔA_2	E_a
Compound	**274** (m)	**278** (ts)	**270** (m)	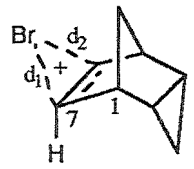	117.0	107.8	6.3	2.9	6.7 (5.7)
ΔH_f	1104.1	1110.8	1109.8						
d_1	1.937	1.995	2.115						
d_2	2.777	2.340	2.113						
Compound	**276** (m)	**279** (ts)	**272** (m)	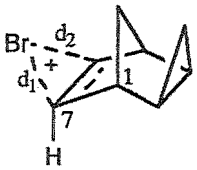	117.5	108.0	6.8	2.7	9.1 (8.2)
ΔH_f	1095.8	1104.9	1104.0						
d_1	1.930	2.000	2.115						
d_2	2.802	2.318	2.111						
Compound	**277** (m)	**280** (ts)	**273** (m)	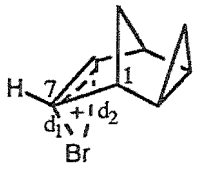	119.8	107.1	9.1	3.6	20.0 (18.1)
ΔH_f	1095.8	1115.8	1113.9						
d_1	1.916	1.992	2.110						
d_2	2.866	2.338	2.110						
Compound	**275** (m)		**271** (ts)	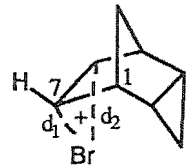	127.3	104.1	16.6	6.6	64.4
ΔH_f	1108.9	-------	1173.3						
d_1	1.911		2.106						
d_2	2.915		2.106						

Table 8.2. Summary of the AM1 results for the possible cations resulting from bromination of the double bond of **68** and **69**. ΔA_1 and ΔA_2 are the deviations of the calculated Br-C7-C1 and Br-C7-H7 angles from the 110.7° angle observed in the ethene bromonium ion **281**. $E_a = \Delta H_f$(Transition state) - ΔH_f(Classical cation). Heats of formation are in kJ mol^{-1}. Numbers in brackets in the E_a column are the difference in heat of formation between the nonclassical and classical cations (ΔH_f(Nonclassical) - ΔH_f(Classical)). Other abbreviations: ts = transition state, m = minima.

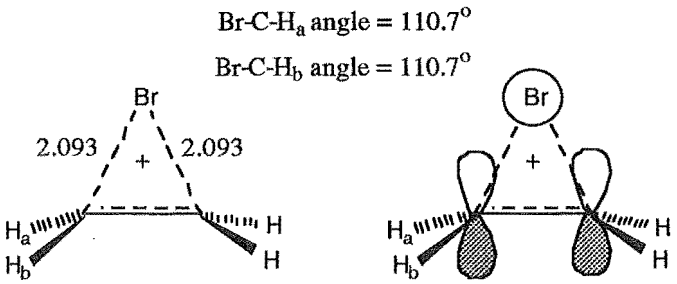

281

Figure 8.6. AM1 calculated bromonium ion **281** formed from Br^+ addition to ethene.

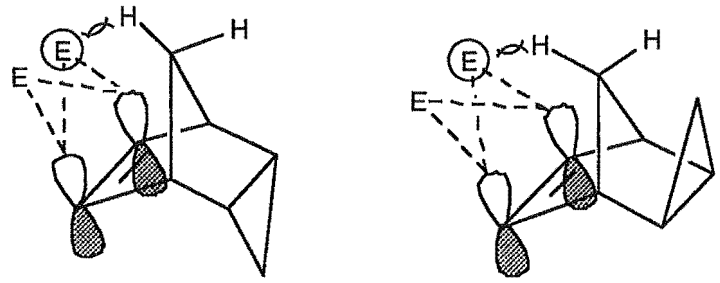

68 **69**

Figure 8.7. Interaction of an attacking electrophile with the double bond of **68** and **69**. The circled "E" would show greater orbital interaction but, due to steric effects, this trajectory is less favourable.

For **68** the semiempirical calculations show *exo* addition of Br^+ to the double bond to result in formation of the most stable carbocation, whether classical or nonclassical, in general agreement with the experimental results[32] which found exclusive *exo* addition to take place. The preference for *exo* addition can be rationalised from consideration of the contour map calculated from mapping the HOMO of **68** onto the electron density surface (Figures 8.8a and b) of the ab initio optimised structures (3-21G(*) basis set). In this case, an area of high correlation (blue/purple) can be seen for *exo* ('top face') addition (Figure 8.8a), whereas a lower correlation is shown for *endo* ('bottom face') addition (Figure 8.8b). Presumably the effects of the orbital distribution and accessibility, combined with steric effects[42] are responsible for exclusive *exo* addition being observed experimentally[32] (Figure 3.2).

For **69**, the HOMO/electron density map‡ shows that some preference for *exo* electrophilic addition (Figure 8.9a) over *endo* addition (Figure 8.9b) would be expected, although this is not as pronounced as in the case of **68**. The cations resulting from *exo* and *endo* addition to the double bond of **69** are predicted to be similar in energy by all three semiempirical methods (PM3, AM1, and MNDO, Tables 8.1 and 8.2). It therefore

‡ Figures 8.9a and b show the surfaces obtained for **69** from ab initio results (3-21(*) basis set).

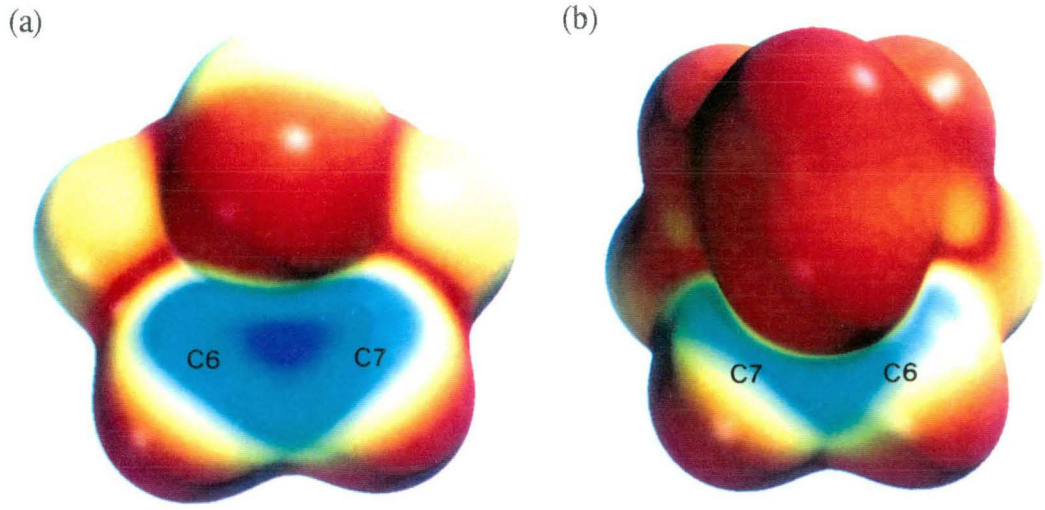

Figure 8.8. HOMO mapped onto the electron density surface of **68** (a) 'top' and (b) 'bottom' face of the double bond.

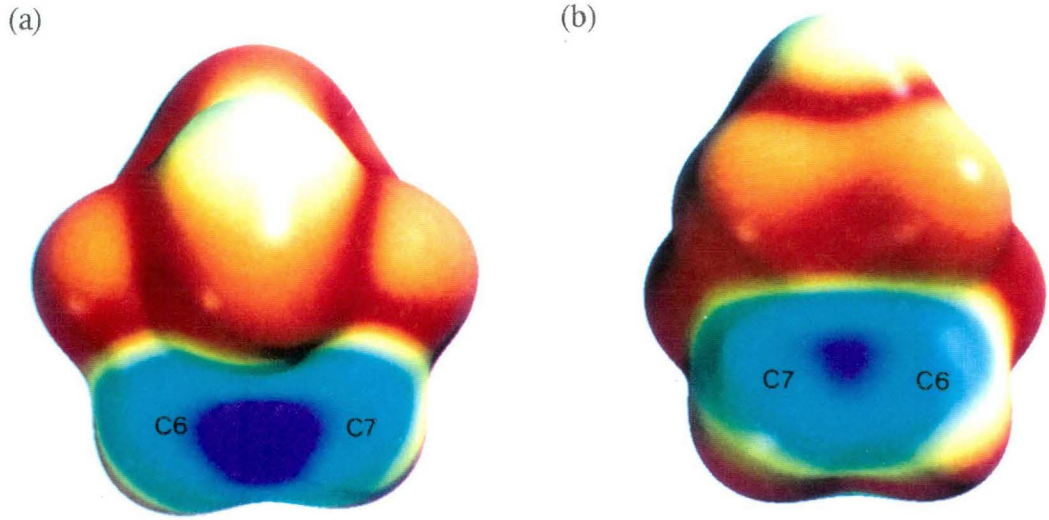

Figure 8.9. HOMO mapped onto the electron density surface of **69** (a) 'top' and (b) 'bottom' face of the double bond.

appears that the calculations are either in error or that the effects governing the trajectory of electrophilic addition present in the TS are absent in the resulting carbocations, as experimentally only *exo* addition is observed.[32] Since orbital effects appear to show little preference for *exo* or *endo* addition it seems likely that steric effects[42] may play an important role in determining the reaction trajectory (Figure 3.3).

From the results of the semiempirical calculations it appears that the regioselectivity of bromine addition to either the cyclopropane ring or double bond of **68** or **69** is not dependent on cation stability (assuming open carbocations are formed), as addition to the cyclopropane ring is calculated to result in formation of a more stable carbocation, and experimentally exclusive addition to the double bond was observed. This therefore suggests that either the calculations are in error or that other factors, such as polarisability of the bond undergoing attack,[17,20,21] may also be important in determining the regiochemistry of electrophilic addition.

Section 8.4 CARBOCATIONS RESULTING FROM PROTON ADDITION TO *exo*-TRICYCLO[3.2.2.0^{2,4}]NON-6-ENE

The possible cations resulting from addition of H^+ to the cyclopropane ring **282**-**284** and double bond **285** of *exo*-tricyclo[3.2.2.0^{2,4}]non-6-ene **47** are shown in Figure 8.10.

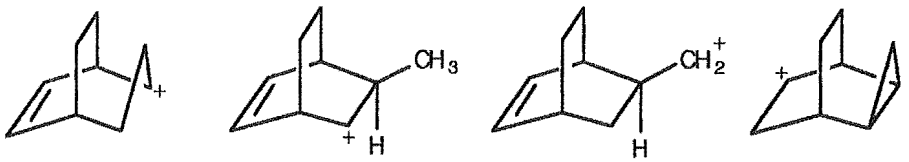

	282	**283**	**284**	**285**
ΔH_f(PM3) kJ mol^{-1}	897.0	907.5	962.6	951.8

Figure 8.10. Possible cations resulting from proton addition to *exo*-tricyclo[3.2.2.0^{2,4}]non-6-ene **47**.

As for **68** and **69**, the most stable carbocation **282** resulted from proton addition to the cyclopropane ring with rupture of the C2-C4 bond. This is in general agreement with the experimental results where the major product (71%), from reaction of **47** with a catalytic amount of PTSA in methanol, was formed from cleavage of the most substituted (C2-C4) cyclopropyl group.‡

‡ Not all the products were identified, as only 70-75% of the products were isolated.

Section 8.5 RELATIVE ENERGIES OF THE CATIONS RESULTING FROM BROMINE ADDITION TO *exo*-TRICYCLO[3.2.2.$0^{2,4}$]NON-6-ENE

Cations **125**, **142**, **286**, and **287** (Figure 8.11) may result from Br^+ addition to the cyclopropane ring of **47**. The cations **118**, **119**, **122**, and **123** resulting from Br^+ addition to the double bond of **47** are also shown (Figure 8.11). Optimisation of cation **288** (Figure 8.12) invariably led to collapse of the initial open primary cation to the bridged structure **287**. The relative stabilities of the cations shown in Figure 8.11 shows a similar trend to that observed for the $C_8H_{10}Br^+$ cations (Figures 8.3 and 8.4) where the lowest energy cations result from bromination of the cyclopropane ring with cleavage of the C2-C4 bond of **47**. Cation **142**, formed from edge addition, was found to be approximately 5 kJ mol^{-1} lower in energy than cation **125** which results from corner attack of Br^+ at the C2-C4 bond.

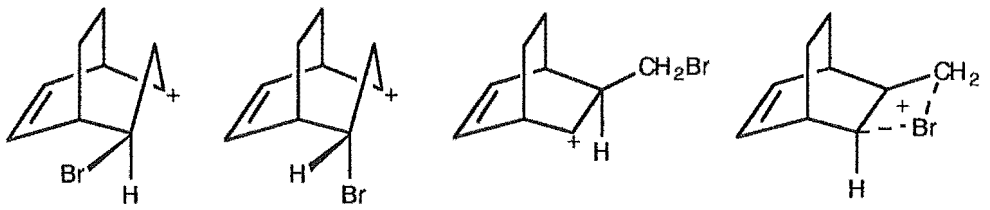

	125	**142**	**286**	**287**
ΔH_f(PM3) kJ mol^{-1}	937.2	931.9	949.2	951.6

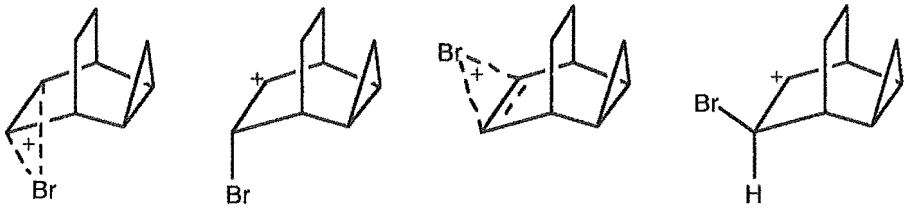

	118	**119**	**122**	**123**
ΔH_f(PM3) kJ mol^{-1}	1018.0	1006.0	1025.7	1007.3

Figure 8.11. Possible cations resulting from Br^+ addition to *exo*-tricyclo[3.2.2.$0^{2,4}$]non-6-ene **47**.

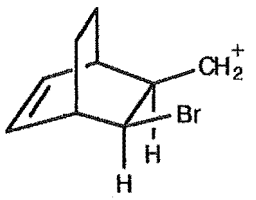

288

Figure 8.12. Possible primary cation resulting from Br^+ addition to the C2-C3 (C3-C4) bond of *exo*-tricyclo[3.2.2.$0^{2,4}$]non-6-ene **47**.

The nonclassical cations **118** and **122** were calculated by PM3 to be transition structures and were higher in energy than the corresponding classical cations **119** and **123**, respectively. The energies of cations **119** and **123**, which result from *endo* and *exo* addition of Br^+ to the double bond, respectively, are similar in energy (ΔH_f(**123**) - ΔH_f(**119**) = 1.3 kJ mol^{-1}). This is in accordance with the experimental results (see Chapter 5) which suggest, although not conclusively, that bromine addition takes place from both *exo* and *endo* modes of addition.

For **47** the HOMO/electron density map (Figure 8.13) shows little preference for *exo* (Figure 8.13a) or *endo* (Figure 8.13b) addition. The difference in steric effects incurred on *exo* or *endo* addition in the tricyclo[3.2.1.$0^{2,4}$]oct-6-ene and norbornene[42] systems, such as the difference in 1,5 interactions of the incoming electrophile with hydrogens H6*endo* or H7*syn* of norbornene (Figure 8.14a), are not present in the tricyclo[3.2.2.$0^{2,4}$]non-6-ene system (Figure 8.14b). Electrophilic addition from both faces of the double bond may therefore be expected.

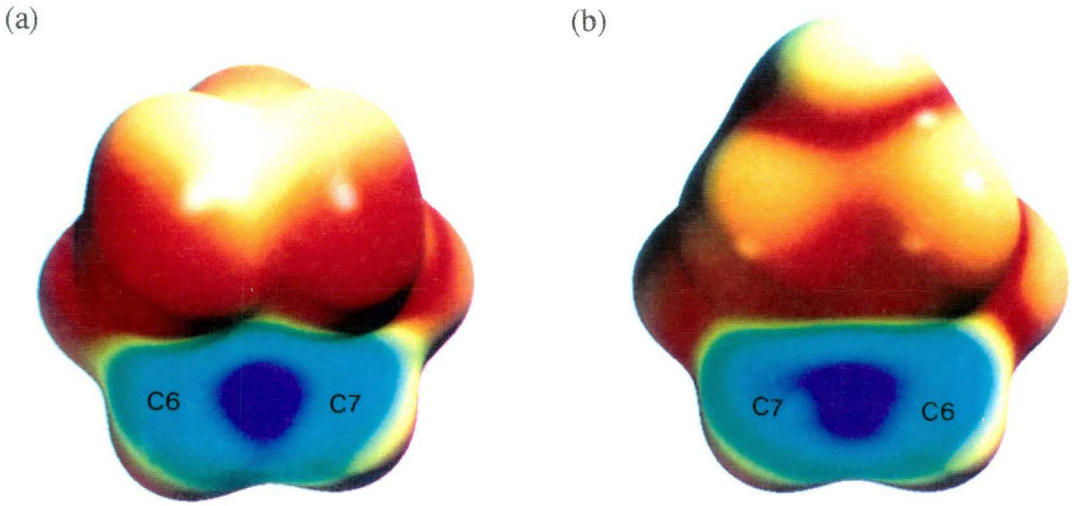

Figure 8.13. HOMO mapped onto the electron density surface of *exo*-tricyclo[3.2.2.$0^{2,4}$]non-6-ene **47**. (a) 'Top' face and (b) 'bottom' face of the alkene group.

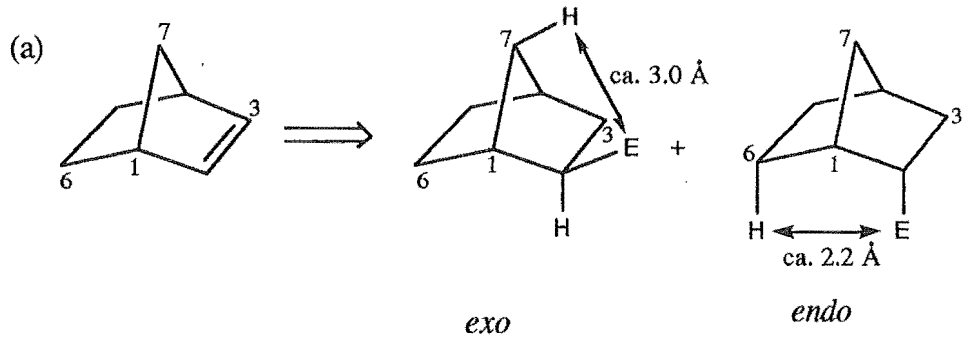

The *exo* addition pathway shows less steric interferance and hence is favoured.

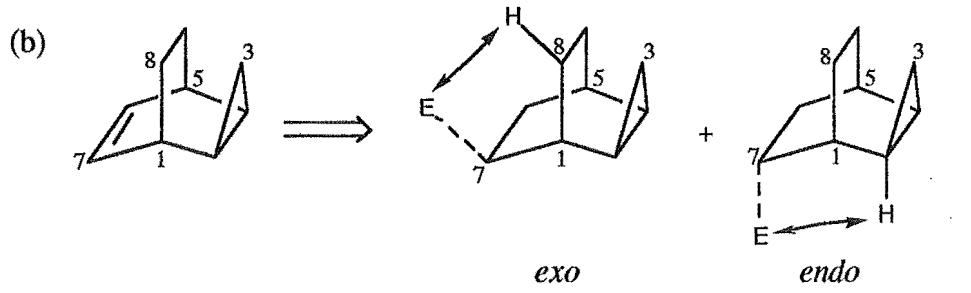

The indicated distances would be expected to be similar and hence neither *exo* or *endo* addition would be sterically disfavoured with respect to the other.

Figure 8.14. Diagram showing the 1,5 interactions incurred by an attacking electrophile on (a) norbornene and (b) *exo*-tricyclo[3.2.2.$0^{2,4}$]non-6-ene **47**. In Figure (a) the increased distance of the incoming electrophile from the methylene bridge H7*syn* proton than from H6*endo* in norbornene makes *exo* addition more favourable. For **47**, Figure (b), the distances of an incoming electrophile from H2 or H8*anti* would be expected to be similar for *endo* and *exo* addition, respectively.

Modelling of some of the rearrangement reactions shown in Figures 5.7, 5.10, and 5.11 indicates that the rearrangement of **119** to **120** (path (a) Figure 8.15) proceeds with a lower activation barrier than the rearrangement to **138** (path b Figure 8.15) (E_a = 46.8 kJ mol^{-1} and 51.4 kJ mol^{-1}, respectively). The transition states **289** (ΔH_f = 1052.8 kJ mol^{-1}) and **290** (ΔH_f = 1057.4 kJ mol^{-1}) for the two rearrangement processes are also shown (Figure 8.15). Of particular note is that only products resulting from nucleophilic capture of **120** from an *endo* trajectory (with respect to the main bridge) were isolated experimentally. Consideration of the accessibility of the LUMO orbital (Figures 8.16a and b) and from the contour map obtained when the LUMO is mapped onto the electron

density surface of **120** (Figures 8.17a and b) indicates that the 'bottom face' (*endo* to the main bridge, Figures 8.16a and 8.17a) of the cationic carbon C5 is more accessible to nucleophilic capture than the 'top face' (*exo* to the main bridge, Figures 8.16b and 8.17b). This is clearly shown in Figure 8.17a which shows a blue/purple area corresponding to a high correlation of the LUMO and electron density surface for 'bottom face' attack. No area of high correlation for 'top face' attack (Figure 8.17b) is observed. Therefore 'bottom face' addition would be expected to be the dominant trajectory for nucleophilic attack, resulting in formation of **113** or **127** for Br^- and MeOH nucleophiles, respectively.

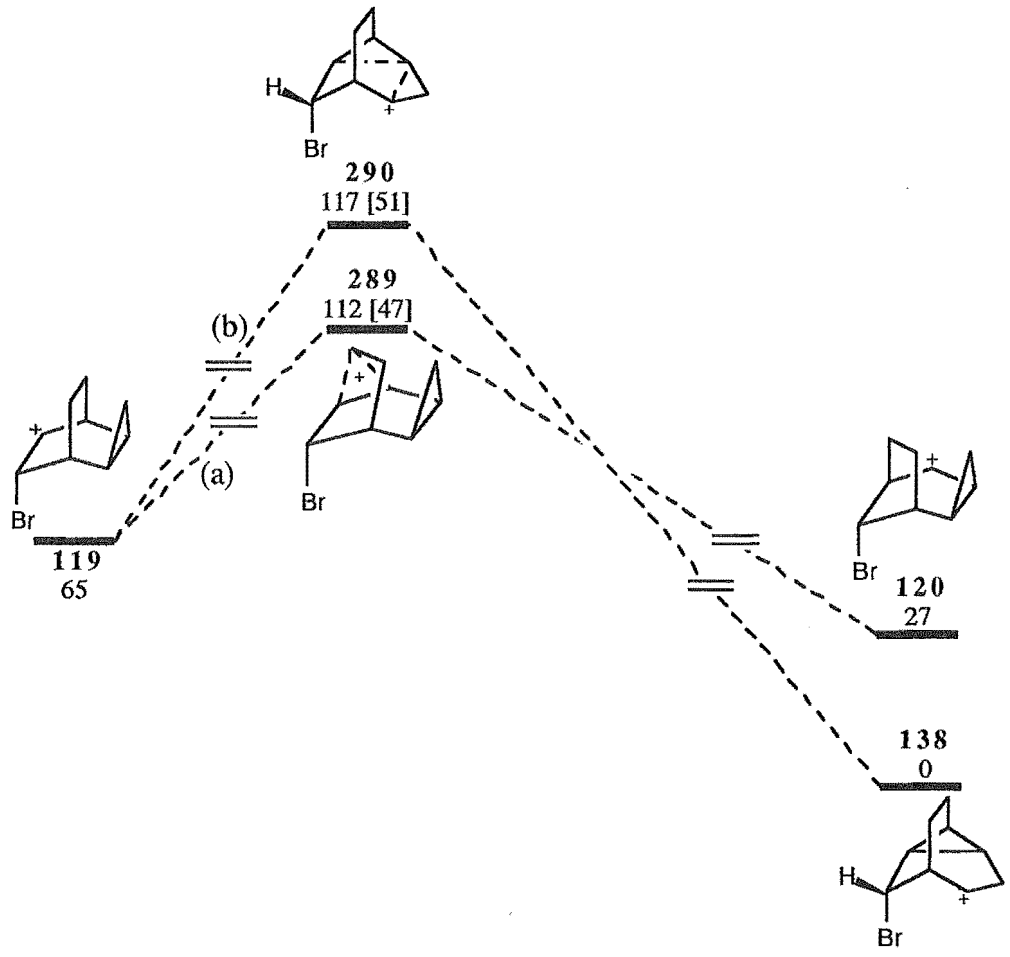

Figure 8.15. PM3 energies, relative to cation **138**, for the rearrangement of cation **119**. Activation barriers (E_a) to transition states **289** and **290** are shown in square brackets. Energies are in kJ mol^{-1}.

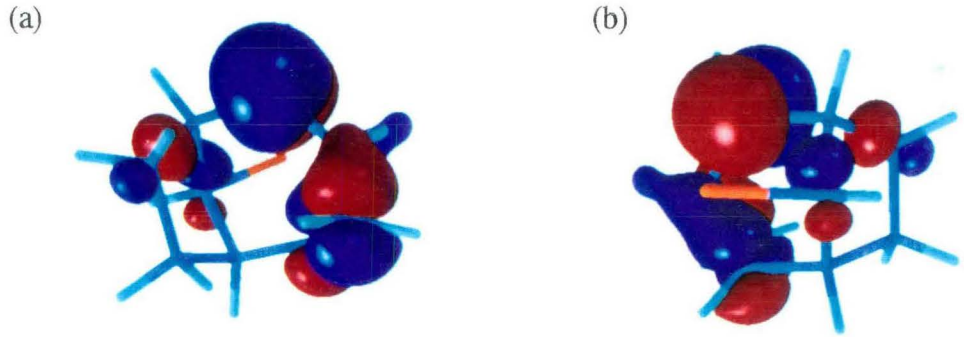

Figure 8.16. LUMO of **120** shown from the (a) 'bottom' and (b) 'top' face of the cation.

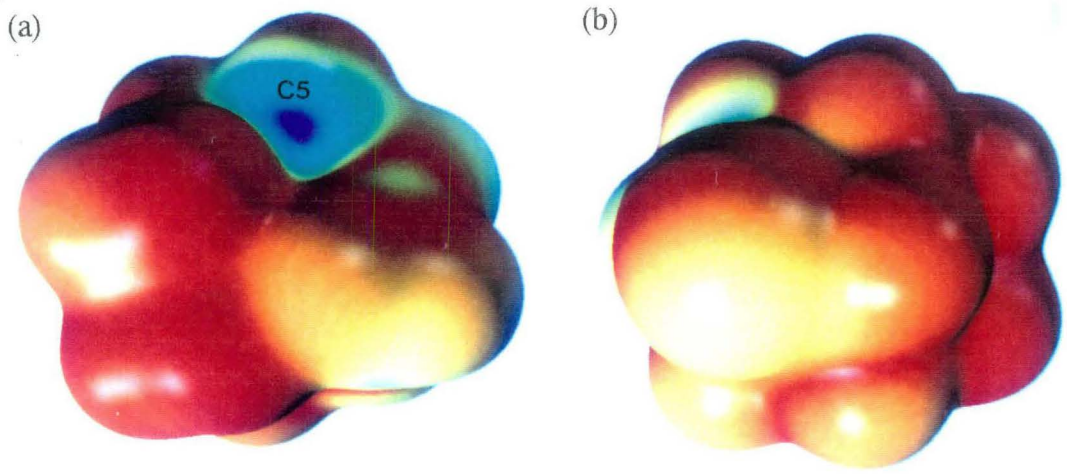

Figure 8.17. LUMO of **120** mapped onto the electron density surface shown from the (a) 'bottom' and (b) 'top' face of the cation.

For cation **123** modelling of the corresponding rearrangement processes to those of cation **119** (Figure 8.15) showed a similar trend. Rearrangement of **123** to the tricyclo[4.2.1.$0^{2,4}$]nonane cation **291** (path (a) Figure 8.18) via TS **292** was calculated to be lower in energy by PM3 than rearrangement to the tricyclo[3.3.1.$0^{2,8}$]nonane structure **124** (path (b) Figure 8.18) via TS **293** (E_a = 38.0 kJ mol^{-1} and 61.3 kJ mol^{-1}, respectively). The relative energies for the rearrangement processes are shown in Figure 8.18.

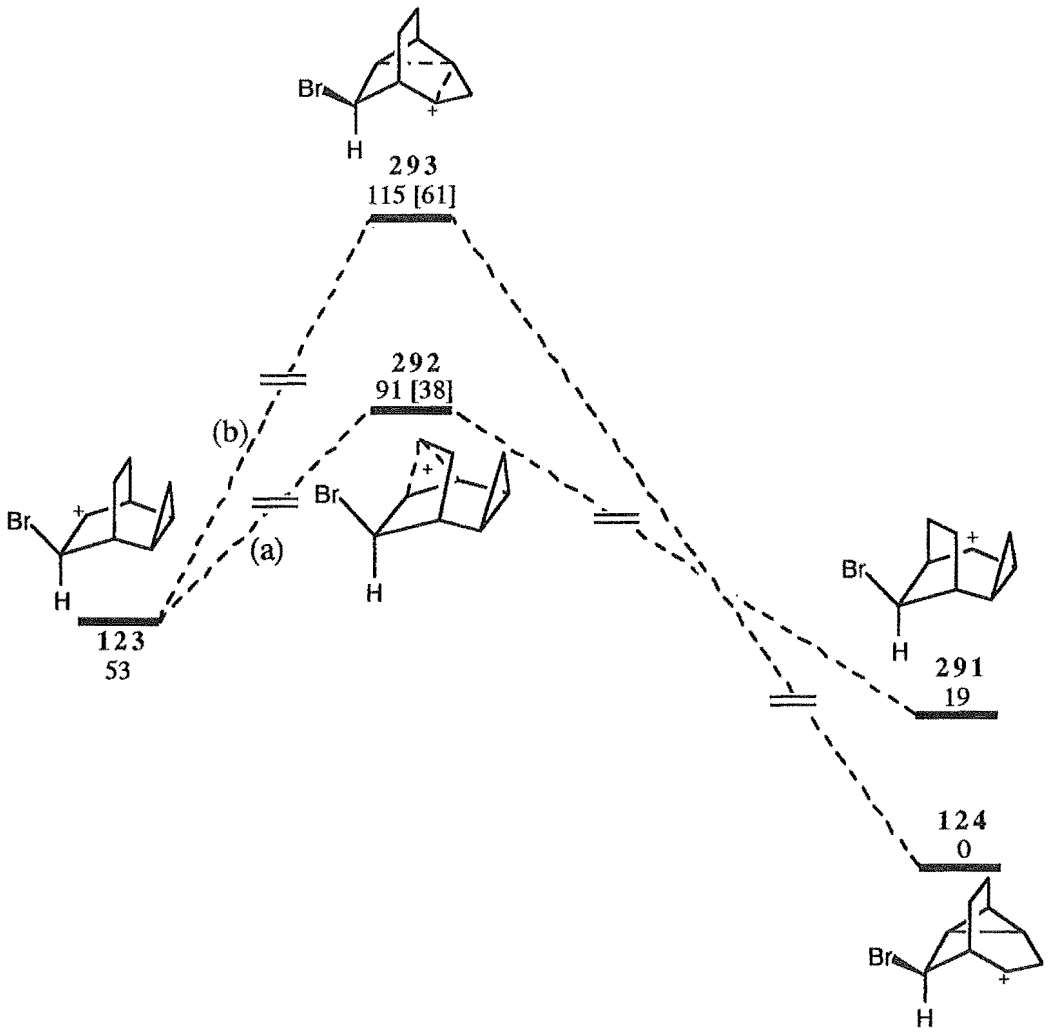

Figure 8.18. PM3 energies, relative to cation **124**, for the rearrangements of cation **123**. Activation barriers (E_a) to transition states **292** and **293** are shown in square brackets. Energies are in kJ mol^{-1}.

The rearrangement of cation **125** to **126** via TS **294** (ΔH_f = 943.5 kJ mol^{-1}) is calculated by PM3 to require only a small activation energy (E_a = 6.3 kJ mol^{-1}, Figure 8.19). From analysis of the PM3 results it would therefore appear that if cation **123** was formed, then products resulting from nucleophilic capture of cation **291** should have been observed if formation of cation **124** occurred (leading to product **114**), as rearrangement to **291** was calculated to be more facile than rearrangement to **124**. Since no products resulting nucleophilic capture of **291** were isolated, the PM3 results suggest that **114** is not formed via cation **124**, as shown in Figure 5.7, and hence may indicate that formation of **114** (or **130** and **131**) occurs from initial Br^+ addition to the cyclopropane ring of **47** to give **125**. Cation **125** may then rearrange to **126** which undergoes nucleophilic capture to give **114** (or **130** and **131**). The small barrier to rearrangement of **125** to **126** would indicate a facile rearrangement to take place. The *endo* orientation of the C4 bromine substituent of **114** is consistent with corner addition

of Br^+ to the cyclopropane ring of **47**, as was observed for **1** and **46**. The absence of any *exo* incorporation of the C4 bromine substituent in the tricyclo[3.3.1.$0^{2,8}$]nonane products isolated (**114**, **130**, **131**), as may have been expected if **124** were formed since nucleophilic attack may be expected to occur from both faces of the cation, is also consistent with initial attack of Br^+ at the cyclopropane ring leading to the formation of these products.‡ However, the mechanism of formation of the tricyclo[3.3.1.$0^{2,8}$]nonane products remains unclear due to the instability of the primary products formed on bromination of **47** in methanol (see Section 5.4.2).

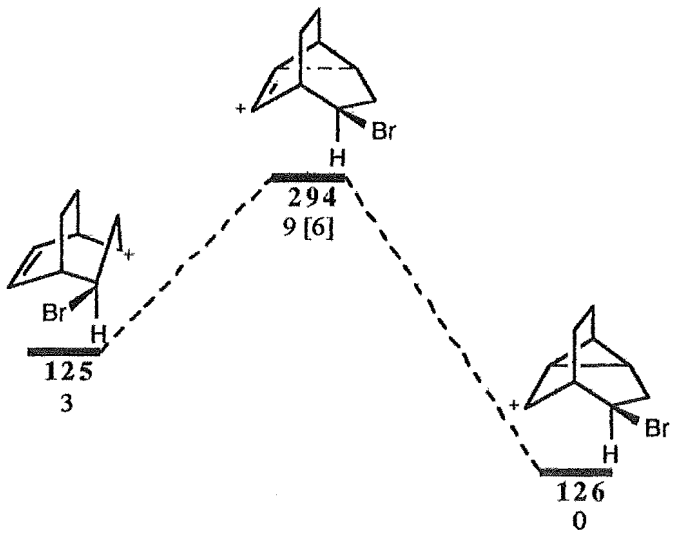

Figure 8.19. PM3 energies, relative to cation **126**, for the rearrangement of cation **125**. The activation barrier (E_a) to the formation of transition state **294** is shown in square brackets. Energies are in kJ mol^{-1}.

‡ The results of semiempirical calculations (not presented here) indicate nucleophilic attack on cation **124** to be preferred from an *exo* orientation and hence **114** would not be the major product expected.

CONCLUSION

The products obtained from bromination of *endo*- and *exo*-tricyclo[3.2.1.$0^{2,4}$]-octane (**1** and **46**, respectively) and 2-methyl-*endo*-tricyclo[3.2.1.$0^{2,4}$]octane **45** indicate that electrophilic addition of bromine occurs via corner attack at the C2-C4 bond of the cyclopropane ring in each case. The preference for corner attack of Br^+ at the C2-C4 bond of **1**, **45**, and **46** is consistent with the results of Coxon et al.[13-16,18] which show H^+ and Hg^{2+} addition to also occur at the most substituted cyclopropyl bond and from this trajectory. Bromination of **1**, **45**, and **46** involves significant charge development in the intermediate cations when the reactions are performed in a polar solvent (MeOH), since significant proportions of rearrangement products were observed for **1** and **46** and nucleophilic capture of an intermediate cation formed in the bromination of **45** appeared to show little selectivity. This is consistent with the conclusion of Skell et al.[24] who have suggested the involvement of essentially classical carbocations in the bromination of simple cyclopropanes. In a nonpolar solvent (CCl_4) acid catalysed ring opening competed more effectively with bromination to the point where for **45** this was the dominant reaction pathway. When bromination of the cyclopropane ring did occur (**1** and **46**), the reaction appeared to be under kinetic and not thermodynamic control as less rearrangement was observed than when the reactions were performed in methanol.

In the case of 2-methyl-*endo*-tricyclo[3.2.1.$0^{2,4}$]oct-6-ene **86** no definitive conclusions can be made about the mechanism of bromine addition due to the complexity of the reaction. However, bromine addition to the double bond is significantly favoured over addition to the cyclopropane ring. Addition of bromine to an alkene moiety in preference to a cyclopropane ring was also observed by Whittington[32] for the bromination of *endo*- and *exo*-tricyclo[3.2.1.$0^{2,4}$]oct-6-ene (**68** and **69**, respectively).

The reaction of *exo*-tricyclo[3.2.2.$0^{2,4}$]non-6-ene **47** with H^+ showed a similar trend to the results obtained by Coxon et al.[13,15] for the reaction of **68** and **69** with H^+-MeOH, whereby, electrophilic addition occurred to the cyclopropane ring with rupture of the most substituted cyclopropyl bond (C2-C4). However, for **47** electrophilic attack took place from both edge and corner trajectories to similar extents, in contrast with **68** and **69** which underwent electrophilic addition exclusively from a corner attack trajectory.[13,15] Bromination of **47** appeared to occur predominantly at the alkene moiety, although the possibility of some addition occurring at the cyclopropane ring could not be ruled out by the present studies, due to the participation of facile side reactions which led to the solvolysis of the initially formed brominated adducts. Attempted reactions of TCNE with **47** and *endo*-tricyclo[3.2.2.$0^{2,4}$]non-6-ene **56** gave little or no product formation. Reaction of tricyclo[3.2.2.$0^{2,4}$]nona-6,8-diene **51** with TCNE gave no products resulting

from addition to the cyclopropane ring, but addition of TCNE to the 1,4-diene moiety in a homo-Diels-Alder reaction was observed.

The results of the semiempirical calculations for the $C_3H_7^+$ cations showed reasonable agreement of the calculated geometries with high level ab initio results; however, the PM3 method showed poor agreement with the ab initio results in characterisation of nonclassical cations. For example, PM3 predicts the corner protonated cation **201** to be a second order saddle point, in contrast with the high level ab initio calculations (MP2/6-311G**) which characterised the corresponding ab initio structure **180** as a minimum.

For the reaction of protonated methanol with cyclopropane, the semiempirical results indicate edge addition to be significantly more favourable than corner attack. This contrasts with the ab initio calculations (HF/3-21G(*) basis set) which favour the corner attack trajectory and predict the PM3 edge transition state **207** to either not have a corresponding stationary point on the HF/3-21G(*) PE surface, or that the barrier to interconversion of the corner and edge transition states is small. In this case high level ab initio calculations using larger basis sets are required to properly characterise the stationary points.

For protonated methanol addition to **1** the PM3 calculations show, in agreement with the experimental results,[13,18] electrophilic addition at the corner of the C2-C4 bond to be more favourable than edge attack. In the case of **46** the semiempirical results predicted the energies of corner and edge attack to be similar. This contrasts with the experimental results[13,14] which show corner addition to the C2-C4 bond to be the predominant reaction pathway. The effect of secondary orbital interactions of the electrophile LUMO with the HOMO-1 orbitals of **1** and **46** were shown to be important. This is in agreement with the conclusions of Wiberg et al.[17,20,21] who calculated that only 50% of the total electron density donated to an incoming proton, on addition to a cyclopropane ring, comes from the HOMO.

The semiempirical calculations show carbocation stability to be important in determining the regioselectivity of cyclopropane ring opening (which cyclopropyl bond is broken) and hence in determining the course of the reaction. For the selectivity of electrophilic addition between a double bond and a cyclopropane ring the calculations predict the cations resulting from H^+ or Br^+ addition to the cyclopropyl moiety of **47**, **68**, and **69** to be more stable than those formed from addition to the double bond. Experimental studies† have shown H^+ addition to occur to the cyclopropane ring and Br^+ addition to occur to the double bond. It therefore appears that the calculations are either in error or that, in the case of Br^+ addition, other factors, such as bond polarisability,

---

† See references 13-16,18, and Chapter 5 Sections 5.4 and 5.5 .

relative HOMO-LUMO energies, etc, may be important in determining the regioselectivity of electrophilic attack.

The results presented in this thesis illustrate the complexity of the factors which govern both the regio- and stereoselectivity of electrophilic addition to cyclopropyl groups. High level calculations are required to better elucidate the factors governing the selectivity of addition, particularly, as the semiempirical molecular orbital techniques may not give an accurate description of the reaction intermediates and transition states involved in the electrophilic addition processes.

Further experimental work is required to more fully elucidate the regiochemical preference of bromine addition to the double bond or cyclopropane ring of **47** and to isolate or synthesise the proposed intermediates (compounds **139** or **140**) so as to enable the study of their solvolysis reactions. In some cases, such as for the bromination of **45** in CCl_4, studies in the presence of an acid scavenger should be carried out to reduce the competition of acid catalysed ring opening with bromination.

The present work was undertaken in order to investigate aspects of the regio-chemistry and stereospecificity of cyclopropane ring opening. With the exception of **47**, which showed little preference (1.3:1.0) for H^+ addition from a corner or edge trajectory, the experimental results are consistent with corner addition of an electrophile to the most substituted cyclopropyl bond (C2-C4 bond) being the dominant mode of ring cleavage (**1**, **45**, and **46**) and hence are in accord with previous investigations.[13-16,18] The results of the theoretical calculations, although showing some deficiencies of the computational methods, provide a useful tool for the investigation of the mechanism of cyclopropane ring opening and the subsequent rearrangement processes.

EXPERIMENTAL

General

NMR spectra were recorded on Varian XL-300 or Varian Unity 300 spectrometers equipped with a 5 mm probe and operating at 300 MHz and 75 MHz for ^{1}H and ^{13}C, respectively. ^{2}H NMR spectra were acquired unlocked at 46 MHz and were proton coupled. Chemical shifts are reported in ppm relative to tetramethylsilane. Difference nOe spectra were obtained in arrayed experiments with the decoupler offset 10 000 Hz and then cycled with low power over the multiplet peaks of the desired proton for irradiation, a procedure based on that of Kinns and Sanders.[224] Carbon detected heteronuclear proton-carbon correlated (HETCOR) spectra were recorded using a pulse sequence which ensures full ^{1}H-^{1}H decoupling.[225] All other experiments were recorded using standard pulse sequences and parameters available with the XL-300 or Unity 300 systems. Proton chemical shifts marked with a superscript asterisk were estimated from nOe or two dimensional NMR experiments (COSY, DQCOSY, HETCOR or HMQC experiments). Proton chemical shifts marked with a superscript hash mark ($^{\#}$) were determined from 1D- or 2D-TOCSY experiments.

Infrared spectra were recorded on a Perkin-Elmer 1600 Series FT-IR spectrometer. Mass spectra were recorded on a Kratos MS80RFA spectrometer using EI. Volatile samples (typically the products obtained from bromination or methanol addition to compounds **1**, **45**, **46**, **47**, and **86**) were run by GCMS using the Kratos MS80RFA spectrometer directly coupled to a Carlo Erba 500 Series GLC fitted with a Restex $R_{tx}1$ 30 m x 0.32 mm capillary column. A programmed run was used for the GCMS (an initial temperature of 60 °C was held for 1 minute and then the column temperature increased at the rate of 20 °C per minute up to 260 °C) to ensure that the sample and all impurities passed through the column to the MS instrument. In some cases molecular ion peaks were not observed in the high resolution mass spectra (HRMS) but were identified in the low resolution spectra (LRMS), in these cases the LRMS and HRMS spectra are shown along with a number of fragment ion peaks which were observed.

A Hewlett Packard HP5890A GLC was used in both analytical and preparative modes with either a 1.5% OV-17, 1.25% QF-1 chromosorb W packed column of 5 mm external diameter and 3.0 m length or a 1.5% OV-17, 1.95% QF-1 chromosorb W packed column of 10 mm external diameter and 2.5 m length.

Melting points were determined on an electrothermal melting point apparatus and are uncorrected. Elemental analyses were performed at the Department of Chemistry, University of Otago, Dunedin.

Radial chromatography was performed on a chromatotron (Harrison and Harrison) using Merck grade $60PF_{254}$ silica gel or polyethylene glycol (PEG, molecular weight

6000 g mol^{-1}) coated silica plates. TLC mesh column chromatography[100] was performed on Merck $60PF_{254+366}$ grade silica gel.

Synthesis of *endo*-tricyclo[3.2.1.$0^{2,4}$]oct-6-ene **68**

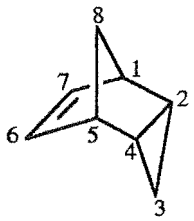

Compound **68** was synthesised according to the literature procedure[63] by Diels-Alder reaction of cyclopentadiene and cyclopropene at -78 °C and was identified by comparison of its ^1H and ^{13}C NMR spectra with those reported.[32]

General Procedure: Cyclopropene was prepared from the reaction of allyl chloride with sodium amide (prepared shortly before use, from the reaction of sodium metal with liquid ammonia in the presence of a catalytic amount of ferric nitrate[226]) in parafin oil at 75 °C and distilled directly into the reaction vessel containing cyclopentadiene and pentane cooled to -78 °C (dry-ice/acetone bath). The reaction was maintained at -78 °C for 12 h after which time the solvent was removed by distillation through a short vigreux column to give **68** which was used without further purification.

Preparation of 2-methyl-*endo*-tricyclo[3.2.1.$0^{2,4}$]oct-6-ene **86**

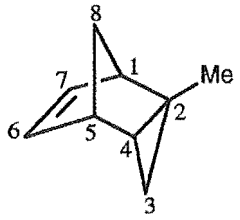

2-Methyl-*endo*-tricyclo[3.2.1.$0^{2,4}$]oct-6-ene **86** was prepared by the literature procedure[16] from the Diels-Alder reaction of cyclopentadiene and 2-methyl-cyclopropene[64] at -78 °C and was identified by comparison of its ^1H and ^{13}C NMR spectra with those reported.[16,32] The general procedure was similar to that outlined above for the synthesis of **68**, except that 3-chloro-2-methylpropene was refluxed with sodium amide in THF to form 2-methylcyclopropene which distilled from the reaction mixture and was trapped at -78 °C in a solution of cyclopentadiene and pentane.

Synthesis of *endo*-tricyclo[3.2.1.$0^{2,4}$]octane **1**

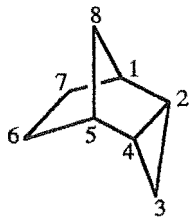

endo-Tricyclo[3.2.1.$0^{2,4}$]octane **1** was prepared using the literature procedure[14,32] by hydrogenation of **68** over 5% palladium on carbon until one equivalent of hydrogen was absorbed. The product was identified by comparison of its ^1H and ^{13}C NMR spectra with those reported.[14,32]

Preparation of 2-methyl-*endo*-tricyclo[3.2.1.0^{2,4}]octane **45**

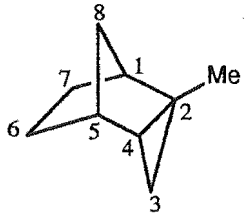

Compound **45** was synthesised by the literature procedure,[16,32] whereby **86** was hydrogenated over 5% palladium on carbon until one equivalent of hydrogen was taken up. Product **45** was identified by comparison of its ^{1}H and ^{13}C NMR spectra with those reported.[16,32]

Synthesis of *exo*-tricyclo[3.2.1.0^{2,4}]octane **46**

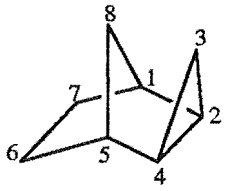

exo-Tricyclo[3.2.1.0^{2,4}]octane **46** was synthesised by the general procedure of Simmons and Smith[65] using a zinc-copper couple prepared by the method of Rawson and Harrison.[66] Compound **46** was identified by comparison of its ^{1}H and ^{13}C NMR spectra with those reported.[14,38]

Synthesis of *exo*-tricyclo[3.2.2.0^{2,4}]non-8-en-6-*exo*-7-*exo*-dicarboxylic acid anhydride **48**

exo-Tricyclo[3.2.2.0^{2,4}]non-8-en-6-*exo*-7-*exo*-dicarboxylic acid anhydride **48** was prepared according to the literature procedure[69] by Diels-Alder reaction of maleic anhydride with cycloheptatriene in refluxing xylene. The product was identified by comparison of its melting point (102-104 °C) with the value reported[69] (102-104 °C).

***exo*-Tricyclo[3.2.2.0^{2,4}]non-8-en-6-*exo*-7-*exo*-dicarboxylic acid anhydride 48**

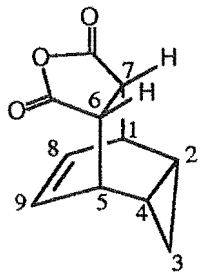

White crystalline needles:

mp 102-104 °C (pet. ether); Lit. 102-104 °C (hexane).[69]

^{1}H NMR $\delta_H(CDCl_3)$: 5.89 (d of d, $^{3}J_{8,1} = {}^{3}J_{9,5} = 4.9$ Hz, $^{4}J_{8,5} = {}^{4}J_{9,1} = 3.3$ Hz, H8, H9), 3.46 (m, H1, H5), 3.24 (t, $^{3}J_{6,5} = {}^{3}J_{7,1} = 1.9$ Hz, H6, H7), 1.12 (m, H2, H4), 0.37 (d of t, $^{2}J_{3endo,3exo} = 6.0$ Hz, $^{3}J_{3endo,2} = {}^{3}J_{3endo,4} = 7.5$ Hz, H3*endo*), 0.26 (d of t, $^{2}J_{3exo,3endo} = 6.1$ Hz, $^{3}J_{3exo,2} = {}^{3}J_{3exo,4} = 3.0$ Hz, H3*exo*).

^{13}C NMR $\delta_C(CDCl_3)$: 172.3 (2 x C=O), 128.4 (C8, C9), 45.8 (C6, C7), 33.6 (C1, C5), 9.4 (C2, C4), 5.1 (C3).

IR (KBr): 3063 (m), 3009 (m), 2944 (m), 1855 (s), 1823 (s), 1775 (s) cm^{-1}.

HRMS : $C_{11}H_{10}O_3$ $M^{+\cdot}$ requires 190.0630; Found 190.0629 (0.3%).

Elemental Analysis: $C_{11}H_{10}O_3$ Calc. C 69.46%, H 5.29%; Found C 69.63%, H 5.25%.

Preparation of *exo*-tricyclo[3.2.2.0^{2,4}]nonan-6-*exo*-7-*exo*-dicarboxylic acid anhydride **49**

exo-Tricyclo[3.2.2.0^{2,4}]nonan-6-*exo*-7-*exo*-dicarboxylic acid anhydride **49** was prepared by hydrogenation of **48** over 5% palladium on carbon (1:10 ratio by weight of catalyst to alkene) until one equivalent of hydrogen had been taken up.[69] The solvent was removed under reduced pressure to give a white solid, mp 139-140 °C (lit. 140 °C).[69]

exo-Tricyclo[3.2.2.0^{2,4}]nonan-6-exo-7-exo-dicarboxylic acid anhydride 49

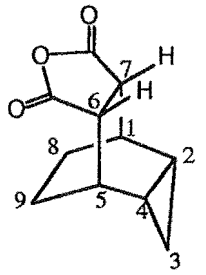

White crystals: mp 139-140 °C; Lit. 140 °C.[69]

^{1}H NMR δ_H(CDCl$_3$): 3.26 (m, H6, H7), 2.57 (m, H1, H5), 1.35 (m, H8*anti*, H8*syn*, H9*anti*, H9*syn*), 1.11 (m, H2 H4), 0.87 (d of t, $^2J_{3exo,3endo}$ = 6.7 Hz, $^3J_{3exo,2}$ = $^3J_{3exo,4}$ = 3.7 Hz, H3*exo*), 0.67 (d of t, $^2J_{3endo,3exo}$ = 6.8 Hz, $^3J_{3endo,2}$ = $^3J_{3endo,4}$ = 7.8 Hz, H3*endo*).

^{13}C NMR δ_C(CDCl$_3$): 173.5 (2 x C=O), 45.9 (C6, C7), 27.6 (C1, C5), 19.5 (C8, C9), 14.3 (C2, C4), 6.6 (C3).

IR (KBr): 3033 (m), 2953 (s), 2885 (s), 1851 (s), 1831 (s), 1772 (s) cm^{-1}.

HRMS: $C_{11}H_{12}O_3$ requires $M^{+\cdot}$ 192.0786; Found 192.0789 (19.6%).

Synthesis of *exo*-tricyclo[3.2.2.0^{2,4}]nonan-6-*exo*-7-*exo*-dicarboxylic acid **50**

To a stirred solution of KOH (8.4 g, 150 mmol) in water (250 ml) was added **49** (7.67 g, 39.9 mmol). The resulting solution was heated to 80 °C until all of the anhydride had dissolved. The hot solution was then carefully acidified with conc. HCl before cooling to room temperature. The precipitate which formed was collected by filtration and dried under vacuum to give a white solid (4.81 g, 57%). The product showed satisfactory ^{1}H, ^{13}C, IR, and mass spectra.

exo-Tricyclo[3.2.2.0^{2,4}]nonan-6-exo-7-exo-dicarboxylic acid 50

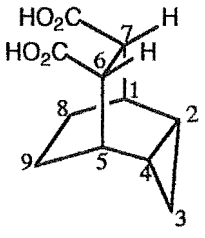

White crystalline solid:

mp 166-167 °C (Water); Lit. 173-174 °C (Water).[68]

^{1}H NMR δ_H(DMSO-d_6): 11.19 (s, $W_{h/2}$ = 19.1 Hz, 2 x OH), 2.12 (s, $W_{h/2}$ = 4.4 Hz, H6, H7), 1.39 (s, $W_{h/2}$ = 8.3 Hz, H1, H5), 0.82 (d, H8*anti*, H9*anti*), 0.32 (d, H8*syn*, H9*syn*), 0.20 (s, $W_{h/2}$ = 16.0 Hz, H2, H4), -0.02 (m, H3*exo*), -0.38 (m, $^2J_{3endo,3exo}$ = 6.4 Hz, $^3J_{3endo,2}$ = $^3J_{3endo,4}$ = 7.3 Hz, H3*endo*).

^{13}C NMR δ_C(DMSO-d_6): 174.9 (2 x C=O), 44.2 (C6, C7), 27.5 (C1, C5), 18.6 (C8, C9), 14.4 (C2, C4), 4.5 (C3).

IR (KBr): 3021 (m), 2952 (m), 2756 (m), 1709 (s) cm^{-1}.

HRMS: $C_{11}H_{14}O_4$ $M^{+\cdot}$ requires 210.0892; Found 210.0873 (0.5%)

$C_{11}H_{12}O_3$ $[M\text{-}18]^{+\cdot}$ requires 192.0786; Found 192.0786 (17.0%).

Preparation of *exo*-tricyclo[3.2.2.0^{2,4}]non-6-ene **47**

exo-Tricyclo[3.2.2.0^{2,4}]non-6-ene **47** was synthesised by the literature procedure.[67,68] To a stirred suspension of **50** (10.9 g, 51.8 mmol), dry benzene (260 ml), and dry pyridine (20.6 ml) at 0 °C (ice bath) was added lead tetraacetate (36.3 g, 91.8 mmol). The reaction was slowly heated to 80 °C over 2 h and maintained at this temperature for a further 5 h. After cooling to room temperature, the mixture was filtered under suction and the solid washed with benzene (50 ml). The benzene fractions were combined and washed with water (200 ml), 5% KOH solution (200 ml), water (200 ml), 10% HCl (200 ml), water (200 ml), saturated $NaHCO_3$ solution (200 ml), and saturated brine solution (200 ml). The resulting benzene extract was dried over $MgSO_4$ and the solvent removed by distillation through a short vigreux column. The brown viscous oil obtained (3.47 g) was shown by GLC analysis to contain **47** (83%), benzene (14%), and another compound which was not identified (3%). This corresponds to a 46% yield of **47** from the diacid **50**. The identity of **47** was confirmed by comparison of its ^{1}H NMR spectra to that reported.[67,68]

***exo*-Tricyclo[3.2.2.0^{2,4}]non-6-ene 47**

Colourless semisolid: bp 165-168 °C; Lit. 162-168 °C.[68]

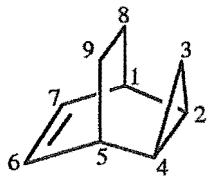

^{1}H NMR $\delta_H(CDCl_3)$: 6.50 (d of d, $^3J_{6,5} = {}^3J_{7,1}$ = 4.5 Hz, $^4J_{6,1} = {}^4J_{7,5}$ = 2.9 Hz, H6, H7), 2.64 (m, H1, H5), 1.39 (m, H8*syn*, H9*syn*), 1.02 (m, H2, H4), 0.86-0.98 (m, H3*exo*, H8*anti*, H9*anti*), 0.58 (d of t, $^2J_{3endo,\,3exo}$ = 5.9 Hz, $^3J_{3endo,2} = {}^3J_{3endo,4}$ = 7.3 Hz, H3*endo*).

^{13}C NMR $\delta_C(CDCl_3)$: 137.8 (C6, C7), 29.9 (C1, C5), 23.2 (C8, C9), 21.5 (C2, C4), 14.1 (C3).

HRMS: C_9H_{12} $M^{+\cdot}$ requires 120.0939; Found 120.0934 (37.5%).

Preparation of *cis*-1,2-bis(phenylmercapto)ethene

cis-1,2-Bis(phenylmercapto)ethene was prepared by the literature procedure[82,83] and identified by comparison of its ^{1}H NMR spectrum with that reported.[75]

Synthesis of *cis*-1,2-bis(phenylsulphonyl)ethene **53**

A procedure similar to that reported by Truce et al.[84] was used. Hydrogen peroxide (30%, 240 ml) was added dropwise to a stirred solution of *cis*-1,2-bis(phenylmercapto)ethene (74.0 g, 303 mmol) in glacial acetic acid (600 ml). The mixture was refluxed for 3 h and then allowed to cool to room

temperature before adding water (ca. 500 ml) until precipitation appeared complete. The precipitate was collected by filtration and dried under vacuum to give a white solid (59.7 g, 194 mmol, 64 %). Recrystallisation from petroleum ether gave white crystalline needles (mp 100-102 °C, lit. 100-101 °C).[75] The ^{1}H and ^{13}C NMR spectra were identical to those published.[75]

Synthesis of *trans*-1,2-bis(phenylsulphonyl)ethene **52**

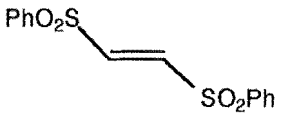

trans-1,2-Bis(phenylsulphonyl)ethene **52** was prepared by the literature procedure,[75] whereby a solution of **53** in CH_2Cl_2 was photolysed in a rayonet photolysis apparatus in the presence of a catalytic amount of iodine. Compound **52** precipitated from the solution and was collected by filtration when the reaction was complete (TLC analysis). The product was identified by comparison of its mp 225-227 °C (lit. mp 219-220 °C, 226-229 °C) and ^{1}H NMR spectra with those published.[75]

Synthesis of 8-*anti*-9-*syn*-bis(phenylsulphonyl)-*endo*-tricyclo[3.2.2.0^{2,4}]non-6-ene **54**

8-*anti*-9-*syn*-Bis(phenylsulphonyl)-*endo*-tricyclo[3.2.2.0^{2,4}]non-6-ene **54** was prepared by the method of De Lucchi et al.[75] by Diels-Alder reaction of **52** with cycloheptatriene in a sealed tube at 120 °C. The product was identified by comparison of its melting point with that reported.[75]

8-*anti*-9-*syn*-Bis(phenylsulphonyl)-*endo*-tricyclo[3.2.2.0^{2,4}]non-6-ene 54

White solid: mp 176-177 °C (ethyl acetate/pet. ether); Lit. 176-177 °C (CH_2Cl_2/ether).[75]

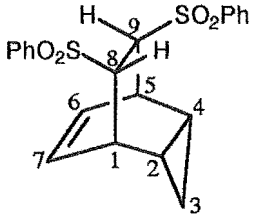

^{1}H NMR δ_H($CDCl_3$): 7.53-7.98 (m, 10 H), 5.80-5.84 (m, H6, H7), 4.04 (d of d, $^{3}J_{8,1}$ = 2.4 Hz, $^{3}J_{8,9}$ = 5.4 Hz, H8), 3.75 (d of d, $^{3}J_{9,5}$ = 2.2 Hz, $^{3}J_{9,8}$ = 5.3 Hz, H9), 3.48 (m, H5), 3.35 (m, H1), 1.65 (m, $^{3}J_{4,3endo}$ = 3.9 Hz, $^{3}J_{4,3exo}$ = 7.8 Hz, $^{3}J_{4,2}$ = 7.8 Hz, H4), 1.08 (m, $^{3}J_{2,3endo}$ = 3.9 Hz, $^{3}J_{2,3exo}$ = 7.3 Hz, $^{3}J_{2,4}$ = 7.8 Hz, H2), 0.19-0.28 (m, H3*endo*, H3*exo*).

^{13}C NMR δ_C($CDCl_3$): 139.6, 133.9$_5$, 133.9$_2$, 129.2 (C6), 128.6$_5$, 128.6$_2$, 128.5$_9$, 126.8 (C7), 66.0 (C8), 65.5 (C9), 33.7 (C5), 33.5 (C1), 8.9 (C2), 6.0 (C4), 3.6 (C3).

HRMS: $C_{15}H_{15}O_2S$ $[M-142]^{+\cdot}$ requires 259.0793; Found 259.0843 (92.5%).

Preparation of 8-*anti*-9-*anti*-bis(phenylsulphonyl)-*endo*-tricyclo[3.2.2.0^{2,4}]non-6-ene **55**

8-*anti*-9-*anti*-Bis(phenylsulphonyl)-*endo*-tricyclo[3.2.2.0^{2,4}]non-6-ene **55** was prepared by the method of De Lucchi et al.[75] by Diels-Alder reaction of **53** with cycloheptatriene in a sealed tube at 120 °C. The product exhibited satisfactory ^{1}H and ^{13}C NMR spectra.

8-*anti*-9-*anti*-Bis(phenylsulphonyl)-*endo*-tricyclo[3.2.2.0^{2,4}]non-6-ene 55

White solid: mp (decomposes) 242-245 °C (toluene); Lit. (partial decomposition) 266-268 °C (toluene).[75]

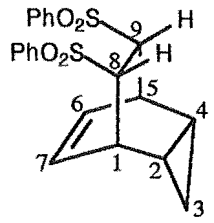

^{1}H NMR δ_H**(CDCl$_3$):** 7.53-8.02 (m, 10 H), 6.05 (d of d, $^3J_{6,5}$ = $^3J_{7,1}$ = 5.0 Hz, $^4J_{6,1}$ = $^4J_{7,5}$ = 3.4 Hz, H6, H7), 3.96 (s, $W_{h/2}$ = 2.9 Hz, H8, H9), 3.35 (s, $W_{h/2}$ = 11.3 Hz, H1, H5), 0.86 (m, H2, H4), 0.12-0.20 (m, H3*endo*, H3*exo*).

^{13}C NMR δ_C**(CDCl$_3$):** 140.9 (C1', C1"), 133.5 (C4', C4"), 128.9 (C3', C3", C5', C5"), 128.8 (C2', C2", C6', C6"), 127.5 (C6, C7), 70.4 (C8, C9), 34.7 (C1, C5), 9.6 (C2, C3), 3.3 (C3).

HRMS: $C_{15}H_{15}O_2S$ [M-142]$^{+\cdot}$ requires 259.0793; Found 259.0769 (2.3%)

C_9H_9 [M-283]$^{+\cdot}$ requires 117.0705; Found 117.0701 (100.0%).

General procedure for lithium in liquid ammonia reductions

To a three neck round bottom flask fitted with a dry ice acetone condenser, ammonia gas inlet, and a magnetic flea, was added the required quantity of disulphone (**54** or **55**). Ammonia gas was condensed into the flask until the required volume of liquid ammonia was obtained. Lithium metal, in small pieces, was then added to the stirred solution of disulphone and liquid ammonia and the reaction continued for the required time (0-4 h) before the condenser was removed and the ammonia allowed to evaporate. When the majority of the ammonia had evaporated, wet ether (obtained by shaking an equal volume of ether and water, and then separating) was cautiously added dropwise until no further reaction was observed. Water was carefully added dropwise to dissolve any solid residue remaining, followed by addition of ether (or pentane). The organic layer was separated, washed with water, dried over $MgSO_4$, and the solvent removed by distillation through a short vigreux column.

Attempted synthesis of *endo*-tricyclo[3.2.2.0^{2,4}]non-6-ene **56** by lithium/NH_3 reduction of **54**

Using the general procedure outlined above, **54** (1.0 g, 2.5 mmol), liquid ammonia (ca. 25 ml), and lithium metal (455 mg, 66 mmol, 26 mole equivalents) were stirred for 3 h before the liquid ammonia was allowed to evaporate. Extraction with ether followed by workup gave a yellow oil (49 mg) which was shown by ^{1}H NMR to contain **56** (28%), **51** (28%), and third compound that was not identified (43%). The identity of **51** and **56** was determined by comparison of their ^{1}H NMR spectra with those reported.[67]

Synthesis of tricyclo[3.2.2.0^{2,4}]nona-6,8-diene **51**

Using the general procedure outlined above, **55** (9.0 g, 22 mmol) and lithium (2.4 g, 346 mmol) were stirred in liquid ammonia (ca. 400 ml) for 2.5 h before allowing the ammonia to evapourate. After workup a yellow oil (550 mg) was obtained whose ^{1}H NMR spectrum showed the presence of **51** (73%), **56** (9%) and another compound which was not identified (18%). This corresponds to a 20% yield of **51** from **55**.

Tricyclo[3.2.2.0^{2,4}]nona-6,8-diene 51

Pale yellow oil.

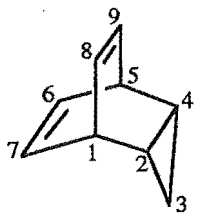

^{1}H NMR δ_H**(CDCl$_3$)**: 6.60 (d of d, $^3J_{8,1} = {}^3J_{9,5} = 4.3$ Hz, $^4J_{8,5} = {}^4J_{9,1} = 3.4$ Hz, H8, H9), 5.97 (d of d, $^3J_{6,5} = {}^3J_{7,1} = 4.6$ Hz, $^4J_{6,1} = {}^4J_{7,5} = 2.9$ Hz, H6, H7), 3.62 (m, H1, H5), 1.16 (m, H2, H4), 0.64 (d of t, $^2J_{3endo,3exo} = 5.5$ Hz, $^3J_{3endo,2} = {}^3J_{3endo,4} = 3.5$ Hz, H3*endo*), 0.48 (d of t, $^2J_{3exo,3endo} = 5.5$ Hz, $^3J_{3exo,2} = {}^3J_{3exo,4} = 7.0$ Hz, H3*exo*).

^{13}C NMR δ_C**(CDCl$_3$)**: 139.3 (C8, C9), 130.6 (C6, C7), 65.2 (C1, C5), 18.0 (C2, C4), 16.8 (C3).

HRMS: C_9H_{10} $M^{+\cdot}$ requires 118.0783; Found 118.0778 (26.0%).

Synthesis of 8-*anti*-methoxycarbonyl-*endo*-tricyclo[3.2.2.0^{2,4}]non-6-ene **58** and 8-*syn*-methoxycarbonyl-*endo*-tricyclo[3.2.2.0^{2,4}]non-6-ene **59**

(a) By Lewis acid catalysed Diels-Alder reaction of methyl acrylate and cycloheptatriene

A procedure similar to that of Bellus et al.[99] was used. To a stirred suspension of $AlCl_3$ (4.83 g, 36.2 mmol) in benzene (250 ml) was added a solution of methyl acrylate (30.0 ml, 330 mmol) and benzene (30 ml) over 15 minutes. The reaction mixture was heated to 30 °C until all of the $AlCl_3$ had dissolved and then cycloheptatriene (34.5 ml, 332 mmol) in benzene (120 ml) added dropwise over 45 minutes. After refluxing for 16 h the benzene was decanted into a separating funnel and washed with water (500 ml portions) until the washings were neutral. The benzene extract was then dried over calcium sulphate and the solvent removed under reduced pressure to give a brown oil (40.19 g). The aqueous washings were extracted with CH_2Cl_2 to give a further 3.91 g of brown oil. Radial chromatography (2 mm silica, 5% ethyl acetate/petroleum ether elution) of a portion (498 mg) of the oil obtained gave a clear colourless oil (290 mg, 44% overall yield) consisting of **58** and **59** in a ratio of 9:1. Separation of the methyl esters **58** and **59** was effected by careful TLC mesh column chromatography[100] (90:1 ratio of TLC grade silica absorbant to compound loaded, 4% ethyl acetate/petroleum ether elution). The products were identified by comparison of their ^{1}H NMR spectra with those reported.[99]

(b) By Diels-Alder reaction of methyl acrylate with cycloheptatriene

Methyl acrylate (1.0 ml, 11 mmol), cycloheptatriene (1.3 ml, 13 mmol), and toluene (2 ml) were placed in a 10 ml thick walled pyrex test tube. The tube was sealed, placed in an oil bath preheated to 130 °C, and the temperature increased to 140 °C. After 30 days the contents of the tube were removed and the solvent distilled under reduced pressure to give a brown oil (860 mg, 44%). A ^{1}H NMR spectrum of the crude reaction mixture showed the presence of **58** and **59** in 3:1 ratio.

8-*anti*-Methoxycarbonyl-*endo*-tricyclo[3.2.2.0^{2,4}]non-6-ene 58

Colourless oil.

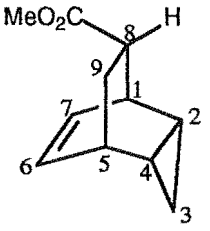

^{1}H NMR δ_H**(CDCl$_3$):** 5.85 (d of t, $^3J_{6,5} = {}^3J_{6,7}$ = 7.3 Hz, $^4J_{6,1}$ = 1.3 Hz, H6), 5.67 (d of t, $^3J_{7,1} = {}^3J_{7,6}$ = 7.3 Hz, $^4J_{7,5}$ = 1.3 Hz, H7), 3.62 (s, $W_{h/2}$ = 0.7 Hz, OMe), 3.15 (m, H1), 2.79 (m, H5), 2.67 (m, $^3J_{8,1}$ = 2.4 Hz, $^3J_{8,9anti}$ = 4.7 Hz, $^3J_{8,9syn}$ = 9.5 Hz, H8), 1.80 (m, $^2J_{9syn,9anti}$ = 12.4 Hz, $^3J_{9syn,5}$ = 2.7 Hz, $^3J_{9syn,8}$ = 9.7 Hz, H9*syn*), 1.67 (m, $^2J_{9anti,9syn}$ = 12.5 Hz, $^3J_{9anti,5}$ = 2.9 Hz, $^3J_{9anti,8}$ = 4.7 Hz, H9*anti*), 0.87-0.94 (m, H2, H4), 0.03-0.09 (m, H3*endo*, H3*exo*).

^{13}C NMR δ_C**(CDCl$_3$):** 175.9 (C=O), 130.4 (C6), 126.4 (C7), 51.6 (OMe), 42.9 (C8), 33.9 (C1), 30.5 (C5), 29.7 (C9), 9.8 (C2 or C4), 9.6 (C4 or C2), 2.9 (C3).

IR (thin film): 3004 (m), 2949 (m), 1736 (s) cm^{-1}.

HRMS: $C_{11}H_{14}O_2$ $M^{+\cdot}$ requires 178.0994; Found 178.0994 (11.4%).

8-*syn*-Methoxycarbonyl-*endo*-tricyclo[3.2.2.0^{2,4}]non-6-ene 59

Colourless oil.

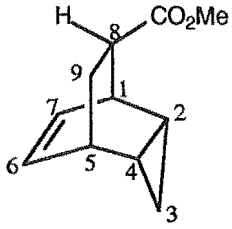

^{1}H NMR δ_H**(CDCl$_3$):** 5.79-5.82 (m, H6, H7), 3.70 (s, $W_{h/2}$ = 0.6 Hz, OMe), 3.10 (m, H1), 2.79 (m, H5), 2.39 (m, $^3J_{8,1}$ = 2.4 Hz, $^3J_{8,9anti}$ = 10.7 Hz, $^3J_{8,9syn}$ = 4.9 Hz, H8), 1.99 (m, $^2J_{9syn,9anti}$ = 12.2 Hz, $^3J_{9syn,8}$ = 4.9 Hz, $^3J_{9syn,5}$ = 2.5 Hz, H9*syn*), 1.51 (m, $^2J_{9anti,9syn}$ = 13.6 Hz, $^3J_{9anti,5}$ = 2.5 Hz, $^3J_{9anti,8}$ = 10.7, H9*anti*), 0.95 (m, $^3J_{4,2}$ = 8.1 Hz, $^3J_{4,3endo} = {}^3J_{4,5}$ = 3.9 Hz, $^3J_{4,3exo}$ = 6.9 Hz, H4), 0.86 (m, $^3J_{2,1} = {}^3J_{2,3endo}$ = 3.9 Hz, $^3J_{2,3exo}$ = 7.3 Hz, $^3J_{2,4}$ = 7.9 Hz, H2), -0.05-0.01 (m, H3*endo*, H3*exo*).

^{13}C NMR δ_C**(CDCl$_3$):** 175.7 (C=O), 130.1 (C6), 128.5 (C7), 51.7 (OMe), 42.8 (C8), 33.7 (C1), 30.1 (C5), 28.3 (C9), 9.4 (C4), 5.5 (C2), 1.5 (C3).

IR (thin film): 2943 (m), 1736 (s) cm^{-1}.

HRMS: $C_{11}H_{14}O_2$ $M^{+\cdot}$ requires 178.0994; Found 178.0994 (7.6%).

Synthesis of 8-*anti*-carboxy-*endo*-tricyclo[3.2.2.0^{2,4}]non-6-ene **60** and 8-*syn*-carboxy-*endo*-tricyclo[3.2.2.0^{2,4}]non-6-ene **61**

A procedure similar to that of Kirmse et al.[101] was used. KOH (229 mg, 4.08 mmol) was dissolved in water (0.3 ml) and ethanol (0.6 ml) added to produce a homogenous solution. The KOH solution was added to a mixture (9:1 ratio) of **58** and **59** (570 mg, 3.20 mmol) in ethanol (4 ml). The resulting solution was refluxed for 3 h after which time TLC analysis showed complete consumption of the starting material. The ethanol was removed under reduced pressure and water (5 ml) added. The resulting solution was acidified with conc. H_2SO_4 and extracted with ether (2 x 5 ml). The ether extracts were combined, washed with saturated brine solution (5 ml), dried over $MgSO_4$, and the ether removed under reduced pressure to give a yellow oil (405 mg, 77%) which was used without further purification. Compound **60** was identified by comparison of its ^{1}H NMR with that reported.[101]

8-*anti*-Carboxy-*endo*-tricyclo[3.2.2.0^{2,4}]non-6-ene 60

Yellow oil.

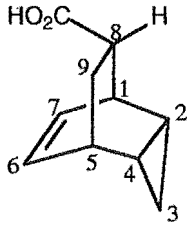

^{1}H NMR δ_H**(CDCl$_3$)**: 5.86 (d of t, $^3J_{6,5} = {}^3J_{6,7}$ = 7.3 Hz, $^4J_{6,1}$ = 1.0 Hz, H6), 5.70 (d of t, $^3J_{7,1} = {}^3J_{7,6}$ = 7.4 Hz, $^4J_{7,5}$ = 1.0 Hz, H7), 3.20 (m, H1), 2.80 (m, H5), 2.70 (m, $^3J_{8,1}$ = 2.4 Hz, $^3J_{8,7anti}$ = 4.7 Hz, $^3J_{8,7syn}$ = 9.6 Hz, H8), 1.81 (m, $^2J_{9syn,\ 9anti}$ = 12.7 Hz, $^3J_{9syn,\ 5}$ = 2.7 Hz, $^3J_{9syn,\ 8}$ = 9.8 Hz, H9*syn*), 1.67 (m, $^2J_{9anti,\ 9syn}$ = 12.7 Hz, $^3J_{9anti,5}$ = 2.9 Hz, $^3J_{9anti,8}$ = 4.9 Hz, H9*anti*), 0.85-0.95 (m, H2, H4), 0.02-0.11 (m, H3*endo*, H3*exo*).

^{13}C NMR δ_C**(CDCl$_3$)**: 181.8 (C=O), 130.5 (C6), 126.4 (C7), 42.9 (C8), 33.8 (C1), 30.4 (C5), 29.4 (C9), 9.8 (C2), 9.5 (C4), 2.9 (C3).

HRMS: $C_{10}H_{12}O_2$ $M^{+\cdot}$ requires 164.0838; Found 164.0823 (1.4%).

8-*syn*-Carboxy-*endo*-tricyclo[3.2.2.0^{2,4}]non-6-ene 61

Compound **61** was not isolated. The following ^{1}H and ^{13}C NMR data were determined from the crude reaction mixture and the assignments made by comparison with **59**. Some protons and carbons were not identified.

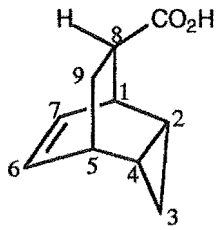

^{1}H NMR δ_H**(CDCl$_3$)**: 3.14 (m, H1), 2.42 (m, H8), 1.96 (m, H9*syn*), 1.52 (m, H9*anti*), -0.05-0.02 (m, H3*endo*, H3*exo*).

^{13}C NMR δ_C**(CDCl$_3$)**: 130.1 (C6), 128.4 (C7), 33.6 (C1), 30.0 (C5), 28.0 (C9), 9.4 (C4), 5.4 (C2), 1.5 (C3).

Preparation of *exo*-tricyclo[3.2.2.0^{2,4}]non-8-en-6-*exo*-carboxylic acid benzophenone oxime ester **62** and *exo*-tricyclo[3.2.2.0^{2,4}]non-8-en-6-*endo*-carboxylic acid benzophenone oxime ester **63**

Oxalyl chloride (16.8 ml, 195 mmol) in dry benzene (20 ml) was added dropwise over 30 minutes to a stirred solution of **60** and **61** (16.0 g, 97.5 mmol, 9:1 ratio respectively) and DMF (1 ml) in dry benzene (200 ml). The reaction was stirred at room temperature for 30 minutes after which time a further portion (8.5 ml, 99 mmol) of oxalyl chloride was added dropwise. The reaction was stirred for 2.5 h after which time the reaction was shown to be complete (^{1}H NMR). The solvent was removed under reduced pressure, the residue redissolved in a further portion of dry benzene (200 ml), and again concentrated under reduced pressure. The mixture of 8-*anti*-chloroformyl-*endo*-tricyclo[3.2.2.0^{2,4}]non-6-ene and 8-*syn*-chloroformyl-*endo*-tricyclo[3.2.2.0^{2,4}]non-6-ene was dissolved in a solution of dry $CHCl_3$ (200 ml) and dry pyridine (8 ml). Benzophenone oxime[227] (19.2 g, 99.9 mmol) in dry $CHCl_3$ (200 ml) was added in portions. The reaction was stirred at room temperature for 2.5 h after which time the reaction was complete. The solvent was removed under reduced pressure to give a viscous brown oil (48.1 g). A sample (1.500 g) was purified by TLC mesh column chromatography (75 g silica absorbant, 10% ethyl acetate/pet. ether elution) to give **62** (545 mg, 52%) and **63** (61 mg, 6%).

8-*anti*-Chloroformyl-*endo*-tricyclo[3.2.2.0^{2,4}]non-6-ene

Yellow oil.

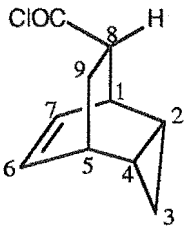

^{1}H NMR δ_H($CDCl_3$): 5.91 (d of t, $^3J_{6,5} = {}^3J_{6,7}$ = 7.6 Hz, $^4J_{6,1}$ = 1.5 Hz, H6), 5.72 (d of t, $^3J_{7,1} = {}^3J_{7,6}$ = 7.4 Hz, $^4J_{7,5}$ = 1.0 Hz, H7), 3.40 (m, H1), 3.15 (m, $^3J_{8,1}$ = 2.5 Hz, $^3J_{8,9anti}$ = 4.9 Hz, $^3J_{8,9syn}$ = 9.5 Hz, H8), 2.87 (m, H5), 1.92 (m, $^2J_{9syn,9anti}$ = 12.7 Hz, $^3J_{9syn,5}$ = 2.9 Hz, $^3J_{9syn,8}$ = 9.8 Hz, H9*syn*), 1.74 ($^2J_{9anti,9syn}$ = 12.7 Hz, $^3J_{9anti,5}$ = 2.7 Hz, $^3J_{9anti,8}$ = 4.9 Hz, H9*anti*), 0.94-1.00 (m, H2, H4), 0.10-0.18 (m, H3*endo*, H3*exo*).

^{13}C NMR δ_C($CDCl_3$): 175.9 (C=O), 131.0 (C6), 125.6 (C7), 55.7 (C8), 34.6 (C1), 30.6 (C9), 30.5 (C5), 9.6 (C2 or C4), 9.4 (C4 or C2), 3.3 (C3).

***exo*-Tricyclo[3.2.2.0^{2,4}]non-8-en-6-*exo*-carboxylic acid benzophenone oxime ester 62**

White solid: mp 99-102 °C (ether).

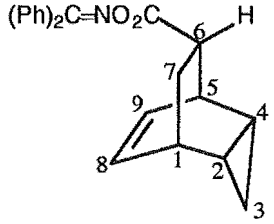

^{1}H NMR δ_H($CDCl_3$): 7.26-7.62 (m, 10 H), 5.77 (d of t, $^3J_{8,1} = {}^3J_{8,9}$ = 7.5 Hz, $^4J_{8,5}$ = 1.4 Hz, H8), 5.48 (d of t, $^3J_{9,5} = {}^3J_{9,8}$ = 7.3 Hz, $^4J_{9,1}$ = 1.5 Hz, H9), 2.96 (m, H5), 2.75 (m, H1), 2.69 (m, $^3J_{6,5}$ = 2.4 Hz, $^3J_{6,7endo}$ = 9.8 Hz, $^3J_{6,7exo}$ = 4.8 Hz, H6), 1.75 (m, $^2J_{7endo,7exo}$ = 12.5 Hz, $^3J_{7endo,1}$ = 2.9 Hz,

$^3J_{7endo,6}$ = 9.7 Hz, H7*endo*), 1.62 (m, $^2J_{7exo,7endo}$ = 12.7 Hz, $^3J_{7exo,1}$ = 2.8 Hz, $^3J_{7exo,6}$ = 4.9 Hz, H7*exo*), 0.82-0.87 (m, H2, H4), -0.01-0.05 (m, H3*endo*, H3*exo*).

^{13}C NMR $\delta_C(CDCl_3)$: 172.5 (C=O), 165.1 (C=N), 134.7, 132.9, 130.8, 130.3 (C8), 129.5, 129.0, 128.6, 128.3, 128.1, 126.3 (C9), 42.1 (C6), 33.5 (C5), 30.3 (C1), 29.6 (C7), 9.7 (C4 or C2), 9.6 (C2 or C4), 2.8 (C3).

IR (KBr): 3043 (m), 3001 (m), 2943 (m), 1756 (s), 1609 (m), 1592 (m), 1568 (m) cm^{-1}.

HRMS: $C_{23}H_{21}O_2N$ $M^{+\cdot}$ requires 343.1572; Found 343.1574 (0.9%).
$C_{22}H_{21}N$ $[M-44]^{+\cdot}$ requires 299.1674; Found 299.1651 (0.4%)
$C_{13}H_{10}NO$ $[M-147]^{+\cdot}$ requires 196.0763; Found 196.0762 (1.2%)
$C_{13}H_{10}N$ $[M-163]^{+\cdot}$ requires 180.0813; Found 180.0805 (100.0%)
$C_{10}H_{11}O$ $[M-196]^{+\cdot}$ requires 147.0809; Found 147.0817 (16.2%)
C_9H_{11} $[M-224]^{+\cdot}$ requires 119.0861; Found 119.0857 (25.6%)
C_7H_8 $[M-251]^{+\cdot}$ requires 92.0626; Found 92.0608 (10.2%)
C_7H_7 $[M-252]^{+\cdot}$ requires 91.0548; Found 91.0547 (26.6%).

Elemental Analysis: $C_{23}H_{21}O_2N$ Calc. C 80.44%, H 6.16%, N 4.08%; Found C 80.39%, H 6.05%, N 4.11%.

***exo*-Tricyclo[3.2.2.0^{2,4}]non-8-en-6-*endo*-carboxylic acid benzophenone oxime ester 63**

Yellow oil.

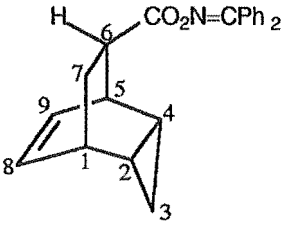

^{1}H NMR $\delta_H(CDCl_3)$: 7.27-7.62 (m, 10 H), 5.69-5.77 (m, H8, H9), 2.92 (m, H5), 2.73 (m, H1), 2.37 (m, $^3J_{6,5}$ = 2.4 Hz, $^3J_{6,7endo}$ = 4.9 Hz, $^3J_{6,7exo}$ = 10.7 Hz, H6), 1.92 (m, $^2J_{7endo,7exo}$ = 12.2 Hz, $^3J_{7endo,1}$ = 2.4 Hz, $^3J_{7endo,6}$ = 4.9, H7*endo*), 1.45 (m, $^2J_{7exo,7endo}$ = 12.2 Hz, $^3J_{7exo,1}$ = 2.9 Hz, $^3J_{7exo,6}$ = 10.8 Hz, H7*exo*), 0.83-0.89 (m, H2, H4), -0.11- -0.05 (m, H3*endo*, H3*exo*).

^{13}C NMR $\delta_C(CDCl_3)$: 172.3 (C=O), 165.1 (C=N), 134.7, 132.8, 130.9, 130.1 (C8), 129.4, 128.9, 128.6, 128.3$_4$, 128.2$_9$ (C9), 128.1$_7$, 41.9 (C6), 33.3 (C5), 30.0 (C1), 28.1 (C7), 9.3 (C2), 5.4 (C4), 1.5 (C3).

IR (KBr): 2976 (m), 1734 (m), 1659 (s), 1598 (m), 1577 (m) cm^{-1}.

LRMS: $C_{23}H_{21}O_2N$ $M^{+\cdot}$ requires 343; Found 343 (8%)
$C_{22}H_{21}N$ $[M-44]^{+\cdot}$ requires 299; Found 299 (100%).

HRMS: $C_{22}H_{21}N$ $[M-44]^{+\cdot}$ requires 299.1674; Found 299.1674 (2.1%)
$C_{13}H_{10}NO$ $[M-147]^{+\cdot}$requires 196.0763; Found 196.0760 (0.7%)
$C_{13}H_{10}N$ $[M-163]^{+\cdot}$ requires 180.0813; Found 180.0830 (100.0%)
$C_{10}H_{11}O$ $[M-196]^{+\cdot}$ requires 147.0809; Found 147.0819 (9.3%)
C_9H_{11} $[M-224]^{+\cdot}$requires 119.0861; Found 119.0860 (26.0%)

C_7H_8 $[M-251]^{+\cdot}$ requires 92.0626; Found 92.0610 (24.3%)
C_7H_7 $[M-252]^{+\cdot}$ requires 91.0548; Found 91.0549 (42.3%).

Synthesis of *endo*-tricyclo[3.2.2.0^{2,4}]non-6-ene by photolysis of benzophenone oxime esters **62** and **63**

The general procedure of Hasebe[94] was used. A mixture of **62** and **63** (303 mg, 0.88 mmol, 9:1 ratio respectively) was dissolved in a solution of isopropanol (3.6 ml) and thiophenol (0.4 ml). The resulting solution was placed in a pyrex photolysis tube, flushed with nitrogen and maintained under a nitrogen atmosphere while photolysed at 0-5 °C (ice bath) with a 450 W low-pressure mercury vapor lamp (Hanovia) for 7.5 h. The reaction mixture was poured into water (4 ml) containing potassium hydroxide (505 mg, 90 mmol) and stirred for 1.5 h. The resulting solution was extracted with pentane, the organic extract washed with water and the solvent carefully removed under reduced pressure at 0-5 °C (ice water bath). Column chromatography (silica gel, pentane elution) of the resulting oil gave pure *endo*-tricyclo[3.2.2.0^{2,4}]non-6-ene **56** (3 mg, 3%) as a colourless solid. Compound **56** was identified by comparison of its ^{1}H NMR spectrum with that reported.[67]

***endo*-Tricyclo[3.2.2.0^{2,4}]non-6-ene 56**

Colourless solid: mp 44-47 °C.

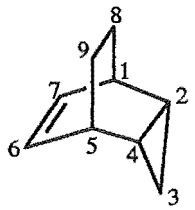

^{1}H NMR δ_H($CDCl_3$): 5.76 (d of d, $^3J_{6,5} = {}^3J_{7,1}$ = 5.2 Hz, $^4J_{6,1} = {}^4J_{4,5}$ = 3.2 Hz, H6, H7), 2.68 (m, H1, H5), 1.51 (m, H8*syn*, H9*syn*), 1.20 (m,H8*anti*, H9*anti*), 0.82 (m, H2, H4), -0.04- -0.11 (m, H3*endo*, H3*exo*).

^{13}C NMR δ_C($CDCl_3$): 129.2 (C6, C7), 30.2 (C1, C5), 25.1 (C8, C9), 9.5 (C2, C4), 1.4 (C3).

HRMS: C_9H_{12} $M^{+\cdot}$ requires 120.0939; Found 120.0936 (41.2%).

Synthesis of phenyl vinyl sulphide

Phenyl vinyl sulphide was prepared according to the literature procedure of Paquette et al.[88,103] by reaction of 1,2-dibromoethane with thiophenol and two equivalents of sodium ethoxide. The product was identified by comparison of its ^{1}H NMR spectrum with that reported.[88]

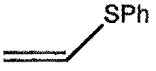

Preparation of phenyl vinyl sulphone **64**

Phenyl vinyl sulphone was synthesised by the literature procedure[88,103] from oxidation of phenyl vinyl sulphide with 30% hydrogen peroxide in glacial acetic acid at 70 °C. ^{1}H NMR as published.[88]

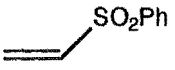

Synthesis of 8-*anti*- and 8-*syn*-phenylsulphonyl-*endo*-tricyclo[3.2.2.0 ^{2,4}]non-6-ene

(a) By Diels-Alder reaction of phenyl vinyl sulphone and cycloheptatriene

Phenyl vinyl sulphone **64** (1.0 g, 5.9 mmol), cycloheptatriene (1.0 ml, 9.6 mmol) and xylene (1 ml, mixed xylenes) were placed in a 10 ml pyrex screw cap test tube. The tube was sealed and heated to 170 °C for 14 days after which time the reaction was allowed to cool to room temperature before being diluted with ether. A small amount of dark solid precipitated and the supernatant solution was removed and evaporated to dryness under reduced pressure. ^{1}H NMR analysis of the precipitate and the solid obtained from evaporation of the solvent, showed both to contain approximately the same ratio of 8-*anti*-phenylsulphonyl-*endo*-tricyclo[3.2.2.0^{2,4}]non-6-ene **65**, 8-*syn*-phenyl-sulphonyl-*endo*-tricyclo[3.2.2.0^{2,4}]non-6-ene **66**, and unreacted **64** (ratio 8.8 : 2.3 : 1.0, respectively).

(b) Reduction of **55** with $NaBH_4$

A vigorously stirred slurry of **55** (5.13 g, 12.8 mmol) and sodium borohydride (8.31 g, 220 mmol, 17 mole equivalents) was refluxed in THF (300 ml) for 14 days under a nitrogen atmosphere. The solvent was removed under reduced pressure, the residue taken up with water (100 ml) and the solution carefully acidified with conc. HCl and extracted with CH_2Cl_2 (2 x 150 ml). The combined CH_2Cl_2 extracts were washed with water (100 ml), saturated $NaHCO_3$ solution (100 ml), water (2 x 100 ml), dried over $MgSO_4$, and the solvent removed under reduced pressure to give a brown viscous oil (3.15 g). TLC mesh column chromatography (75 g TLC grade silica, 25% ethyl acetate/pet. ether elution) gave a mixture of **65** and **66** (1.072 g, 32%) in a ratio of 2.1:1.0, respectively, and a small amount of **54** (157 mg, 3%). Compounds **65** and **66** were further purified by TLC mesh column chromatography (125:1 ratio of silica absorbant to sample loaded, 10% ethyl acetate/ pet. ether elution).

8-*anti*-Phenylsulphonyl-*endo*-tricyclo[3.2.2.0^{2,4}]non-6-ene 65

Colourless oil.

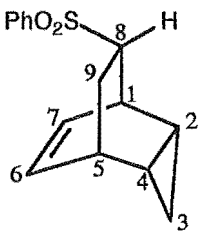

^{1}H NMR δ_H(CDCl$_3$): 7.87 (m, $^3J_{2',3'} = {}^3J_{6',5'} = 7.6$ Hz, $^4J_{2',4'} = {}^4J_{6',4'} = 1.5$ Hz, H2', H6'), 7.64 (m, $^3J_{4',3'} = {}^3J_{4',5'} = 7.5$ Hz, $^4J_{4',2'} = {}^4J_{4',6'} = 1.5$ Hz, H4'), 7.55 (m, $^3J_{3',2'} = {}^3J_{3',4'} = {}^3J_{5',4'} = {}^3J_{5',6'} = 7.6$ Hz, H3', H5'), 5.89 (d of t, $^3J_{6,5} = {}^3J_{6,7} = 7.1$ Hz, H6), 5.69 (d of t, $^3J_{7,1} = {}^3J_{7,6} = 6.9$ Hz, $^4J_{7,5} = 1.5$ Hz, H7), 3.34* (H8), 3.32* (H1), 2.89 (m, H5), 1.89 (m, $^2J_{9syn,9anti} = 12.7$ Hz, $^3J_{9syn,5} = 3.0$ Hz, $^3J_{9syn,8} = 9.7$ Hz, H9*syn*), 1.75 (m, $^2J_{9anti,9syn} = 13.2$ Hz, $^3J_{9anti,\ 5} = 2.5$ Hz, $^3J_{9anti,8} = 5.9$ Hz, H9*anti*), 0.85-0.93 (m, H2, H4), 0.07-0.14 (m, H3*endo*, H3*exo*).

^{13}C NMR δ_C(CDCl$_3$): 139.1 (C1'), 133.4 (C4'), 129.8 (C6), 129.1 (C3', C5'), 128.6 (C2', C6'), 125.2 (C7), 64.7 (C8), 31.3 (C1), 30.7 (C5), 28.8 (C9), 9.9 (C2), 9.0 (C4), 2.9 (C3).

IR (KBr): 3005 (m), 2942 (m), 1305 (s), 1147 (s) cm^{-1}.

HRMS: $C_{15}H_{16}O_2S$ $M^{+\cdot}$ requires 260.0871; Found 260.0873 (1.7%).

8-*syn*-Phenylsulphonyl-*endo*-tricyclo[3.2.2.0^{2,4}]non-6-ene 66

Colourless oil.

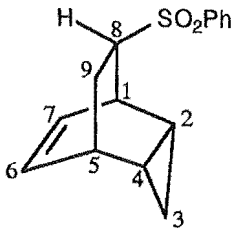

^{1}H NMR δ_H(CDCl$_3$): 7.90 (m, H2', H6'), 7.61, (m, H4'), 7.55 (m, H3', H5'), 5.79* (H6), 5.78* (H7), 3.24 (m, H1), 2.98* (H8), 2.95* (H5), 2.07 (m, $^2J_{9syn,9anti}$ = 12.7 Hz, $^3J_{9syn,5}$ = 2.5 Hz, $^3J_{9syn,8}$ = 5.8 Hz, H9*syn*), 1.53 (m, $^2J_{9anti,9syn}$ = 12.9 Hz, $^3J_{9anti,5}$ = 3.0 Hz, $^3J_{9anti,8}$ = 10.3 Hz, H9*anti*), 1.44 (m, $^3J_{2,3exo}$ = $^3J_{2,4}$ = 7.8 Hz, $^3J_{2,1}$ = $^3J_{2,3endo}$ = 3.9 Hz, H2), 1.15 (m, $^3J_{4,2}$ = $^3J_{4,3exo}$ = 7.8 Hz, $^3J_{4,3endo}$ = $^3J_{4,5}$ = 3.9 Hz, H4), 0.10 (d of t, $^2J_{3exo,\ 3endo}$ = 5.4 Hz, $^3J_{3exo,\ 2}$ = $^3J_{3exo,\ 4}$ = 7.3 Hz, H3*exo*), 0.00 (d of t, $^2J_{3endo,3exo}$ = 5.4 Hz, $^3J_{3endo,2}$ = $^3J_{3endo,4}$ = 3.7 Hz, H3*endo*).

^{13}C NMR δ_C(CDCl$_3$): 139.9 (C1'), 133.4 (C4'), 130.5 (C6), 129.2 (C3', C5'), 128.2 (C2', C6'), 127.8 (C7), 63.7 (C8), 31.7 (C1), 30.4 (C5), 26.6 (C9), 10.0 (C4), 4.8 (C2), 2.1 (C3).

IR (KBr): 3005 (m), 2948 (m), 1306 (s), 1146 (s) cm^{-1}.

HRMS: $C_{15}H_{16}O_2S$ $M^{+\cdot}$ required 260.0871; Found 260.0875 (1.2%).

Synthesis of 6-phenylsulphonyl-*exo*-tricyclo[3.2.2.0^{2,4}]nona-6,8-diene 67

(a) Reaction of **55** with NaOH at room temperature

8-*anti*-9-*anti*-Bis(phenylsulphonyl)-*endo*-tricyclo[3.2.2.0^{2,4}]non-6-ene **55** (1.25 g, 3.12 mmol) was added to a stirred solution of dioxan (90 ml), water (90 ml), and NaOH (1.8 g, 45 mmol) at room temperature. After 4.5 h the solution was diluted with water and extracted with CH_2Cl_2 (3 x 50 ml). The CH_2Cl_2 extracts were combined, dried over $MgSO_4$ and the solvent removed under vacuum to give a brown oil. A ^{1}H NMR of the oil showed the presence of starting material **55** and *trans* disulphone **54** in a ratio of 2.7:1.0, respectively. No formation of **67** was observed.

(b) Reaction of **55** with NaOH in refluxing aqueous dioxan solution

Compound **55** (1.05 g, 2.62 mmol) was added to a stirred solution of water (30 ml), dioxan (45 ml), and NaOH (1.14 g, 28.5 mmol). The reaction was heated to reflux for 1 h after which time a ^{1}H NMR spectrum showed the presence of **55** and **54** in a ratio of 2:3, respectively. No formation of **67** was observed.

(c) Reaction of **55** with K_2CO_3 at 50 °C

Compound **55** (1.0 g, 2.5 mmol) in dioxan (30 ml) was added as a slurry to a solution of K_2CO_3 (2.8 g, 20 mmol) in water (15 ml). The reaction mixture was heated to 50 °C for 3.5 h after which time a ^{1}H NMR spectrum showed only **55** and **54** to be present (5:1 ratio, respectively). A further portion of dioxan (30 ml) was added and the

heating continued for a further 1.5 h. A ^{1}H NMR spectrum after this time showed only **5 5** and **5 4** to be present (ratio **5 5**:**5 4** 3.5:1).

(d) Reaction of **5 5** with NaOH/pyridine/water at room temperature

Compound **5 5** (600 mg, 1.50 mmol) was added to a stirred solution of pyridine (32 ml), NaOH (215 mg, 5.38 mmol), and water (1 ml). The reaction was stirred at room temperature for 48 h after which time the resulting solution was diluted with water (20 ml), carefully acidified with conc. HCl (ca. 50 ml), and then extracted with CH_2Cl_2 (2 x 100 ml). The CH_2Cl_2 extracts were combined, washed with water (50 ml), saturated $NaHCO_3$ solution (50 ml), water (50 ml), dried over $MgSO_4$, and the solvent removed under reduced pressure to give a brown oil (409 mg). Radial chromatography (2 mm silica plate, 15% ethyl acetate/pet. ether elution) gave pure 6-phenylsulphonyl-*exo*-tricyclo[3.2.2.0^{2,4}]nona-6,8-diene **6 7** (205 mg, 53%).

(e) Reaction of **5 5** with pyridine/water at room temperature

8-*anti*-9-*anti*-Bis(phenylsulphonyl)-*endo*-tricyclo[3.2.2.0^{2,4}]non-6-ene **5 5** (304 mg, 0.76 mmol) was dissolved in pyridine (16 ml) and the resulting solution stirred at room temperature. After 7 days a ^{1}H NMR spectrum showed no formation of **6 7**. Water (1 ml) was then added and the reaction continued for a further 9 days. The reaction was then poured into water (10 ml), acidified with conc. HCl, and extracted with CH_2Cl_2 (2 x 45 ml). The combined CH_2Cl_2 extracts were washed with water (20 ml), saturated $NaHCO_3$ solution (20 ml), water (20 ml), dried over $MgSO_4$, and the solvent removed under reduced pressure to give a brown solid (217 mg). A ^{1}H NMR of the residue showed only starting material **5 5** to be present.

6-Phenylsulphonyl-*exo*-tricyclo[3.2.2.0^{2,4}]nona-6,8-diene 67

Colourless crystals: mp 85-86 °C (pet. ether).

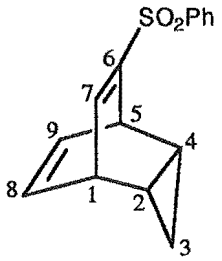

^{1}H NMR δ_H(CDCl$_3$): 7.84 (m, H2', H6'), 7.62* (H4'), 7.56* (H7), 7.54* (H3', H5'), 5.86-5.95 (m, H8, H9), 3.84-3.90 (m, H1, H5), 1.21 (m, $^3J_{4,2} = {}^3J_{4,3endo} = 7.7$ Hz, $^3J_{4,3exo} = 3.8$ Hz, H4), 1.09 (m, $^3J_{2,3endo} = {}^3J_{2,4} = 7.4$ Hz, $^3J_{2,3exo} = 3.8$ Hz, H2), 0.68 (d of t, $^2J_{3exo,3endo} = 6.0$ Hz, $^3J_{3exo,2} = {}^3J_{3exo,4} = 3.6$ Hz, H3*exo*), 0.52 (d of t, $^2J_{3endo,3exo} = 6.2$ Hz, $^3J_{3endo,2} = 7.1$ Hz, H3*endo*).

^{13}C NMR δ_C(CDCl$_3$): 152.8 (C6), 149.8 (C7), 139.6 (C1'), 133.1 (C4'), 129.6$_9$ (C8, C9), 129.1 (C3', C5'), 127.7 (C2', C6'), 39.6 (C5 or C1), 39.1 (C1 or C5), 18.6 (C2), 17.3 (C4), 17.1 (C3).

IR (KBr): 3066 (m), 2982 (m), 2966 (m), 1616 (w), 1581 (m), 1302 (s), 1153 (s) cm^{-1}.

HRMS: $C_{15}H_{14}O_2S$ $M^{+\cdot}$ requires 258.0715; Found 258.0714 (21.4%).

Elemental Analysis: Calc. C 69.74%, H 5.46%, S 12.41%; Found C 69.52%, H 5.64%, S 12.42%.

Synthesis of 8-*anti*- and 8-*syn*-phenylsulphonyl-*endo*-tricyclo[3.2.2.0^{2,4}]non-6-ene by reduction of **67** with $NaBH_4$

A vigorously stirred solution of **67** (107 mg, 0.41 mmol) and sodium borohydride (235 mg, 6.21 mmol, 15 mole equivalents) in THF (30 ml) was refluxed under a nitrogen atmosphere for 6 days. The solvent was removed under reduced pressure, the residue taken up with water (10 ml), and the aqueous solution extracted with CH_2Cl_2 (3 x 20 ml). The combined CH_2Cl_2 extracts were washed with water (2 x 30 ml), 5% $NaHCO_3$ solution (30 ml), water (30 ml), and dried over $MgSO_4$. The CH_2Cl_2 was removed under reduced pressure to give a cloudy white semisolid (107 mg). TLC mesh column chromatography (10 g TLC grade silica, 10% ethyl acetate/pet. ether elution) gave **65** (25 mg, 23%) and **66** (37 mg, 35%).

Synthesis of *endo*-tricyclo[3.2.2.0^{2,4}]non-6-ene **56** by sodium amalgam reduction of 8-*anti*-phenylsulphonyl-*endo*-tricyclo[3.2.2.0^{2,4}]non-6-ene **65**

The general method outlined by Paquette et al.[88] was used. Sulphone **65** (263 mg, 1.01 mmol), anhydrous disodium hydrogen phosphate (580 mg, 4.08 mmol), and 6% sodium amalgam (5.275 g, 13.7 mmol of Na, 13.6 mole equivalents) were stirred in dry methanol (10 ml, distilled immediately before use from magnesium methoxide) at room temperature under a nitrogen atmosphere for 49 h. The solution was decanted into a beaker, diluted with water (30 ml), and flask rinsed with pentane (2 x 20 ml) and ether (10 ml). The organic extracts were combined and used to extract the aqueous solution which was then further extracted with ether (25 ml). The ether and pentane extracts were combined, washed with water (2 x 15 ml), saturated brine solution (15 ml), dried over $MgSO_4$, and the solvent removed by distillation through a short vigreux column. Column chromatography (5 g neutral alumina, pentane elution) of the resulting oil gave **56** (47 mg, 39% isolated yield) which was identified by comparison of its ^1H NMR spectra with that reported.[67]

Reaction of *exo*-tricyclo[3.2.1.0^{2,4}]octane **46** with bromine in carbon tetrachloride

Bromine (371 mg, 2.32 mmol) in CCl_4 (10 ml) was added dropwise over 10 minutes to a stirred solution of **46** (313 mg, 2.89 mmol, 1.1 mole equivalent) in CCl_4 (5 ml). The reaction was stirred in the dark at room temperature for 3 h after which time it was washed with an aqueous sodium metabisulphite solution and twice with water. The CCl_4 was separated, dried over $MgSO_4$, and carefully removed under reduced pressure to give a yellow oil (491 mg, ca. 79% recovery). GLC analysis showed the presence of

three products, 2-*exo*-4-*endo*-dibromobicyclo[3.2.1]octane **70a** (58%), 2-*exo*-4-*exo*-dibromobicyclo[3.2.1]octane **71a** (36%), and one other compound (ca. 6%) which was not identified. The major products were separated by column chromatography (silica gel, 67:1 ratio absorbant to sample loaded, pentane elution).

2-*exo*-4-*endo*-Dibromobicyclo[3.2.1]octane 70a

Colourless oil.

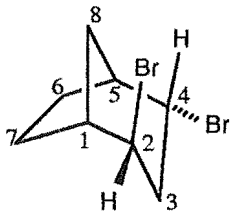

^{1}H NMR $\delta_H(CDCl_3)$: 4.52 (m, $^3J_{4,3endo}$ = 11.1 Hz, $^3J_{4,3exo}$ = 5.8 Hz, $^4J_{4,6exo}$ = 1.0 Hz, H4), 4.24 (m, $^4J_{2,8anti}$ = 2.0 Hz, H2), 2.57* (H5), 2.53* (H1), 2.33-2.45 (m, H3*endo*, H3*exo*), 2.30 (d, $^2J_{8syn,8anti}$ = 12.5 Hz, H8*syn*), 1.87 (m, $^4J_{6endo,8syn}$ =2.1 Hz, H6*endo*), 1.82* (H7*exo*), 1.71 (m, H6*exo*), 1.58 (m, $^2J_{8anti,8syn}$ = 12.5 Hz, $^3J_{8anti,1} = {}^3J_{8anti,5}$ = 5.0 Hz, $^4J_{8anti,2}$ = 2.0 Hz, H8*anti*), 1.47 (m, $^4J_{7endo,8syn}$ = 2.0 Hz, H7*endo*).

^{13}C NMR $\delta_C(CDCl_3)$: 55.9 (C4), 53.0 (C2), 44.1 (C5), 42.1 (C1), 39.7 (C3), 35.2 (C8), 28.8 (C7), 23.8 (C6).

HRMS: $C_8H_{12}{}^{81}Br_2$ $M^{+\cdot}$ requires 269.9267; Found 269.9180 (2.6%).

$C_8H_{12}{}^{79}Br\,{}^{81}Br$ $M^{+\cdot}$ requires 267.9287; Found 267.9235 (7.0%)

$C_8H_{12}{}^{79}Br_2$ $M^{+\cdot}$ requires 265.9307; Found 265.9240 (4.6%).

$C_8H_{11}{}^{81}Br_2$ $[M-1]^{+\cdot}$ requires 268.9189; Found 268.9187 (36.0%).

$C_8H_{11}{}^{79}Br{}^{81}Br$ $[M-1]^{+\cdot}$ requires 266.9209; Found 266.9208 (78.8%)

$C_8H_{11}{}^{79}Br_2$ $[M-1]^{+\cdot}$ requires 264.9229; Found 264.9231 (41.9%).

2-*exo*-4-*exo*-Dibromobicyclo[3.2.1]octane 71a

Colourless crystals: mp 109-111 °C (CCl_4).

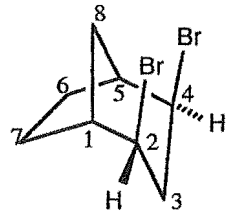

^{1}H NMR $\delta_H(C_6D_6)$: 3.77 (m, H2, H4), 3.03 (d, $^2J_{8syn,8anti}$ = 12.4 Hz, H8*syn*), 2.31 (m, H1, H5), 2.18 (d, $^2J_{3exo,3endo}$ = 17.7 Hz, H3*exo*), 1.84 (d of t, $^2J_{3endo,3exo}$ = 17.8 Hz, $^3J_{3endo,2} = {}^3J_{3endo,4}$ = 5.5 Hz, H3*endo*), 1.29 (m, H6*exo*, H7*exo*), 1.10 (m, $^2J_{8anti,8syn}$ = 12.4 Hz, $^3J_{8anti,1} = {}^3J_{8anti,5}$ = 5.6 Hz, $^4J_{8anti,2} = {}^4J_{8anti,4}$ = 1.5 Hz, H8*anti*), 0.80 (m, $^2J_{6endo,6exo} = {}^2J_{7endo,7exo}$ = 15.6 Hz, $^4J_{6endo,8syn} = {}^4J_{7endo,8syn}$ = 2.1 Hz, H6*endo*, H7*endo*).

^{13}C NMR $\delta_C(C_6D_6)$: 52.1 (C2, C4), 44.0 (C1, C5), 35.5 (C3), 29.8 (C8), 28.7 (C6, C7).

IR (KBr): 2958 (m), 2620 (m), 1653 (m), 1628 (m) cm^{-1}.

HRMS: $C_8H_{12}{}^{81}Br_2$ $M^{+\cdot}$ requires 269.9267; Found 269.9288 (2.6%)

$C_8H_{12}{}^{79}Br\,{}^{81}Br$ $M^{+\cdot}$ requires 267.9287; Found 267.9295 (5.5%)

$C_8H_{12}{}^{79}Br_2$ $M^{+\cdot}$ requires 265.9307; Found 265.9311 (3.1%).

Reaction of *exo*-tricyclo[3.2.1.0^{2,4}]octane **46** with bromine in methanol

Bromine (348 mg, 2.18 mmol) in dry methanol (10 ml) was added dropwise over 10 minutes to a stirred solution of **46** (296 mg, 2.74 mmol, 1.26 mole equivalents) in dry methanol (5 ml) at room temperature. The reaction was stirred in the dark for 1.5 h after which time it was diluted with an aqueous solution of sodium metabisulphite (15 ml) and extracted with ether (2 x 20 ml). The ether extracts were combined, washed with saturated brine solution (5 ml), dried over $MgSO_4$, and the solvent removed under reduced pressure to give a yellow oil (355 mg, ca. 74 % recovery). GLC analysis showed the presence of four products, 2-*endo*-bromo-5-*endo*-methoxybicyclo-[2.2.2]octane **72b** (50%), 2-*exo*-bromo-4-*exo*-methoxybicyclo[3.2.1]octane **71b** (46%), 2-*exo*-4-*exo*-dibromobicyclo[3.2.1]octane **71a** (2%) and one other compound (2%) which was not identified. A crude separation was effected by radial chromatography (2 mm silica plate, gradient elution starting with 2% ether/pentane) after which the major products were further purified by column chromatography (silica gel, 100:1 ratio absorbant to sample, 2% ether/pet. ether elution). 2-*exo*-4-*exo*-Dibromobicyclo-[3.2.1]octane **71a** was identified by comparison of its ^{1}H NMR data with that reported above for the reaction of **46** with bromine in CCl_4.

2-*endo*-Bromo-5-*endo*-methoxybicyclo[2.2.2]octane 72b

Colourless oil.

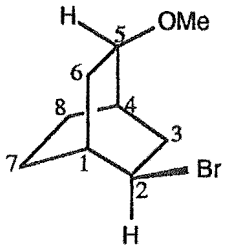

^{1}H NMR $\delta_H(C_6D_6)$: 4.07 (m, $^3J_{2,1}$ = 2.1 Hz, $^3J_{2,3endo}$ = 6.2 Hz, $^3J_{2,3exo}$ = 10.3 Hz, $^4J_{2,6exo}$ = 2.1 Hz, H2), 3.16 (s, $W_{h/2}$ = 0.8 Hz, OMe), 3.12 (m, H5), 2.62 (d of d, $^2J_{3endo,3exo}$ = 14.4 Hz, $^3J_{3endo,2}$ = 6.2 Hz, H3*endo*), 2.24 (m, $^2J_{6endo,6exo}$ = 14.1 Hz, H6*endo*), 1.91 (m, $^2J_{3exo,3endo}$ = 14.2 Hz, $^3J_{3exo,2}$ = 10.3 Hz, $^3J_{3exo,4}$ = 3.9 Hz, $^4J_{3exo,5}$ = 1.7 Hz, H3*exo*), 1.83 (m, H1), 1.72 (m, $^2J_{6exo,6endo}$ = 13.5 Hz, $^3J_{6exo,5}$ = 9.5 Hz, $^3J_{6exo,1}$ = 4.1 Hz, $^4J_{6exo,2}$ = 2.0 Hz, H6*exo*), 1.55 (m, H4) 1.14-1.23 (m, H7*anti*, H7*syn*), 1.04-1.13 (m, H8*anti*, H8*syn*).

^{13}C NMR $\delta_C(C_6D_6)$: 78.1 (C5), 55.8 (OMe), 53.2 (C2), 35.1 (C1), 33.2 (C3), 30.5 (C4), 30.2 (C6), 25.6 (C7), 22.1 (C8).

LRMS: $C_9H_{15}{}^{81}BrO$ $M^{+\cdot}$ requires 220; Found 220 (85%)

$C_9H_{15}{}^{79}BrO$ $M^{+\cdot}$ requires 218; Found 218 (84%).

HRMS: $C_9H_{15}{}^{79}BrO$ $M^{+\cdot}$ requires 218.0307; Found 218.0300 (3.6%).

2-*exo*-Bromo-4-*exo*-methoxybicyclo[3.2.1]octane 71b

Colourless oil.

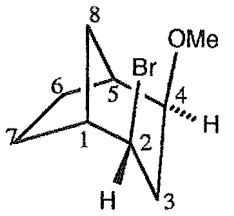

^{1}H NMR δ_H**(CDCl$_3$):** 4.21 (m, H2), 3.34 (s, $W_{h/2}$ = 0.7 Hz, OMe), 3.26 (m, H4), 2.53 (d, $^2J_{8syn,8anti}$ = 12.0 Hz, H8*syn*), 2.50* (H1), 2.45 (m, H5), 2.21 (d, $^2J_{3exo,3endo}$ = 16.5 Hz, H3*exo*), 2.05 (d of t, $^2J_{3endo,3exo}$ = 16.5 Hz, $^3J_{3endo,2} = {}^3J_{3endo,4}$ = 5.0 Hz, H3*endo*), 1.75-1.80 (m, H6*exo*, H7*exo*), 1.45 (m, $^4J_{7endo,8syn}$ = 1.8 Hz, H7*endo*), 1.34 (m, $^4J_{6endo,8syn}$ = 1.8 Hz, H6*endo*), 1.22 (m, $^2J_{8anti,8syn}$ = 12.0 Hz, $^3J_{8anti,1} = {}^3J_{8anti,5}$ = 4.7 Hz, $^4J_{8anti,2} = {}^4J_{8anti,4}$ = 1.8 Hz, H8*anti*).

^{13}C NMR δ_C**(CDCl$_3$):** 79.7 (C4), 56.0 (OMe), 53.7 (C2), 43.3 (C1), 38.0 (C5), 30.6 (C3), 28.1 (C7), 27.9 (C8), 25.9 (C6).

HRMS: $C_9H_{15}{}^{81}BrO$ $M^{+\cdot}$ requires 220.0287; Found 220.0279 (16.4%)
$C_9H_{15}{}^{79}BrO$ $M^{+\cdot}$ requires 218.0307; Found 218.0297 (16.8%).

Reaction of *endo*-tricyclo[3.2.1.0^{2,4}]octane **1** with bromine in carbon tetrachloride

To stirred solution of **1** (150 mg, 1.39 mmol) in CCl_4 (2 ml) was added bromine (186 mg, 1.16 mmol, 0.83 mole equivalents) in CCl_4 (5 ml) dropwise over 10 minutes. The reaction was stirred in the absence of light for 4 h and then washed with a solution of sodium metabisulphite, water (5 ml), and dried over $MgSO_4$. The solvent was carefully removed under reduced pressure to give a yellow oil (268 mg, ca. 86% recovery) which was shown by GLC analysis to consist of four compounds, 2-*exo*-3-*endo*-dibromobicyclo[3.2.1]octane **75a** (48%), 2-*endo*-4-*endo*-dibromobicyclo[3.2.1]octane **76a** (29%), 2-*endo*-6-*endo*-dibromobicyclo[3.2.1]octane **77a** (15%), and one other compound (8%) which was not identified. A crude separation of the products was effected by radial chromatography (1 mm PEG coated silica plate, pentane elution). 2-*exo*-3-*endo*-Dibromobicyclo[3.2.1]octane **75a** was further purified by preparative GLC. Compounds **76a** and **77a** were separated by preparative TLC (analytical grade silica TLC plates, multiple elution with 3% ethyl acetate/pentane).

2-*exo*-3-*endo*-Dibromobicyclo[3.2.1]octane 75a

Colourless oil.

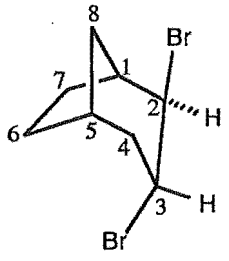

^{1}H NMR δ_H**(CDCl$_3$):** 4.84 (s, $W_{h/2}$ = 6.9 Hz, H2), 4.66 (d, $^3J_{3,4exo}$ = 6.3 Hz, H3), 2.64 (m, H1), 2.51 (m, $^2J_{4exo,4endo}$ = 15.9 Hz, $^3J_{4exo,3}$ = 6.4 Hz, $^3J_{4exo,5}$ = 3.2 Hz, H4*exo*), 2.34 (m, H5), 2.19-2.29 (m, H6*endo*, H7*endo*), 2.10 (m, $^2J_{4endo,4exo}$ = 15.7 Hz, $^3J_{4endo,5}$ = 3.4 Hz, H4*endo*), 2.06 (d, $^2J_{8syn,8anti}$ = 11.7 Hz, H8*syn*), 1.85* (H7*exo*), 1.77* (H6*exo*), 1.44 (m, H8*anti*).

^{13}C NMR δ_C(CDCl$_3$): 60.1 (C2), 48.8 (C3), 43.6 (C1), 36.7 (C4), 33.9 (C5), 33.1 (C8), 29.1 (C7), 27.4 (C6).

LRMS: $C_8H_{12}{}^{81}Br_2$ $M^{+\cdot}$ requires 270; Found 270 (0.3%)
$C_8H_{12}{}^{79}Br{}^{81}Br$ $M^{+\cdot}$ requires 268; Found 268 (0.5%)
$C_8H_{12}{}^{79}Br_2$ $M^{+\cdot}$ requires 266; Found 266 (0.3%)
$C_8H_{12}{}^{81}Br$ $[M\text{-}Br]^{+\cdot}$ requires 189; Found 189 (66%)
$C_8H_{12}{}^{79}Br$ $[M\text{-}Br]^{+\cdot}$ requires 187; Found 187 (67%).

HRMS: $C_8H_{12}{}^{79}Br{}^{81}Br$ $M^{+\cdot}$ requires 267.9287; Found 267.9249 (1.3%)
$C_8H_{12}{}^{81}Br$ $[M\text{-}Br]^{+\cdot}$ requires 189.0103; Found 189.0097 (100.0%)
$C_8H_{10}{}^{79}Br$ $[M\text{-}83]^{+\cdot}$ requires 184.9966; Found 184.9949 (2.1%).

2-*endo*-4-*endo*-Dibromobicyclo[3.2.1]octane 76a

Colourless oil.

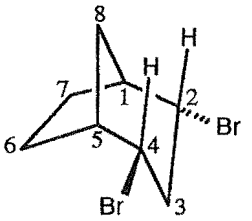

^{1}H NMR δ_H(CDCl$_3$): 4.09 (m, $^3J_{2,1} = {}^3J_{4,5} = 2.8$ Hz, $^3J_{2,3endo} = {}^3J_{4,3endo} = 11.8$ Hz, $^3J_{2,3exo} = {}^3J_{4,3exo} = 5.2$ Hz, H2, H4), 2.64 (m, $^2J_{3exo,3endo} = 13.4$ Hz, $^3J_{3exo,2} = {}^3J_{3exo,4} = 5.3$ Hz, H3*exo*), 2.55 (m, H1, H5), 2.24 (d of t, $^2J_{3endo,3exo} = 13.3$ Hz, $^3J_{3endo,2} = {}^3J_{3endo,4} = 11.7$, H3*endo*), 1.91 (m, H6*endo*, H7*endo*), 1.83 (d of t, $^2J_{8anti,8syn} = 12.7$ Hz, $^3J_{8anti,1} = {}^3J_{8anti,5} = 5.3$ Hz, H8*anti*), 1.73 (m, H6*exo*, H7*exo*), 1.55 (d, $^2J_{8syn,8anti} = 12.7$ Hz, H8*syn*).

^{13}C NMR δ_C(CDCl$_3$): 53.2 (C2, C4), 42.7 (C1, C5), 41.3 (C3), 38.7 (C8), 24.4 (C6, C7).

HRMS: $C_8H_{12}{}^{81}Br_2$ $M^{+\cdot}$ requires 269.9267; Found 269.9278 (2.1%)
$C_8H_{12}{}^{79}Br{}^{81}Br$ $M^{+\cdot}$ requires 267.9287; Found 267.9457 (4.7%)
$C_8H_{12}{}^{79}Br_2$ $M^{+\cdot}$ requires 265.9307; Found 265.9384 (3.4%).

2-*endo*-6-*endo*-Dibromobicyclo[3.2.1]octane 77a

White solid.

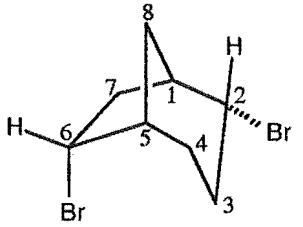

^{1}H NMR δ_H(CDCl$_3$): 4.38 (m, $^3J_{6,5} = {}^3J_{6,7endo} = 5.6$ Hz, $^3J_{6,7exo} = 10.7$ Hz, H6), 4.25 (m, $^4J_{2,7exo} = 1.0$ Hz, H2), 2.56 (m, H1), 2.49 (m, $^3J_{7exo,6} = 11.0$ Hz, $^4J_{7exo,2} = 1.2$ Hz, H7*exo*), 2.33 (m, H5), 2.12* (H7*endo*), 2.14-2.22 (m, H3*endo*, H3*exo*), 1.99 (m, $^2J_{4endo,4exo} = 16.2$ Hz, $^4J_{4endo,8anti} = 2.9$ Hz, H4*endo*), 1.77 (m, H8*anti*), 1.65* ($^4J_{8syn,7endo} = 3.0$ Hz, H8*syn*), 1.57* (H4*exo*).

^{13}C NMR δ_C(CDCl$_3$): 56.5 (C2), 51.1 (C6), 44.8 (C1), 38.8 (C5), 38.0 (C8), 36.4 (C7), 30.9 (C3), 30.4 (C4).

LRMS: $C_8H_{12}{}^{81}Br_2$ $M^{+\cdot}$ requires 270; Found 270 (0.2%)
$C_8H_{12}{}^{79}Br{}^{81}Br$ $M^{+\cdot}$ requires 268; Found 268 (0.3%)
$C_8H_{12}{}^{79}Br_2$ $M^{+\cdot}$ requires 266; Found 266 (0.2%)

$C_8H_{12}{}^{81}Br$ $[M\text{-}Br]^{+\cdot}$ requires 189; Found 189 (85%)

$C_8H_{12}{}^{79}Br$ $[M\text{-}Br]^{+\cdot}$ requires 187; Found 187 (86%).

HRMS: $C_8H_{12}{}^{81}Br$ $[M\text{-}Br]^{+\cdot}$ requires 189.0103; Found 189.0102 (100.0%).

Attempted synthesis of bicyclo[3.2.1]oct-2-ene **79** by reaction of *endo*-tricyclo-[3.2.1.$0^{2,4}$]octane **1** with acid in carbon tetrachloride

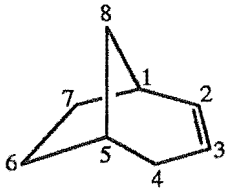

Trifluoroacetic acid (1 drop) was added to a solution of **1** (16 mg, 0.15 mmol) in CCl_4 (1 ml), the solution was stirred at room temperature and the progress of the reaction monitored by ^1H NMR. After 6 days a ^1H NMR spectrum showed no significant reaction. The reaction was then heated to 70 °C for a further 6 days after which time a ^1H NMR spectrum of the resulting mixture again showed that no reaction had occurred. A catalytic amount of HBr in acetic acid was added and the reaction continued at room temperature for 12 days. A ^1H NMR spectrum after this time showed no reaction. The solution was heated to 70 °C for a further 14 days, but again no significant reaction was observed by ^1H NMR after this time.

Reaction of *endo*-tricyclo[3.2.1.$0^{2,4}$]octane **1** with bromine in methanol

To a stirred solution of **1** (117 mg, 1.08 mmol) in dry methanol (3 ml) was added bromine (154 mg, 0.96 mmol, 0.89 mole equivalents) in dry methanol (5 ml) dropwise over 10 minutes. The solution was stirred at room temperature for 2 h after which time the reaction was diluted with water (8 ml) and sodium metabisulphite added until all of the bromine colour had dissipated. The solution was extracted with ether (20 ml), the ether extracts washed with water, dried over $MgSO_4$, and the solvent removed under reduced pressure to give a yellow oil (132 mg, ca. 60% recovery). GLC analysis showed the presence of three products, 2-*endo*-bromo-4-*endo*-methoxybicyclo[3.2.1]octane **76b** (53%), 6-*endo*-bromo-2-*endo*-methoxybicyclo[3.2.1]octane **77b** (44%), and 2-*endo*-4-*endo*-dibromobicyclo[3.2.1]octane **76a** (3%). A crude separation was effected by radial chromatography (2 mm PEG coated silica plate, pentane elution). The major products were further purified by preparative TLC (analytical grade silica TLC plates, 1% ethyl acetate/pentane elution). 2-*endo*-4-*endo*-Dibromobicyclo[3.2.1]octane **76a** was identified by comparison of its ^1H NMR data with that reported above.

2-*endo*-Bromo-4-*endo*-methoxybicyclo[3.2.1]octane 76b

Colourless oil.

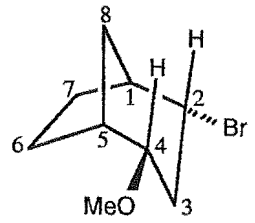

^{1}H NMR δ_H($CDCl_3$): 4.12 (m, $^3J_{2,1}$ = 2.0 Hz, $^3J_{2,3endo}$ = 11.3 Hz, $^3J_{2,3exo}$ = 5.4 Hz, H2), 3.29 (s, $W_{h/2}$ = 1.0 Hz, OMe), 3.17 (m, $^3J_{4,3endo}$ = 12.2 Hz, $^3J_{4,3exo}$ = 5.2 Hz, $^3J_{4,5}$ = 2.3 Hz, H4), 2.46* (H1), 2.44# (m, H3*exo*), 2.41* (H5), 1.80* (H7*endo*), 1.75* (H6*endo*), 1.71# (d of t, $^2J_{8anti,8syn}$ = 11.7 Hz, $^3J_{8anti,1}$ = $^3J_{8anti,5}$ = 5.9 Hz, H8*anti*), 1.69# (d of t, $^2J_{3endo,3exo}$ = 13.0 Hz, $^3J_{3endo,2}$ = $^3J_{3endo,4}$ = 10.9 Hz, H3*endo*), 1.62* (H7*exo*), 1.56* (H6*exo*), 1.33 (d, $^2J_{8syn,8anti}$ = 12.2 Hz, H8*syn*).

^{13}C NMR δ_C($CDCl_3$): 80.5 (C4), 55.8 (OMe), 53.8 (C2), 43.4 (C1), 37.1 (C5), 37.0 (C3), 35.6 (C8), 24.7 (C7), 22.8 (C6).

HRMS: $C_9H_{15}{}^{79}BrO$ $M^{+\cdot}$ requires 218.0307; Found 218.0375 (46.0%)

$C_9H_{15}O$ $[M\text{-}Br]^{+\cdot}$ requires 139.1123; Found 139.1133 (55.6%).

6-*endo*-Bromo-2-*endo*-methoxybicyclo[3.2.1]octane 77b

Colourless oil.

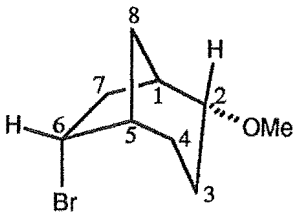

^{1}H NMR δ_H($CDCl_3$): 4.36 (m, $^3J_{6,7endo}$ = 5.7 Hz, $^3J_{6,7exo}$ = 10.7 Hz, H6), 3.30 (s, $W_{h/2}$ = 0.6 Hz, OMe), 3.24 (m, $^3J_{2,1}$ = $^3J_{2,3exo}$ = 3.4 Hz, $^3J_{2,3endo}$ = 10.3 Hz, H2), 2.37 (m, H1), 2.29 (m, H7*exo*), 2.20 (m, H5), 1.99 (m, $^2J_{7endo,7exo}$ = 14.5 Hz, $^3J_{7endo,6}$ = 5.6 Hz, $^4J_{7endo,8syn}$ = 2.5 Hz, H7*endo*), 1.97* (H4*endo*), 1.89* (H3*exo*), 1.70 (m, $^2J_{8anti,8syn}$ = 12.3 Hz, $^3J_{8anti,1}$ = $^3J_{8anti,5}$ = 5.4 Hz, $^4J_{8anti,4endo}$ = 2.9 Hz, H8*anti*), 1.51* (H3*endo*), 1.47* (H4*exo*), 1.44 (d of d, $^2J_{8syn,8anti}$ = 12.0 Hz, $^4J_{8syn,7endo}$ = 2.7 Hz, H8*syn*).

^{13}C NMR δ_C($CDCl_3$): 80.8 (C2), 55.4 (OMe), 52.5 (C6), 39.4 (C5), 38.6 (C1), 35.2 (C8), 35.0 (C7), 27.7 (C4), 25.2 (C3).

LRMS: $C_9H_{15}{}^{81}BrO$ $M^{+\cdot}$ requires 220; Found 220 (0.7%)

$C_9H_{15}{}^{79}BrO$ $M^{+\cdot}$ requires 218; Found 218 (0.7%).

HRMS: $C_9H_{15}{}^{79}BrO$ $M^{+\cdot}$ requires 218.0307; Found 218.0327 (30.9%).

Reaction of 2-methyl-*endo*-tricyclo[3.2.1.0^{2,4}]oct-6-ene **8 6** with bromine in carbon tetrachloride

A solution of bromine (396 mg , 2.48 mmol) in CCl_4 (10 ml) was added dropwise over 10 minutes to a stirred solution of **8 6** (320 mg, 2.66 mmol, 1.1 mole equivalents) in CCl_4 (5 ml) at room temperature. After 1 h the solvent was removed under reduced pressure to give a brown oil (696 mg, ca. 100% recovery). A ^{1}H NMR spectrum showed the oil to consist of one major product which was later identified as 7-*exo*-8-*anti*-dibromo-2-methylbicyclo[3.2.1]oct-2-ene **8 7** (ca. 80%). The major product was purified

by rapid radial chromatography (2 mm silica plate, 10% ether/pentane elution). The product ratios could not be determined by GLC analysis due to the instability of the major product (GLC analysis showed five products, 10-20% each, to be present which was not in agreement with the ^{1}H NMR spectrum). A large number of minor products were also present but these were estimated (^{1}H NMR) to comprise not more than 20% of the overall reaction mixture.

7-*exo*-8-*anti*-Dibromo-2-methylbicyclo[3.2.1]oct-2-ene 87

Colourless oil.

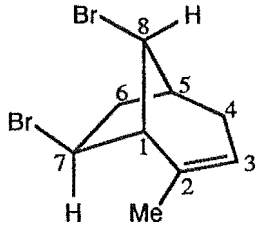

^{1}H NMR δ_H(CDCl$_3$): 5.14 (s, $W_{h/2}$ = 8.0 Hz, H3), 4.42 (s, $W_{h/2}$ = 3.1 Hz, H8), 4.27 (m, $^3J_{7,6endo}$ = 8.3 Hz, $^3J_{7,6exo}$ = 3.8 Hz, H7) 2.88 (m, $^2J_{6exo,6endo}$ = 14.8 Hz, H6*exo*), 2.84 (s, $W_{h/2}$ = 4.1 Hz, H1), 2.71 (m, H5), 2.54 (m, $^2J_{4exo,4endo}$ = 17.9 Hz, H4*exo*), 2.43 (d of d, $^2J_{6endo,6exo}$ = 14.9, $^3J_{6endo,7}$ = 8.3 Hz, H6*endo*), 1.92 (m, $^2J_{4endo,4exo}$ = 17.8 Hz, H4*endo*), 1.73 (d of d, $^4J_{Me,3}$ = 3.9 Hz, Me).

^{13}C NMR δ_C(CDCl$_3$): 140.0 (C2), 119.1 (C3), 57.5 (C1), 55.9 (C8), 48.9 (C7), 44.8 (C5), 43.3 (C6), 36.2 (C4), 22.2 (Me).

HRMS: $C_9H_{12}{}^{81}Br_2$ $M^{+\cdot}$ requires 281.9267; Found 281.9244 (5.8%)

$C_9H_{12}{}^{79}Br^{81}Br$ $M^{+\cdot}$ requires 279.9287; Found 279.9241 (11.8%)

$C_9H_{12}{}^{79}Br_2$ $M^{+\cdot}$ requires 277.9307; Found 277.9240 (6.9%).

Reaction of 2-methyl-*endo*-tricyclo[3.2.1.0^{2,4}]oct-6-ene **86** with bromine in carbon tetrachloride at -10 °C

The reaction procedure was similar to that used for the reaction of **86** with bromine in carbon tetrachloride at room temperature, except that the reaction was carried out at -10 °C (ice-NaCl bath) using **86** (126 mg, 1.05 mmol), bromine (138 mg, 0.86 mmol, 0.82 mole equivalents), and gave a yellow oil (309 mg). A ^{1}H NMR spectrum showed a complex reaction mixture consisting of 7-*exo*-8-*anti*-dibromo-2-methylbicyclo[3.2.1]oct-2-ene **87** (30-40%), two other major products (ca. 10% and 20%), 6-*exo*-bromo-4-methyltricyclo[3.2.1.0^{2,7}]oct-3-ene **90** (ca. 5%) and numerous other minor products. Attempted purification by column chromatography (silica gel, gradient elution with ether/pentane, initially 100% pentane) failed to give any significant separation. Compound **90** was not isolated, but was identified from a ^{1}H NMR spectrum of the crude reaction mixture.

Reaction of 2-methyl-*endo*-tricyclo[3.2.1.0^{2,4}]oct-6-ene **86** with bromine in methanol

A solution of bromine (280 mg, 1.75 mmol) in dry methanol (10 ml) was added dropwise over 10 minutes to a stirred solution of **86** (235 mg, 1.96 mmol, 1.1 mol

equivalents) in dry methanol (5 ml) at room temperature. The reaction was stirred for 2.5 h after which time the methanol was removed under reduced pressure to give a yellow oil (669 mg, some MeOH still present). A ^{1}H NMR spectrum of the oil showed a complex reaction mixture with numerous products. Attempted separation by radial chromatography (2 mm silica plate, ether/pentane gradient elution) followed by further purification by dry column flash chromatography gave two products, 7-*anti*-bromo-5-*endo*-methoxy-1-methylbicyclo[2.2.2]oct-2-ene **91** (ca. 15%) and 6-*exo*-bromo-4-methyltricyclo-[3.2.1.0^{2,7}]oct-3-ene **90** (ca. 10%), no other products were isolated.

7-*anti*-Bromo-5-*endo*-methoxy-1-methylbicyclo[2.2.2]oct-2-ene 91

Colourless oil.

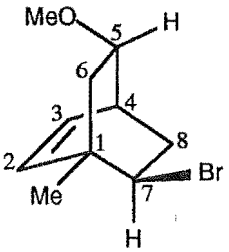

^{1}H NMR δ_H(CDCl$_3$): 6.23 (t, $^3J_{3,2} = {}^3J_{3,4} = 8.1$ Hz, H3), 6.07 (d, $^3J_{2,3} = 8.0$ Hz, H2), 3.80 (m, $^3J_{7,8syn} = 10.1$ Hz, $^3J_{7,8anti} = 4.3$ Hz, $^4J_{7,6endo} = 2.4$ Hz, H7), 3.69 (d of t, $^3J_{5,4} = {}^3J_{5,6endo} = 3.0$ Hz, $^3J_{5,6exo} = 8.1$ Hz, H5), 3.29 (s, $W_{h/2} = 0.6$ Hz, OMe), 2.82 (m, H4), 2.36 (d of d, $^2J_{6exo,6endo} = 13.7$ Hz, $^3J_{6exo,5} = 8.1$ Hz, H6*exo*), 2.25 (m, $^2J_{8syn,8anti} = 14.4$ Hz, $^3J_{8syn,7} = 10.2$ Hz, $^3J_{8syn,4} = 4.1$ Hz, H8*syn*), 1.81 (m, $^2J_{8anti,8syn} = 14.6$ Hz, $^3J_{8anti,7} = 4.3$ Hz, $^3J_{8anti,4} = 2.1$ Hz, H8*anti*), 1.24 (s, $W_{h/2} = 1.1$ Hz, Me), 1.07 (d of t, $^2J_{6endo,6exo} = 13.7$ Hz, $^3J_{6endo,5} = {}^3J_{6endo,7} = 2.7$ Hz, H6*endo*).

^{13}C NMR δ_C(CDCl$_3$): 136.7 (C2), 132.4 (C3), 80.1 (C5), 58.1 (C7), 55.8 (OMe), 39.4 (C1), 37.3 (C6), 36.8 (C8), 34.8 (C4), 24.1 (Me).

LRMS: $C_{10}H_{15}{}^{81}BrO$ $M^{+\cdot}$ requires 232; Found 232 (0.6%)

$C_{10}H_{15}{}^{79}BrO$ $M^{+\cdot}$ requires 230; Found 230 (0.6%).

HRMS: $C_{10}H_{15}{}^{79}BrO$ $M^{+\cdot}$ requires 230.0307; Found 230.0259 (1.5%).

6-*exo*-Bromo-4-methyltricyclo[3.2.1.0^{2,7}]oct-3-ene 90

Colourless oil.

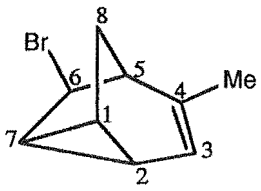

^{1}H NMR δ_H(CDCl$_3$): 5.51 (m, $^3J_{3,2} = 4.8$ Hz, $^4J_{3,Me} = 1.6$ Hz, H3), 3.69 (s $W_{h/2} = 2.5$ Hz, H6), 2.53 (d, $^3J_{5,8anti} = 4.9$ Hz, H5), 2.22 (m, $^2J_{8anti,8syn} = 11.8$ Hz, $^3J_{8anti,1} = 2.3$ Hz, $^3J_{8anti,5} = 4.7$ Hz, H8*anti*), 1.72 (d, $^4J_{Me,3} = 1.7$ Hz, Me), 1.68* (H7), 1.63* (H2), 1.59* (H1), 0.91 (d, $^2J_{8syn,8anti} = 11.8$ Hz, H8*syn*).

^{13}C NMR δ_C(CDCl$_3$): 136.5 (C4), 115.9 (C3), 56.5 (C6), 47.2 (C5), 25.5 (C8), 22.5 (C7), 20.1 (Me), 18.5 (C2), 15.4 (C1).

Reaction of 2-methyl-*endo*-tricyclo[3.2.1.0^{2,4}]oct-6-ene **86** with bromine in methanol at -20 °C and -78 °C

A procedure similar to that used for the reaction of **86** with bromine in MeOH at room temperature was used except that the reactions were cooled to -20 C (CCl_4/dry-ice

bath) or -78 C (acetone/dry-ice bath) and performed in methanol-d_4 to allow analysis of the reaction mixtures by NMR directly without workup. ^{1}H NMR spectra of the crude reactions showed the formation of a complex mixture of products in both cases. The products were not further investigated.

Reaction of 2-methyl-*endo*-tricyclo[3.2.1.0^{2,4}]octane **45** with bromine in carbon tetrachloride

To a stirred solution of **45** (100 mg, 0.82 mmol) in CCl_4 (5 ml) was added bromine (121 mg, 0.76 mmol, 0.93 mole equivalents) in CCl_4 (5 ml) dropwise over 10 minutes. The reaction was stirred in the absence of light for 1.5 h after which time the colourless solution was washed with water (7 ml). The organic extract was separated, dried over $MgSO_4$, and the solvent carefully removed under reduced pressure to give a brown oil (207 mg, ca. 97% recovery). A ^{1}H NMR spectrum showed the oil to consist of 2-*exo*-3-*endo*-dibromo-2-*endo*-methylbicyclo[3.2.1]octane **94** (ca. 80%). A number of minor products were also present (all less than 5%) but were not identified. Purification was effected by radial chromatography (2 mm PEG coated silica plate, pentane elution).

2-*exo*-3-*endo*-Dibromo-2-*endo*-methylbicyclo[3.2.1]octane 94

Colourless oil.

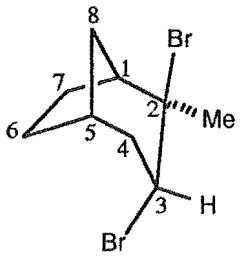

^{1}H NMR $\delta_H(C_6D_6)$: 4.85 (d, $^3J_{3,4exo}$ = 5.8 Hz, H3), 2.47 (m, $^2J_{4exo,4endo}$ = 16.6 Hz, $^3J_{4exo,3}$ = 5.9 Hz, $^3J_{4exo,5}$ = 3.7 Hz, $^4J_{4exo,6exo}$ = 1.2 Hz, H4*exo*), 2.34* (H1), 2.33* (H8*syn*), 2.25* (H6*endo*) 2.12* (H7*endo*), 2.08 (s, $W_{h/2}$ = 1.0 Hz, Me), 2.04 (m, $^2J_{4endo,4exo}$ = 16.6 Hz, $^3J_{4endo,3}$ = 1.2 Hz, $^3J_{4endo,5}$ = 4.9 Hz, $^4J_{4endo,8anti}$ = 2.4 Hz, H4*endo*), 2.03* (H5), 1.50* (H6*exo*), 1.43* (H7*exo*), 1.32 (m, $^2J_{8anti,8syn}$ = 11.6 Hz, $^3J_{8anti,1}$ = $^3J_{8anti,5}$ = 4.9 Hz, $^4J_{8anti,4endo}$ = 2.4 Hz, H8*anti*).

^{13}C NMR $\delta_C(C_6D_6)$: 76.7 (C2), 56.6 (C3), 50.6 (C1), 38.7 (C8), 38.3 (C4), 35.6 (Me), 34.6 (C5), 27.8 (C6), 26.7 (C7).

LRMS: $C_9H_{14}{}^{81}Br_2$ $M^{+\cdot}$ requires 284; Found 284 (0.4%)
$C_9H_{14}{}^{79}Br{}^{81}Br$ $M^{+\cdot}$ requires 282; Found 282 (0.6%)
$C_9H_{14}{}^{79}Br_2$ $M^{+\cdot}$ requires 280; Found 280 (0.4%)
$C_9H_{14}{}^{81}Br$ $[M\text{-}Br]^{+\cdot}$ requires 203; Found 203 (62%)
$C_9H_{14}{}^{79}Br$ $[M\text{-}Br]^{+\cdot}$ requires 201; Found 201 (64%)
C_9H_{14} $[M\text{-}Br_2]^{+\cdot}$ requires 122; Found 122 (13%)
C_9H_{13} $[M\text{-}161]^{+\cdot}$ requires 121; Found 121 (100%).

HRMS: $C_9H_{14}{}^{81}Br$ $[M\text{-}Br]^{+\cdot}$ requires 203.0260; Found 203.0263 (37.2%)
C_9H_{14} $[M\text{-}Br_2]^{+\cdot}$ requires 122.1096; Found 122.1059 (11.5%)
C_9H_{13} $[M\text{-}161]^{+\cdot}$ requires 121.1018; Found 121.1026 (100.0%).

Column chromatography of 2-*exo*-3-*endo*-dibromo-2-*endo*-methylbicyclo[3.2.1]octane **94** on silica

The products from the reaction of 2-methyl-*endo*-tricyclo[3.2.1.$0^{2,4}$]octane **45** with bromine in carbon tetrachloride (207 mg, containing approximately 80% **94**) were subjected to column chromatography (silica gel, 100:1 ratio absorbant to sample loaded, pentane elution). The resulting major product was identified as 2-*exo*-6-*endo*-dibromo-1-methylbicyclo[2.2.2]octane **93**. Compound **94** was not present in any of the fractions collected.

2-*exo*-6-*endo*-Dibromo-1-methylbicyclo[2.2.2]octane 93

Colourless crystals: mp 60-61 °C (pentane).

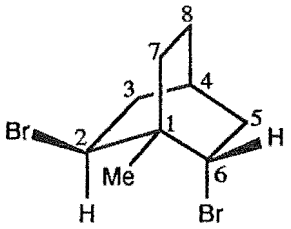

^{1}H NMR δ_H($CDCl_3$): 4.63 (d of t, $^3J_{2,3endo}$ = 9.8 Hz, $^4J_{2,7anti}$ = 2.5 Hz, H2), 4.36 (d of d, $^3J_{6,5endo}$ = 3.9 Hz, $^3J_{6,5exo}$ = 9.8 Hz, H6), 2.59 (m, $^2J_{3endo,3exo}$ = 15.1 Hz, $^3J_{3endo,2}$ = 9.8 Hz, $^3J_{3endo,4}$ = 2.6 Hz, $^4J_{3endo,8anti}$ = 2.6 Hz, H3*endo*), 2.43 (m, $^2J_{5exo,5endo}$ = 15.2 Hz, $^3J_{5exo,4}$ = 2.7 Hz, $^3J_{5exo,6}$ = 9.8 Hz, $^4J_{5exo,3exo}$ = 2.7 Hz, H5*exo*), 2.19* (H3*exo*), 2.18* (H5*endo*), 2.10* (H7*syn*), 1.77* (H8*syn*), 1.71* (H4), 1.52 (m, H8*anti*), 1.32 (m, $^2J_{7anti,7syn}$ = 13.6 Hz, $^3J_{7anti,8anti}$ = 11.3 Hz, $^3J_{7anti,8syn}$ = 2.5 Hz, $^4J_{7anti,2}$ = 2.5 Hz, H7*anti*), 1.08 (s, $W_{h/2}$ = 1.0 Hz, Me).

^{13}C NMR δ_C($CDCl_3$): 59.2 (C6), 56.4 (C2), 39.9 (C5), 39.2 (C3), 37.8 (C1), 28.3 (C7), 26.7 (C4), 26.4 (Me), 24.5 (C8).

LRMS: $C_9H_{14}{}^{81}Br_2$ $M^{+\cdot}$ requires 284; Found 284 (0.4%)
$C_9H_{14}{}^{79}Br{}^{81}Br$ $M^{+\cdot}$ requires 282; Found 282 (0.8%)
$C_9H_{14}{}^{79}Br_2$ $M^{+\cdot}$ requires 280; Found 280 (0.4%)
$C_9H_{14}{}^{81}Br$ $[M\text{-}Br]^{+\cdot}$ requires 203; Found 203 (83%)
$C_9H_{14}{}^{79}Br$ $[M\text{-}Br]^{+\cdot}$ requires 201; Found 201 (85%).

HRMS: $C_9H_{14}{}^{81}Br$ $[M\text{-}Br]^{+\cdot}$ requires 203.0260; Found 203.0222 (100.0%).

Reaction of 2-methyl-*endo*-tricyclo[3.2.1.$0^{2,4}$]octane **45** with trifluoroacetic acid and bromine in carbon tetrachloride

2-Methyl-*endo*-tricyclo[3.2.1.$0^{2,4}$]octane **45** (50 mg, 0.41 mmol) was added to a stirred solution of TFA (5 mg, 0.04 mmol) in CCl_4 (3 ml). The solution was stirred at room temperature for 3 h after which time a ^{1}H NMR spectrum of a sample (0.4 ml) showed that approximately 50% of the starting material had been consumed. The major product was identified as 2-methylbicyclo[3.2.1]oct-2-ene **97** (ca. 80% of the observed reaction gave this product) by comparison of its ^{1}H and ^{13}C NMR spectra with those published.[16]

The remaining solution was stirred for a further 1 h before bromine (39 mg, 0.24 mmol) in CCl_4 (0.8 ml) was added dropwise. The solution was stirred at room temperature for 15 minutes after which time all of the starting material had been consumed (^{1}H NMR). The major product, 2-*exo*-3-*endo*-dibromo-2-*endo*-methylbicyclo[3.2.1]-octane **94** (ca. 80%), was identified by comparison of its ^{1}H and ^{13}C NMR spectra with those reported above. A small amount of **97** (ca. 2%) was also present, along with a number of minor products which were not identified.

Reaction of 2-methyl-*endo*-tricyclo[3.2.1.0^{2,4}]octane **45** with bromine in methanol

Bromine (181 mg, 1.13 mmol) in dry methanol (5 ml) was added dropwise over 10 minutes to a stirred solution of **45** (154 mg, 1.26 mmol, 1.1 mole equivalents) at room temperature. The reaction was stirred in the dark for 30 minutes, diluted with water (7 ml), and extracted with pentane (8 ml) and ether (2 x 8 ml). The organic extracts were combined, dried over $MgSO_4$, and the solvent carefully removed under reduced pressure to give a pale yellow oil (258 mg, ca. 98% recovery). GLC analysis showed the presence of two major products, 4-*endo*-bromo-2-*exo*-methoxy-2-*endo*-methylbicyclo[3.2.1]-octane **98** (50%), 4-*endo*-bromo-2-*endo*-methoxy-2-*exo*-methylbicyclo[3.2.1]octane **99** (45%), and two minor products which were not isolated. The two major products were separated by preparative GLC.

4-*endo*-Bromo-2-*exo*-methoxy-2-*endo*-methylbicyclo[3.2.1]octane 98

Colourless oil.

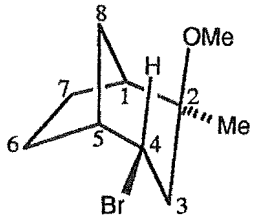

^{1}H NMR δ_H(CDCl$_3$): 4.40 (m, $^3J_{4,1}$ = 3.0 Hz, $^3J_{4,3endo}$ = 12.0 Hz, $^3J_{4,3exo}$ = 5.4 Hz, $^4J_{4,6exo}$ = 1.0 Hz, H4), 3.16 (s, $W_{h/2}$ = 0.6 Hz, OMe), 2.49 (m ,H5), 2.17* (H1), 2.14 (d of d, $^2J_{3exo,3endo}$ = 14.2 Hz, $^3J_{3exo,4}$ = 5.4 Hz, H3*exo*), 2.04 (d, $^2J_{8syn,8anti}$ = 12.2 Hz, H8*syn*), 1.84* (H6*endo*), 1.69* (H7*exo*), 1.64* (H6*exo*), 1.62* (H3*endo*), 1.42* (H7*endo*), 1.37 (d of t, $^2J_{8anti,8syn}$ = 11.8 Hz, $^3J_{8anti,1} = {}^3J_{8anti,5}$ = 5.1 Hz, H8*anti*), 1.08 (s, $W_{h/2}$ = 1.0 Hz, Me).

^{13}C NMR δ_C(CDCl$_3$): 78.2 (C2), 55.7 (C4), 48.6 (OMe), 43.2 (C5), 42.0 (C1), 41.5 (C3), 33.5 (C8), 26.2 (C7), 24.2 (C6), 21.5 (Me).

LRMS: $C_{10}H_{17}{}^{81}BrO$ $M^{+\cdot}$ requires 234; Found 234 (0.6%)
$C_{10}H_{17}{}^{79}BrO$ $M^{+\cdot}$ requires 232; Found 232 (0.6%)
$C_9H_{14}{}^{81}BrO$ $[M-15]^{+\cdot}$ requires 219; Found 219 (10%)
$C_9H_{14}{}^{79}BrO$ $[M-15]^{+\cdot}$ requires 217; Found 217 (10%).

HRMS: $C_9H_{14}{}^{81}BrO$ $[M-15]^{+\cdot}$ requires 219.0209; Found 219.0219 (100.0%).

4-*endo*-Bromo-2-*endo*-methoxy-2-*exo*-methylbicyclo[3.2.1]octane 99

Colourless oil.

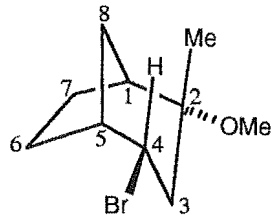

^{1}H NMR δ_H($CDCl_3$): 4.18 (m, $^3J_{4,3endo}$ = 12.2 Hz, $^3J_{4,3exo}$ = 5.4 Hz, $^3J_{4,5}$ = 2.4 Hz, H4), 3.16 (s, $W_{h/2}$ = 0.6 Hz, OMe), 2.50 (m, H5), 2.18 (m, H1), 2.10 (m, $^2J_{3exo,3endo}$ = 13.2 Hz, $^3J_{3exo,4}$ = 5.4 Hz, $^4J_{3exo,1}$ = $^4J_{3exo,5}$ = 1.4 Hz, H3*exo*), 1.84* (H6*endo*), 1.83* (H3*endo*), 1.82* (H7*endo*), 1.65* (H7*exo*), 1.50-1.58 (H8*anti*, H8*syn*), 1.50* (H6*exo*), 1.20 (d, *J* = 1.2 Hz, Me).

^{13}C NMR δ_C($CDCl_3$): 76.8 (C2), 54.6 (C4), 48.5 (OMe), 44.0 (C5), 43.0 (C3), 42.0 (C1), 34.7 (C8), 23.9$_4$ (C6 or C7), 23.8$_5$ (C7 or C6), 21.3 (Me).

The quaternary carbon (C2, 76.8 ppm) was not observed in the ^{13}C NMR spectra but its chemical shift was calculated from a correlation observed in an HMBC experiment.

LRMS: $C_{10}H_{17}{}^{81}BrO$ $M^{+\cdot}$ requires 234; Found 234 (0.6%)
$C_{10}H_{17}{}^{79}BrO$ $M^{+\cdot}$ requires 232; Found 232 (0.6%)
$C_9H_{14}{}^{81}BrO$ $[M-15]^{+\cdot}$ requires 219; Found 219 (15%)
$C_9H_{14}{}^{79}BrO$ $[M-15]^{+\cdot}$ requires 217; Found 217 (14%).

HRMS: $C_9H_{14}{}^{81}BrO$ $[M-15]^{+\cdot}$ requires 219.0209; Found 219.0208 (100.0%).

Reaction of *exo*-tricyclo[3.2.2.0^{2,4}]non-8-en-6-*exo*-7-*exo*-dicarboxylic acid anhydride **48** with bromine in CCl_4

To a solution of anhydride **48** (504 mg, 2.65 mmol) in CCl_4 (30 ml) was added bromine (380 mg, 2.38 mmol, 0.90 mole equivalents) in CCl_4 (10 ml) dropwise over 10 minutes. The reaction was stirred in the absence of light at room temperature for 50 days after which time a ^{1}H NMR spectrum of the reaction mixture showed less then 10% reaction had occurred. The products were not investigated further.

Reaction of *exo*-tricyclo[3.2.2.0^{2,4}]non-8-en-6-*exo*-7-*exo*-dicarboxylic acid anhydride **48** with bromine in methanol

A solution of bromine (243 mg, 1.52 mmol) in dry methanol (10 ml) was added dropwise to a stirred solution of **48** (312 mg, 1.64 mmol, 1.01 mole equivalents) in dry methanol (10 ml). The resulting solution was stirred at room temperature for 23 h after which time it was poured into an aqueous solution of sodium metabisulphite (0.70 g, 3.7 mmol, dissolved in 45 ml of water) and then extracted with ether (2 x 50 ml). The ether extracts were combined, washed with water (50 ml), dried over $MgSO_4$, and the solvent carefully removed under reduced pressure to give a yellow oil (252 mg). Analysis of the ^{1}H NMR spectra of the oil showed the presence of *exo*-tricyclo[3.2.2.0^{2,4}]non-8-en-6-*exo*-7-*exo*-dicarboxylic acid monomethyl ester **104** (62%), *exo*-tricyclo[3.2.2.0^{2,4}]non-8-en-6-*exo*-7-*exo*-dicarboxylic acid dimethyl ester **105** (11%), and 8-*syn*-bromo-9-*anti*-

methoxy-*exo*-tricyclo[3.2.2.$0^{2,4}$]nona-6-*exo*-7-*exo*-dicarboxylic acid anhydride **106** (9%). Separation was achieved by dry column flash chromatography (TLC grade silica, gradient elution, initially using 50% ether/pentane). Compound **105** was identified by comparison of its mp and ^{1}H NMR spectra with those reported.[140,141]

exo-Tricyclo[3.2.2.$0^{2,4}$]non-8-en-6-_exo_-7-_exo_-dicarboxylic acid mono-methyl ester 104

White crystals: mp 113-115 °C (pet. ether).

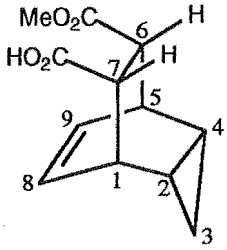

^{1}H NMR δ_H(CDCl$_3$): 5.93 (t, $^3J_{8,1} = {}^3J_{8,9}$ = 7.5 Hz, $^4J_{8,5}$ = 1.1 Hz, H8), 5.84 (t, $^3J_{9,5} = {}^3J_{9,8}$ = 6.9 Hz, $^4J_{9,1}$ = 1.1 Hz, H9), 3.59 (s, $W_{h/2}$ = 1.2 Hz, OMe), 3.05-3.17 (m, H1, H5, H6, H7), 0.94-1.00 (m, H2, H4), 0.10-0.21 (m, H3*endo*, H3*exo*).

^{13}C NMR δ_C(CDCl$_3$): 179.1 (CO_2H), 173.5 ($\underline{C}O_2$Me), 128.1 (C8), 127.1 (C9), 51.5 (OMe), 48.1 (C6), 47.9 (C7), 34.4 (C1 or C5), 33.7 (C5 or C1), 9.4 (C2), 9.2 (C4), 2.8 (C3).

IR (KBr): 3010 (m), 2942 (m), 2898 (m), 1739 (s), 1701 (s) cm^{-1}.

HRMS: $C_{12}H_{14}O_4$ $M^{+\cdot}$ requires 222.0892; Found 222.901 (1.1%).

Elemental Analysis: $C_{12}H_{14}O_4$ Calc. C 64.85%, H 6.35%; Found C 64.59%, H 6.20%.

exo-Tricyclo[3.2.2.$0^{2,4}$]non-8-en-6-_exo_-7-_exo_-dicarboxylic acid dimethyl ester 105

White solid: mp 67-71 °C (pet. ether); Lit. 69-70 °C (methanol).[140]

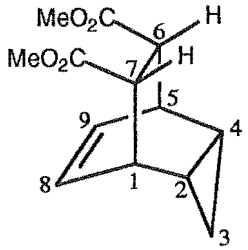

^{1}H NMR δ_H(CDCl$_3$): 5.89 (d of d, $^3J_{8,1} = {}^3J_{9,5}$ = 5.0 Hz, $^4J_{8,5} = {}^4J_{9,1}$ = 3.4 Hz, H8, H9), 3.60 (s, $W_{h/2}$ = 1.1 Hz, 2 x OMe), 3.14 (m, H1, H5), 3.09 (s, $W_{h/2}$ = 2.6 Hz, H6, H7), 0.96 (m, H2, H4), 0.20 (d of t, $^2J_{3exo,3endo}$ = 5.6 Hz, $^3J_{3exo,2} = {}^3J_{3exo,4}$ = 3.6 Hz, H3*exo*), 0.13 (d of t, $^2J_{3endo,3exo}$ = 5.6 Hz, $^3J_{3endo,2} = {}^3J_{3endo,4}$ = 7.3 Hz, H3*endo*).

^{13}C NMR δ_C(CDCl$_3$): 173.5 (2 x C=O), 127.5 (C8, C9), 51.5 (2 x OMe), 48.1 (C6, C7), 34.1 (C1, C5), 9.4 (C2, C4), 2.8 (C3).

IR (thin film): 3006 (s), 2950 (s), 2842 (m), 1747 (s) cm^{-1}.

HRMS: $C_{13}H_{16}O_4$ $M^{+\cdot}$ requires 236.1049; Found 236.1044 (4.3%).

Elemental Analysis: $C_{13}H_{16}O_4$ requires C 66.08%, H 6.83%; Found C 66.19%, H 6.55%.

8-*syn*-Bromo-9-*anti*-methoxy-*exo*-tricyclo[3.2.2.0^{2,4}]nona-6-*exo*-7-*exo*-dicarboxylic acid anhydride 106

Colourless oil.

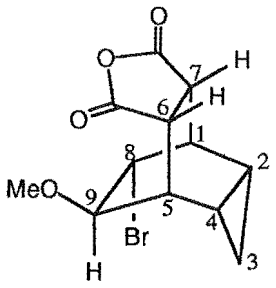

^{1}H NMR δ_H(CDCl$_3$): 4.67 (d, $^3J_{8,1}$ = 3.5 Hz, $^3J_{8,9}$ = 2.2 Hz, $^4J_{8,2}$ = 1.2 Hz, H8), 4.58 (d, $^3J_{9,5}$ = 5.0 Hz, $^3J_{9,8}$ = 2.5 Hz, $^4J_{9,6}$ = 1.3 Hz, H9), 3.74 (s, $W_{h/2}$ = 1.1 Hz, OMe), 3.15* (H5), 3.10 (d of d, $^3J_{7,1}$ = 1.5 Hz, $^3J_{7,6}$ = 9.7 Hz, H7), 2.89 (m, $^3J_{6,5}$ = 4.8 Hz, $^3J_{6,7}$ = 9.7 Hz, $^4J_{6,9}$ = 1.4 Hz, H6), 2.87* (H1), 1.27 (d of t, $^2J_{3exo,3endo}$ = 7.0 Hz, $^3J_{3exo,2}$ = $^3J_{3exo,4}$ = 3.9 Hz, H3*exo*), 1.13-1.20 (m, H2, H4), 0.78 (d of t, $^2J_{3endo,3exo}$ = 7.0 Hz, $^3J_{3endo,2}$ = $^3J_{3endo,4}$ = 8.0 Hz, H3*endo*).

^{13}C NMR δ_C(CDCl$_3$): 176.2 (C=O), 171.9 (C=O), 83.9 (C9), 52.4 (OMe), 46.3 (C8), 45.9 (C7), 41.7 (C5), 39.6 (C6), 35.4 (C1), 11.5 (C4), 8.1 (C2), 6.3 (C3).

LRMS: $C_{12}H_{13}{}^{81}BrO_4$ $M^{+\cdot}$ requires 302; Found 302 (21%)
$C_{12}H_{13}{}^{79}BrO_4$ $M^{+\cdot}$ requires 300; Found 300 (22%)
$C_{12}H_{13}O_4$ $[M\text{-}Br]^{+\cdot}$ requires 221; Found 221 (92%).

HRMS: $C_{12}H_{13}{}^{81}BrO_4$ $M^{+\cdot}$ requires 301.9978; Found 301.9980 (4.0%)
$C_{12}H_{13}O_4$ $[M\text{-}Br]^{+\cdot}$ requires 221.0814; Found 221.0820 (41.2%).

Diels-Alder reaction of cycloheptatriene and dimethyl maleate

Dimethyl maleate was refluxed in xylene with cycloheptatriene for 48 h after which time a ^{1}H NMR spectrum of a sample showed the reaction to be approximately 30% complete. The major product exhibited identical ^{1}H NMR data to **105**, isolated as a product from the reaction of **48** with bromine in methanol.

Synthesis of *exo*-tricyclo[3.2.2.0^{2,4}]non-8-en-6-*exo*-7-*exo*-dicarboxylic acid mono-methyl ester **104**

exo-Tricyclo[3.2.2.0^{2,4}]non-8-en-6-*exo*-7-*exo*-dicarboxylic acid anhydride **48** (171 mg) was refluxed for 48 h in dry methanol (15 ml). The solvent was removed under reduced pressure to give essentially pure **104** (197 mg, 98%) as a pale yellow solid. The product was identified by comparison of its ^{1}H NMR with that reported above.

Synthesis of 8-*anti*-9-*anti*-bis(hydroxymethyl)-*endo*-tricyclo[3.2.2.0^{2,4}]non-6-ene **107**

A procedure similar to that used by Russell et al.[144] was used. To a vigorously stirred solution of lithium aluminium hydride (1.2 g, 32 mmol) in dry THF (30 ml) was added a solution of **48** (5.00 g, 26.3 mmol) in dry THF (50 ml) at such a rate as to maintain a gentle reflux. After the addition was complete the reaction was heated to reflux for 1 h after which time a ^{1}H NMR spectrum showed little reaction had occurred. The

solution was allowed to cool and a further portion of $LiAlH_4$ (1.0 g, 26 mmol) added. The reaction was heated to reflux and monitored by ^1H NMR. After 5 days the reaction was cooled and ethyl acetate (5 ml) added slowly with stirring, followed by ethanol (10 ml), and water (30 ml). Dilute H_2SO_4 was then added to dissolve any remaining precipitate and the aqueous layer was extracted with ether (100 ml). The organic extract was washed with water, dried over $MgSO_4$, and the solvent removed under reduced pressure to give a cloudy white oil (3.87 g) which gradually solidified on standing. A ^1H NMR spectra showed the presence of **107** (62%) and 7-*exo*-hydroxymethyl-*exo*-tricyclo[3.2.2.$0^{2,4}$]non-8-en-6-*exo*-carboxylic acid lactone **108** (38%). The products were separated by column chromatography (silica gel, ether elution). Compound **107** was identified from comparison of its melting point and ^1H NMR with those reported.[144]

8-*anti*-9-*anti*-Bis(hydroxymethyl)-*endo*-tricyclo[3.2.2.$0^{2,4}$]non-6-ene 107

White crystals: mp 112-116 °C (pet. ether); Lit. 113-114 °C (benzene).[144]

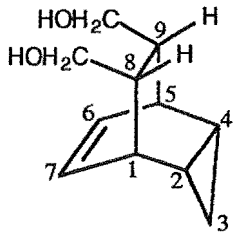

^1H NMR $\delta_H(CDCl_3)$: 5.66 (d of d, $^3J_{6,5} = {}^3J_{7,1}$ = 4.9 Hz, $^4J_{6,1} = {}^4J_{7,5}$ = 3.4 Hz, H6, H7), 3.52-3.65 (m, 2 x $C\underline{H}_2OH$), 2.68 (s, $W_{h/2}$ = 11.3 Hz, H1, H5), 2.29 (m, H8, H9), 0.96 (m, $^3J_{2,1} = {}^3J_{4,5}$ = 2.4 Hz, $^3J_{2,3exo} = {}^3J_{4,3exo}$ = 8.8 Hz, $^3J_{2,3endo} = {}^3J_{4,3endo}$ = 4.4.Hz, H2, H4), -0.03-0.03 (m, H3*endo*, H3*exo*).

^{13}C NMR $\delta_C(CDCl_3)$: 128.1 (C6, C7), 65.1 (2 x $\underline{C}H_2OH$), 46.1 (C1, C5), 35.8 (C8, C9), 10.1 (C2, C4), 1.8 (C3).

IR (KBr): 3317 (s), 3074 (m), 3014 (m), 2944 (s), 2883 (m) cm^{-1}.

HRMS: $C_{11}H_{16}O_2$ $M^{+\cdot}$ requires 180.1150; Found 180.1151 (2.6%).

7-*exo*-Hydroxymethyl-*exo*-tricyclo[3.2.2.$0^{2,4}$]non-8-en-6-*exo*-carboxylic acid lactone 108

White solid: mp 124-126 °C (pet. ether).

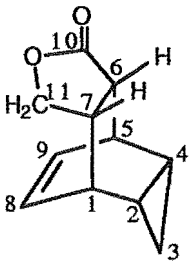

^1H NMR $\delta_H(CDCl_3)$: 5.90 (m, $^3J_{9,5} = {}^3J_{9,8}$ = 7.2 Hz, H9), 5.83 (m, $^3J_{8,1} = {}^3J_{8,9}$ = 7.2 Hz, H8), 4.35 (t, $^2J_{11a,11b}$ = 9.3 Hz, $^3J_{11a,7}$ = 4.4 Hz, H11a), 3.87 (d of d, $^2J_{11b,11a}$ = 9.3 Hz, $^3J_{11b,7}$ = 9.3 Hz, H11b), 3.30 (m, H5), 2.96 (m, H1), 2.88* (H6), 2.84* (H7), 1.03 (m, $^3J_{4,2}$ = 7.8 Hz, $^3J_{4,3endo}$ = 7.3 Hz, $^3J_{4,3exo} = {}^3J_{4,5}$ = 3.9 Hz, H4), 0.94 (m, $^3J_{2,1} = {}^3J_{2,3exo}$ = 3.7 Hz, $^3J_{2,3endo}$ = 7.6 Hz, $^3J_{2,4}$ = 7.8 Hz, H2), 0.24 (d of t, $^2J_{3endo,3exo}$ = 5.3 Hz, $^3J_{3endo,2} = {}^3J_{3endo,4}$ = 7.4 Hz, H3*endo*), 0.19 (d of t, $^2J_{3exo,3endo}$ = 5.3 Hz, $^3J_{3exo,2} = {}^3J_{3exo,4}$ = 3.7 Hz, H3*exo*).

^{13}C NMR $\delta_C(CDCl_3)$: 178.6 (C=O), 129.8 (C9), 127.8 (C8), 71.9 (C11), 45.9 (C6), 39.4 (C7), 34.8 (C1), 33.5 (C5), 9.4_1 (C2 or C4), 9.3_8 (C4 or C2), 4.5 (C3).

IR (KBr): 2999 (m), 2946 (m), 1752 (s) cm^{-1}.

HRMS: $C_{11}H_{12}O_2$ $M^{+\cdot}$ requires 176.0837; Found 176.0840 (6.1%).

Elemental analysis: $C_{11}H_{12}O_2$ Calc. C 74.98%, H 6.86%; Found C 74.92%, H 6,94%.

Reaction of 8-*anti*-9-*anti*-bis(hydroxymethyl)-*endo*-tricyclo[3.2.2.0^{2,4}]non-6-ene **107** with bromine in methanol

Bromine (142 mg, 0.89 mmol) in dry methanol (10 ml) was added dropwise to a stirred solution of **107** (174 mg, 0.97 mmol, 1.1 mole equivalents) in dry methanol (5 ml). The reaction was stirred at room temperature for 25 h, diluted with an aqueous solution of sodium metabisulphite (0.2 g in 30 ml of water), and extracted with ether (2 x 40 ml). The ether extracts were combined, washed with water, dried over $MgSO_4$, and solvent carefully removed under reduced pressure to give a yellow oil (174 mg) which consisted of starting material **107** (11%), 7-*endo*-bromo-11-*anti*-hydroxymethyl-9-oxa-*endo*-tetracyclo[4.4.1.0^{2,8}0^{3,5}]undecane **109** (78%), and a number of minor products which were not identified. The major product was purified by column chromatography (silica gel, gradient elution starting with 80% ether/pentane).

7-*endo*-Bromo-11-*anti*-hydroxymethyl-9-oxa-*endo*-tetracyclo-[4.4.1.0^{2,8}0^{3,5}]undecane 109

Colourless oil.

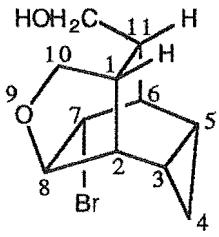

^{1}H NMR δ_H($CDCl_3$): 4.03 (d, $^3J_{8,2}$ = 4.8 Hz, H8), 3.78 (d of d, $^3J_{7,6}$ = 3.4 Hz, $^3J_{7,8}$ = 1.0 Hz, H7), 3.62-3.74 (m, H10*endo*, H10*exo*, C$\underline{H}_2$OH), 2.51 (m, $^3J_{2,8}$ = 4.5 Hz, H2), 2.44 (m, H1), 2.32 (m, H6), 2.28 (m, H11), 1.05* (H3), 1.03* (H4*endo*), 0.98* (H5), 0.61 (d of t, $^2J_{4exo,4endo}$ = 6.1 Hz, $^3J_{4exo,3}$ = $^3J_{4exo,5}$ = 7.6 Hz, H4*exo*).

^{13}C NMR δ_C($CDCl_3$): 83.6 (C8), 67.8 (C10), 61.8 (C$\underline{H}_2$OH), 53.7 (C7), 44.6 (C11), 41.3 (C2), 35.5 (C1), 32.7 (C6), 12.9 (C5), 9.3 (C4), 6.3 (C3).

HRMS: $C_{11}H_{15}{}^{81}BrO_2$ $M^{+\cdot}$ requires 260.0236; Found 260.0220 (0.4%)

$C_{11}H_{15}{}^{79}BrO_2$ $M^{+\cdot}$ requires 258.0256; Found 258.0255 (0.3%).

Attempted cyclisation of 7-*endo*-Bromo-11-*anti*-hydroxymethyl-9-oxa-*endo*-tetracyclo-[4.4.1.0^{2,8}0^{3,5}]undecane **109**

(a) Reaction with potassium tertiarybutoxide

Compound **109** (300 mg, 1.16 mmol) in dry ether (10 ml) was stirred at room temperature with KOBu^t (130 mg, 1.16 mmol) for 14 days after which time a ^{1}H NMR spectrum showed only starting material **109** to be present.

(b) Reaction with sodium amide

Bromide **109** (150 mg, 0.58 mmol) in dry ether (5 ml) was stirred at room temperature with $NaNH_2$ (80 mg, 2.1 mmol) and the reaction monitored by ^{1}H NMR.

After 2 days a ^{1}H NMR showed the presence of starting material **109** and numerous minor products. The reaction was not investigated further.

Reaction of *exo*-tricyclo[3.2.2.0^{2,4}]non-6-ene **47** with bromine in carbon tetrachloride

Bromine (366 mg, 2.29 mmol) in CCl_4 (10 ml) was added dropwise to stirred solution of **47** (312 mg, 2.60 mmol, 1.1 mole equivalents) in CCl_4 (5 ml) at room temperature. The reaction was stirred for 1 h and then washed with an aqueous solution of sodium metabisulphite, water, dried over $MgSO_4$, and the solvent removed under reduced pressure to give a yellow oil (560 mg, ca. 87% recovery). GLC analysis showed four products, 5-*endo*-9-*syn*-dibromo-*endo*-tricyclo[4.2.1.0^{2,4}]nonane **113** (38%), 4-*endo*-9-*anti*-dibromotricyclo[3.3.1.0^{2,8}]nonane **114** (26%), 6-*exo*-7-*endo*-dibromo-*exo*-tricyclo[3.2.2.0^{2,4}]nonane **115** (15%), the fourth product (10%) was not identified. A number of minor products were also present, of which 5-*endo*-9-*syn*-dibromo-bicyclo[4.2.1]non-2-ene **116** (ca. 5%) was the only one isolated. A ^{1}H NMR spectrum of the reaction mixture indicated the presence of a number of minor products, which presumably had coincident retention times with those of the major products, but showed four major products in approximately the same ratio as obtained from the GLC analysis. Column chromatography (silica gel, 100:1 ratio absorbant to sample, pentane elution) gave pure **115** and **116** but resulted in rearrangement of the two other major products. Radial chromatography on PEG coated silica plates (pentane elution) gave a crude separation of the major products and pure **113** was obtained by recrystallisation (pentane) of an enriched fraction. The third major product **114** was not isolated in high purity, but was assigned from an enriched fraction (ca. 70%) obtained from radial chromatography on a PEG coated silica plate.

5-*endo*-9-*syn*-Dibromo-*endo*-tricyclo[4.2.1.0^{2,4}]nonane 113

Colourless crystals: mp 79-80 °C (pentane).

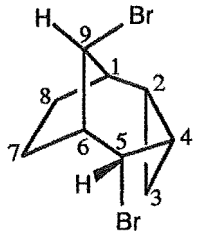

^{1}H NMR δ_H(CDCl$_3$): 5.28 (t, $^3J_{5,4}$ = 7.4 Hz, $^3J_{5,6}$ = 5.7 Hz, H5), 4.03 (t, $^3J_{9,1} = {}^3J_{9,6}$ = 4.3 Hz, H9), 2.75 (m, H1), 2.47 (m, H6), 1.87 (m, H7*endo*), 1.69* (H2), 1.62* (H7*exo*, H8*exo*), 1.56* (H8*endo*), 1.41 (m, H4), 0.78 (d of t, $^2J_{3exo,3endo}$ = 6.0 Hz, $^3J_{3exo,2} = {}^3J_{3exo,4}$ = 9.4 Hz, H3*exo*), 0.57 (d of t, $^2J_{3endo,3exo}$ = 5.8 Hz, $^3J_{3endo,2} = {}^3J_{3endo,4}$ = 5.8 Hz, H3*endo*).

^{13}C NMR δ_C(CDCl$_3$): 59.0 (C5), 56.9 (C9), 44.1 (C6), 37.5 (C1), 25.7 (C8), 24.6 (C2), 23.5 (C7), 15.3 (C4), 12.5 (C3).

LRMS: $C_9H_{12}{}^{81}Br_2$ $M^{+\cdot}$ requires 282; Found 282 (1%)

$C_9H_{12}{}^{79}Br^{81}Br$ $M^{+\cdot}$ requires 280; Found 280 (3%)

$C_9H_{12}{}^{79}Br_2$ $M^{+\cdot}$ requires 278; Found 278 (1%).

HRMS: $C_9H_{12}{}^{79}Br^{81}Br$ $M^{+\cdot}$ requires 279.9287; Found 279.9275 (78.0%)

$C_9H_{12}{}^{79}Br_2$ $M^{+\cdot}$ requires 277.9307; Found 277.9311 (28.9%).

4-*endo*-9-*anti*-Dibromotricyclo[3.3.1.$0^{2,8}$]nonane 114

This compound was identified from an enriched mixture (ca. 70%) and a complete assignment was not obtained.

Colourless oil.

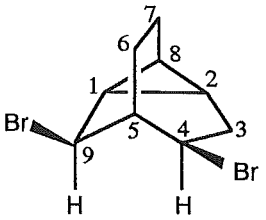

^{1}H NMR δ_H($CDCl_3$): 4.76 (m, $^3J_{9,1} = {}^3J_{9,5}$ = 3.7 Hz, H9), 4.15 (m, $^3J_{4,3endo}$ = 10.7 Hz, $^3J_{4,3exo}$ = 8.3 Hz, $^3J_{4,5}$ = 2.7 Hz, H4), 2.60 (m, H3*exo*), 2.34 (m, H5), 2.12* (H3*endo*), 1.50 (m, H1), 1.21-1.27 (m, H2, H8).

^{13}C NMR δ_C($CDCl_3$): 54.0 (C9), 51.0 (C4), 42.1 (C5), 28.2 (C3).

The following ^{13}C NMR signals were observed but not assigned: 18.1, 16.1, 15.9, 14.4, 14.0.

6-*exo*-7-*endo*-Dibromo-*exo*-tricyclo[3.2.2.$0^{2,4}$]nonane 115

Colourless oil.

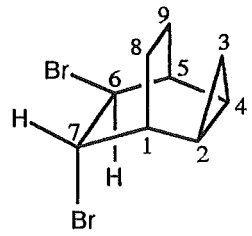

^{1}H NMR δ_H($CDCl_3$): 4.53 (m, $^3J_{6,5}$ = 3.5 Hz, $^3J_{6,7}$ = 3.3 Hz, $^4J_{6,9syn}$ = 2.5 Hz, H6), 4.39 (t, $^3J_{7,1} = {}^3J_{7,6}$ = 3.2 Hz, H7), 2.27* (H5), 2.25* (H1), 1.80 (m, $^4J_{9anti,4}$ = 1.1 Hz, H9*anti*), 1.43-1.54 (m, H8*anti*, H8*syn*), 1.34* (H2), 1.29* (H9*syn*), 1.10 (m, H4), 0.84 (d of t, $^2J_{3exo,3endo}$ = 6.1 Hz, $^3J_{3exo,2} = {}^3J_{3exo,4}$ = 3.8 Hz, H3*exo*), 0.61 (d of t, $^2J_{3endo,3exo}$ = 5.6 Hz, $^3J_{3endo,2} = {}^3J_{3endo,4}$ = 8.5 Hz, H3*endo*).

^{13}C NMR δ_C($CDCl_3$): 61.7 (C6), 61.1 (C7), 35.9 (C5), 35.3 (C1), 24.4 (C8), 17.3 (C9), 14.5 (C4), 9.2 (C2), 6.3 (C3).

HRMS: $C_9H_{12}{}^{81}Br_2$ $M^{+\cdot}$ requires 281.9267; Found 281.9327 (36.6%)

$C_9H_{12}{}^{79}Br^{81}Br$ $M^{+\cdot}$ requires 279.9287; Found 279.9289 (77.4%)

$C_9H_{12}{}^{79}Br_2$ $M^{+\cdot}$ requires 277.9307; Found 277.9298 (38.6%).

5-*endo*-9-*syn*-Dibromobicyclo[4.2.1]non-2-ene 116

Colourless oil.

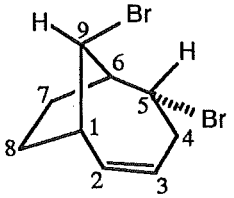

^{1}H NMR δ_H($CDCl_3$): 5.85 (m, $^3J_{2,1}$ = 8.7 Hz, $^3J_{2,3}$ = 11.2 Hz, $^4J_{2,4endo}$ = 2.8 Hz, H2), 5.59 (m, $^3J_{3,2}$ = 11.2 Hz, $^3J_{3,4exo}$ = 8.6 Hz, $^3J_{3,4endo}$ = 3.4 Hz, H3), 4.74 (m, $^3J_{5,4endo}$ = 11.2 Hz, $^3J_{5,4exo}$ = 5.2 Hz, $^3J_{5,6}$ = 2.0 Hz, H5), 4.25 (t, $^3J_{9,1} = {}^3J_{9,6}$ = 6.7 Hz, H9), 3.03 (m, $^3J_{6,9}$ = 6.8 Hz, H6), 2.88 (m, H1), 2.80 (m, $^3J_{4endo,2}$ = 3.3 Hz, $^3J_{4endo,3}$ = 3.3 Hz, $^3J_{4endo,5}$ = 11.4 Hz, H4*endo*), 2.70 (m, $^2J_{4exo,4endo}$ = 16.2 Hz, $^3J_{4exo,3}$ = 8.5 Hz, $^3J_{4exo,5}$ = 5.7 Hz, $^3J_{4exo,6}$ = 1.0 Hz, H4*exo*), 2.04-2.20 (m, H7*endo*, H8*exo*), 1.84-1.95 (m, H7*exo*, H8*endo*).

^{13}C NMR δ_C($CDCl_3$): 137.0 (C2), 127.5 (C3), 56.6 (C9), 53.1 (C6), 52.0 (C5), 42.0 (C1), 36.0 (C4), 29.7 (C8), 23.7 (C7).

HRMS: $C_9H_{12}{}^{81}Br_2$ $M^{+\cdot}$ requires 281.9267; Found 281.9307 (54.4%)
$C_9H_{12}{}^{79}Br^{81}Br$ $M^{+\cdot}$ requires 279.9287; Found 279.9289 (100.0%)
$C_9H_{12}{}^{79}Br_2$ $M^{+\cdot}$ requires 277.9307; Found 277.9332 (61.9%).

Reaction of *exo*-tricyclo[3.2.2.0^{2,4}]non-6-ene **47** with bromine in methanol at room temperature

A solution of bromine (359 mg, 2.25 mmol) in dry methanol (5 ml) was added dropwise over 10 minutes to a stirred solution of **47** (329 mg, 2.74 mmol, 1.2 mole equivalents) in dry methanol (7 ml) at room temperature. The resulting solution was stirred for 2 h and then poured into an aqueous solution of sodium metabisulphite before being extracted with ether (2 x 15 ml). The ether extracts were combined, washed with a saturated NaCl solution (10 ml), dried over $MgSO_4$, and the solvent carefully removed under reduced pressure to give a yellow oil (617 mg). GLC analysis showed the presence of three major products as well as a number of minor products. Due to the overlap of the peaks observed in the GLC (under a variety of conditions) the product ratios were estimated from a ^1H NMR spectrum of the reaction mixture. A crude separation of the products was effected by radial chromatography on a PEG coated silica plate (pentane elution). The products were further purified by preparative GLC. The following compounds were identified: 9-*syn*-bromo-5-*endo*-methoxy-*endo*-tricyclo[4.2.1.0^{2,4}]-nonane **127** (34%), 4-*endo*-9-*anti*-dimethoxytricyclo[3.3.1.0^{2,8}]nonane **128** (24%), 4-*endo*-9-*syn*-dimethoxytricyclo-[3.3.1.0^{2,8}]nonane **129** (14%), 4-*endo*-bromo-9-*anti*-methoxytricyclo[3.3.1.0^{2,8}]nonane **130** (5%), 4-*endo*-bromo-9-*syn*-methoxytricyclo-[3.3.1.0^{2,8}]nonane **131** (5%), 9-*syn*-bromo-5-*endo*-methoxybicyclo[4.2.1]non-2-ene **132** (3%), and 5-*endo*-9-*syn*-dibromo-*endo*-tricyclo[4.2.1.0^{2,4}]nonane **113** (3%). A number of other minor products were also present but were not identified. 5-*endo*-9-*syn*-Dibromo-*endo*-tricyclo[4.2.1.0^{2,4}]nonane **113** was identified by comparison with the ^1H NMR data reported above.

9-*syn*-Bromo-5-*endo*-methoxy-*endo*-tricyclo[4.2.1.0^{2,4}]nonane 127

Colourless oil.

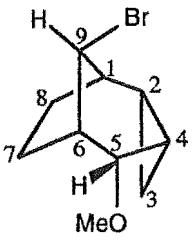

^1H NMR $\delta_H(CDCl_3)$: 4.12 (t, $^3J_{5,4} = {}^3J_{5,6} = 6.7$ Hz, H5), 4.04 (t, $^3J_{9,1} = {}^3J_{9,6} = 4.9$ Hz, H9), 3.40 (s, $W_{h/2} = 1.0$ Hz, OMe), 2.63 (m, $^3J_{1,2} = 6.9$ Hz, $^3J_{1,8} = {}^3J_{1,9} = 4.3$ Hz, H1), 2.44 (m, $^3J_{6,5} = {}^3J_{6,7} = {}^3J_{6,9} = 6.3$ Hz, H6), 1.57* (H7*endo*), 1.53* (H8*endo*), 1.42* (H2), 1.40* (H8*exo*), 1.34* (H7*exo*), 1.16 (m, $^3J_{4,3endo} = 5.6$ Hz, $^3J_{4,3exo} = 8.9$ Hz, $^3J_{4,5} = 7.2$ Hz, H4), 0.58 (d of t, $^2J_{3exo,3endo} = 5.4$ Hz, $^3J_{3exo,2} = {}^3J_{3exo,4} = 8.8$ Hz, H3*exo*), 0.44 (m, $^2J_{3endo,3exo} = 5.4$Hz, $^3J_{3endo,2} = {}^3J_{3endo,4} = 5.4$ Hz, H3*endo*).

^{13}C NMR δ_C($CDCl_3$): 76.4 (C5), 56.5 (C9), 55.0 (OMe), 39.4 (C6), 37.5 (C1), 25.5 (C8), 19.9 (C7), 19.6 (C2), 10.3 (C4), 7.6 (C3).

LRMS: $C_{10}H_{15}{}^{81}BrO$ $M^{+\cdot}$ requires 232; Found 232 (0.3%)
$C_{10}H_{15}{}^{79}BrO$ $M^{+\cdot}$ requires 230; Found 230 (0.2%)
$C_{10}H_{15}O$ $[M\text{-}Br]^{+\cdot}$ requires 151; Found 151 (0.5%).

HRMS: $C_{10}H_{15}O$ $[M\text{-}Br]^{+\cdot}$ requires 151.1123; Found 151.1130 (39.7%).

4-*endo*-9-*anti*-Dimethoxytricyclo[3.3.1.0^{2,8}]nonane 128

Colourless oil.

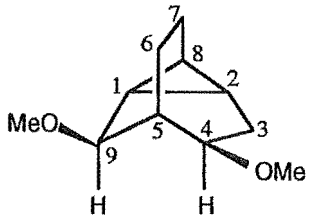

^{1}H NMR δ_H($CDCl_3$): 3.57 (t, $^3J_{9,1} = {}^3J_{9,5}$ = 3.7 Hz, H9), 3.41 (s, $W_{h/2}$ = 0.7 Hz, OMe), 3.31 (s, $W_{h/2}$ = 0.7 Hz, OMe), 3.23 (d of t, $^3J_{4,3endo} = {}^3J_{4,3exo}$ = 8.8 Hz, $^3J_{4,5}$ = 3.0 Hz, H4), 2.34 (m, $^2J_{3exo,3endo}$ = 14.2 Hz, $^3J_{3exo,4}$ = 8.8 Hz, H3*exo*), 2.19 (s, $W_{h/2}$ = 10.4 Hz, H5), 2.02 (m, H7*exo*), 1.54* (H7*endo*), 1.53* (H6*endo*), 1.52 (d of d, $^2J_{3endo,3exo}$ = 14.2 Hz, $^3J_{3endo,4}$ = 9.3 Hz, H3*endo*), 1.41 (m, H6*exo*), 1.15 (d of t, $^3J_{1,2} = {}^3J_{1,8}$ = 8.3 Hz, $^3J_{1,9}$ = 3.4 Hz, H1), 0.97* (H8), 0.96* (H2).

^{13}C NMR δ_C($CDCl_3$): 78.8 (C4), 76.7 (C9), 55.7 (OMe), 55.6 (OMe), 33.9 (C5), 23.7 (C3), 15.0 (C7), 13.8 (C6), 13.7 (C1), 13.1 (C8), 11.4 (C2).

HRMS: $C_{11}H_{18}O_2$ $M^{+\cdot}$ requires 182.1307; Found 182.1315 (6.8%)
$C_{10}H_{14}O$ $[M\text{-}32]^{+\cdot}$ requires 150.1045; Found 150.1112 (69.9%).

4-*endo*-9-*syn*-Dimethoxytricyclo[3.3.1.0^{2,8}]nonane 129

Colourless oil.

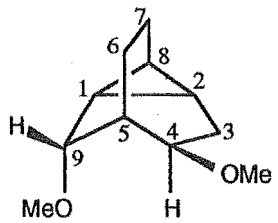

^{1}H NMR δ_H($CDCl_3$): 3.75 (t, $^3J_{9,1} = {}^3J_{9,5}$ = 3.4 Hz, H9), 3.55 (m, $^3J_{4,3endo}$ = 7.7 Hz, $^3J_{4,3exo}$ = 9.2 Hz, $^3J_{4,5}$ = 4.2 Hz, H4), 3.40 (s, $W_{h/2}$ = 0.6 Hz, OMe), 3.29 (s, $W_{h/2}$ = 0.7 Hz, OMe), 2.48 (m, $^2J_{3exo,3endo}$ = 14.2 Hz, $^3J_{3exo,2}$ = 6.8 Hz, $^3J_{3exo,4}$ = 9.3 Hz, H3*exo*), 2.21 (m, H5), 1.80* (H7*exo*), 1.78* (H6*endo*), 1.54* (H7*endo*), 1.46 (d of d, $^2J_{3endo,3exo}$ = 14.2 Hz, $^3J_{3endo,4}$ = 7.8 Hz, H3*endo*), 1.32 (m, H6*exo*), 1.15 (m, H1), 1.08* (H8), 1.00* (H2).

^{13}C NMR δ_C($CDCl_3$): 78.7 (C9), 73.0 (C4), 55.7 (OMe), 55.6 (OMe), 34.0 (C5), 23.9 (C3), 21.4 (C6), 15.2 (C7), 14.7 (C8), 13.5 (C1), 11.6 (C2).

LRMS: $C_{11}H_{18}O_2$ $M^{+\cdot}$ requires 182; Found 182 (1%)
$C_{10}H_{14}O$ $[M\text{-}32]^{+\cdot}$ requires 150; Found 150 (100.0%).

HRMS: $C_{10}H_{14}O$ $[M\text{-}32]^{+\cdot}$ requires 150.1045; Found 150.1051 (100.0%).

4-*endo*-Bromo-9-*anti*-methoxytricyclo[3.3.1.0^{2,8}]nonane 130

Colourless oil.

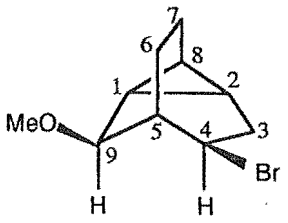

^{1}H NMR δ_H(CDCl$_3$): 4.09 (d of t, $^3J_{4,3endo}$ = 10.4 Hz, $^3J_{4,3exo}$ = 8.6 Hz, $^3J_{4,5}$ = 2.4 Hz, H4), 3.64 (t, $^3J_{9,1}$ = $^3J_{9,5}$ = 3.9 Hz, H9), 3.39 (s, $W_{h/2}$ = 0.7 Hz, OMe), 2.55 (m, H3*exo*), 2.28 (s, $W_{h/2}$ = 9.5 Hz, H5), 2.09 (d of d, $^2J_{3endo,3exo}$ =14.7 Hz, $^3J_{3endo,4}$ = 10.6 Hz, H3*endo*), 2.08* (H7*exo*), 1.65-1.78 (m, H6*endo*, H6*exo*, H7*endo*), 1.20 (m, $^3J_{1,2}$ = $^3J_{1,8}$ = 7.8 Hz, $^3J_{1,9}$ = 3.4 Hz, H1), 1.04* (H2), 1.02* (H8).

^{13}C NMR δ_C(CDCl$_3$): 76.9 (C9), 55.8 (OMe), 52.0 (C4), 39.2 (C5), 28.6 (C3), 14.7$_6$ (C6 or C7), 14.7$_2$ (C7 or C6), 14.3 (C8), 13.4 (C1), 13.2 (C2).

LRMS: $C_{10}H_{15}{}^{81}BrO$ $M^{+\cdot}$ requires 232; Found 232 (1%)
$C_{10}H_{15}{}^{79}BrO$ $M^{+\cdot}$ requires 230; Found 230 (1%)
$C_9H_{11}{}^{81}Br$ $[M-32]^{+\cdot}$ requires 200; Found 200 (49%)
$C_9H_{11}{}^{79}Br$ $[M-32]^{+\cdot}$ requires 198; Found 198 (50%).

HRMS: $C_9H_{11}{}^{81}Br$ $[M-32]^{+\cdot}$ requires 200.0025; Found 200.0026 (34.2%)
$C_9H_{11}{}^{79}Br$ $[M-32]^{+\cdot}$ requires 198.0045; Found 198.0028 (36.7%).

4-*endo*-Bromo-9-*syn*-methoxytricyclo[3.3.1.0^{2,8}]nonane 131

Colourless oil.

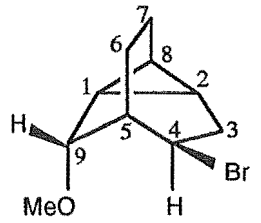

^{1}H NMR δ_H(CDCl$_3$): 4.56 (d of t, $^3J_{4,3endo}$ = $^3J_{4,3exo}$ = 9.3 Hz, $^3J_{4,5}$ = 2.9 Hz, $^4J_{4,6exo}$ = 1.0 Hz, H4), 3.76 (t, $^3J_{9,1}$ = $^3J_{9,5}$ = 3.4 Hz, H9), 3.38 (s, $W_{h/2}$ = 0.7 Hz, OMe), 2.70 (m, $^2J_{3exo,3endo}$ = 14.0, $^3J_{3exo,2}$ = 7.1 Hz, $^3J_{3exo,4}$ = 9.3 Hz, H3*exo*), 2.23 (m, H5), 2.11 (d of d, $^2J_{3endo,3exo}$ = 13.2 Hz, $^3J_{3endo,4}$ = 9.3, H3*endo*), 2.09* (H6*endo*), 1.93 (m, H7*exo*), 1.62 (m, $^2J_{7endo,7exo}$ = 14.7 Hz, $^3J_{7endo,6endo}$ = $^3J_{7endo,6exo}$ = 9.1 Hz, H7*endo*), 1.51* (H6*exo*), 1.19 (m, H1), 1.08* (H8), 1.04* (H2).

^{13}C NMR δ_C(CDCl$_3$): 78.7 (C9), 55.8 (OMe), 49.5 (C4), 39.3 (C5), 28.7 (C3), 22.7 (C6), 14.9 (C7), 14.5 (C8), 14.0 (C2), 13.0 (C1).

LRMS: $C_{10}H_{15}{}^{81}BrO$ $M^{+\cdot}$ requires 232; Found 232 (1%)
$C_{10}H_{15}{}^{79}BrO$ $M^{+\cdot}$ requires 230; Found 230 (1%)
$C_9H_{11}{}^{81}Br$ $[M-32]^{+\cdot}$ requires 200; Found 200 (15%)
$C_9H_{11}{}^{79}Br$ $[M-32]^{+\cdot}$ requires 198; Found 198 (15%).

HRMS: $C_9H_{11}{}^{81}Br$ $[M-32]^{+\cdot}$ requires 200.0025; Found 200.0039 (19.0%)
$C_9H_{11}{}^{79}Br$ $[M-32]^{+\cdot}$ requires 198.0045; Found 198.0037 (20.7%).

9-*syn*-Bromo-5-*endo*-methoxybicyclo[4.2.1]non-2-ene 132

Compound **132** was identified from a mixture with **127** (ca. 7:3 ratio **132**:**127**).

Colourless oil.

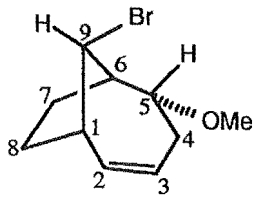

^{1}H NMR δ_H($CDCl_3$): 5.84 (m, $^3J_{2,1}$ = 8.3 Hz, $^3J_{2,3}$ = 11.7 Hz, $^4J_{2,4endo}$ = 2.9 Hz, H2), 5.63 (m, $^3J_{3,2}$ = 11.7 Hz, $^3J_{3,4endo}$ = 3.2 Hz, $^3J_{3,4exo}$ = 8.8 Hz, H3), 4.31 (t, $^3J_{9,1}$ = $^3J_{9,6}$ = 6.9 Hz, H9), 3.63 (m, $^3J_{5,4endo}$ = 10.7 Hz, $^3J_{5,4exo}$ = 4.4 Hz, $^3J_{5,6}$ = 2.5 Hz, H5), 3.35 (s, $W_{h/2}$ = 0.5 Hz, OMe), 2.84 (m, $^3J_{1,2}$ = 8.3 Hz, $^3J_{1,8exo}$ = $^3J_{1,9}$ = 7.6 Hz, H1), 2.72 (m, $^3J_{6,7exo}$ = $^3J_{6,9}$ = 6.4 Hz, H6), 2.43* (H4*exo*), 2.26 (m, $^2J_{4endo,4exo}$ = 16.1 Hz, $^3J_{4endo,5}$ = 10.7 Hz, $^3J_{4endo,3}$ = 3.1 Hz, $^4J_{4endo,2}$ = 3.1 Hz, H4*endo*), 2.03* (H8*exo*), 2.00* (H7*endo*), 1.79* (H8*endo*), 1.71* (H7*exo*).

^{13}C NMR δ_C($CDCl_3$): 136.2 (C2), 125.3 (C3), 75.9 (C5), 56.9 (OMe), 55.8 (C9), 47.0 (C6), 41.8 (C1), 30.2 (C4), 29.3 (C8), 22.8 (C7).

HRMS: $C_{10}H_{15}{}^{81}BrO$ $M^{+\cdot}$ requires 232.0287; Found 232.0285 (7.2%)
$C_{10}H_{15}{}^{79}BrO$ $M^{+\cdot}$ requires 230.0307; Found 230.0337 (8.3%).

Reaction of *exo*-tricyclo[3.2.2.0^{2,4}]non-6-ene **47** with bromine in methanol at 0 °C

A solution of bromine (263 mg, 1.65 mmol) in dry methanol (7 ml) was added dropwise to a solution of **47** (225 mg, 1.87 mmol, 1.1 mole equivalents) in dry methanol (10 ml) cooled in an ice bath (0-5 °C). The reaction was stirred for 5 minutes after which time sodium metabisulphite was added until no bromine colour was observed. The solvent was removed under reduced pressure at 0-5 °C and the residue extracted with ether. The ether extract was dried over $MgSO_4$ and the solvent removed under reduced pressure while cooled in an ice bath. The resulting oil (366 mg) was shown by GLC analysis to contain one major product and a number of minor products. Due to the overlap of the compounds on GLC the ratio of products was estimated from a ^{1}H NMR spectrum of the crude reaction mixture. The following compounds were identified: 9-*syn*-bromo-5-*endo*-methoxy-*endo*-tricyclo[4.2.1.0^{2,4}]nonane **127** (30%), 2-*exo*-bromo-4-*exo*-methoxybicyclo[3.2.2]non-6-ene **146** (8%), 4-*endo*-9-*syn*-dimethoxytricyclo[3.3.1.0^{2,8}]-nonane **129** (7%), 9-*syn*-bromo-5-*endo*-methoxybicyclo[4.2.1]non-2-ene **132** (7%), 5-*endo*-9-*syn*-dibromo-*endo*-tricyclo[4.2.1.0^{2,4}]nonane **113** (7%), 2-*exo*-4-*exo*-dimethoxybicyclo[3.2.2]non-6-ene **147** (6%), 4-*endo*-9-*anti*-dimethoxytricyclo[3.3.1.0^{2,8}]-nonane **128** (6%), 4-*endo*-bromo-9-*syn*-methoxytricyclo[3.3.1.0^{2,8}]nonane **131** (5%), 4-*endo*-bromo-9-*anti*-methoxytricyclo[3.3.1.0^{2,8}]nonane **130** (3%), and 2-*exo*-bromo-9-*syn*-methoxybicyclo[3.2.2]non-6-ene **148** (3%). A crude separation was effected by radial chromatography on a PEG coated silica plate (pentane elution). The following compounds were further purified by preparative GLC **127**, **128**, **129**, **130**, **131**, and **147**. Compounds **146** and **148** were isolated from TLC mesh column chromatography on silica. Compounds **113**, **127**, **128**, **129**, **130**, **131**, and **132** were identified from

the ^1H and ^{13}C NMR data of the products obtained from the reaction of **47** with Br_2 in methanol at room temperature.

2-*exo*-Bromo-4-*exo*-methoxybicyclo[3.2.2]non-6-ene 146

Colourless oil.

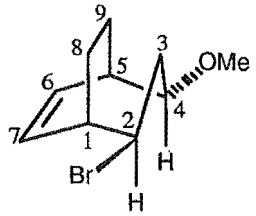

^1H NMR $\delta_H(CDCl_3)$: 6.13-6.17 (m, H6, H7), 4.17 (d of d, $^3J_{2,3endo}$ = 5.2 Hz, $^3J_{2,3exo}$ = 11.7 Hz, H2), 3.29 (s, $W_{h/2}$ = 0.9 Hz, OMe), 3.08 (d of d, $^3J_{4,3endo}$ = 5.2 Hz, $^3J_{4,3exo}$ =10.8 Hz, H4), 2.73 (m, H1), 2.68 (m, $^2J_{3endo,3exo}$ = 13.2 Hz, $^3J_{3endo,2}$ = $^3J_{3endo,4}$ = 5.3 Hz, $^4J_{3endo,1}$ = $^4J_{3endo,5}$ =1.3 Hz, H3*endo*), 2.50 (m, H5), 2.28 (d of t, $^2J_{3exo,3endo}$ =13.2 Hz, $^3J_{3exo,2}$ = $^3J_{3exo,4}$ = 11.2 Hz, H3*exo*), 2.18 (t, H8*syn*), 2.02 (t, H9*syn*), 1.63* (H8*anti*), 1.62* (H9*anti*).

^{13}C NMR $\delta_C(CDCl_3)$: 133.7 (C7), 133.3 (C6), 78.8 (C4), 56.3 (OMe), 52.7 (C2), 42.1 (C3), 40.9 (C1), 35.6 (C5), 19.7_2 (C8 or C9), 19.6_8 (C9 or C8).

LRMS: $C_{10}H_{15}{}^{81}BrO$ $M^{+\cdot}$ requires 232; Found 232 (1%)
$C_{10}H_{15}{}^{79}BrO$ $M^{+\cdot}$ requires 230; Found 230 (1%)
$C_9H_{11}{}^{81}Br$ $[M-32]^{+\cdot}$ requires 200; Found 200 (2%)
$C_9H_{11}{}^{79}Br$ $[M-32]^{+\cdot}$ requires 198; Found 198 (2%)
$C_7H_9{}^{81}Br$ $[M-58]^{+\cdot}$ requires 174; Found 174 (8%)
$C_7H_9{}^{79}Br$ $[M-58]^{+\cdot}$ requires 172; Found 172 (8%).

HRMS: $C_7H_9{}^{79}Br$ $[M-58]^{+\cdot}$ requires 171.9888; Found 171.9890 (11.1%).

2-*exo*-4-*exo*-Dimethoxybicyclo[3.2.2]non-6-ene 147

Colourless oil.

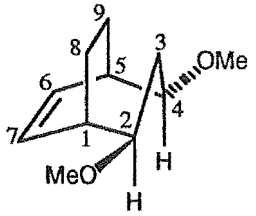

^1H NMR $\delta_H(CDCl_3)$: 6.11 (d of d, $^3J_{6,5}$ = $^3J_{7,1}$ = 5.6 Hz, $^4J_{6,1}$ = $^4J_{7,5}$ = 3.2 Hz, H6, H7), 3.31 (s, $W_{h/2}$ = 0.8, 2 x OMe), 3.11 (d of d, $^3J_{2,3endo}$ = $^3J_{4,3endo}$ = 5.1 Hz, $^3J_{2,3exo}$ = $^3J_{4,3exo}$ = 11.5 Hz, H2, H4), 2.46 (m, H1, H5), 2.40 (m, $^2J_{3endo,3exo}$ =13.2, $^3J_{3endo,2}$ = $^3J_{3endo,4}$ = 5.2 Hz, H3*endo*), 1.91 (m, H8*syn*, H9*syn*), 1.61* (H3*exo*), 1.52* (H8*anti*, H9*anti*).

^{13}C NMR $\delta_C(CDCl_3)$: 132.8 (C6, C7), 78.8 (C2, C4), 56.2 (2 x OMe), 36.6 (C3), 35.4 (C1, C5), 19.9 (C8, C9).

HRMS: $C_{11}H_{18}O_2$ $M^{+\cdot}$ requires 182.1307; Found 182.1306 (9.5%).

2-*exo*-Bromo-9-*syn*-methoxybicyclo[3.2.2]non-6-ene 148

Colourless oil.

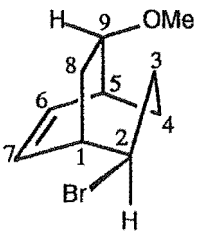

^1H NMR $\delta_H(CDCl_3)$: 6.19 (t, $^3J_{6,5}$ = $^3J_{6,7}$ = 7.8 Hz, H6), 6.09 (t, $^3J_{7,1}$ = $^3J_{7,6}$ = 7.8 Hz, H7), 4.32 (d of d, $^3J_{2,3endo}$ = 5.4 Hz, $^3J_{2,3exo}$ = 11.3 Hz, H2), 3.67 (m, $^3J_{9,5}$ = $^3J_{9,8syn}$ = 4.9 Hz, $^3J_{9,8anti}$ = 9.8 Hz, H9), 3.39 (s, $W_{h/2}$ = 0.6 Hz, OMe), 2.84 (m, H1), 2.78 (m, H3*exo*), 2.62 (m, H5), 2.30 (m, H3*endo*), 2.17*

(H8*anti*), 2.12 (m, $^2J_{8syn,\ 8anti}$ = 14.7 Hz, $^3J_{8syn,1}$ = 1.7 Hz, $^3J_{8syn,9}$ = 4.6 Hz, H8*syn*), 1.78 (m, H4*exo*), 1.52* (H4*endo*).

^{13}C NMR δ_C(CDCl$_3$): 136.3 (C6), 132.4 (C7), 78.3 (C9), 56.5 (OMe), 55.4 (C2), 42.2 (C1), 36.1 (C3), 34.0 (C5), 27.8 (C8), 27.6 (C4).

LRMS: $C_{10}H_{15}{}^{81}BrO$ $M^{+\cdot}$ requires 232; Found 232 (1%)
$C_{10}H_{15}{}^{79}BrO$ $M^{+\cdot}$ requires 230; Found 230 (1%)
$C_9H_{11}{}^{81}Br$ $[M-32]^{+\cdot}$ requires 200; Found 200 (2%)
$C_9H_{11}{}^{79}Br$ $[M-32]^{+\cdot}$ requires 198; Found 198 (2%)
$C_7H_9{}^{81}Br$ $[M-58]^{+\cdot}$ requires 174; Found 174 (6%)
$C_7H_9{}^{79}Br$ $[M-58]^{+\cdot}$ requires 172; Found 172 (6%).

HRMS: $C_7H_9{}^{79}Br$ $[M-58]^{+\cdot}$ requires 171.9888; Found 171.9888 (10.8%).

Stability of the products from bromination of *exo*-tricyclo[3.2.2.0^{2,4}]non-6-ene **47** in methanol

A mixture of products obtained from bromination of **47** (103 mg) consisting of **127** (ca. 34%), **128** (ca. 24%), and **129** (ca. 14%) was refluxed in 99.5% methanol-d_4 for 1 h. The solvent was removed under reduced pressure to give a yellow oil (99 mg). Comparison of the ^{1}H and ^{13}C NMR spectra of the products before and after reflux indicated the complete loss of **128** and some loss of **129** (ca. 60%). The appearance of a compound with ^{1}H and ^{13}C NMR data nearly identical to that of **147** was observed in the ^{1}H and ^{13}C NMR spectra of the crude reaction mixture and hence the compound was tentatively assigned to 4-*exo*-methoxy-2-*exo*-trideuteriomethoxybicyclo[3.2.2]non-6-ene **150**. Compound **150** was not isolated. GCMS analysis of the reaction mixture showed a product with an identical retention time (7.4 minutes on a Restex R_{tx}1 30 m x 0.32 mm capillary column) to that of **147** with a molecular ion peak consistent with structure **150**.

4-*exo*-methoxy-2-*exo*-trideuteriomethoxybicyclo[3.2.2]non-6-ene 150

This compound was not isolated but was identified from the crude reaction mixture. The following ^{1}H and ^{13}C NMR assignments were made:

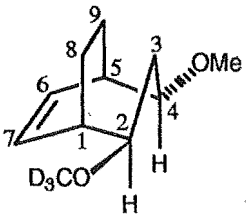

^{1}H NMR δ_H(CDCl$_3$): 6.11 (d of d, H6, H7), 3.11 (d of d, H2, H4).

^{13}C NMR δ_C(CDCl$_3$): 132.8 (C6, C7), 78.7 (C2, C4), 56.1 (OMe), 36.5 (C3), 35.3 (C1, C5), 19.8 (C8, C9).

^{2}H NMR δ_D(CCl$_4$): 3.25 (s, OCD$_3$).

HRMS: $C_{11}H_{15}{}^2H_3O_2$ $M^{+\cdot}$ requires 185.1495; Found 185.1492 (16.9%).

Deuterium Incorporation: 1% D_0, 0% D_1, 0% D_2, 99% D_3.

Low temperature NMR of the reaction of *exo*-tricyclo[3.2.2.0^{2,4}]non-6-ene **47** with bromine in methanol-d_4

Bromine (27 mg, 0.17 mmol) in methanol-d_4 (0.2 ml) was added to a solution of **47** (22 mg, 0.18 mmol) in methanol-d_4 (0.4 ml) contained in an NMR tube and cooled in a dry-ice isopropanol bath. The NMR tube was rapidly transferred to the NMR probe which was precooled to -20 °C. A ^{1}H NMR spectrum run after approximately 5 minutes showed no starting material to be present. The sample was slowly warmed to room temperature and the reaction monitored by ^{1}H NMR spectroscopy. No significant change in the ^{1}H NMR spectrum was observed on warming. When equilibrated to room temperature the the sample was removed, sodium metabisulphite added, and the solvent removed under reduced pressure at 0-5 °C. The resulting residue was divided in two; one half was extracted with $CDCl_3$ (0.7 ml) and the other with methanol-d_4 (0.7 ml). A ^{1}H NMR spectrum of the methanol-d_4 extract showed no change from that obtained before workup. ^{1}H and ^{13}C NMR spectra of the $CDCl_3$ extract allowed identification of the deuterated reaction products by comparison with those of the nondeuterated compounds previously isolated. The deuterated analogues of the following products were identified and the product ratios estimated from the ^{1}H and ^{13}C NMR spectra of the $CDCl_3$ extract: **127**, **128**, **129** in a ratio of 10:7:4, respectively.

Reaction of *exo*-tricyclo[3.2.2.0^{2,4}]non-6-ene **47** with a catalytic amount of *p*-toluenesulphonic acid in methanol

A solution of **47** (305 mg, 2.54 mmol) and *p*-toluenesulphonic acid monohydrate (PTSA) (30 mg, 0.16 mmol, 0.06 mole equivalents) in dry methanol (3 ml) was heated in a sealed tube at 80 °C for 21 days. The methanol was removed under reduced pressure and the resulting brown oil taken up with pentane, washed with a saturated solution of sodium bicarbonate (3 ml), water (3 ml), dried over $MgSO_4$, and the solvent removed under reduced pressure to give a yellow oil (149 mg, ca. 39% recovery) which was shown by GLC analysis to contain three products. The major product, 2-*exo*-methoxybicyclo[3.2.2]non-6-ene **152** (75 %) was isolated by preparative GLC. The remaining two products (15% and 10 %) were not identified.

2-*exo*-methoxybicyclo[3.2.2]non-6-ene 152

Colourless oil.

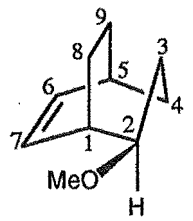

^{1}**H NMR** δ_H**(CDCl$_3$):** 6.28 (t, $^3J_{6,5} = {}^3J_{6,7} = 8.1$ Hz, H6), 6.04 (t, $^3J_{7,1} = {}^3J_{7,6} = 8.4$ Hz, H7), 3.30 (s, $W_{h/2} = 1.4$ Hz, OMe), 3.08 (d of d, $^3J_{2,3endo} = 5.3$ Hz, $^3J_{2,3exo} = 10.4$ Hz, H2), 2.48 (m, H1), 2.30 (m, H5), 2.03* (H8*syn*), 1.99# (m, H3*endo*), 1.79# (d of d of t, $^2J_{3exo,3endo} = 13.3$ Hz, $^3J_{3exo,2} = {}^2J_{3exo,4endo} = 9.8$ Hz,

$^3J_{3exo,4exo}$ = 6.0 Hz, H3*exo*), 1.72* (H9*syn*), 1.61# (m, H4*exo*), 1.58* (H9*anti*), 1.57* (H8*anti*), 1.50# (m, H4*endo*).

^{13}C NMR $\delta_C(CDCl_3)$: 138.5 (C6), 131.1 (C7), 79.5 (C2), 56.0 (OMe), 36.1 (C1), 30.6 (C3), 30.5 (C5), 30.3 (C4), 24.3 (C9), 20.3 (C8).

HRMS: $C_{10}H_{16}O$ $M^{+\cdot}$ requires 152.1201; Found 152.1203 (24.7%).

Reaction of *exo*-tricyclo[3.2.2.0^{2,4}]non-6-ene **47** with a catalytic amount of *p*-toluenesulphonic acid in methanol-d_1

A solution of **47** (424 mg, 3.53 mmol) and *p*-toluenesulphonic acid monohydrate (50 mg, 0.26 mmol, 0.07 mole equivalents) in 95% methanol-d_1 (3 ml) was heated for 10 days at 80 °C in a sealed tube, after which time GLC analysis showed the reaction to be complete. The reaction mixture was poured into water (7 ml) and extracted with ether (16 ml). The ether extract was washed with a saturated brine solution, dried over $MgSO_4$, and the solvent removed under reduced pressure to give a brown oil (292 mg, ca. 54% recovery). GLC analysis of the resulting oil showed three peaks, 71%, 16%, and 13%. The major peak was collected by preparative GLC and shown (^{13}C and ^{2}H NMR) to contain two products, 4-*exo*-deuterio-2-*exo*-methoxybicyclo[3.2.2]non-6-ene **154** (40%) and 4-*endo*-deuterio-2-*exo*-methoxybicyclo[3.2.2]non-6-ene **155** (31%). The ratio of the two products was estimated from integration of the ^{2}H NMR spectrum (ratio 1.3:1.0). The two other products (16% and 13%) were not identified.

4-*exo*-deuterio-2-*exo*-methoxybicyclo[3.2.2]non-6-ene 154 and **4-*endo*-deuterio-2-*exo*-methoxybicyclo[3.2.2]non-6-ene 155**

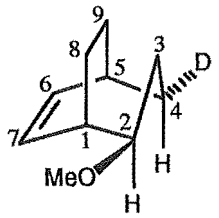

154

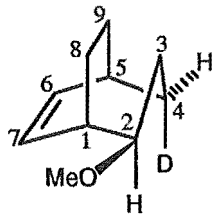

155

Colourless oils.

The following assignments were made for both molecules:

^{1}H NMR $\delta_H(CCl_4)$: 6.21 (t, $^3J_{6,5} = {}^3J_{6,7}$ = 8.3 Hz, H6), 5.97 (t, $^3J_{7,1} = {}^3J_{7,6}$ = 8.5 Hz, H7), 3.20 (s, $W_{h/2}$ = 1.2 Hz, OMe), 2.98 (d of d, $^3J_{2,3endo}$ =10.3 Hz, $^3J_{2,3exo}$ = 5.4 Hz, H2), 2.42 (m, H1), 2.28 (m, H5), 1.97* (H8*syn*), 1.90* (H3*endo*), 1.74* (H3*exo*), 1.52-1.62 (m, H8*anti*, H9*anti*, H9*syn*).

The following proton chemical shifts were assigned to the indicated compounds:

154: 1.46 ppm (H4*endo*).

155: 1.59 ppm (H4*exo*)

^{13}C NMR $\delta_C(CCl_4)$: 137.9 (C6), 131.0$_8$ and 131.1$_1$ (C7), 78.8 (C2), 55.4 (OMe), 35.9$_2$ (C1), 30.3$_0$, 30.2$_8$, 30.1$_8$, 30.0$_6$, 24.4 (C9), 20.1 and 20.0 (C8).

^{2}H NMR $\delta_D(CCl_4)$: 154 1.80 (D4*exo*)

155 1.65 (D4*endo*).

HRMS: $C_{10}H_{15}{}^2H_1O$ $M^{+\cdot}$ requires 153.1264; Found 153.1264 (29.9%).

Deuterium Incorporation: 10% D_0, 90% D_1.

The following assignments were made using $CDCl_3$ as the NMR solvent:

^{1}H NMR $\delta_H(CDCl_3)$: 6.29 (m, H6), 6.04 (m, H7), 3.30 (s, OMe), 3.10 (m, H2), 2.49 (m, H1), 2.30 (m, H5).

^{13}C NMR $\delta_C(CDCl_3)$: 138.5 (C6), 131.1 (C7), 79.5 (C2), 56.0 (OMe), 36.1 (C1), 30.6, 30.5, 30.3, 24.3 (C9), 20.3 and 20.2 (C1).

Reaction of tricyclo[3.2.2.0^{2,4}]nona-6,8-diene **51** with tetracyanoethene

A solution of **51** (376 mg, 3.18 mmol) and tetracyanoethene (TCNE) (408 mg, 3.19 mmol) in CH_2Cl_2 (15 ml) was stirred at room temperature for 8 days after which time the solution was filtered and the filtrate evaporated under reduced pressure to give a brown solid (502 mg). A small portion (60 mg) was purified by column chromatography (silica gel, $CHCl_3$ elution) to give 10,10,11,11-tetracyanopentacyclo[5.4.0.0^{2,9}0^{3,5}0^{6,8}]-undecane **158** (41 mg, 44%).

10,10,11,11-Tetracyanopentacyclo[5.4.0.0^{2,9}0^{3,5}0^{6,8}]undecane 158

White crystalline solid: mp 223-224 °C (ethyl acetate/pet. ether).

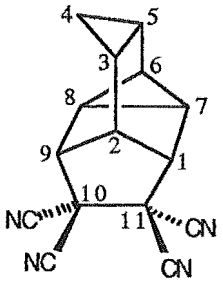

^{1}H NMR δ_H(DMSO-d_6): 3.61 (s, $W_{h/2}$ = 3.3 Hz, $^3J_{1,2}$ = 1.5 Hz, H1), 3.58 (s, $W_{h/2}$ = 3.7 Hz, $^3J_{9,2}$ = $^3J_{9,8}$ = 1.6 Hz, H9), 2.53 (d, $^3J_{2,1}$ = $^3J_{2,9}$ = 1.4 Hz, $^3J_{2,3}$ = 5.6 Hz, H2), 1.70 (d of t, $^3J_{6,5}$ = 4.1 Hz, $^3J_{6,7}$ = $^3J_{6,8}$ = 7.4 Hz, H6), 1.62 (t, $^3J_{7,6}$ = $^3J_{7,8}$ = 6.3 Hz, H7), 1.44 (m, H8), 1.26 (m, $^3J_{5,3}$ = $^3J_{5,4exo}$ = 8.6 Hz, $^3J_{5,4endo}$ = $^3J_{5,6}$ = 4.1 Hz, H5), 1.16 (m, $^3J_{3,2}$ = $^3J_{3,4endo}$= 4.5 Hz, $^3J_{3,4exo}$ = $^3J_{3,5}$ = 8.7 Hz, H3), 0.60 (d of t, $^2J_{4exo,4endo}$ = 5.0 Hz, $^3J_{4exo,3}$ = $^3J_{4exo,5}$ = 7.8 Hz, H4*exo*), 0.30 (d of t, $^2J_{4endo,4exo}$ = 5.0 Hz, $^3J_{4endo,3}$ = $^3J_{4endo,5}$ = 4.1 Hz, H4*endo*).

^{13}C NMR δ_C (DMSO-d_6): 112.9 (CN), 112.8 (CN), 111.7 (CN), 111.5 (CN), 50.2 (C1), 49.6 (C9), 47.6 (C11 or C10), 46.9 (C10 or C11), 37.6 (C2), 15.7 (C6), 15.0 (C7), 14.9 (C8), 8.0 (C4), 6.6 (C3), 5.4 (C5).

IR (KBr): 3023 (m), 2936 (m), 2252 (m) cm^{-1}.

HRMS: $C_{15}H_{10}N_4$ $M^{+\cdot}$ 246.0905; Found 246.0907 (18.3%).

Elemental analysis: Calc. C 73.15%, H 4.09%, N 22.75%; C 71.49%, H 3.68%, N 22.00%.

Reaction of *exo*-tricyclo[3.2.2.0^{2,4}]non-6-ene **47** with TCNE

(a) At 40 °C

exo-Tricyclo[3.2.2.0^{2,4}]non-6-ene **47** (100 mg, 0.83 mmol) and TCNE (106 mg, 0.83 mmol) were refluxed in CH_2Cl_2 (15 ml) for 7 days. A ^{1}H NMR (DMSO-d_6) of a sample showed no reaction had taken place.

(b) At 80 °C

The reaction mixture of part (a) was carefully concentrated under reduced pressure. Benzene (15 ml) and TCNE (110 mg, 0.86 mmol) were added and the solution refluxed for 40 days after which time a ^{1}H NMR showed no observable product formation.

(c) Sealed tube, 110 °C

exo-Tricyclo[3.2.2.0^{2,4}]non-6-ene **47** (50 mg, 0.42 mmol), TCNE (188 mg, 1.47 mmol, 3.5 mole equivalents), a few crystals of hydroquinone, and toluene (3 ml) were heated in a sealed tube at 110 °C for 9 days. The solvent was removed under reduced pressure to give a dark brown solid (221 mg). A ^{1}H NMR spectrum (acetone-d_6) of the crude reaction mixture showed little reaction had occurred. The reaction was not further investigated.

Reaction of *endo*-tricyclo[3.2.2.0^{2,4}]non-6-ene **56** with TCNE

(a) At room temperature

A solution of **56** (12 mg, 0.10 mmol) and TCNE (15 mg, 0.12 mmol, 1.2 mole equivalents) in CH_2Cl_2 (3 ml) was stirred at room temperature for 17 days. The solvent was carefully removed under reduced pressure to give a white solid (22 mg) which was dissolved in acetone-d_6. A ^{1}H NMR spectrum showed only the presence of starting material **56**.

(b) At 70 °C

A solution of **56** and TCNE in acetone-d_6 (obtained from part (a) above) was heated at 70 °C in sealed tube for 7 days. A ^{1}H NMR spectrum of the solution after this time showed no discernable product formation.

(c) Sealed tube, 110 °C

endo-Tricyclo[3.2.2.0^{2,4}]non-6-ene **56** (30 mg, 0.25 mmol), TCNE (138 mg, 1.08 mmol, 4.3 mole equivalents), a few crystals of hydroquinone, and toluene (2 ml) were heated in a sealed tube at 110 °C for 9 days. The solvent was removed under reduced pressure to give a dark brown solid (146 mg). TLC mesh column chromatography (silica gel, 20% ethyl acetate/pet. ether elution) gave 5-*exo*-methyl-9,9,10,10-tetracyanotricyclo[4.4.0^{1,6}0^{2,8}]dec-3-ene **159** (1 mg, 2%) and a mixture of two other products (3 mg) which were not identified.

5-*exo*-Methyl-9,9,10,10-tetracyanotricyclo[4.4.0.^{1,6}0^{2,8}]dec-3-ene 159

White solid.

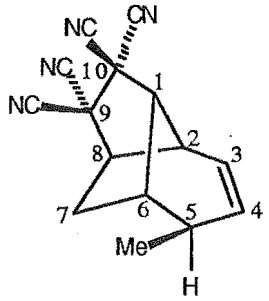

^{1}H NMR δ_H(CDCl$_3$): 5.76* (H4), 5.74* (H3), 3.18 (m, $^3J_{8,7endo}$ = 5.4 Hz, H8), 3.02 (m, H2), 2.85 (s, $W_{h/2}$ = 4.0 Hz, H1), 2.48 (d, $^3J_{6,7exo}$ = 7.8 Hz, H6), 2.31 (m, H5), 2.08 (m, $^2J_{7exo,7endo}$ = 15.2 Hz, $^3J_{7exo,6}$ = 7.8 Hz, $^4J_{7exo,2}$ = 1.5 Hz, H7*exo*), 1.73 (m, $^2J_{7endo,7exo}$ = 15.1 Hz, $^3J_{7endo,8}$ = 5.3 Hz, $^3J_{7endo,6}$ = 2.4 Hz, H7*endo*), 1.14 (d, $^3J_{Me,5}$ = 6.8 Hz, Me).

^{13}C NMR δ_C(CDCl$_3$): 134.8 (C4), 121.0 (C3), 54.6 (C8), 48.8 (C1), 44.6 (C2), 41.0 (C5), 38.5 (C6), 28.9 (C7), 19.1 (Me).

The following quaternary carbons were identified from an HMBC experiment but were not observed in the ^{13}C NMR spectrum: 45.8 (C9), 45.5 (C10).

IR (CDCl$_3$): 3015 (w), 2967 (m), 2929 (s), 2852 (m), 2256 (s), 1729 (w), 1604 (w) cm^{-1}.

HRMS: $C_{15}H_{12}N_4$ $M^{+\cdot}$ requires 248.1062; Found 248.1057 (33.3%).

CRYSTALLOGRAPHY

Table C.1 lists the crystal data and X-ray experimental details for the structure determinations. Intensity data were collected with a Nicolet R3m four-circle diffractometer by using monochromatised Mo Kα radiation. Cell parameters were determined by least squares refinement, the setting angles of at least 20 accurately centred reflections ($2\theta > 20°$) being used. Throughout data collections (ω scans; ±h, +k, +l) the intensities of three standard reflections were monitored at regular intervals and in both cases this indicated no significant crystal decomposition. The intensities were corrected for Lorentz and polarization effects and for absorption based on azimuthal psi-scans. The space groups followed from systematic absences.

The structures were solved by conventional direct methods, and refined on |F| by full matrix least squares procedures. The dibromide **71a** possessed a crystallographic mirror plane. All non-hydrogen atoms were refined with anisotropic thermal parameters. Hydrogen atoms were included in calculated positions with isotropic thermal parameters 1.25 times the isotropic equivalent of their carrier carbon atoms. The functions minimised $\Sigma w(|F_o| - |F_c|)^2$, with $w = [\sigma^2(F_o) + 0.0006F_o^2]^{-1}$. All calculations were performed on an IBM PC computer using SHELXTL PC.

Final atom coordinates and bonding geometries are listed in Tables C.2-C.5. Perspective views and atom labelling are shown in Figures C.1 and C.2.

	71a	**113**
Formula	$C_8H_{12}Br_2$	$C_9H_{12}Br_2$
Molecular weight (g mol^{-1})	268.0	280.0
Crystal System	monoclinic	monoclinic
Space Group	$P2_1/m$	$P2_1/m$
a (Å)	5.927(2)	6.5210(10)
b (Å)	11.281(4)	11.217(2)
c (Å)	6.868(3)	12.751(2)
β (°)	106.60(3)	96.020(10)
V ($Å^3$)	440.1(3)	927.6(3)
Dc (g cm^{-3})	2.022	2.005
Z	2	4
F (000)	260	544
μ (cm^{-1})	0.91	0.86
Diffractometer	Nicolet R3m	Nicolet R3m
Radiation	Mo Kα	Mo Kα
Wavelength (Å)	0.71073	0.71073
Temperature (°C)	-80	-143
Crystal dimensions (mm)	0.76 x 0.32 x 0.21	0.44 x 0.42 x 0.18
Scan mode	ω	ω
2θ range (°)	3-60	4-50
Transmission factors	0.95-0.54	1.00-0.53
Solution method	Direct methods	Direct methods
Unique data	1342	1636
Observed data ($I > 3\sigma(I)$)	1120	1273
Observed criterion	$I > 3\sigma(I)$	$I > 3\sigma(I)$
Number of parameters	69	100
R	0.031	0.024
wR	0.040	0.030

Table C.1. Crystal data and X-ray experimental details.

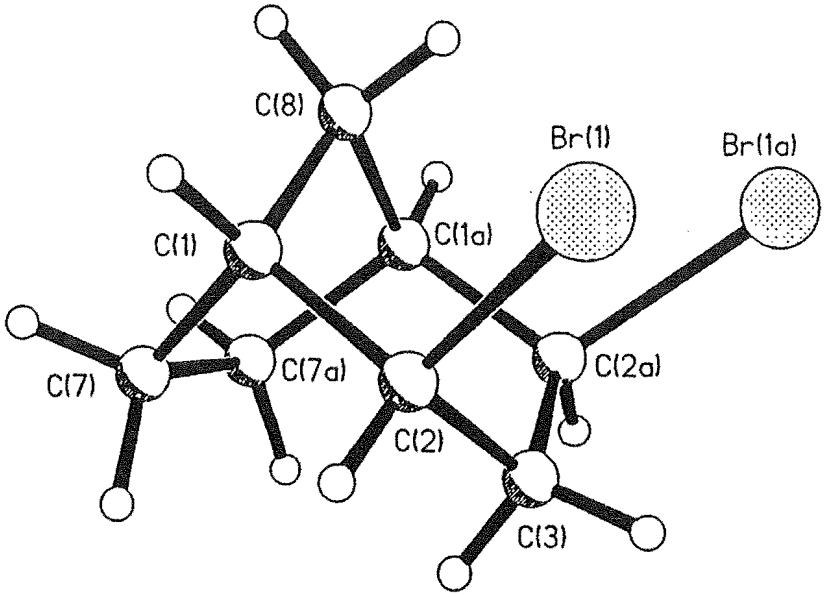

Figure C.1. X-Ray crystal structure of 2-*exo*-4-*exo*-dibromobicyclo[3.2.1]octane **71a**.

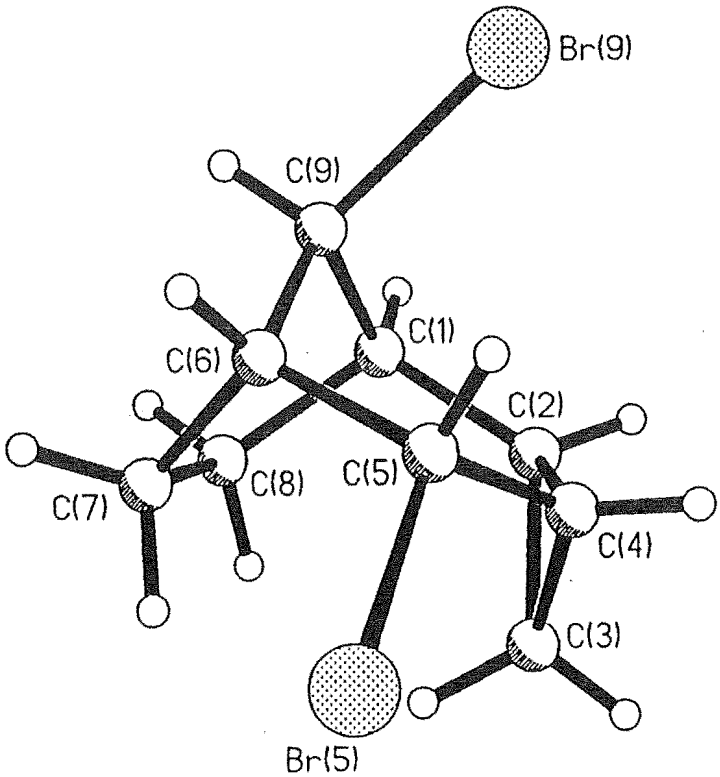

Figure C.2. X-Ray crystal structure of 5-*exo*-9-*syn*-dibromo-*endo*-tricyclo[4.2.1.$0^{2,4}$]nonane **113**.

Atomic Coordinates

Atom	x	y	z	U_{eq}[a]
Br(1)	33573(5)	8167(3)	64491(4)	27(1)
C(1)	17260(49)	14443(23)	99182(40)	18(1)
C(2)	7943(49)	13528(25)	76023(41)	19(1)
C(3)	-3598(69)	25000	65990(56)	18(1)
C(7)	-3200(53)	18077(25)	107685(42)	22(1)
C(8)	34211(71)	25000	105182(59)	21(1)

Table C.2. Atomic coordinates (x 10^5) and equivalent isotropic displacement coefficients ($Å^2$ x 10^3) for **71a** with e.s.d.'s in parentheses.

[a] Equivalent isotropic U defined as one third of the trace of the orthogonalised U_{ij} tensor.

Bond Lengths (Å)

Br(1)-C(2)	1.997(3)	C(2)-C(3)	1.532(3)
C(1)-C(2)	1.531(4)	C(3)-C(2A)	1.532(3)
C(1)-C(7)	1.544(5)	C(7)-C(7A)	1.562(6)
C(1)-C(8)	1.537(4)	C(8)-C(1A)	1.537(4)

Bond Angles (°)

C(2)-C(1)-C(7)	108.8(2)	C(1)-C(2)-C(3)	113.1(2)
C(2)-C(1)-C(8)	110.2(3)	C(2)-C(3)-C(2A)	115.2(3)
C(7)-C(1)-C(8)	102.5(2)	C(1)-C(7)-C(7A)	105.4(1)
Br(1)-C(2)-C(1)	110.1(2)	C(1)-C(8)-C(1A)	101.6(3)
Br(1)-C(2)-C(3)	111.7(2)		

Table C.3. Bond lengths (Å) and angles (°) for **71a** with e.s.d.'s in parentheses.

Atomic Coordinates

Atom	x	y	z	U_{eq}[a]
Br(5)	67081(6)	42936(4)	38268(3)	19(1)
Br(9)	16562(6)	17266(4)	56850(3)	17(1)
C(1)	20386(58)	11986(36)	34578(29)	13(1)
C(2)	42910(57)	8565(34)	37785(28)	12(1)
C(3)	60215(60)	12829(36)	31745(30)	15(1)
C(4)	57567(57)	18244(35)	42377(29)	13(1)
C(5)	48961(57)	30497(34)	43646(31)	12(1)
C(6)	26544(57)	32381(35)	38930(30)	13(1)
C(7)	22615(62)	31786(35)	26782(32)	17(1)
C(8)	16740(63)	18637(36)	23996(31)	18(1)
C(9)	13628(59)	21676(35)	41780(29)	14(1)

Table C.4. Atomic coordinates (x 10^5) and equivalent isotropic displacement coefficients ($Å^2$ x 10^3) for **113** with e.s.d.'s in parentheses.

[a] Equivalent isotropic U defined as one third of the trace of the orthogonalised U_{ij} tensor.

Bond Lengths (Å)

Br(5)-C(5)	1.996(4)	C(3)-C(4)	1.512(5)
Br(9)-C(9)	1.974(4)	C(4)-C(5)	1.500(5)
C(1)-C(2)	1.532(5)	C(5)-C(6)	1.536(5)
C(1)-C(8)	1.538(5)	C(6)-C(7)	1.545(6)
C(1)-C(9)	1.518(6)	C(6)-C(9)	1.532(6)
C(2)-C(3)	1.509(6)	C(7)-C(8)	1.556(6)
C(2)-C(4)	1.522(5)		

Bond Angles (°)

C(2)-C(1)-C(8)	114.3(3)	Br(5)-C(5)-C(4)	111.2(3)
C(2)-C(1)-C(9)	110.4(3)	Br(5)-C(5)-C(6)	110.0(3)
C(8)-C(1)-C(9)	98.9(3)	C(4)-C(5)-C(6)	115.8(3)
C(1)-C(2)-C(3)	122.1(3)	C(5)-C(6)-C(7)	116.0(3)
C(1)-C(2)-C(4)	118.0(3)	C(5)-C(6)-C(9)	108.9(3)
C(3)-C(2)-C(4)	59.8(3)	C(7)-C(6)-C(9)	99.6(3)
C(2)-C(3)-C(4)	60.5(3)	C(6)-C(7)-C(8)	106.3(3)
C(2)-C(4)-C(3)	59.7(3)	C(1)-C(8)-C(7)	104.3(3)
C(2)-C(4)-C(5)	117.9(3)	Br(9)-C(9)-C(1)	113.9(3)
C(3)-C(4)-C(5)	123.0(3)	Br(9)-C(9)-C(6)	115.3(2)
C(1)-C(9)-C(6)	102.5(3)		

Table C.5. Bond lengths (Å) and angles (°) for **113** with e.s.d.'s in parentheses.

GENERAL CALCULATION METHODS

All semiempirical calculations were performed using MOPAC Ver. 6.0 or SPARTAN Ver. 2.01 running on IBM RS6000 320 or 320H RISC computers. MOPAC Ver. 6.0 was ported to run under a UNIX environment by Dr D. Q. McDonald from the original VAX VMS code obtained from the Quantum Chemistry Program Exchange (QCPE, program number 455, 1990). SPARTAN is available from Wavefunction Inc., 18401 Von Karmen Ave, Suite 370, Irvine, CA 92715, U.S.A.

Ab initio calculations were performed using the "Ab initio" module available in SPARTAN using "direct" calculation procedures. Structure input to MOPAC was generally accessed through PCMODEL Ver. 4.0 (available from Serena Software, P.O. Box 3076, Bloomington, Indiana, U.S.A.). Molecular mechanics minimisations were performed by this program using the MMX force field.

The geometries of the stationary points located using MOPAC were refined with the "PRECISE" keyword specified. Transition states were refined using Bartel's nonlinear least squares gradient minimisation procedure, accessed with the "NLLSQ" keyword in MOPAC, or by eigenvector following routines using the "TS" keyword. In both cases the convergence criteria of the gradient norm was set to 0.1 using the "GNORM = 0.1" keyword.

Structure optimisations ("geometry optimisation" or "transition state optimisation") in SPARTAN were performed according to the standard features and convergence criteria available in this program. All commands were accessed via the standard graphical interface which was also used to construct the initial geometries. Molecular mechanics optimisations in SPARTAN were performed using the Sybyl force field.

All semiempirical or ab initio optimised structures were characterised by calculation of the associated force constants and vibrational frequencies using the "FORCE" keyword in MOPAC or the "Frequency" option available in the properties module of SPARTAN. The vibrational descriptions obtained were visualised by either using SPARTAN or, from MOPAC, using the MOLVIB program written by Dr D. Q. McDonald. Transition states were characterised by the presence of one negative force constant (one imaginary frequency) and minima were assigned by all force constants being positive. First approximations to transition states were obtained from construction of a crude model in PCMODEL, by use of the linear synchronous approximation to transition states available in SPARTAN, or from possible stationary points observed on potential energy surfaces.

Potential energy surfaces were calculated by using the grid search facilities available in MOPAC ("STEP1" and "STEP2" keywords), from the path calculation facility of MOPAC (setting the optimisation flag of the required variable in the molecules Z-matrix to "-1" and listing the required values of the variable beneath the geometry specification in

the input file), or from multiple single point calculations where the geometry of each successive point was optimised, independently of the preceding points, using MOPAC. The input files for the PE surface single point calculations were derived using the program "grid2x" and the output processed using the program "retrievex" (see program descriptions in Appendix 1).

Molecular orbitals and orbital 'maps' were visualised using standard procedures available in SPARTAN. Contour plots were constructed using the Macintosh based graphing program Deltagraph Professional. Three dimensional surfaces were either constructed from Deltagraph or from the Xsurface (or Surface) program written by Dr D. Q. McDonald running on an IBM RS6000 computer.

Molecular mechanics conformational searches were performed using BAKMDL Ver. 2.99 (1992) with the MM2 force field on IBM RS6000 computers. Geometry format interconversions were performed using the program MDLFMTS which is part of the suite of programs available with PCMODEL.

APPENDIX 1
Program Descriptions

grid2x

The program "grid2x" is used to construct multiple input files for calculation of potential energy surfaces. Each geometry file is constructed from an initial input file in the MOPAC Z-matrix format output by PCMODEL.‡ The FORTRAN input format is shown below (Figure A.1), where "a2" is two characters, "f12.6" is twelve digit floating point format with six decimal places (twelve spaces overall), "i3" is a three digit integer format, and "i4" is a four digit integer format.

The program is run interactively and prompts the user for the following input (also see Figure A.2): input file name (no extensions), a general output file name (no extensions), number of the first variable to be controlled, initial and final values of this variable, and the increment size for the first variable. The initial value, final value, and increment are input on one line separated by commas. The variable may be a bond length, bond angle or dihedral angle (Cartesian coordinate input is not supported). The program then prompts the user for the number, initial value, final value, and increment size for the second variable. The number of atoms in the molecule is then input followed by the number of symmetry relations present in the input geometry. Note that the value of each variable in the original geometry specification should by equal to the initial value specified in the input file. The variable number is derived from the following: the bond length of the first atom is variable one, the bond angle of atom one is variable two, the dihedral angle of the first atom is variable three (all of the first three variables are set to zero in the Z-matrix). For the second atom, its bond length is variable four, bond angle is variable five, and dihedral angle is variable six. For the third atom, its bond length is variable seven, bond angle is variable eight, and dihedral angle is variable nine. This continues to the end of the geometry definition (also see the example geometry input Figure A.1).

Once all of the data has been supplied the program generates the input geometries for the variable ranges specified. For example, the input shown in Figure A.2 will create 169 individual input files named m2400s01-01,.., m2400s01-13 to m2400s13-01,.., m2400s13-13.† For the example in Figure A.1, the file has 30 atoms (including dummy atoms), variable 15 is incremented from 0° to 360° in 30° increments (12 increments gives 13 values for variable 15), the second variable 24 is incremented from 0° to 120° in

---

‡ Free format input is not supported.

† The input shown in Figure A.2 was used to setup the geometry specifications for the calculation of the PE surface shown in Figure 7.15 and relates to the Z-matrix shown in Figure A.1.

```
PM3 symmetry charge=1 t=28800 precise                          {* Keywords *}
meoh2+ attack on tricyclo[3.2.1.0(2,4)]octane epimerised oxygen {* Title *}
                                                               {* Blank line *}
XX    0.000000 0      .000000 0      .000000 0   0  0  0
XX    0.519000 0      .000000 0      .000000 0   1  0  0
H     0.991000 0    90.000000 0      .000000 0   2  1  0
O     1.306101 0   100.716174 0    92.130000 0   3  2  1
H     0.955096 1   106.081216 1     0.000000 0   4  3  2
XX    0.705000 0    90.000000 0  -150.220000 0   5  4  3
C     1.428992 1   108.234426 1    88.120422 0   4  5  6
H     1.095133 1   104.296087 1     0.000000 0   7  4  5
H     1.096680 1   111.578136 1   120.000000 0   7  4  5
H     1.095651 1   108.726388 1   240.000000 0   7  4  5
C     1.417576 0    73.120012 0   -87.267155 0   3  2  1
C     1.596260 0    87.473431 0   128.922642 0  11  3  2
C     1.454525 0    64.407623 0  -177.836433 0  12 11  3
C     1.528371 1   121.385982 1   -89.456254 1  13 12 11
C     1.542458 1   110.609294 1    -1.754148 1  14 13 12
C     1.545588 1   103.870443 1    71.748648 1  15 14 13
C     1.539803 1   103.577321 1    -2.110555 1  16 15 14
C     1.548312 1   100.915397 1    36.667340 1  17 16 15
H     1.111349 1    87.591012 1     6.664417 1  11  3  2
H     1.103406 1   120.681318 1   107.945527 1  13 12 11
H     1.098689 1   116.318699 1   -65.641026 1  12 11  3
H     1.103548 1   117.708779 1    69.689020 1  12 11  3
H     1.106565 1   113.143362 1  -131.486550 1  14 13 12
H     1.104002 1   110.988080 1  -167.750661 1  15 14 13
H     1.107728 1   111.839966 1   -48.895914 1  15 14 13
H     1.105360 1   111.561290 1   116.725990 1  16 15 14
H     1.106374 1   113.079015 1  -124.125733 1  16 15 14
H     1.106243 1   114.648404 1   161.540974 1  17 16 15
H     1.103279 1   113.550127 1  -177.067122 1  18 14 13
H     1.102981 1   114.176574 1    60.072530 1  18 14 13

8,7,9                                                  {* Symmetry relation*}
8,11,10                                                {* Symmetry relation*}
|  |          |  |          |  |          |  |  |  |  |
a2    f12.6    i3    f12.6    i3    f12.6    i3 i4 i3 i3   {* Format *}
```

Figure A.1. Input format required by the grid2x program. The FORTRAN input format is also shown. Variables 15 and 24 are underlined.

```
m2400s          {* Input file name *}
m2400s          {* General output file name *}
15              {* First variable number *}
0,360,30        {* initial, final, and increment values for variable 1 *}
24              {* Second variable number *}
0,120,12        {* initial, final, and increment values for variable 2 *}
30              {* Number of atoms in geometry specification *}
2               {* Number of symmetry elements *}
```

Figure A.2. Example command input for the program grid2x.

10° increments (12 increments, 13 values of variable 24), and two symmetry relations were specified (see Figure A.1). Note that the program works in a similar way to the grid molecular mechanics conformational searches whereby the first variable is fixed at its initial value and the second incremented until the upper limit of this variable is reached. The first variable is then incremented to its second value (30° in this case) and the second variable is incremented from its initial to final values. The program also writes a file which contains the commands required to run each single calculation ("*filename*x", e.g. "m2400sx" for the example shown above). This file is made executable by the following UNIX command:

chmod u+x *filename*
(e.g. chmod u+x m2400sx)

The executable file is then submitted to the "batch" queue and will run each calculation in turn. MOPAC then produces the '*filename*.out' and '*filename*.sum' files. The output from MOPAC should be kept to a minimum as the calculations may use large amounts of disk space. The ".sum" files are used for further processing by the "retrievex" program (see later this section); however, the ".out" files are generally not required further and may be deleted when the calculations are complete. An intermediate file "*filename*.ipt" is also generated by "grid2x" and is required by the "retrievex" program.

retrievex

Once the calculations obtained from MOPAC and grid2x have completed successfully‡ the "retrievex" program is then run to extract all of the energies from the ".sum" files. The program requires only the general file name to be input ("m2400s" for the above example) and runs interactively to produce two files, "*filename*.del" and "*filename*.sur" ("m2400s.del" and "m2400s.sur" for the above example). Note that the ".del" and ".sur" files must not already exist or the program will stop so as not to overwrite any potentially useful information (an error message "trouble writing file tfile" will be displayed). The ".del" file gives the values of the adjusted variables and the

---

‡ If all of the calculations have not been completed successfully, i.e. a structure has not converged and thus has not produced a ".sum" file, the "retrievex" program will not run and will output the error message "trouble reading dfile". If this occurs it may be useful to resubmit the point that has not converged but using a successfully completed structure with similar values of the variables being incremented as a starting geometry. The required variable values of the unsuccessful point are then input into the new starting geometry and the MOPAC calculation resubmitted.

corresponding energies in kcal mol^{-1} in a format readable by Deltagraph Professional.§ The second output file, the ".sur" file, is in the format required by the Xsurface program, except that the square root of the number of calculated points needs to be put on the first line of the file. Note that the Xsurface program of Dr. D. Q. McDonald requires a square grid and may require some scaling of the graph axes values.

§ Conversion to kJ mol^{-1} can be accomplished using the "formula" function of Deltagraph Professional.

APPENDIX 2
Program Listings

grid2x Fortran Listing

```
      program grid
*
*  program sets up seperate files for grid calculations
*  and reads specified symmetry relations
*
      integer inlen,numatms,i,j,k,l,numi1,numi2,var1,var2
      integer bdf(80),baf(80),daf(80),con1(80),con2(80),con3(80)
      real init1,final1,init2,final2
      real*16 incrmt1,incrmt2
      real da(80),bd(80),ba(80),t
      character infile*17,line1*80,line2*80,line3*80,atms(80)*2
      character symtry(31)*80
      integer nsym
*
*  get input file name and determine length of name
*
       write(*,*) 'input filename (max. 12 characters,no extensions)'
      read(*,1000) infile
      write(*,*)
      inlen=0
      do 100 i=1,12
        if(infile(i:i).ne.' ') inlen=inlen+1
 100  continue
*
*  get variable #1 to form grid and interval,etc
*
      write(*,*) 'input first variable number'
      read(*,*) var1
      write(*,*) 'input lowest,highest and increment for this variable'
      read(*,*) init1,final1,incrmt1
      write(*,*) 'input number of increments for first variable'
      read(*,*) numi1
*
*  get variable #2 to form second dimension of grid
*
      write(*,*) 'input second variable number'
      read(*,*) var2
      write(*,*) 'input lowest,highest and incrment for this variable'
      read(*,*) init2,final2,incrmt2
      write(*,*) 'input number of increments for second variable'
      read(*,*) numi2
*
*  get the total number of atoms in molecule
*
      write(*,*) 'input number of atoms in the molecule'
      read(*,*) numatms
      write(*,*) numatms
*
*  get symmetry if present
*
```

```
      write(*,*) 'input number of symmetry relations'
      read(*,*) nsym
*
* now read the original file
*
      call gfile(line1,line2,line3,atms,bd,bdf,ba,baf,da,daf,con1,
     *     con2,con3,infile,numatms,nsym,symtry)
*
*    set up grid of files
*
      call wfile(inlen,infile,incrmt1,incrmt2,line1,line2,line3,
     *  bd,bdf,ba,baf,da,daf,var1,var2,atms,con1,con2,con3,
     * numi1,numi2,numatms,init1,final1,init2,final2,nsym,symtry)
*
*     the end
*
      stop

 1000 format(a17)
 1100 format(a1)

      end


      subroutine increment(incrmx,rvtcx,nvtcx,bd,ba,da,
     *  tbd,tbdf,tba,tbaf,tda,tdaf,idx)
*
*  subroutine to inrement variables
*
      real bd(80),da(80),ba(80),tbd(80),tda(80),tba(80)
      real*16 incrmx
      integer rvtcx,nvtcx,tbdf(80)
      integer tbaf(80),tdaf(80),idx

      if(nvtcx.eq.1) then
        tbd(rvtcx)=bd(rvtcx)+((idx-1)*incrmx)
        tbdf(rvtcx)=0
      else
        if(nvtcx.eq.2) then
          tba(rvtcx)=ba(rvtcx)+((idx-1)*incrmx)
          tbaf(rvtcx)=0
        else
          tda(rvtcx)=da(rvtcx)+((idx-1)*incrmx)
          tdaf(rvtcx)=0
        endif
      endif

      return

      end


      character*17 function mkfname(finlen,k,tinfile)
*
*  function to make file names for input geometries
*
      character tinfile*17,infile*17
      integer temp,k,l,filelen,ept,finlen,numlet
```

```
      temp=k
      l=0
700   l=l+1
      if((temp.ge.10).and.(temp.lt.100)) then
        ept=1
      else
        ept=0
        if(l.eq.1)then
          tinfile(finlen+1:finlen+1)='0'
          l=l+1
        endif
      endif
      numlet=int(temp/(10**ept))+48
      tinfile(finlen+1:finlen+1)=char(numlet)
      temp=temp-(numlet-48)*(10**ept)
      if(ept.gt.0) goto 700
      mkfname=tinfile

      return

200   format(a17)
      end


      subroutine wfile(inflen,infle,incr1,incr2,line1,line2,line3,
     *    bd,bdf,ba,baf,da,daf,var1,var2,atms,wcn1,wcn2,wcn3
     *   ,numinc1,numinc2,natms,intl1,fin1,intl2,fin2,ttnsym,
     *   ttsymtry)
*
*  subroutine writes separate input files
*
      character  infle*17,tinfle*17,mkfname*17,outfile*17,toutfile*17
      character atms(80)*2,line1*80,line2*80,line3*80
      integer inflen,rvtc1,rvtc2,nvtc1,nvtc2,opflen,topflen
      character opfile*17,txfile*13
      real*16 incr1,incr2
      real intl1,fin1,intl2,fin2
      integer tinlen,i,j,k,l,txlen
      character first*5
      integer baf(80),bdf(80),daf(80),tinflen,outlen
      integer tdaf(80),tbdf(80),tbaf(80),var1,var2
      integer wcn1(80),wcn2(80),wcn3(80),natms,numinc1,numinc2
      real bd(80),ba(80),da(80),tbd(80),tda(80),tba(80)
      character ttsym,ttsymtry(31)*80
      integer ttnsym

      rvtc1=int(var1/3)
      nvtc1=mod(var1,3)
      nvtc2=mod(var2,3)
      rvtc2=int(var2/3)

      if(nvtc1.gt.0) rvtc1=rvtc1+1
      if(nvtc2.gt.0) rvtc2=rvtc2+1
*
*  set up input file for extraction program
*
        opflen=inflen+4
```

```
      opfile(1:opflen)=infle(1:inflen)//'.ipt'
      open(21,file=opfile(1:opflen),status='new',err=997)
      write(21,102) var1
      write(21,103) intl1,fin1,incr1,numinc1
      write(21,102) var2
      write(21,103) intl2,fin2,incr2,numinc2
      write(21,102) natms
      topflen=opflen+1
      write(21,102) topflen
*
* open executable file
*
      txlen=inflen+1
      txfile(1:txlen)=infle(1:inflen)//'x'
      open(22,file=txfile(1:txlen),status='unknown',err=997)
      do 600 i=1,numinc1+1
        first='TRUE '
        do 605 l=1,natms
          tbd(l)=bd(l)
          tbdf(l)=bdf(l)
          tba(l)=ba(l)
          tbaf(l)=baf(l)
          tda(l)=da(l)
          tdaf(l)=daf(l)
605     continue

        do 610 j=1,numinc2+1
        tinfle=infle
        tinlen=inflen
        tinfle=mkfname(tinlen,i,tinfle)
        tinlen=tinlen+2
        tinfle(tinlen+1:tinlen+1)='-'
        tinlen=tinlen+1
        tinfle=mkfname(tinlen,j,tinfle)
        tinlen=tinlen+2
        write(21,105) tinfle(1:tinlen)
        write(22,106) 'runmopac ',tinfle(1:tinlen)
        open(20,file=tinfle(1:tinlen),err=997)
        write(20,1000)line1
        write(20,1000)line2
        write(20,1000)line3
        if(first.eq.'TRUE ') then
          call increment(incr1,rvtc1,nvtc1,bd,ba,da,tbd,tbdf,tba
     *          ,tbaf,tda,tdaf,i)
            first='FALSE'
        endif
        do 620 k=1,natms
            if(k.eq.rvtc2)then
          call increment(incr2,rvtc2,nvtc2,bd,ba,da,tbd,tbdf,
     *          tba,tbaf,tda,tdaf,j)
          endif
          write(20,101) atms(k),tbd(k),tbdf(k),tba(k),
     *          tbaf(k),tda(k),tdaf(k),wcn1(k),wcn2(k),wcn3(k)
620     continue

        if (ttnsym.gt.0) then
          do 630 k=1,ttnsym+1
            write(20,1000) ttsymtry(k)
```

```
630         continue
           endif

610       continue

600   continue

      close(21,status='keep')
      close(22,status='keep')
     return

997    write(*,*) 'problem writing file'
1000   format(a80)
101    format(a2,f12.6,i3,f12.6,i3,f12.6,i3,i4,i3,i3)
102   format(i3)
103   format(3f9.2,i4)
104   format(a17)
105   format(a17)
106   format(a9,a17)
     end


     subroutine gfile(11,12,13,atms,bd,bdf,ba,baf,da,daf,cn1,
    *                 cn2,cn3,ifile,natms,tnsym,tsymtry)
*
*   subroutine to read input file
*
     integer natms,bdf(80),baf(80),i,j
     integer daf(80),cn1(80),cn2(80),cn3(80)
     real bd(80),ba(80),da(80)
     character  ifile*17,11*80,12*80,13*80,atms(80)*2
     character tsym,tsymtry(31)*80
     integer tnsym

     write(*,*) ifile
     write(*,*) natms
     open(19,file=ifile,status='OLD',err=998)
     read(19,500) 11
     read(19,500) 12
     read(19,500) 13
          do 501 i=1,natms
       read(19,510) atms(i),bd(i),bdf(i),ba(i),baf(i),da(i),daf(i)
    *            ,cn1(i),cn2(i),cn3(i)
       write(*,510) atms(i),bd(i),bdf(i),ba(i),baf(i),da(i),daf(i)
    *            ,cn1(i),cn2(i),cn3(i)
501   continue
     if (tnsym.gt.0) then
       do 502 j=1,tnsym+1
         read(19,500) tsymtry(j)
502     continue
      write(*,*) 'done read'
     endif

     return
998 write(*,*) 'error finding file'
500 format(a80)
510 format(a2,f12.6,i3,f12.6,i3,f12.6,i3,i4,i3,i3)
511 format(a17)
```

```
      end
```

retrievex Fortran Listing

```
      program retrieve
*
*  program reads MOPAC ".sum" files from grid calc.'s & writes results
*  in Deltagraph and Xsurface formats
*
      integer var1,var2,natms,ttf
      integer inlen,fcount,dflen,topflen,toflen
      integer i,j,k,numinc1,numinc2,tlen
      real deltah(80,80),incr1,incr2,init1,init2,final2,final1
      character infile*21,tfile*21,ofile1*21,ofile2*21,dfile*21
      character dline*80,dummy*40,tdfile*17
*
*  get input file name & length
*
      write(*,*) 'input general filename (max.12 chars,no extensions)'
      read(*,104) infile
      write(*,*)
      inlen=0
      do 100 i=1,12
        if(infile(i:i).ne.' ') inlen=inlen+1
  100 continue
*
*  read '.ipt' file
*
      tlen=inlen+4
      tfile(1:tlen)=infile(1:inlen)//'.ipt'
      open(20,file=tfile(1:tlen),status='old',err=997)
      read(20,102) var1
      read(20,103) init1,final1,incr1,numinc1
      read(20,102) var2
      read(20,103) init2,final2,incr2,numinc2
      read(20,102) natms
      read(20,102) topflen
      write(*,*) natms,topflen
*
*  read '.sum' files
*
      do 110 i=1,numinc1+1
        do 120 j=1,numinc2+1
           read(20,104) tdfile
          ttf=17-topflen+1
          toflen=topflen+4
          dfile(1:toflen)=tdfile(ttf:17)//'.sum'
          open(21,file=dfile(1:toflen),status='old',err=998)
          do 130 k=1,18
            read(21,105) dline
  130       continue
          read(21,106) dummy,deltah(i,j)
          close(21,status='keep')
  120   continue
  110 continue
*
*  write output files
*
      call dout(deltah,numinc1,numinc2,init1,init2,infile,inlen,incr1
```

```
     *  ,incr2)
        call qout(deltah,numinc1,numinc2,init1,init2,infile,inlen,incr1
     *  ,incr2)

        stop

  102  format(i3)
  103  format(3f9.2,i4)
  104  format(a17)
  105  format(a80)
  106  format(a40,f9.2)

  997  write(*,*) 'trouble writing file tfile'
  998  write(*,*) 'trouble reading file dfile'

        end


        subroutine dout(dh,numic1,numic2,intl1,intl2,ifile,ilen,inc1
     *              ,inc2)
*
* subroutine writes Deltagraph input format
*
        character*21 ifile,dofle
        real dh(80,80),intl1,intl2,temp(80),v1
        integer numic1,numic2,ilen,dlen
        integer k,i,j,l
        real inc1,inc2
        character dd*8,dsp(80)

        do 207 l=1,80
           dsp(l)=','
  207  continue
        dd='       '
        dlen=ilen+4
        dofle(1:dlen)=ifile(1:ilen)//'.del'
        open(22,file=dofle(1:dlen),status='new',err=996)

        write(*,*) 'about to do do loop',inc2
        do 200 k=1,numic2+1
         temp(k)=intl2+(k-1)*inc2
         write(*,*) temp(k)
  200  continue

        write(22,260) dd,(temp(k),k=1,numic2+1)

        do 202 i=1,numic1+1
           v1=intl1+(i-1)*inc1
           write(22,250) v1,(dh(i,j),j=1,numic2+1)
  202  continue

        close(22,status='keep')

        return

  996  write(*,*) 'problem writing deltagraphfile'

  250  format(80f8.2)
```

```
260  format(a8,80f8.2)

     end


     subroutine qout(dh,numic1,numic2,intl1,intl2,ifile,ilen,
    *     inc1,inc2)
*
*  subroutine writes output for Quentins Xsurface program
*
     character*21 ifile,qfile
     real intl1,intl2,dh(80,80),t1,t2,inc1,inc2
     integer qlen,ilen,numic1,numic2,i,j

     qlen=ilen+4
     qfile(1:qlen)=ifile(1:ilen)//'.sur'
     open(23,file=qfile(1:qlen),status='new',err=995)

     do 301 i=1,numic1+1
       t1=intl1+(i-1)*inc1
       do 302 j=1,numic2+1
         t2=intl2+(j-1)*inc2
         write(23,300) t1
         write(23,300) t2
         write(23,300) dh(i,j)
302    continue
301  continue

     close(23,status='keep')
     return

995  write(*,*) 'problem writing file for Xsurface'
300  format(f8.2)

     end
```

REFERENCES

1. Förster, T. *Z. Phys. Chem., Abt. B* **1939**, *43*, 58.
2. Coulson, C. A; Moffit, W. E. *Philos. Mag.* **1949**, *40*, 1.
3. Walsh, A. D. *Trans. Faraday Soc.* **1949**, *45*, 179.
4. Hoffmann, R. *J. Chem. Phys.* **1964**, *40*, 2480.
5. Newton, M. D.; Switkes, E.; Lipscomb, W. N. *J. Chem. Phys.* **1970**, *53*, 2645.
6. Newton, M. D. In *Modern Theoretical Chemistry*; Schaefer, H. F., Ed.; Plenium: New York, 1977; Vol. 4, Chapter 6.
7. Battiste, M. A.; Coxon, J. M. In *The Chemistry of the Cyclopropyl Group*; Rappoport, Z., Ed.; Wiley and Sons: Chichester, 1987; Chapter 6.
8. Cremer, D.; Kraka, E. *J. Am. Chem. Soc.* **1985**, *107*, 3800.
9. Dewar, M. J. S. *J. Am. Chem. Soc.* **1984**, *106*, 669.
10. Edmiston, C.; Ruedenberg, K. *Rev. Mod. Phys.* **1963**, *35*, 457.
11. Hamilton, J. G.; Palke, W. E. *J. Am. Chem. Soc.* **1993**, *115*, 4159.
12. Dewar, M. J. S. *Bull. Soc. Chim. Belg.* **1979**, *88*, 957.
13. Burritt, A.; Coxon, J. M.; Steel, P. J. In *Trends in Organic Chemistry*, in press.
14. Coxon, J. M.; Steel, P. J.; Whittington, B. I. *J. Org. Chem.* **1989**, *54*, 1383.
15. Coxon, J. M.; Steel, P. J.; Whittington, B. I. *J. Org. Chem.* **1989**, *54*, 3702.
16. Coxon, J. M.; Steel, P. J.; Whittington, B. I. *J. Org. Chem.* **1990**, *55*, 4136.
17. Wiberg, K. B.; Kass, S. R. *J. Am. Chem. Soc.* **1985**, *107*, 988.
18. Coxon, J. M.; Steel, P. J.; Whittington, B. I.; Battiste, M. A. *J. Am. Chem. Soc.* **1988**, *110*, 2988.
19. Baird, R. L.; Aboderin, A. A. *J. Am. Chem. Soc.* **1964**, *86*, 252.
20. Wiberg, K. B.; Kass, S. R.; Bishop, K. C. *J. Am. Chem. Soc.* **1985**, *107*, 996.
21. Wiberg, K. B.; Kass, S. R.; Bishop, K. C. *J. Am. Chem. Soc.* **1985**, *107*, 1003.
22. Zimmerman, M. P.; Li, H.-T.; Duax, W. L.; Weeks, C. M.; Djerassi, C. *J. Am. Chem. Soc.* **1984**, *106*, 5602.
23. Fukui, K. *Acc. Chem. Res.* **1971**, *4*, 57.
24. Skell, P. S.; Day, J. C.; Shea, K. J. *J. Am. Chem. Soc.* **1976**, *98*, 1195.
25. Lambert, J. B.; Black, R. D. H.; Shaw, J. H.; Papay, J. T. *J. Org. Chem.* **1970**, *35*, 3214.
26. DePuy, C. H. *Förtschr. Chem. Försch.* **1973**, *40*, 73.
27. Lambert, J. B.; Iwanetz, B. A. *J. Org. Chem.* **1972**, *37*, 4082.

28. Deno, N. C.; Lincoln, D. N. *J. Am. Chem. Soc.* **1966**, *88*, 5357.
29. Shea, K. J.; Skell, P. S. *J. Am. Chem. Soc.* **1973**, *95*, 6728.
30. Nagorski, R. W.; Brown, R. S. *J. Am. Chem. Soc.* **1992**, *114*, 7773.
31. Vardhan, H. B.; Bach, R. D. *J. Org. Chem.* **1992**, *57*, 4948.
32. Whittington, B. I. Ph.D. Thesis, University of Canterbury, 1989.
33. Lambert, J. B.; Chelius, E. C.; Schulz, Jr., W. J.; Carpenter, N. E. *J. Am. Chem. Soc.* **1990**, *112*, 3156.
34. DeBoer, A.; De Puy, C. H. *J. Am. Chem. Soc.* **1970**, *92*, 4008.
35. DePuy, C. H.; McGirk, R. H. *J. Am. Chem. Soc.* **1974**, *96*, 1121.
36. Lambert, J. B.; Chelius, E. C.; Bible, Jr., R. H.; Hajdu, E. *J. Am. Chem. Soc.* **1991**, *113*, 1331.
37. Yamabe, S.; Minato, T.; Seki, M.; Inagaki, S. *J. Am. Chem. Soc.* **1988**, *110*, 6047.
38. Ouellette, R. J.; Robins, R. D.; South, Jr., A. *J. Am. Chem. Soc.* **1968**, *90*, 1619.
39. Nesmeyanova, O. A.; Lukina, M. Y.; Kazanskii, B. A. *Dokl. Akad. Nauk SSSR* **1963**, *153*, 114.
40. Nesmeyanova, O. A.; Lukina, M. Y.; Kazanskii, B. A. *Dokl. Akad. Nauk SSSR* **1963**, *153*, 357.
41. Wardell, J. L. In *Comprehensive Organometallic Chemistry*; Wilkinson, G., Ed.; Pergamon: Oxford, 1982; Vol. 2, p 863.
42. Traylor, T. G. *Acc. Chem. Res.* **1969**, *2*, 152.
43. Balsamo, A.; Battistini, C.; Crotti, P.; Macchia, B.; Macchia, F. *J. Org. Chem.* **1975**, *40*, 3233.
44. Danishefsky, S. *Acc. Chem. Res.* **1979**, *12*, 66.
45. Verhé, R.; De Kimpe, N. In *The Chemistry of the Cyclopropyl Group*; Rappoport, Z., Ed.; Wiley and Sons: Chichester, 1987; Chapter 9.
46. Vilsmaier, E. In *The Chemistry of the Cyclopropyl Group*; Rappoport, Z., Ed.; Wiley and Sons: Chichester, 1987; Chapter 22.
47. Clark, R. D.; Heathcock, C. H. *Tetrahedron Lett.* **1975**, 529.
48. Cristol, S. J.; Jarvis, B. B. *J. Am. Chem. Soc.* **1967**, *89*, 5885.
49. Koser, G. F.; Relenyi, A. G. *J. Org. Chem.* **1976**, *41*, 1266.
50. Stewart, J. M.; Westberg, H. H. *J. Org. Chem.* **1965**, *30*, 1951.
51. Danishefsky, S.; Singh, R. K. *J. Am. Chem. Soc.* **1975**, *97*, 3239.
52. Singh, R. K; .Danishefsky, S. *J. Org. Chem.* **1975**, *40*, 2969.
53. Danishefsky, S.; Singh, R. K. *J. Org. Chem.* **1975**, *40*, 3807.
54. Corey, E. J.; Fuchs, P. L. *J. Am. Chem. Soc.* **1972**, *94*, 4014.
55. Trost, B. M.; Taber, D. F.; Alper, J. B. *Tetrahedron Lett.* **1976**, 3857.

56. Reissig, H.-U. In *The Chemistry of the Cyclopropyl Group*; Rappoport, Z., Ed.; Wiley and Sons: Chichester, 1987; Chapter 8.
57. de Meijere, A. *Angew. Chem. Int. Ed. Engl.* **1979**, *18*, 809.
58. Allen, F. H. *Acta Cryst.* **1980**, *B36*, 81.
59. Hoffmann, R. *Tetrahedron Lett.* **1970**, 2907.
60. Günther, H. *Tetrahedron Lett.* **1970**, 5173.
61. Clark, T.; Spitznagel, G. W.; Klose, R.; Schleyer, P. v. R. *J. Am. Chem. Soc.* **1984**, *106*, 4412.
62. Liu, H.-W.; Walsh, C. T. In *The Chemistry of the Cyclopropyl Group*; Rappoport, Z., Ed.; Wiley and Sons: Chichester, 1987; Chapter 16.
63. Closs, G. L.; Krantz, K. D. *J. Org. Chem.* **1966**, *31*, 638.
64. Fischer, F.; Applequist, D. E. *J. Org. Chem.* **1965**, *30*, 2089.
65. Simmons, H. E.; Smith, R. D. *J. Am. Chem. Soc.* **1959**, *81*, 4256.
66. Rawson, R. J.; Harrison, I. T. *J. Org. Chem.* **1970**, *35*, 2057.
67. Rhodes, Y. E.; Schueler, P.E.; DiFate, V. G. *Tetrahedron Lett.* **1970**, 2073.
68. Schueler, P. E.; Rhodes, Y. E. *J. Org. Chem.* **1974**, *39*, 2063.
69. Kohler, E. P.; Tishler, M.; Potter, H.; Thompson, H. T. *J. Am. Chem. Soc.* **1939**, *61*, 1057.
70. Radlick, P.; Klem, R.; Spurlock, S.; Sims, J. J.; van Tamelen, E. E.; Whitesides, T. *Tetrahedron Lett.* **1968**, 5117.
71. Westberg, H. H.; Dauben, Jr., H. J. *Tetrahedron Lett.* **1968**, 5123.
72. Daub, J.; Schleyer, P. v. R. *Angew. Chem. Int. Ed. Engl.* **1968**, *7*, 468.
73. de Meijere, A.; Schallner, O.; Weitemeyer, C. *Tetrahedron Lett.* **1973**, 3483.
74. Daub, J.; Trautz, V.; Erhardt, U. *Tetrahedron Lett.* **1972**, 4435.
75. De Lucchi, O.; Lucchini, V.; Pasquato, L.; Modena, G. *J. Org. Chem.* **1984**, *49*, 596.
76. Walborsky, H. M.; Loncrini, D. F. *J. Am. Chem. Soc.* **1954**, *76*, 5396.
77. De Lucchi, O.; Modena, G. *J. Chem. Soc., Chem. Commun.* **1982**, 914.
78. Paquette, L. A.; Moerck, R. E.; Harirchian, B.; Magnus, P. D. *J. Am. Chem. Soc.* **1978**, *100*, 1597.
79. Davis, A. P.; Whitham, G. H. *J. Chem. Soc., Chem. Commun.* **1980**, 639.
80. Colter, A. K.; Miller, Jr., R. E. *J. Org. Chem.* **1971**, *36*, 1898.
81. Paquette, L. A.; Williams, R. V. *Tetrahedron Lett.* **1981**, *22*, 4643.
82. Truce, W. E.; McManimie, R. J. *J. Am. Chem. Soc.* **1954**, *76*, 5745.
83. Parham, W. E.; Heberling, J. *J. Am. Chem. Soc.* **1955**, *77*, 1175.
84. Truce, W. E.; McManimie, R. J. *J. Am. Chem. Soc.* **1953**, *75*, 1672.
85. Brown, A. C.; Carpino, L. A. *J. Org. Chem.* **1985**, *50*, 1749.
86. De Lucchi, O.; Pasquato, L. *Gazz. Chim. Ital.* **1984**, *114*, 349.

87. Wakefield, B. J. In *Best Synthetic Methods: Organolithium Methods*; Katritsky, A. R.; Meth-Cohn, O.; Rees, C. W., Eds.; Academic: London, 1988; Chapter 3, p 23..
88. Carr, R. V. C.; Williams, R. V.; Paquette, L. A. *J. Org. Chem.* **1983**, *48*, 4976.
89. Simpkins, N. S. *Tetrahedron* **1990**, *46*, 6951.
90. Carr, R. V. C.; Paquette, L. A. *J. Am. Chem. Soc.* **1980**, *102*, 853.
91. De Lucchi, O.; Pasquato, L. *Tetrahedron* **1988**, *44*, 6755.
92. Barton, D. H. R.; Crich, D.; Motherwell, W. B. *Tetrahedron* **1985**, *41*, 3901.
93. Dauben, W. G.; Bridon, D. P.; Kowalczyk, B. A. *J. Org. Chem.* **1990**, *55*, 376.
94. Hasebe, M.; Tsuchiya, T. *Tetrahedron Lett.* **1987**, *28*, 6207.
95. Yates, P.; Eaton, P. *J. Am. Chem. Soc.* **1960**, *82*, 4436.
96. Fray, G. I.; Robinson, R. *J. Am. Chem. Soc.* **1961**, *83*, 249.
97. Inukai, T.; Kasai, M. *J. Org. Chem.* **1965**, *30*, 3567.
98. Inukai, T.; Kojima, T. *J. Org. Chem.* **1966**, *31*, 2032.
99. Bellus, D.; Helferich, G.; Weis, C. D. *Helv. Chim. Acta* **1971**, *54*, 463.
100. Taber, D. F. *J. Org. Chem.* **1982**, *47*, 1351.
101. Kirmse, W.; Wahl, K.-H. *Chem. Ber.* **1974**, *107*, 2768.
102. Hasebe, M.; Tsuchiya, T. *Tetrahedron Lett.* **1986**, *27*, 3239.
103. Paquette, L. A.; Carr, R. V. C. *Org. Synth.* **1986**, *64*, 157.
104. Konovalov, A. I. *Dokl. Akad. Nauk SSSR* **1965**, *162*, 343.
105. Becker, S.; Fort, Y.; Caubère, P. *J. Org. Chem.* **1990**, *55*, 6194.
106. Whitesell, J. K.; Minton, M. A. *Stereochemical Analysis of Alicyclic Compounds by C-13 NMR Spectroscopy*; Chapman and Hall: London, **1987**.
107. Garratt, D. G. *Can. J. Chem.* **1980**, *58*, 1327.
108. Mark, V. *Tetrahedron Lett.* **1974**, 299.
109. Tori, K.; Ueyama, M.; Tsuji, T.; Matsumura, H.; Tanida, H.; Iwamura, H.; Kushida, K.; Nishida, T.; Satoh, S. *Tetrahedron Lett.* **1974**, 327.
110. Subramanian, P. M.; Emerson, M. T.; LeBel, N. A. *J. Org. Chem.* **1965**, *30*, 2624.
111. Smart, B. E. *J. Org. Chem.* **1973**, *38*, 2027.
112. Stirling, C.J.M. *Radicals in Organic Chemistry*; Oldbourne; London, 1965; Chapter 6.
113. Brown, H. C. *Acc. Chem. Res.* **1983**, *16*, 432.
114. Dewar, M. J. S.; Merz, Jr., K. M. *J. Am. Chem. Soc.* **1986**, *108*, 5634.
115. Saunders, M.; Johnson, Jr., C. S. *J. Am. Chem. Soc.* **1987**, *109*, 4401.
116. Brown, H. C. *Acc. Chem. Res.* **1986**, *19*, 34.
117. Dewar, M. J. S. *Acc. Chem. Res.* **1985**, *18*, 292.

118. Olah, G. A.; Prakash, G. K. S.; Saunders, M. *Acc. Chem. Res.* **1985**, *18*, 292.
119. Koch, W.; Liu, B.; DeFrees, D. J. *J. Am. Chem. Soc.* **1989**, *111*, 1527.
120. Olah, G. A.; Prakash, G. K. S.; Saunders, M. *Acc. Chem. Res.* **1983**, *16*, 440.
121. Walling, C. *Acc. Chem. Res.* **1983**, *16*, 448.
122. Yoshimine, M.; McLean, A. D.; Liu, B.; DeFrees, D. J.; Binkley, J. S. *J. Am. Chem. Soc.* **1983**, *105*, 6185.
123. Raghavachari, K.; Haddon, R. C.; Schleyer, P. v. R.; Schaefer, H. F. *J. Am. Chem. Soc.* **1983**, *105*, 5915.
124. Kato, M.; Yamamoto, S.; Yoshihara, T.; Furuichi, K.; Miwa, T. *Chem. Lett.* **1987**, 1823.
125. Lippmaa, E.; Pehk, T.; Belikova, N. A.; Bobyleva, A. A.; Kalinichenko, A. N.; Ordubadi, M. D.; Platé, A. F. *Org. Magn. Reson.* **1976**, *8*, 74.
126. Strothers, J. B.; Tan, C. T. *Can. J. Chem.* **1977**, *55*, 841.
127. Tori, K.; Aono, K.; Kitahonoki, K.; Muneyuki, R.; Takano, Y.; Tanida, H.; Tsuji, T. *Tetrahedron Lett.* **1966**, 2921.
128. Tori, K.; Aono, K.; Hata, Y.; Muneyuki, R.; Tsuji, T.; Tanida, H. *Tetrahedron Lett.* **1966**, 9.
129. Kwart, H.; Kaplan, L. *J. Am. Chem. Soc.* **1954**, *76*, 4072.
130. Kwart, H.; Miller, R. K. *J. Am. Chem. Soc.* **1956**, *78*, 5678.
131. Kaplan, L.; Kwart, H.; Schleyer, P. v. R. *J. Am. Chem. Soc.* **1960**, *82*, 2341.
132. Japenga, J.; Klumpp, G. W.; Stapersma, J. *Tetrahedron* **1977**, *33*, 2847.
133. Marchand, A. P. *Methods in Stereochemical Analysis 1; Stereochemical Applications of NMR Studies in Rigid Bicyclic Systems*; Verlag Chemie International: Florida, 1982; Chapter 4.
134. Ruasse, M.-F. *Acc. Chem. Res.* **1990**, *23*, 87.
135. Hendrickson, J. B.; Boeckman, Jr., R. K. *J. Am. Chem. Soc.* **1969**, *91*, 3269.
136. McManus, L. D.; Rogers, N. A. J. *Tetrahedron Lett.* **1969**, 4735.
137. Müller, E. *Chem. Ber.* **1976**, *109*, 3793.
138. Gleiter, R.; Bohm, M. C.; de Meijere, A.; Pruess, T. *J. Org. Chem.* **1983**, *48*, 796.
139. Srinivasan, R.; Ors, J. A.; Brown, K. H.; Baum, T.; White, L. S.; Rossi, A. R. *J. Am. Chem. Soc.* **1980**, *102*, 5297.
140. Verma, S. M.; Singh, M. D. *Recl. Trav. Chim. Pays-Bas* **1978**, *97*, 238.
141. Tori, K.; Kitahonoki, K. *J. Am. Chem. Soc.* **1965**, *87*, 386.
142. Alder, K.; Jacobs, G. *Chem. Ber.* **1953**, *86*, 1528.
143. March, J. In *Advanced Organic Chemistry*, 3rd ed.;Wiley and Sons: New York, 1985; p 347.

144. Russell, G. A.; Keske, R. G.; Holland, G.; Mattox, J.; Givens, R. S.; Stanley, K. *J. Am. Chem. Soc.* **1975**, *97*, 1892.
145. Silverstein, R. M.; Bassler, G. C.; Morrill, J. C. *Spectrometric Identification of Organic Compounds*, 4th ed.; Wiley and Sons: New York, 1981; p 269.
146. Henbest, H. B.; Nicholls, B. *J. Chem. Soc.* **1959**, 227.
147. Bly, R. K.; Bly, R. S. *J. Org. Chem.* **1963**, *28*, 3165.
148. Bly, R. S.; Bly, R. K.; Bedenbaugh, A. O.; Vail, O. R. *J. Am. Chem. Soc.* **1967**, *89*, 880.
149. Factor, A.; Traylor, T. G. *J. Org. Chem.* **1968**, *33*, 2607.
150. Sasaki, T.; Kanematsu, K.; Kondo, A.; Nishitani, Y. *J. Org. Chem.* **1974**, *39*, 3569.
151. Berson, J. A. *J. Am. Chem. Soc.* **1954**, *76*, 5748.
152. Berson, J. A.; Swidler, R. *J. Am. Chem. Soc.* **1954**, *76*, 4060.
153. Kwart, H.; Kaplain, L. *J. Am. Chem. Soc.* **1954**, *76*, 4078.
154. Berson, J. A. *J. Am. Chem. Soc.* **1954**, *76*, 4069.
155. Haasnoot, C. A. G.; De Leeuw, F. A. A. M.; Altona, C. *Tetrahedron* **1980**, *36*, 2783.
156. Garbisch, Jr., E. W. *J. Am. Chem. Soc.* **1964**, *86*, 5561.
157. Olah, G. A.; Reddy, V. P.; Prakash, G. K. S. *Chem. Rev.* **1992**, *92*, 69.
158. Tidwell, T. T. In *The Chemistry of the Cyclopropyl Group*; Rappoport, Z., Ed.; Wiley and Sons: Chichester, 1987; Chapter 10.
159. Haywood-Farmer, J. *Chem. Rev.* **1974**, *74*, 315.
160. Musso, H.; Biethan, U. *Chem. Ber.* **1967**, *100*, 119.
161. Fry, J. L.; Karabatos, G. J. In *Carbonium Ions*; Olah, G. A.; Schleyer, P. v. R.; Eds.; Wiley and Sons: New York, 1970; Vol. 2, Chapter 14.
162. Berson, J. A.; Luibrand, R. T.; Kundu, N. G.; Morris, D. G. *J. Am. Chem. Soc.* **1971**, *93*, 3075.
163. Künzer, H.; Cottrell, C. E.; Paquette, L. A. *J. Am. Chem. Soc.* **1986**, *108*, 8089.
164. Aydin, R.; Frankmölle, W.; Schmalz, D.; Gunther, H. *Magn. Reson. Chem.* **1988**, *26*, 408.
165. Battiste, M. A.; Coxon, J. M.; Posey, R. G.; King, R. W.; Mathew, M.; Palenik, G. J. *J. Am. Chem. Soc.* **1975**, *97*, 945.
166. Coxon, J. M.; de Bruijn, M.; Lau, C. K. *Tetrahedron Lett.* **1975**, 337.
167. Fickes, G. N.; Metz, T. E. *J. Org. Chem.* **1978**, *43*, 4057.
168. Tabushi, I.; Yamamura, K.; Yoshida, Z.; Togashi, A. *Bull. Chem. Soc. Jpn.* **1975**, *48*, 2922.

169. Carey, F. A.; Sundberg, R. J. *Advanced Organic Chemistry: Part A: Structure and Mechanisms*; Plenium: New York, 1990; p 313-319.
170. Traegar, J. C.; McLoughin, R. G. *J. Am. Chem. Soc.* **1981**, *103*, 3647.
171. Halim, H.; Heinrich, N.; Koch, W.; Schmidt, J.; Frenking, G. *J. Comp. Chem.* **1986**, *7*, 93.
172. Stewart, J. J. P. *J. Comp. Chem.* **1989**, *10*, 200.
173. Bingham, R. C.; Dewar, M. J. S.; Lo, D. H. *J. Am. Chem. Soc.* **1975**, *97*, 1294.
174. Bischof, P. K.; Dewar, M. J. S. *J. Am. Chem. Soc.* **1975**, *97*, 2278.
175. Al-Khowaiter, S. H.; Wellington, C. A. *Tetrahedron* **1977**, *33*, 2843.
176. Schwarz, H.; Franke, W.; Chandrasekhar, J.; Schleyer, P. v. R. *Tetrahedron* **1979**, *35*, 1969.
177. Radom, L.; Pople, J. A.; Buss, V.; Schleyer, P. v. R. *J. Am. Chem. Soc.* **1971**, *93*, 1813
178. Radom, L.; Pople, J. A.; Buss, V.; Schleyer, P. v. R. *J. Am. Chem. Soc.* **1972**, *94*, 311.
179. Hariharan, P. C.; Radom, L.; Pople, J. A.; Schleyer, P. v. R. *J. Am. Chem. Soc.* **1974**, *96*, 599.
180. Lischka, H.; Kohler, H.-J. *J. Am. Chem. Soc.* **1978**, *100*, 5297.
181. Raghavachari, K.; Whiteside, R. A.; Pople, J. A.; Schleyer, P. v. R. *J. Am. Chem. Soc.* **1981**, *103*, 5649.
182. Møller, C.; Plesset, M. S. *Phys. Rev.* **1934**, *46*, 618.
183. Binkley, J. S.; Pople, J. A. *Int. J. Quantum Chem.* **1975**, *9*, 229.
184. Pople, J. A.; Binkley, J. S.; Seeger, R. *Int. J. Quantum Chem. Symp.* **1976**, *10*, 1.
185. Krishnan, R.; Pople, J. A. *Int. J. Quantum Chem.* **1978**, *14*, 91.
186. Rosenstock, H. M.; Draxl, K.; Steiner, B. W.; Herron, J. T. *J. Phys. Chem. Ref. Data, Suppl. 1* **1977**.
187. Chong, S.-L.; Franklin, J. L. *J. Am. Chem. Soc.* **1972**, *94*, 6347.
188. Viviani, D.; Levy, J. B. *Int. J. Chem. Kinet.* **1979**, *11*, 1021.
189. Attinà, M.; Cacace, F.; Giacomello, P. *J. Am. Chem. Soc.* **1980**, *102*, 4768.
190. Dewar, M. J. S.; Healy, E. F.; Ruiz, J. M. *J. Chem. Soc., Chem. Commun.* **1987**, 943.
191. Dewar, M. J. S.; Ford, G. P. *J. Am. Chem. Soc.* **1979**, *101*, 783.
192. Koch, W.; Liu, B.; Schleyer, P. v. R. *J. Am. Chem. Soc.* **1989**, *111*, 3479.
193. DePuy, C. H.; Fünfschilling, P. C.; Andrist, A. H.; Olson, J. M. *J. Am. Chem. Soc.* **1977**, *99*, 6297.

194. Hopkinson, A. C. In *The Chemistry of Alkanes and Cycloalkanes*; Rappoport, Z., Ed.; Wiley and Sons: Chichester, 1992; p 535-537.
195. Saunders, M.; Vogel, P.; Hagen, E. L.; Rosenfeld, J. *Acc. Chem. Res.* **1973**, *6*, 53.
196. Vogel, P. *Carbocation Chemistry*; Elsevier: Amsterdam, 1985.
197. Schleyer, P. v. R.; Laidig, K. E.; Wiberg, K. B., Saunders, M.; Schindler, M. *J. Am. Chem. Soc.* **1988**, *110*, 300.
198. Saunders, M.; Laidig, K. E.; Wiberg, K. B.; Schleyer, P. v. R. *J. Am. Chem. Soc.* **1988**, *110*, 7652.
199. Schultz, J. C.; Houle, F. A.; Beauchamp, J. L. *J. Am. Chem. Soc.* **1984**, *106*, 3917.
200. Stewart, J. J. P. *J. Comp. Chem.* **1989**, *10*, 209.
201. Stewart, J. J. P. *J. Comp. Chem.* **1991**, *12*, 320.
202. Dewar, M. J. S.; Zoebisch, E. G.; Healy, E. F.; Stewart, J. J. P. *J. Am. Chem. Soc.* **1985**, *107*, 3902.
203. Stewart, J. J. P. In *Reviews in Computational Chemistry*; Lipkowitz, K. B.; Boyd, D. B., Eds.; VCH: New York, 1990; Vol. 1, Chapter 2.
204. Stewart, J. J. P. MOPAC Ver. 6.0 manual and references cited therein.
205. Bingham, R. C.; Dewar, M. J. S.; Lo, D. H. *J. Am. Chem. Soc.* **1975**, *97*, 1285.
206. Pople, J. A.; Beveridge, D. L.; Dobosh, P. A. *J. Chem. Phys.* **1967**, *47*, 2026.
207. Pople, J. A.; Santry, D. P.; Segal, G. A. *J. Chem. Phys.* **1965**, *43*, S129.
208. Clark, T. In *A Handbook of Computational Chemistry*; Wiley and Sons, New York, 1985; Chapter 4.
209. Dewar, M. J. S.; Storch, D. M. *J. Chem. Soc., Chem. Commun.* **1985**, 94.
210. Cramer, C. J.; Truhlar, D. G. *J. Am. Chem. Soc.* **1991**, *113*, 8305.
211. Cramer, C. J.; Truhlar, D. G. *J. Am. Chem. Soc.* **1991**, *113*, 8552.
212. Cramer, C. J.; Truhlar, D. G. *Science* **1992**, *256*, 213.
213. Cramer, C. J.; Truhlar, D. G. *J. Comp. Chem.* **1992**, *13*, 1089.
214. Dewar, M. J. S.; Jie, C.; Yu, J. *Tetrahedron* **1993**, *49*, 5003.
215. Lambert, J. B.; Schulz, Jr., W. J.; Mueller, P. H.; Kobayashi, K. *J. Am. Chem. Soc.* **1984**, *106*, 792.
216. Battiste, M. A.; Coxon, J. M. *Tetrahedron. Lett.* **1986**, *27*, 517.
217. Galland, B.; Evleth, E. M.; Ruasse, M.-F. *J. Chem. Soc., Chem. Commun.* **1990**, 898.
218. Poirier, R. A.; Demaré, G. R.; Yates, K.; Csizmadia, I. G. *J. Mol. Struct. (THEOCHEM)* **1983**, *94*, 137.

219. Poirier, R. A.; Mezey, P. G.; Yates, K.; Csizmadia, I. G. *J. Mol. Struct. (THEOCHEM)* **1981**, *85*, 153.
220. Yamabe, S.; Minato, T.; Inagaki, S. *J. Chem. Soc., Chem. Commun.* **1988**, 532.
221. Wünsch, E.; Sodupe, M.; Lluch, J. M.; Oliva, A.; Bertrán, J. *J. Mol. Struct. (THEOCHEM)* **1988**, *170*, 225.
222. Hehre, W. J.; Hiberty, P. C. *J. Am. Chem. Soc.* **1974**, *96*, 2665.
223. Bach, R. D.; Henneike, H. F. *J. Am. Chem. Soc.* **1970**, *92*, 5589.
224. Kinns, M.; Sanders, J. K. M. *J. Magn. Reson.* **1984**, *56*, 518.
225. Perpick-Dumont, M.; Reynolds, W. F.; Eriquez, R. G. *Magn. Reson. Chem.* **1988**, *26*, 358.
226. Hauser, C. R.; Adams, J. T.; Levine, R. *Org. Synth. Collective Vol. 3*; **1964**, p 291.
227. Vogel, A.; Furniss, B. S.; Hannaford, A. J.; Rogers, V.; Smith, P. W. G.; Tatchell, A. R. *Vogel's Textbook of Practical Organic Chemistry*, 4th ed.; Longman: London, 1987; p 812.

ACKNOWLEDGEMENTS

I would like to thank the academic and technical staff of the Department of Chemistry at the University of Canterbury for their help and cooperation during the course of this work, particularly, Rewi Thompson and Mike Van der Colk for their help in the operation of the NMR and GLC instruments.

I would also like to express my appreciation to Dr John Blunt for his help with the more elaborate NMR experiments and to Drs Alan Happer and Robert Maclagan for many helpful discussions.

I would also like to thank my supervisor Prof. Jim Coxon for his expert supervision and guidance throughout this work.

I would particularly like to thank Dr Peter Steel for his help in all aspects of this work, for performing the X-ray crystal structure analyses, and for his help in the preparation of this thesis.

My thanks also go out to the following students, both past and present, for their help and interesting thought provoking conversations: Quentin McDonald, Siew Tai Fong (Mowthorpe), Ian Phillips, Kiawan Gan, Edward Coxon, and Jane Taylor.

I would like to acknowledge the financial support of a University of Canterbury postgraduate scholarship.

Finally, I would like to thank my parents and brother for their continuous and unending support and encouragement throughout the duration of this work, without which completion of this thesis would not have been possible.